ASPECTS OF THE DRAINAGE PROCESS IN SOILS

Submitted to the University of Cape Town in partial fulfilment of the requirements for the degree of Master of Science in Engineering.

Gavin Roger Wardle

Febuary 1986.

DECLARATION BY CANDIDATE

'I, Gavin Roger Wardle, hereby declare that this thesis represents my own work, carried out under the supervision of Prof A.D.W. Sparks of the University of Cape Town, and is according to the requirements of the regulations of the University for the award of the degree, Master of Science in Engineering.'

Signed

G.R. Wardle

Febuary 1985.

DEDICATION

TO NEIL, IRENE, AND ELAINE

SYNOPSIS

The initial portion of this thesis contains a review of basic theory. An experimental programme was also undertaken to measure soil parameters; and to observe heads and seepage rates during transient flow conditions in experiments. These experimental values were compared with results from finite element calculations. It was necessary for the candidate to devise a system for modifying an existing main-frame finite element package (ADINAT) in order to cope with the transient partly saturated draining state which exists above a falling water table. Good agreement was found between observed and computed transient heads. The experimental work of other investigators was also analysed by using this Finite Element program, and again good agreement was found between observed and computed transient conditions. It was decided in conjunction with the supervisor to limit this thesis to two-dimensional flow in the vertical plane.

ACKNOWLEDGEMENTS

I would like to express my sincere gratitude to the following:

Professor A.D.W. Sparks, under whose supervision this thesis was conducted.

Mr N. Hassen, for his assistance in the laboratory.

Mr C. Doig and Mr G. Jack, for their suggestions and advice, in relation to the design of the electrical circuitary needed for the experiments.

Mr D Joubert, for the use of the electrical pressure transducers he had designed and built.

Professor W.S. Doyle, for his encouragement and permission, in relation to the use of ADINAT.

Miss D Sutherland, for her patience and immaculate typing of this thesis.

All the staff of the Department of Civil Engineering for their help and friendship during this period.

The Council of Scientific and Industrial Research for their financial assistance.

CONTENTS

APPENDIX F

CHAPTER 1

INTRODUCTION.

1.1 General.

The flow of water or seepage through a rigid porous media is of great importance in many fields of engineering, agriculture and groundwater geology. Traditionally attention was focused on the saturated zone in analyzing seepage through earth structures and the subsurface. However, the unsaturated zone also plays a big part in the movement of moisture. This is important when we have a changing water table (phreatic surface) in transient problems, e.g., earth dam with a variable reservoir head, or a land mass being drained to a ditch or to a river. Also a large number of problems take place in the unsaturated zone, e.g., above the water table (phreatic surface). Examples are the recharge of the water table from a ditch, canal or pond; the irrigation of land, and the movement of toxic leachates beneath sanitary landfills. An understanding of the flow in the unsaturated region is also important because of negative pore-water pressures that are important for stability analysis, but cannot be calculated from the classical free-surface approach. Most problems are one of an unconfined aquifer with flow taking place both above and below the phreatic surface.

In general the problem is to determine the pressure distribution and velocity of the water in the interior of a soil mass with given boundary conditions. Mathematically speaking the problem is in the class known as boundary-value problems. However, before it is possible to make a theoretical analysis of the flow of water in a rigid porous medium, it is necessary to understand the soil-moisture relationship.

1.2 Aims and Objectives.

The aim of this thesis was to describe both the parameters that are important for the flow of water in a draining saturated-unsaturated

rigid porous media, and to develop an effective method for solving this type of problem. The investigation was taken further, and the actual parameters for a soil were measured; an experimental program was planned; and a theoretical verification was made by using the finite element method.

In order to achieve this, the principal aim was divided into a number of initial secondary objectives, namely:-

a) A literature survey on soil-moisture relationships, in connection with drainage.

b) A literature survey on the methods for obtaining the parameters that are important in the drainage of soils.

c) A review of the finite element method with application to the solution of two-dimensional seepage problems.

d) An experimental program to investigate the flow of water in a saturated-unsaturated rigid porous medium.

e) Design and construction of experimental equipment needed for the experimental program.

f) The design and construction of a data-acquisition unit to record the output signals from pressure transducers.

g) The finite element method program packages available at the University of Cape Town were investigated to seek one that might be used for the solving of seepage problems.

h) The existing finite element method program packages were not suitable for transient seepage with partly saturated zones above the phreatic surface. The candidate therefore decided to modify and add an extra option to an existing computer package.

i) Verification of the experimental results with the finite element method was undertaken.

j) It was hoped that useful suggestions in the use of the finite element method for different flow problems, will arise from this thesis.

CHAPTER 2

A REVIEW OF THE PHYSICAL PROCESS OF DRAINAGE.

2.1 Introduction.

The parameters that affect the drainage process are numerous. In this thesis the porous medium through which seepage (drainage) occurs is assumed to be rigid and made up of solid particles. The fluid used for the examples and the analysis considered is water. The air phase in the medium is assumed to be free to move and at atmospheric pressure. (ie. A one-phase flow is considered.) The fluid (water) remains a liquid and no phase change is considered as its temperature is near room temperature. (18 ^{o}C)

2.2 Properties of a Porous Media.

A porous medium is assumed to consist of a mass of discrete solid particles, which form voids of varying sizes. Each void or pore is taken to be connected to others by constricted passages. The whole forms a complex of irregular interconnected passages through which fluids may flow. A void that is isolated from others will not allow fluid to pass through it. Fluid flowing through these tortuous three-dimensional passages is subjected to acceleration and deceleration, accompanied by a dissipation of mechanical energy.

The velocity distribution of the fluid flowing through the passages may resemble that in a capillary tube, but it is essentially non-uniform in the direction of flow, although the flow may be steady. On the macroscopic level taken over an area large enough compared with the pore sizes, the discharge per unit area normal to the direction of flow will be much more uniform. This area on the macroscopic level, surrounding a point P, must be smaller than the size of the entire flow domain, otherwise the resulting average cannot represent what happens at P. On the other hand, it should also be large enough to include a sufficient number of voids (passages) to permit a meaningful statistical average.

With this generalization, details of the flow are lost, but much is gained, in that this macroscopic behaviour can be described more easily mathematically than the microscopic behaviour.

It was noted earlier that the porous medium consists of discrete solid particles in the form of a matrix with voids between. These voids may be filled completely with water and air. If the voids are completely filled with water then the medium is saturated, but if only partially filled then it is unsaturated (partially-saturated).

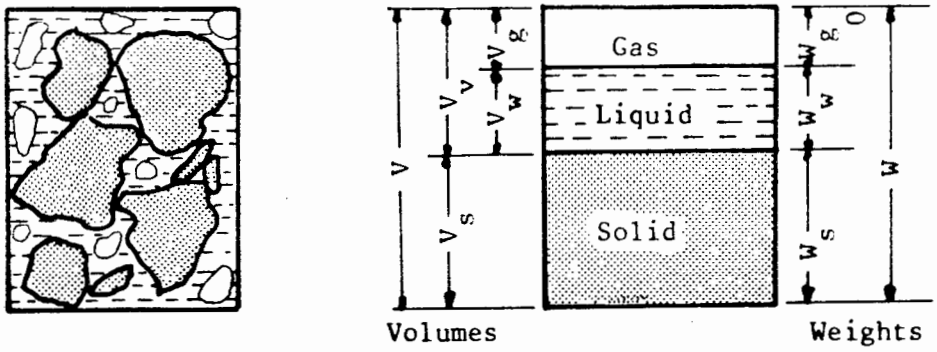

Fig 2.1: Relationship among phases in soil. (a) Element of natural soil. (b) Idealised form, element separated into phases.

In this thesis a one-phase drainage flow approach is considered, meaning that the air phase in the voids is considered to be at atmospheric pressure and free to move in the voids. To understand the properties of a porous medium it is advantageous to adopt an idealized form of diagram as shown in figure (2.1). The porous medium has a total volume V and a volume of solid particles that summates to V_s. The volume of the voids, V_v, is $(V - V_s)$. From a study of figure (2.1) the following may be defined:

Void ratio (e)

$$e = \frac{\text{volume of voids}}{\text{volume of solids}} = \frac{V_v}{V_s} \qquad (2.1)$$

Porosity (n)

$$n = \frac{\text{volume of voids}}{\text{total volume}} \tag{2.2}$$

$$n = \frac{V_v}{V} = \frac{V_v}{V_v + V_s} = \frac{e}{1 + e} \tag{2.3}$$

Degree of saturation (S_r)

$$S_r = \frac{\text{volume of water}}{\text{volume of voids}} = \frac{V_w}{V_v} \quad \text{(usually expressed as a percentage.)} \tag{2.4}$$

Volumetric moisture content or water content (θ)

$$\theta = \frac{\text{volume of water}}{\text{total volume}} = \frac{V_w}{V} \tag{2.5}$$

Classification of a porous medium is a difficult task. This is because the range of particles that could make up a soil is very large. As an example, sand and clay could be considered for simplicity.

Sands are mainly composed of macroscopic particles that are rounded or angular in shape. Sands drain readily, do not swell, possess a small capillary potential and when dry exhibit little or no shrinkage. Forces acting on fluids flowing in the pore passages are mainly due to mechanical forces (eg. forces due to pressure gradients, gravity, inertia and friction.)

Clays on the other hand, are composed of microscopic particles of platelike shape. Clays are highly impervious, exhibit considerable swelling, possess a high capillary potential, and have a considerable volume reduction upon drying. In addition to mechanical forces, molecular and electro-chemical forces are important in acting on seeping fluids and the particles of the clay. In clays, both the chemistry of the percolating water and the mineralogical structure of the clay are important.

A quantitative description of the voids in a porous medium can be given by its porosity, defined above. A definition of the void sizes appears impossible at present. The particle sizes of the medium are often used to try and characterize the void sizes, ignoring the fact that the different packings of the particles yield a wide range of void sizes. Harr [16] gives references to a number of studies that have been undertaken to try to calculate the permeability and porosity of natural soils, based on their sieve analyses and various packings of uniform spheres. Natural soils contain particles that can deviate considerably from the idealized spherical shape and, in addition, are far from uniform in size. While it is not possible to derive significant permeability estimates from porosity measurements alone, the void characteristics of these ideal packings do present some of the prominent features of natural soils.

2.3 Properties of water.

Water itself is a complex liquid, made up of two hydrogen atoms and one oxygen atom. The two hydrogen atoms are bonded at an angle with the oxygen atom, so that the H-O-H bond is not linear, but at an angle of $104{,}5^{\circ}$. The arrangement of electrons in the water molecule give it an electrical dipole nature although there is no net charge. This polarity of water molecules makes them mutually attractive. Compared with other common liquids, water has unusually high melting and boiling points, heats of fusion and vaporization, specific heat, viscosity and surface tension.

The density ρ, of a material is defined as the mass per unit volume. For water, its maximum density is at $4^{\circ}C$. Below this the substance expands due to hydrogen bonds forming an hexagonal lattice structure (eg. ice crystals). Above this temperature, expansion in the water is due to increased thermal motion of the water molecules. Still, the change in density is very small and in the normal temperature range of say $4\text{-}50^{\circ}C$, the density only decreases from 1,000 to 0,988 gm/cm^3. (See Table B-1). This change is neglected in this thesis.

The compressibility of water is defined as the relative change in the density with a change in pressure. In the soil-water relationships considered in this thesis, where the pressure changes are not great, (about one to two metres head of water) the water is assumed to be incompressible. This assumption cannot always be made, as for example, with confined aquifers the water may be subjected to very large pressures and then the compression of the water must be considered.

At the interface of the water and air a phenomenon occurs called surface tension. The water surface behaves as if it were covered by an elastic membrane in a constant state of tension, tending to cause the surface to contract. If the interface between water and air is not planar, but curved (eg. concave or convex), a pressure difference between the two phases is indicated, since equilibrium normal to the surface must exist. This pressure difference is balanced by the curved surface, surface tension forces, that have a resultant force, normal to the surface. For example, water with a bulging (convex) surface to the atmosphere indicates a pressure greater than atmospheric, and vice-versa, a dished (concave) surface indicates the water has a sub-atmospheric pressure just under the surface.

If a drop of water is placed on a solid surface it will spread to a certain extent, coming to rest with the water-air surface forming a typical angle at the edges where it makes contact with the solid surface. This angle is called the contact angle. (See figure 2.2a). The angle can vary between 0^{o}, where the drop of water would completely flatten for a perfect wetting of the solid, to 180^{o} (if it were possible) for a completely non-wetting liquid, and the drop retains a spherical shape (assuming no gravity effects). The contact angle can be different between the condition when water is advancing upon the solids (the wetting or advancing angle) and the condition when water is receding upon the solid surface (the retreating or receding angle).

If a thin clean capillary tube is dipped in water, the water level will rise in the tube, due to capillary forces. Capillary forces depend on the contact angle between the water and the tube wall and the surface-tension of the water.

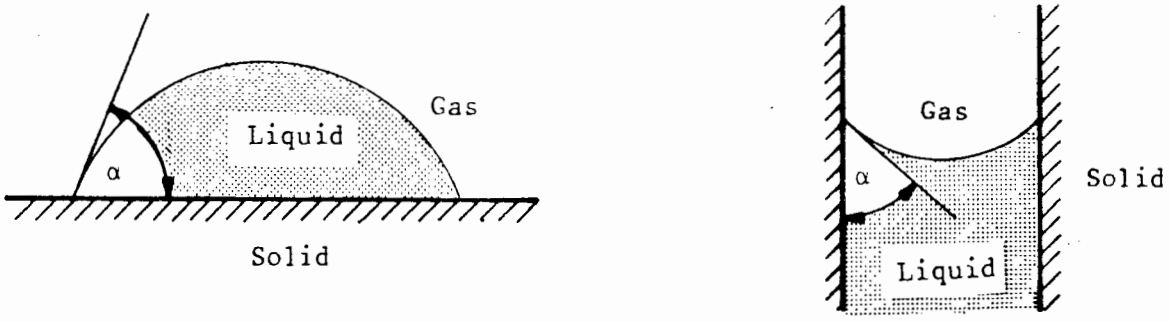

Fig 2.2: The contact angle of the water-air surface with a solid surface. (a) Of a drop resting upon a plane surface. (b) Of a meniscus in a capillary tube.

In the case of the clean capillary tube, an acute contact angle forms, with a concave water surface towards the air. (See figure 2.2b). Due to surface tension and a curved water surface, the level of the water is forced up the tube, as the water and the air are both at atmospheric pressure. The water level will come to rest in the tube where the downward force due to the weight of the raised column of water will balance the resultant upward force from the surface tension in the concave water surface. The resultant force which develops due to the contact angle being acute and the surface tension is known as the capillary force.

For water to flow through a porous medium, viscous forces have to be overcome. This is because the fluid is forced to move against shear forces (ie adjacent layers of the water are made to slide over each other). The activating force required is proportional to the shear forces. The proportionality factor is called the viscosity η. Also the ratio of the viscosity η to the density of the water is called the kinematic viscosity ν. With water, as with any fluid, the viscosity is a function of temperature, decreasing with a rise in temperature. (See Table B-2).

2.4 Flow of water in saturated soils.

The movement or flow of water through a saturated porous medium can be expressed by Darcy's Law. Henry Darcy was a French hydraulic engineer who investigated the flow of water through horizontal beds of sand to be used for water filtration. In 1856 he reported (see Todd [37]):

> "I have attempted by precise experiments to determine the law of the flow of water through filters... The experiments demonstrated positively that the volume of water which passes through a bed of sand of a given nature is proportional to the pressure and inversely proportional to the thickness of the bed traversed; thus in calling s the surface area of a filter, k a coefficient depending on the nature of the sand, e the thickness of the sand bed, $P - H_o$ the pressure below the filtering bed, $P + H$ the atmospheric pressure added to the depth of water on the filter; one has for flow of this last condition $Q = (ks/e)(H + e + H_o)$, which reduces to $Q = (ks/e)(H + e)$ when $H_o = 0$, or when the pressure below the filter is equal to the weight of the atmosphere."

This statement, that the flow rate in a porous media is proportional to the head loss and inversely proportional to the length of the flow path, is known as Darcy's Law. Figure (2.3) shows an experimental set up to show:

$$Q = \frac{k A (\phi_1 - \phi_2)}{L} \tag{2.6}$$

where k, (a coefficient of proportionality), is known as the hydraulic conductivity or coefficient of permeability, A is the constant cross-sectional area of the porous media through which flow is taking place, $\Delta\phi = (\phi_1 - \phi_2)$ is the total head loss or energy loss per unit weight of fluid and L is the length over which this total head loss occurs.

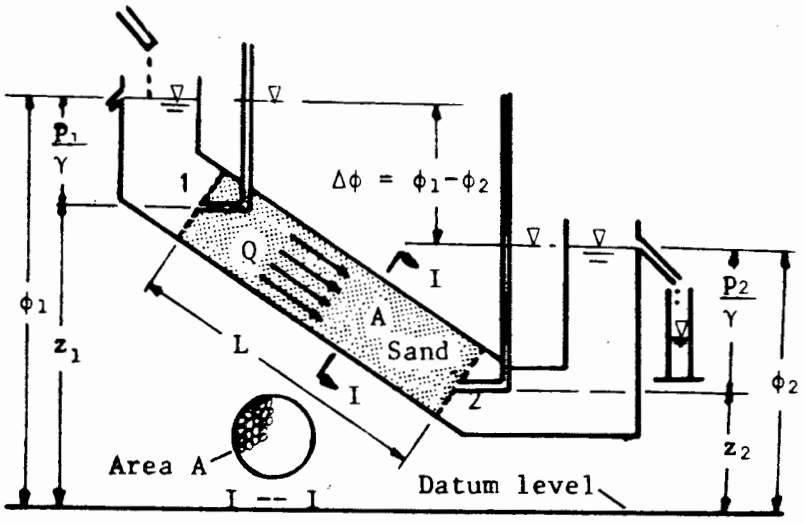

Fig 2.3: Seepage through a inclined filter due to a total head difference. (Darcy's Experiment.)

The total energy heads above a datum plane may be expressed by the Bernoulli equation:

$$\frac{p_1}{\gamma} + \frac{v_1^2}{2g} + z_1 = \frac{p_2}{\gamma} + \frac{v_2^2}{2g} + z_2 + \Delta\phi \qquad (2.7)$$

where p is pressure, γ the specific weight of water, v the velocity of flow, g the acceleration of gravity, z the elevation head above a chosen datum level, and $\Delta\phi$ the head loss. Because velocities in porous media are usually low, velocity heads may be neglected without appreciable error. Therefore the total head ϕ, is defined as:

$$\phi = \frac{p_w}{\gamma} + z \qquad (2.8)$$

or

$$\phi = \psi + z \qquad (2.9)$$

where ϕ, the pressure head or suction head is defined as:

$$\phi = \frac{p_w}{\gamma} \tag{2.10}$$

which could be negative or positive depending on the pore-water pressure p_w. Hence, rewriting equation (2.7), the total head loss becomes:

$$\Delta\phi = \left(\frac{p_1}{\gamma} + z_1\right) - \left(\frac{p_2}{\gamma} + z_2\right) \tag{2.11}$$

The macroscopic fluid velocity (flux) is given as:

$$q = \frac{Q}{A} = k\frac{\Delta\phi}{L} \tag{2.12}$$

or expressed in general terms:

$$q = -k\frac{d\phi}{dL} \tag{2.13}$$

where $d\phi/dL$ is the hydraulic gradient and is negative as flow is in the direction of decreasing head. Equation (2.13) can be rewritten as:

$$k = \frac{q}{\left(-\frac{d\phi}{dL}\right)} \tag{2.14}$$

so that the hydraulic conductivity k, is defined as the ratio of the flux to the hydraulic gradient. Plotting the flux q, versus the hydraulic gradient $-d\phi / dL$, for different flow rates, gives a linear relationship where the gradient of the line is the hydraulic conductivity.

The hydraulic conductivity can be affected by a number of parameters;

The structure and texture of the porous medium. (eg. The hydraulic conductivity is greater when a soil is highly porous and fractured then when it is compacted and dense.)

The porosity and size of conducting pores. (eg. The hydraulic conductivity of a sandy soil with large pores is greater than that of a clayey soil with small pores, even though the total porosity of the clay is generally greater.)

The chemical, physical and biological changes that can occur due to water flowing through the soil. (eg. Ion-exchange can occur in the water. Also entrapped air in the soil or air given off from the water due to a temperature change can block the pore passages, decreasing the hydraulic conductivity.)

The viscosity of the water. (eg. A change in temperature causes a change in the viscosity of water and therefore the boundary friction forces acting on the fluid will change.)

2.5 Generalization of Darcy's Law.

If the hydraulic conductivity is the same throughout the domain of a porous medium, that is, if it is independent of position within the domain, the medium is said to be homogeneous with respect to the hydraulic conductivity. Otherwise if it varies from point to point, the medium is said to be heterogeneous. If the hydraulic conductivity, at a point is the same in all directions throughout the domain of a porous medium, the medium is said to be isotropic with respect to the hydraulic conductivity. But if the hydraulic conductivity at each point in the domain varies with direction, (eg. the horizontal hydraulic conductivity at each point may be greater, or smaller, than the vertical hydraulic conductivity), then the medium is said to be anisotropic with respect to the hydraulic conductivity.

2.5.1 Isotropic medium.

The experimentally derived form of Darcy's Law (for an homogeneous material and incompressible fluid) was limited to one-dimensional flow. Generalisation of Darcy's Law to three dimensions, the flux at a point, which is a vectorial quantity, can be characterized by its magnitude and its direction. (see Bear [6]). In cartesian coordinates, equation (2.13) results in the form:

$$\underset{\sim}{q} = - k \text{ grad } \phi = - k \nabla\phi \tag{2.15}$$

where $\underset{\sim}{q}$ is the specific flux vector (macroscopic fluid velocity) with components q_x, q_y and q_z in the directions of the Cartesian x, y and z coordinates respectively, and gradϕ is the hydraulic gradient with components $-\frac{\partial\phi}{\partial x}$, $-\frac{\partial\phi}{\partial y}$, $-\frac{\partial\phi}{\partial z}$, in the x, y and z directions respectively. The total head ϕ, is given as before by:

$$\phi = \psi + z \tag{2.16}$$

where, the z-axis is taken as positive upwards from a chosen datum level, so that gravity acts in the negative z-direction.

When flow takes place through a homogeneous isotropic medium, the coefficient k, is a scalar constant and we may write equation (2.15) as three equations:

$$q_x = - k \frac{\partial\phi}{\partial x} \tag{2.17a}$$

$$q_y = - k \frac{\partial\phi}{\partial y} \tag{2.17b}$$

$$q_z = - k \frac{\partial\phi}{\partial z} \tag{2.17c}$$

Equations (2.17) remain valid for three-dimensional flow through a nonhomogeneous isotropic medium where k = k(x,y,z).

2.5.2 Anisotropic medium.

Equations (2.17) are not the most general equations incorporating Darcy's Law, since all three of the equations use the same hydraulic conductivity constant k. From equations (2.17) it follows that the influence of $\partial\phi/\partial x$ upon q_x, is equal to that of $\partial\phi/\partial y$ upon q_y and that of $\partial\phi/\partial z$ upon q_z. However, not all soils have an isotropic hydraulic conductivity. In a layered soil for example, the hydraulic conductivity is greater in the direction parallel to the layers, than in the direction perpendicular to the layers. To allow for an anisotropic hydraulic conductivity in equations (2.17), (see Bear [6]) they can be rewritten as:

$$q_x = - k_{xx} \frac{\partial\phi}{\partial x} - k_{xy} \frac{\partial\phi}{\partial y} - k_{xz} \frac{\partial\phi}{\partial z} \tag{2.18a}$$

$$q_y = - k_{yx} \frac{\partial\phi}{\partial x} - k_{yy} \frac{\partial\phi}{\partial y} - k_{yz} \frac{\partial\phi}{\partial z} \tag{2.18b}$$

$$q_z = - k_{zx} \frac{\partial\phi}{\partial x} - k_{zy} \frac{\partial\phi}{\partial y} - k_{zz} \frac{\partial\phi}{\partial z} \tag{2.18c}$$

where x, y, z are Cartesian coordinates and k_{xx} k_{xy} ... k_{zz} are nine constant numerical coefficients. Equations (2.18) can be written in a more compact form:

$$\underset{\sim}{q} = - \underset{\approx}{k} \nabla\phi \tag{2.19}$$

where $\underset{\approx}{k}$ is the hydraulic conductivity tensor:

$$\underset{\approx}{k} = \begin{bmatrix} k_{xx} & k_{xy} & k_{xz} \\ k_{yx} & k_{yy} & k_{yz} \\ k_{zx} & k_{zy} & k_{zz} \end{bmatrix} \tag{2.20}$$

Because the hydraulic conductivity tensor $\underset{\approx}{k}$, to satisfy the conservation of energy, is a symmetrical tensor (ie.: $k_{xy} = k_{yx}$), only six different coefficients are necessary to define it.

If the direction of the axes is changed to x', y' and z', then the specific flux vector in the direction of the new axes, can be found as:

$$\underset{\sim}{q'} = \begin{bmatrix} q'_x \\ q'_y \\ q'_z \end{bmatrix} \tag{2.21}$$

$$= \underset{\approx}{L}\ \underset{\sim}{q} \tag{2.22}$$

where $\underset{\approx}{L}$ is a transformation matrix of direction cosines. Similarly, the new vector of the hydraulic gradients is:

$$-\nabla\phi' = -\begin{bmatrix} \frac{\partial\phi}{\partial x'} \\ \frac{\partial\phi}{\partial y'} \\ \frac{\partial\phi}{\partial z'} \end{bmatrix} \tag{2.23}$$

$$= -\underset{\approx}{L}\ \nabla\phi \tag{2.24}$$

combining equations (2.22) and (2.24) yields:

$$\underset{\sim}{q'} = -\underset{\approx}{k'}\ \nabla\phi' \tag{2.25}$$

where the new hydraulic conductivity tensor:

$$\underset{\approx}{k'} = \underset{\sim}{L}\ \underset{\approx}{k}\ \underset{\sim}{L}^{-1} \tag{2.26}$$

With this type of transformation, it is possible to find three orthogonal directions x', y' and z' for which $\underset{\approx}{k}'$ reduces to a diagonal matrix:

$$\underset{\approx}{k}' = \begin{bmatrix} k_{x'x'} & 0 & 0 \\ 0 & k_{y'y'} & 0 \\ 0 & 0 & k_{z'z'} \end{bmatrix} \tag{2.27}$$

substituted into equation (2.25) gives:

$$\underset{\sim}{q}' = - \begin{bmatrix} k_{x'x'} & 0 & 0 \\ 0 & k_{y'y'} & 0 \\ 0 & 0 & k_{z'z'} \end{bmatrix} \nabla\phi' \tag{2.28}$$

These directions are known as the principal axes of the porous medium. Thus knowing the hydraulic conductivity of an anisotropic porous media in its three principal directions, the hydraulic conductivity tensor can be found with respect to a differently orientated orthogonal axes system, by means of a simple transformation matrix.

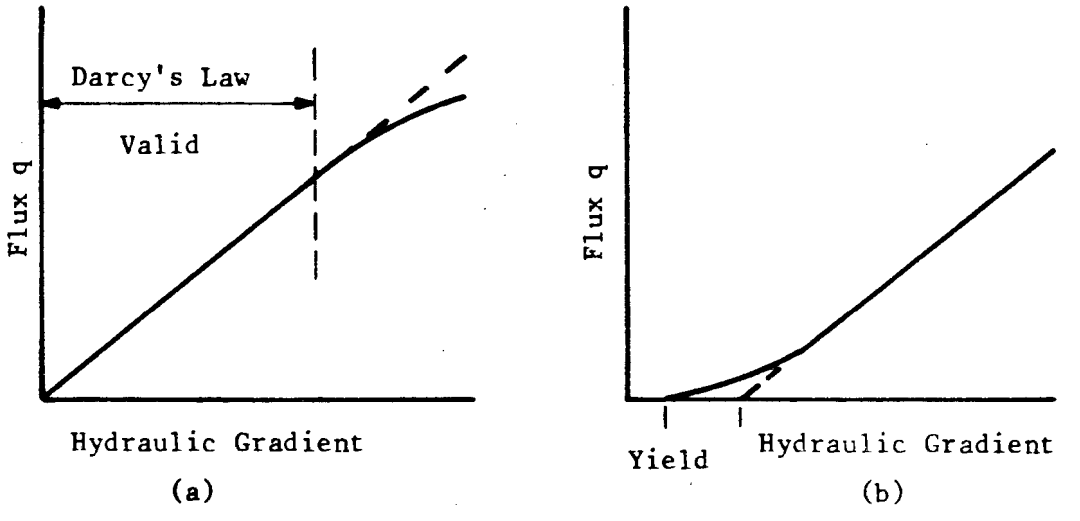

Fig 2.4: Limits of Darcy's law. (a) Deviation from Darcy's law at high flux, where flow becomes turbulent. (b) Possible deviations from Darcy's law at low gradients. (Exhibiting a Bingham liquid property.)

2.5.3 Range of validity of Darcy's Law.

Darcy's Law only applies as long as the flow of water is laminar within the pore passages. (See figure 2.4a). With turbulent flow through the pore passages, which may occur at high flux rate, (eg. In coarse sands with hydraulic gradients near or in excess of unity) Darcy's Law will not always be valid.

Also at low hydraulic gradients and with a soil that has very small pore passages, it has been reported (and disputed) that the flow rates of the water can be zero or less than proportional to the hydraulic gradient. A possible reason for this (see Hillel [18]) is that the water in close proximity to the particles acts more rigid than ordinary water, and exhibits the properties of a Bingham liquid (ie. having a yield value), rather than a Newtonian liquid. See figure (2.4b)

2.6 **Flow of water in unsaturated soil.**

Movement of water above the water table (in the zone of aeration) takes place in an unsaturated porous medium. Such flow is in general quite complicated and difficult to describe quantitatively. This is because changes in the state of the soil and the water can occur during flow. These changes involve the complex relationship between the volumetric moisture content θ, suction head (negative pressure head) ϕ, and conductivity k, whose interrelationships may be further complicated by hysteresis.

It was stated in a previous section that flow in the saturated soil takes place in the direction of decreasing total head, that the rate of flow (flux) is proportional to the hydraulic gradient and is affected by the geometric properties of the pore channels through which flow takes place. These principles also apply in unsaturated soils. In saturated soils the moving force is the total head ϕ, which is the sum of the pressure head and elevation head ($\psi + z$), the pressure head being positive below the phreatic surface. The same total head is the driving force in unsaturated soils, but the local pressure head is

subatmospheric. This subatmospheric pressure head is sometimes referred to as the suction head. In the unsaturated soil there is a matrix suction due to the physical affinity of water to the soil particle surfaces and capillary pores. This means that water tends to be drawn from zones where the capillary menisci are less curved to where they are more highly curved. This means that at the same elevation, water flows from a lower matrix suction to a zone of higher matrix suction. (ie. If the soil is homogeneous, then water will migrate horizontally from zones where thicker layers of water surround the particles, to the zones where those water layers are thinner.) If there is a change in elevation, this must be taken into account and movement will only occur where there is a difference in total head ϕ.

One of the most important differences between saturated and unsaturated soils is the hydraulic conductivity. When the soil is saturated, all of the pores are water filled and conducting, so that continuity and hence conductivity is at a maximum. In an unsaturated soil, some of the pores are partly air filled and the conductive cross-sectional area of the soil decreases correspondingly. As a soil becomes more unsaturated, the matrix suction develops, emptying the largest pores first, which are the most conductive and leaving water to flow in the smaller pores only. As more pores empty, (in a more unsaturated soil) discontinuous pockets of water, as shown in figure (2.5), may remain almost entirely in capillary wedges at the contact points of the particles. For these reasons, the transition from saturation to unsaturation generally has a steep drop in hydraulic conductivity as shown in figure (2.6). At very high suction or low volumetric moisture content, the moisture left in a soil may all be bound to soil particles, by capillary forces and as bonded moisture. The conductivity is therefore very low (approaching zero) near the residual saturation, indicating no flow.

At saturation, soils with the largest continuous pore passages are normally the most conductive, while the least conductive are soils with very small pore passages (eg. sands and clays, respectively). However, the opposite may be true when the soils are unsaturated. As a suction develops, a soil with large pores empties more quickly, compared with a soil with small pores which can retain the water against the applied

suction. Thus the initially high hydraulic conductivity of a large pore soil decreases steeply and, at a particular suction, may be less than that of a soil with very small pores, whose hydraulic conductivity has not decreased as drastically.

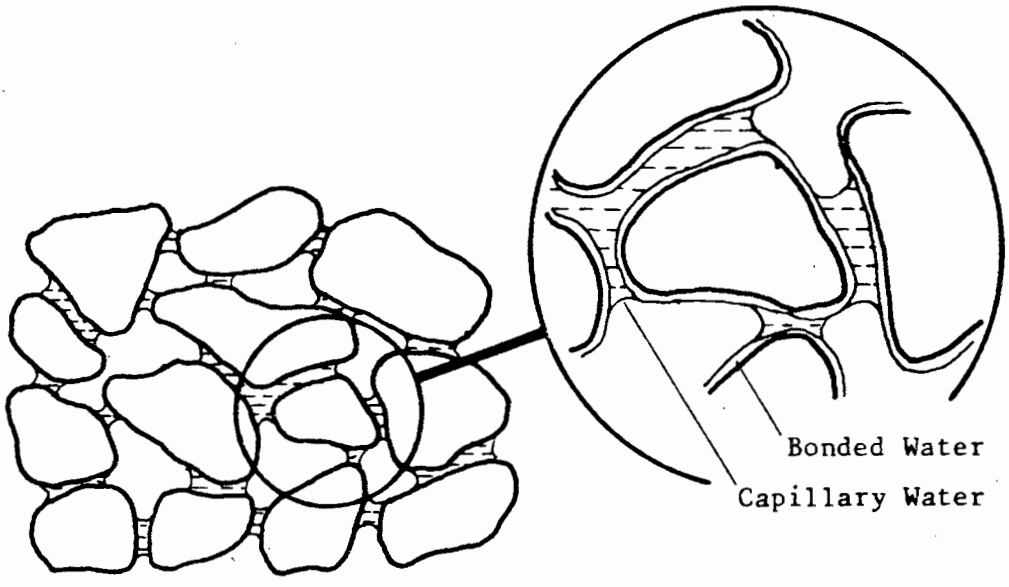

Fig 2.5: **Illustration of: (a) Water in an unsaturated coarse-textured soil; (b) Bonded and Capillary water.**

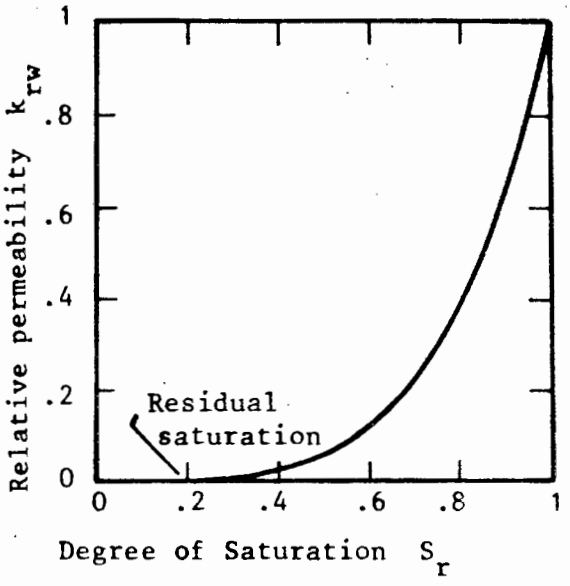

Fig 2.6: **Relative hydraulic conductivity, (Ratio of the unsaturated to the saturated hydraulic conductivity) as a function of saturation.**

2.7 Extension of Darcy's Law.

The hydraulic conductivity k, originally introduced by Darcy for saturated soils, was extended by Buckingham (1907) and Richards, (See Richards [36]), to unsaturated flow, with the provision that the conductivity is now a function of the volumetric moisture content, i.e. $k = k(\theta)$. From a theoretical viewpoint, $k(\theta)$ can be expressed as:

$$k(\theta) = k\, k_{rw}(\theta) \tag{2.29}$$

where k is the hydraulic conductivity or coefficient of permeability of a saturated soil, and $k_{rw}(\theta)$ is the relative hydraulic conductivity which varies from 0, for a completely dry soil (below the residual saturation), to 1, for a fully saturated soil. See figure (2.6). The specific flux vector in three dimensions can now be extended to an unsaturated soil by substituting equation (2.29) into (2.19) in the form:

$$\underset{\sim}{q} = - k(\theta)\, \nabla \phi \tag{2.30}$$

or

$$\underset{\sim}{q} = - \underset{\approx}{k}\, [\, k_{rw}(\theta)\, \nabla \phi\,] \tag{2.31}$$

where $\underset{\approx}{k}$ is the hydraulic conductivity tensor for the saturated soil. There is just one problem in that the relationship of $k_{rw} = k_{rw}(\theta)$, is affected by wetting and drying hysteresis. The degree of hysteresis is much less than the hysteresis between the suction head ϕ, and volumetric moisture content θ. Because of the hysteresis in the relationship of $k_{rw} = k_{rw}(\theta)$, being much less, compared with the relationship of $\phi = \phi(\theta)$, it is assumed in most literature that a single relationship exists between k_{rw} and θ, but which still leaves the problem of dealing with the hysteresis in the relationship between ϕ and θ.

2.8 Soil moisture characterstic curve.

The total head for water in a rigid soil as defined previously is given as:

$$\phi = \psi + z \qquad (2.32)$$

where ψ is the pressure head and z the elevation head above some datum plane. ψ takes on negative values in the unsaturated zone and positive values in the saturated zone. If we consider a point P, in a soil mass that is initially saturated and then becomes unsaturated, we get a plot of the suction head versus volumetric moisture θ, as shown in figure (2.7) for the pressure at point P. Initially as the negative pressure increases, little or no change in the saturation will occur (i.e. no air will penetrate the sample) until the critical suction is exceeded at which time the largest pores begin to drain. This critical suction can be called one of the following; air-entry suction, critical capillary head, bubbling pressure or the air-entry pressure.

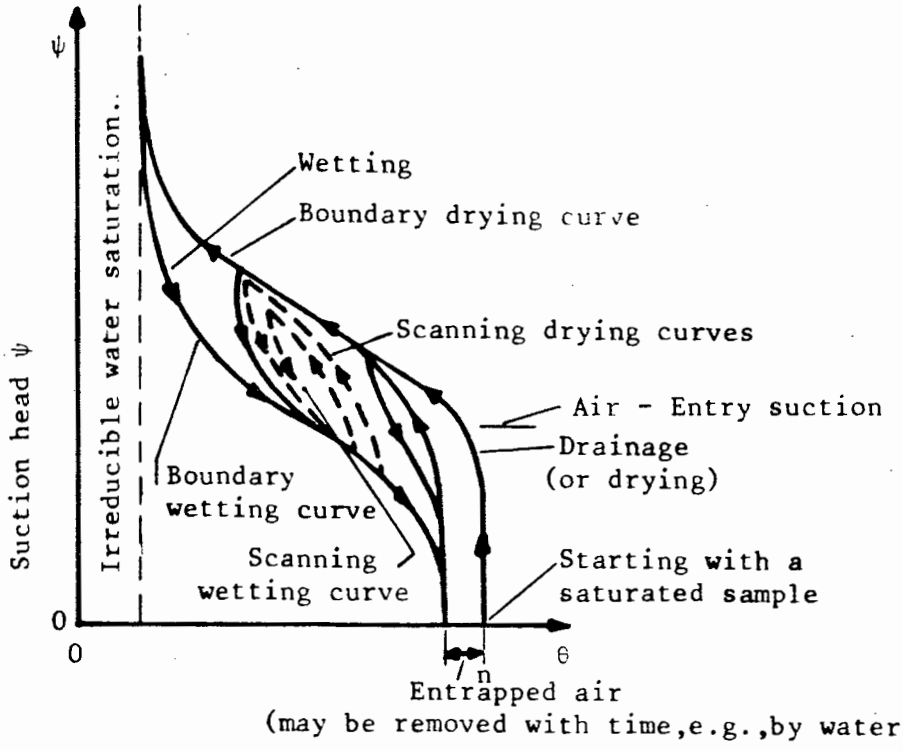

Fig 2.7: Soil-moisture characteristic curve. Hysteresis in the relationship of $\phi = \phi(\theta)$.

With the increase in suction, more water will drain out of the relatively large pores. This gradual increase in suction will result in the emptying of progressively smaller pores until, at high suction values, the only water remaining is held as bonded moisture to the particles and by large capillary forces between the particles. See figure (2.5b).

2.8.1 Hysteresis.

The relationship between the suction head (i.e. the negative pressure head) ψ and the volumetric moisture content θ, is not a single valued function, but has different curves for wetting and drying, See figure (2.7). The equilibrium moisture content θ, at a given pressure head ψ, is path dependent and this dependency is called hysteresis.

The hysteresis effect may be attributed to several causes (Hillel [18]):

1) Geometric nonuniformity of the individual pores resulting in the "inkbottle" effect, figure (2.8a).
2) The contact-angle effect which is different for an advancing meniscus as opposed to a receding one. The angle is smaller for the receding one and therefore exhibits greater suction than an advancing one, figure (2.8b).
3) Entrapped air upon rewetting.
4) If the soil is not rigid, compaction or consolidation can change the total volume and soil structure.

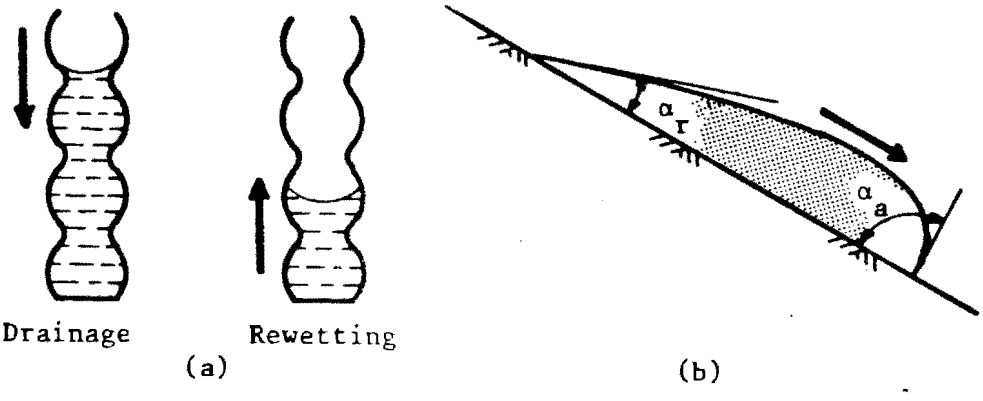

Fig 2.8: **Factors causing hysteresis in the soil-moisture characteristic curve: (a) The ink-bottle effect; (b) The raindrop effect.**

If the last two cases are not considered then the drainage and wetting curves form a closed loop, figure (2.9b). If we consider the inkbottle effect with hypothetical pores shown in figure (2.8a) The pores consist of relatively wide voids with narrow channels. If initially saturated, the pores will only drain when the suction exceeds the tension due to capillary forces in the narrow channels. However, for the pores to be rewet, the suction must be decreased to below the tension due to capillary forces of the relatively large pores, and then only will the pores fill. The tension due to capillary forces for the small channels is greater than that of the larger pores, and therefore drainage and rewetting occurs at two different suction pressures.

The two main complete characteristic curves, from saturation to dryness and vice versa, are called the Main or Boundary curves of the hysteretic soil moisture characteristic curve. When a partially wetted soil begins to drain or a partially drying soil is rewetted, the relation $\psi = \psi(\theta)$ follows some intermediate curve (scanning curve) as it moves from one Boundary curve to another. Cyclic changes often involve wetting and drying scanning curves, which may form closed loops between the main branches. As long as the soil remains rigid (i.e. there is no consolidation) the hysteresis loop can usually be repeatedly traced. The relationship of $\psi = \psi(\theta)$ is seen to be very complicated. If there is only monotonic wetting or drying in a particular problem, it may be justifiable to use only one of the main soil moisture characterstic curves. This thesis will deal with monotonic drainage (ie. drying curves apply).

2.8.2 Specific moisture capacity.

The specific moisture capacity c, is generally defined as the slope of the soil-moisture characteristic curve, which is the change of volumetric moisture content θ, per unit change of pressure head ψ:

$$c(\theta) = \frac{d\theta}{d\psi} \tag{2.33}$$

The specific moisture capacity c is also non-linear and is path dependent (ie. Hysteresis effects apply). (See figure 2.9c).

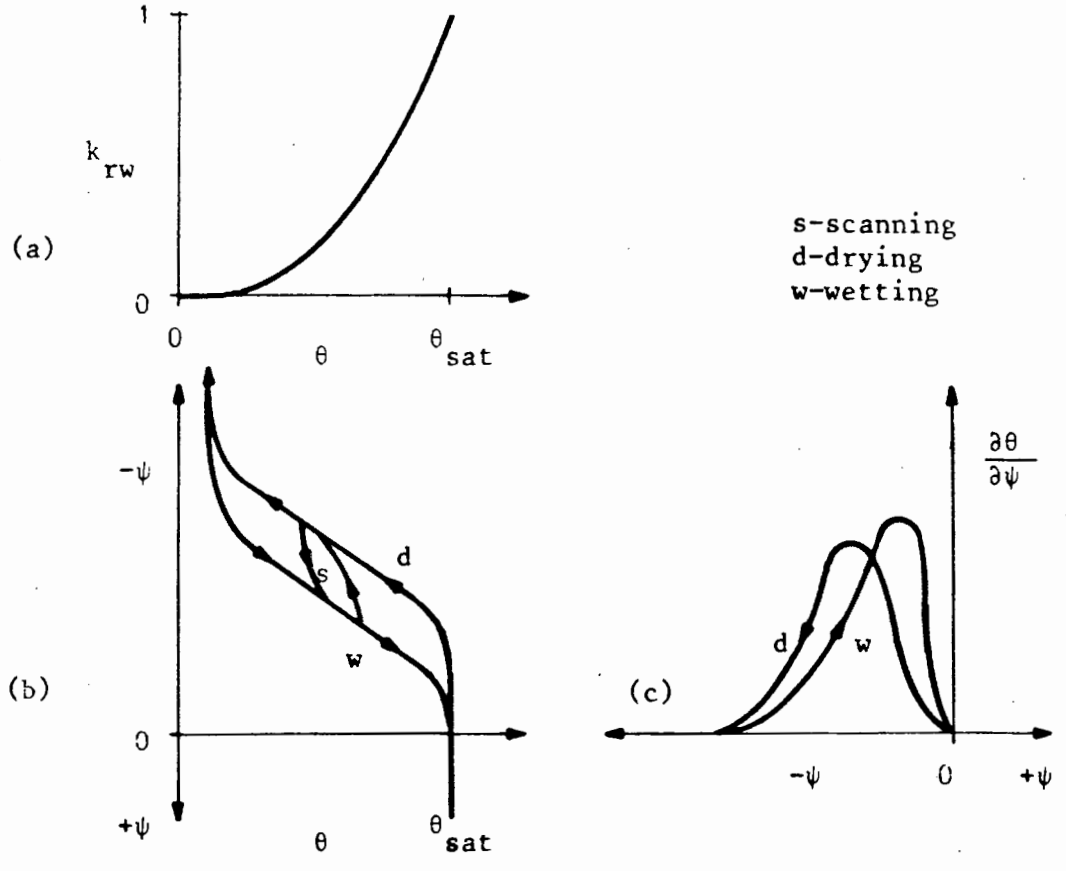

Fig 2.9: **Typical functional relationships for saturated-unsaturated soils: (a) Relative hydraulic conductivity versus volumetric moisture content; (b) Pressure head versus volumetric moisture content; (c) Specific moisture capacity versus pressure head.**

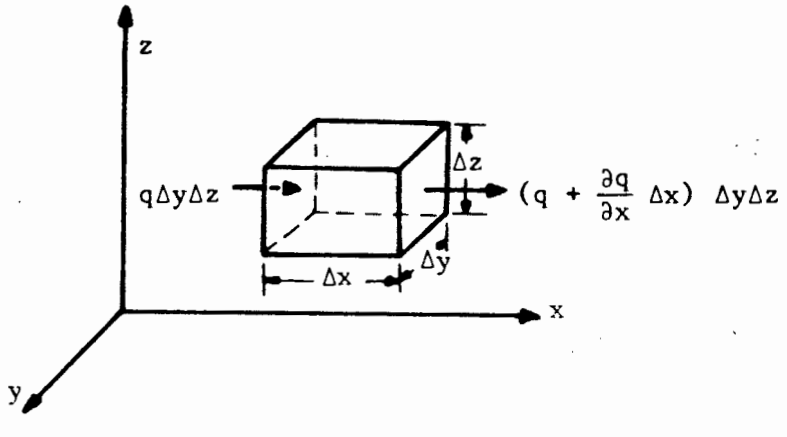

Fig 2.10: **The continuity principle: A volume of soil gaining or losing water in accordance with the divergence of the flux.**

2.9 General equation of saturated-unsaturated flow.

2.9.1 The continuity equation.

Considering, for a moment, only the net flow in the x direction through a volume element of a porous medium, with sides of length Δx, Δy and Δz, as shown in figure (2.10). If the flux leaving the right-hand face exceeds the flux entering the left-hand face by the amount $\frac{\partial q}{\partial x} \Delta x$, then the net rate of inflow into the element in the x direction is given by:

$$q_x \Delta y \, \Delta z - \left[q_x + \left(\frac{\partial q_x}{\partial x}\right) \Delta x \right] \Delta y \, \Delta z \qquad (2.34)$$

or

$$- \left(\frac{\partial q_x}{\partial x}\right) \Delta x \, \Delta y \, \Delta z \qquad (2.35)$$

where q_x is the flux in the x direction. This rate of inflow into the element must equal the rate at which water (moisture) is being stored in the element, which can be expressed in terms of the rate of change of volumetric moisture content θ, multiplied by the volume of the element:

$$\left(\frac{\partial \theta}{\partial t}\right) \Delta x \, \Delta y \, \Delta z \qquad (2.36)$$

If the porous medium is incompressible, then combining equations (2.35) and (2.36), gives:

$$\left(\frac{\partial \theta}{\partial t}\right) \Delta x \, \Delta y \, \Delta z = - \left(\frac{\partial q_x}{\partial x}\right) \Delta x \, \Delta y \, \Delta z \qquad (2.37)$$

or

$$\frac{\partial \theta}{\partial t} = - \frac{\partial q_x}{\partial x} \qquad (2.38)$$

If the fluxes in the y and z directions are also considered, the three-dimensional form of the continuity equation is obtained, namely:

$$\frac{\partial \theta}{\partial t} = -\left(\frac{\partial q_x}{\partial x} + \frac{\partial q_y}{\partial y} + \frac{\partial q_z}{\partial z}\right) \tag{2.39}$$

where q_x, q_y, q_z are the fluxes in the x, y, z directions, respectively. Equation (2.39) can be rewritten as:

$$\frac{\partial \theta}{\partial t} = -\nabla \cdot \underset{\sim}{q} \tag{2.40}$$

or

$$\frac{\partial \theta}{\partial t} = -\operatorname{div} \underset{\sim}{q} \tag{2.41}$$

2.9.2 The combined flow equation.

The equation for the generalized Darcy's Law for saturated-unsaturated flow was given by equation (2.30) as:

$$\underset{\sim}{q} = -\underset{\approx}{k}(\theta)\, \nabla \phi \tag{2.42}$$

where $\underset{\approx}{k}$ the hydraulic conductivity tensor is a function of the volumetric moisture content θ, and the total head gradient $\nabla\phi$. The hysteresis of the soil-moisture characteristic curve is taken into account in the relationship between ϕ and θ. By substituting equation (2.42) into the continuity equation (2.40) we obtain the general flow equation:

$$\frac{\partial \theta}{\partial t} = \nabla \cdot [\, \underset{\approx}{k}(\theta)\, \nabla \phi \,] \tag{2.43}$$

where θ is the volumetric moisture content, t the time, ϕ the total head ($\phi + z$) and $\underset{\approx}{k}(\theta)$ the hydraulic conductivity. The air in the voids is assumed to be at atmospheric pressure and free to move, and the water is incompressible.

2.10 Calculation of the hydraulic conductivity of saturated soils.

2.10.1 Theoretical prediction.

Since the hydraulic conductivity is a physical characteristic property of a porous medium, it could be reasonably assumed that it relates to the soil pore geometry in some functional way. A universal functional relation does not seem to have been found. A further complication is that whatever relationship is found it must relate to measurable properties of the soil pore geometry (eg. porosity, pore-size distribution, internal surface area of the voids, etc) as the actual pore geometry cannot be measured. Most approaches are empirically based.

The simplest approach is to find a relationship between the saturated hydraulic conductivity and the porosity or void ratio. As for example the following equation:

$$k = c \frac{e^3}{(1 + e)} \quad \text{cm/s} \tag{2.44}$$

where e is the void ratio of the soil, k the hydraulic conductivity and c a proportionality constant. This approach holds for the comparison of the same soil, (ie. two soils having the same particle size distribution) with different porosities, but the proportionality constant differs for each individual soil with a different particle size distribution.

The next approach that is used, is to find the correlations between the hydraulic conductivity and particle size distribution. As for example the following equation. (Hazen's equation):

$$k = c \, (D_{10})^2 \quad \text{cm/s} \tag{2.45}$$

where c is a coefficient in the range between 45 for clayey sands and 140 for pure sands (often the value of c = 100 is used as an average),

and D_{10} is the effective grain size diameter in cm. (See section 4.2). Problems with this approach are that the particles of a soil having the same effective grain size diameter D_{10}, can be packed differently, yielding a different hydraulic conductivity to that predicted.

Purely theoretical formulae have been obtained from theories based on the relation of the hydraulic conductivity to the geometric properties of the porous media (ie. from theoretical derivations of Darcy's Law). One such example is the Kozeny-Carman equation. (see Bear [6]):

$$k = c \frac{n^3}{(1 - n)^2 a^2} \qquad (2.46)$$

where n is the porosity, a the specific surface exposed to the fluid and c a constant representing a particle shape factor. The theory is based on the concept of a hydraulic radius. The hydraulic radius is measured by the ratio of the volume to the surface of the voids, or the average ratio of the cross-sectional area of the voids to their circumferences.

Other approaches have also been investigated, but each has some or other limitation that prevents it from being universally used.

2.10.2 Laboratory measurement.

Methods have been devised to measure the hydraulic conductivity of a soil sample in the laboratory. Problems with these measurements made in the laboratory are that they often do not correspond to the hydraulic conductivity of the soil in the field. (ie. In-situ soil) This is because soil samples are disturbed and repacked in the laboratory with porosities, packing and grain orientations markedly changed, and consequently the hydraulic conductivity is modified. Laboratory tests however permit the relationship between the hydraulic conductivity and the void ratio to be studied.

Two commonly used laboratory methods for the determination of the

hydraulic conductivity are the "Constant head permeameter" and "Variable head permeameter" tests;

a) Constant head permeameter.

The constant head permeameter as shown in figure (2.11a) is used to measure the hydraulic conductivity. By noting the head loss Δh over the sample length L, and the flow rate of the water through the soil sample, it is possible to calculate the hydraulic conductivity from Darcy's Law:

$$k = \frac{\frac{Q_t}{A\ t}}{\frac{\Delta h}{L}} \qquad (2.47)$$

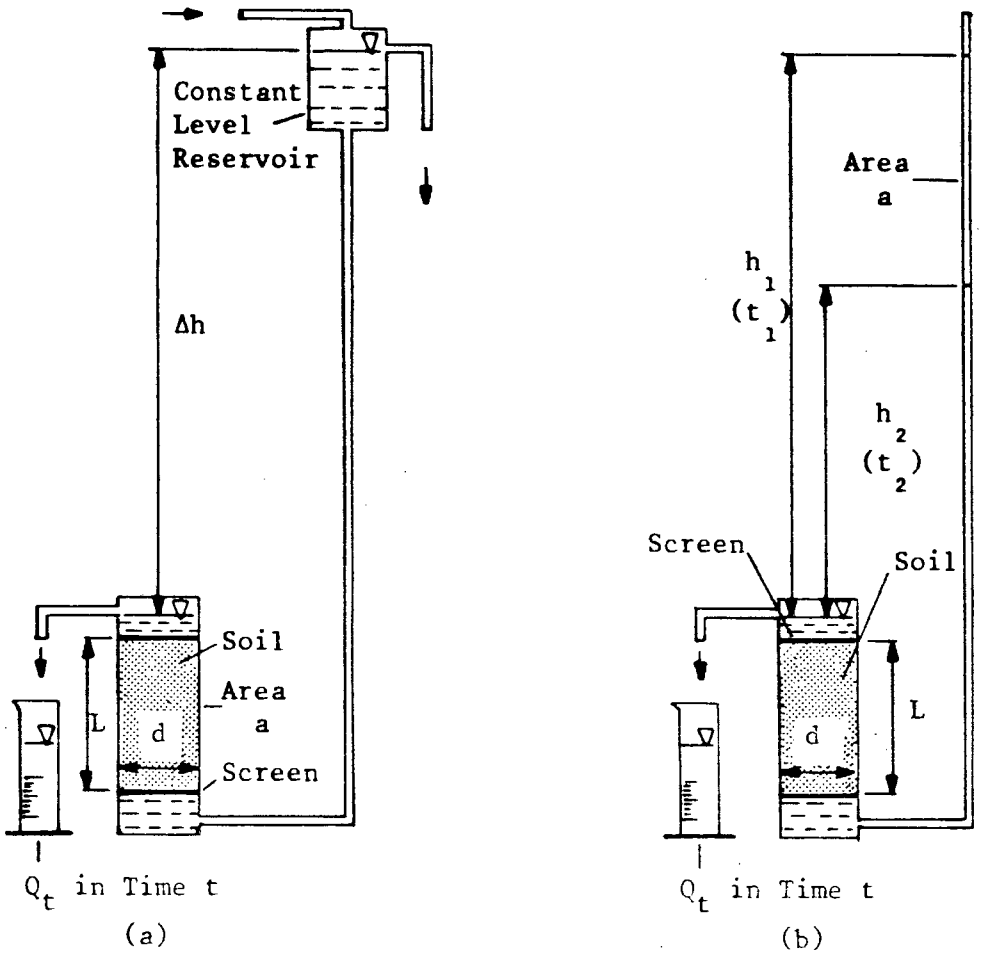

Fig 2.11: Laboratory permeameter tests: (a) Constant head; (b) Variable head.

where k is the hydraulic conductivity, Q_t the quantity of water to flow through the sample in time t and A the cross-sectional area of the sample. By repeating the test using different flow rates $q = Q_t/t$, a plot of Q_t/At versus $\Delta h/L$ can be made. The gradient of a straight line fitted to the plotted points is the hydraulic conductivity.

b) Variable head permeameter.

The variable head permeameter uses a similar lay-out to that of the constant head permeameter, except that instead of a constant supply head, a falling head is used, as shown in figure (2.11b). Here the water is added to a tall column of known cross-sectional area. The water then passes upwards through the sample and is collected as it overflows. The test consists of noting times at which the water level passes various height graduations on the tube. The cross-sectional area and the length of the sample are measured. If two graduations are used, as shown in figure (2.11b), then h_1 and h_2 must be known. The time required for the water level in the tube to fall from h_1 to h_2 is measured as t.

The differential form of Darcy's Law can be written as:

$$dQ_t = k \frac{A\ h\ dt}{L} \qquad (2.48)$$

If a is the cross-sectional area of the tube and the water level height changes by -dh, then:

$$dQ_t = - a\ dh \qquad (2.49)$$

Substituting into equation (2.48) gives:

$$- a\ dh = k \frac{A\ h\ dt}{L} \qquad (2.50)$$

Rearranging and simplifying, equation (2.50) becomes:

$$-\frac{dh}{h} = k\frac{A\,dt}{a\,L} \qquad (2.51)$$

Integrating yields:

$$-\ln h = k\frac{At}{aL} + C \qquad (2.52)$$

when $t = o$, $h = h_1$, thus:

$$C = -\ln h_1 \qquad (2.53)$$

Inserting this into equation (2.52) and rearranging gives:

$$k = \frac{aL}{At}\ln\frac{h_1}{h^2} \qquad (2.54)$$

Therefore, by measuring the time for the water level to drop from h_1 to h_2 and knowing the cross-sectional area's of the tube and the soil sample, plus its length, the hydraulic conductivity can be calculated from equation (2.54).

2.10.3 Field measurement.

The pumping tests on wells, that extend below the water table, are important for the evaluation of the hydraulic properties of an aquifer. Parameters predicted by these tests are well yields; position of the water table or piezometric surface; and recharge rates of the aquifer. Other techniques for use in the field have been developed, for determining more specifically the hydraulic conductivity of the soil in situ. The tests differ, depending on where the water table is. If the water table is near the surface, the tests are done below the water table in the saturated zone. If the water table is relatively deep, the

hydraulic conductivity is measured above the water table, (ie. the vadose zone) using tests that first artificially wet an area until saturated. The in situ test results are mainly used for surface-subsurface water relations (eg. Infiltration), to design drainage systems and to estimate seepage from channels. Some methods, for the measuring of the hydraulic conductivity in soils, as near as possible to saturation, either above or below the phreatic surface, are given below.

a) Pumping tests

Pumping tests are done with wells, to determine the hydraulic properties of the aquifer. By pumping the water out of the well, at a constant rate, and observing the drawdown of the piezometric surface or the water table in observation wells at some distance from the pumped well, the aquifer's hydraulic properties can be determined. The type of the test can vary, either being a steady state or transient test and applied to a confined or unconfined aquifer. A number of methods for the evaluation of the aquifer parameters from the pumping tests results have been developed by several investigators (eg. Theis solution; Chow solution; Jacob solution; etc). Most of the methods are based on a graphical method for the solution.

The same measurements can be made during a recovery test. This is a test started when the pumping of a well is stopped and the rise of the water levels in the observation wells are recorded.

b) Rate of rise tests

Tests in this category are to do with wells that penetrate below the water table. To do the tests, the static water table level must be visible in the well. A quantity of water is removed from the well (to lower the water level) and the rate at which the water level rises is recorded.

A number of tests based on the above are given in Bouwer [7], for example, the Slug test, Auger-hole method and Piezometer method. With each of these methods there are variations adopted by different investigators.

With the Slug test, (See figure 2.12) both vertical and horizontal conductivity is measured. Water is removed from the well and the rate of rise is noted. Using type curves (ie. graphical method) similar to the Theis procedure for pumping tests, the solution of the Transmissivity and Storativity of a

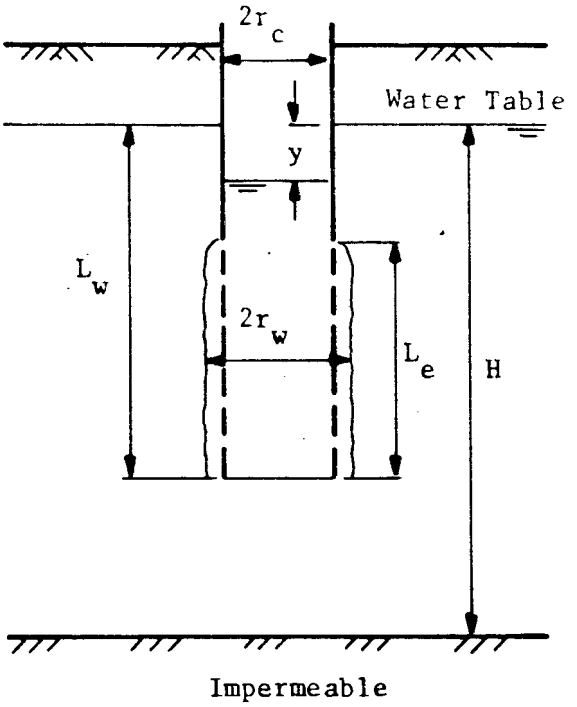

Fig 2.12: Schematic diagram of slug test. Bouwer [7]

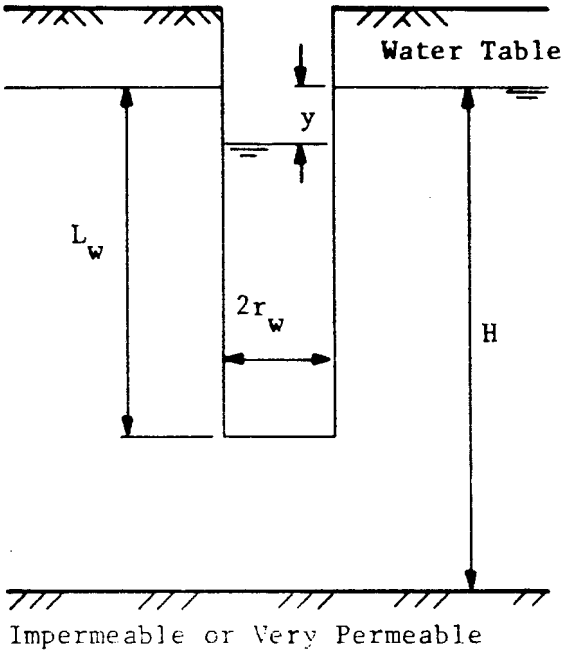

Fig 2.13: Schematic diagram of auger-hole method. Bouwer [7]

confined aquifer can be found. Bouwer [7] and Rice developed a slug-test procedure applicable to both confined and unconfined aquifers, from which the hydraulic conductivity can be obtained.

The Auger-hole method (See figure 2.13) is similar to the Slug test method for wells, but the water level rise is measured in an unlined auger hole. This test has been developed by different investigators, and the water level rise in the auger-hole and the geometry thereof are related to the hydraulic conductivity.

The Piezometer method (See figure 2.14) is just a variation on the Auger-hole method, in that a pipe is jetted into the soil, instead of an augered hole, and the water level is rapidly lowered. Its rise back to the water table level is recorded. From this the value of the hydraulic conductivity around the pipe tip is calculated by a given equation.

c) Hydraulic conductivity in the vadose zone

Measurement of the hydraulic conductivity in the vadose zone is important if infiltration or seepage through this zone needs to be predicted. The basis of calculating the hydraulic conductivity of the soil is to artificially wet a portion of the soil and to evaluate the hydraulic conductivity from a flow system created within the wetted zone. A problem with this method is that it is difficult to achieve full saturation of the soil and so the resulting hydraulic conductivity measured is less than that at saturation. A few of the methods described by Bouwer [7], are the Air-entry permeameter method; Infiltration-gradient technique; Double-tube method and Well Pump-in technique.

The Air-entry permeameter (See figure 2.15) is a surface device. It consists of a metal cylinder with one end opened, which is pressed into the soil, and the top end is closed. A stand pipe with a reservoir is fixed to the cylinder. The soil within the cylinder is wet with water via the stand pipe. Noting the drop of the water level in the reservoir, the flow rate of

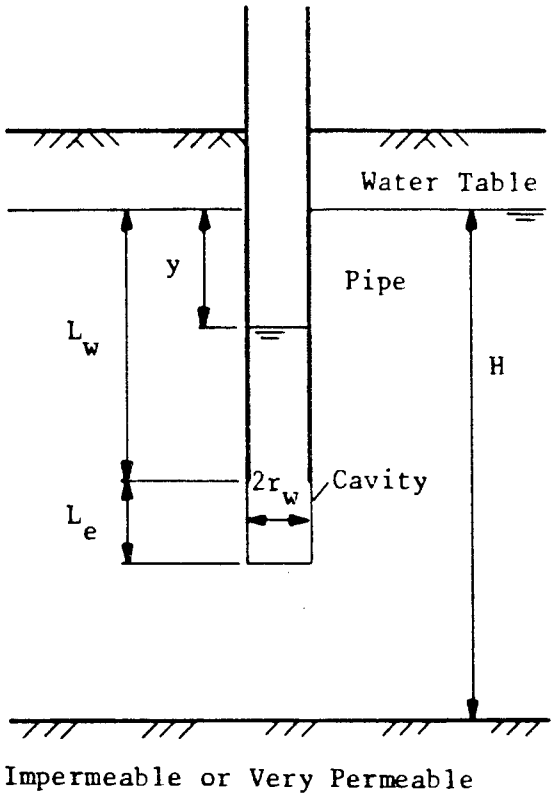

Fig 2.14: Schematic diagram of the piezometer method. Bouwer [7]

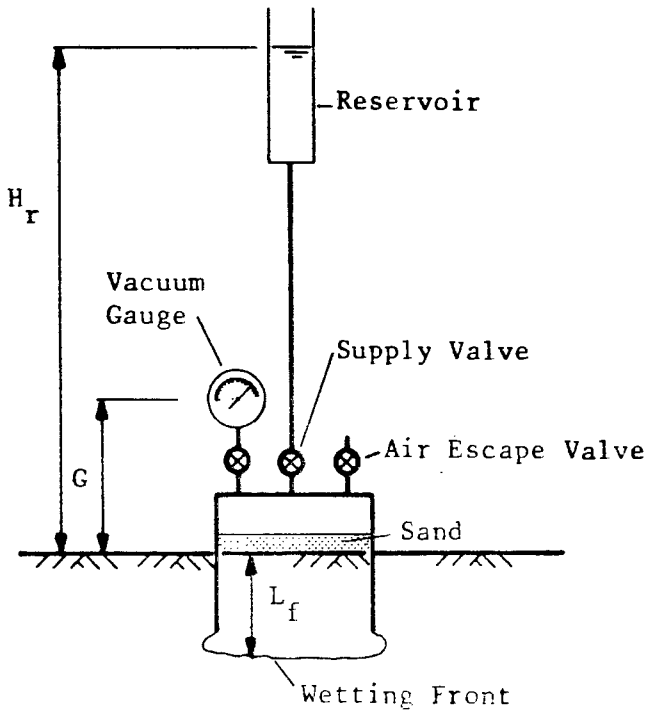

Fig 2.15: Schematic diagram of the air-entry permeameter. Bouwer [7]

the water entering the cylinder can be determined. Once the wetting front, in the soil, reaches the open end of the cylinder, the stand pipe is closed and the build up of negative pressure is noted. The highest recorded negative value is the air-entry value. With this reading and measuring the depth of the wetting front from the surface, the hydraulic conductivity can be calculated using a modified form of Darcy's equation. This modified form takes the air-entry value into account.

The infiltration-gradient technique (See figure 2.16) is similar to the air-entry permeameter in principle, but the vertical gradient is measured directly with tensiometers. To ensure vertical flow, two concentric cylinders are used to wet the soil. The open ends of the cylinders are pushed into the soil. The infiltration rate for the inner cylinder is measured, while the water level in both cylinders is kept level as they drop. From the measurement of the infiltration rate and the vertical gradient (from the tensiometer readings) the hydraulic conductivity can be calculated.

The double-tube method allows the hydraulic conductivity of the soil to be measured without the use of tensiometers or knowing the air-entry value and wet depth of the soil. The test is performed by first wetting the soil below both cylinders. (as with the infiltration-gradient technique.) The water level in the outer cylinder is kept at a constant height while that in the inner cylinder is allowed to drop. This infiltration rate is noted. The test is then repeated, but this time the water level in the outer cylinder is adjusted so that it falls at the same rate as the inner cylinder. By noting the different flow rates, (ie. the dropping rate of the water level) and knowing the geometry of the equipment the hydraulic conductivity can be calculated.

The well pump-in technique (See figure 2.17) is the reverse test to the auger-hole method. Water is added to an augered-hole and the flow rate necessary to keep the water level constant in the

hole is measured. By knowing the physical dimensions of the augered hole, the hydraulic conductivity can be calculated.

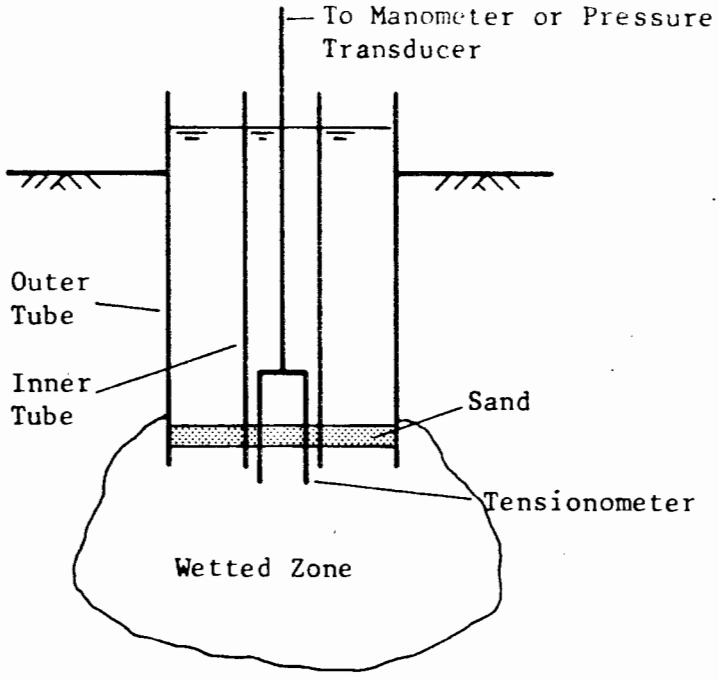

Fig 2.16: Schematic diagram of the infiltration-gradient technique. Bouwer [7]

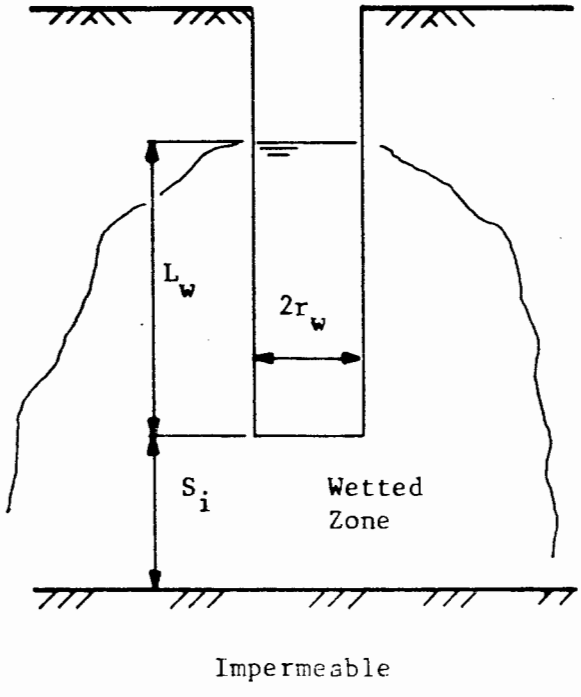

Fig 2.17: Schematic diagram of well pump-in method. Bouwer [7]

2.11 Calculation of the hydraulic conductivity of unsaturated soils.

2.11.1 Theoretical prediction.

Various models are used for predicting the hydraulic conductivity of unsaturated soils. The models are either theoretical, empirical or semi-empirical based. (See Mualem [27] and [28]). The approaches can be divided into two main groups. The first is based on the relative hydraulic conductivity k_{rw}, being a power function of the effective saturation S_e, ie.:

$$k_{rw} = \left(\frac{k(\theta)}{k_{sat}} \right) \tag{2.55}$$

$$= S_e^{\alpha} \tag{2.56}$$

where

$$S_e = \frac{(\theta - \theta_r)}{(\theta_{sat} - \theta_r)} \tag{2.57}$$

where θ and θ_r are the actual and the residual volumetric moisture contents respectively. Mualem [28] gives references to various investigations in which the value for α has been derived theoretically as well as empirically. A value within the range of 2 to 24 is reported by Mualem for 50 soil samples investigated, with α = 3,5 being the most common value.

A theoretical analysis reported by Mualem [28] showed that α may be lower than 3 for a granular porous medium and higher than 3 for a fine-grained soil. These findings are verified by experimental data presented for the 50 soils.

The second approach makes use of the measured capillary head versus volumetric moisture content relation (ie. $\psi = \psi(\theta)$, the soil-moisture characteristic curve) to derive the hydraulic conductivity of the

unsaturated soil. The underlying concept of this method is relating the relative hydraulic conductivity k_{rw} with the porous medium's pore-size distribution. From the soil-moisture characteristic curve, using a statistical approach, the number of conducting interconnected pores is determined. This is related to the relative hydraulic conductivity. (See Mualem [27]; Jackson [21] and King [23]).

Using the ratio of the measured to the calculated saturated hydraulic conductivity k_{sat}/k_1, as a matching factor, to adequately represent experimental data, Jackson's [21] formulation is as follows:

$$k_i = k_s\left(\frac{\theta_i}{\theta_{sat}}\right)^{\beta} \frac{\sum_{j=1}^{m} [(2j + 1 - 2i)\,\phi_j^{-2}]}{\sum_{j=1}^{m} [(2j - 1)\,\phi_j^{-2}]} \qquad (2.58)$$

where k_i is the hydraulic conductivity at a volumetric moisture content value θ_i, m is the number of increments of θ (ie. equal intervals from dryness to saturation of θ), ϕ_i is the suction head at the midpoint of each θ increment, and j and i are summation indices. Finally β is an arbitrary constant assigned a value of between 0 to 4/3 by various investigators. Jackson [21] found that the value of 1 is satisfactory.

Hillel [18] notes that as this second approach is based on the pore sizes, it can be expected that the above theory referenced, applies more to coarse-grained than to fine-grained soils, whereas the power function approach can be applied to both.

A problem with the theoretical predictions is that even if a certain formula is suitable for a particular class of soils, the coefficients may vary form soil to soil within that class. Therefore the merit of most empirical and semi-empirical methods is there use in an analytical solution, based on experimental data from which coefficients are found, rather than being an effective solitary tool for predicting.

2.11.2 Laboratory measurement.

Laboratory tests can be done on a sample of soil to find the relation between the hydraulic conductivity k and the volumetric moisture content θ or suction head ψ. Bouwer [7] and Youngs [40] report on a most direct method of measuring the hydraulic conductivity of an unsaturated soil. The technique also used by Childs, consists of a long, soil-filled vertical column. Water is applied to the top of the column, at a constant rate less than that required to saturate the sample. The water is allowed to drain freely from the bottom of the column.

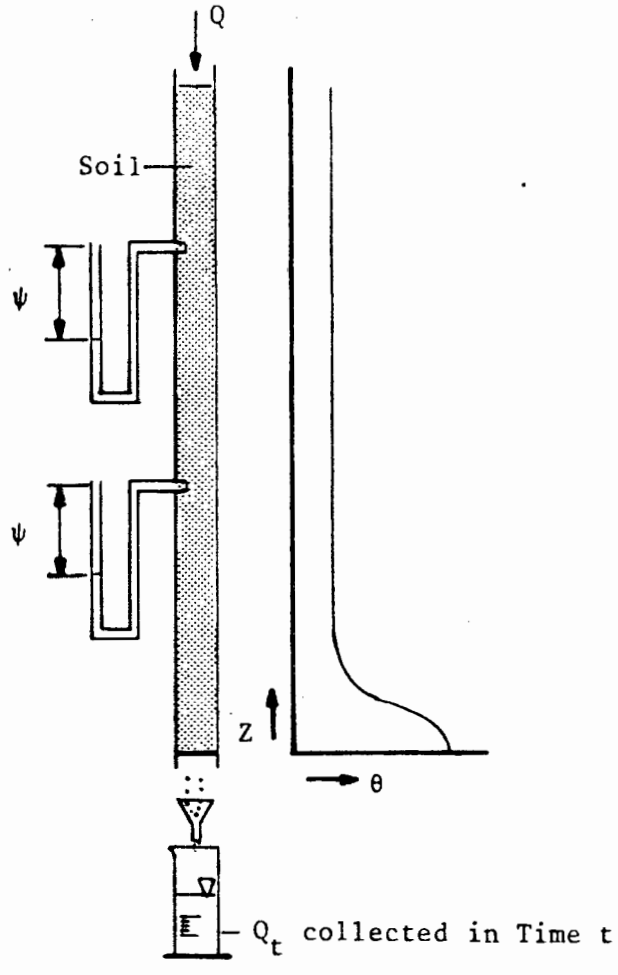

Fig 2.18: Long soil column to determine the unsaturated hydraulic conductivity k, in relation to the suction head $k = k(\phi)$, or volumetric moisture content $k = k(\theta)$

When equilibrium conditions are established, the bottom of the soil column will essentially be saturated due to a capillary fringe, but the rest of the soil will be at a uniform water content θ, and suction head ϕ. (See figure 2.18). A constant suction head in the soil column means an hydraulic gradient of one and so the hydraulic conductivity must be equal to the downward flow rate q/A, of the water in the column. The value of the suction head ϕ can be measured with tensiometers, giving one point of the relationship between the hydraulic conductivity and the suction head. Measurement of the volumetric moisture content in the column (eg. with a gamma-ray technique) then also yields a point of the hydraulic conductivity and the volumetric moisture content relationship. The experiment can be repeated using different flow rates which change the degree of saturation and correspondingly the hydraulic conductivity. A disadvantage of the above method is the long time it takes for equilibrium conditions to be reached.

Another method is to estimate the hydraulic conductivity of an unsaturated soil, based on experiments with horizontal infiltration of water into a horizontal soil column. A plot of the square of the distance from the water source to the wetting front as a function of the time is made. From this plot a soaking factor is obtained which permits an estimation of the hydraulic conductivity as a function of the volumetric moisture content of the soil. (See Lambe [24]). A slight variation to the method is given by Reichardt et al [35].

Other techniques have also been developed for determining the hydraulic conductivity versus suction head or volumetric moisture content relations. These include pressure-plate-outflow; instantaneous-profile and transient flow methods. (See Corey [11] and Brooks et al [10]). The conductivity can be measured by applying a constant hydraulic head difference across a sample of soil and measuring the resulting steady flow rate of water flowing through the soil. The soil sample is then de-saturated either by tension-plate devices or in a pressure chamber. Measurements made at successive levels of suction and wetness give the results for the relationship of the hydraulic conductivity versus volumetric moisture content or suction head.

As the relationship is hysteretic (path dependent) the tests must be done in both directions (ie. from a saturated sample to a dry sample and vice versa), to obtain the complete relationship.

2.11.3 Field Measurement.

Field tests are important because small disturbed samples tested in the laboratory often are not fully representative of actual field conditions. Several in situ methods have been developed to measure the hydraulic conductivity of unsaturated soils. (See Hillel [18]).

a) Sprinkling infiltration.
With this method, described in principle by Youngs [40], water is sprinkled on the surface at a constant rate, less than that to cause saturation of the soil (ie. no ponding on the surface). Eventually, once steady-state conditions are established, a constant flux and a steady moisture distribution in the conducting soil will result. In a uniform soil, the suction head gradients will tend to zero and with only a unit elevation head gradient in effect, the hydraulic conductivity becomes equal to the flow rate. The test is normally started with a dry soil and a series of successively increased flow rates are used. By measuring the volumetric moisture content of the soil, it is possible to obtain the relationship of the hydraulic conductivity versus the volumetric moisture content. The problem with this test is the rather elaborate equipment needed to be able to apply the very small sprinkling flow rates.

b) Infiltration through an impeding layer.
This method suggested by Hillel and Gardner [19] is based on a similar principle to the sprinkling infiltration method above. The difference is that instead of using elaborate equipment to supply a flow rate lower than that needed to saturate the soil, a layer of soil with a lower saturated hydraulic conductivity is spread over the soil being tested. This means that the infiltration rates applied to the lower soil being tested can be adjusted by the capping crust used. By using a series of

different impeding layers, a series of tests are performed, giving different flow rates. This gives the results for the relationship of the hydraulic conductivity versus the volumetric moisture content.

The volumetric moisture content may be determined, in both cases, by a neutron probe or gamma-ray technique.

c) Internal drainage.

This method is based on the approach of monitoring the transient state internal drainage of a soil profile. (See Hillel et al [20] for a detailed description of a simplified procedure). The method is performed by selecting a large enough surface area so that processes at the centre of the site are not affected by the boundaries. A neutron access tube is placed in the centre so that the volumetric moisture content can be measured at different depths. Next to the tube, but far enough away so that the neutron readings are not affected, a vertical row of tensiometers are placed, so that the soil suction can be monitored at different depths. Water is then ponded on the plot, until the tensiometer readings indicate that steady state conditions exist. Irrigation is then stopped. The surface is then covered to prevent any further flux crossing the surface (eg. water evaporation). As the internal drainage process proceeds, periodic readings of the volumetric moisture content and tensiometers are made. The volumetric moisture content readings are made at depths corresponding to the tensiometers. From the volumetric moisture content readings at different times, the soil moisture movement between each depth increment can be calculated. From the tensiometer readings, the hydraulic gradient at each depth can be calculated. From the above, the hydraulic conductivity can be calculated at different depths for the corresponding volumetric moisture content.

By plotting the results corresponding to the different depths, for each time step, the hydraulic conductivity versus the volumetric moisture content relationship for each depth is

found. For each depth, the relationship could be different if the soil is heterogenous. Otherwise the relationship for each depth should be the same if the soil is homogeneous.

2.12 Calculation of the soil-moisture characteristic curve.

2.12.1 Theoretical prediction.

The soil-moisture characteristic curve is strongly affected by soil texture. The greater the clay content in general, the greater the water retention at any particular suction, and the more gradual the slope of the curve. In a sandy soil, most of the pores are relatively large and once these large pores have been emptied at a given suction, only a small amount of water remains. In a clayey soil, the pore-size distribution is more uniform and more of the water is retained, so that by increasing the soil moisture suction only a gradual decrease is caused in the volumetric moisture content.

There seems to be no satisfactory theory that exists for the prediction of the soil moisture suction head ϕ, versus the volumetric moisture content relationship, from the basic soil properties. Several empirical equations have been proposed, but they only describe the soil-moisture characteristic curve for some soils within limited suction ranges. One such equation presented by Brookes and Corey [10] is:

$$\frac{(\theta - \theta_r)}{(\theta_{sat} - \theta_r)} = \left(\frac{\phi_e}{\phi}\right)^{\lambda} \qquad (2.59)$$

where the suction head ϕ must be greater than the air-entry suction ϕ_e. The exponent λ is termed the pore-size distribution index, θ the volumetric moisture content (a function of the suction head ϕ), θ_{sat} the saturated volumetric moisture content and θ_r is the residual volumetric moisture content.

Theoretical methods proposed normally fall short in not being able to

account for the hysteresis effect between the relationship of the suction head and volumetric moisture content. Not only being limited to particular suction ranges, the equations only describe either the wetting or drying curve of the relationship.

A hysteresis model is introduced by Mualem [26] and expanded by Mualem and Miller [29]. The hysteresis model is based on the independent domain concept, to account for the hysteresis. With this method, only the main drying and wetting curves and one drying scanning curve is needed to calibrate the model. Using the data from these curves, the method predicts the wetting and drying scanning curves.

Parlange [34] extended the method used by Mualem, so that only one of the main boundary curves is needed, instead of two, to predict the wetting and drying scanning curves.

With most of the theoretical methods published, some actual measurements are required from the soil being investigated, in order to be able to use the methods for prediction.

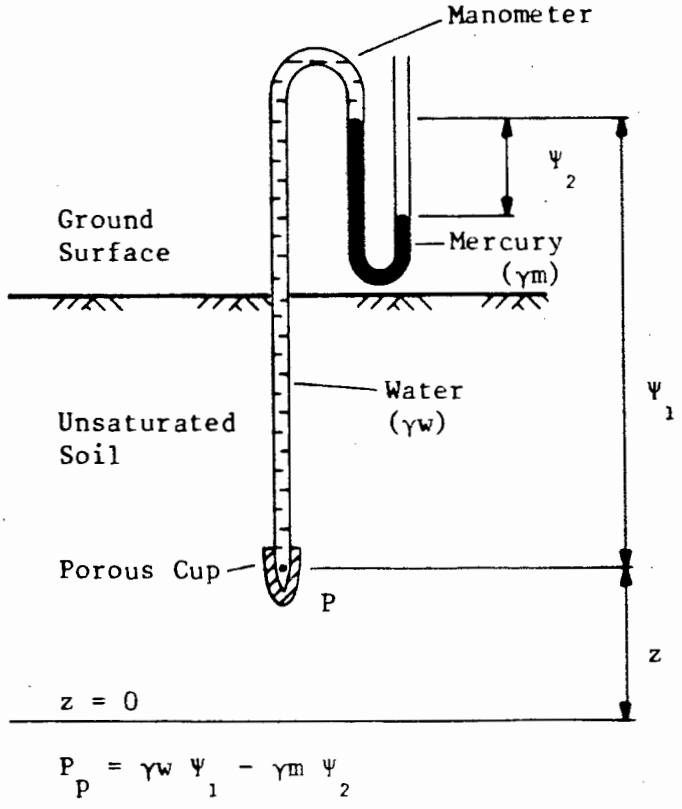

Fig 2.19: Schematic diagram of a tensiometer.

2.12.2 Laboratory and field measurement.

Two methods are mainly used to measure the suction head. In the field an instrument known as a tensiometer is used, whereas in the laboratory use is often made of a tension plate or pressure plate apparatus. A tensiometer can also be used in the laboratory.

A gamma-ray or neutron moisture meter can be used for measuring the volumetric moisture content while tests are in progress.

By testing the soils's suction head at different volumetric moisture contents, the soil-moisture characteristic curve can be found. A test done must be made in both directions (ie. from a saturated soil to a dry soil and vice versa) because of the hysteresis nature of the curve.

a) The tensiometer (See figure 2.19)

The tensiometer is used for measuring the capillary pressure (suction head) in an unsaturated soil. The tensiometer consists of a porous cup, with which contact with the soil is established. The tensiometer is filled with water that comes into hydraulic contact with the soil-moisture through the pores of the porous cup walls. As the water is in hydraulic contact, the pressure of the water in the tensiometer tends to equilibrate with the soil-moisture pressure. The soil-moisture of an unsaturated soil is at sub-atmospheric pressure and this is balanced by a negative hydrostatic pressure in the instrument. The pressure in the instrument can be indicated by a manometer, which may be a simple water or mercury-filled U-tube, a vacuum gauge or an electrical pressure transducer.

There is normally a time lag between the initial instant when the porous cup is placed in contact with the soil and for the water pressure in the tensiometer to equilibrate with the soil water. This lag can be minimized by the use of a null-flow tensiometer. With this type of device, rigid tubing and a transducer type manometer is used. This is so that the tensiometer water can adjust to the soil-moisture pressure

changes with practically no flow of water through the porous cup.

The suction range of the tensiometer is limited by two things mainly. One is the air-entry value of the porous cup. The tensiometer cannot measure suctions lower than this value as air is drawn into the instrument. The second is that the water pressure within the instrument cannot go below about 0.8 bar suction pressure because of general macroscopic failure of the water (ie. cavitation) in the instrument below this pressure.

b) Tension plate

The tension plate works on the same principle as the tensiometer. The soil-moisture suction head is determined by means of a tension plate which is the same as the porous cup in a tensiometer. A sample of soil is placed on the plate. The soil-moisture then comes into contact with the water in the tension plate assembly through the pores of the plate. The pressures are allowed to equilibrate and thus the suction can be measured.

For samples that have very high suction heads (eg. below 1 bar) a pressure plate is used. (See figure 2.20) The instrument is similar to that of the tension plate, but instead of atmospheric pressure surrounding the sample, a pressure cell is placed around both the sample and porous plate. The air pressure around the sample is increased and the suction head of the soil-moisture is determined from the difference between the applied pressure and that measured through the porous plate.

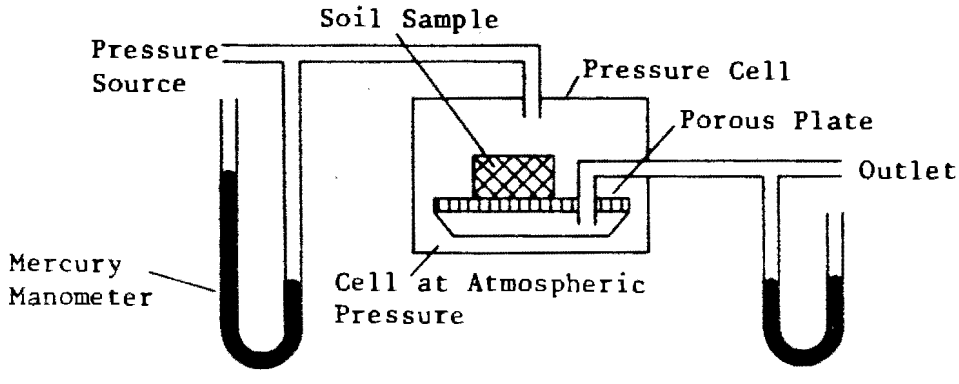

Fig 2.20: Schematic diagram of a pressure plate apparatus.

c) Vapour pressure measurement.

The vapour pressure within the air phase in the soil sample can be measured to provide an indirect method for estimating the tension in the porewater. This method is suited to measuring high tensions in fairly dry samples.

CHAPTER 3

PRESSURE RECORDING APPARATUS.

3.1 Introduction.

The ability to measure the soil-moisture pressure was of great importance in the experiments and some of the tests conducted for this thesis. If the pressure had changed slowly, and there was an abundance of time in which to take a reading, then a manometer or pressure gauge with pencil and paper to record the data could have been used. However, manual sampling was impractical because of the high rate of pressure change and the number of different pressure readings required at one instance. A joint decision with the author's supervisor was therefore made to automate the system of getting pressure readings. This would be done by using a computer-based data-collection scheme that would reduce the amount of operator interaction and still allow the collection of large amounts of data. The number of pressure points requiring sampling was greater than one, therefore some form of switching system was required so that the data from the different points could be collected.

A computer based system to achieve the above aims is illustrated in figure (3.1). Taking the point at which the value of the pressure (be it air or water) is to be measured as the starting point, then the system is as follows:

First a **transducer** is required so that the measured value (pressure in this case) is converted into a convenient form or signal (eg. electrical potential). This signal is then transmitted to a recording device via electrical conducting wires (serial connection). The value of the signal can also be **amplified** to increase its strength and to match that of the converter.

The **converter** (in this case an analog to digital) converts the signal (electrical voltage) to that of a digital equivalent (a binary number). The digital equivalent which appears on the output bus of the converter is read by the **computer** via a parallel

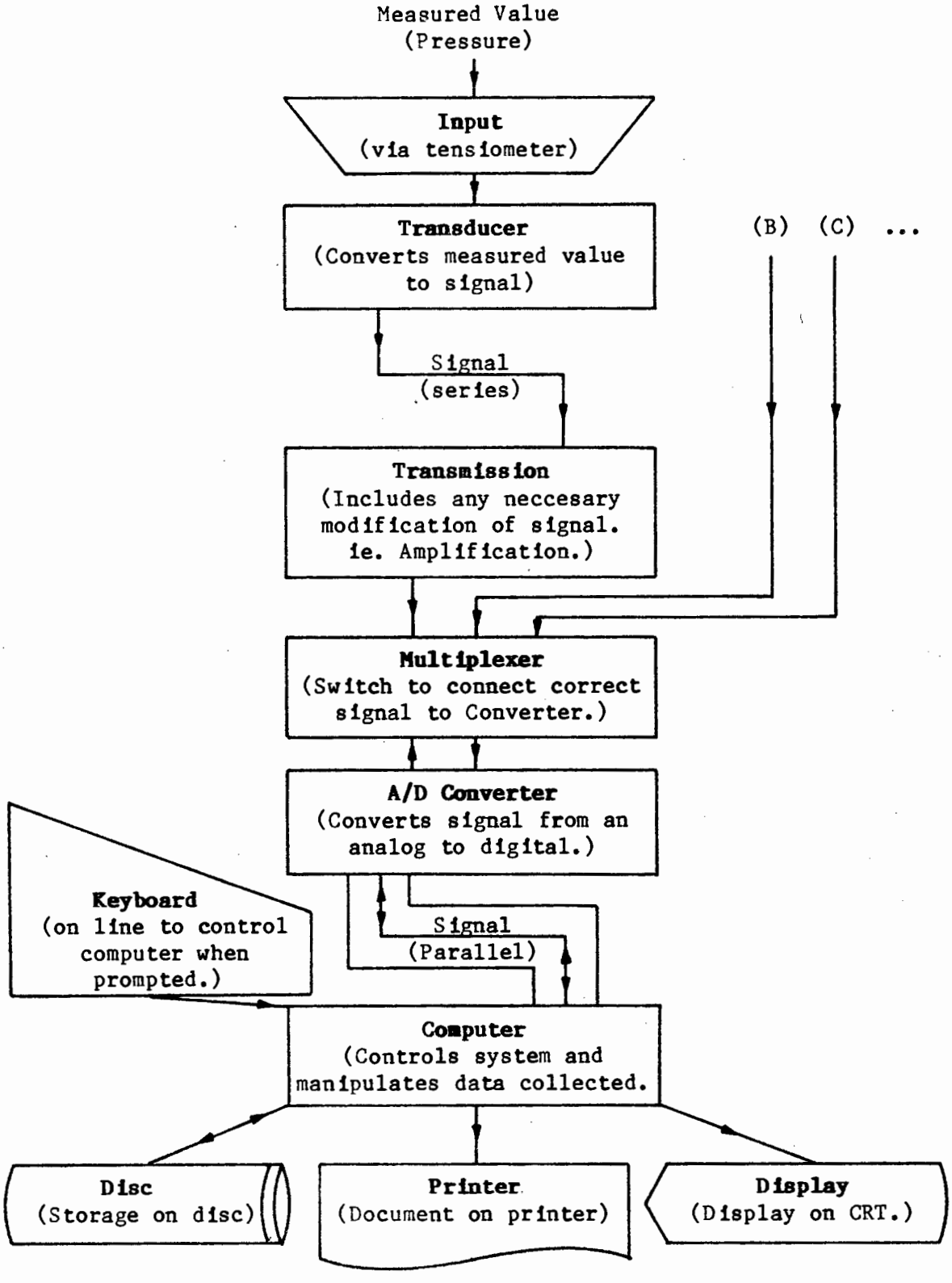

Fig 3.1: Generalized measuring system.

connection. This digital equivalent, read into the computer, is then either manipulated, sent to an **output device** such as the screen, to a **storage device** or a storage area. The method of storage depends on memory availability of the computer and whether the data is required again for manipulation. As there is more than one transducer, a **multiplexer** is required, so that the signal from only one transducer is sent to the converter at any one time.

Both the switching of the multiplexer and the conversion operation of the converter is controlled by the computer, allowing full automation.

Each component in the system is discussed more fully below.

The advantage of the automated data-collection system, is that the pressures which cannot be measured and recorded by conventional means, due to rapidly varying conditions, can be recorded by rapid sampling and data storage to allow for later analysis.

A system was designed and constructed to measure low heads of water, utilizing up to seventeen pressure transducers and connected to a micro-computer. The layout of the design was based on the system shown in figure (3.1).

3.2 Transducers.

A transducer is defined by Bass [3] as being:

> "a device which converts a measured value (measurand) into a convenient form (signal)"

This signal is usually, but not necessarily, electrical. There are a vast number of different transducers for applications in all fields of measurement.

The classification of transducers could be done in a number of ways. (See Joubert [22]). For example, to classify according to:

a) Their input circuitry. Those requiring an external power source and those extracting the power from the measurand.

b) The nature of the process measured.

c) The nature of the output signal, eg. Analog (constantly varying) or Digital (piecewise varying).

d) The physical (electrical) principle behind their operation, eg. resistance, capacitance or inductance.

e) Their use, eg. displacement, pressure or force transducers.

This last classification system is for those interested in the application of the transducer and who are not really concerned about the workings of it.

3.2.1 Selection criteria.

The transducers used for experimental work in this thesis were selected by Sparks and Joubert [22]. The following set of criteria, whereby a suitable transducer system, for the use in soil mechanics experimentation should be selected by, was given:

a) Size, such that it can be used in (relatively) small experiments.

b) Insulated from water, as water pressure is to be measured.

c) Adaptable for use in a variety of different experiments.

d) Relative ease of assembly and maintenance.

e) Reliability and repeatability of results.

Further criteria the author considered important are:

f) A near null-flow pressure measurement system. (eg. if the transducer uses a force-displacement measurement, then the strains to operate the transducer must be very small.)

g) The output signal must be an electrical analog voltage, which can be converted to an equivalent digital signal which the computer can read.

Once a transducer system had been selected, it could be checked to see if the above criteria were satisfied.

3.2.2 Transducer requirements.

Joubert [22] gives the requirements of a transducer, subdivided into two groups, static and dynamic quantities.

Static quantities:

a) The relationship between the measured and the output signal should be linear, over the range of interest.

b) The sensitivity should be such that a sufficient electrical output signal be produced for the expected mechanical input.

c) The sensitivity should be constant with respect to time, temperature and extraneous sources.

Dynamic quantities:

a) All the requirements for static quantities as outlined above.

b) The transducer should not interfere with the process being measured.

c) The device must be capable of operating at frequencies greater than the internal frequencies of measurements required.

d) The phase difference (ie. the time a response takes to occur) should be constant between mechanical input and signal output and should, ideally, be small.

e) The natural frequency of the transducer should differ markedly from the operating frequency of the other equipment involved in the system. (eg. if the frequency is near that of the alternating current supply, the output signal could be affected).

f) The transducer should have a good transient reponse (ie. the electrical output signal should follow as closely as possible to the mechanical input, which varies with time).

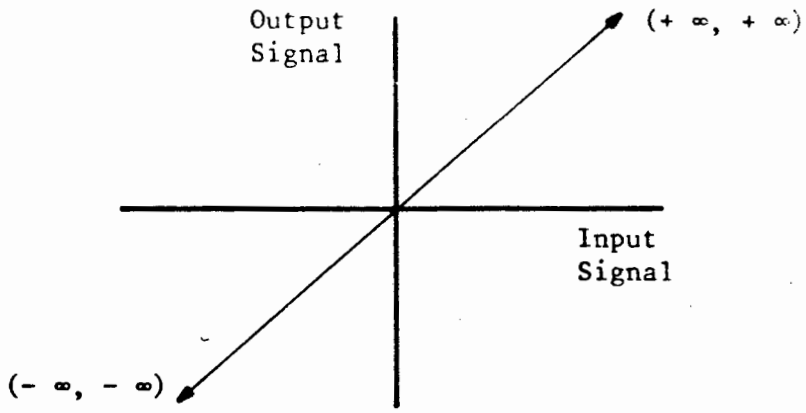

Fig 3.2: Performance curve for a perfect transducer.

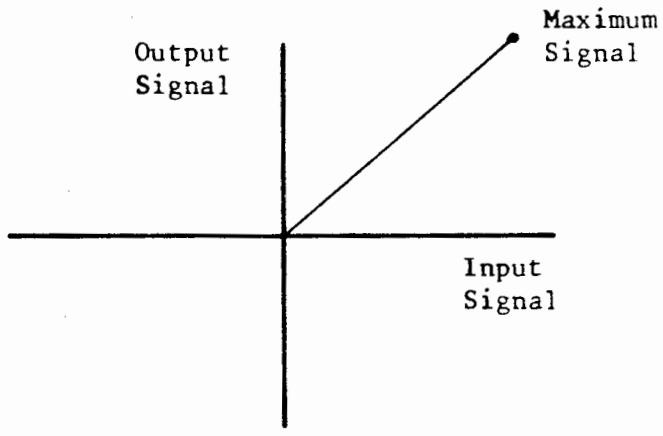

Fig 3.3: Performance curve for a realistic transducer.

3.2.3 Transducer performance. (See Bragg [9])

As stated above, a linear relationship should exist between the measurement (input) and the output signal, over the range of interest. An ideal transducer would have an infinite reading and response range, as shown in figure (3.2). This is umrealistic as an infinite input would be required. A realistic response is, as shown in figure (3.3), where a value of maximum signal anticipated is specified. Many tranducers are, however, not necessarily linear, but tend to have a proportional relationship, as shown in figure (3.4). (This is occasionally done on purpose. If a transducer is responding to x^2 and we wish to obtain x eventually, it is often possible to arrange the device to measure x^2 and give x as the output signal).

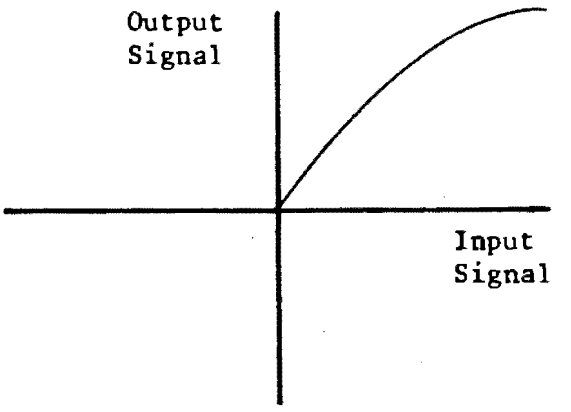

Fig 3.4: Nonlinear transducer performance curve.

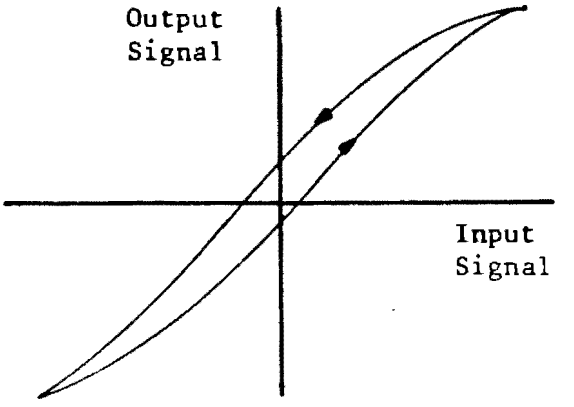

Fig 3.5: Transducer performance curve with hysteresis. (A hysterical transducer.)

Should the transducer have differing values of signal output for the same input, depending upon the direction of approach to the input signal, the transducer is said to have hysteresis, as shown in figure (3.5). This type of transducer response should be avoided as the direction of the signal must be known, so that the output signal can be properly interpreted. Care should be exercised to avoid extraneous effects (generally called noise) that could affect the general performance of the transducer output, as shown in figure (3.6).

A further important characateristic in the performance of transducers is their time dependency. To evaluate this a series of test input signals have been devised, as shown in figure (3.7) (see Bass [3]). These input signals are applied to the transducer input and the output signal response is measured.

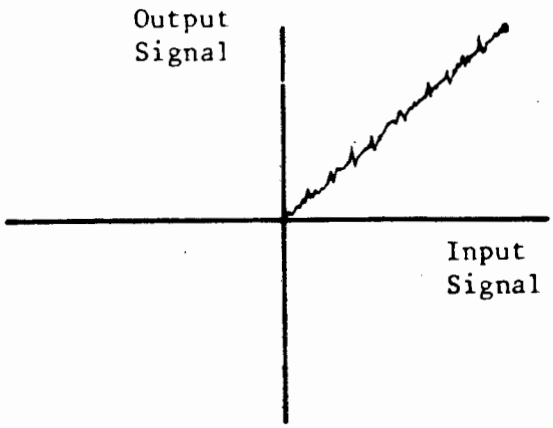

Fig 3.6: Transducer performance affected by noise.

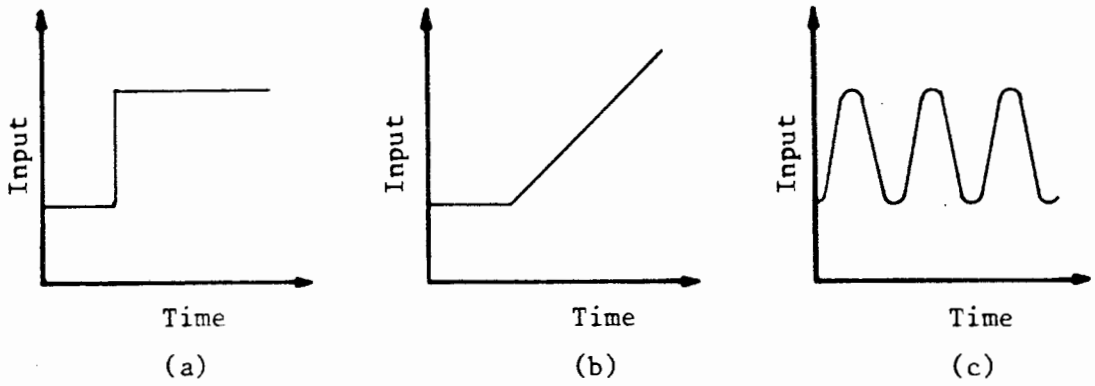

Fig 3.7: Standard test input signals: (a) Step; (b) Ramp; (c) Sinusoid.

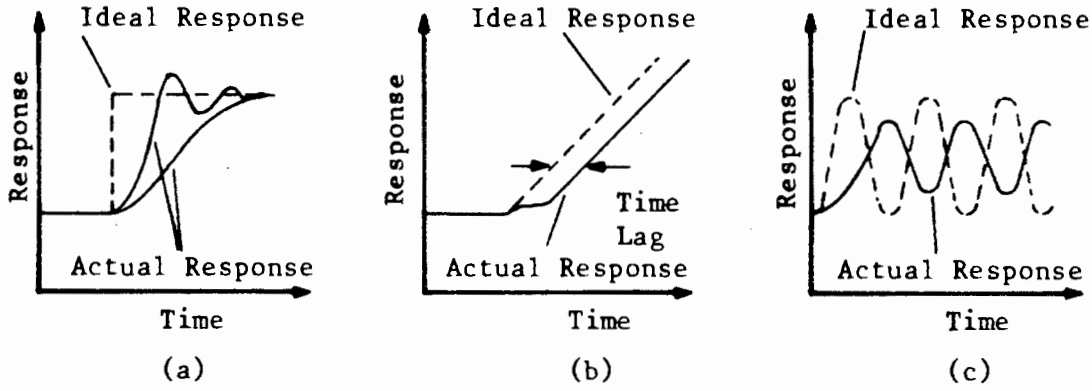

Fig 3.8: Output responses to standard input signals.

The general form (the exact form can be analysed theoretically) of the responses is shown in figure (3.8). On applying a change in signal input, there is a time lag before the output signal starts indicating a change. These effects are important when considering dynamic situations. A dynamic calibration must be performed if the transducer is going to be used in a dynamic situation. (A static calibration for a rapidly varying input is incorrect).

The performance characteristics of a transducer are important as a false performance assumption can cause large errors.

3.2.4 Transducer selection and recommendation.

Types of transducers available; the physical property that they can measure; their method of construction and operation, as well as their output signal, is covered by Joubert [22]. A commercially available semiconductor pressure transducer was decided on by Sparks and Joubert [22] for soil mechanics experimental work. The reasons for his choice are as follows:

a) These transducers are extremely versatile in application.

b) They can be isolated against water.

c) The high manufacturing standard of semiconductor integrated circuits (IC), and therefore their reliability.

d) The size of the units.

e) The application to various experiments would only require minor changes.

f) The availability of the transducers commercially.

g) The ability to be assisted by Mr C Doig in solving technical problems.

Semiconductor pressure transducers are the most recently developed of all pressure transducers. The heart of the transducer is a monolithic silicon chip with a cavity etched out to form a diaphragm. The effect of pressure on the diaphragm causes it to deform and this in turn results in a change in current (or voltage) passing through the crystal.

The device selected was a National Semiconductor LX0503A pressure transducer. The LX0503A converts an applied pressure into an output voltage signal. The operating range of the input pressure is 0 to 30 pounds per square inch (psi). Normal atmospheric pressure is about 14,7 psi. The device is pictured in figure (3.9), having an inlet port on the top and eight leads coming out the bottom, five being active.

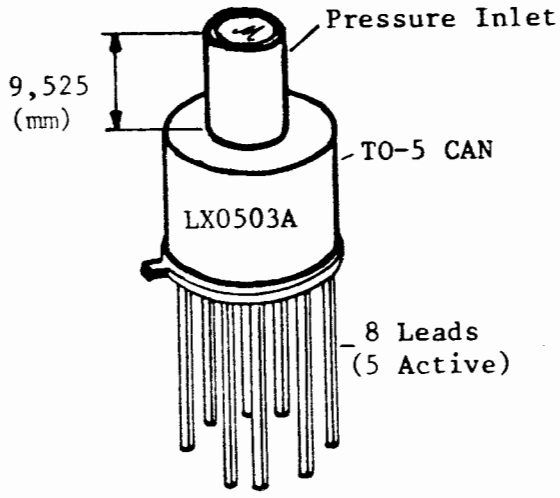

Fig 3.9: **National Semiconductor LX0503A pressure transducer, having a TO-5 metal-can transistor with a single inlet pressure port on top. Suitable for use with non-ionic working fluids.**

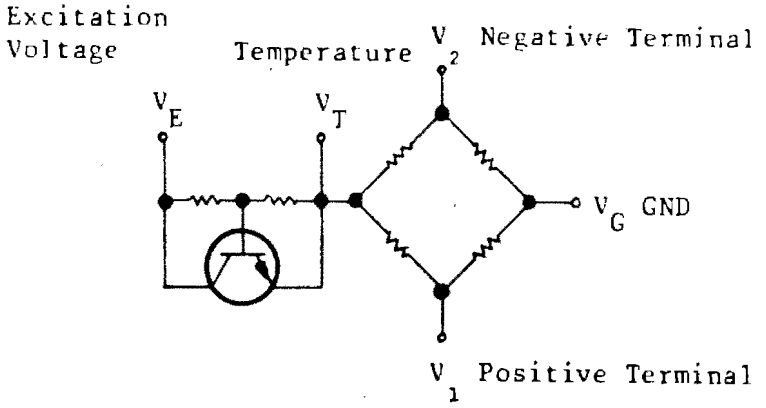

Fig 3.10: Schematic diagram of the LX0503A pressure transducer, showing that the device is essentially a bridge with a piezoelectric element.

Figure (3.10) shows a schematic diagram of the LX0503A. A piezoelectric crystal element forms one leg of the bridge. A voltage supply to the transducer can be supplied directly either to the V_E or V_T terminal. Voltage output is measured between V_2 and V_1. This is a differential type of output in which V_2 goes more negative and V_1 goes more positive as the pressure increases. The output voltage changes by approximately between 2 to 8 mV per 1 psi pressure change. Therefore over a range of 30 psi there will be a change in output of 60 to 240 mV. This voltage range is very small and some amplification is therefore required.

An amplification circuit was designed by Mr C Doig for Joubert [22], as shown in appendix (C-1). The amplification circuit is a linear inverting amplification circuit, increasing the output signal of the LX0503A by about 30 times. The output voltage after amplification is therefore between 60 and 240 mV per psi pressure change. See figure (3.11) Also provided with the amplification circuit is a variable resistor, which allows the offset of the output signal to be set.

The output signal from each transducer and amplification circuit is connected to a switching device (multiplexer). This is so that the output signal from each transducer, can in turn be recorded via a converter, by the computer.

3.2.5 Transducer input interfacing.

The problem with the LX0503A pressure transducer selected is that the top side of the diaphragm contains the pressure sensing circuitry. The pressure inlet allows the working fluid to make contact with the circuit side of the diaphragm. Therefore water, ionic and other aqueous fluids must be kept out of the pressure inlet to avoid electrical failure.

The author overcame this problem by using an intermediate fluid between the water whose pressure is being measured, and the diaphragm. A circuit, as shown in figure (3.12), was designed and constructed using heavy gauge nylon tubing, brass connectors and an interface block housing various valves and a stop-cock. Within the interface block, which is constructed from perspex, the interface between the water being measured and the intermediate fluid can be observed.

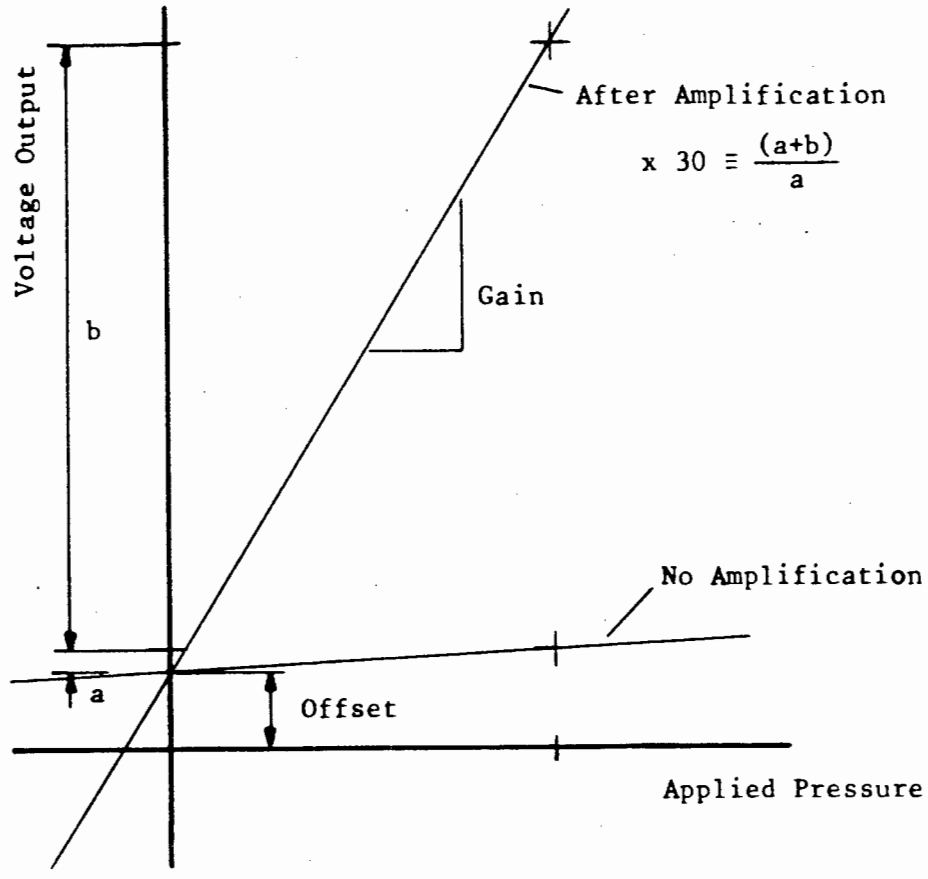

Fig 3.11: Typical voltage output signal versus pressure input before and after linear amplification.

One of the selection criteria was that the measuring system be a null-flow system. This immediately excludes the use of air as the intermediate fluid, as a change in pressure at the point of measurement would cause the air to compress or expand and flow to occur, in or out of the system. Joubert [22], in consultation with his supervisor (Prof. A D W Sparks), decided to use oil as the intermediate fluid. A pure mineral oil (with no additives at all), a Mobil product "Rubex 100", was decided on by Sparks and Joubert [22]. This was after discussion with Mr N Jones of Mobil-Oil (SA) (Pty) Ltd and Dr Harper from the Special Projects Department within Mobil. The main reason for selecting oil was that it would not affect the electrical circuitry. Pure mineral oil was selected, so that no gases would be given off which could form air bubbles in the piping system. The intermediate fluid used was therefore "Rubex 100". The interface between the oil and the water is visible through the clear perspex of the interface block.

The method used for filling the transducer input interface tubing with oil, water and excluding the air from the system is given in appendix (C-2).

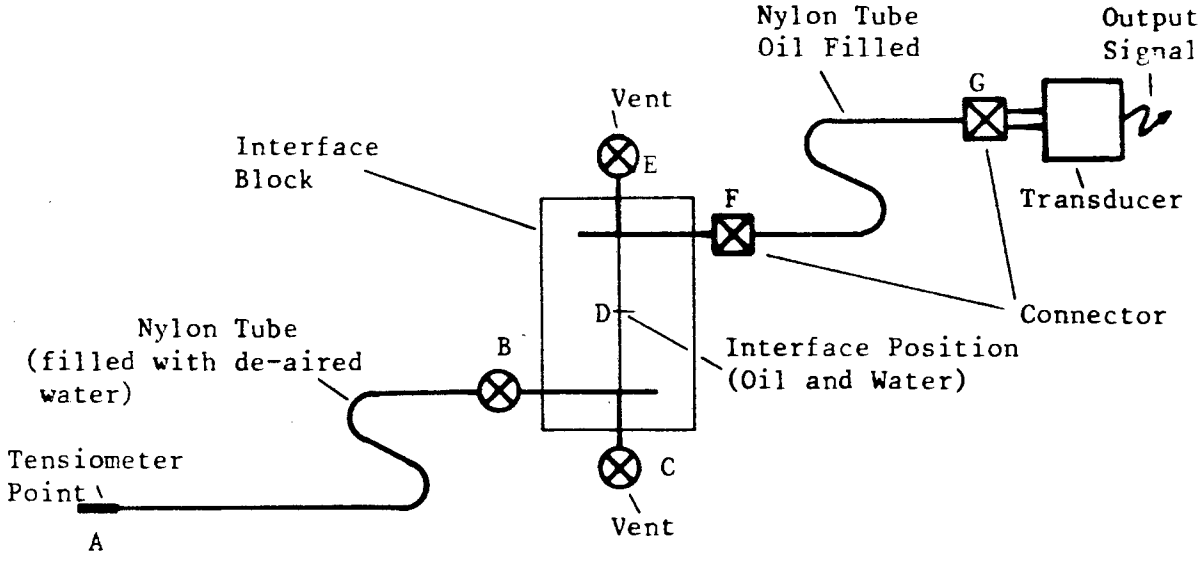

Fig 3.12: Circuit diagram of the transducer input interfacing with a tensiometer.

As the system is a null-flow one, the interface between the oil and water does not move, therefore the densities of the oil and water or the ratio thereof does not need to be known. Pressure is transmitted via the water and oil from the point of measurement to the diaphragm in the transducer. A change at the measuring point causes an exact pressure change in the transducer input port (at the diaphragm).

3.3 Analog to digital conversion and multiplexing.

3.3.1 Introduction.

The system as shown in figure (3.1) is used to measure the pressure, at pressure measuring points, which can vary as a function of time. A transducer is used, which takes the physical parameter pressure and converts it into an electrical voltage or current. The computer, while quite proficient when handling binary voltages is not directly able to handle the analog type of voltage that comes from the transducers being used. To resolve this problem an interface called an analog to digital (A/D) converter is needed.

The function of an A/D converter is to transform an analog quantity (voltage) into a digital equivalent which can be accepted by a computer. This transformation involves sampling the continuous analog voltage, representing the voltage as a discrete value and then formating this quantity for the computer. Figure (3.13) shows a continuous analog signal, represented by discrete values.

The design criteria for the A/D converter needed is based on the particular application for which it is required. The criteria being the resolution (dR), relative system error and sampling frequency (Fs).

a) Resolution.

The resolution of an A/D converter is the smallest analog voltage difference that can be detected with the converter. The resolution will therefore be equal to the magnitude of a unit change in the least significant digit of the digital output from

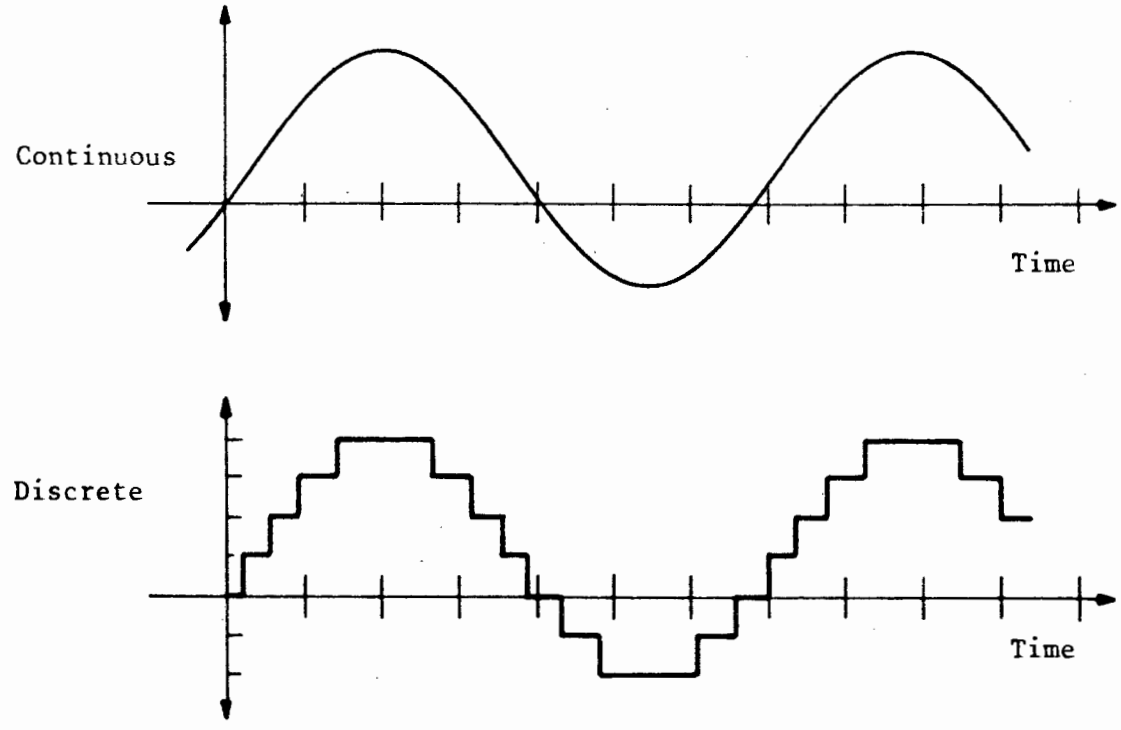

Fig 3.13: A continuous analog signal and a discrete representation thereof.

the converter. The resolution is determined by dividing the maximum analog input voltage range (Vmax) that the A/D converter can accept, by the maximum number of digit intervals (k) that represent the input range. That is:

$$\text{Resolution } dR = \frac{V_{max}}{k}$$

b) Relative system error.

Accuracy of the total system is related to the ability to represent the actual value of the unknown pressure by a digital equivalent. Accuracy is therefore a function of the linearity of the system, gain and offset errors, A/D resolution and the magnitude of the signal being measured. In general the resolution of the A/D converter is the main source of system inaccuracy. For a given system, the relative system error will be minimized when the unknown input voltage range to the A/D converter from the transducer output nearly matches the input range of the A/D converter.

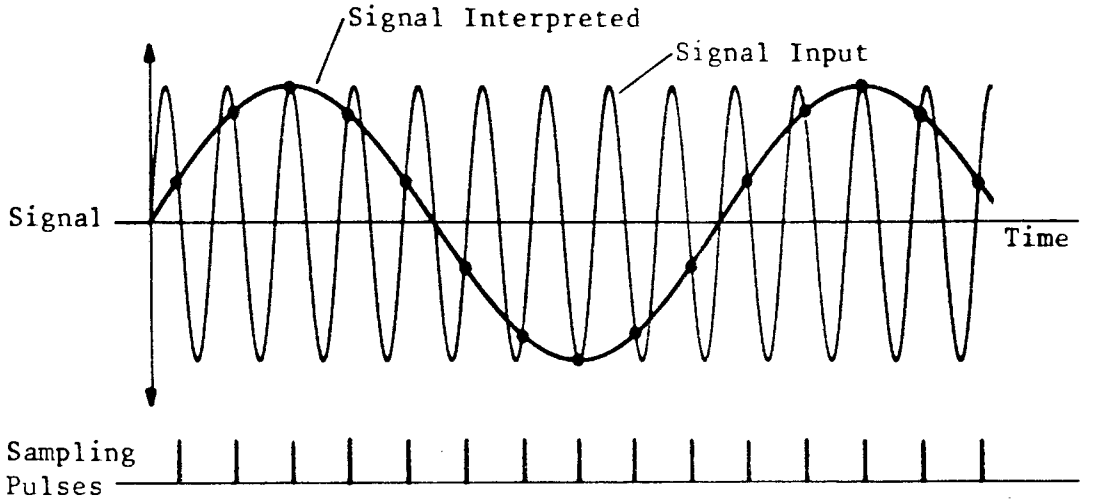

Fig 3.14: Aliasing error caused by an inadequate sampling rate.

c) Sampling theory.

An A/D converter samples the analog input signal, sequentially with respect to time. The sampling rate determines the ability to detect time dependent changes in the input signal. Therefore the sampling rate determines the maximum frequency component which can theoretically be detected. If the sampling rate is too slow, aliasing errors can occur, which result when a high frequency input signal impersonates a low frequency signal. See figure (3.14). A good rule of thumb is to set the sampling rate at least greater than twice the maximum frequency component of the input signal. (See Hallgren [15])

3.3.2 A/D converter selection criteria.

The original selection criteria for the A/D converter, at the start of the author's thesis was given by his supervisor as follows:

a) 17 transducers needed to be monitored, and from each one at least 5 readings taken within a second.

b) It was hoped that the resolution of the system would allow detention of a 0,5 mm water head change of pressure in the transducer input port.

To satisfy the first criteria, two separate designs are needed. One is the design of a switching device, so that each of the transducer's output signal can sequentially be connected to the input port of the A/D converter for conversion. The second is the design of the A/D converter for its speed.

The A/D converter can only sample the next transducer's signal, once it has finished converting the present signal it is sampling. Also, after each conversion, the digital output has to be read and stored by the computer. All of this takes time, how long is not known until a system is constructed and tested. To overcome this problem, an A/D converter is chosen, a circuit designed and then it is calculated to check if the sampling rate is within limits (ie. 5 x 17 = 85 samples/sec).

The second criteria, the resolution of the system is also dependent on what A/D converter is used in the circuit design. A similar approach is adopted with this criteria as with the above.

An A/D converter is therefore chosen, a circuit designed and a check then made to see if the above requirements are satisfied. If not, the process is repeated by selecting a different A/D converter and repeating the design.

3.4 System hardware.

After studying the literature of various A/D converter integrated chips commercially available, and consulting the various supply agents, the author decided to use the following. A fast, complete 12-bit A/D converter with a built-in microprocessor interface, from ANALOG Devices Inc. The AD574A from ANALOG devices is a successive approximation type A/D converter. The highlights of the product are as follows:

a) The AD574A interfaces to most popular microprocessors with an 8-, 12- or 16-bit bus without external buffers or peripheral interface controllers.

b) Four calibrated input ranges are provided, 0 to +10 and 0 to +20 volts uni-polar or -5 to +5 and -10 to +10 volts bi-polar.

c) An internal buried zener reference trimmed to 10 volt with 1% maximum error and 15 ppm/^{o}C typical temperature compensation.

d) The two-chip construction renders the AD574A inherently more relaible than hybrid multi-chip designs.

The switching device selected was two, 16 channel CMOS Analog Multiplexers. The DG506 selected, from Siliconix, is a single-pole 16-position (plus OFF) electronic switch array, designed to function as analog switches. The ON-OFF state of each switch is controlled by drivers, which are in turn controlled by a 4-bit binary word plus an enable-inhibit input.

By using two 16 channel multiplexers it was possible to design a switching device for 32 input channels. The binary control of the multiplexers is done through the output bus of a Peripheral interface adaptor (PIA).

The PIA used was the MC6821. The MC6821 PIA selected, from Motorola, is designed to provide a universal means of interfacing peripheral equipment to the MC6800 Microprocessing unit (MPU). The author used this chip with the 6502 MPU (Apple IIe Computer) to provide a means of interfacing peripheral equipment to it. The device is capable of interfacing the MPU to peripherals via two 8-bit bidirectional peripheral data buses and four control lines, two of them being bidirectional. In the design one of the two 8-bit bidirectional peripheral data buses is programmed, in software, as an output bus for controlling the two DG506 multiplexers. Via the PIA with software in the computer it is possible to select any one of the 32 channels.

As a PIA is being used for the interface of the multiplexers to the MPU, the second 8-bit bidirectional bus could be used for interfacing the A/D converter chip to the MPU, even though this was not necessary. The 8-bit bidirectional bus is programmed in software to be an input bus to

receive digital data output from the A/D converter for the computer. The control of the A/D converter, namely the start and end of conversion is done by using the control lines provided on the PIA. The A/D converter (AD574A) is a 12-bit converter and the Apple Computer has only an 8-bit input bus. It is therefore necessary to transfer the 8 Most Significant Bits (MSB) via the PIA to the MPU, first and then the 4 Least Significant Bits (LSB).

A circuit layout for the multiplexers, A/D converter, peripheral interface adaptor and connection to the 6502 MPU was designed by the author, as shown in appendix (C-3). The circuit layouts were discussed with Mr G Jack (Post-graduate, Dept. of Electrical Eng. U.C.T.), to confirm whether they were feasible and if no errors had been made. Software (in 6502 machine code) was then written (See appendix C-4) to perform the following very simple operations:

Initialise the PIA so one 8-bit bus is an output bus and the other an input bus.
Switch the multiplexer to the input channel number one.
Control the A/D converter to do a conversion of the input signal.
Once conversion is complete, to transfer the digital binary output from the PIA to the MPU and store the result in memory.
Then to switch off the multiplexer.

Table. 3.1: Delays expected in the execution of one read cycle

DELAY	Time (μsec)
Software to initialize the PIA:	108
Software to switch the Multiplexer to a channel:	6
Multiplexer delay:	882
Software to initiate conversion of the A/D converter:	37
Maximum time for a conversion by the A/D converter:	1
Software to take a reading via the MPU of the 8 MSB digits output by the A/D converter and storing them:	10
Software to take a reading via the MPU of the 4 LSB digits output by the A/D converter and storing them:	18
Software to switch off the Multiplexer:	6
Multiplexer delay:	6
Total:	1076

Once the layout of the circuit was complete with the corresponding software, it could be checked to see if it satisfied the selection criteria.

The first criteria being that at least 85 readings per second be made by the system. This could be checked by giving a layout of the approximate delays that would be expected from a read cycle. (See Table 3.1).

The sampling rate is 1076.10^{-6} seconds, therefore in 1 second $1/1076.10^{-6}$ = 929 readings could be made. This is much greater than the selection criteria of 85 readings per second, even with a very long delay routine included. It must just be noted that until a complete system is constructed and tested, filters incorporated to smooth out any noise in the input signal and changes in the software (for more flexible switching of the multiplexer and manipulation of the recorded data), the exact number of readings per second cannot be predicted accurately. With 929 readings per second the author was confident that the final system, when built, would still satisfy the above requirement.

The second criteria is that the system resolution must be less than 0,5 mm head of water. The minimum output from the transducer after initial amplification is about 60 to 160 mV per psi. (See section 3.2.4). Using the conversion factor of 1 psi ≈ 6,9 KN/m^2 or 1 psi ≈ 690 mm head of water, the transducer output is therefore about 0,087 mV to 0,232 mV per mm head of water. If the 0 to 10 Volt input calibration range is used on the A/D converter (AD574A), the resolution of the 12-bit A/D converter is 10V/4096 = 2,44 mV. (2^{12} = 4096). Therefore to get the required system accuracy required, the output signal from the transducer would need further amplification. The amplification to give the required resolution is therefore between 56 and 21 times (2,44/(0,087x0,5) = 56). An amplification of 33 times was designed for by the author. This does not satisfy the selection criteria of a 0,5 mm head of water resolution, for all the transducers performing within specification. The author however adopted 33 because any further amplification would correspondingly also amplify noise. Also, with 33 times amplification a resolution of 1 mm is achieved for all transducers. The author was satisfied with a 1 mm head of water

resolution for the experimental work he envisaged performing for this thesis. Also, in these preliminary calculations it is assumed that some of the transducers give the lowest specification output. (About 2 mV per psi). Most of the transducers perform better than this and a further increase in the resolution of the system is gained. Only once a calibration of the individual transducers is done (see section 3.7) would it be possible to know the exact resolution of each transducer.

3.5 Real Time.

3.5.1 Introduction.

In experimental work that has transient changes, it is required that there be some form of time base with which to be able to identify collected data. The collected data in this case is the output from the pressure transducers. As the computer used (an Apple IIe) does not have a clock that can be referenced to obtain the time, another method had to be developed.

One method which could be used, would be to use Software Timing. This is accomplished by putting a delay routine in the software, which would give a specified delay between each set of readings. There are problems with this approach, as the time taken for a program to be executed by the processor can vary, depending on the hardware attached. Another limitation is that while the computer is busy with a delay routine it cannot carry out other tasks.

To overcome the problems of the software approach a hardware circuit or a hardware/software combination that accurately records time with respect to an external observer is needed. This is known as a real-time clock.

Hardware circuits can take on many forms, but generally such real-time clocks fall into two categories, namely, the heartbeat-interrupt or time-of-day clocks. The heartbeat-interrupt clock is less expensive and uses fewer or simpler components, but more software interaction is

needed to perform all the housekeeping chores. The output line from the clock circuit is connected to an interrupt input on the processr. Every time the clock ticks, the processor stops what it is doing and increments an elapsed-ticks counter in memory. When the processor needs to know the real time, it must calculate the time from the number of ticks counted. The time-of-day clock on the other hand, does almost everything with hardware, requiring relatively little interaction with software. The time is stored directly in memory. (usually in the hardware circuit) When the processor needs the time it just reads the relevant memory register.

3.5.2 Real time clock design.

The author decided to build a time-of-day clock that would keep track of the time in hardware and free the processor for other operations. A battery back-up ensures that the time is kept even when the processor is switched off. Therefore the clock does not require setting each time the processor is switched on. The device used for the design was the MM58167A versatile real-time clock chip by National Semiconductor Corporation, which has been designed for connection to the data buses of common MPU. The MM58167A is a low threshold metal gate CMOS circuit that functions as a real-time clock. It contains a 14-digit counter chain, clocked from a 32 768Hz crystal-reference oscillator. The time is kept in increments from 1 / 10 000 of a second to months. To be able to address the MM58167A with the 6502 MPU, a PIA is needed to interface the two. A similar PIA chip (6821) as used with the A/D converter and two multiplexer is used. Appendix (C-5) shows the layout of the Clock circuit. To reset the clock chip and then to read its various registers, to obtain the time, software is needed. Appendix (C-6) shows a listing of software needed (coded in 6502 machine code) to initialize the PIA, reset the clock registers and read them.

3.6 Data Acquisition Software.

The computer used for the acquisition system is an Apple IIe, which uses a 6502 MPU. Because the A/D converter works at speeds faster than the

high level language (BASIC) that the Apple IIe works with, the subroutines controlling the acquisition system are mostly written in machine language via the 6502 Assembler language. The speeds at which the MPU processes the machine language instructions is compatible with the speeds of the A/D converter.

The general layout for the acquisition software is as follows:

The user writes his own high-level BASIC program. In this program he can select to read or reset the time, specify which transducer channels he is going to read and then read them. This is done by using the relevant subroutines given below. A subdivision of the software is shown in figure (3.15).

There are two subroutines written in highlevel language BASIC, one for the operations dealing with the clock (TIME) and the other for operations of the A/D converter (DATA). These two subroutines call various machine language coded subroutines. Once the user has obtained the time or data requested, he can then display it on a screen or store it on a disc.

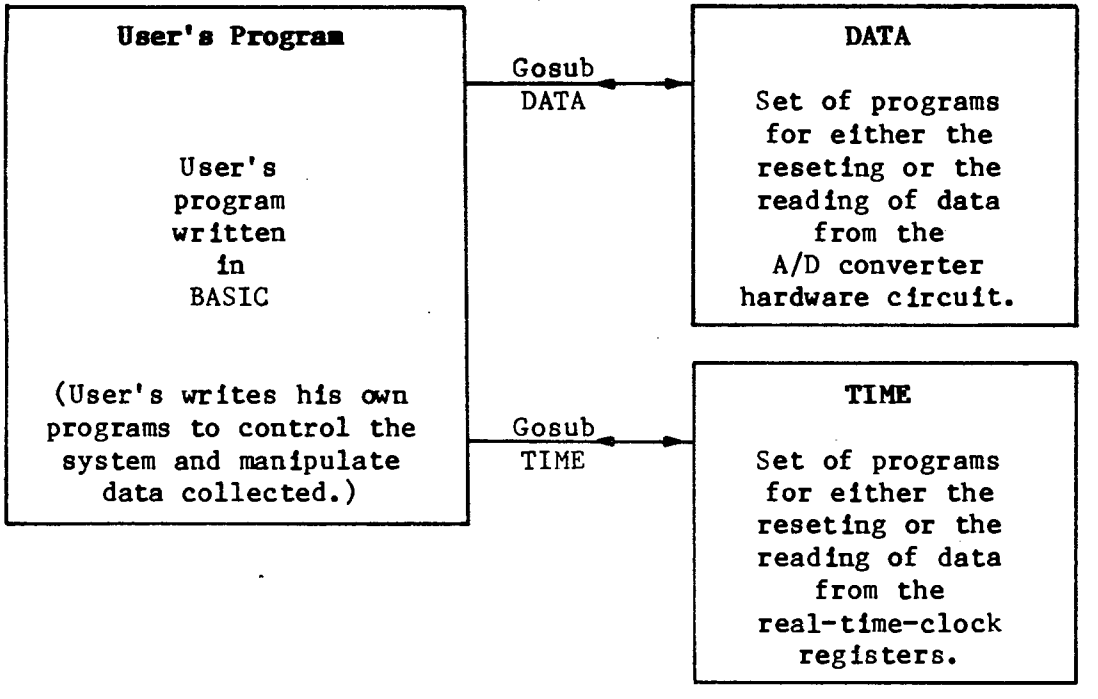

Fig 3.15: Subdivision of the software to control the data-acquistion system.

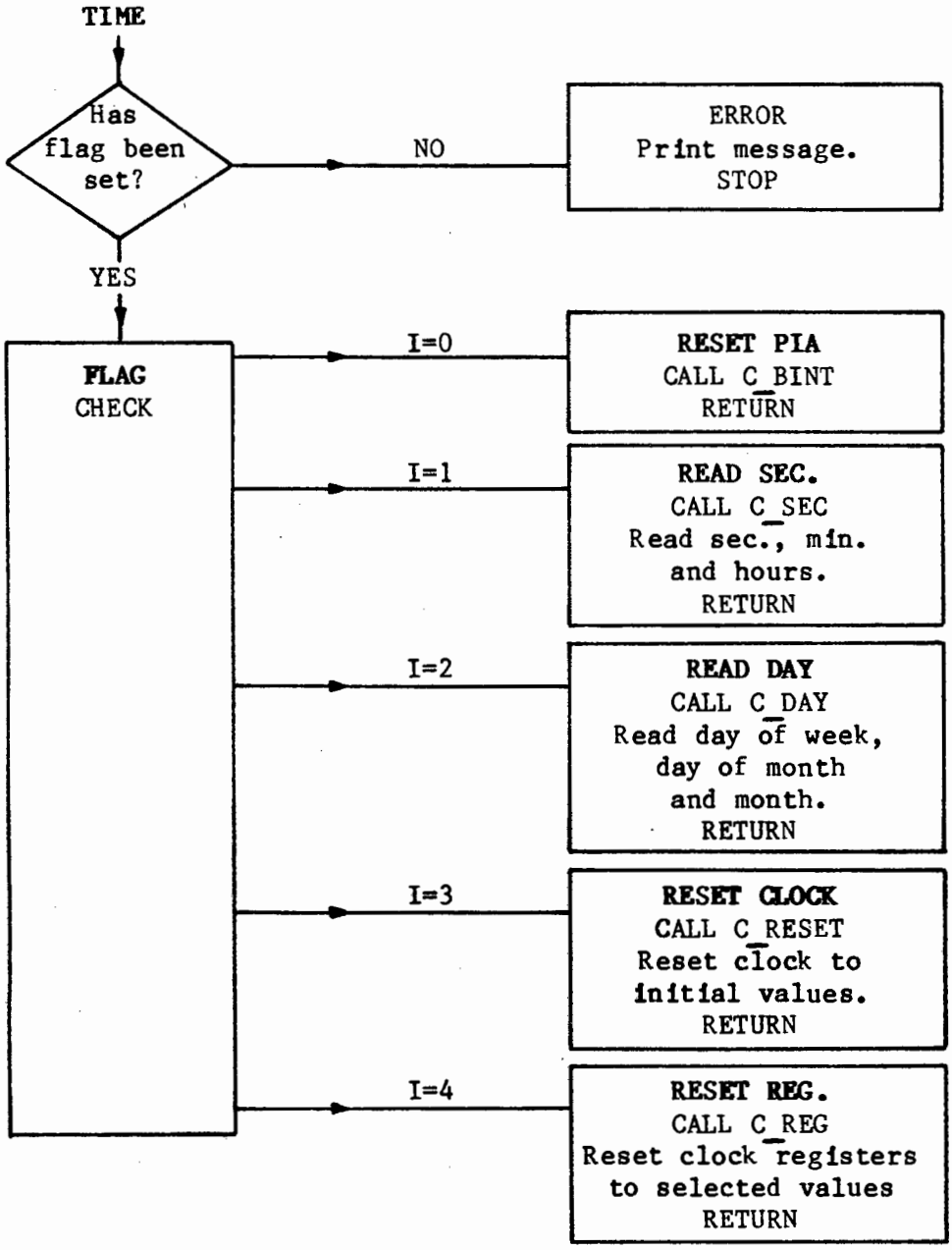

Fig 3.16: Flowchart of the software programs' "TIME".

a) Subroutine "TIME"

This subroutine is for selecting, via a flag, which operation must be performed in connection with the clock hardware circuit. The flag used is the integer I and can have a value from 0 to 4. A flowchart is shown in figure (3.16). The various operations are, briefly, as follows:

I = 0 The PIA is reset (used after the MPU has been switched on or a CONTROL-RESET performed on the keyboard of the Apple IIe)

I = 1 The time in seconds (0 - 60); minutes (0 - 60); and hours (1 - 24) is read and passed back to the user's program.

I = 2 The time in Day of the week (1 - 7); Day of the month (1 - ?); and Month of the year (1 - 12) is read and passed back to the user's program.

I = 3 A full reset of the clock is done setting all readings to their initial values.

I = 4 The user can specify which register he wants to reset and to which value. (ie. Register 2 is seconds, register 3 is minutes,... and register 7 is months.)

Appendix (C-7) gives a listing of the subroutine "TIME" and all the supporting assembler language subroutines needed are in appendix (C-6).

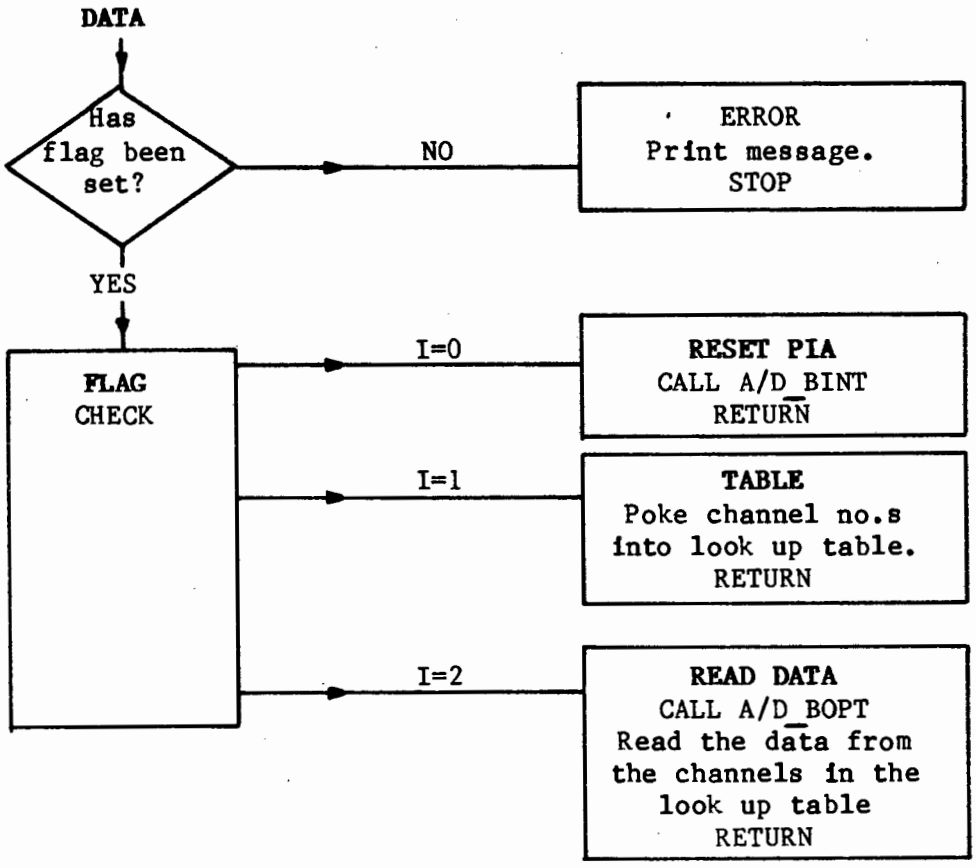

Fig 3.17: **Flowchart of the software programs' "DATA".**

b) Subroutine "DATA"

This subroutine is for selecting, via a flag, what operations must be performed in connection with the A/D converter circuit. The flag used is the integer I and can have the value from 0 to 2. A flowchart is shown in figure (3.17). The various operations are, briefly, as follows:

I = 0 The PIA is reset (used after the MPU has been switched on or a CONTROL- RESET performed on the keyboard of the Apple IIe)

I = 1 The look up table of the channels to be recorded is set. (Before data is read a look up table must be set so that the multiplexer knows which channels to switch to during a read-cycle).

I = 2 The channels listed in the look up table are read via the A/D converter and passed back to the user's program. (The value read is a decimal number between 0 and 4 095. By using the calibration of the transducer this number can be converted to a pressure).

Appendix (C-8) gives a listing of the subroutine "DATA" and all the supporting assembler language subroutines needed are in appendix (C-4).

Table. 3.2: Time taken for 85 (5 X 17) transducer readings.

Time	Readings recorded of 17 transducers																
(sec)	1	2	3	4	5	6	7	8	9	10	11	12	13	14	15	16	17
0,35	79	130	80	12	44	2	60	58	55	58	39	86	2	98	155	53	139
	79	130	80	12	44	2	60	58	55	58	39	86	2	98	155	53	139
	79	130	80	12	44	2	61	57	55	58	39	86	2	99	155	53	139
	79	130	80	12	44	2	60	58	55	58	39	86	2	98	155	53	139
0,81	79	130	80	12	44	2	61	57	55	57	39	86	2	98	155	54	139

0,46 sec total differance in time between first and last set of readings

c) Testing the whole system.

Once the system had been constructed and the software written, the system could be tested to see if the selection criteria were satisfied.

A short user program was written to make a time reading and five sets of readings, of all 17 transducers, so that the speed of the readings could be checked. Table (3.2) shows the results and it can be seen that all the readings taken are within 1 second. This therefore satisfies the first selection criteria.

In section (3.7) a calibration of all the semiconductor pressure transducer is done. It can be seen that all the transducers satisfy the author's requirement of 1 mm head of water pressure resolution. About 50 % of the transducers have a resolution of better than 0,5 mm head of water.

The hardware as described earlier and the supporting software as given in appendix (C-7) and (C-8) was therefore used by the author for the work in this thesis.

d) Using the data acquistion software.

The two subroutines described above with their supporting assembler language subroutines are stored on a floppy disc. To use the system with the programs provided, the following is a way in which this could be done.

The computer, printer and A/D converter would be switched on. (An initialized disc must be in the disc drive when the computer is switched on.) The user would then either write a program for collecting data and the time, or a pre-written one would be loaded from disc storage into the computer memory. The program written or loaded from disc storage, must include the subroutines TIME and DATA if they are going to be used. The subroutines TIME and DATA can be loaded (eg. LOAD TIME) into the computer memory from the disc provided with the system. Before the program, that has been written by the user, is run, the following machine

language routines must be loaded (eg. BLOAD A/D_BOPT) into the computer memory. If the subroutine TIME is going to be used then the following must be loaded into memory:

C_BINT
C_READ
C_RESET
C_REG

If the subroutine DATA is going to be used then the following must be loaded into memory:

A/D_BINT
A/D_BOPT

After these subroutines have been loaded into memory from disc, the user can then run his program.

3.7 Calibration.

In order to be able to use the pressure transducers, they need to be calibrated. Calibration is necessary, so that the digital equivalent which the A/D converter outputs can be related to the physical pressure being measured.

The purpose of calibrating the pressure transducers is two-fold. One, is to show that the transducer output is linear to the input, and therefore no hysteresis, and secondly, to get the calibration of the transducer. To do the actual calibration, each transducer was connected up to an absolute pressure measuring device (ie. A U-tube manometer) and the inlet port was subjected to a series of different known pressures. The pressure was recorded by the acquisition unit. Appendix (C-9) gives a listing of recordings made for the calibration of the transducers.

The apparatus used for the calibration consisted of a U-tube manometer filled with de-aired water, and a metre rule. See figure (3.18). The pressure applied to the transducer was measured as the difference in water heads (in mm) of the U-tube. (The density of water taken as one: $\rho = 1{,}000\ g/cm^3$).

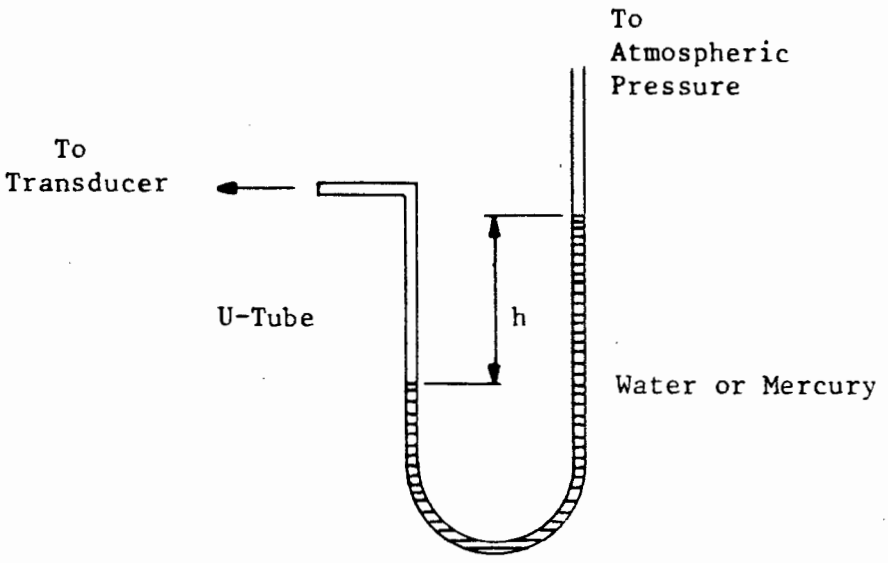

Fig 3.18: A manometer used to supply a known pressure to the transducers for calibration purposes.

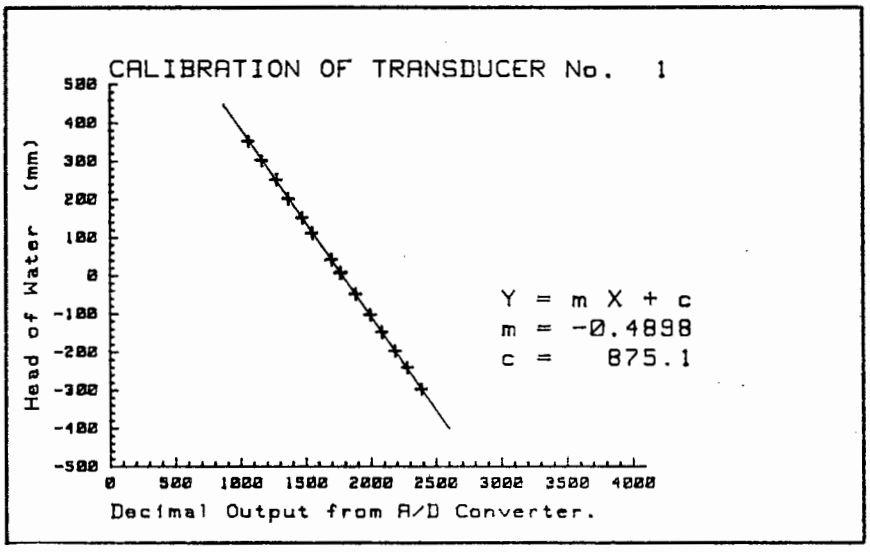

Fig 3.19: Calibration result for transducer no. 1. Plot of known pressures supplied to the transducer as a head of water versus the digital equivalent output, read by the computer.

By making a number of pressure readings at various applied pressures and by the use of the "least-squares approximation method", a straight line could be fitted to the data. Figure (3.19) shows the calibration curve for transducer no. 1. In appendix (C-9) the calibration curves for all 17 transducers are shown.

The actual calibration was carried out in a very short space of time and start and ending applied pressures were approximately the same. The author therefore made no correction for any change in the atmospheric pressure that may have occured during the calibration of the transducers.

3.8 Limitations.

There are various limitations on the different components used in the data acquisition system.

a) Transducers.

The main limitation to the transducer is the applied pressure to the inlet port. This is limited to between 0 and 30 psi absolute pressure. When the transducer is connected to the A/D converter this range is further limited in range. This is because the output voltage of the transducer is amplified, but the input range of the A/D converter is only 0 to 10 Volts.

b) Multiplexers.

The multiplexers can only switch a voltage of less then 12 volts supply through to the A/D converter, because the supply voltages to them are only 12 Volts.

c) A/D converter.

The input range of the A/D converter is limited to between 0 and 10 Volts. The output is a 12-bit binary number between 0 and 4096 decimal. The resolution is therefore 2,44 mV per digit.

d) Clock circuit

The clock can only keep real time for four years (No leap year).

e) Apple IIe.

Memory is very limited and the architecture of it is very badly laid out. Strings used in BASIC use up memory very rapidly, as old ones are not deleted from the memory. Programs have to be extremely small if it is intended to use graphics, as the graphics page uses up a lot of programming memory and is located in the centre of the memory stack. Editing of programs is extremely difficult and time consuming. These problems are compounded by the poor manuals supplied.

CHAPTER 4

EXPERIMENTAL APPARATUS AND TESTING PROCEDURE.

4.1 Introduction.

In this chapter, the apparatus and procedures of the various tests and experiments performed for this thesis are discussed. The tests are necessary to find the parameters that are important in analysing saturated-unsaturated flow in a porous medium. The experiments are to study the seepage of water in saturated-unsaturated domains. For these tests and experiments a porous medium is required. The medium selected was a coarse grained sand, with a fairly high hydraulic conductivity. A relatively high hydraulic conductivity was selected so that experiments could be performed without too much delay in waiting for the soil to drain. The sand was also selected for a capillary fringe compatible with the experimental apparatus the author intended to use.

The material used was a whitish-yellow (pearl coloured) coarse sand consisting of well rounded particles. This material is from a limited stock of special sand used by Prof. Sparks for seepage experiments. It is apparently a washed river sand obtained some years ago from a supplier near Stellenbosch. The aim of the testing program was to find the parameters of the soil, namely:-

a) a rough classification of the soil in terms of grain size;
b) the saturated hydraulic conductivity of the soil;
c) the relative hydraulic conductivity of the unsaturated soil;
d) and the soil-moisture characteristic curve.

4.2 Classification properties of Cape Flat's sand.

Two "standard" tests were performed, to classify the soil. A specific gravity test and a grain size analysis. Appendix (D) gives the procedure of these tests and the results obtained.

The averages of the results obtained are as follows:-

Particle size distribution:

Sieve aperture size (mm)	% Passing (by mass)
2	100
1	81
0,850	46
0,710	7
0,600	3
0,425	0,6
0,300	0,3

Figure (4.1) shows a distribution curve of the particle sizes.

Specific gravity: 2,64

Effective size (D_{10}): 0,72 mm

Uniformity coefficient (U): (D_{60}/D_{10})

= 0,91 / 0,72 = 1,3 (uniform soil)

Description: whitish-yellow (pearl coloured) coarse sand, uniformly graded, rounded particles.

4.3 Saturated hydraulic conductivity.

The hydraulic conductivity can be measured (in the laboratory) by two methods:

-Falling head permeameter

-Constant head permeameter

The reason the laboratory tests were done, was to find the relationship of the saturated hydraulic conductivity of the soil with the void ratio. The test used by the author was the Constant head method. See Lambe and Whitman [25].

PARTICLE SIZE DISTRIBUTION.

SUMMARY OF RESULTS.

U.C.T. SOIL MECHANICS LABORATORY

TEST No. PSD/A01/A02/A03/A04

DATE. 8/85

TESTED By. G WARDLE

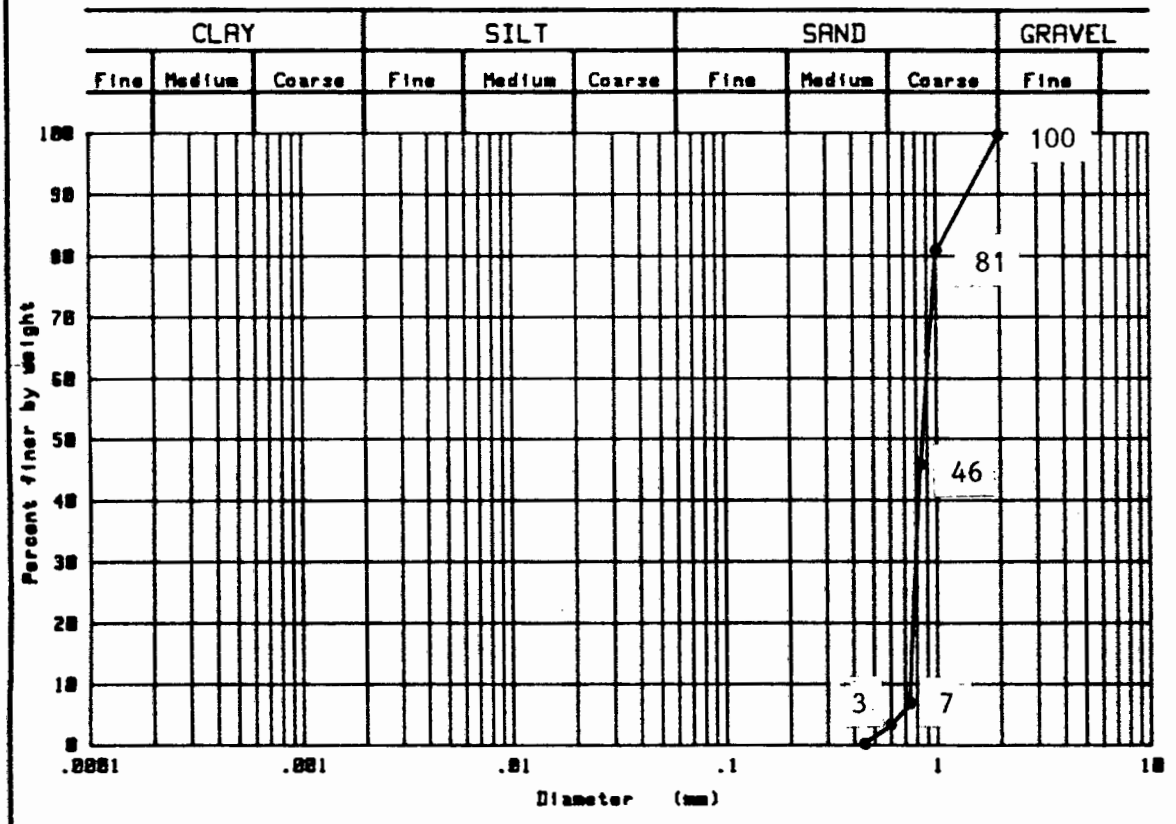

REMARKS: SUMMARY OF RESULTS FROM PARTICLE SIZE TESTS.

Sieve aperture size (mm)	Percent passing (By mass)
2	100
1	81
0,850	46
0,710	7
0,600	3
0,425	0,6
0,300	0,3

G.B.Wardle.
M.Sc. Thesis
U.C.T. 1986/88

Fig 4.1: Particle size distribution curve for the soil used.

Figure (4.2) shows the experimental set-up needed to do the Constant head test. The sample of soil to be tested is placed in a tube that has piezometers within the sample length. A constant head supply tank of water is connected to one end of the sample tube. At the outlet a facility is required to collect the water leaving the sample.

The procedure adopted for doing the tests is as follows:

A dry sample of soil, mass W_s, is placed with a loose uniform density in the sample tube (permeameter). The sample is then saturated with water. This can be done by two methods. In the first method, the sample tube is sealed and a vacuum applied. After waiting a while for the removal of air, the soil is saturated by introducing de-aired water from the bottom of the sample.

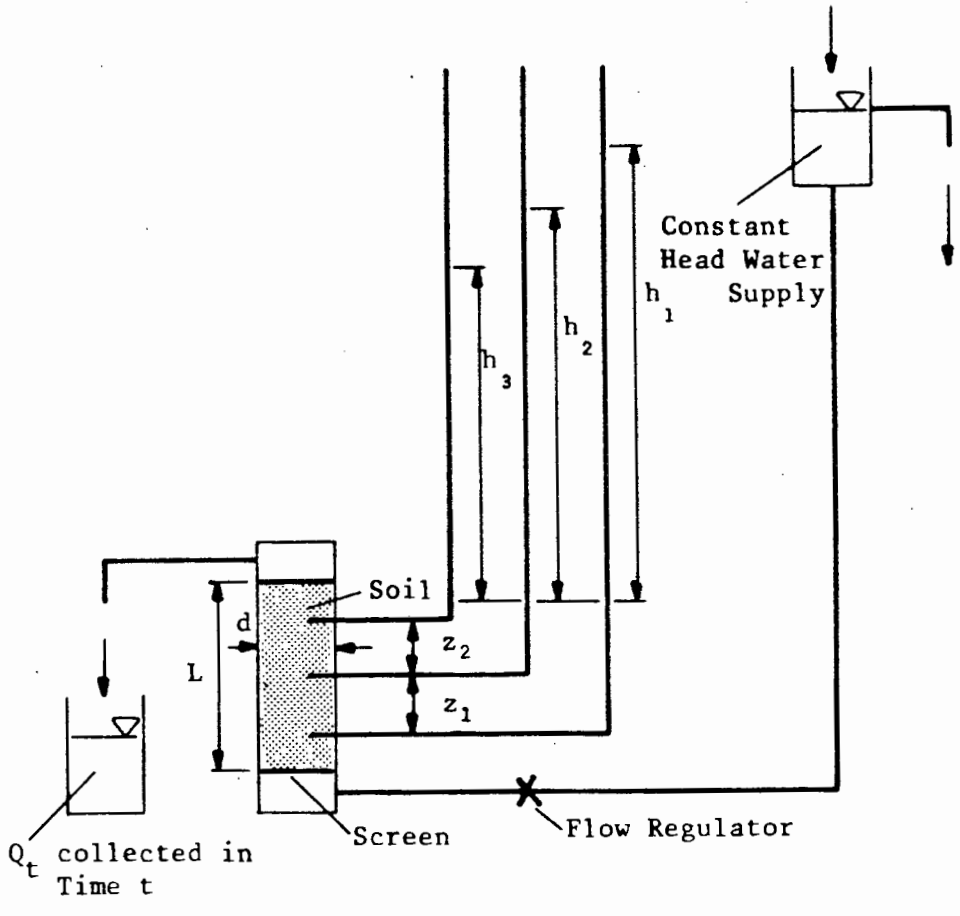

Fig 4.2: Schematic diagram of a constant head permeability set-up.

The second method is to pass de-aired water through the sample so that quick sand conditions develop. With the soil in this agitated condition, any air within the sample of soil is removed with the passing water. The second method of flushing the air out of the sample was used for the test.

After saturating the soil, the flow regulator is closed. Measurements are made of the tube diameter d, and the total length L, of the soil sample. The distances z_1 and z_2 between the piezometer points are also measured.

Flow is started by opening the flow regulator (See figure 4.2). The flow regulator must not be opened too much, or quick sand conditions will occur. After the flow has reached equilibrium conditions, the flow rate is measured. This is done by measuring the time t, taken for a quantity of water Q_t, to be collected, from the outlet of the sample tube. The temperature T, of the water is also recorded every few minutes. While the water is being collected from the outlet of the sample tube, the heights h, of the water levels in the piezometer tubes is recorded.

The flow rate is then altered, by changing the setting of the flow regulator. The test is repeated by waiting for equilibrium conditions to be reached, and a new set of readings taken. After the test has been repeated for 3 or more different flow rates, the void ratio of the sample is changed.

The flow of water through the soil is stopped and the void ratio of the soil is decreased by tapping the side of the sample tube or by rodding the saturated sand in the permeameter. The new sample length L is measured and the test repeated for different flow rates.

The saturated hydraulic conductivity can be determined by applying Darcy's Law:

$$k = \frac{Q_t \, z}{t \, h \, A} \qquad (4.1)$$

where k is the hydraulic conductivity to be calculated, Q_t is the total quantity of water which flowed through the soil in time t. h is the total head loss between two piezometers separated by a length z. A is the cross-sectional area of the sample tube. The values for Q_t and t are measured directly. h, the total head loss, is the vertical distance between the water levels in the piezometer tubes ($h_1 - h_2$). A, the cross-sectional area, is calculated from the tube diameter ($\pi d^2/4$). For a series of tests, equation (4.1) is not used directly to calculate the hydraulic conductivity, but the results of the tests are plotted as the Darcian velocity versus the hydraulic gradient. The slope of a line fitted to the plotted points gives the coefficient of permeability k. This can be shown by rewriting equation (4.1) as:

$$k = \frac{\frac{Q_t}{A\ t}}{\frac{h}{z}} \tag{4.2}$$

or

$$k = \frac{v}{i} \tag{4.3}$$

where $v = Q_t/At$ is the Darcian velocity and $i = h/z$ is the hydraulic gradient. The effect of temperature has not been considered yet. With a change in temperature the viscosity η of the water changes. Therefore to standardise all the tests to 20 ^{0}C the viscosity change is considered. If at temperature T the Darcian velocity $v_T = v$. Then at temperature T = 20 ^{0}C, the Darcian velocity is:

$$v_{20} = v_T \frac{\eta_T}{\eta_{20}} \tag{4.4}$$

where η_T is the viscosity of the water at temperature T. See Lambe [24].

Equation (4.3) is therefore rewritten as:

$$k_{20} = \frac{v_T \frac{\eta_T}{\eta_{20}}}{i}$$

$$= \frac{v_{20}}{i} \qquad (4.5)$$

The results from the tests are plotted as the Darcian velocity at 20^0C v_{20}, versus hydraulic gradient i. For each different Darcian velocity there is a corresponding hydraulic gradient. For a particular void ratio of the soil, at least 3 tests are done. Therefore, using the method of "least squares approximation" a straight line can be fitted to the plot of the data. The slope of the line is the coefficient of permeability k_{20} in Darcy's Law (ie. hydraulic conductivity):

$$v_{20} = k_{20} i \qquad (4.6)$$

The void ratio is calculated from the mass of the dry soil and its volume V, in the sample tube:

$$V = L \pi \frac{d^2}{4} \qquad (4.7)$$

$$V_s = \frac{W_s}{\rho} \qquad (4.8)$$

$$V_v = V - V_s \qquad (4.9)$$

$$e = \frac{V_v}{V_s} \qquad (4.10)$$

where V_s is volume of the solids, ρ the mass density of the solids, V_v the volume of the voids and e the void ratio. The void ratio can therefore be determined and the corresponding hydraulic conductivity obtained from the plot of the Darcian velocity versus the hydraulic gradient.

4.4 Unsaturated hydraulic conductivity.

The unsaturated hydraulic conductivity can be expressed as a function of either the volumetric moisture content $k = k(\theta)$ or the suction head $k = k(\phi)$. The functional relationship depends on whether the volumetric moisture content or the suction head is considered. The relationship between the hydraulic conductivity and volumetric moisture content is physically more meaningful, but in flow calculations the relation between the hydraulic conductivity and suction head is more useful.

The relationship between the volumetric moisture content and the suction head is dependent on the pore configuration and this relationship displays hysteresis. The method therefore employed in this test is to determine the hydraulic conductivity as a function of the volumetric moisture content. The relation between the volumetric moisture content and the suction head is determined from the soil-moisture characteristic curve. (See section 4.5). By combining the two relationships, the relationship between the hydraulic conductivity and the suction head can therefore also be estimated.

To determine the hydraulic conductivity versus the volumetric moisture content relationship, a direct experimental method is used. (See Bouwer [7] and Youngs [40]). The apparatus consists of a long, soil-filled vertical column, with tensiometers or pressure tappings, as shown in figure (4.3). A constant flow of water is applied to the top of the sand column, but less then that required to saturate the soil. (ie. It must not cause ponding on the surface). The water is allowed to drain freely from the bottom of the column, but provision is made for collecting it.

As no neutron or gamma-ray technique for determining the volumetric moisture content was available, an alternative had to be used. The method suggested by the author's supervisor was used. That is, the volumetric moisture content was determined by obtaining the mass the complete apparatus. See figure (4.3).

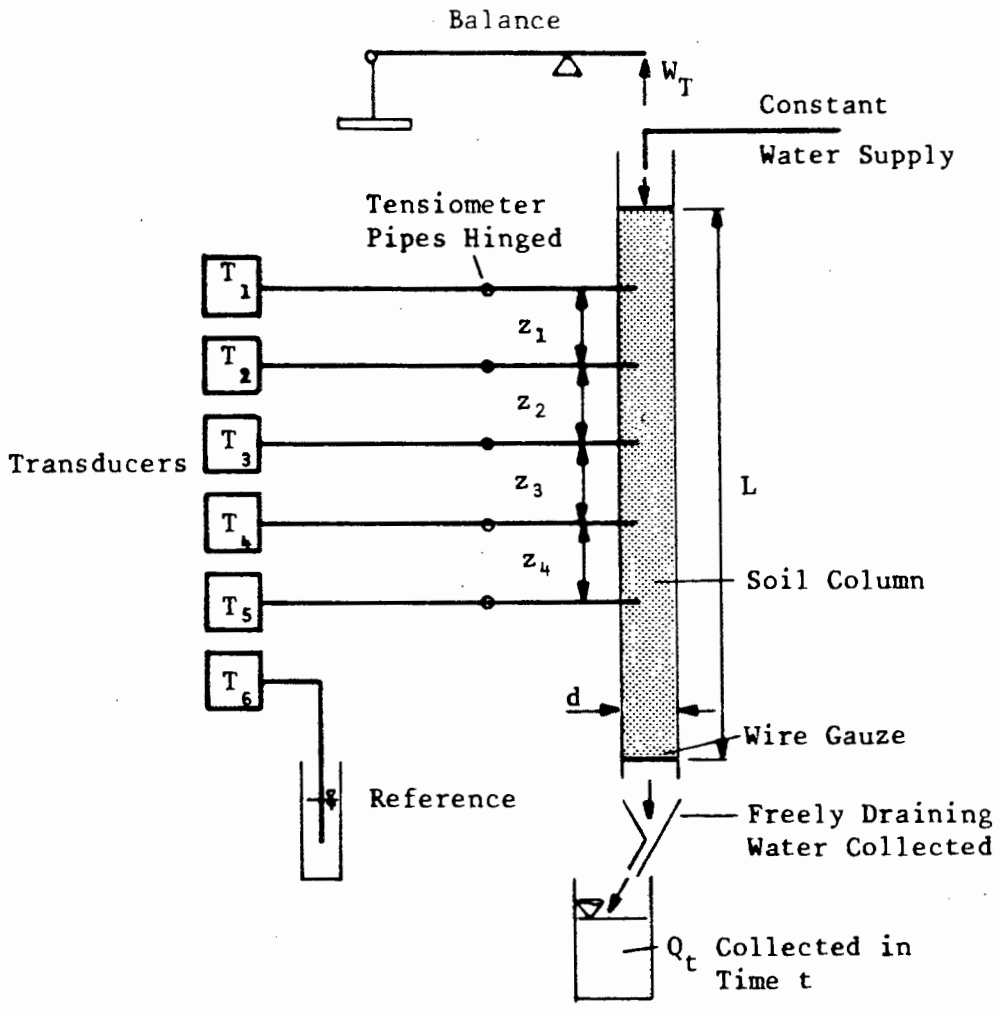

Fig 4.3: Schematic diagram of the experimental apparatus for determining the unsaturated hydraulic conductivity.

The procedure adopted for the test is as follows:

The mass W_a of an empty vertical column, with tensiometers connected, was found. A dry sample of soil, mass W_s, is placed with a loose, uniform density in the vertical column. The soil is then saturated with de-aired water. This is done by closing the top and bottom of the column and applying a vacuum to the soil. After waiting a while for the air to be removed, the soil is saturated by introducing de-aired water from the bottom of the soil column. After saturating the soil column, the bottom is opened, allowing water to drain, while at the same time water is applied to the top of the sand column, at a flow rate less than that which would cause ponding on the surface. This produces an unsaturated flow of water

within the sand column. Measurements are made of the column tube diameter d, the length L of the soil column and the distances z between the tensiometer points. If the flow rate is kept constant and the bottom of the column is free to drain, equilibrium conditions will be established. The upper portion of the soil column will have a uniform volumetric moisture content θ, and suction head ϕ (See figure 2.18). The water content will be higher at the bottom of the soil column due to the capillary effect at an outflow surface. The flow rate is measured after equilibrium conditions have been reached, by measuring the time t, taken for a quantity of water Q_t, to be collected from the bottom of the soil column. The temperature T, of the water is also recorded. While the water is being collected from the bottom of the sand column, the local heights h, of the tensiometer readings are recorded. The total mass W_T, of unsaturated sand and apparatus is also recorded.

The test is then repeated for a different flow rate to yield another point in the unsaturated hydraulic conductivity versus suction head relationship.

It must be noted that at very small flow rates, a very long time is needed for equilibrium conditions to be established before readings can be made.

After the test has been repeated for a sufficient number of times to get a relationship of the hydraulic conductivity versus the volumetric moisture content, the void ratio of the sample is changed. This is done by tapping the side of the column tube and noting the new sample length L. The complete test is then repeated for the new void ratio.

The unsaturated hydraulic conductivity is calculated by applying Darcy's Law even though the soil is not saturated. The hydraulic conductivity is therefore determined corresponding to a certain volumetric moisture content of the soil. The volumetric moisture content is determined from the total mass of the system recorded for each flow rate.

The volume of the soil sample is:

$$V = L \pi \frac{d^2}{4} \tag{4.11}$$

where L is the length of the soil sample during the test. The volume of moisture in the soil at a particular flow rate is determined from the mass of the moisture. The mass of moisture is:

$$W_w = W_T - (W_a + W_s) \tag{4.12}$$

and the volume of moisture is therefore

$$V_w = \frac{W_w}{\rho} \tag{4.13}$$

where ρ is the mass density of water, taken as 1,000 g/cm^3. (See section 2.3). The volumetric moisture content is therefore:

$$\theta = \frac{V_w}{V} \tag{4.14}$$

Darcy's Law can be written as:

$$k = \frac{Q_t z}{t\ h\ A} \tag{4.15}$$

where k is the hydraulic conductivity to be calculated, Q_t is the total quantity of water (millilitres) collected in time t. h is the total head loss between the tensiometers separated by the vertical length z. A is the cross-sectional area of the column tube. The values of Q and t are measured directly. A, the cross-sectional area, is calculated from the tube diameter ($\pi\ d^2/4$).

Equation (4.15) can be rewritten in the following form:

$$k = \frac{\frac{Q_t}{A\ t}}{\frac{h}{z}} \tag{4.16}$$

or

$$k = \frac{v}{i} \tag{4.17}$$

where $v = Q_t/At$ is the Darcian velocity of the unsaturated soil and $i = h/z$ is the hydraulic gradient. The calculation of the hydraulic gradient, at equilibrium, should be equal to one. The reason is h, the total head loss between two tensiometers T_1 and T_2 in figure (4.3), can be rewritten as:

$$h = \phi_1 + z - \phi_2 \tag{4.18}$$

where ϕ_1 and ϕ_2 are the suction heads at tensiometers 1 and 2, and z the vertical distance between the two. At equilibrium the volumetric moisture content and the suction head are constant along the whole length of the column of soil except at the bottom where the capillary effect causes a higher saturation. At equilibrium therefore throughout most of the column $\phi_1 \simeq \phi_2$. Therefore $i = h/z = z/z = 1$.

The effect of temperature also needs to be considered. As in section (4.3) Equation (4.17) can be rewritten as:

$$k_{20} = \frac{v_T \frac{\eta_T}{\eta_{20}}}{i} \tag{4.19}$$

$$= \frac{v_{20}}{i} \tag{4.20}$$

to take temperature into account. At each flow rate the hydraulic gradient i, is calculated. (Should be 1). The Darcian velocity standardised to 20 ^{0}C is also determined from:

$$v_{20} = \frac{Q_t}{A\ t} \frac{\eta_T}{\eta_{20}} \tag{4.21}$$

The unsaturated hydraulic conductivity can therefore be obtained which corresponds to the volumetric moisture content of the unsaturated soil calculated above. The test is repeated at a different flow rate causing a change in the degree of saturation. A new unsaturated hydraulic conductivity, which corresponds to the changed volumetric moisture content, is then obtained by repeating the above calculations.

The void ratio at which the set of tests are done can be determined from the sample length. The volume of the soil sample is given as V, in equation (4.11). The volume of solids is:

$$V_s = \frac{W_s}{\rho} \tag{4.22}$$

where ρ is the mass density of the solids. The volume of voids in the soil is:

$$V_v = V - V_s \tag{4.23}$$

The void ratio is therefore:

$$e = \frac{V_v}{V_s} \tag{4.24}$$

To repeat all the tests at a different void ratio, this is done by just changing the length of the soil sample in the column.

4.5 Soil moisture characteristic curve.

To find the soil-moisture characteristic curve in the laboratory, a sample of soil must be subjected to various suction heads and the corresponding volumetric moisture content measured. The suctions imposed must either be in increasing or decreasing increments so that the envelopes of the hysteresis can be observed. (eg. the soil must either be drained from a saturated case or wetted from a dry state). Secondary scanning curves in the relationship are determined by a change in direction of wetting or drying during a test. (See figure 2.7)

The apparatus used to determine the relation between the volumetric moisture content θ, and the moisture suction head ϕ, is a pot to contain a soil sample; a drainage pipe with which to apply a suction; and a tensiometer to measure the suction head. The complete apparatus is mounted on a scale so that its mass can be measured at any time. See figure (4.4). The pot used is a short, large diameter perspex tube with a flat base. At the base of the tube two holes are made. Through one, a nylon drainage tube is passed and a tensiometer through the other.

The test is started by measuring the mass of the empty pot W_a. A sample of dry sand, mass W_s, is placed loosely with a uniform density into the pot.

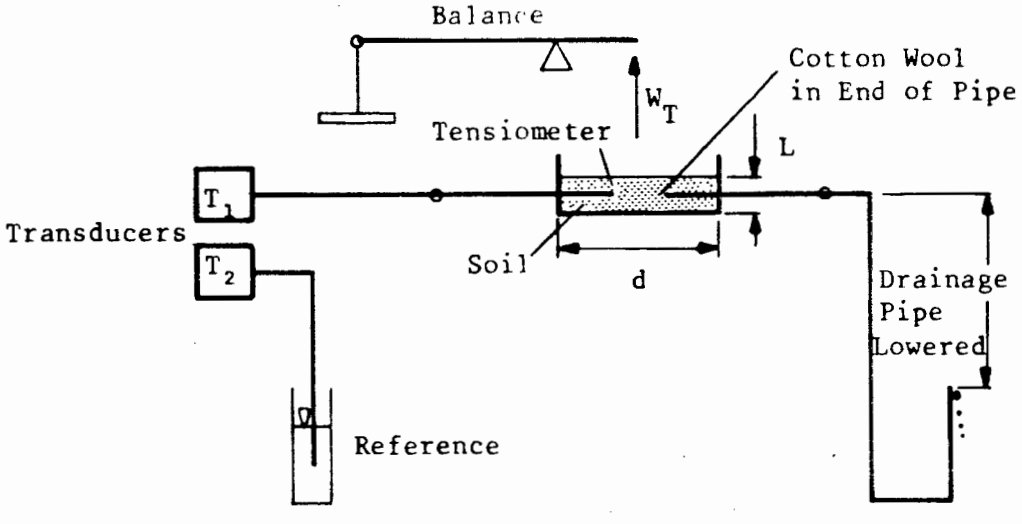

Fig 4.4: Schematic diagram of the experimental apparatus for determining the soil-moisture characteristic curve.

The sample of sand in the pot is then saturated. This is done by closing off the top of the pot and applying a vacuum to the pot for a while, to remove the air. De-aired water is then introduced via the drainage pipe to saturate the sand. The tensiometer is referenced, by recording the pressure of the water, with its level just above the sand in the pot. The water level is then lowered to the surface of the sand in the pot (zero datum level) and the mass of the total saturated system is found. The diameter d, of the pot and the height L, of the sand therein is recorded.

The measurements of the relation between the volumetric moisture content and suction head is started by applying a suction to the soil in the pot. This is done by lowering the drainage pipe outlet in small increments (10 to 20 mm). Between each increment of lowering the outlet there is a time delay, so that the system can drain until an equilibrium is reached. Once an equilibrium condition has been reached (ie. no more flow out the drainage pipe), a tensiometer reading is taken and the total mass of the system W_T, recorded. The lowering of the drainage tube outlet is continued until further lowering of the tube causes very little change in the total mass of the system.

The reverse process is then proceeded with. In this case the drainage tube outlet is raised a small increment and de-aired water added to the open end of the tube. When equilibrium is reached (ie. no water level change in the drainage tube) a tensiometer reading is taken and the total mass of the system, measured. The raising of the drainage tube outlet is continued until the water level is at the top of the soil sample in the pot (ie. back to zero suction head).

The process of draining the soil and rewetting it can be repeated to obtain secondary curves in the soil-moisture characteristic curve.

The calculations needed are to find the volumetric moisture content, corresponding to a tensiometer reading. This then allows a plot to be made of the soil-moisture characteristic curve. At the start of the test the dry mass of the soil and apparatus is recorded. During the test the total mass is measured, which includes the mass of the water in

the pot. Therefore the mass of water is:

$$W_w = W_T - (W_s + W_a) \tag{4.25}$$

The volume of water is therefore:

$$V_w = \frac{W_w}{\rho} \tag{4.26}$$

where ρ is the mass density of water, taken as 1,000 g/cm^3. (See section 2.3) The volume of the soil in the pot is:

$$V = L \pi \frac{d^2}{4} \tag{4.27}$$

Therefore the volumetric moisture content is:

$$\theta = \frac{V_w}{V} \tag{4.28}$$

The tensiometer reading is given in mm head of water and is a negative value, being the suction head ϕ. Plotting the volumetric moisture content versus the suction head, the soil-moisture characteristic curve is obtained. (See figure 2.7)

The void ratio of the soil in the pot can also be calculated. The volume of solids is:

$$V_s = \frac{W_s}{\rho} \tag{4.29}$$

Where ρ is the mass density of the solids. The volume of voids in the soil is:

$$V_v = V - V_s \tag{4.30}$$

The void ratio is therefore:

$$e = \frac{V_v}{V_s} \tag{4.31}$$

4.6 Experimental apparatus.

Experimental work was carried out on the flow of water through coarse sand in an open flume. (The flow conditions were then analysed by the finite element method and the experimental and calculated results compared).

The open flume used in the laboratory was 312,4 mm (12,3 inches) wide, 450 mm (17,7 inches) deep and 2885 mm (113,6 inches) long. See figure (4.5). The sides were made of clear perspex for viewing purposes. Within the perspex of the one side wall, a set of piezometers had been constructed on a 50,8 by 101,6 mm (2 by 4 inch) grid. This allowed positive water heads to be measured. For the experiments performed, a vertical embankment was considered on the drainage end of the flume. A vertical wire screen was therefore positioned to hold the soil in this position and to prevent scouring of the material when drainage occurred out of the face. Flow through the vertical face was removed by a large diameter drainage pipe, resulting in a zero tailwater depth. (No analysis of the stability of the embankment was considered).

At the other end of the flume, two types of embankment were used. For the one, a vertical screen similar to the drainage face was used. This allowed water to flow in or out of the soil, depending on the level of the upstream water level. The second embankment used was an impermeable barrier. This allowed no flow in or out of the "upstream" face and was used to represent a line of symmetry.

Preliminary experiments showed that it was essential to use de-aired water in these seepage models. If de-aired water was not used (eg. tap water) then air bubbles came out of solution during the experiment and the coefficient of permeability to water flow changed during these model experiments. (Note that in is not essential to use de-aired water in an upwards flow permeameter if the soil is periodically brought to the quick sand boiling condition which drives off the air bubbles.)

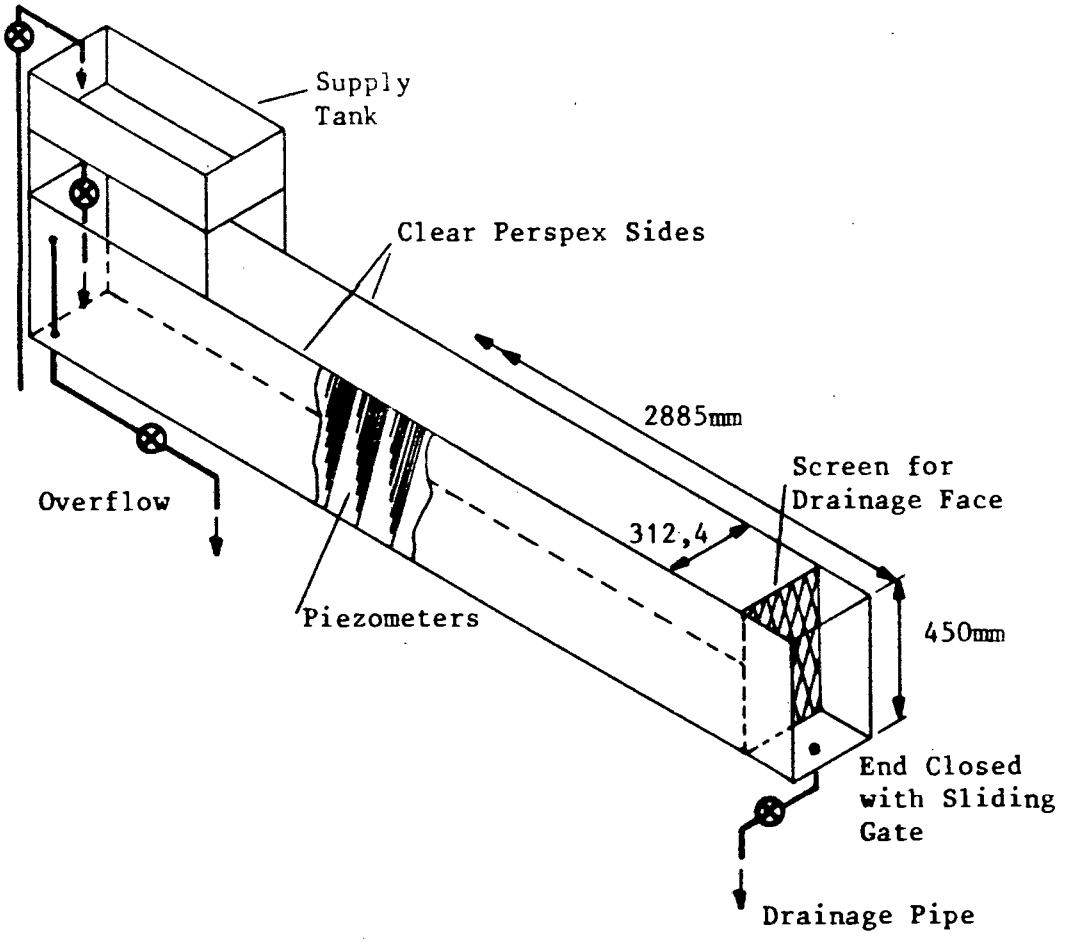

Fig 4.5: Lay-out of the Open Flume used for the drainage experiments.

4.7 Experiment number 1.

4.7.1 Definition of problem.

Figure (4.6) shows a schematic diagram of the first flow domain considered. It consists of a rectangular dam of homogenous, isotropic soil, underlain by a horizontal impermeable layer. The upstream water level is maintained constant with time. The downstream water level is the same as the upstream level for time $t<0$ (ie. a horizontal phreatic surface). At time $t = 0$ the downstream water level is lowered to the level of the impervious layer and drainage out of the embankment occurs through the vertical face. The seepage of the water within the domain was investigated.

4.7.2 Experimental simulation.

The experiment was performed in the laboratory on the rectangular dam which was 1066,8 mm (42 inches) long, 355,6 mm (14 inches) high and 312,4 mm (12,3 inches) wide. (See figure 4.6). The soil was placed as uniformly as possible in the flume between the perspex walls on the sides, and the vertical screens at the two ends. (The base of the flume is impervious). The upstream end of the flume was supplied with an overflow pipe to provide an upstream reservoir with a constant head for the upstream face of the dam. At the downstream end the stop cock of the drainage pipe was kept closed, for the time $t<0$, keeping the water level, and the same as the upstream side. At time $t = 0$ the stop cock was opened very rapidly and the water level in the downstream reservoir dropped rapidly to zero. Flow within the soil started to occur as the dam drained.

The boundary conditions applied to the dam were as follows:

a) Vertical upstream face.
   A constant head of water was kept in contact with this face and the water was allowed to flow into the soil.

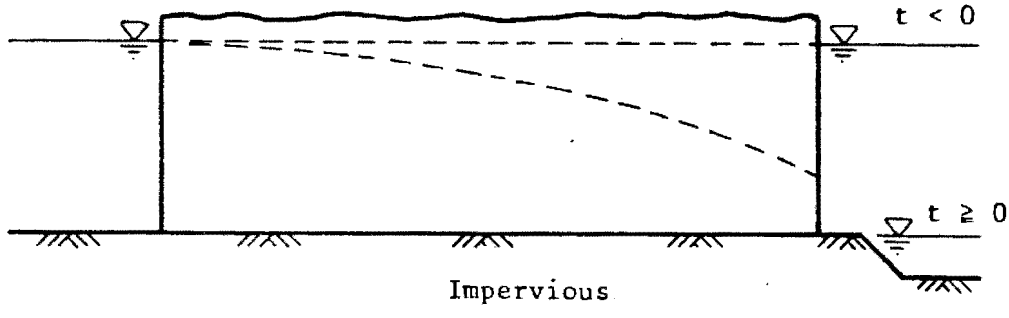

Fig 4.6: **Schematic diagram of the drainage experiment no. 1 with a declining water table due to a instantaneous drop in the down-stream water level.**

b) Vertical downstream face.
Seepage out of the face was allowed and the outflow rate was recorded.

c) Top surface.
No flow took place across this face.

d) Horizontal bottom.
This was a horizontal impervious base, allowing no flow across it.

From the time when the stop cock was opened, the following measurements were made:

a) the outflow volume with respect to the time;
b) the heights of the water levels in the side wall piezometers;
c) the pressure at pressure points (tensiometers) located at specific points within the dam.

This experiment was repeated several times. On each occasion de-aired water was initially placed in the system.

4.7.3 Measurement techniques.

The methods of making the different measurements in the experiment were as follows:

The outflow from the drainage face was collected in calibrated containers from time t = 0. Initially, with a large outflow, the containers were alternated every 5 seconds. Therefore the quantity of water seeping out of the face in a 5 second interval was recorded, as well as the cumulative outflow. As the rate of seepage decreased, the intervals over which the water was collected were lengthened.

The water levels in the side-wall piezometers were marked straight onto the perspex. Thus, as the water level dropped during an

experiment, the levels in the piezometers were marked at different time intervals. Then at a later stage, after the experiment was over, the heights at different time steps could be measured by measuring the markings on the side walls. The pencil used to make the markings on the perspex was a "DERMATOGRAPH" LIBERTY * 7600 (China-marker) which does not leave a permanent mark.

The method of measuring the pressure at specific points within the dam was done by using the transducers and data-acquisition system that had been constructed. Each tensiometer consisted of a nylon pipe going from the pressure point within the soil to a transducer interface block located on a table next to the experiment. Each nylon tube was filled with de-aired water between the experiment (pressure point) and the transducer interface block. (See figure 4.7)

At the pressure point end of the nylon tube, a tensiometer was simply made by pressing cotton wool into the end of the nylon tube to provide a form of porous tip. The pressure at the other end of the tube was therefore recorded, via the transducers, by the computer. The pressure could be either positive or negative with respect to atmospheric pressure as the tensiometers and transducers can measure both. The actual digital readings made by the computer first have to be converted via software to a pressure reading using the calibration of the transducer. (See section 3.7). To ensure that atmospheric pressure did not affect the transducer readings, a reference was used. One of the transducers measured the atmospheric pressure and any changes were added to the tensiometer readings made.

From the readings from the piezometers in the side-walls and the tensiometers at specific points within the soil, the pressure distribution within the soil could be found.

In each case corrections to the readings were necessary because of the relative height difference between the elevation of the tip of the tensiometer within the soil and the elevation of the oil-water

interface. (ie. the elevation of the transducer) This correction due to relative elevation was taken into account as follows:

Before the experiment was performed the flume was filled with de-aired water. A reading was made of the pressure acting on each transducer and recorded to zero all future readings made. These zero reference readings were adjusted so as to give the total hydraulic head above the base of the flume for each transducer. The adjustment was made by measuring the depth of the water in the flume at the time when a reference reading was made.

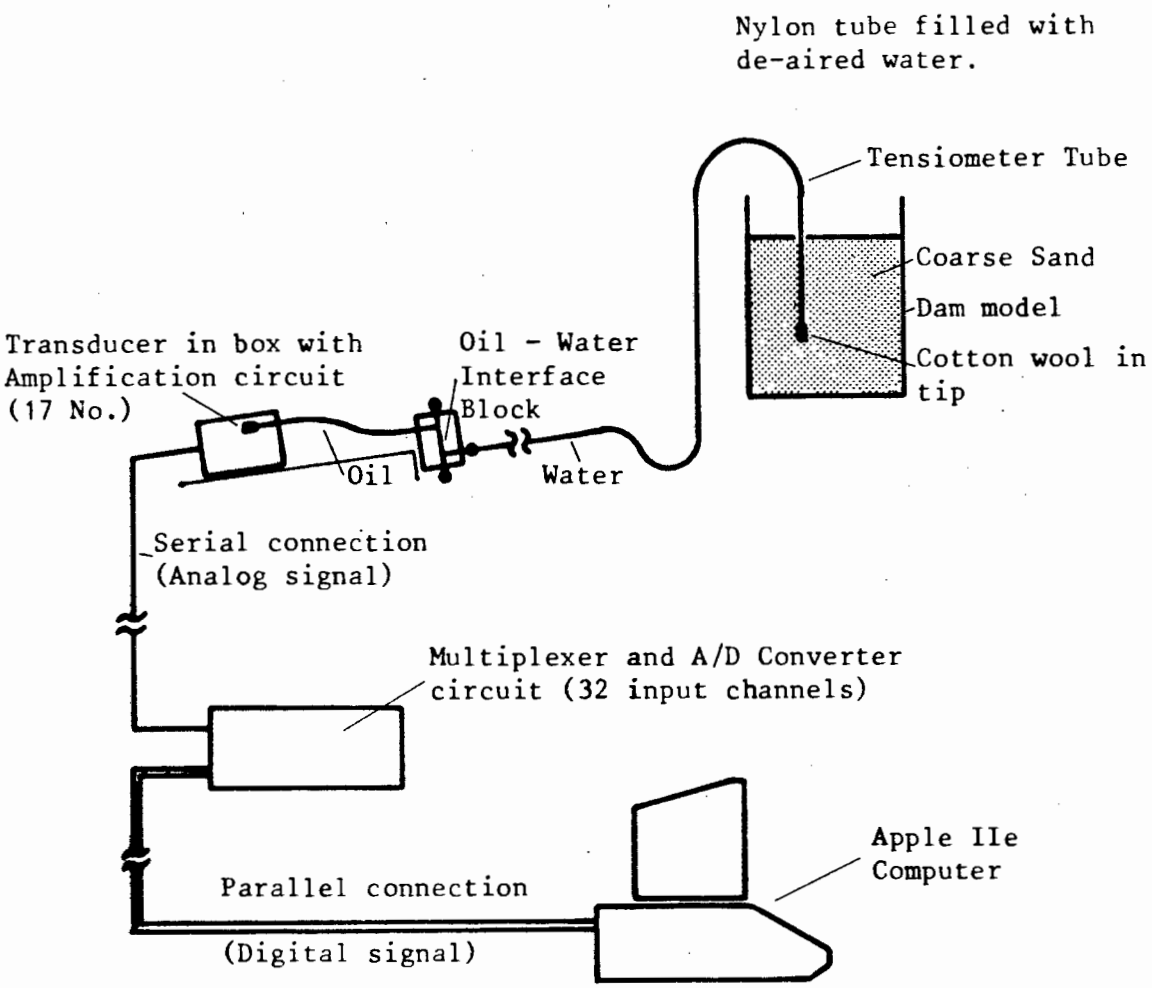

Fig 4.7: Schematic diagram of the data-acquisition lay-out in connection with an experiment in the flume

4.8 Experiment number 2.

4.8.1 Definition of problem.

Figure (4.8) shows a schematic diagram of the second flow domain considered. It consists of a slab of homogenous isotropic soil underlain by a horizontal impermeable layer and divided by equaly spaced trenches. At time $t<0$, the waterlevel in the trenches is at a initial height above the impervious layer. At time $t = 0$ the water level in the trenches is dropped to the height of the slab base. The water level within the slab therefore drops as drainage takes place. Because of symmetry, only the cross-hatched section in figure (4.8) need be considered.

4.8.2 Experimental simulation.

An experiment was performed in the laboratory on a slab of soil, 2717,8 mm (107 inches) long, 401,3 mm (15,8 inches) high and 312,4 mm (12,3 inches) wide, which corresponds to the cross-hatched domain in figure (4.8). The soil was placed as uniformly as possible in the flume, between the perspex walls on the sides, the vertical screen at the drainage end and an impermeable barrier at the other end of the flume. (The base of the flume is impervious).

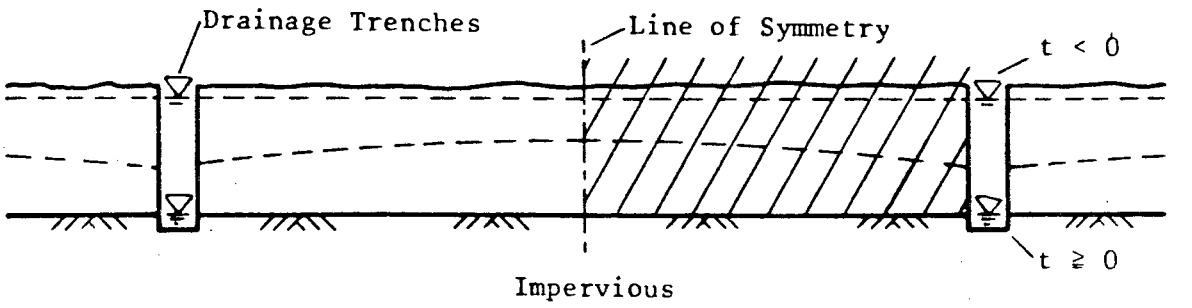

Fig 4.8: **Schematic diagram of the drainage experiment no. 2 with a declining water table due to the instantaneous drop of the water level in the drainage trenches.**

At the drainage end the stop cock was initially kept closed and the flume was filled with de-aired water to a height of 381 mm (15 inches) above the base.

At time t = 0 the stop cock was opened very rapidly and the water level in the reservoir dropped rapidly to zero. Drainage of the soil started as the water was allowed to seep out of the vertical embankment.

The boundary conditions applied to the dam were as follows:

a) Vertical "upstream" face.
   No flow took place across this boundary as an impervious boundary was used. (line of symmetry.)

b) Vertical drainage end.
   Seepage was allowed out of this face and the outflow rate was recorded.

c) Top surface.
   No flow took place across this face.

d) Horizontal bottom.
   This was a horizontal impervious base, allowing no flow across it.

From the time when the stop cock was opened, the following measurements were made:

a) the outflow volume with respect to the time;
b) the heights of the water levels, in the side-wall piezometers;
c) the pressure at pressure points (tensiometers) located at specific points within the dam.

The experiment was repeated several times. Each time de-aired water was placed initially within the soil.

4.8.3 Measurement techniques.

The method of making the different measurements in the experiment are the same as for experiment number 1. The outflow was measured by using calibrated containers and noting the quantity collected for each time interval.

The water levels in the side-wall piezometer were marked onto the perspex at different time intervals.

The pressure at specific points within the soil were measured using the transducers and data-acquisition system.

From the results of the piezometers in the side-wall and the tensiometers at specific points within the soil, the pressure distribution within the soil could be found.

Later analysis of the results showed that the response time of the sidewall piezometers was not fast enough to accurately portray the dynamic transient pressure distributions in the soil whereas the tensiometers attached to the transducers were most satisfactory.

CHAPTER 5

ANALYSIS OF EXPERIMENTAL AND TEST RESULTS.

5.1 Introduction.

In this chapter the results obtained from the preliminary tests and subsequent experiments are analysed. The results from the tests are analysed first. This is to obtain the soil-moisture parameters that are used in the theoretical analysis of the experiments. The tests (see Chapter 4) were as follows:

a) Saturated hydraulic conductivity
   Nine - Constant head tests with varying void ratio.
b) Unsaturated hydraulic conductivity
   Two - Direct experimental tests with differing void ratio.
c) Soil-moisture characteristic curve
   Three - Direct experimental tests.

The two subsequent experiments were to study the flow of water in a draining soil. The first experiment was on a rectangular dam with an instantaneous dropping tail-water level. The second experiment was on a rectangular slab of soil with drainage from one face being considered. The monotonic lowering of the phreatic surface (water table) was investigated in both cases.

5.2 Saturated hydraulic conductivity.

Nine tests were performed to determine the relationship of the saturated hydraulic conductivity of the soil, versus the void ratio. (See appendix E-1). The lowest void ratio tested was 0,452 and the highest was 0,663.

A constant head test was used and the procedure is given in section (4.3). Figure (4.2) shows a schematic diagram of the constant head permeability test set-up. If we consider test number "CHPA01" given in

appendix (E-1), the following is an example of the typical calculations involved in determining the saturated hydraulic conductivity and the corresponding void ratio:

Data from experimental set-up (See figure 4.2)

Inside diameter of permeameter tube	d	=	7,366	cm
Path length between piezometer tips	z_1	=	12,75	cm
	z_2	=	12,70	cm
Mass density (See section 4.2)	ρ	=	2,64	g/cm^3
Mass of dry soil	W_s	=	2 658,2	g
Soil sample length	L	=	34,3	cm

Data for run no. 1

Temperature	T	=	15,5	^0C
Quantity of water collected from outlet	Q_t	=	880	cm^3
Time in which water was collected	t	=	270	sec
Piezometer readings	h_1	=	46,6	cm
	h_2	=	42,5	cm
	h_3	=	38,3	cm

Calculations

Cross-sectional area of permeameter tube $A = \pi.d^2/4$

$= \pi \cdot 7,366^2/4 = 42,61 \ cm^2$

Bulk volume of soil sample $V = L.A$

$= 34,3 \cdot 42,61 = 1\,461,7 \ cm^3$

Volume of solid soil particles $V_s = W_s/\rho$

$= 2\,658,2/2,64 = 1\,006,9 \ cm^3$

Volume of voids $V_v = V - V_s$

$= 1\,461,7 - 1\,006,9 = 454,8 \ cm^3$

Therefore void ratio $e = V_v/V_s$

= 454,8/1 006,9 = 0,452

Flow rate $Q = Q_t/t$

= 880/270 = 3,26 cm^3/s

Darcian velocity at 15,5 ^0C $v_T = Q/A$

= 3,26/42,61 = 0,076 cm^3/s

Darcian velocity at 20 ^0C $v_{20} = v_T \cdot \eta_T/\eta_{20}$

(See Table B-2)

= 0,076 . 1,1 202 = 0,086 cm^3/sec

Hydraulic gradient between piezometers 1 & 2

$i_1 = (h_1 - h_2)/z_1$

= (46,6 - 42,5)/12,75 = 0,322

Similarly i_2 and $i_3 = (h_1 - h_2)/(z_1 + z_2)$

= (46,6 - 38,3)/(12,75 + 12,70) = 0,326

Therefore the average hydraulic gradient

$i_{average} = (i_1 + i_2 + i_3)/3$

= (0,322 + 0,331 + 0,326)/3 = 0,326

The above calculations were repeated for each data run made. Figure (5.1) shows a graph of the hydraulic gradient ($i_{average}$) versus the Darcian velocity (v_{20^oC}) for test no. CHPA01. A straight line has been fitted to the data, (v versus i) using the method of "least squares approximation". The slope of the line, shown in figure (5.1), is 0,269. As k = v/i, the hydraulic conductivity is represented by the slope of the line. Therefore k_{20} = 0,269 cm/sec when this void ratio is 0,452.

The data and the results for all nine tests performed, are given in appendix (E-1). Also shown with the data for each test, is a plot of the results. The results from the plots are summarised in Table (5.1),

giving the void ratio of the soil and the corresponding hydraulic conductivity determined from the tests.

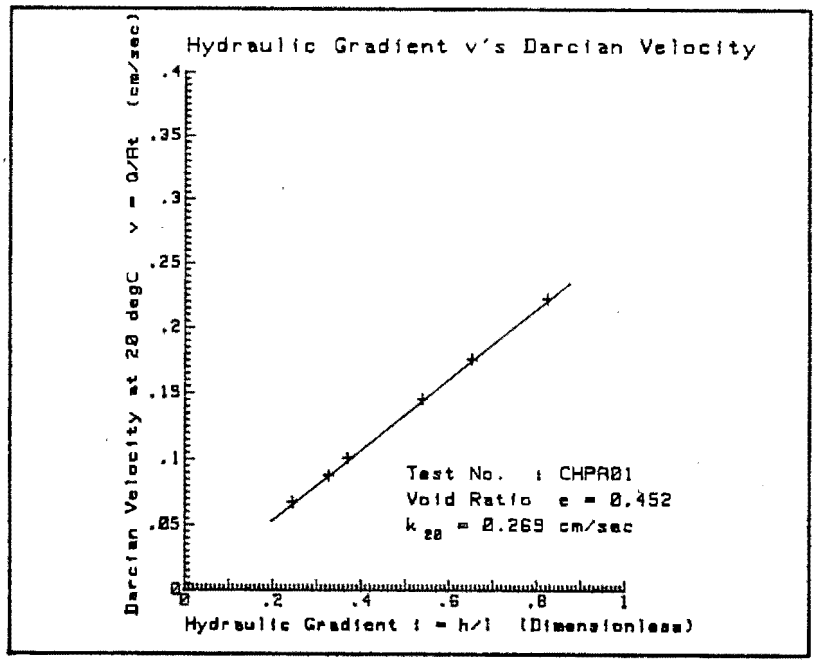

Fig 5.1: The hydraulic gradient versus the Darcian velocity (at 20 °C) for the constant-head test no. "CHPA01".

Table. 5.1: Listing of the saturated hydraulic conductivity (at 20 °C) versus the void ratio of the soil, obtained from the constant-head tests.

Test no.	e	k_{sat} (cm/sec)
CHPA01	0,452	0,269
CHPA02	0,604	0,562
CHPA03	0,549	0,433
CHPA04	0,493	0,286
CHPA05	0,583	0,506
CHPA06	0,663	0,740
CHPA07	0,516	0,358
CHPA08	0,595	0,563
CHPA09	0,570	0,515

To find a relationship between the void ratio and the hydraulic conductivity, the results presented in Table (5.1) are plotted in the form of some function of the void ratio e, against some function of the hydraulic conductivity. Two plots drawn (See figures 5.2 and 5.3) show the relationship of k versus $e^3/(1 + e)$, $e^2/(1 + e)$, e^2 and e on one plot and e versus log (k) on the other. By a visual observation of figures (5.0) and (5.3), the plot of the hydraulic conductivity k versus $e^3(1 + e)$, gives the best relationship. This is observed by looking at the straight line fitted to the relationships plotted, using the method of "least squares approximation". The relation used for the straight line is y = m x + c, where y is the vertical axis, x the horizontal, m is the slope of the line and c the y intercept of figures (5.2) and (5.3). Except for the two tests "CHPA01" and "CHPA04" with the lowest void ratios (0,452 and 0,493 respectively), the results from the tests match the straight line relation of k versus $e^3/(1 + e)$ very well.

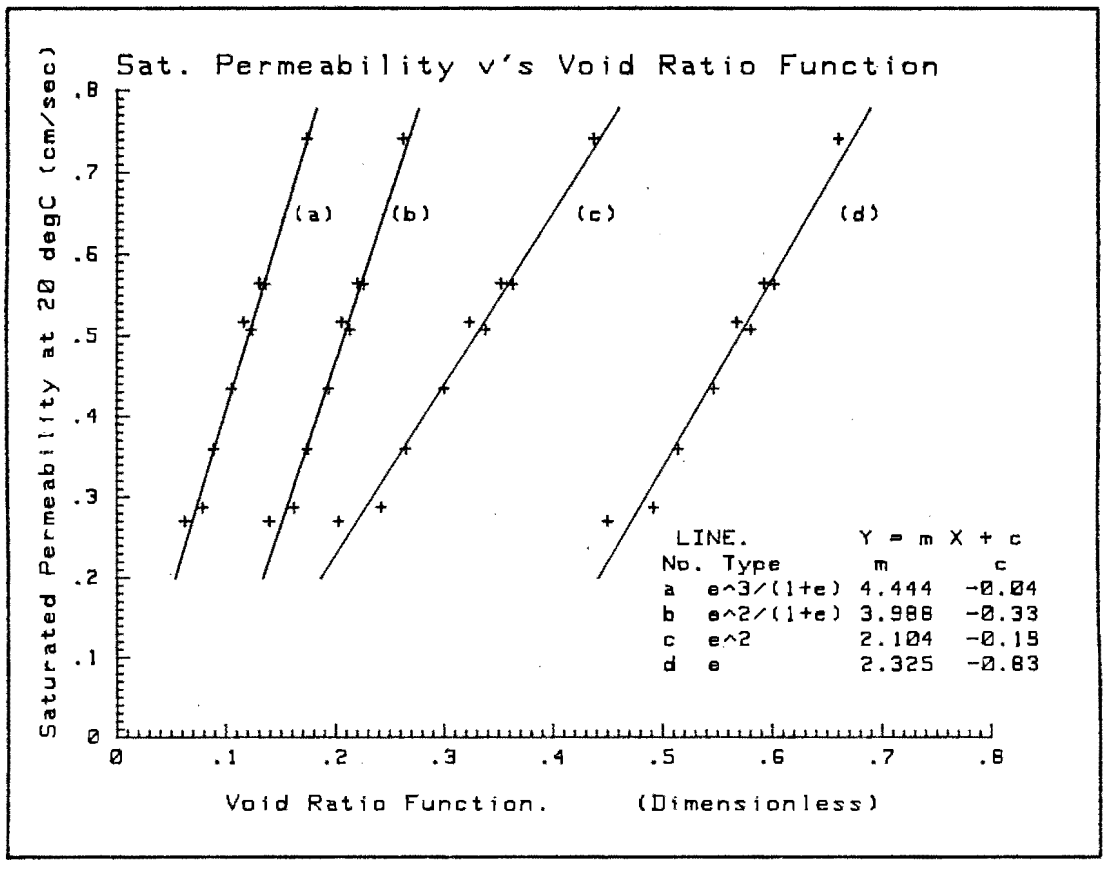

Fig 5.2: **Saturated permeability (at 20°C) versus trial functions of the void ratio for the results from the constant-head tests.**

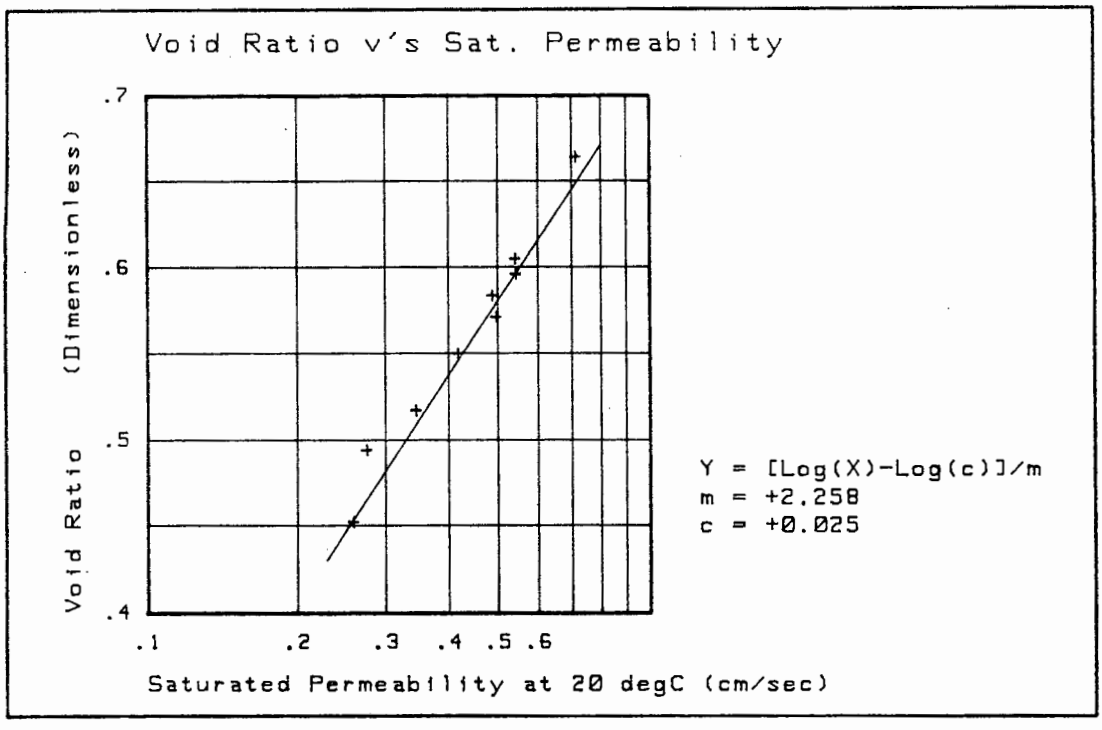

Fig 5.3: The void ratio versus the log of the saturated permeability for the results from the constant head tests.

Also the y intercept is very close to zero, which it should be, if the water is an ideal Newtonian fluid.

For the experiments performed, the relationship of the saturated hydraulic conductivity versus the void ratio is taken as (See figure 5.2):

$$k_{sat} = 4{,}444 \left(\frac{e^3}{1+e}\right) - 0{,}04 \quad \text{cm/sec} \qquad (5.1)$$

In section (2.10.1) Hazen's formula was introduced. Namely:

$$k = c\, D_{10}^2 \quad \text{cm/sec} \qquad (5.2)$$

where D_{10} is the 10 % finer from the grain-size distribution curve, given in centimetres and c a constant between 45 for clayey sands and

140 for pure sands. A value of c = 100 is often used as an average even for clean sands. For the soil used in this thesis the D_{10} = 0,072 cm (See section 4.2). Therefore if c = 100 is used:

$$k = 100\ D_{10}^{2}$$
$$= 100 \cdot (0,072)^{2}$$
$$= 0,518 \quad cm/sec$$

If we consider figure (5.2) and k = 0,518 cm/sec, we see that this corresponds to a void ratio of about e = 0,580, which is mid-range of the void ratio's tested. This indirectly confirms that the results obtained are correct in terms of order of magnitude.

5.3 Unsaturated hydraulic conductivity.

To determine the relationship of the unsaturated hydraulic conductivity, versus the volumetric moisture content of the sand, two tests were performed. (See appendix E-2).

A direct method of testing was used which consisted of a vertical column of sand. The vertical unsaturated flow rate in the sand was then measured to determine the unsaturated hydraulic conductivity. The procedure of the test is given in section (4.4). Figure (4.3) gives a schematic diagram of the test equipment set-up.

The tensiometers used in the vertical column were connected to transducers via a nylon pipe filled with de-aired water. One extra transducer, connected to an open reservoir of water, was used as a reference to measure any change in atmospheric pressure. Section (3.6) gives the operation of the transducers and data-acquisition system. To reference all transducers to zero, a reading was taken with the tensiometers located at their correct heights, but with the open sensing end, open to atmospheric pressure. Saturated cotten wool existed in each open end of these nylon tubes. This was known as the "zero" reference reading. All subsequent readings were scaled to this reading so that the print-out from the computer gave the local pressure change

from "zero", at the tensiometer point.

If we consider test no. "USPA01", given in appendix (E-2), the following is an example of the typical calculations involved in determining the unsaturated hydraulic conductivity and the corresponding degree of saturation:

Data from experimental set-up (See figure 4.3)

Inside diameter of permeameter tube	d	=	4,40	cm
Path length between tensiometer tips	z_1	=	15,00	cm
	z_2	=	15,05	cm
	z_3	=	15,00	cm
	z_4	=	15,00	cm
Mass density (See section 4.2)	ρ	=	2,64	g/cm^3
Mass of empty apparatus	W_a	=	631,1	g
Mass of dry soil	W_s	=	2 102,8	g
Soil sample length	L	=	83,7	cm
Tensiometers readings of reference run.	T_1	=	h_{1r}	
("zero" readings, run no. "r"	T_2	=	h_{2r}	
made before the first run	T_3	=	h_{3r}	
of the test.)	T_4	=	h_{4r}	
	T_5	=	h_{5r}	
	T_{ref}	=	h_{rr}	

Data for run no. 1

Temperature	T	=	15,5	^0C
Quantity of water collected from outlet	Q_t	=	318	cm^3
Time in which water was collected	t	=	957	sec
Mass of wet soil and apparatus	W_t	=	2 982,9	g
Tensiometer readings of run no. "1"	T_1	=	h_{11}	
	T_2	=	h_{21}	
	T_3	=	h_{31}	
	T_4	=	h_{41}	
	T_5	=	h_{51}	

$T_{ref} = h_{r1}$

Calculations

Cross-sectional area of permeameter tube $A = \pi.d^2/4$

$= \pi \cdot (4,4)^2/4 = 15,21 \ cm^2$

Bulk volume of soil sample $V = L.A$

$= 83,7 \cdot 15,21 = 1\,272,7 \ cm^3$

Volume of solid soil particles $V_s = W_s/\rho$

$= 2\,102,8/2,64 = 796,5 \ cm^3$

Volume of voids $V_v = V - V_s$

$= 1\,272,7 - 796,5 = 476,2 \ cm^3$

Therefore void ratio $e = V_v/V_s$

$= 476,2/796,5 = 0,598$

Tensiometer reading $h_1 = (h_{11} - h_{1r}) - (h_{r1} - h_{rr})$

(ie. local heads; suction negative) $= -9,6$ cm

Similarly $h_2 = -9,0$ cm

$h_3 = -9,7$ cm

$h_4 = -9,6$ cm

$h_5 = -10,9$ cm

Flow rate $Q = Q_t/t$

$= 318/957 = 0,332 \ cm^3/s$

Darcian velocity at 15,5 ^{0}C $v_T = Q/A$

$= 0,332/15,21 = 0,022 \ cm^3/s$

Darcian velocity at 20 ^{0}C $v_{20} = v_T \cdot \eta_T/\eta_{20}$

(See Table B-2)

$= 0,022 \cdot 1,1\,202 = 0,024 \ cm^3/sec$

Hydraulic gradient between tensiometer 1 & 2

$i_1 = (h_1 - h_2)/z_1$

$= (- 9,6 + 15,00 + 9,0)/15,00 = 0,96$

Similarly

$i_2 = 1,05$

$i_3 = 0,99$

$i_4 = 1,09$

Average hydraulic gradient $i_{average} = (i_1 + i_2 + i_3 + i_4)/4$

$= (0,96 + 1,05 + 0,99 + 1,02)/4 = 1,02$

Mass of water in the whole soil sample $W_w = W_T - (W_a + W_s)$

$= 2\ 982,9 - (631,1 + 2\ 102,8) = 249,0$ g

Volume of water in the soil sample $V_w = W_w/\rho$

(ρ the mass density of water is taken as 1,000 g/cm^3)

$= 249,0/1 = 249,0$ cm^3

Therefore the volumetric moisture content $\theta = V_w/V$

$= 249,0/1\ 272,7 = 0,196$

and the degree of saturation $S_r = V_w/V_v$

$= 249,0/476,2 = 0,523$

The unsaturated hydraulic conductivity $k(\theta) = v_{20}/i_{average}$

(at 20 ^{0}C)

$= 0,024/1,02 = 0,024$ cm/sec

The saturated hydraulic conductivity $k_{sat} = 4,444 \frac{e^3}{(1+e)} - 0,04$

(at 20 ^{0}C) (See section 5.2)

$= 4,444 \cdot 0,598^3/(1 + 0,598) - 0,04 = 0,556$ cm/sec

Therefore the relative permeability $k_{rw} = k(\theta)/k_{sat}$

at volumetric moisture content θ

$= 0,024/0,556 = 0,043$

The above calculations are repeated for each data run made. A plot is made of the results to show the relationship between the unsaturated hydraulic conductivity and the volumetric moisture content. The plot could either show the unsaturated hydraulic conductivity versus the volumetric moisture content or the relative permeability (k_{rw} = unsaturated hydraulic conductivity/saturated hydraulic conductivity) versus the degree of saturation S_r. A plot in figure (5.4) shows the relationship of the relative permeability versus the degree of saturation, from the results for test no. "USPA01".

A scatter of the results is observed. This can be attributed to two main reasons. The first is the effect of hysteresis in soil suction pressures between the drying and the wetting soil. This can be seen in figure (5.4) by the relative positions of the drying and the wetting

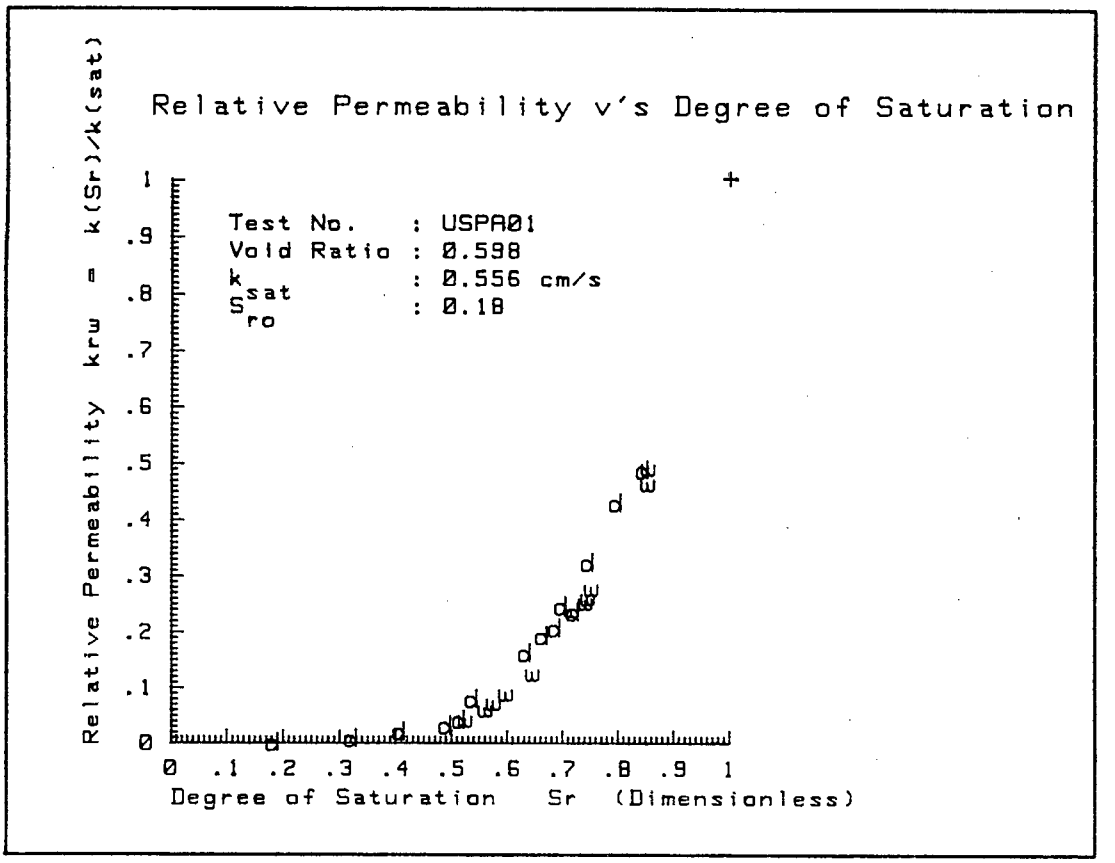

Fig 5.4: The relative permeability versus the degree of saturation for test no. "USPA01". (key: w = wetting, d = drying)

Table. 5.2: Residual saturation, recorded in the tests for determining the unsaturated hydraulic conductivity, versus the void ratio of the soil.

Test no.	e	S_{ro}
USPA01	0,598	0,18
USPA02	0,527	0,22

points. The second is the long time that is needed for equilibrium conditions to be reached. Readings may have been made before equilibrium had been reached, as a slight scatter of the tensiometer readings is noticed for some of the data runs (See appendix E-2).

In section (2.11.1) a power function of the effective saturation was introduced. Namely:

$$k_{rw} = (S_e)^{\alpha} \tag{5.3}$$

where S_e is the effective saturation defined in equation (2.57), rewritten as:

$$S_e = \frac{(S_r - S_{ro})}{(1 - S_{ro})} \tag{5.4}$$

where S_r and S_{ro} are the actual and residual saturation respectively. Equation (5.3) is used to try to find a relationship between the relative permeability and the degree of saturation (or effective saturation).

Table (5.2) gives the residual saturation recorded for the two unsaturated hydraulic conductivity tests performed. Using the values in Table (5.2) and the results from tests "USPA01" and "USPA02", a graph is plotted of the relative permeability versus the effective saturation, as shown in figure (5.5). Also shown in figure (5.5) are the curves for

equation (5.3) where α = 3; 3,5; and 4. By a visual observation, the curve for α = 3, fits the test data best. If there were more results a numerical approximation method could have been used to find the best fitting curve. A value for the residual saturation S_{ro} needs to be selected before equation (5.3) can be used. This is done in a subsequent section. (See section 5.5). It is also assumed that the water phase is non-continuous at the degree of saturation S_{ro}, hence k_{rw} is zero at this saturation value.

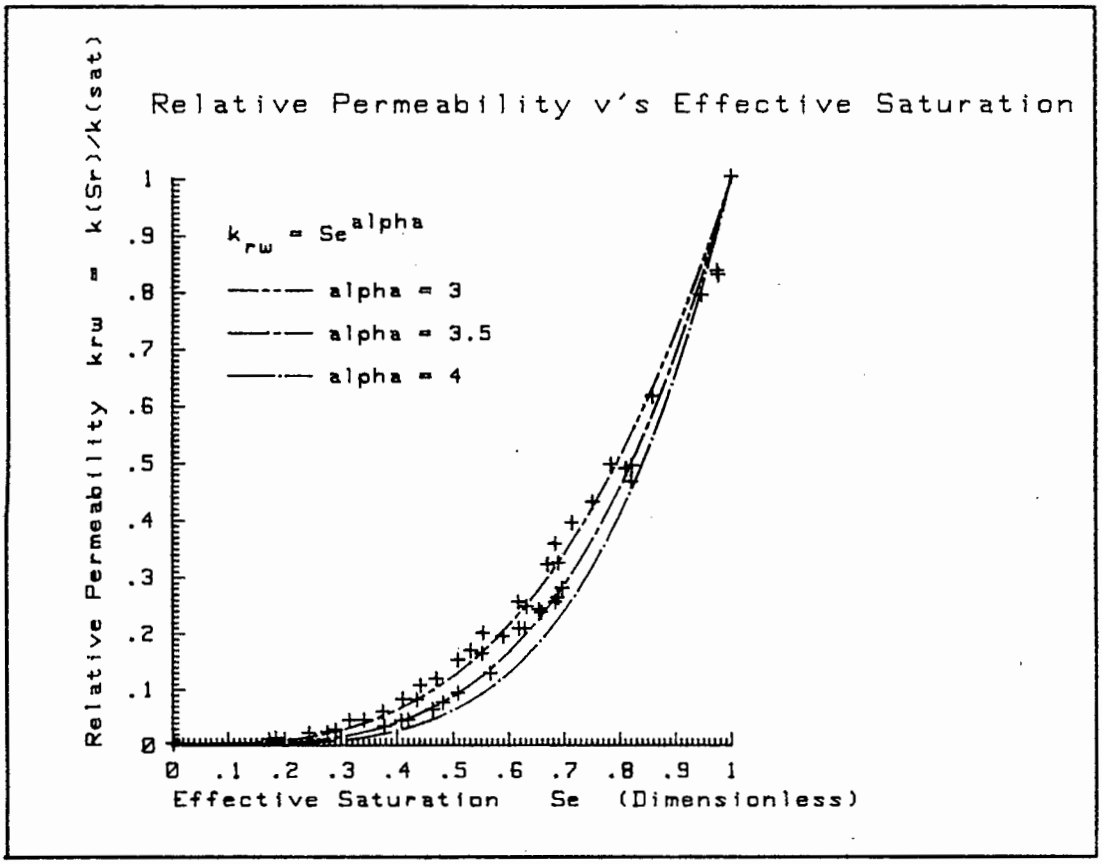

Fig 5.5: **The relative permeability versus the effective saturation for the unsaturated hydraulic conductivity tests. (Effective saturation S_e is defined in equation 5.4).**

5.4 Soil-moisture characteristic curve.

To determine the relationship of the soil-moisture suction head versus the volumetric moisture content of the soil, three tests were performed. (See appendix E-3).

A direct method of testing was used for measuring the suction head in a sample of unsaturated soil. Figure (4.4) gives a schematic diagram of the test equipment set-up. The equipment consists of a pot with a tensiometer into which the soil sample to be tested is placed. The tensiometer in the pot was connected to a transducer via a nylon pipe, filled with de-aired water. A second transducer, connected to an open reservoir of water, was used as a reference to measure any change in atmospheric pressure. The procedure that was used in the test is given in section (4.5).

To reference the tensiometer to zero head, a reading was taken of the "zero" pressure, when the soil in the pot was saturated and the water table was at the surface of the soil. This reading was known as the reference reading. All the other readings were scaled to this reading, so that the print-out from the computer gives the local pressure changes from "zero" at the tensiometer point.

If we consider test number "SMHA01" from appendix (E-3), the following is an example of the typical calculations involved in determining the relationship of the suction head versus the volumetric moisture content or degree of saturation:

Data from experimental set-up

Inside diameter of pot	d	=	8,35	cm
Mass density (See section 4.2)	ρ	=	2,64	g/cm^3
Mass of empty apparatus	W_a	=	239,3	g
Mass of dry soil	W_s	=	329,4	g
Soil sample height	L	=	3,63	cm

Tensiometer readings of reference run. ("zero" readings, run no. "1" made for the first run of the test.)	T_1	=	h_{11}
	T_{ref}	=	h_{r1}

Data for run no. 2

Temperature	T	=	20,0	^oC
Mass of wet soil and apparatus	W_t	=	642,5	g
Tensiometer readings of run no. "2"	T_1	=	h_{12}	
	T_{ref}	=	h_{r2}	

Calculations

Cross-sectional area of pot	A	=	$\pi.d^2/4$	
= π . $8,35^2/4$		=	54,76	cm^2
Bulk volume of soil sample in pot	V	=	L.A	
= 3,63 . 54,76		=	198,8	cm^3
Volume of solid soil particles	V_s	=	W_s/ρ	
= 329,4/2,64		=	124,8	cm^3
Volume of voids	V_v	=	$V - V_s$	
= 198,8 - 124,8		=	74,0	cm^3
Therefore void ratio	e	=	V_v/V_s	
= 74,0/124,8		=	0,593	
Tensiometer reading	h_1	=	$(h_{12} - h_{11}) - (h_{r2} - h_{r1})$	
(ie. local head; suction negative)		=	- 7	mm
Mass of water in the soil sample	W_w	=	$W_T - (W_a + W_s)$	
= 642,5 - (239,3 + 329,4)		=	73,8	g

Volume of water in the soil sample $V_w = W_w/\rho$

(ρ the mass density of water is taken as 1,000 g/cm^3)

= 73,8/1 = 73,8 cm^3

Therefore the volumetric moisture content $\theta = V_w/V$

= 73,8/198,8 = 0,371

and the degree of saturation $S_r = V_w/V_v$

= 73,8/74,0 = 0,997

The above calculations were repeated for each data run of readings made. A plot was made of the results to show the relationship between the soil suction head and the volumetric moisture content. The plot could either show the suction head versus the volumetric moisture content or the degree of saturation. The relationship obtained for the suction head versus the degree of saturation from the results of test no. "SMHA01", is shown in figure (5.6).

A scatter of the results is observed. This can be attributed to the long time that is needed for equilibrium conditions to be reached. Readings may have been made before equilibrium had been reached.

To be able to fit a curve to the results from the tests (See appendix E-3), a plot is made of the suction head versus the effective saturation. (See figure 5.7). The effective saturation S_e defined in equation (5.4). Table (5.3) gives the residual saturation recorded for

Table. 5.3: Residual saturation, recorded in the tests for determining the soil-moisture characteristic curve, versus the void ratio of the soil.

Test no.	e	S_{ro}
SMHA01	0,593	0,11
SMHA02	0,557	0,10
SMHA03	0,569	0,11

the tests. A curve (Dotted line in figure 5.7) is fitted to the drying curve of the plotted results. Table (5.4) gives the co-ordinates for the average curve fitted to the results. The drying curve is selected because the chosen experiments in this thesis deal with a draining soil

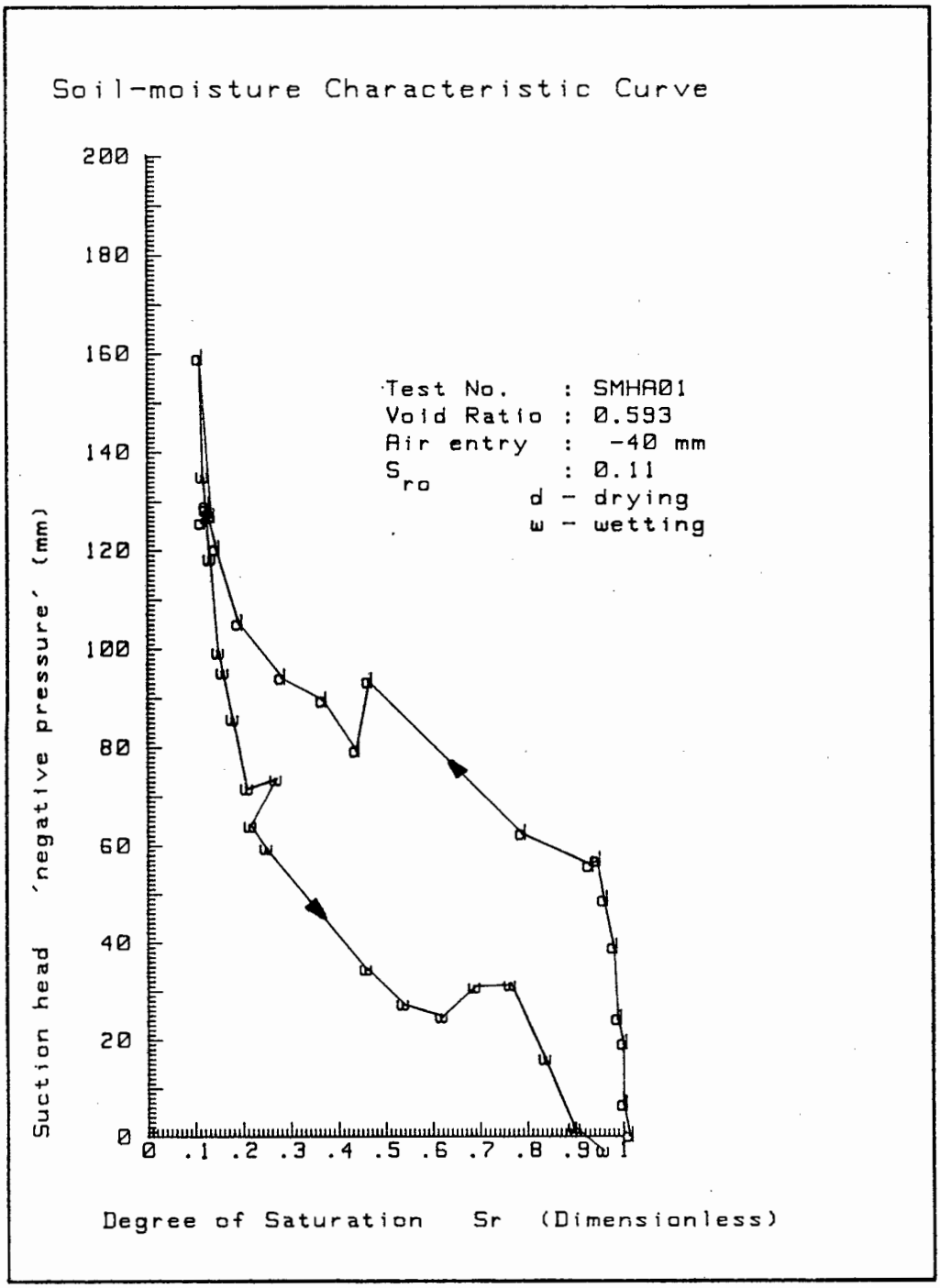

Fig 5.6: **The soil-moisture charcteristic curve for test no. "SMHA01". The suction head versus the degree of saturation.**

(drying soil). The curve is fitted to the two tests that show matching results. The first test "SMHA01" gives the impression that the results obtain from it are not correct (See figure 5.6). Air could have entered

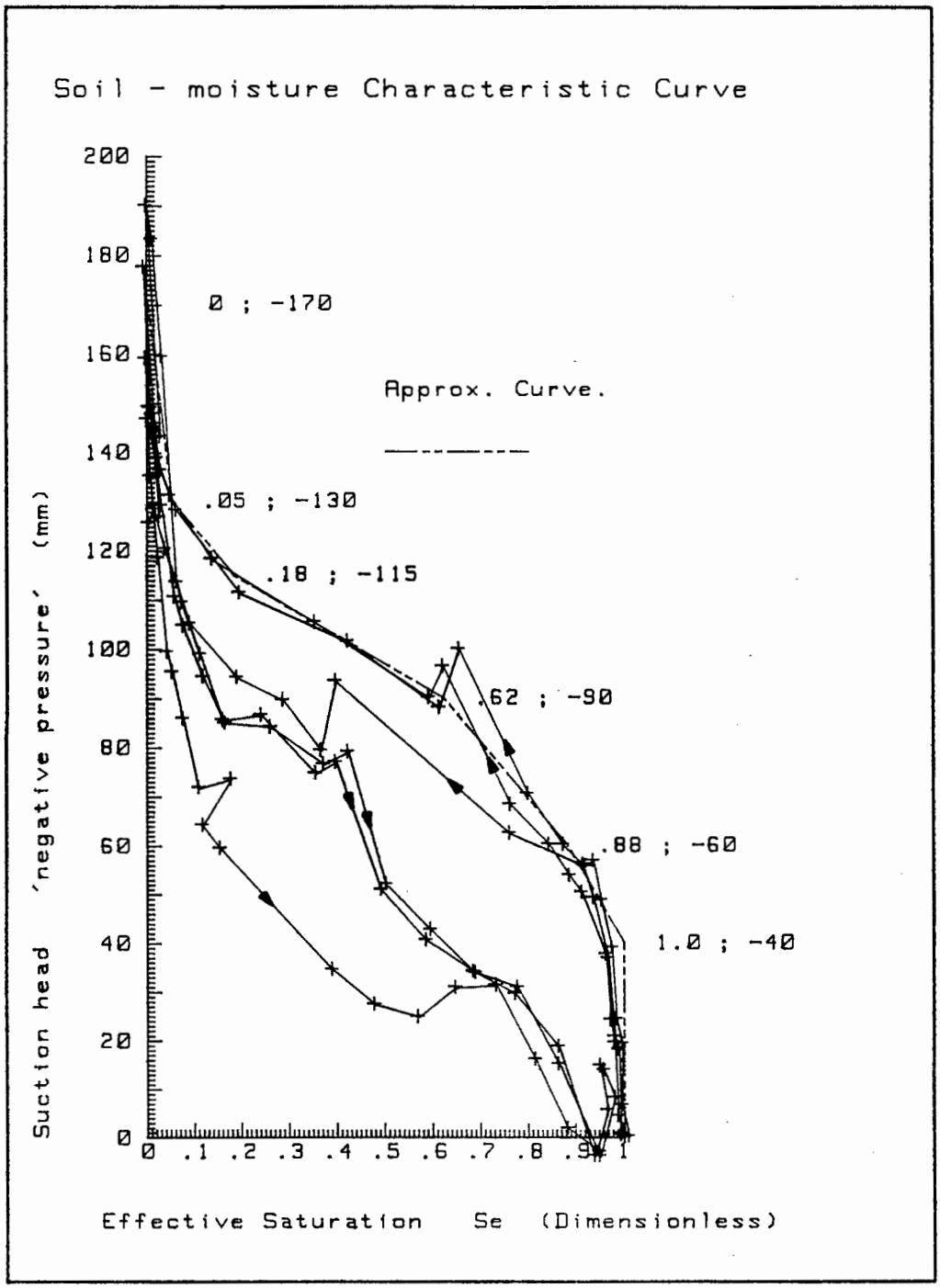

Fig 5.7: **The soil-moisture characteristic curve, of the suction head versus the effective saturation for the tests done. (Effective saturation is defined in equation 5.4)**

Table. 5.4: Tabulated soil-moisture characteristic curve. Suction head ϕ versus the effective saturation S_e (Equation 5.4) of the soil.

ϕ (mm)	S_e
- 170	0
- 130	0,05
- 115	0,18
- 90	0,62
- 60	0,88
- 40	1,00
0	1,00

the tensiometer and caused the recorded suction not to be as great as it should have been. The results for the first test are therefore neglected.

The average curve of the results (Tabulated in Table 5.4) is given with respect to the effective saturation. Therefore to use Table (5.4) in the analysis of experiments (See later), a residual saturation is selected, based on the void ratio of the experiment. Table (5.4) is then rewritten as a function of the degree of saturation.

For the average curve, proposed in Table (5.4), the air-entry value is taken as 40 mm of water head. If we consider Table (5.5) from Harr [16], we see that the air-entry value of the soil used, is of the

Table. 5.5: Typical values of height of capillary rise. Harr. [16]

Soil type.	Height of capillary rise (mm)
Coarse sand	20 - 50
Sand	120 - 350
Fine sand	350 - 700
Silt	700 - 1500
Clay	2000 - 4000 & greater.

same order as the capillary heights of a coarse sand. The sand used for the test was a coarse sand (See section 4.2) and therefore the result show an agreement in order of magnitude.

5.5 Experiment No. 1 Analysis.

5.5.1 Introduction.

The set up and procedure for the experiment has been given in section (4.7). The basic problem is to observe the drainage flow through a rectangular dam, as shown in figure (4.6), with a constant upstream water level and a tail water level that has dropped to zero elevation at time t = 0.

No attempt has been made to model an actual large scale drainage problem (ie. a large dam scaled down in the laboratory) as the purpose of this investigation was to monitor an actual laboratory drainage problem and to try and verify the observation with a numerical analysis. To make any analysis, the soil-moisture parameters of the soil used in the experiment are needed. For the soil used these have been obtained in sections (4.2), (5.2), (5.3) and (5.4).The shape of the dam is rectangular with length 1 066,8 mm (42 inches), height 355,6 mm (14 inches) and a width of 312,4 mm (12,3 inches). The dry mass of sand used to construct the dam was 202,2 kg. The lay-out of the experiment is shown in figure (5.8). The void ratio of the dam is calculated as follows:

Bulk volume of soil V = Length x height x width
= 1 066,8 mm x 355,6 mm x 312,4 mm = $118,5 \cdot 10^3$ cm^3

Mass of sand used W_s = $202,2 \cdot 10^3$ g

Volume of solid particles V_s = W_s/ρ
(Mass density ρ = 2,64 g/cm^3, see section 4.2)
= $202,2 \cdot 10^3/2,64$ = $76,6 \cdot 10^3$ cm^3

Volume of voids within the soil $V_v = V - V_s$

$= 118,5 \cdot 10^6 - 76,6 \cdot 10^6 = 41,9 \cdot 10^3 \text{ cm}^3$

Therefore the void ratio $e = V_v/V_s$

$= 41,9/76,6 = 0,547$

Using equation (5.1) from section (5.2), the saturated hydraulic conductivity at 20 ^{o}C is obtained. The saturated hydraulic conductivity k_{sat} at 20 ^{0}C is therefore:

$$k_{sat} = 4,444 \left(\frac{e^3}{1 + e}\right) - 0,04$$

$$= 4,444 \left(\frac{0,547^3}{1 + 0,547}\right) - 0,04$$

$$= 0,430 \text{ cm / sec}$$

The temperature of the experiment differed from that of 20 ^{0}C and was measured at 16,6 ^{0}C. The saturated hydraulic conductivity is therefore adjusted for this difference, by considering the ratio of viscosity of the water at 16,6 ^{0}C and 20 ^{0}C. The saturated hydraulic conductivity k_s at 16,6 ^{0}C is therefore:

$$k_s = k_{sat} \frac{\eta_{20}}{\eta_T}$$

$$= 0,430 \frac{1}{1,0887}$$

$$= 0,395 \text{ cm / sec}$$

where k_s is the hydraulic conductivity at 16,6 ^{0}C and the ratio of the viscosities is given in Table (B-2).

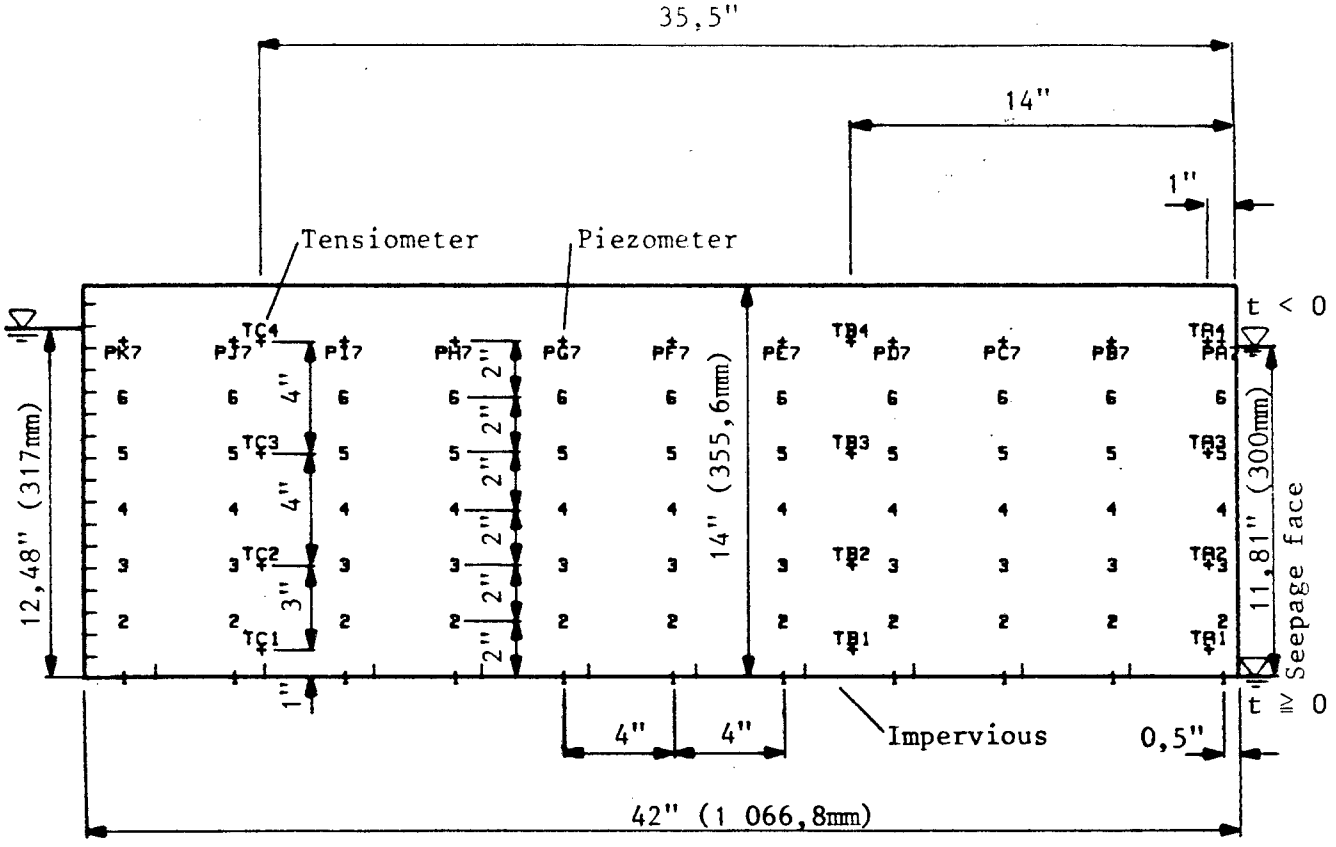

Fig 5.8: Lay-out of experiment no. 1, giving the dimensions and showing the locations of the piezometers and tensiometers.

In this thesis the factors affecting the residual saturation S_{ro} have not been studied. Therefore there is no relationship presented relating it to the void ratio or particle size distribution (eg. as the hydraulic conductivity is related to the void ratio). For the tests done in sections (5.3) and (5.4), (See Tables 5.2 and 5.3), the residual saturation varies between 0,1 and 0,22. A value for the residual saturation is therefore assumed to be 0,15. This value is used in the analysis of the experiment.

From section (5.3), the relationship for the hydraulic conductivity

versus the effective saturation is given as a power function. Namely:

$$k_{rw} = (S_e)^{\alpha}$$

$$= \left(\frac{S_r - S_{ro}}{1 - S_{ro}}\right)^{\alpha}$$

Based on the results of tests "USPA01" and "USPA02" shown in figure (5.5), the value of $\alpha = 3$ is selected for equation (5.3) to be used in the analysis of the experiments performed. S_{ro} the residual saturation is taken as 0,15 (see above) and S_r is the degree of saturation of the soil. Therefore

$$k_{rw} = \left(\frac{S_r - 0,15}{0,85}\right)^{\alpha} \qquad (5.5)$$

is used for the relationship of the relative hydraulic conductivity versus the degree of saturation.

The soil-moisture characteristic curve for the relationship of the suction head versus the effective saturation of the soil is given by Table (5.4) in section (5.4). As the residual saturation of the soil used in the experiment is taken as 0,15, Table (5.4) can be rewritten as the relationship of the suction head versus the degree of saturation of the soil. Table (5.6) therefore shows the relationship used in the analysis of this experiment with $S_{ro} = 0,15$.

Table. 5.6: Tabulated soil-moisture characteristic curve. Suction head ϕ versus the degree of saturation S_r of the soil. Residual saturation $S_{ro} \simeq 0,15$

ϕ (mm)	S_r
- 170	0,15
- 130	0,19
- 115	0,30
- 90	0,68
- 60	0,90
- 40	1,00
0	1,00

The experiment was performed 5 times. Each time the experiment was started from the same initial position. The initial position was taken at complete saturation with the water table in the upstream reservoir at 317 mm and due to a leak, the downstream reservoir at 300 mm. To reach this position the dam was first completely flooded for a day or two and then the water level was lowered to 317 mm and 300 mm for the upstream and downstream reservoirs respectively. Each time the experiment was performed various measurements were recorded. The average of the readings made was then used in the analysis of the experiment. The actual readings recorded while the experiment was underway were that of the outflow of the water, at the drainage face; and the change in pressure at various pressure points. The recordings made are listed in appendix (E-4), (E-5), (E-6) and (E-7).

The experiment was run until the outflow drainage rate stopped changing by an appreciable amount. This was after about 150 sec from time t = 0. Steady state flow conditions were soon achieved.

5.5.2 Drainage outflow.

The drainage outflow is the water that left the dam via the vertical drainage face of the dam. This water seeping out of the drainage face was measured to find its flow rate. The technique of collecting the water with respect to time is given in section (4.7.3). If a quantity of water ΔQ_t was collected in a time interval of Δt, then the flow rate at the center of the time interval is taken as approximately equal to:

$$Q = \frac{\Delta Q_t}{\Delta t} \qquad (5.6)$$

In appendix (E-4) the quantities of water collected for the different time intervals are listed. Also listed is the average flow rate for the intervals, calculated by using equation (5.6) and the mid-interval times.

From the results a plot is made of the outflow seepage rate, as shown in figure (5.9). The results for more than one run of the experiment have been plotted on the graph. By averaging the results, an approximate

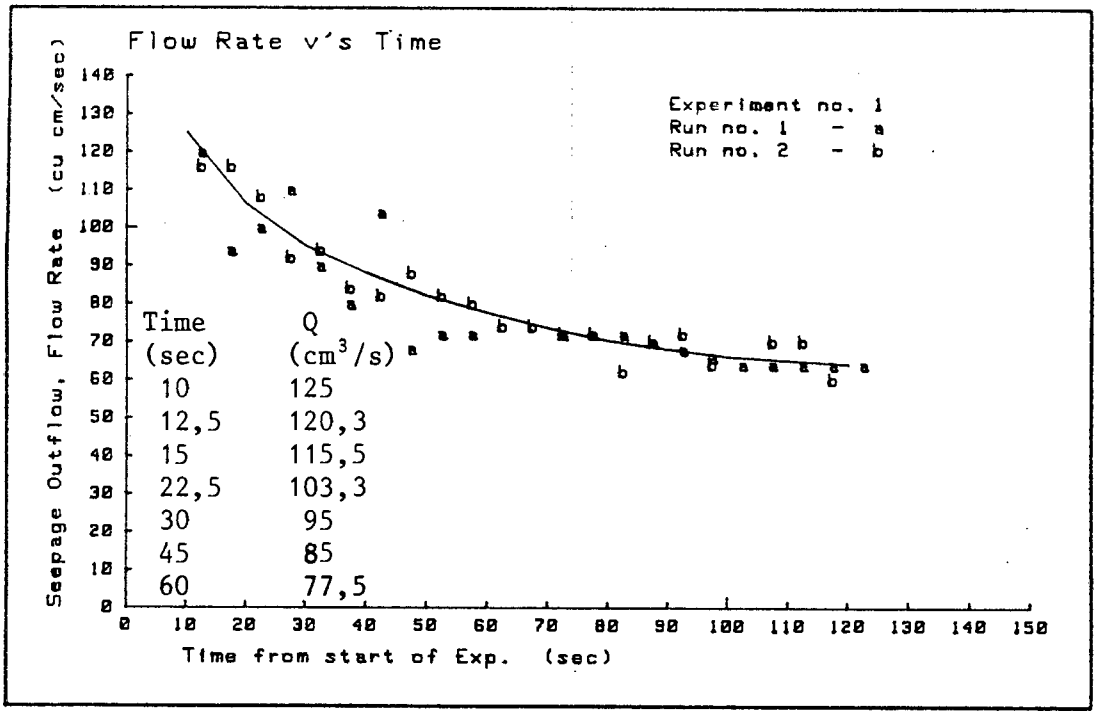

Fig 5.9: Seepage outflow, flow rate versus time measured at the drainage face for experiment no. 1.

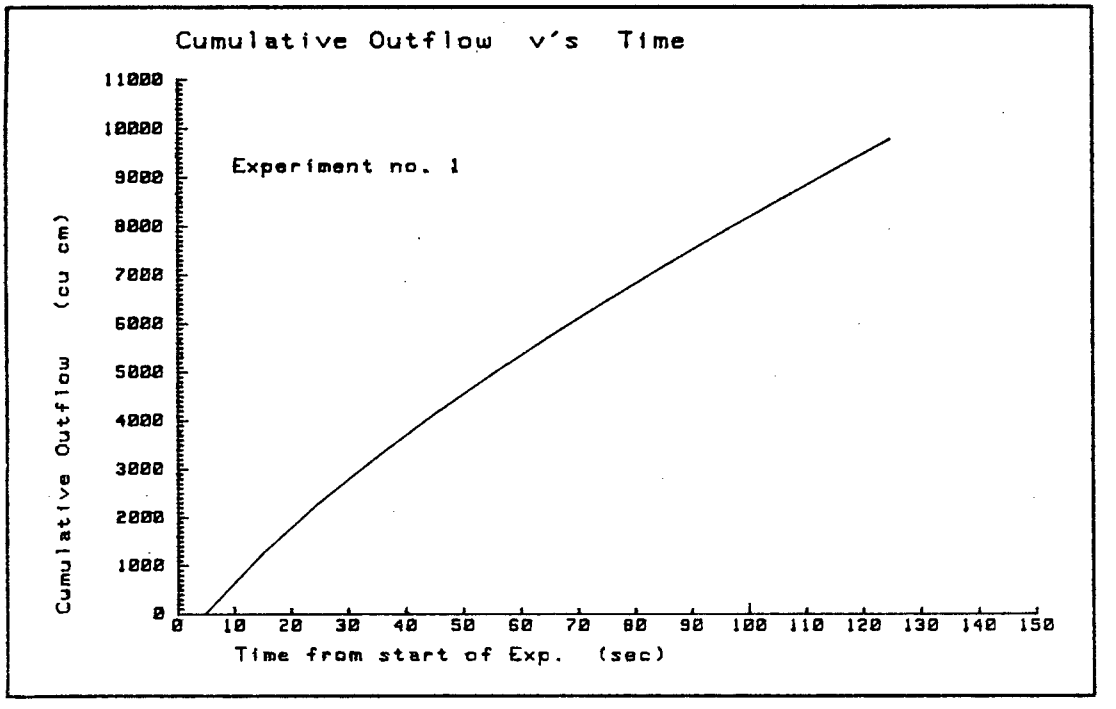

Fig 5.10: Cumulative seepage outflow, at the drainage face versus time for experiment no. 1.

outflow curve is also shown. By integrating under the curve with respect to time, the curve for the cumulative outflow can be plotted, as shown in figure (5.10). With time the outflow rate decreases and tends to a value which represents the flow rate for steady state flow through the dam. Therefore the flow rates above this value are all due to the water draining out of the soil above the steady state phreatic surface.

5.5.3 Sidewall piezometers.

While the experiment was in progress, the water levels in the piezometer tubes were recorded. Figure (5.8) gives the locations of the piezometers in the experimental lay-out. The technique of making the recordings is given in section (4.7.3). The results for the experiment are listed in appendix (E-5). Some of the piezometers are shown as faulty in the listing of the results. These were piezometers which were blocked and whose water levels did not drop, and so no recording could be made. As the water table in the soil dropped with time, some of the piezometers ended up above the water table and drained empty. These piezometers are shown as above the water table (AWT), from the time the water level dropped below the piezometer point. (ie. Their water levels coincided with the levels of the connecting holes to the soil.)

The results from the sidewall piezometers are used later for the plotting of contours of the total pressure heads in the experiment. The results are used more as a guide for transient heads, because the results recorded were erratic. The reason for this could be due to the fact that the piezometers are not null-flow devices, and they are unable to quickly match the dynamic changes occurring within the soil.

5.5.4 Transducer monitored tensiometers.

At specific points within the soil mass of the dam a set of tensiometers were located. The set-up and technique of recording the pressure is given in section (4.7.3). The results of the pressures recorded with respect to the time for the 5 independent runs are listed in appendix (E-6). The positions at which the tensiometers were located is shown in figure (5.8). Each transducer is referenced according to its

position (eg. TA1 for column A of A, B and C and 1 for the lower row of 4 tensiometer rows).

Figure (5.11) shows the results for transducer "TB4", of the total pressure head versus time elapsed from time t = 0. The elapsed time was measured from the instant when the drainage outlet of the downstream reservoir was opened. The results for all 5 runs have been plotted on the single graph. The results plotted for the rest of the transducers are given in appendix (E-6).

The results obtained from the tensiometers were relatively consistent and accurate for the repeated runs, but problems were encountered. In some tensiometers, not all the air was removed when primed with de-aired water and so the result is correct until the entrapped air came out of solution. This affects the result in that the pressure being transferred to the transducer from the tensiometer was not the same as that being experienced at the tensiometer point. A second problem encountered was that at a certain suction, air could enter the tensiometer through the cotton wool and have the same effect as described above. This could have been overcome by using a finer porous

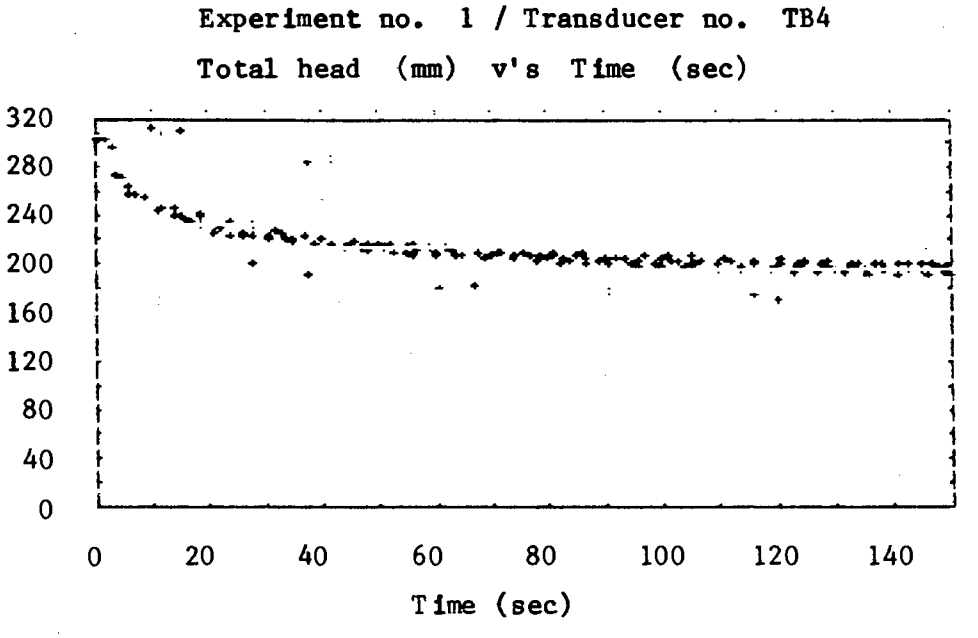

Fig 5.11: **Total head above the base of the flume versus time, measured by transducer "TB4", for experiment no. 1.**

medium than cotton wool. A third problem was encountered only when all the transducers were connected up to the A/D converter via the multiplexer switch. The problem was that, for certain readings made, the result recorded would randomly be a value of about 80 to 100 mm below that which it should have been. This last error was caused by some sort of electrical noise in the data acquisition system, and was only observed by the author in the later stages of experimental analysis. Some of the errors discussed above can be observed in figure (5.11) and also in the plots given in appendix (E-6).

5.5.5 Analysis of results.

To analyse and get some sort of confirmation of the experimental results, the mass transfer of the water within the dam is studied. The dam is considered as a rectangular brick volume with 6 sides. 4 of the sides do not need to be considered, because no flow takes place across them (ie. the sides and the bottom of the flume are impermeable and no external water flows out or into the top surface. Neglecting evaporation). The transfer of moisture is therefore considered by looking at the transfer of water flowing in and out of the upstream and downstream faces respectively and the change of the phreatic surface and the total volume of water within the dam with respect to time.

To be able to do this study of the mass transfer of water, the analysis is made on the following line:

> A contour plot of the total heads within the dam at a specific time after t = 0, is made. This is done by using the results from the piezometers and tensiometers. Then, by using the soil-moisture characteristic curve, a contour plot is made of the degree of saturation of the soil. The movement of the water is then considered in 3 specific areas. That is, the volume of water flowing in and out of the soil and change of water volume within the soil.

The method of doing this can be shown more clearly if we consider a specific time after the start of the experiment and show the full

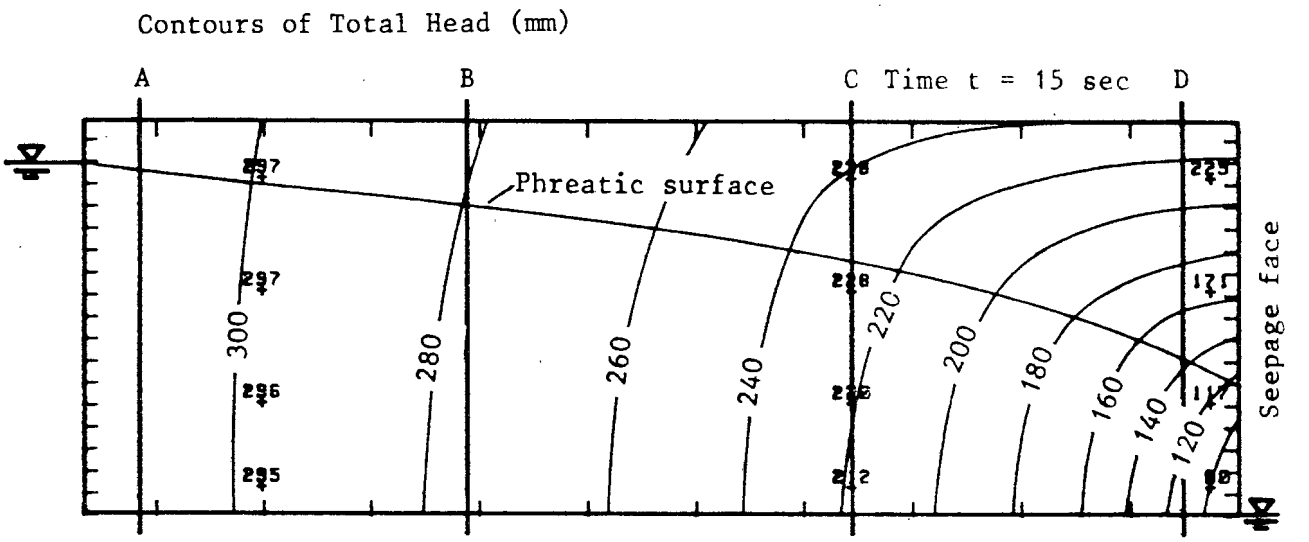

Fig 5.12: **Contour plot of the total head for experiment no. 1 at 15 seconds after the start of the experiment. Contour plot based on the results of the pressure recorded at specific points.**

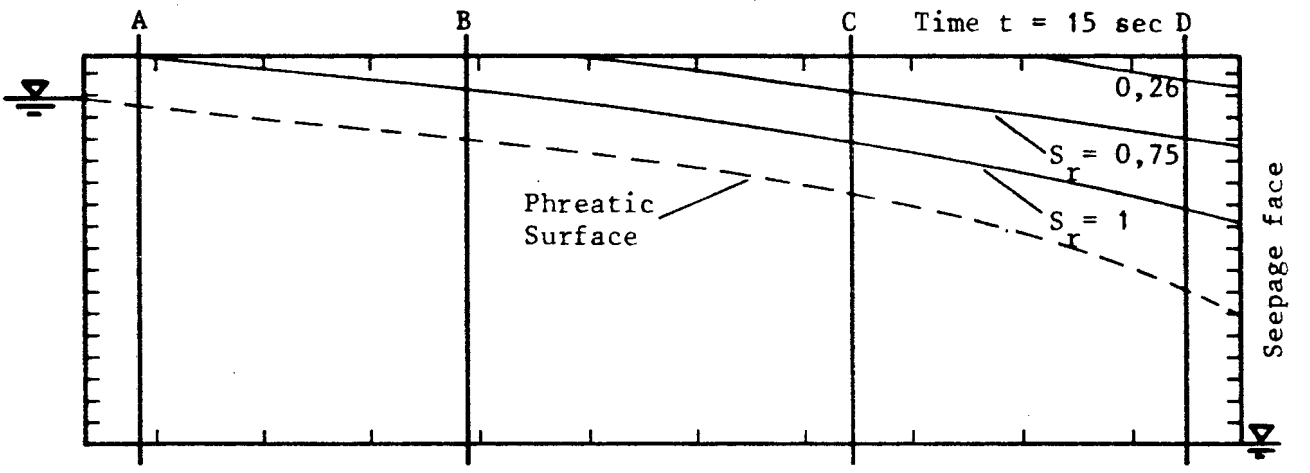

Fig 5.13: **Contour plot of the degree of saturation for experiment no. 1 at 15 seconds after the start of the experiment. Plot made from the pressure head distribution via the soil-moisture characteristic curve.**

procedure. If we consider the time 15 sec after the start of the experiment, then the following is an example of the analyses done. (or for other time steps.)

Figure (5.12) shows a contour plot of the total heads recorded within the dam. Also shown is the phreatic surface and the results from the tensiometers. The contour map is plotted by using the results of the tensiometer readings and the sidewall piezometer readings (Not shown). The final result shown was obtained by a trial and error process, similar to that used for plotting a flow net for a steady state flow problem. The actual readings recorded were used as the bases for the contour plot.

It can be seen in figure (5.12), that the total head contours are all sloping towards the drainage face. The value of the contours decrease from the upstream face which is at 317 mm to the drainage face. The instantaneous seepage flow within the dam, which is perpendicular to the contour lines of the total pressure heads, varies in direction from horizontal along the base of the dam to nearly vertical within the unsaturated zone near the drainage face. By converting the total heads to local pressure heads and using the soil-moisture characteristic curve a contour plot of the degree of saturation is made, as shown in figure (5.13). The local pressure head is obtained by subtracting the value of the elevation head from the total head (eg. $\phi = \phi - z$). The soil-moisture drainage characteristic curve is used in that a given suction head corresponds to a degree of saturation. See Table (5.6). Below the phreatic surface the local pressure is positive and therefore the soil is taken as saturated. As the air entry value of the soil used is greater than zero, ($\simeq$ 40 mm) full saturation extends above the phreatic surface. This can be seen in figure (5.13), as the phreatic surface is shown, by a dotted line, below the start of the unsaturated zone.

To study the flow of water into and out of the dam, an approximate method is used. The method is shown by considering the upstream face as an example. The flow across a section A-A shown in figures (5.12) and (5.13) is considered. A profile of the local pressure head along A-A with respect to the elevation is made from figure (5.12).

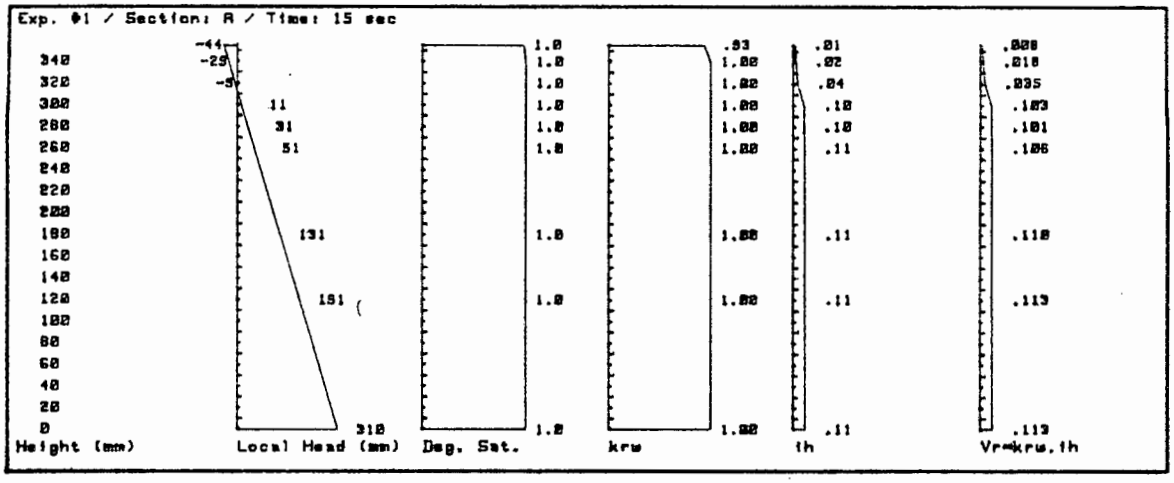

Fig 5.14: **Profile plots made for section A-A (Fig 5.12) in experiment no. 1 at 15 seconds after the start. All with respect to elevation: (a) Local head; (b) Degree of saturation; (c) Relative hydraulic conductivity; (d) Horizontal hydraulic gradient; (e) Relative horizontal Darcian velocity.**

Table. 5.7: Results listed of the values for the profile plots, with respect to elevation, made in figure (5.14), at section A-A in experiment no. 1, 15 seconds after the start.

Height (mm)	Local Head (mm)	Deg. Sat.	Rel. Perm.	Hydraulic Grad.	k_{rw} x i_h
356	-44	0,98	0,926	0,01	0,008
340	-29	1,00	1,000	0,02	0,018
320	-9	1,00	1,000	0,04	0,035
300	11	1,00	1,000	0,10	0,103
280	31	1,00	1,000	0,10	0,101
260	51	1,00	1,000	0,11	0,106
180	131	1,00	1,000	0,11	0,110
120	191	1,00	1,000	0,11	0,113
0	310	1,00	1,000	0,11	0,113

Width	: 312,4	mm	Temp T	: 16,6	°C
Void Ratio e	: 0,547		Sat. Perm. k_s	: 0,395	cm/sec
Eff. Sat. Area	: 125,7	mm	Rel. Flow Rate	: 35,2	mm
			Flow Rate	: 43,4	cm^3/sec

Figure (5.14a) shows a plot of the profile of the local pressure heads. Next a profile of the degree of saturation along A-A with respect to the elevation is made. This can be made either from the local pressure head profile, using the soil-moisture characteristic curve Table (5.6) or from figure (5.13). From the profile of the degree of saturation with respect to elevation, a profile of the relative hydraulic conductivity can be made. This is done by using equation (5.5) which relates the relative hydraulic conductivity to the degree of saturation. Namely:

$$k_{rw} = \left(\frac{S_r - 0,15}{0,85}\right)^3 \qquad (5.7)$$

As the soil was placed very carefully with a uniform density, it is assumed to be homogenous and isotropic with respect to the hydraulic conductivity.

The hydraulic gradient in the horizontal direction is determined next. This is done by calculating the head loss and scaling its corresponding horizontal path length across section A-A in figure (5.12). Figure (5.15) shows graphically how this is done. By doing this at different elevations a profile plot is made of the horizontal hydraulic gradient acting across A-A with respect to the elevation, as shown in figure (5.14d).

From the two profiles of the relative hydraulic conductivity and the horizontal hydraulic gradient, a profile of the relative horizontal Darcian velocity can be determined.

This is done by taking the multiple of the relative hydraulic conductivity and the horizontal hydraulic gradient at each elevation, (eg. $v_r = k_{rw} \times i_h$). Figure (5.14e) shows a plot of this profile with respect to elevation. To obtain the horizontal Darcian velocity at any elevation, the relative hydraulic Darcian velocity is multiplied by the saturated hydraulic conductivity of the soil, determined from the void ratio. (See section 5.5.1).

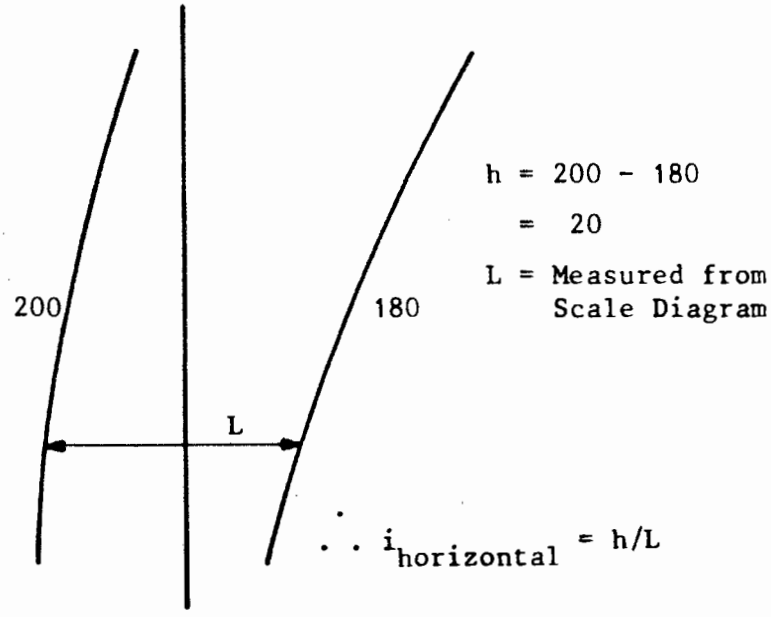

Fig 5.15: Horizontal hydraulic gradient determined graphically across a section by scaling off the pathlength from the contour plot of the total pressure head.

Having determined the relative horizontal Darcian velocity across section A-A with respect to elevation, the quantity of water flowing across a unit width of the section is calculated. This is done by multiplying the horizontal Darcian velocity at each elevation by the width (in this case Unit 1) and then integrating over the full elevation of the section. Therefore the flow rate of water across section A-A is given as:

$$Q = \int_0^{355,6} k_{rw} \cdot i_h \, dz \cdot k_s \cdot (\text{Width}) \qquad (5.8)$$

The integral ($\int k_{rw} \cdot i_h \, dz$) is determined by the area of the profile plot shown in figure (5.14e). This area is determined by summing the area of the profile plot in the form of trapeziums for each slope of the curve. In the experiment the width of the flume is 312,4 mm and

Table (5.7) gives the value of the integral as 35,2 mm. (Relative flow rate). Therefore using k_s = 0,395 cm/s in equation (5.8):

$$Q = \int_0^{355,6} k_{rw} \cdot i_h \, dh \cdot k_s \quad \text{(Width)}$$

$$= \frac{35,2}{10} \cdot \frac{312,4}{10} \cdot 0,395 \quad \text{cm}^3 / \text{sec}$$

$$= 43,4 \quad \text{cm}^3 / \text{sec}$$

(Across the whole width and height of section A-A)

The above calculations are repeated for section D-D in figure (5.12), located at the drainage face. The respective profiles determined with respect to elevation are shown in figure (5.16) and the values in Table (5.8).

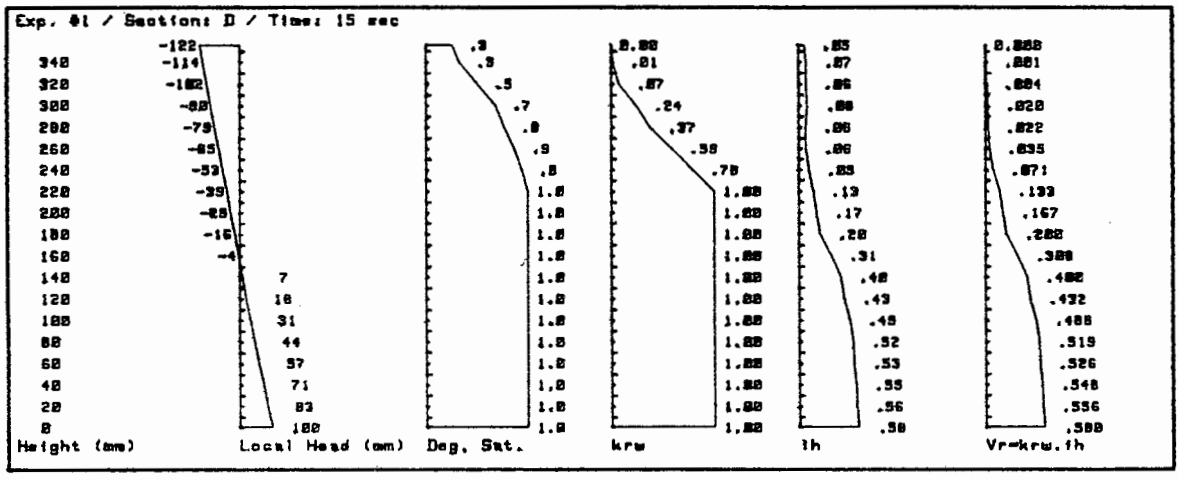

Fig 5.16: **Profile plots made for section D-D (Fig 5.12) in experiment no. 1 at 15 seconds after the start. All with respect to elevation: (a) Local head; (b) Degree of saturation; (c) Relative hydraulic conductivity; (d) Horizontal hydraulic gradient; (e) Relative horizontal Darcian velocity.**

Table. 5.8: Results listed of the values for the profile plots, with respect to elevation, made in figure (5.16), at section D-D in experiment no. 1, 15 seconds after the start.

Height (mm)	Local Head (mm)	Deg. Sat.	Rel. Perm.	Hydraulic Grad.	$k_{rw} \times i_h$
356	-122	0,25	0,002	0,05	0,000
340	-114	0,32	0,008	0,07	0,001
320	-102	0,50	0,069	0,06	0,004
300	-90	0,68	0,238	0,08	0,020
280	-79	0,76	0,373	0,06	0,022
260	-65	0,86	0,586	0,06	0,035
240	-53	0,93	0,784	0,09	0,071
220	-39	1,00	1,000	0,13	0,133
200	-29	1,00	1,000	0,17	0,167
180	-16	1,00	1,000	0,20	0,200
160	-4	1,00	1,000	0,31	0,308
140	7	1,00	1,000	0,40	0,400
120	18	1,00	1,000	0,43	0,432
100	31	1,00	1,000	0,49	0,488
80	44	1,00	1,000	0,52	0,519
60	57	1,00	1,000	0,53	0,526
40	71	1,00	1,000	0,55	0,548
20	83	1,00	1,000	0,56	0,556
0	100	1,00	1,000	0,58	0,580

Width	: 312,4	mm	Temp T	: 16,6	°C
Void Ratio e	: 0,547		Sat. Perm. k_s	: 0,395	cm/sec
Eff. Sat. Area	: 110,4	mm	Rel. Flow Rate	: 94,4	mm
			Flow Rate	: 116,5	cm^3/sec

Also in Table (5.8) is the value for the integral (Relative flow rate.) given as 94,4 mm. Therefore using k_s = 0,395 cm/s in equation (5.8):

$$Q = \int_0^{355,6} k_{rw} \cdot i_h \, dh \cdot k_s \cdot (\text{Width})$$

$$= \frac{94,4}{10} \cdot \frac{312,4}{10} \cdot 0,395 \quad cm^3 / sec$$

$$= 116,5 \quad cm^3 / sec$$

(Across the whole width and height of section D-D)

This computed result (116,5 cm^3/sec) compares very well with the outflow rate determined previously ($Q \approx 115\ cm^3/sec$), as shown in figure (5.9).

The next problem is to determine the quantity of water within the soil (between sections A and D), at the time of 15 sec after the start. This is done by an approximate method of considering the effective volumetric moisture content at 4 sections indicated in figure (5.12) and taking an average value of this between the sections. The volumetric moisture content at a specific elevation is obtained from the degree of saturation profile. The volumetric moisture content is obtained by multiplying the degree of saturation by the porosity of the soil. The effective volumetric moisture for a unit width of soil at a section is obtained by summing vertically the volumetric moisture content over the full elevation. (Effective Saturated Area.) This is the same as integrating the area under the degree of saturation profile with respect to elevation and multiplying by the constant porosity n. Written as:

$$\text{Eff. Sat. Area} = \int_0^{355,6} S_r \, dz \cdot n \qquad (5.9)$$

where the porosity is determined from the void ratio of the soil. If we consider section B-B in figure (5.13), the profile of the degree of saturation is given in figure (5.17b) and the values in Table (5.9). The method of integrating the area under the curve is the same as that used to determine the area under the relative horizontal Darcian velocity profile given earlier. Table (5.9) gives the result for the integral of the profile given in figure (5.17b) as:

$$= \int_0^{355,6} S_r \, dz \cdot n$$

$$= 124,7 \quad mm$$

Once the effective volumetric moisture (Effective Saturated Area) at two sections has been determined, the volume of moisture between the two sections is calculated. This is done by taking the average of the

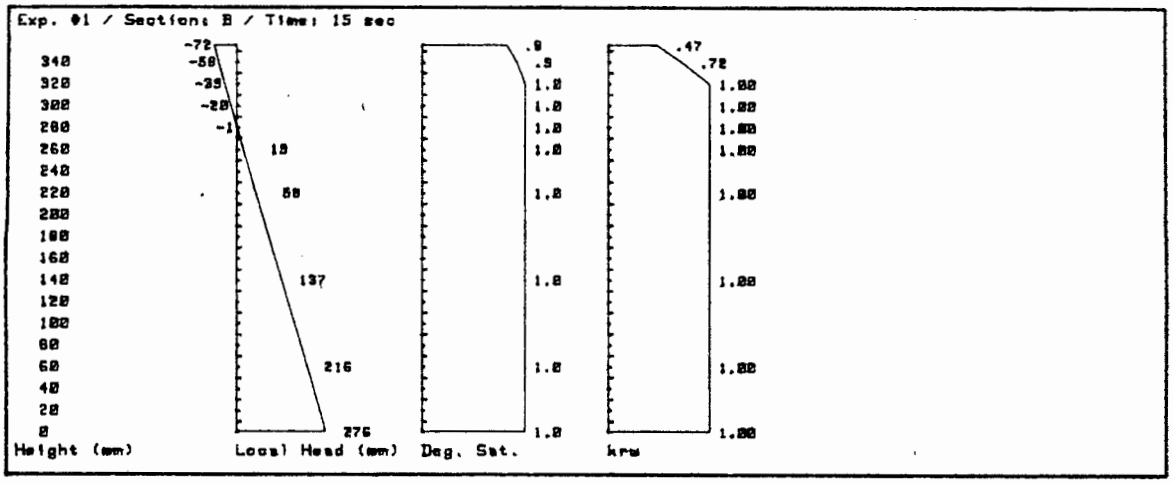

Fig 5.17: Profile plots made for section B-B (Fig 5.12) in experiment no. 1 at 15 seconds after the start. All with respect to elevation: (a) Local head; (b) Degree of saturation; (c) Relative hydraulic conductivity.

Table. 5.9: Results listed of the values for the profile plots, with respect to elevation, made in figure (5.17), at section B-B in experiment no. 1, 15 seconds after the start.

Height (mm)	Local Head (mm)	Deg. Sat.	Rel. Perm.
356	-72	0,81	0,474
340	-58	0,91	0,717
320	-39	1,00	1,000
300	-20	1,00	1,000
280	-1	1,00	1,000
260	19	1,00	1,000
220	58	1,00	1,000
140	137	1,00	1,000
60	216	1,00	1,000
0	276	1,00	1,000

Width : 312,4 mm
Void Ratio e : 0,547
Eff. Sat. Area : 124,7 mm

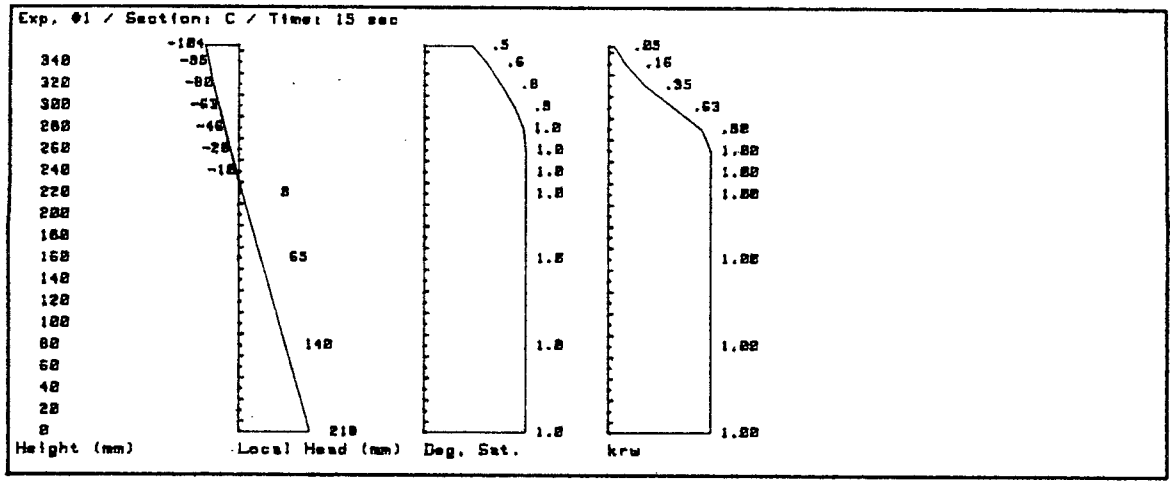

Fig 5.18: **Profile plots made for section C-C (Fig 5.12) in experiment no. 1 at 15 seconds after the start. All with respect to elevation: (a) Local head; (b) Degree of saturation; (c) Relative hydraulic conductivity.**

Table. 5.10: Results listed of the values for the profile plots, with respect to elevation, made in figure (5.18), at section C-C in experiment no. 1, 15 seconds after the start.

Height (mm)	Local Head (mm)	Deg. Sat.	Rel. Perm.	Hydraulic Grad.	$k_{rw} \times i_h$
356	-104	0,46	0,050		
340	-95	0,61	0,158		
320	-80	0,75	0,353		
300	-63	0,88	0,627		
280	-46	0,97	0,903		
260	-28	1,00	1,000		
240	-10	1,00	1,000		
220	9	1,00	1,000		
160	65	1,00	1,000		
80	140	1,00	1,000		
0	218	1,00	1,000		

Width : 312,4 mm
Void Ratio e : 0,547
Eff. Sat. Area : 119,0 mm

---

effective volumetric moisture of the two sections and multiplying this by the distance between the two sections and the width of the flume.

For figure (5.13) the effective volumetric moisture at the sections A, B, C, and D for a unit width are calculated as: 125,7; 124,7; 119,0 and 110,4 mm respectively. (See Tables 5.7, 5.8, 5.9 and 5.10). Therefore the total volume of moisture between sections A and D is the sum of the moisture between sections AB, BC, and CD. The distances between sections A, B, C and D as shown in figure (5.12), are 304,8 mm (12 inches), 355,6 mm (14 inches) and 304,8 mm respectively. The width is 312,4 mm. The total moisture between sections AB is determined as:

$$V_w(AB) = 304{,}8 \cdot \frac{125{,}7 + 124{,}7}{2} \cdot 312{,}4 \quad mm^3$$

$$= 11{,}92 \cdot 10^6 \quad mm^3$$

$$= 11{,}92 \cdot 10^3 \quad cm^3$$

Table (5.11) shows the results for the volume of moisture calculated between the sections BC and CD as well. Also shown is the total sum of the volume of moisture calculated, between sections A-A and D-D for the time of 15 seconds after the start, time t = 0. This volume is given as $36{,}372 \cdot 10^3$ cm^3.

Table. 5.11: Summary of results calculated for the sections at different times considered in experiment no. 1.

Time t (sec)	Volume of moisture between: AB	BC	CD	Total (cm^3)	Flow rate at: A-A	D-D (cm^3/sec)
10	11 921	13 642	11 259	36 822	34,8	131,4
15	11 918	13 532	10 922	36 372	43,4	116,5
30	11 884	13 290	10 274	35 448	49,0	93,9
60	11 838	12 895	9 483	34 216	64,3	80,1

All these results are computed from the observed flow field.

Other times of 10, 30 and 60 seconds after the start are also considered (See appendix E-7) and the final results obtained are also presented in Table (5.11). The methods of calculation used for those times are similar to those for the example given above. (ie. for the time of 15 sec after the start.)

The difference in the result for the inflow and outflow rate at sections A and D respectively should be compensated for by the rate of change of the volume of moisture within the soil mass between sections A and D. If we consider the results in Table (5.11) for the time at 10 seconds, then the rate of change in the volume of moisture at the 10 second time step, should be equal to the difference of 34,8 and 131,4 = 96,6 cm^3/sec. Similarly, at 15 seconds the rate of change in the volume of moisture is 73,1 cm^3/sec. The total volume of moisture calculated at the 10 and 15 seconds time steps is given in Table (5.11) as $36{,}822 . 10^3$ and $36{,}372 . 10^3$ cm^3 respectively. The change in the volumes occurs during the 5 seconds between the 10 and 15 second time step. The average rate of change of the volume of moisture between these intervals is therefore:

$$\frac{\Delta Q}{\Delta t} = \frac{(36{,}822 . 10^3 - 36{,}372 . 10^3)}{5}$$

$$= 90 \quad cm^3 / sec$$

This value lies within the bounds of the rate of change in moisture determined as 96,6 and 73,1 cm^3/sec at the 10 and 15 seconds time steps respectively. (As shown in Table 5.12)

The above calculations are repeated for the time intervals between 15 and 30, and 30 and 60 seconds. The results are presented in Table (5.12). For the results shown in Table (5.12), good agreement is shown for both the outflow predicted to that measured (See figure 5.9). The average rate of change in the volume of moisture, (last column in Table 5.12) compares reasonably with the range in

Table. 5.12: Results calculated for the moisture transfer in experiment no. 1 at different times.

Time t (sec)	Inflow (A-A) (cm^3/s)	Outflow (B-B) (cm^3/s)	Difference (cm^3/s)	Total storage (A-D) (cm^3)	"Storage" change (cm^3)	Average change rate (cm^3/sec)
10	34,8	131,4	96,6	36 822		
					450	90
15	43,4	116,5	73,1	36 372		
					924	62
30	49,0	93,9	44,9	35 448		
					1232	41
60	64,3	80,1	15,8	34 216		

All these results are computed from the observed flow field.

column 4 of Table (5.12) calculated by the difference in the inflow and outflow rates at different times.

5.5.6 Summary and conclusion.

The calculations made on the results obtained for the experiment were made to confirm that the contouring of the total heads was done correctly. Also to show that the different readings made are consistent with each other. The results from the tensiometers were far more accurate than the piezometer readings. The latter even contradicted each other in places. The reason for the erratic piezometer readings, as noted before, could be due to partially blocked tubes in the walls of the seepage tank.

Based on the above, the author felt that if more tensiometers connected to transducers could have been used, the contouring of the total pressure heads could have been done more easily and more accurately. A further verification of the results obtained is made in Chapter 6, by using the finite element method.

5.6 Experiment No. 2 analysis.

5.6.1 Introduction.

The arrangement and procedure for the experiment has been given in section (4.8). The basic problem (See figure 4.8) in this second experiment is similar to the first, in that drainage is to be observed, but in this case the upstream face of the rectangular slab is impermeable and the soil is allowed to completely drain. Figure (5.19) shows the lay-out of the problem.

As with the first experiment, no attempt has been made to model an actual large scale drainage problem. The experiment is done to observe the actual drainage encountered in this tank and to make a numerical verification.

Attempts were made to overcome some of the problems encountered in the first experiment. The main problem was that there were too few tensiometers. To overcome this, in the second experiment, sets of tensiometers (ie. nylon pipes with cotton wool pressed into the front) were located on a regular grid. See figure (5.19). The experiment was then repeated a number of times, each time the transducers were connected to a different set of tube tensiometers. In this way it was hoped to increase the amount of data collected, without increasing the number of transducers required.

The soil-moisture parameters of the soil used, are as given in sections (4.2), (5.2), (5.3) and (5.4). The shape of the slab drained is rectangular, with length 2 717,8 mm (107 inches); height 401,3 mm (15,8 inches) and a width of 312,4 mm (12,3 inches). The mass of the sand used to construct the slab was 571,5 kg. The void ratio of the slab of soil is calculated the same way as shown in section (5.5.1):

Bulk volume of soil	V	$= 340{,}8 \cdot 10^3$ cm^3
Mass of sand used	W_s	$= 571{,}5 \cdot 10^3$ g
Volume of solid particles	V_s	$= 216{,}5 \cdot 10^3$ cm^3
Volume of voids within the soil	V_v	$= 124{,}3 \cdot 10^3$ cm^3

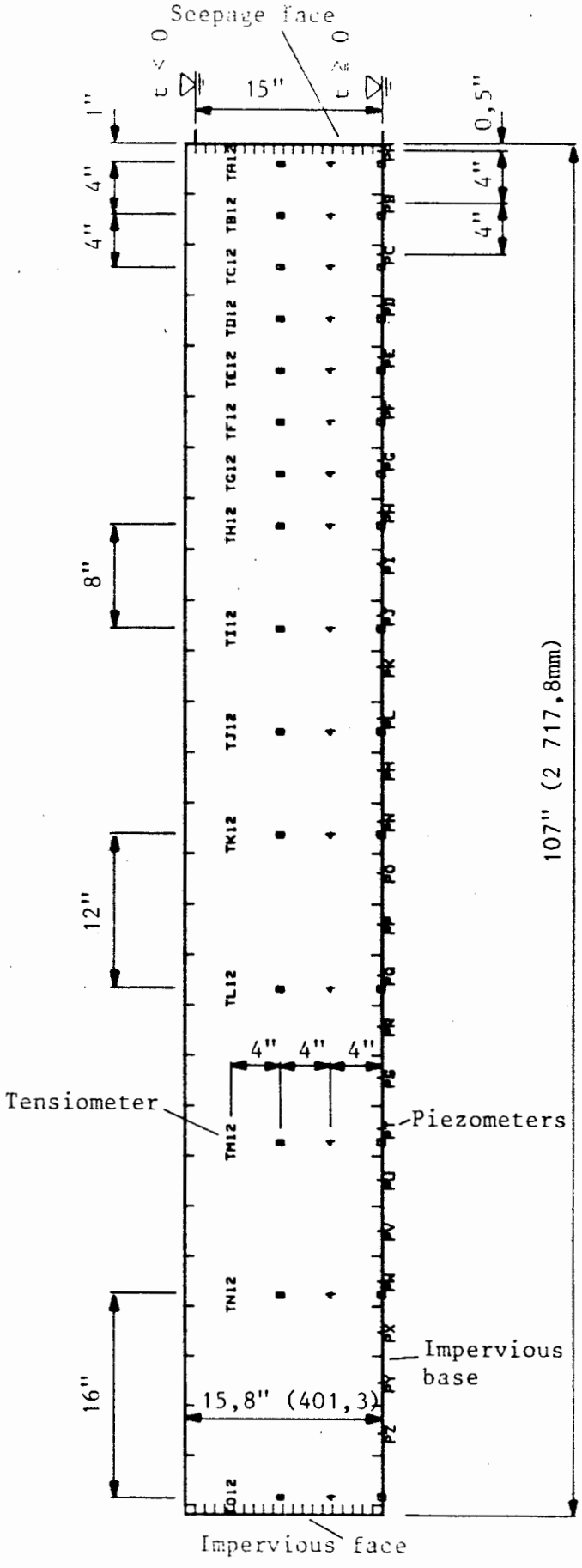

Fig 5.19: Lay-out of experiment no. 2, giving the dimensions and showing the locations of the piezometers and tensiometers.

Therefore the void ratio $e = 0,574$

Using equation (5.1) from section (5.2), the saturated hydraulic conductivity at 20 ^{0}C is:

$$k_{sat} = 4,444 \left(\frac{0,574}{1,574}\right)^3 - 0,04$$

$$= 0,494 \quad \text{cm / sec}$$

The temperature of the experiment differed from that of 20 ^{0}C and was measured at 18 ^{0}C. Using the viscosity of the water at the different temperatures, the hydraulic conductivity is adjusted for this temperature difference as before. The saturated hydraulic conductivity k_s at 18 ^{0}C is therefore:

$$k_s = k_{sat} \frac{\eta_{20}}{\eta_T}$$

$$= 0,494 \frac{1}{1,0507}$$

$$= 0,470 \quad \text{cm / sec}$$

where η_{20}/η_T the ratio of the viscosities is given in Table (B-2).

The residual saturation is taken as:

$$S_{ro} = 0,15$$

for the same reasons as given in the first experiment, section (5.5.1). As the residual saturation is the same as before, the relative hydraulic conductivity is given by equation (5.5), written as:

$$k_{rw} = \left(\frac{S_r - 0,15}{0,85}\right)^3$$

This equation gives the relationship of the relative hydraulic conductivity as a function of the degree of saturation.

The soil-moisture characteristic curve from the first experiment can be used again for this experiment, as the residual saturation is the same. Table (5.6) in section (5.5.1), therefore shows the relationship of the suction head versus the degree of saturation of the soil used in the analysis of this experiment.

In most respects this second experiment is similar to the first. The experiment was performed 4 times. Each time the experiment was started from the same initial position. The difference was that the transducers were connected up to different tensiometers for each run. The same recordings were made, as before, while the test was in progress. Namely, the outflow with respect to time and the change in pressure at various pressure points was measured. The main difference in the set-up was that the upstream face of the soil was impermeable. Therefore no water flowed into the soil through the upstream face, and as drainage continued, a corresponding drop in the phreatic surface took place.

The initial position of the experiment was with the phreatic surface at 381 mm (15 inches) above the base of the flume and the soil saturated. The experiment was started by dropping the drainage reservoir at time $t = 0$ to zero elevation and measuring the outflow of the water seeping out of the drainage face. The initial position for the experiment was reached by first submerging the complete slab of soil in the flume for a few days with de-aired water. The water level was then lowered to the position of 381 mm above the flume base. This level was kept for a while in the drainage reservoir to make certain that the phreatic surface within the soil had also achieved the level of 381 mm. Once these equilibrium conditions had been reached the experiment could be performed.

The recordings made while the experiment was underway are listed in appendices (E-8), (E-9) and (E-10). The experiment was run until the outflow drainage rate had dropped to a very small value. This was after about 3 600 seconds (1 hour) from time $t = 0$.

5.6.2 Drainage outflow.

The determination of the approximate flow rate from the drainage outflow was performed the same way as described in section (5.5.2), for the first experiment. Appendix (E-8) lists the quantities of water collected for the different time intervals and also the calculated average flow rates.

From the results, a plot is made, as shown in figure (5.20). The results from the repeated runs are all plotted on the one graph. To this data an approximate outflow curve is fitted. By integrating under the curve with respect to time, the curve for the cumulative outflow is plotted, as shown in figure (5.21).

The curve of the drainage flow rate tends towards zero with respect to time, because the soil tends to a completely drained state and no more water can drain out. The curve for the cumulative outflow plot tends to a horizontal line, which corresponds to the total volume of water in drainable storage within the soil at time t = 0.

5.6.3 Sidewall piezometers.

While the experiment was in progress, the water level in the piezometer tubes was recorded, as before. Appendix (E-9) gives a listing of the results. The results are listed as a single value for each vertical set of piezometers. This is because the drop in the water levels in the piezometers was much slower than in experiment one and the results for a vertical set were all nearly the same. An average of the results was therefore recorded. The results are used later for the plotting of the total head contours in the experiment at different times.

5.6.4 Transducer monitored tensiometers.

The tensiometers were located at specific points within the soil. Figure (5.19) shows where the tensiometers were located. As noted earlier, for each run a different set of tensiometers were connected to the transducers. Therefore for each run a different set of tensiometers

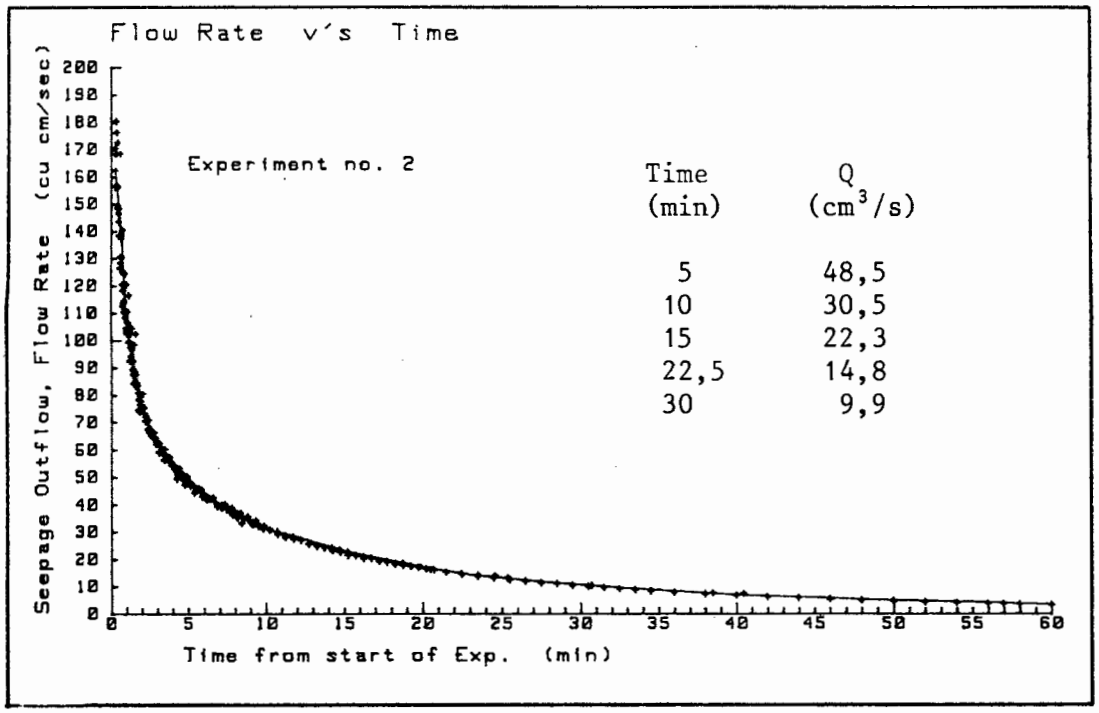

Fig 5.20: Seepage outflow, flow rate versus time measured at the drainage face for experiment no. 2.

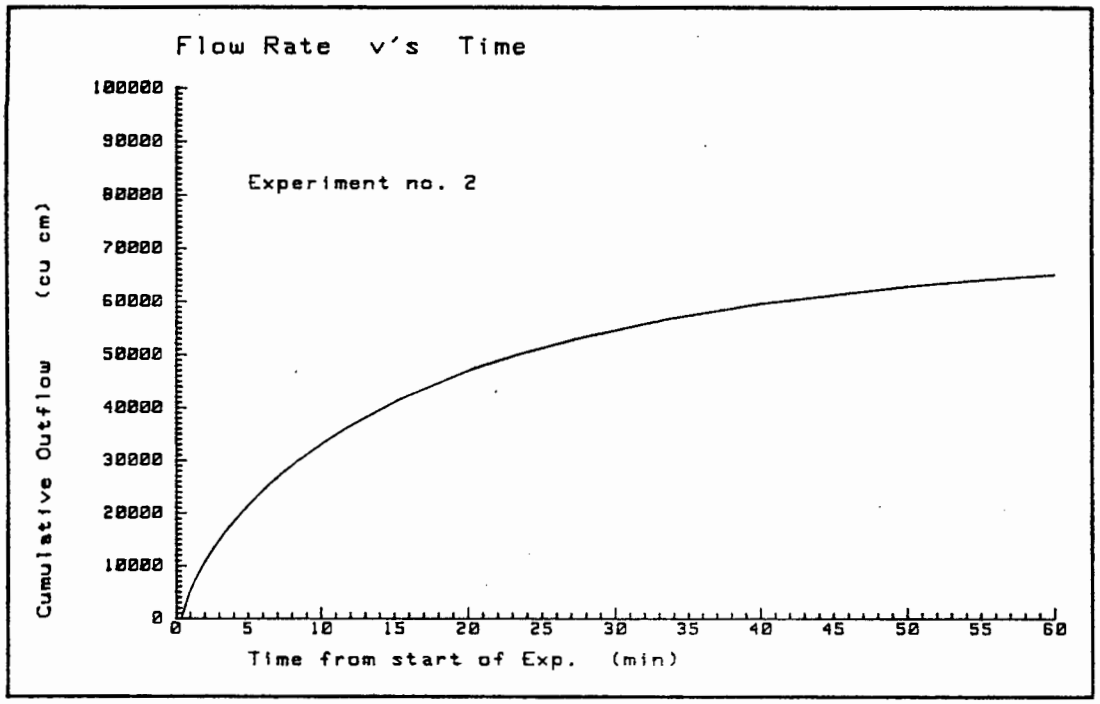

Fig 5.21: Cumulative seepage outflow, at the drainage face versus time for experiment no. 2.

were monitored. Appendix (E-10) gives a listing of the results for the respective experimental runs. The readings are listed with respect to time and are referenced to which tensiometer was monitored. From the listing the results can be plotted with respect to time. Figure (5.22) shows a plot of the total pressure head above the flume base for tensiometer "TE4" with respect to time. The results plotted for the rest of the tensiometers are shown in appendix (E-10).

The results obtained from the tensiometers show the same problems as encountered before. Namely, that certain readings have been affected by erratic electrical noise or air has come out of solution in the connecting nylon pipe between the tensiometer and transducer. The readings made for experiment run No. 2, (See appendix E-10) are for certain of the readings, most erratic due to electrical noise. This seems to be, because the reference transducer's reading must have been affected and this in turn affected all the other readings. The transducers affected due to air coming out of solution cannot be seen straight off from the results. These are only discovered when a contour plot is attempted and a reading does not seem to fit in with the general pattern of the readings made.

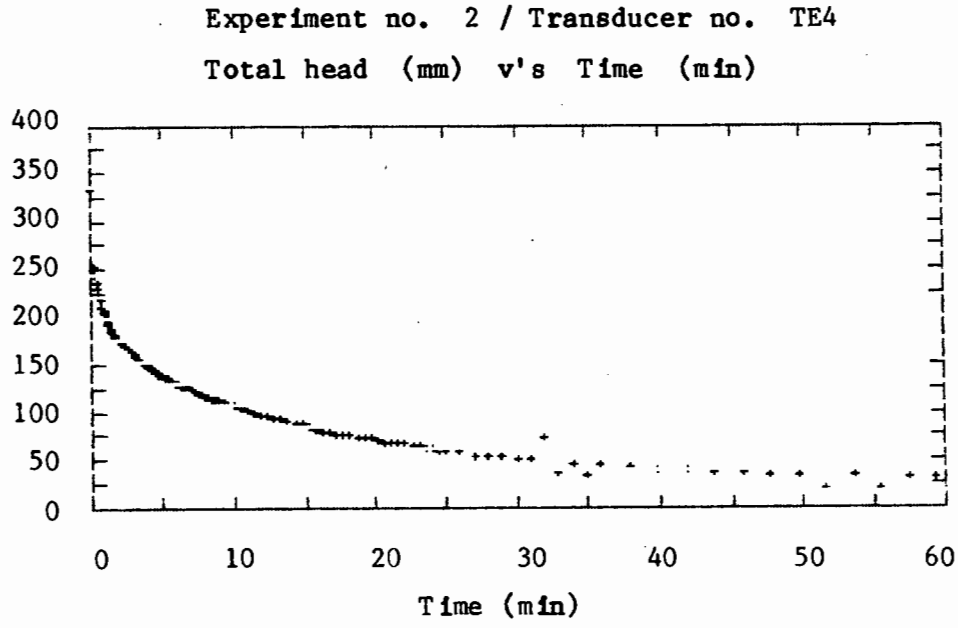

Fig 5.22: **Total head above the base of the flume versus time, measured by transducer "TE4", for experiment no. 2.**

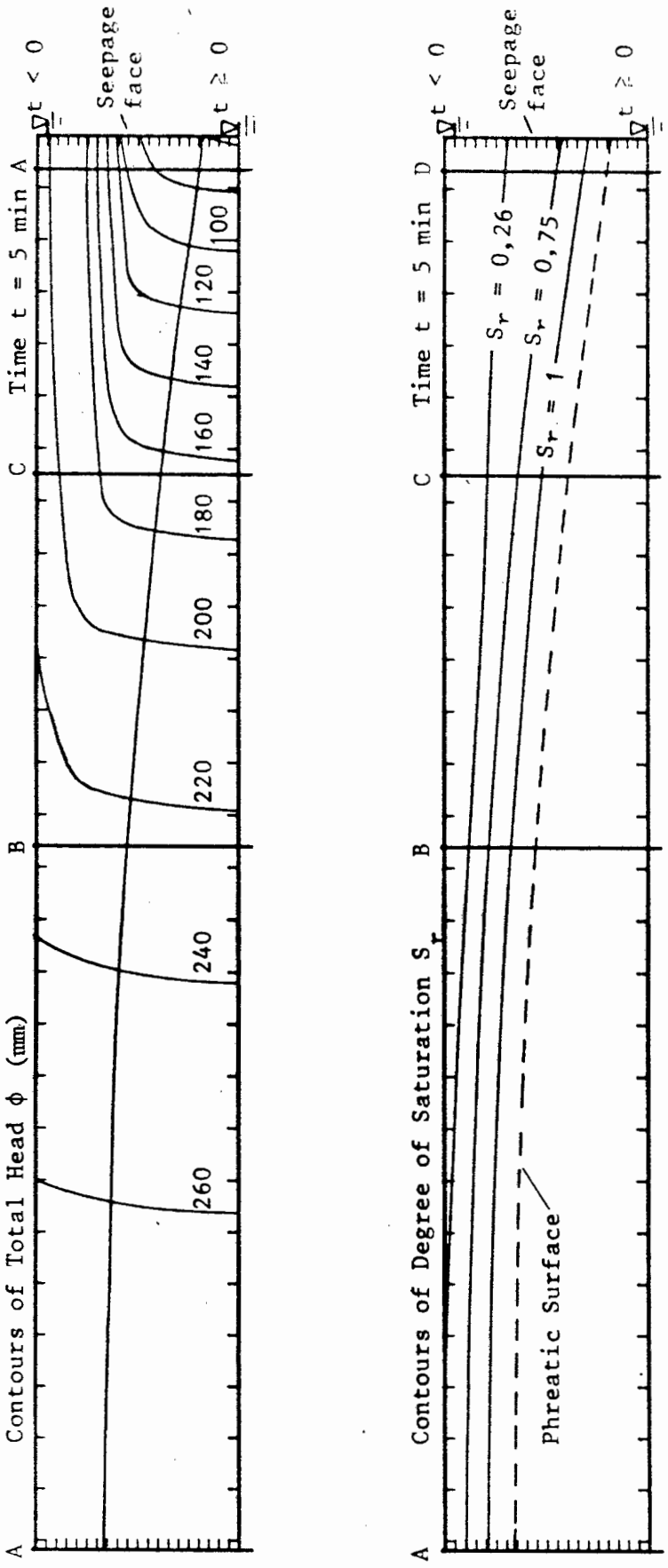

Fig 5.23: Contour plot of the total head for experiment no. 2 at 300 seconds (5 minutes) after the start of the experiment. Contour plot based on the results of the pressure recorded at specific points.

5.6.5 Analysis of results.

To analyse and get some sort of confirmation of the experimental results, once again the mass transfer of the water within the soil is studied. As the soil has only one face across which flow can take place (the drainage face), only this face need be considered in terms of water flowing in or out of the soil. The in or out-flow must be matched with a corresponding rate of volume changes of water within the soil.

The approximate method, as used in experiment one, is used again. The outflow out of the drainage face is determined by taking a section near the face and plotting the relative horizontal Darcian velocity. From this, the flow rate across the section is determined. Section (5.5.5) of experiment one, discusses how this is done. The volume of water within the soil is determined by taking an average of the effective volume of moisture determined at a number of sections. This is also discussed in section (5.5.5) for experiment one.

For this experiment, three times are considered. Namely, 5; 15; and 30 minutes after the start of the experiment. Figure (5.23) shows the contour plot for the 5 minute time step and where the sections are located for this analysis. Table (5.13) gives the final results obtained for the calculations performed at the different times.

Table. 5.13: Results calculated for the moisture transfer in experiment no. 2 at different times.

Time t (min)	Outflow (cm^3/s)	Total storage (A-D) (cm^3)	"Storage" change (cm^3)	Average change rate (cm^3/sec)
05	47,9	96 995		
			20 601	34,3
15	21,3	76 394		
			13 873	15,4
30	10,0	62 521		

All these results are computed from the observed flow field.

Appendix (E-11) lists the tables and values used in the various calculations. Also shown are the contour plots of the total pressure heads and degree of saturation for the different time steps analysed.

5.6.6 Summary and conclusions.

For this second experiment, the results for the mass transfer calculation show agreement with the outflow measured. This is seen by the results given in Table (5.13) and the values measured as shown in figure (5.20). The analysis done therefore indirectly confirms that the contour plots made could be correct. A verification of the results is done in chapter 6. using a numerical method of analysis (The finite element method.).

The problem of not having enough tensiometers in experiment one was not really overcome by using a larger number of tensiometers. The reason for this is that a lot of the readings obtained were incorrect due to air being entrapped when connected up to the transducer. To overcome this, a better system is needed for priming the tensiometers already located within the soil. For this second experiment the heads changed slowly in the piezometer tubes located far from the drainage face, hence the heads in these tubes were not subject to signficant response time errors, and they were used to check the transducer readings.

CHAPTER 6

MODELLING OF FLUID FLOW IN A SATURATED-UNSATURATED DOMAIN USING THE FINITE ELEMENT METHOD.

6.1 Introduction.

In section (2.9.2) the combined flow equation was developed in the form of a partial differential equation, based on a set of assumptions which simplified the complex real world. (Equation 2.43). To find the unknown total head ϕ, a function of space and time, the partial differential equation, subject to specific initial and boundary conditions needs to be solved. The geometry of the flow domain and its various storage and transport coefficients must be known. (ie. specific moisture capacity and hydraulic conductivity). Three classes of methods exist for solving such problems. (Bear [6]):

- analytical methods
- methods based on the use of models and analogs
- numerical methods.

Each method has its advantages and the method used depends on the problem encountered and the facility available, (eg. skilled manpower). A brief paragraph is given to introduce each method. The method selected by the writer and expanded in this chapter is a numerical method, and more specifically, the finite element method.

a) Analytical methods.

The analytical method is the most superior of all the methods. An advantage of using it is that the solution can be applied to different values of the parameters defining the problem. The influence of each parameter can then clearly be seen. Problems with this method are that for irregularly shaped domains, encountered in practice, an analytical solution is sometimes not possible. Also, the partial differential equation for saturated-unsaturated flow is non-linear. As a result of these problems, analytical methods are seldom used in practice.

b) Analog methods.

Analogs (and models) may be regarded as special purpose computers, when compared with digital computers. An analog system is usually constructed to solve a particular flow problem. Once this has been done, as long as the geometry of the system considered does not change, a number of cases (eg. with different inputs and outputs) can be considered. In models used, the dependent variable and its derivatives are related to each other in a similar manner to the system being investigated, therefore allowing it to be solved.

The following models and analogs could be used for studying various flow problems:

- Sand box model
- Vertical and horizontal Hele-Shaw analogs
- Electric analogs of the elctrolytic tank type; of the conducting paper type; of the RC-network type (ie. Resistor and Capacitor network)
- Ion motion analog
- Membrane analog

The use of the sand box model involves many technical difficulties. The vertical Hele-Shaw analog can only be used for two-dimensional flows in the vertical plane, but is a useful tool for studying sea water intrusion in coastal aquafiers. Also, problems with a phreatic surface can be solved. The horizontal Hele-Shaw analog is used essentially to study two-dimensional flow in a confined aquafier. The electrolytic tank and conducting paper are usually used for steady flow only. The presence of a phreatic surface requires special techniques. The RC-network is used for the solution of regional forecasting problems. A disadvantage of the RC-network is its cost, especially that of the peripheral equipment for input, output and boundary conditions.

c) Numerical methods.

Numerical methods are merely tools used to enable one to replace the partial differential equations valid in a domain with an approximate set of algebraic equations in a similar domain which are then solved. The two most popular methods are:

- Finite difference method
- Finite element method.

Both of theses methods are merely structured procedures for approximating the differential system. Computer based numerical methods are the most practically used tools for solving flow problems at the moment. They are used because they allow for the solution of problems involving irregularly shaped boundaries; materials with high variations in properties; non-linear partial differential equations; and complex boundary conditions which may be insolvable by analytical means. Furthermore, with a numerical method, changes in the problem - geometry and physical parameters - are more easily accommodated than with an analytical method which may require a complete re-analysis of the problem. However, analytical solutions are useful for serving as standards for comparisons of numerically computed results.

Numerical methods for the solving of partial differential equations have often been published and, in many cases, these are in the form of computer programs. The use of these programs for the solving of saturated flow problems is relatively easy and can be done with a minimal background knowledge in numerical methods. For unsaturated flow, the equations become more involved and care needs to be exercised when dealing with such problems.

Finite difference method

The finite difference method involves the process of replacing a derivative based on a small differential distance dx by an approximation of a difference based on some finite

distances Δx. In making this approximation, an error is introduced. The finite difference theory is concerned with ensuring that the error is of a magnitude tolerable within the constraints of the problem under study. The differential equation which holds for the entire domain is replaced by a number of discrete approximations to the differential equation for the domain. The domain is subdivided (discretized) by selecting points or nodes at which the approximations are used. The approximation at one point depends to some degree on the values at nearby points. The continuous unknown variable appearing in the partial differential equation is therefore replaced by a discrete variable at the nodes. The set of simultaneous finite difference equations is then solved numerically on a digital computer to yield the results of the unknown variable at the nodes.

Finite element method

An object within the finite element method is to transform the partial differential equation into an integral equation which involves derivatives of the first order only. The integration is performed numerically over elements into which the domain has been subdivided. The functions selected are typically polynomials of some sort and the solution required can be expressed as a sum involving these polynomials. The differential equation is approximated and is not necessarily satisfied exactly, hence the solution may contain an error. The solution to the problem is obtained by requiring that the average error over the entire domain be as small as possible.

The methods of finite difference and finite element have a lot in common and borrowing of concepts by one method from the other has taken place. This cross-breeding of the two methods, which has been accelerated in the last decade makes it difficult to point out the unique features of either method. Table (6.1) reproduced from Gray [14] gives a list of elementary differences between the two methods.

Table. 6.1: A finite list of elementary differences: The elements of finite differences which are different from finite elements. Gray [14].

Finite Difference.	Finite Element.
Approximates derivatives of functions directly.	Approximates the functions themselves.
Provides approximations at points which borrow information from neighboring points to whatever degree desired.	Provides global approximations which are restricted to neighborhoods of the grid to whatever degree desired.
Traditionally uses a regular mesh	Structure of method readily lends itself to irregular, curved grids.
Approximations developed via curve fitting or Taylor Series expansions.	Approximations developed from families of basis functions and integration over grid.
Resultant difference expression explicitly provided by the programmer to the code. Approximations may be "seen".	Resultant difference expression provided implicitly to the code which performs the integrations. Approximation is buried in the integrals.
Complete freedom to select nodes to be used in a discrete approximation provided	Nodes included in discrete approximation determined by basis functions, integration rule, and weighting function.
On a regular grid, similar approximations are made at different nodes.	Even on a regular grid, different approximations may be made at different nodes (eg. 9-node Lagrangian elements).
Difference expressions are generally in terms of function values only.	Difference expressions are often written in terms of function values and derivatives of the functions (eg. Hermitian cubic elements).
Though not typically done, derivatives with respect to one independent variable may be weighted over another variable (eg. a time derivative approximation may be a sum of time derivatives evaluated at different spatial locations).	Though typically weighted over different coordinates, derivatives may sometimes be lumped by selection of an appropriate nodal integration formula (eg. trapezoidal rule for bilinear elements).

Table 6.1: Cont.

Commonly uses ADI requiring a tridiagonal matrix solver.	Commonly uses banded, frontal, or sparse matrix solver.
Staggered grid easily implemented because of regular rectangular nodal placement.	Staggered grid virtually impossible because of grid irregularities. However mixed interpolation is a partially staggered grid.
Boundary conditions applied by altering the basic computational molecule.	Boundary conditions are applied through the boundary integral obtained after application of Green's theorem
Moving boundary problems are traditionally difficult.	Moving boundary problems are conceptually straightforward.
Large gradients require a fine mesh for resolution.	Functional implanting may minimize need for fine mesh near steep gradients.
For a regular mesh, a zone requiring high resolution determines grid spacing.	Localized refinement of computational grid is easily accomplished
Data input may be simple because of regularity.	Data input is complex and undiscovered data errors can be a cause of trouble.
Regular grid interfaces easily with computer graphics.	Graphics interface may be complicated by an irregular mesh and isoparametric elements.

The finite element method is discussed in more detail in the rest of this chapter. Its use is shown in solving some saturated-unsaturated flow problems and in the verification of the experimental work covered in earlier chapters.

6.2 History of the finite element method.

The finite element method was first developed in the 1950s, mainly by structural engineers in the aircraft industry, for solving stress

analysis problems of complex geometrical configurations of solids. Although little related work was published by mathematicians, it was the practical demands of the engineer coupled with the development of the electronic digital computer which caused rapid development in the method. It was only in the late sixties that mathematicians took a widespread interest in the method and subsequently contributed to the theoretical understanding of the method. Initially the method was strongly related to variational methods which rely on the calculus of variations and the finding of a stationary value of a given functional for the solution of a physical problem. (eg. Rayleigh Ritz). The variational method, though having mathematical advantages (i.e. providing existence proofs) also has inherent limitations. In some cases it is very difficult to find the variational formulation which parallels a partial differential equation whose solution is required. This disadvantage was overcome by the use of Weighted Residual methods, which begin with the governing differential equation of the problem and gives the identical equations to those given by the variational method. The Galerkin method is used extensively with the Weighted Residual method.

A description and the application of the basic steps of the finite element method are discussed later. First the theoretical development of the Galerkin Weighted Residual method is discussed.

6.3 Basic formulation of the partial differential equation.

For a numerical solution of equation (2.43) (Section 2.9.2), and because both saturated and unsaturated regions in the domain are of interest, it is necessary to consider the total head ϕ, instead of the volumetric moisture content θ, as the independent variable. The governing equation for the movement of water (moisture) in a saturated-unsaturated porous rigid medium can therefore be written as:

$$c\,(\phi)\,\frac{\partial \phi}{\partial t} = \nabla\,[\,\underset{\approx}{k}\,(\phi)\cdot\nabla\,\phi\,] \qquad (6.1)$$

where ϕ is the independent variable, c is the specific moisture

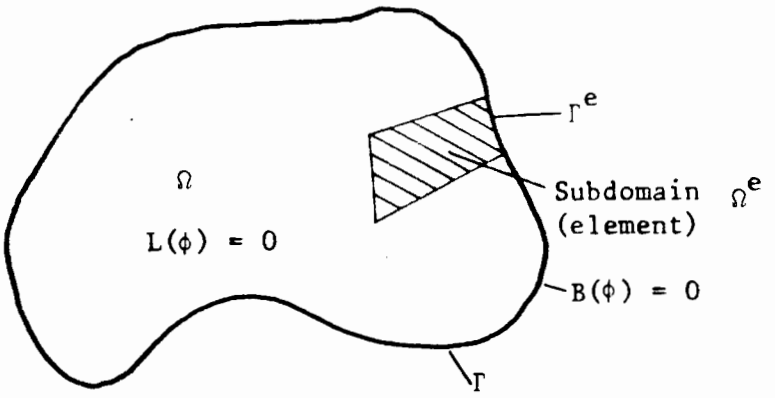

Fig 6.1: Problem domain Ω enclosed by a boundary Γ.

capacity and the local pressure head $\psi = \phi - z$, z being the elevation from a reference datum level. The specific moisture capacity c is defined as:

$$c(\phi) = \frac{d\theta}{d\phi} \tag{6.2}$$

The problem to be solved, is that we seek an unknown function ϕ such that it satisfies equation (6.1) in the domain Ω enclosed by a boundary Γ, on which three types of boundary conditions are generally encountered (Yeh [39]). See figure (6.1).

With the first type of boundary condition (Dirichlet), the local pressure head or total head is prescribed as:

$$\phi = \bar{\phi}(t) \qquad \text{on} \quad \Gamma_1 \tag{6.3}$$

where Γ_1 is a portion of the boundary Γ and $\bar{\phi}(t)$ is a given function of time of the total head. With the second type of boundary condition (Neumann), the flux $\bar{q}(t)$, is prescribed as:

$$-\underset{\sim}{n}\,[\,\underset{\approx}{k}(\phi)\cdot\nabla\phi\,] = \bar{q}(t) \qquad \text{on} \quad \Gamma_2 \tag{6.4}$$

where $\underset{\sim}{n}$ is the directional cosine of the outward unit vector, normal on the Γ_2 portion of the boundary Γ. With the third type of boundary

condition, it's a variable boundary condition, in the sense that, either the Neumann or Dirichlet conditions may prevail:

$$\phi = \bar{\phi}(t) \qquad \text{on} \quad \Gamma_3 \tag{6.5a}$$

or

$$-\underset{\sim}{n}\,[\,\underset{\approx}{k}(\phi)\cdot\nabla\phi\,] = \bar{q}(t) \qquad \text{on} \quad \Gamma_3 \tag{6.5b}$$

where $\bar{\phi}(t)$ and $\bar{q}(t)$ are two known input functions of time on Γ_3 which is a portion of boundary Γ.

6.4 General representation.

The partial differential equation (6.1) governs the behaviour of the unknown ϕ over the domain Ω. Our next step is to find the approximation $\hat{\phi}$ to the unknown ϕ. As noted earlier there are two methods to perform this derivation. The variational method (energy method) and the Weighted Residual method. The more commonly adopted approach, that of the Galerkin Weighted Residual method, is adopted in the discussion that follows. Equation (6.1) can be rewritten as:

$$L(\hat{\phi}) = \nabla\,[\,\underset{\approx}{k}\cdot\nabla\hat{\phi}\,] - c\frac{\partial\hat{\phi}}{\partial t} \qquad \text{in} \quad \Omega \tag{6.6}$$

and with boundary conditions:

$$B(\hat{\phi}) = -\bar{q} - \underset{\sim}{n}\,[\,\underset{\approx}{k}\cdot\nabla\hat{\phi}\,] \qquad \text{on} \quad \Gamma_q \tag{6.7a}$$

$$\text{and} \quad \hat{\phi} = \bar{\phi} \qquad \text{on} \quad \Gamma_\phi \tag{6.7b}$$

where $L(\hat{\phi})$ and $B(\hat{\phi})$ are the respective errors involved in satisfying equations (6.1),(6.3),(6.4) and (6.5), by an approximation of ϕ.

We therefore seek to find the unknown $\hat{\phi}$ which satisfies the differential equation:

$$L\ (\hat{\phi}) \approx 0 \tag{6.8}$$

within the domain Ω and also satisfies the boundary conditions:

$$B\ (\hat{\phi}) \approx 0 \tag{6.9}$$

on the boundary Γ. Since equation (6.1) holds throughout the domain Ω, it follows that:

$$\int_{\Omega} w\ L\ (\hat{\phi})\ d\Omega \equiv 0 \tag{6.10}$$

where w is a arbitrary function. We can assert that if equation (6.10) is satisfied for any w then the differential equation (6.6) must be satisfied by $\hat{\phi}$ at all points of the domain. The proof of the validity of this statement is obvious if one considers the possibility that $L(\hat{\phi}) \neq 0$ at any point or part of the domain. Immediately a function w can be found, which makes the integral of equation (6.10) non-zero and hence, the point is proved. Similar reasoning, applied to the boundary conditions results in the integral statement:

$$\int_{\Omega} w\ \ L\ (\hat{\phi})\ d\Omega + \int_{\Gamma} \bar{w}\ \ B\ (\hat{\phi})\ d\Gamma \equiv 0 \tag{6.11}$$

Thus if equation (6.11) is satisfied for any w and $\bar{w}$, then $\hat{\phi}$ satisfies both the differential equation and the boundary conditions. Of course, reasonable restrictions are placed on w and $\bar{w}$, and $\hat{\phi}$ for the integral to exist. We limit the choice of w and $\bar{w}$, to single finite value fuctions, where as $\hat{\phi}$ must have the degree of continuity required so that its derivatives, to the order of differentiation involved in $L(\phi)$ and $B(\phi)$, are finite and single valued. It is possible to reduce the order of differentiation in the integrands of equation (6.11) via integration by parts (e.g. Green's Theorem) and replace it by an alternative statement of the following form:

$$\int_{\Omega} C\ (w)\ \ D\ (\hat{\phi})\ d\Omega + \int_{\Gamma} E\ (\bar{w})\ \ F\ (\hat{\phi})\ d\Gamma \equiv 0 \tag{6.12}$$

Thus, the continuity requirements on $\hat{\phi}$ have been relaxed, but those of w and $\bar{w}$, have been constrained further. i.e. The operators D and F contain lower order derivatives than those occuring in the operators L and B. The integral statement equation (6.12) is termed a "weak form" of the equation (6.11). Sometimes this "weak form" represents a physical quantity, not immediately apparent from the differential equation. (Zienkiewicz [41].)

Thus far, in equation (6.6) to (6.12), the approximate function $\hat{\phi}$ has been arbitrary, apart from the continuity restrictions. If the unknown function ϕ is approximated by the expansion:

$$\phi \approx \hat{\phi} = \sum_{i=1}^{r} N_i \phi_i = \underset{\sim}{N} \underset{\sim}{\phi} \tag{6.13}$$

where N_i are interpolation functions over the domain Ω and r is some finite value, then it is impossible to satisfy both the differential equation (6.1), and the boundary conditions in a general case. However the integral statement (6.11) or (6.12) allows an approximation to be made if, in place of any function w, we put a finite set of prescribed functions:

$$w = w_j \; ; \quad \bar{w} = \bar{w}_j \qquad , j = 1,2 \ldots n \tag{6.14}$$

where n is the number of unknown parameters ϕ_i entering the problem ($n \leq r$). Substituting equations (6.13) and (6.14) into equations (6.11) and (6.12) yields a set of equations from which the parameter ϕ_i can be determined. i.e. For equation (6.11) we have a set of n equations:

$$\int_{\Omega} w_j L(\underset{\sim}{N}\,\underset{\sim}{\phi})\, d\Omega + \int_{\Gamma} \bar{w}_j B(\underset{\sim}{N}\,\underset{\sim}{\phi})\, d\Gamma = 0 \quad j = 1,n \tag{6.15}$$

or from equation (6.12):

$$\int_{\Omega} C(w_j)\, D(\underset{\sim}{N}\,\underset{\sim}{\phi})\, d\Omega + \int_{\Gamma} E(\bar{w}_j)\, F(\underset{\sim}{N}\,\underset{\sim}{\phi})\, d\Gamma = 0 \quad j = 1,n \tag{6.16}$$

Clearly, almost any set of independent functions w_j and $\bar{w}_j$, could be used for the purpose of weighting. Depending on which choice of

functions are used, a different name is given for the process. (e.g. Point collocation, subdomain collocation, Galerkin method...) The choice adopted here is the Galerkin method. In the Galerkin method we choose the weights to correspond to the approximating functions N_i so that:

$$w_j = N_j \qquad j = 1,2, \ldots n \tag{6.17a}$$

and

$$\bar{w}_j = N_j \qquad j = 1,2, \ldots n \tag{6.17b}$$

Substituting for $\phi \approx \underset{\sim}{N}\underset{\sim}{\phi}$, expansion (6.13), into equation (6.15) and setting $w_j = N_j$ gives:

$$\int_\Omega N_j \{ \nabla [\underset{\approx}{k} \cdot \nabla (\underset{\sim}{N}\,\underset{\sim}{\phi})] - c \frac{\partial(\underset{\sim}{N}\,\underset{\sim}{\phi})}{\partial t} \} \, d\Omega$$

$$- \int_\Gamma N_j \{ \bar{q} + \underset{\sim}{n} [\underset{\approx}{k} \cdot \nabla (\underset{\sim}{N}\,\underset{\sim}{\phi})] \} \, d\Gamma = 0 \qquad j = 1,n \tag{6.18}$$

where Ω is the domain of interest, Γ_q are parts of the boundary Γ on which Neumann boundary conditions are imposed and assuming that the boundary condition $\phi = \bar{\phi}$ is automatically satisfied by the choice of functions $\underset{\sim}{N}\underset{\sim}{\phi}$ on the boundary Γ_ϕ. There are $j = 1,n$ equations of this form. By rearranging (the order of summation) and integrating by parts (Green's Theorem), as with equation (6.16), we obtain:

$$\int_\Omega \nabla^T N_j [\underset{\approx}{k} \nabla \underset{\sim}{N} \, d\Omega] \underset{\sim}{\phi} + [\int_\Omega c \, N_j \underset{\sim}{N} \, d\Omega] \frac{\partial \underset{\sim}{\phi}}{\partial t}$$

$$- \int_{\Gamma_q} N_j \, \bar{q} \, d\Gamma = 0 \qquad j = 1,n \tag{6.19}$$

which can be expressed in matrix form as:

$$\underset{\approx}{M} \dot{\underset{\sim}{\phi}} + \underset{\approx}{S} \underset{\sim}{\phi} + \underset{\sim}{Q} = 0 \tag{6.20}$$

where the time derivative of the total head ϕ is given by:

$$\dot{\underset{\sim}{\phi}} = \frac{\partial \underset{\sim}{\phi}}{\partial t} \tag{6.21}$$

and the components of the matrices are:

$$M_{ij} = \int_\Omega c\, N_i\, N_j\, d\Omega \tag{6.22a}$$

$$S_{ij} = \int_\Omega \nabla^T N_i \underset{\approx}{k} \nabla N_j\, d\Omega \tag{6.22b}$$

$$Q_i = - \int_{\Gamma_q} N_i\, \bar{q}\, d\Gamma \tag{6.22c}$$

where prescribed values of ϕ are imposed on boundaries Γ_ϕ. The unknown ϕ_j , $j = 1,n$ can be obtained by solving the set of equations (6.20). Having found ϕ_j, the approximation to ϕ is given by:

$$\phi \approx \hat{\phi} = \underset{\sim}{N}\, \underset{\sim}{\phi} \tag{6.23}$$

The above method has one serious shortcoming. There is no systematic method for the choosing of interpolation functions N_j, which could be difficult over complex domains. (e.g. three-dimensional). The above difficulty is resolved by the finite element method.

6.5 **The finite element method.**

6.5.1 The finite element concept.

The main idea of the finite element method, is to define interpolation functions N_j as piecewise functions over subregions Ω^e, (finite elements), of the domain Ω. Over these subregions use is made of very simple functions. (e.g. polynomials). This provides a general and systematic technique for constructing basis functions. (Interpolation functions). Nodes are located along the boundaries and within each subdomain. Each basis function is identified with a specific node. Depending on the form of the basis functions, certain of their derivatives may also be continuous across element boundaries.

6.5.2 Discretisation.

The domain Ω is subdivided into a number of distinct non-overlapping regions Ω^e known as finite elements, interconnected at a discrete number of points or nodes, over which the variable ϕ is interpolated. The shape and type of element employed depends to a large extent on the nature of the domain. For example, a triangular or rectangular element would be used for a two-dimensional domain, whereas a terahedral or hexahedral "brick" element would be chosen for a three-dimensional domain. The nodes are distributed in a logical manner around the perimeter of an element and in some instances within the element itself. Using coordinate transformations, a complex or awkward domain can be discretised into a complete finite element mesh from fixed master elements.

6.5.3 Approximation and interpolation.

The unknown ϕ is approximated throughout the domain Ω, by approximating it piecewise over each element Ω^e. The nodes provide a convenient way for utilising interpolation functions. This is done by the approximation of the unknown ϕ over each element as:

$$\phi \approx \hat{\phi} = \sum_{i=1}^{n} N_i \phi_i \qquad (6.24)$$

where N_i are the appropriate interpolation functions (e.g. Lagrange interpolation polynomials) defined piecewise element by element and ϕ_i are the nodal values of ϕ. $N_i = N_i^e$ when the point concerned is within a particular element e and i is a point (Node) associated with that element. If the point (Node) i does not occur within the element $N_i = 0$. The outcome of the finite element method is eventually to give the nodal values ϕ_i of the unknown ϕ. The assumed distribution then gives an approximation for ϕ over the whole of the discretised domain. (Using equation 6.24).

6.5.4 Derivation of element equations.

The integral form of equation (6.11) permits approximation to be

obtained element by element providing the function $L(\hat{\phi})$ and $B(\hat{\phi})$ are integrable. By virtue of the property of definite integrals requiring that the total be the sum of the parts:

$$\int_{\Omega} w\, L\,(\hat{\phi})\, d\Omega \;+\; \int_{\Gamma} \bar{w}\, B\,(\hat{\phi})\, d\Gamma$$

$$= \sum_{e=1}^{m} \left\{ \int_{\Omega^e} w\, L\,(\hat{\phi})\, d\Omega \;+\; \int_{\Gamma^e} \bar{w}\, B\,(\hat{\phi})\, d\Gamma \right\} \qquad (6.25)$$

where Ω^e is the domain of each element, Γ^e its boundary and m is the number of elements.

Using a similar procedure (The Galerkin method) as adopted in equations (6.11) to (6.22) for the domain Ω, we can consider an element of domain Ω^e. This procedure leads to a system of equations, for a particular element, which can be expressed as:

$$\underset{\approx}{M}^e \underset{\sim}{\dot{\phi}} \;+\; \underset{\approx}{S}^e \underset{\sim}{\phi} \;+\; \underset{\sim}{Q}^e \;=\; 0 \qquad (6.26)$$

where the components of the matrices are:

$$M^e_{ij} = \int_{\Omega^e} c\, N^e_i\, N^e_j\, d\Omega \qquad (6.27a)$$

$$S^e_{ij} = \int_{\Omega^e} \nabla^T N^e_i\, \underset{\approx}{k}\, \nabla N^e_j\, d\Omega \qquad (6.27b)$$

$$Q^e_i = -\int_{\Gamma^e} N^e_i\, \bar{q}\, d\Gamma \qquad (6.27c)$$

and prescribed values of ϕ satisfy boundary conditions Γ^e_{ϕ}.

6.5.5 Assembly of global equations and boundary conditions.

The next step is to assemble the element equations into a single global system governing the entire mesh. This global system of equations is obtained by summing equation (6.26) over all m elements in the mesh. This is done by expanding the element matrices in equations (6.27), to (n X n) and (n X 1) order matrices corresponding to the order of the global matrices in equations (6.22). e.g. $\underset{\approx}{S}^e$ will become a (n X n)

matrix $\underset{\approx}{\bar{S}}^e$ with zeros everywhere except those rows and columns corresponding to nodes within element Ω^e. The global matrix equation representing the domain Ω, may be written as:

$$\underset{\approx}{M}\ \dot{\underset{\sim}{\phi}} + \underset{\approx}{S}\ \underset{\sim}{\phi} + \underset{\sim}{Q} = 0 \qquad (6.28)$$

which is similar to equation (6.20), but where the global matrices $\underset{\approx}{M}$, $\underset{\approx}{S}$ and $\underset{\sim}{Q}$ are assembled from the various element matrices $\underset{\approx}{M}^e$, $\underset{\approx}{S}^e$ and $\underset{\sim}{Q}^e$ respectively:

$$\underset{\approx}{M} = \sum_{e=1}^{m} \underset{\approx}{M}^e \qquad (6.29a)$$

$$\underset{\approx}{S} = \sum_{e=1}^{m} \underset{\approx}{S}^e \qquad (6.29b)$$

$$\underset{\sim}{Q} = \sum_{e=1}^{m} \underset{\sim}{Q}^e \qquad (6.29c)$$

Prescribed boundary conditions on boundary Γ_ϕ are directly translated into their equivalent positions, for the global system, in equation (6.28). The next step is to solve the resulting system of equations for the unknown nodal values.

6.5.6 Solution of equations.

The system is now a set of algebraic equations from which the unknown ϕ may be solved for. Boundary conditions are first imposed and then the solving of the equations can be done in a variety of ways. Direct methods (e.g. Gaussian elimination), or iterative methods may be employed. If the time dependence from equation (6.28) is removed ,then the unknown ϕ can be solved for, from a set of simultaneous equations. If not, then the initial values of ϕ at $t = 0$ are generally specified and a numerical recurrence process is required to find the solution at subsequent times.

Two approaches can be adopted. One is by extending the Galerkin finite element process, so that the unknown ϕ is not only a function of spatial

Table. 6.2: Listing of Alternative Numerical Schemes. Yeh [39].

	Time Marching			Mass Matrix	
Numerical Schemes	Central Difference	Backward Difference	Mid-Difference	Without Lumping	With Lumping
1	X			X	
2		X		X	
3	X				X
4		X			X
5			X	X	
6			X		X

position in x, y and z, but also a function of time t. The domain used would be subdivided into finite elements in both space and time. This method is not that common as a vast amount of computer storage is required. The second and more common approach is to discretize the time domain into a sequence of finite intervals Δt, and nodal values of ϕ are solved, subject to initial conditions at $t = 0$, by using a finite difference "time marching" , or "time stepping", technique. (e.g. the Runge - Kutta and "predictor - correction" methods). Table (6.2), by Yeh [39] lists six alternative numerical schemes by which equation (6.28) could be solved. Each one dependent on the method of time marching and treatment of the mass matrix $\underset{\approx}{M}$. If a one-step method is used, in which it is assumed that:

$$\dot{\underset{\sim}{\phi}}^{(t + \alpha \Delta t)} = \frac{\left({}^{t + \Delta t}\underset{\sim}{\phi} - {}^{t}\underset{\sim}{\phi} \right)}{\Delta t} \tag{6.30a}$$

and

$$\underset{\sim}{\phi}^{(t + \alpha \Delta t)} = (1-\alpha)\, {}^{t}\underset{\sim}{\phi} + \alpha\, {}^{(t + \Delta t)}\underset{\sim}{\phi} \tag{6.30b}$$

where $(0 \leq \alpha \leq 1)$, and ${}^{t}\underset{\sim}{\phi}$ is the value of the unknown at time t. Then

these assumptions correspond to the following time integration techniques, [2],[4]:

$\alpha = 0$ Euler forward-difference (explicit)
$\alpha = 1/2$ Mid-difference or Crank-Nicolson (implicit)
$\alpha = 1$ Euler backward-difference (implicit)

On solving for the unknown ϕ at a specific time step t, the specific flux vector (macroscopic fluid velocity), can be obtained from equation (2.42), by using:

$$\underset{\sim}{q} = - \underset{\approx}{k} \nabla \phi \tag{6.31}$$

This approach gives good results for the flux (velocity) at the optimal (integration) points of the element, but yields discontinuity in the flux at the nodal points and element boundaries. (See Zienkiewiez [41].) If the flux is required at nodal points and element boundaries, then the nodal gradient $\partial\phi$, must also be treated as an unknown in the solution process.

Results of the flux are usually only given at the optimal points within an element. (ie. The Gauss Numerical integration points.)

6.5.7 Summary.

It has been shown that the flow of water in the saturated-unsaturated domain can be expressed by a governing differential equation. This equation can then be numerically solved by the Galerkin finite element method, which gives an approximation to the solution of the flow problem. From the solution, secondary values such as the flux, can be relatively easily obtained. What makes the finite element method of great value, is that it can be easily coded, as a computer program, which can then be used for solving a variety of flow problems.

6.6 A simple example.

To show the application of the finite element method, a simple example of steady state vertical saturated flow through 3 layers of soil is considered, as shown in figure (6.2). The problem considered consists of three layers, each of a different hydraulic conductivity, placed on top of each other. At the bottom face (Face A), the total seepage head is prescribed to equal 8,0 units and at the top face (Face B), the total seepage head is prescribed to equal 20,0 units. The thickness of the layers is 4 units each, and the hydraulic conductivity is: 2,0; 1,0 and 0,5 from the top layer down, respectively.

The governing differential equation is a one-dimensional steady state version of equation (6.1) and can be written as:

$$\frac{d}{dz}\left[k \left(\frac{d\phi}{dz}\right) \right] = 0 \qquad (6.32)$$

where ϕ is the unknown total head distribution. Two types of boundary conditions may exist. Namely, Dirichlet, where the total head is

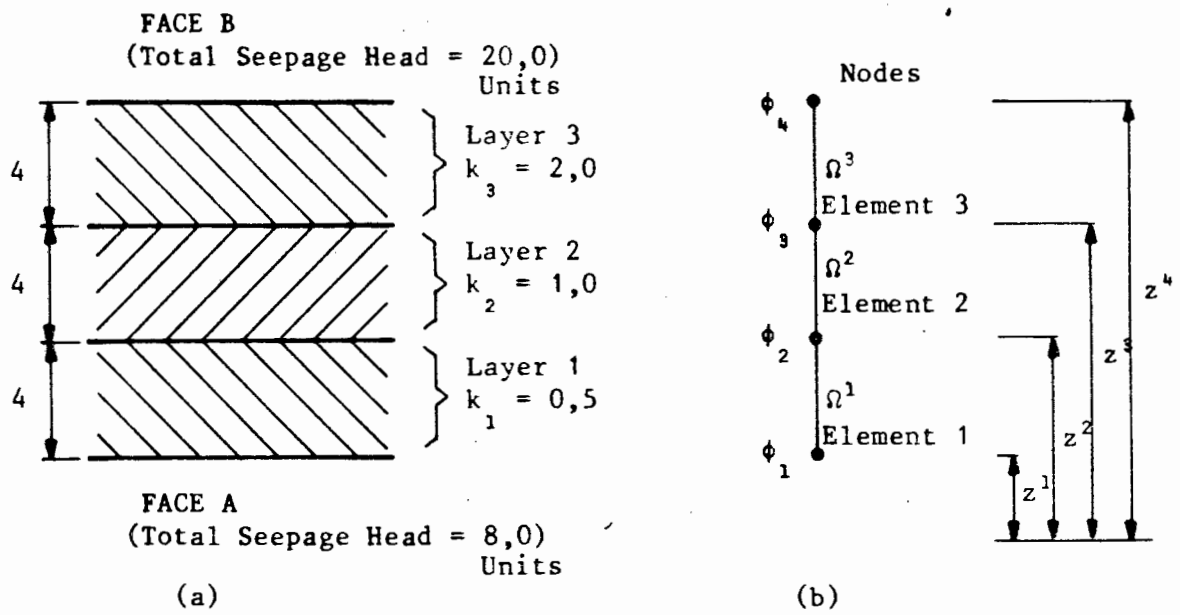

Fig 6.2: **Problem considered: (a) A three layered soil with prescribed total heads at top and bottom faces; (b) Modelled using three, two noded one-dimensional elements.**

prescribed as:

$$\phi(z_j) = \bar{\phi}_j \tag{6.33}$$

where z_j is the position (ie. node) of the boundary at which the total seepage head is prescribed. In the example considered the total seepage head boundary conditions are equal to 20 and 8 at the top and bottom boundaries of the 3 layers, respectively. The second boundary condition that may exist is Neumann, where the flux is prescribed as:

$$-k\left(\frac{d\phi}{dz}\right) = \bar{q} \tag{6.34}$$

where $\bar{q}$ is the prescribed flux boundary condition. In the example considered no such boundary condition is imposed.

For the sake of simplicity and to show the finite element method, a 2-node-one-dimensional element, which has a node at each end, is used. If a single element is first considered, the linear shape functions over the element are shown in figure (6.3) where:

$$N_1^e = \frac{(z_2^e - z^e)}{\ell^e} \tag{6.35}$$

$$N_2^e = \frac{(z^e - z_1^e)}{\ell^e} \tag{6.36}$$

and the length of the element is:

$$\ell^e = \left| z_2^e - z_1^e \right| \tag{6.37}$$

where Z is the coordinate in the direction of the element. It is noticed that:

$$N_i^e (z_j^e) \begin{cases} = 0 & i \neq j \\ = 1 & i = j \end{cases} \tag{6.38}$$

By equation (6.24), given earlier, the total seepage head over the element can be approximated by the expression:

$$\phi^e = N_1^e \phi_1^e + N_2^e \phi_2^e \qquad (6.39)$$

where N_1^e and N_2^e are the shape functions over the element, given above and ϕ_1^e and ϕ_2^e are the nodal values of ϕ.

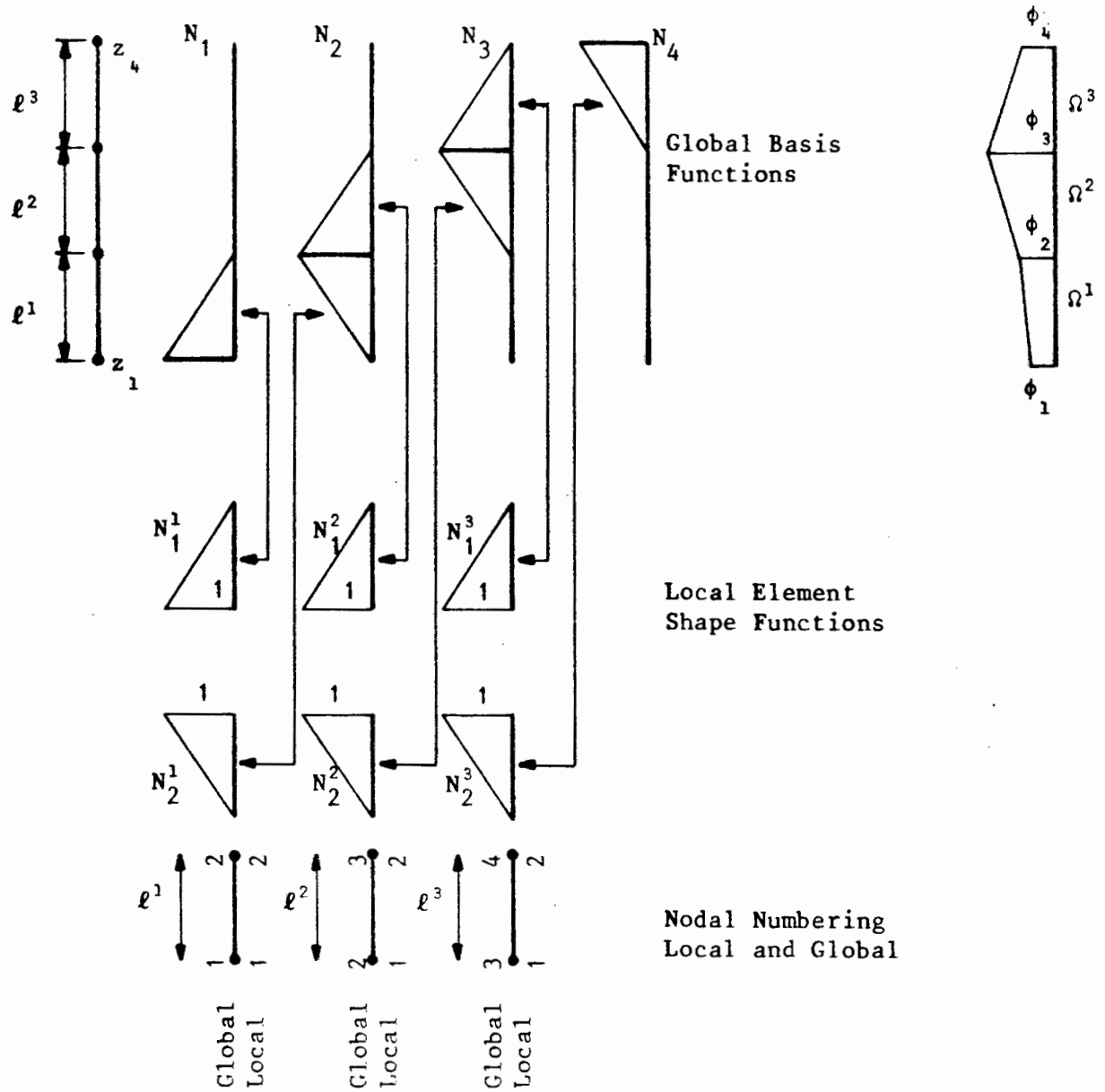

Fig 6.3: Three element representation of problem. (In Figure 6.2)

If the derivative of the total head is required, within an element, then it can be obtained from equation (6.39) by simply differentiating so that:

$$\frac{d\phi^e}{dz} = \frac{dN_1^e}{dz}\phi_1^e + \frac{dN_2^e}{dz}\phi_2^e \tag{6.40}$$

$$= \left[\frac{dN_1^e}{dz}, \frac{dN_2^e}{dz}\right] \begin{bmatrix} \phi_1^e \\ \phi_2^e \end{bmatrix}$$

$$= \left[-\frac{1}{\ell^e}, \frac{1}{\ell^e}\right] \begin{bmatrix} \phi_1^e \\ \phi_2^e \end{bmatrix}$$

The problem given in figure (6.2) can be subdivided into 3 elements, each layer being an element. Figure (6.3) shows the three element representation of the problem, with 4 nodes located at z_1, z_2, z_3 and z_4. These nodes correspond to the boundaries of the layers.

For each element, there are local shape functions which make up the global basis functions for the problem. This can be seen by noting that:

Consider any point P (at height z) where the total head is required;

N_1 coincides with $N_1^{(1)}$ when P is element 1, $z_1 < z < z_2$
N_1 is zero when P is elsewhere, $z_2 < z < z_4$

N_2 coincides with $N_2^{(1)}$ when P is element 1, $z_1 < z < z_2$
N_2 coincides with $N_1^{(2)}$ when P is element 2, $z_2 < z < z_3$
N_2 is zero when P is elsewhere, $z_3 < z < z_4$ (6.41)

N_3 coincides with $N_2^{(2)}$ when P is element 2, $z_2 < z < z_3$
N_3 coincides with $N_1^{(3)}$ when P is element 3, $z_3 < z < z_4$
N_3 is zero when P is elsewhere, $z_1 < z < z_2$

N_4 coincides with $N_2^{(3)}$ when P is element 3, $z_3 < z < z_4$

N_4 is zero when P is elsewhere, $z_1 < z < z_3$

Thus at any point P (at height z) within the mesh (ie. domain of three elements) the total head is given as:

$$\hat{\phi}_4 = N_1\phi_1 + N_2\phi_2 + N_3\phi_3 + N_4\phi_4 \qquad (6.42)$$

A solution to the approximation of the unknown ϕ, given by equation (6.42) can be found by using the Galerkin Weighted Residual method. If equation (6.42) is inserted into equation (6.32), then the left-hand side of equation (6.32) will not necessarily be zero but will have a resulting error which may be written as:

$$L(\hat{\phi}_4) = \frac{d}{dz}\left(k \frac{d\hat{\phi}_4}{dz} \right) \qquad (6.43)$$

and with boundary conditions:

$$B(\hat{\phi}_4) = -\bar{q} - k\left(\frac{d\hat{\phi}}{dz}\right) \qquad (6.44)$$

and

$$\hat{\phi}_i = \bar{\phi}_i \qquad (6.45)$$

A solution for the set of unknown ϕ_i is therefore needed to satisfy the equation:

$$\int_0^{z_4} w_j L(\hat{\phi}_4)\, dz + \int_\Gamma \bar{w}_j\, B(\hat{\phi}_4)\, d\Gamma \equiv 0 \quad \text{for} \quad j = 1,.. 4 \qquad (6.46)$$

where typically with the Galerkin Weighted Residual method, the weights w_j are taken as the basis functions N_j. It is therefore possible to write:

$$\int_0^{z_4} N_j\left[\frac{d}{dz}\left(k \frac{d\hat{\phi}_4}{dz} \right) \right] dz$$

$$+ \int_\Gamma N_j\left[-\bar{q} - k\left(\frac{d\hat{\phi}_4}{dz}\right) \right] d\Gamma \equiv 0 \qquad j = 1,.. 4 \qquad (6.47)$$

This formulation (equation 6.47) requires second derivatives of $\hat{\phi}_4$. A "weak" formulation is therefore considered, based only on the first derivative of $\hat{\phi}_4$. By integrating by parts and rearranging, equation (6.47) can be rewritten in the form:

$$\int_0^{z_4} k \frac{dN_j}{dz} \frac{d\hat{\phi}_4}{dz} dz - \int_\Gamma N_j \bar{q} \, d\Gamma \equiv 0 \quad j = 1,.. 4 \qquad (6.48)$$

Substituting for the basis functions, equation (6.48) can be rewritten as:

$$\int_0^{z_4} k \frac{dN_j}{dz} \left[\frac{dN_1}{dz}, \ldots \frac{dN_4}{dz}\right] \begin{bmatrix} \phi_1 \\ \phi_2 \\ \phi_3 \\ \phi_4 \end{bmatrix} dz$$

$$- \int_\Gamma N_j \bar{q} \, d\Gamma \equiv 0 \qquad j = 1,.. 4 \qquad (6.49)$$

This integration holds for the total system. If the relationships given by (6.41) are used, then the basis functions can be replaced by the relevant shape functions. Thus if only one element is considered for the moment with the shape functions of figure (6.3), then equation (6.49) for one element can be written as:

$$\int_{z_1^e}^{z_2^e} k^e \frac{dN_j^e}{dz} \left[\frac{dN_1^e}{dz}, \frac{dN_2^e}{dz}\right] \begin{bmatrix} \phi_1^e \\ \phi_2^e \end{bmatrix} dz$$

$$- \int_{\Gamma^e} N_j \bar{q} \, d\Gamma \equiv 0 \qquad j = 1,2 \qquad (6.50)$$

The shape functions and their derivatives have been given in equations (6.35) and (6.36) above. On substituting equations (6.35), (6.36) and (6.40) into equation (6.50) a system of two equations for an element is obtained in the form:

$$\underset{\approx}{S}^e \underset{\sim}{\phi} = \underset{\sim}{Q}^e \qquad (6.51)$$

where $\underset{\approx}{S}^e$ is the element stiffness matrix composed of four entries:

$$S_{ij}^e = \int_{z_1^e}^{z_2^e} (k^e \frac{dN_i^e}{dz} \frac{dN_j^e}{dz}) \, dz \tag{6.52}$$

and $\underset{\sim}{Q}^e$ is the force vector due to boundary conditions:

$$Q^e = \begin{bmatrix} q_1^e \\ q_2^e \end{bmatrix} \tag{6.53}$$

The integral in equation (6.52) is evaluated over the element. If one element is considered, then the first entry in the stiffness matrix in equation (6.51) is:

$$S_{11}^e = \int_{z_1^e}^{z_2^e} (k^e \frac{dN_1^e}{dz} \frac{dN_2^e}{dz}) \, dz$$

$$= k^e \int_{z_1^e}^{z_2^e} (-\frac{1}{\ell^e} \cdot -\frac{1}{\ell^e}) \, dz$$

$$= \frac{k^e}{\ell^e} \tag{6.54}$$

Similarly

$$S_{12}^e = \int_{z_1^e}^{z_2^e} (k^e \frac{dN_1^e}{dz} \frac{dN_2^e}{dz}) \, dz$$

$$= k^e \int_{z_1^e}^{z_2^e} (-\frac{1}{\ell^e} \cdot +\frac{1}{\ell^e}) \, dz$$

$$= -\frac{k^e}{\ell^e} \tag{6.55}$$

Similarly

$$S_{21}^e = -\frac{k^e}{\ell^e} \tag{6.56}$$

and

$$S_{22}^e = \frac{k^e}{\ell^e} \tag{6.57}$$

The element stiffness matrix for a single element can therefore be written as:

$$S^e = \frac{k^e}{\ell^e} \begin{bmatrix} 1 & -1 \\ -1 & 1 \end{bmatrix} \tag{6.58}$$

By virtue of the property of definite integrals, the total integral given in equation (6.46) must be equal to the sum of the parts:

$$\int_\Omega w\, L(\hat{\phi})\, d\Omega + \int_\Gamma \bar{w}\, B(\hat{\phi})\, d\Gamma$$

$$= \sum_{e=1}^{4} \left\{ \int_{\Omega^e} w\, L(\phi)\, d\Omega + \int_{\Gamma^e} \bar{w}\, B(\phi)\, d\Gamma \right\} \tag{6.59}$$

The element stiffness matrix that is obtained from equation (6.46) can be assembled from the stiffness matrix obtained for each element. On assembling:

$$S_{ij} = \sum_{e=1}^{4} \underset{\approx}{S}{}^e_{ij} \tag{6.60}$$

or where the global stiffness matrix for all the elements is:

$$\underset{\approx}{S} = \begin{bmatrix} S^1_{11} & S^1_{12} & & \\ S^1_{21} & S^1_{22} + S^2_{11} & S^2_{12} & \\ & S^2_{21} & S^2_{22} + S^3_{11} & S^3_{12} \\ & & S^3_{21} & S^3_{22} \end{bmatrix} \tag{6.61}$$

If we consider the example where $\ell^e = 4$ units for all three elements. Then the stiffness matrix for each element is:

$$S^e = \frac{k^e}{4} \begin{bmatrix} 1 & -1 \\ -1 & 1 \end{bmatrix} \tag{6.62}$$

The global stiffness matrix for the example in figure (6.2) is therefore:

$$\underset{\approx}{S} = 1/4 \begin{bmatrix} k^1 & -k^1 & & \\ -k^1 & k^1 + k^2 & -k^2 & \\ & -k^2 & k^2 + k^3 & -k^3 \\ & & -k^3 & k^3 \end{bmatrix} \qquad (6.63)$$

The values for k^e have been given earlier as:

$$k^1 = 0,5 \text{ units}$$
$$k^2 = 1,0 \text{ units}$$
$$k^3 = 2,0 \text{ units}$$

The global system of equations is written as a combination of all the pertinent element equations (from equation 6.51). ie. The global system of equations is:

$$\underset{\approx}{S}\ \underset{\sim}{\phi} = \underset{\sim}{Q} \qquad (6.64)$$

where boundary conditions imposed are:

$$\phi_1 = 8,0 \text{ units}$$
$$\phi_4 = 20,0 \text{ units}$$

Therefore using the assembled global stiffness matrix as given in equation (6.63) and the boundary conditions imposed, the set of global equations to be solved are:

$$\begin{bmatrix} 0,5/4 & -0,5/4 & & \\ -0,5/4 & 0,5/4 + 1,0/4 & -1,0/4 & \\ & -1,0/4 & 1,0/4 + 2,0/4 & -2,0/4 \\ & & -2,0/4 & 2,0/4 \end{bmatrix} \begin{bmatrix} 8 \\ \phi_2 \\ \phi_3 \\ 20 \end{bmatrix} = \begin{bmatrix} q_1 \\ 0 \\ 0 \\ q_4 \end{bmatrix} \qquad (6.65)$$

where q_1 and q_4 are the unknown fluxes at the boundary nodes and ϕ_1 and ϕ_4 (Prescribed total heads) have been inserted in their correct locations. By removing the equations 1 and 4 (ϕ_1 and ϕ_4 are already known) from the set of equations alters the terms on the right hand side and, the following set of equations need to be solved:

$$\begin{bmatrix} 1,5 & -1,0 \\ -1,0 & 3,0 \end{bmatrix} \begin{bmatrix} \phi_2 \\ \phi_3 \end{bmatrix} = \begin{bmatrix} 4 \\ 40 \end{bmatrix} \qquad (6.66)$$

Solving for ϕ_2 and ϕ_3 gives:

$$\phi_2 = 14,857 \text{ units}$$
$$\phi_3 = 18,286 \text{ units}$$

Knowing ϕ_1 ϕ_2 ϕ_3 and ϕ_4 the flux at any point can be calculated. If element number one is considered:

$$\phi_1 = 8 \text{ units}$$
$$\phi_2 = 14,857 \text{ units}$$
$$k^1 = 0,5$$
$$\ell^1 = 4$$

Then

$$q = k^1 \frac{\Delta\phi}{\ell} \qquad (6.67)$$

$$= 0,5 \frac{(14,857 - 8)}{4}$$

$$= 0,857 \text{ unit length/time}$$

For element number three:

$$\phi_1 = 18,286 \quad \text{units}$$
$$\phi_2 = 20 \quad \text{units}$$
$$k^1 = 2,0$$
$$\ell^1 = 4$$

Then

$$q = k^3 \frac{\Delta\phi}{\ell^3} \tag{6.68}$$

$$= 2,0 \frac{(20 - 18,286)}{4}$$

$$= 0,857 \quad \text{unit length/time}$$

The flux in element one equals that in element three as there is no storage in any element and the continuity equation must hold. The results obtain here are the same as those given in appendix (F-1) for the same example analysed by using a finite element program ADINAT [2]. (See section 6.8).

6.6.1 Summary of the basic steps of the finite element method.

The following is a brief summary of the main steps which are followed in a finite element analysis, which does not include changes in the time domain:

a) The structure is divided into a mesh of finite elements;
b) For each element the "stiffness" matrix and the "load" vector are evaluated;
c) The element stiffness matrices and load vectors are assembled into their respective positions in the overall stiffness matrix and load vector;
d) The prescribed boundary conditions are imposed and the set of equations solved for the unknown values of total head at the

nodes;

e) The subsidiary element quantities, such as fluxes, are evaluated. (eg. at internal points within the elements.)

6.7 Application to flow in porous media.

The numerical solution of equation (6.1) with applied boundary conditions, and all the features as described above, for a two-dimensional vertical domain, are incorporated in the code of a computer program. The program used is ADINAT [2], which is a program for the "Automatic Dynamic Incremental Non-linear Analysis of Temperatures". The program ADINAT, was written to solve the same governing differential equation (6.1), as this is also the governing equation for the temperature distribution ϕ, over a domain Ω. For seepage the unknown ϕ, is the total head, defined as the local pressure head plus the elevation head ($\psi + z$). Some changes have had to be made to the coding of ADINAT to take this into account. The changes have been incorporated into ADINAT, for two-dimensional elements orientated in the vertical plane, in the form of a new non-linear material model. (See appendix F-2).

The relative hydraulic conductivity $k_{rw}(\theta)$ is a function of the volumetric moisture content θ, but the volumetric moisture content θ, is also a function of the local pressure head ψ, see figure (2.9). Therefore the relative hydraulic conductivity k_{rw}, is also a function of the local pressure head ψ. If the hysteresis nature of the relationship between ψ and θ is neglected, the relative hydraulic conductivity k_{rw}, is a single value function of the local pressure head ψ. Similarly, the specific moisture capacity c, is a single value function of the pressure head ψ. See figure (6.4). The assumption to neglect hysteresis is possible, if either a monotonic wetting or drying domain is being considered, as only a primary wetting or drying curve, of the soil moisture characteristic curve, is being considered. (Ref Hillel [18]). See figure (2.9). Depending on the accuracy of the solution required this assumption could also be made for a simultanuous wetting and drying domain.

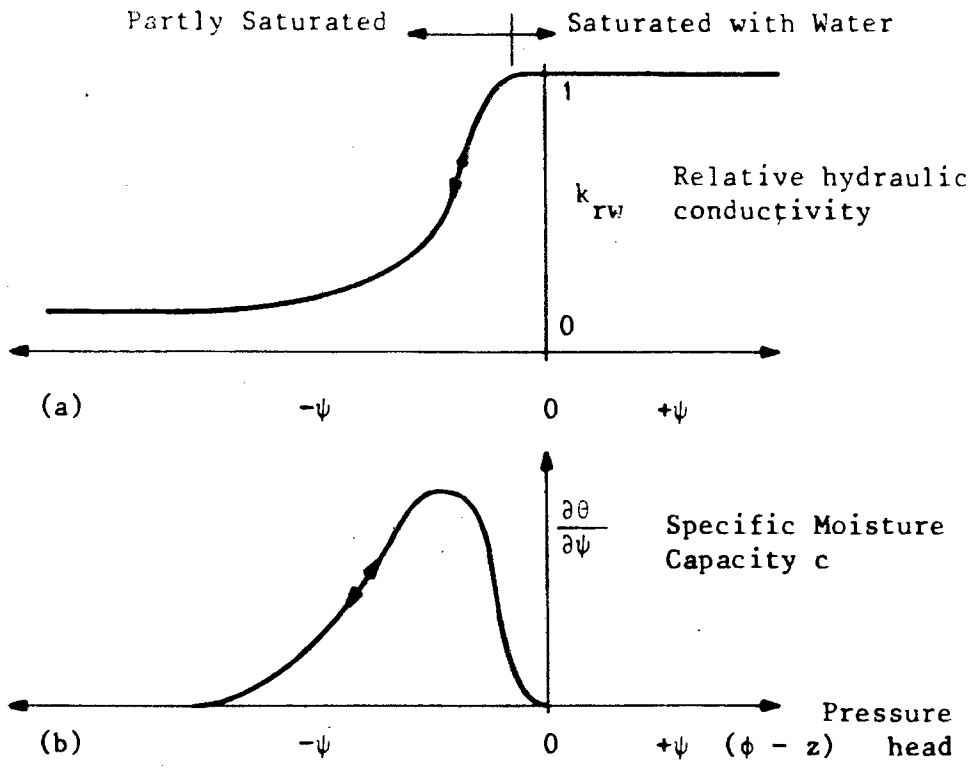

Fig 6.4: Single value function relationships for a saturated-unsaturated soils (all versus pressure head ϕ): (a) Relative hydraulic conductivity; (b) Specific moisture capacity.

Hysteresis is not considered in the present analysis. Only a single functional relationship is considered between ϕ, k_{rw} and c. This is incorporated into the program analysis by linear interpolation between discrete tabulated values in the input data of the program, where $k_{rw}(\phi)$ and $c(\phi)$ are considered as non-linear material parameters in the model. It is therefore assumed that:

$$k_{rw}(\phi) = 1 \qquad \text{for} \quad \phi \geq 0 \qquad (6.69a)$$

and

$$0 \leq k_{rw}(\phi) \leq 1 \qquad \text{for} \quad \phi \leq 1 \qquad (6.69b)$$

where $k_{rw}(\phi)$ is assumed as a non-linear material. see figure (6.4).

The nature of ADINAT, allows both confined and unconfined problems to be

solved. The candidate incorporated saturated-unsaturated conditions within ADINAT. In the program, the total head ϕ, is treated as the unknown variable. Specific values of $\bar{\phi}$ or $\bar{q}$ can be specified as a function of time for the nodes and boundary surfaces with Dirichlet or Neumann boundary conditions respectively. (See figure 6.5). The relative hydraulic conductivity k_{rw} and the specific moisture capacity c, can be tabulated as functions of: either time t; the unknown total head ϕ; or the pressure head ψ ($\psi = \phi - z$, where z is the vertical elevation), with constant material model parameters over each element within the saturated-unsaturated domain.

Some of these features are demonstrated later by examples. Firstly the input and output data for the program ADINAT is discussed.

6.8 Operation of the finite element program package.

The finite element program package used for the finite element analysis done, was ADINAT, version 84.00 [2]. Modifications were made to the program material model (see Section 6.9), so that the material parameters could be entered as functions not only of total head, but of pressure head as well. This program package was loaded on the

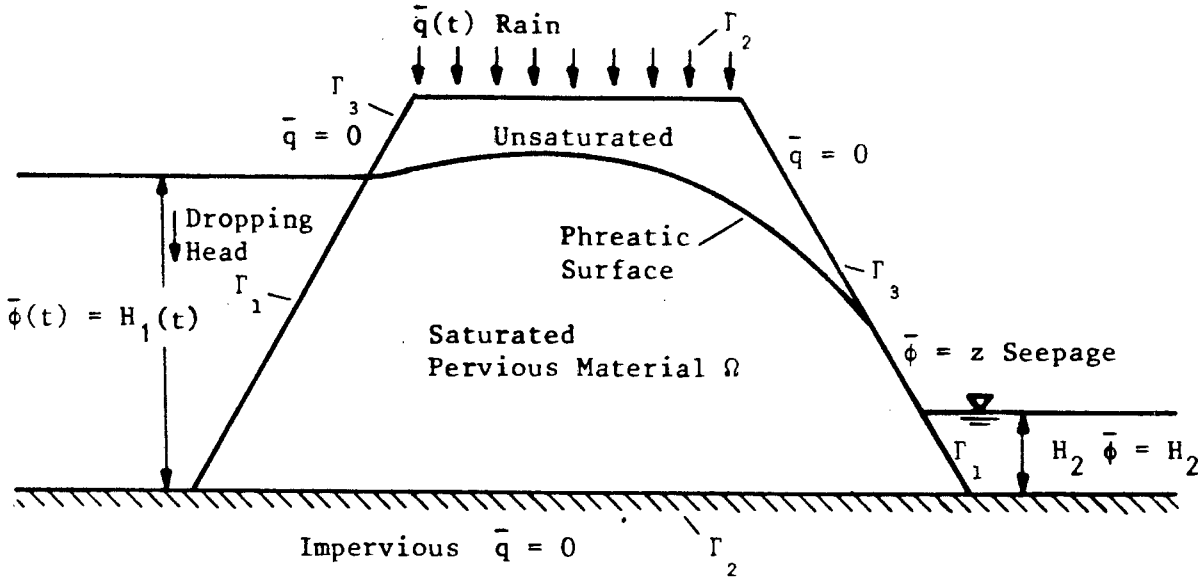

Fig 6.5: **Saturated-unsaturated flow domain Ω enclosed by a boundary Γ.**

University of Cape Town's mainframe computer (Sperry Univac 1100) and permission to use the program was granted by Prof. W S Doyle.

Data input is entered in fixed format as specified by the users' manual [2]. Character variables may appear anywhere in the space set aside. Integer variables must be right-adjusted in the spaces set aside. Real number variables may be written with or without a decimal point in the space set aside. If the decimal point is not included then the real number must be right-adjusted. In the users' manual [2] each card or card group is identified by name and the format used on the card(s), with the name of the variables being given. The meaning of the variables and notes are also provided.

The general groups of data input are as follows:

Group 1: Heading

Group 2: Master Control Data
This group is always input and includes the following: number of nodes; number of linear and non-linear element groups; solution mode; number of time-steps; time of solution start and output interval; form of generated input data, output; analysis type; convergence tolerances; method of time integration; and control of output.

Group 3: Time step Data
This controls the number and size of the time step.

Group 4: Nodal point Data
This is the nodal coordinate data.

Group 5: Initial Conditions
This specifies the initial conditions for the total heads at all nodes.

Group 6: Boundary Condition Control Data
This specifies the number of nodes involved with boundary conditions.

Group 7: Definition of Time Functions
This specifies the time function curves for the various boundary conditions.

Group 8: Applied Seepage Flow Data
This includes the prescribed nodal values and flux conditions.

Group 9: Element Group Data and Topology
This includes the following: element type; number of elements in group; problem type; number of nodes per element; order of integration; material poperties (see sections 6.9.1, 6.9.2 and 6.9.3); and nodes that make up each element (topology).

An example of an input data file, for the problem considered in section (6.6), is given in appendix (F-1).

6.9 Finite element material models.

For the analysis of seepage problems presented in this thesis, three different material models were used. The range is from saturated seepage problems - where the material properties do not change during the analysis, to a highly saturated-unsaturated problem with varying material properties which depend on the total head or pressure head. (Time dependent properties can also be considered by the program ADINAT [2]).

6.9.1 Constant saturated hydraulic conductivity model.

This is a linear model defined by one hydraulic conductivity constant for an isotropic material. The model is used for steady-state linear

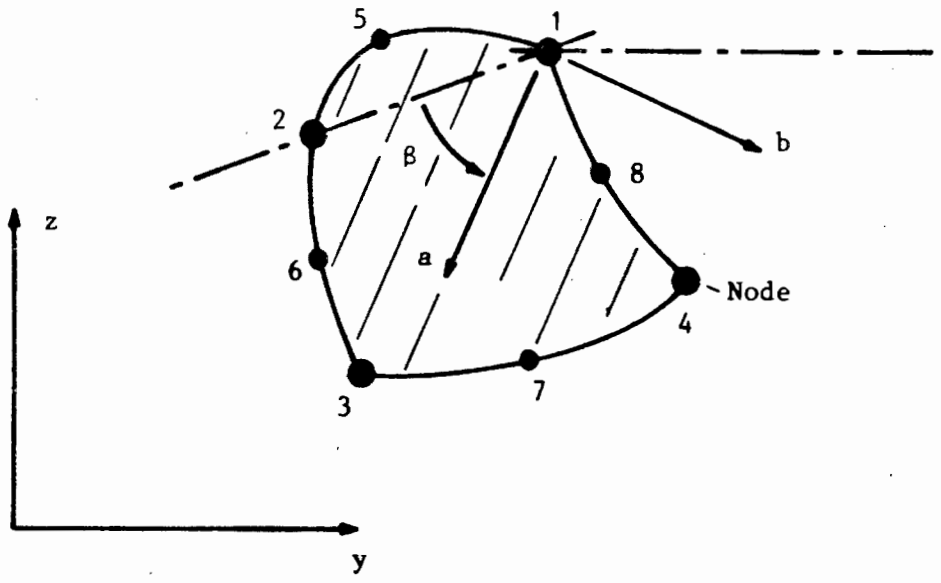

Fig 6.6: **Principal in-plane material axes orientation for the linear orthotropic material model. ADINAT [2].**

analysis and no time stepping is required. This is because the specific moisture capacity term is zero in equation (6.28), and therefore the time domain is not considered. The solution of the unknown total heads over the domain can be directly solved with the applied boundary conditions.

The terms required for the material properties for an analysis are:

Saturated hydraulic conductivity for an isotropic material

$$k$$

or Saturated hydraulic conductivity in the two orthotropic directions

In direction a: k_a
In direction b: k_b

and for each element the angle

$$\beta$$

for an anisotropic material, as shown in figure (6.6).

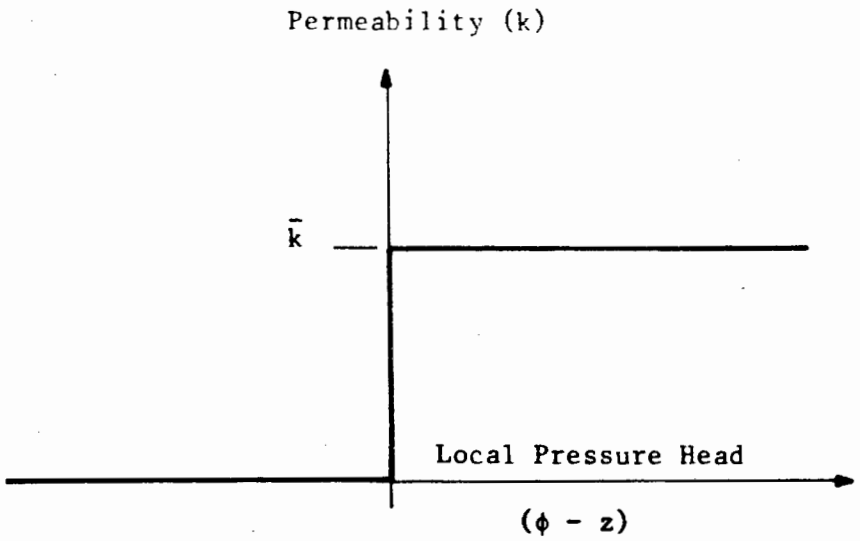

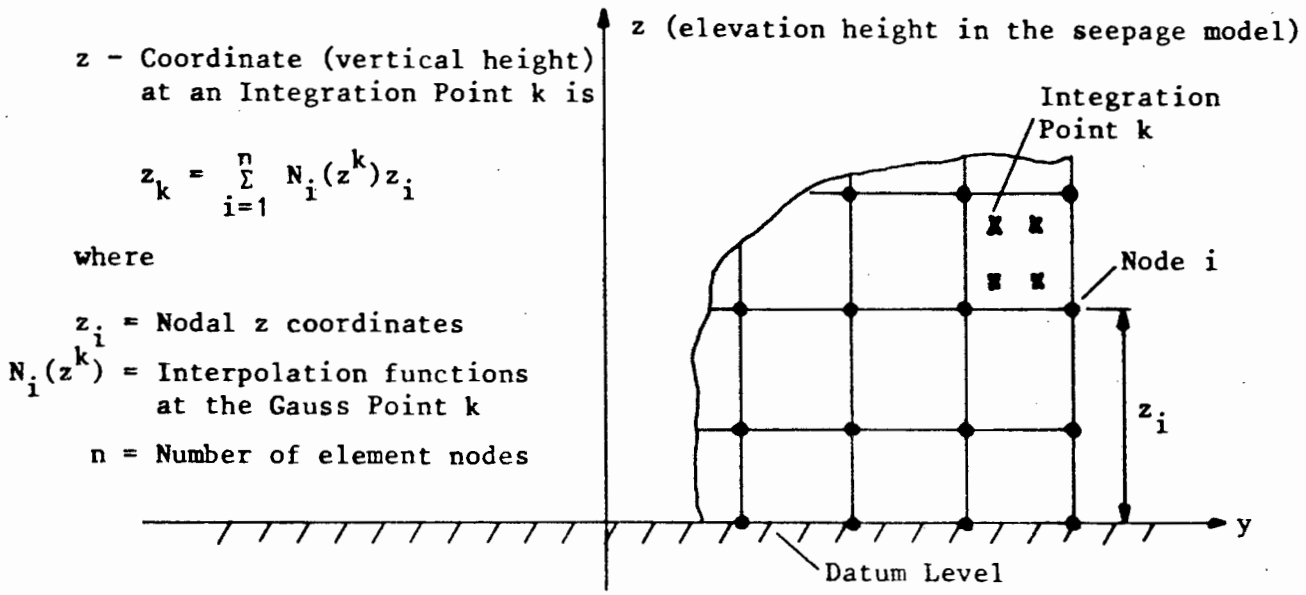

Fig 6.7: Material behavior and element modelling for two-dimensional seepage model. ADINAT [2].

6.9.2 Steady-state phreatic surface seepage model.

This is a non-linear model developed by Bathe et al [5] for the solving of steady-state unconfined seepage problems with a phreatic surface. No mesh re-organising is required during the analysis, as the hydraulic conductivity is modelled by a non-linear material model. In the non-linear material model the hydraulic conductivity k, used in the calculation of the seepage flow vector is defined as:

$$k = \begin{cases} 0 & \text{for} \quad \phi < z \\ \bar{k} & \text{for} \quad \phi > z \end{cases} \tag{6.70}$$

where ϕ is the total potential head and z is the elevation head, see figure (6.7). It is noticed that the line $\phi = z$ corresponds to the phreatic surface (free surface) in the model, above which no flow can occur.

The model can only be used for isotropic material and the only term required for the material property for an analysis is the:

Saturated hydraulic conductivity

$$k$$

6.9.3 Saturated-unsaturated flow model.

This is a non-linear material model incorporated into the program by the writer for the solving of saturated-unsaturated flow problems. No mesh re-organising is required during the analysis, as the hydraulic conductivity is defined by a non-linear material model and the complete saturated-unsaturated domain is treated as a single problem.

With this model, transient analysis is involved and the specific moisture capacity is therefore (See figure 6.4) also required. For an isotropic analysis figure (6.8) shows the material behaviour for the

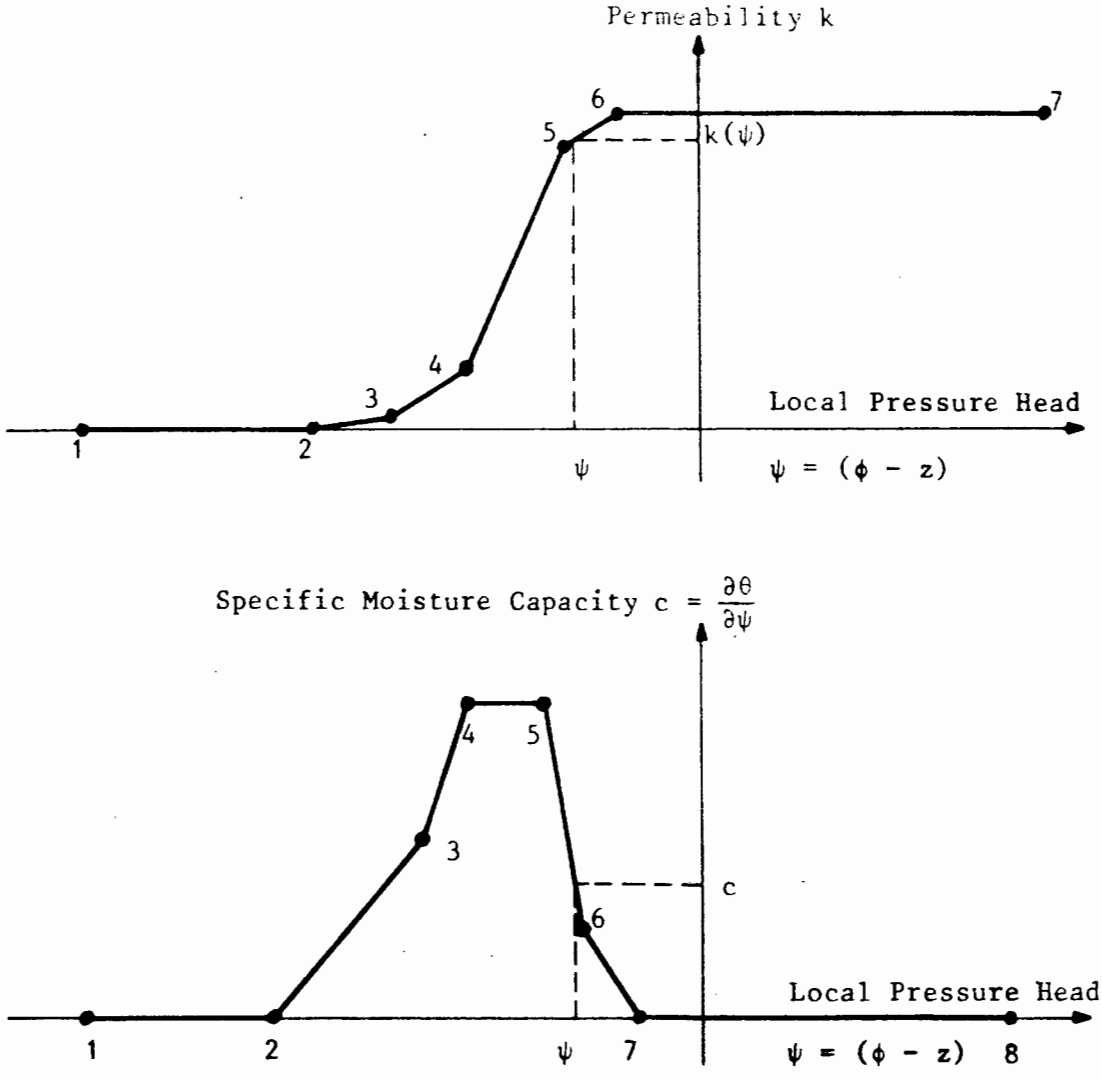

Fig 6.8: **Material** behaviour **for two-dimensional saturated-unsaturated seepage model. Interpolation shown as a function of pressure head for: (a) The current conductivity; (b) The specific moisture capacity.**

model. With this non-linear model both the hydraulic conductivity and specific moisture capacity are functions of the pressure head. Linear interpolation is used in figure (6.8) to obtain the hydraulic conductivity and specific moisture capacity of the material at intermediate positions between the points for which data is entered in tabular form.

For isotropic hydraulic conductivity material, only a tabular entry of the hydraulic conductivity and the specific moisture

and for each element one must specify the angle (See figure 6.9):

β

where k_a and k_b are the hydraulic conductivities in the two principle directions of the anisotropic medium.

6.10 Output from finite element package.

The output of results depends on the analysis done. For a steady-state analysis the following is the output:

- the total seepage head at each node;
- the pressure heads at the element integration points;
- the flux at the integration points within the elements.

For a transient analysis the above is also the output, but only at the time steps requested. The extent of output is controlled by the user (eg. the nodes and elements for which output is required can be specified).

The flux output at the Gauss integration points is determined by using equation (6.31).

For the analyses done in this thesis, the flux values were usually not needed as the pressure heads were used for comparing results. This was because in the experiments done by the writer, pressure heads were usually measured. The horizontal flux values were however compared, as shown in figure (6.25), in the verification of experiment number one.

The finite element package did have a flag to output the nodal and element results into a file for post-processing, but the post-processor was not yet available at the University of Cape Town. This is because the version of ADINAT [2] used was a new version and the post-processor had not yet been released.

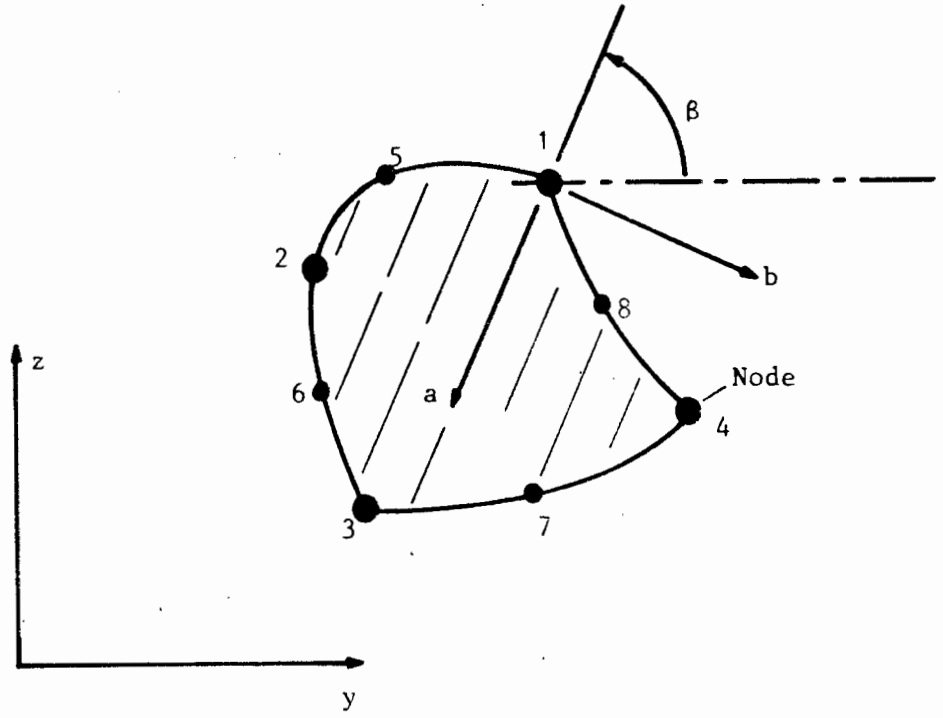

Fig 6.9: Principal in-plane material axes orientation for the saturated-unsaturated orthotropic seepage material model.

capacity is needed. Namely values of:

$$k(\phi)$$
$$c(\phi)$$

For anisotropic hydraulic conductivity material, a tabular form of the hydraulic conductivity and specific moisture capacity is still required. Namely:

$$k_a(\phi)$$
$$c(\phi)$$

but the ratio between $k_a(\phi)$ and $k_b(\phi)$ is also needed:

$$\text{Ratio} = k_a/k_b$$

6.11 Finite element examples and program verification.

6.11.1 Introduction.

To show some of the features of the finite element program package ADINAT [2] and also to verify the material model implemented by the writer, a few varied seepage problems were considered. The problems considered included:

a) The analysis of steady-state confined saturated flow around a raking sheet pile in a stratified, anisotropic foundation. (See figure 6.10);
b) The analysis of steady unconfined free surface flow through an earth dam with a toe drain. (See figure 6.11);
c) The transient analysis of saturated-unsaturated flow in a rectangular dam caused by a change in tail-water level. This causes a decline of the phreatic surface towards a new steady-state flow system. (See figure 6.13);
d) The analysis of non-steady saturated-unsaturated flow between drains after rapid drawdown. (Using observations by others. See figure 6.16).
e) The transient analysis in a rectangular dam caused by a change in tail-water level. This is for a saturated-unsaturated transient flow system. (Experiment by candidate. See figure 6.19).
f) Analysis and observation of non-steady saturated-unsaturated flow into drains after rapid-drawdown. (Work by candidate. See figure 6.26)

The results are presented mainly as a function of the total or pressure head. Where possible comparisons are shown with the results obtained by other investigators for experimental or theoretical analysis done.

Note: Only two-dimensional flow in a vertical plane is considered.

The (implicit) backward difference time marching scheme is used with lumping of the Mass matrix for the transient examples considered. This method is suggested by Neuman [31] so that

oscillatory and instability problems of two point recurrence schemes are overcome.

6.11.2 Example No. 1: Saturated confined seepage.

In this example (See figure 6.10a), the total head distribution in a stratified, anisotropic foundation with an inclined wall of sheet piling is studied. It is possible to compute the analytical solution for the flow by using conformal mapping. The analytical solution was not found.

The problem consists of a sheet pile inclined at 52^{o}, and a stratified soil with the inclination of the orthotropic axis for the principal hydraulic conductivity of the soil at 60^{o}. (See figure 6.10a). The ratio of the hydraulic conductivities is taken as 4. A prescribed total hydraulic head of 100 and 0 at the upstream and downstream surfaces is applied respectively.

The problem is solved as a steady-state problem with a constant material model and prescribed total head boundaries. The results obtained by a finite element analysis of the total head distribution, using ADINAT, are given at the appropriate nodes, as shown in figures (6.10a and b). From these results the equipotentials have been drawn, which are distorted due to the stratified foundation. As the stratification of the foundation and the sheet pile are inclined in a similar direction, it would be expected that the mid-equipotential line between the upstream and downstream total heads corresponds to this direction. This has been predicted by the results from the analysis as shown in figures (6.10a and b).

6.11.3 Example No. 2: Unconfined free surface steady state flow.

The total head distribution below the free surface of steady-state seepage through a dam with a toe drain, as shown in figure (6.11), is analysed. The dam consists of an upstream water level, constant with time at an elevation of unit 1 and a toe drain at the downstream face of the dam with a tail water level at elevation 0,1. The material model used for the analysis is that described in section (6.9.2), with the

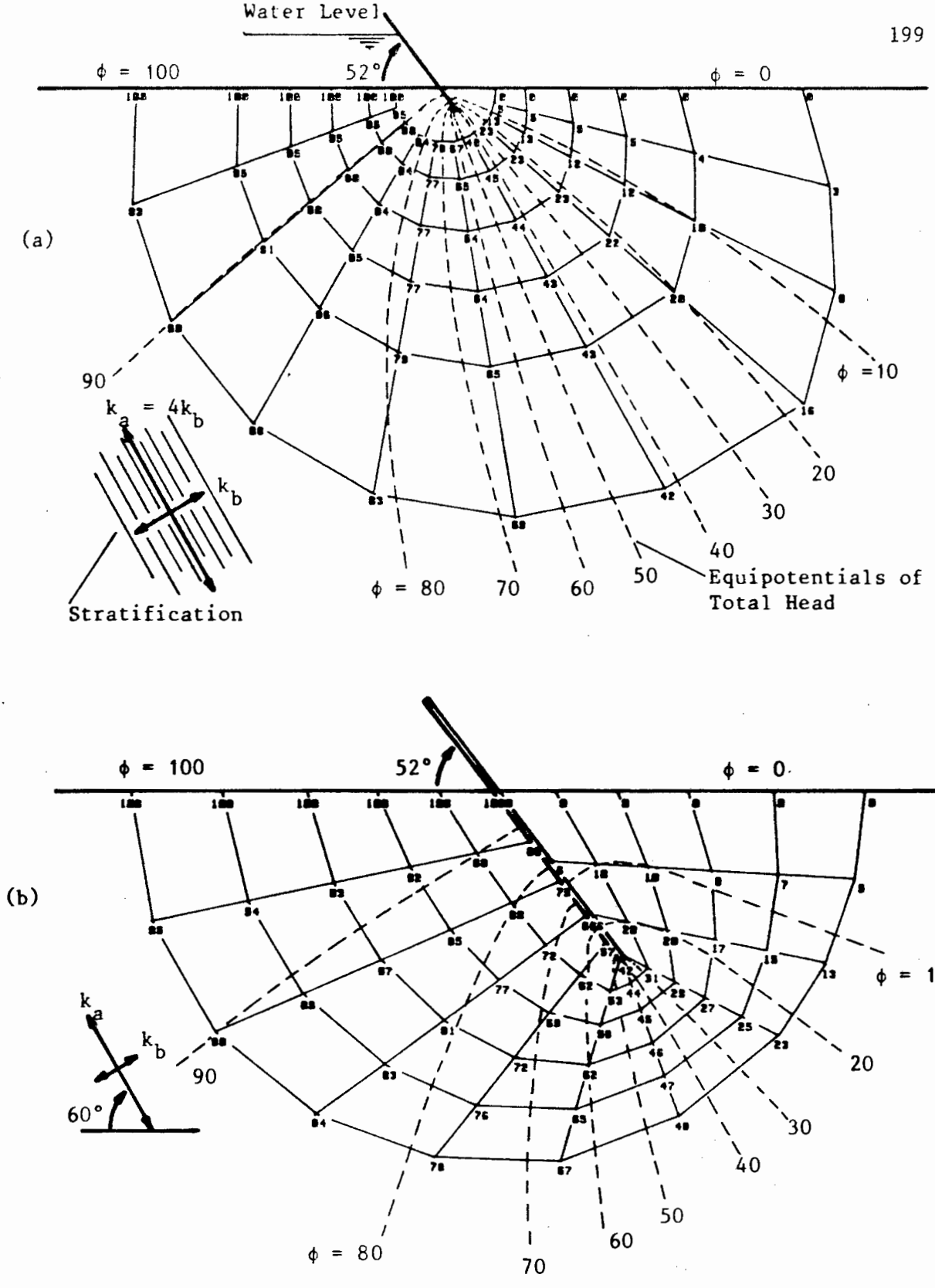

Fig 6.10: Flow around an inclined sheet pile wall in a stratified (anisotropic) foundation. (a) Complete region analysed. (b) Finer mesh near tip of pile. (This analysis by the candidate using ADINAT). The angle of 52° for inclination of pile wall may be different from that used by previous workers.

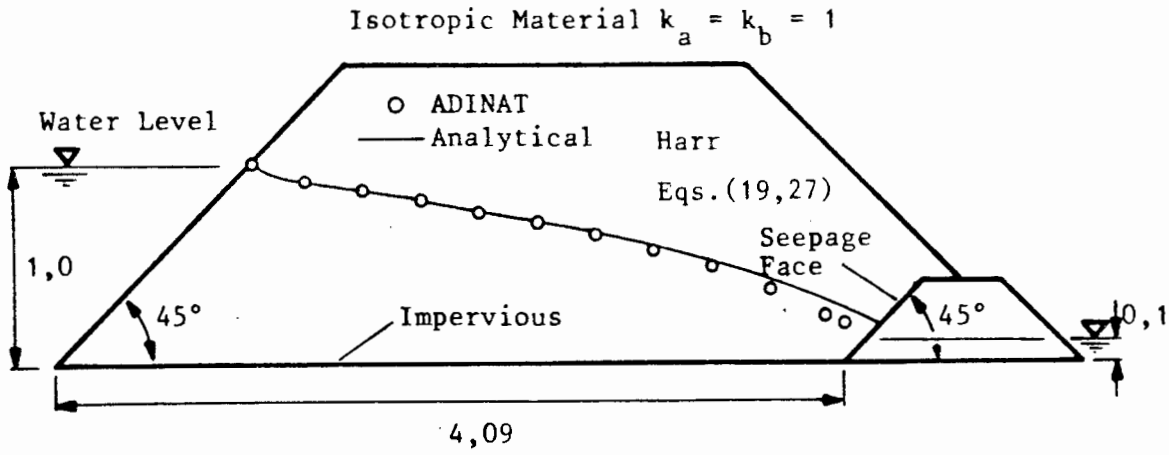

Fig 6.11: Seepage analysis of the unconfined free surface steady-state flow through an earth dam with a toe drain.

saturated hydraulic conductivity taken as 1,0. Figure (6.11) shows the results of the free surface obtained numerically by ADINAT, using the finite element mesh as shown in figure (6.12). The results are compared with that obtained from an analytical solution using conformal mapping. The charts and tables for the analytical solution are given in Harr [16]. Using these charts and tables a plot of the free surface could be made as shown in figure (6.11).

The results obtained from the finite element method show a good comparison with that of the analytical solution, except near the seepage face of the toe drain. Near the seepage face some of the elements have been reduced to triangles from four noded elements. Also the mesh used is not very fine. The reason for the discrepancy in the solutions could be caused by the reasons given above or partly caused by them. In this outflow zone the first node above the tailwater level is located at a height of 0,2 units. (See figure 6.12). It is possible that ADINAT regards this node as having no flux. At the lowest node (submerged) the tailwater level is 0,1 units and hence ADINAT will regard the outflow surface as being up to the tailwater level. (ie 0,1 units high). In practice there will also be an outflow surface above the tailwater levels which does not seem to have been simulated by ADINAT in this instance. The problem could be re-analysed using a finer mesh near the seepage face, to check the above.

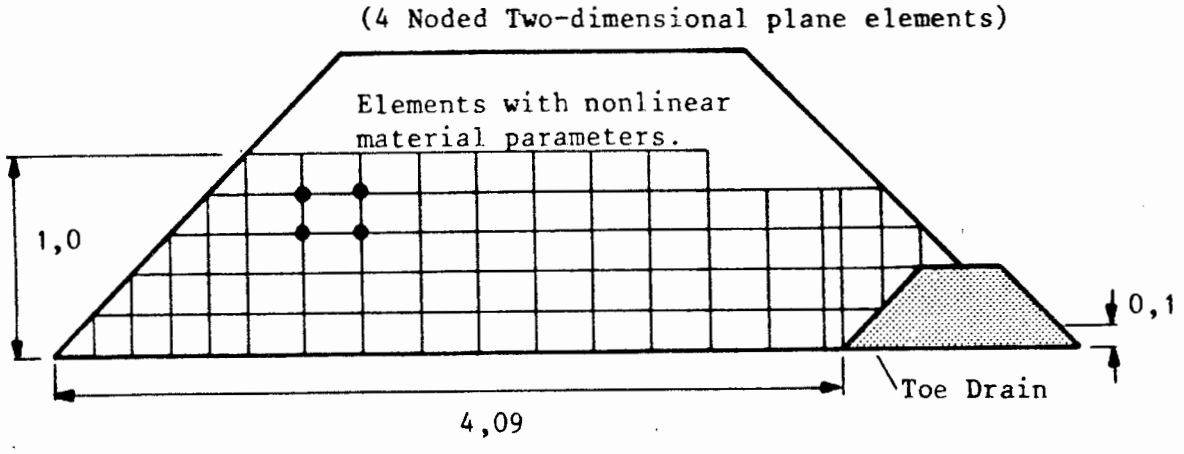

Fig 6.12: Finite element mesh used by candidate for the analysis of the dam. (Figure 6.11).

6.11.4 Example No. 3: Drainage from a saturated-unsaturated system.

In this example a vertical domain is considered, in which part of the domain is saturated and part is unsaturated. Figure (6.13) shows schematically the lay-out of the problem. Initially, the water table in the problem is at an elevation 143 cm . At time t = 0 the water level in one reservoir is lowered to an elevation of 80 cm and this situation is maintained indefinitely. The resulting hydraulic gradient causes the water table to drop gradually at a rate indicated by the solid curves in figure (6.13). The sand below the water table remains saturated during the drainage, while the region above has varying degrees of saturation.

This problem was also studied by Narasimhan et al [30] in which he gives the data for the highly non-linear relationship between ϕ, k_{rw} and c, see Table (6.3). Figure (6.14) shows the layout of the finite element mesh used in the present analysis, which is the same as the mesh used by Narasimhan et al. for simulating the experiment. The unkown total head ϕ at all nodes is given an initial value of 143 cm at t = 0. The problem is then solved for t > 0. Fixed nodal values of total head (143 cm) are imposed on the RHS boundary of the problem. Along the LHS for the zone below the water level in the reservoir, nodal values for the total head are fixed at 80 cm and the seepage face above the water

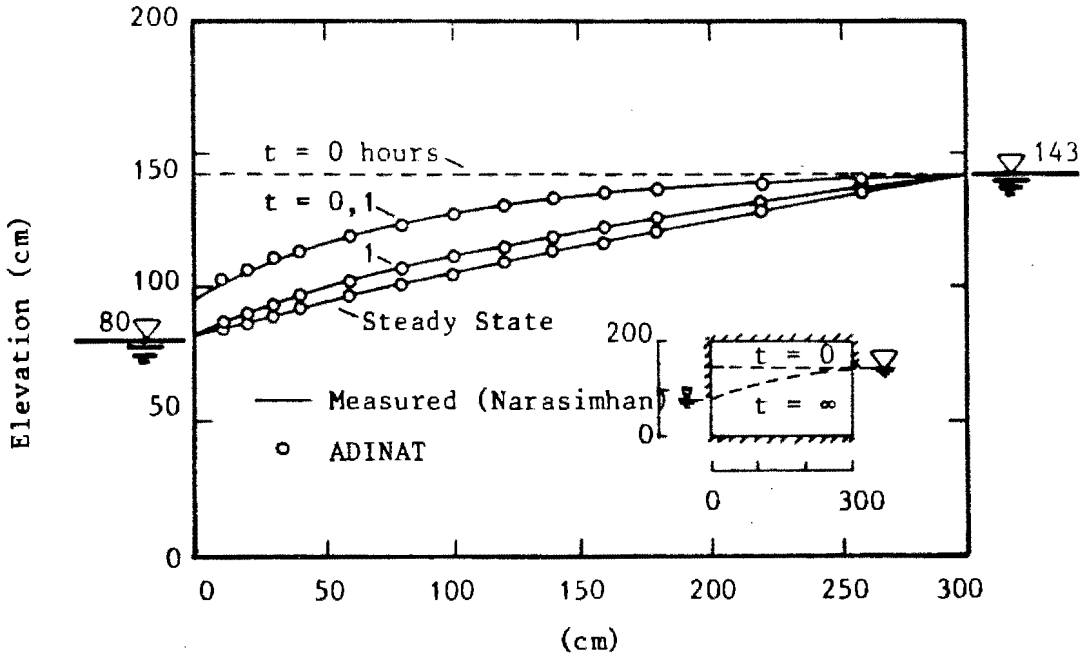

Fig 6.13: Decline of water table in a drainage experiment of a saturated-unsaturated system. Numerical results from ADINAT compared with measured results from Narasimhan et al. [30].

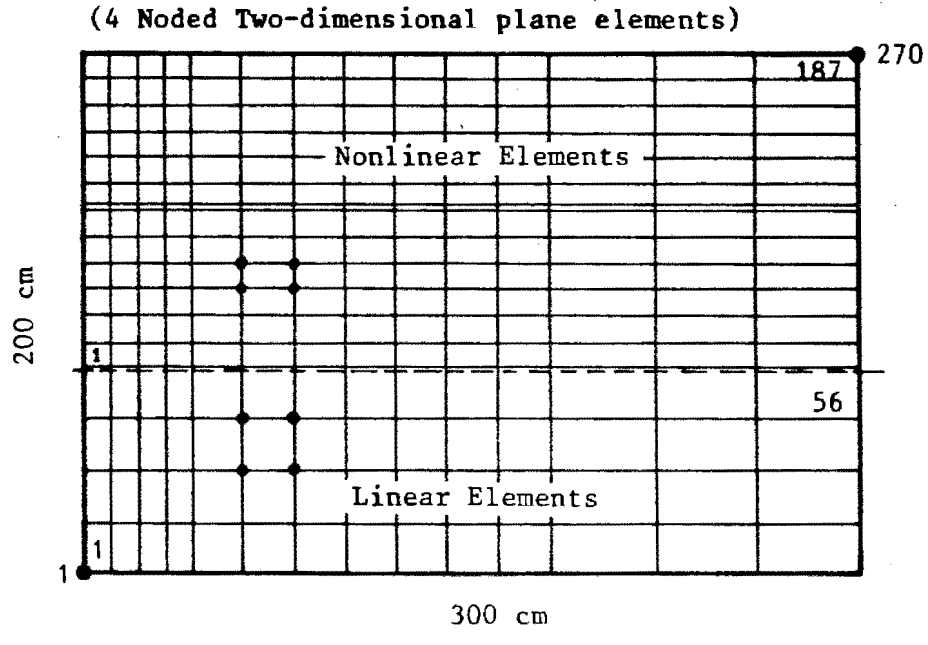

Fig 6.14: Finite element mesh used by candidate to simulate the experiment reported in Narasimhan et al. [30]. Flow in the saturated-unsaturated domain.

level is treated as a flux boundary condition. The flux boundary condition, only allows flow out of the boundary and the flux is zero if the local pressure head becomes negative.

The problem was solved using Euler backward difference time stepping and the results were printed at time t = 0,1 hours and 1 hours. The steady state water table is obtained by assuming no specific moisture capacity (i.e. taking the time dependence out) and solving the problem as a linear problem with non-linear, material properties and boundary conditions. Figure (6.13) shows the various positions of the water table, as given by the numerical results from this analysis using ADINAT, and the corresponding experimental data. [30]. The two are in excellent agreement with each other.

Table 6.3: Relationships between ϕ, k and c for drainage problem. Narasimhan et al. [30]

ϕ (cm)	c (cm^3/cm)	k (cm/s)
-90	7×10^{-4}	
-80		$1,94 \times 10^{-7}$
-75	$1,3 \times 10^{-3}$	
-65	$2,0 \times 10^{-3}$	
-60		$6,94 \times 10^{-6}$
-55	$3,1 \times 10^{-3}$	
-50		$1,94 \times 10^{-5}$
-45	$4,6 \times 10^{-3}$	
-40		$6,94 \times 10^{-5}$
-30	$5,9 \times 10^{-3}$	$8,33 \times 10^{-4}$
-25		$1,73 \times 10^{-3}$
-20		$3,72 \times 10^{-3}$
-17,5	$4,2 \times 10^{-3}$	
-12,5	$2,5 \times 10^{-3}$	
-10		$1,02 \times 10^{-2}$
-7,5	$1,0 \times 10^{-3}$	
-4		$1,12 \times 10^{-2}$
-2,5	$1,6 \times 10^{-4}$	
0	$1,0 \times 10^{-5}$	$1,12 \times 10^{-2}$

6.11.5 Example No. 4: Non-steady state flow betweens drains after rapid drawdown.

A problem of this type arises when parallel drains or ditches are placed, as shown in figure (6.15), to lower the water table. The depth and spacing of the drains are two important factors that control the lowering of the water table. The problem can be considered as a two-dimensional problem in the vertical plane with only half the distance between the drains taken for modelling, because the line of symmetry acts as an impervious layer. This problem is considered by subdividing the domain, into a mesh of 4 noded elements, as shown in figure (6.18). The initial total head is 19.7 inches. At time t = 0, the water level in the ditch is lowered to the base and the ditch face treated as a seepage face. The line of symmetry and the base are treated as impervious boundaries (i.e. $\bar{q} = 0$).

This problem has also been considered by other authors, Desai [12] and France et al [13], but only the saturated hydraulic conductivities and specific yields are given in these references:

Hydraulic conductivity: $k = 0{,}0674$ inches/sec
Specific yield: $S_y = 0{,}886$

To be able to use the program ADINAT, not only must the saturated hydraulic conductivity be known, but the relative conductivity k_{rw} as well, so that the problem can be solved as a saturated-unsaturated problem over the domain. Since this is not given the relative curves are assumed for analysing the problem.

The assumed functions for the relationships of ϕ, k_{rw} and c are shown in figure (6.17). The relationship between ϕ and c was assumed so that the area under the graph yielded the specific yield (i.e. $S_y = 0{,}1 \times 0{,}866 + 0{,}9 \times 0{,}866$). Using these assumed relationships, the problem was solved using ADINAT. Figure (6.16) shows the results for the solution of the problem, given by; Desai [12] a one-dimensional finite element solution, France et al [13] a three-dimensional finite element

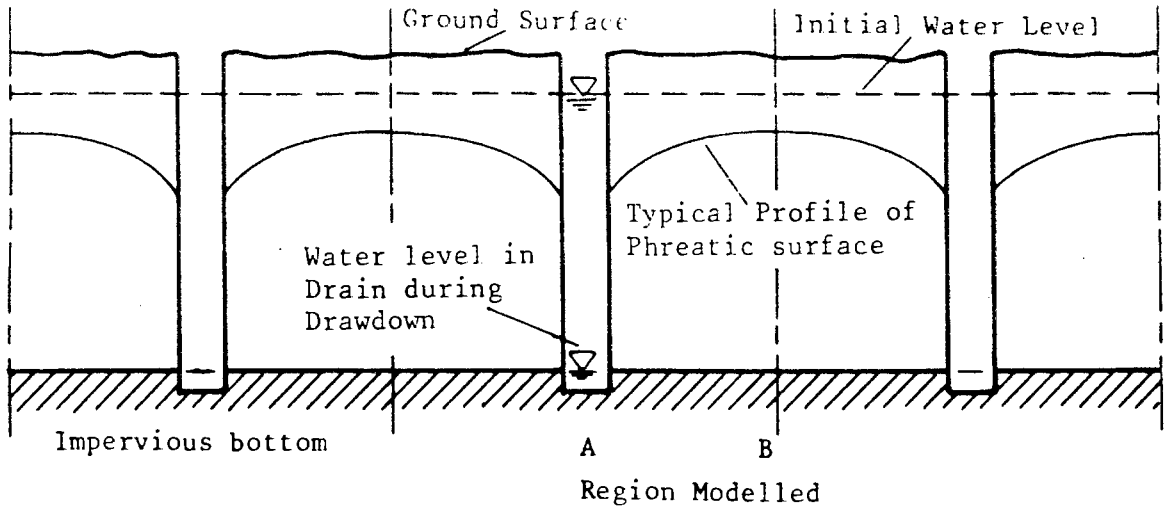

Fig 6.15: Rapid drawdown between parallel drains.

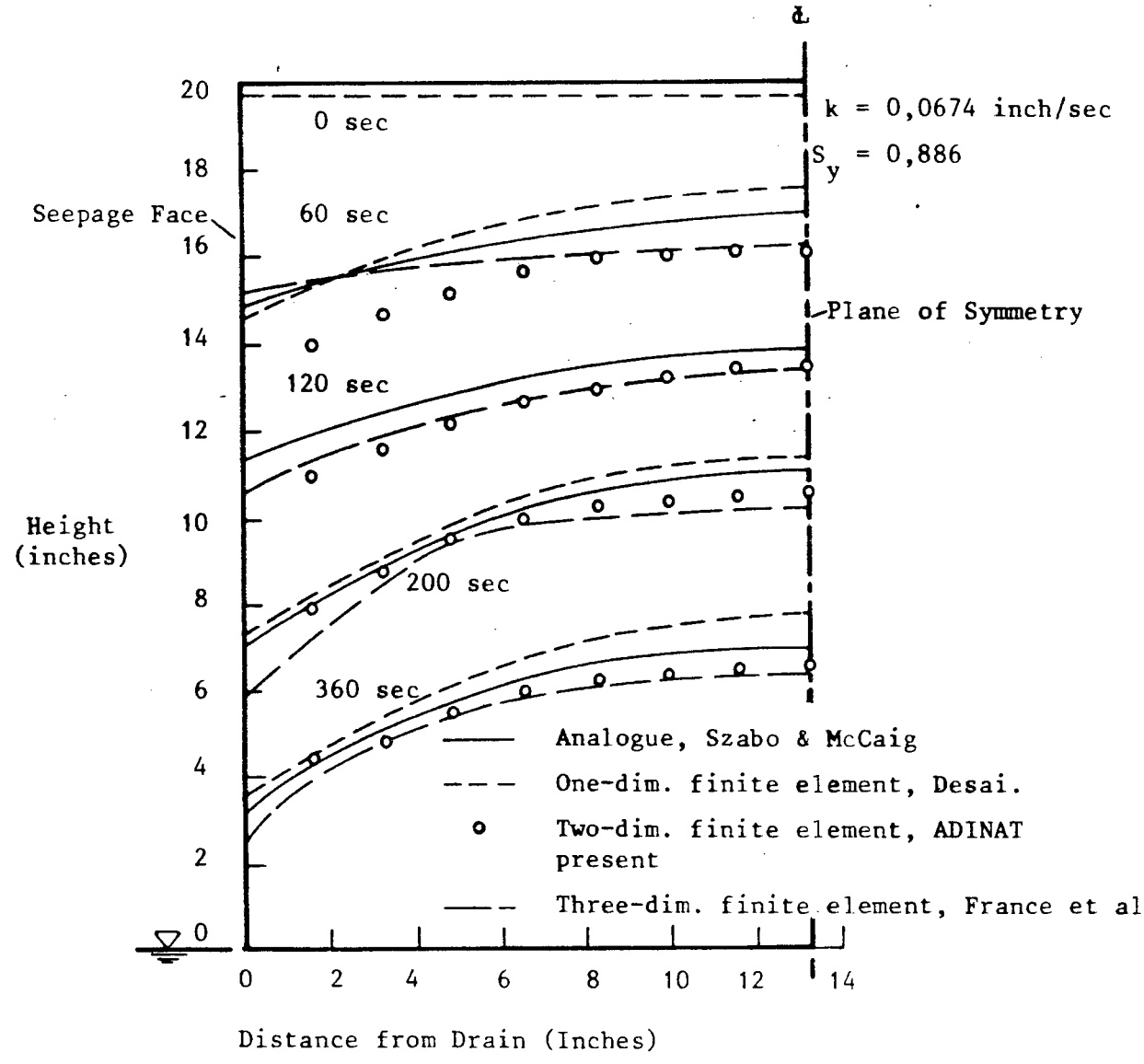

Fig 6.16: Comparisons of the decline of the phreatic surface with rapid drawdown between parallel drains.

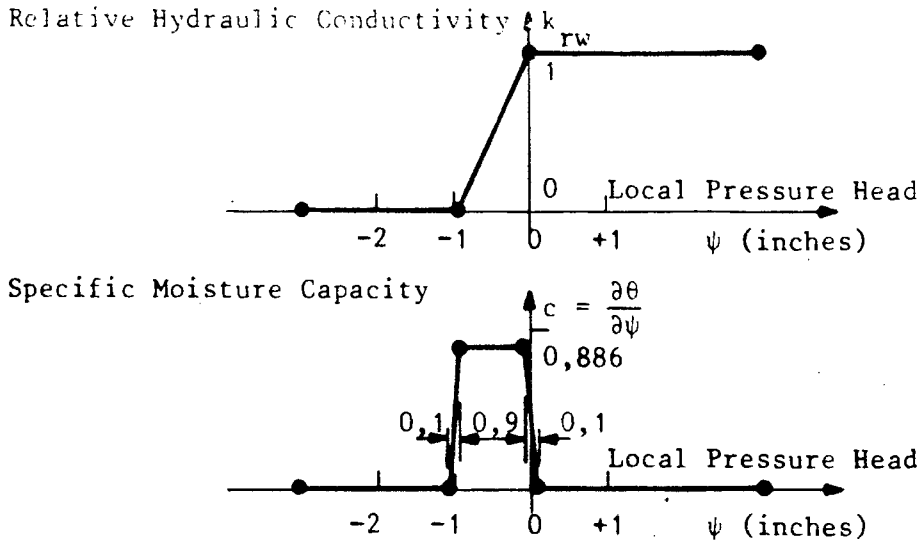

Fig 6.17: **Assumed functional relationships between ϕ, k_{rw} and c for drainage problem of rapid drawdown between drains. (Section 6.11.5)**

solution, the reported analogue solution by Szabo and McCaig, and the solution by ADINAT using two-dimensional finite elements.

For the early stages of the simulation by ADINAT (eg. time t = 60 sec), the predicted drainage rate is too great. (See figure 6.16). As time progresses the predicted solution improves and shows good agreement with the reported results. This discrepency at the start of the predication could be caused by the coarse mesh and the method of modelling the seepage face as nodal fluxes. For the time t = 60 sec, the solution predicted by the reported results from references all coincide at the drainage seepage face with the midpoint of the element face of the mesh used in the finite element model by ADINAT. The phreatic surface for ADINAT at this seepage face tends to a lower node. (See figure 6.16). For later time steps, the predicted results are good near this outflow surface, but boundary effects can still be observed. These boundary effects are most noticeable at time t = 360 sec, where a kink in the predicted results occurs near the seepage face. Because ADINAT is based on the concept that on the seepage face, above the tailwater level, the nodes either allow a seepage flux (when the local pressure head is zero) or have no seepage flux (when the local pressure head is less than zero)

the boundary effects on the outflow surface can lead to incremental errors when using ADINAT. The phreatic surface at the outflow surface, above the tailwater level, must coincide with a nodal point of the finite element mesh. For example when time t = 360 seconds the phreatic surface passes through the node at the z height of four inches on the drainage surface. (Aside: Below the phreatic surface the local pressure head must be equal to zero, ie. atmospheric pressure, on the drainage surface above the tailwater level.)

A method of overcoming this could be to use a finer mesh near the seepage boundary, particularly in the vertical direction, so that the

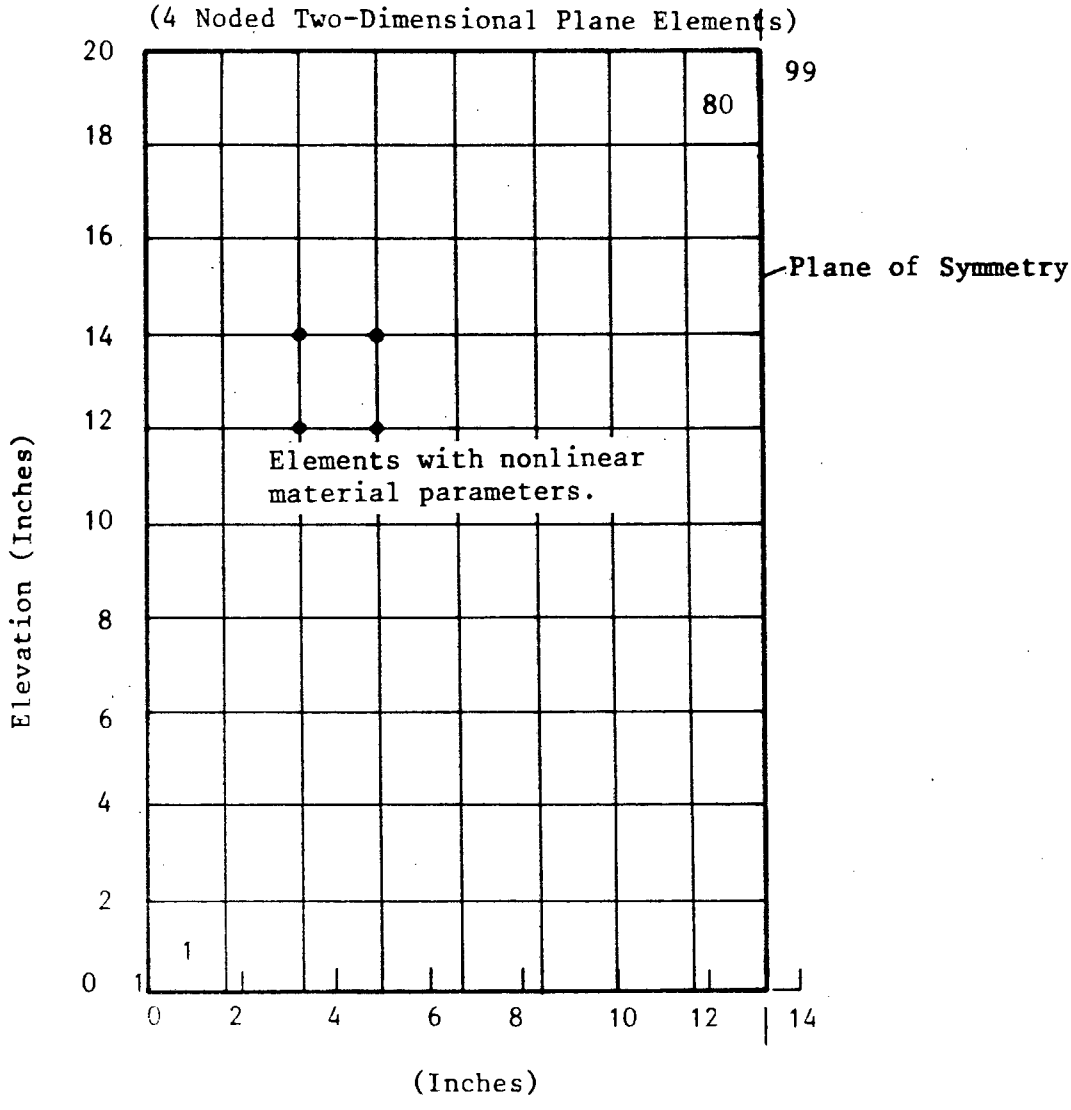

Fig 6.18: Finite element mesh used by candidate to model rapid drawdown between drains. (Figure 6.16).

seepage face can be modelled more accurately. The assumed relationships of ψ, k_{rw} and c, as shown in figure (6.17), could also have affected the results.

6.11.6 Summary and conclusion.

It can be seen from the examples given that the use of the finite element method, is relatively easy, for the solving of seepage problems, when in the form of a computer program. Examples of both saturated steady-state and transient saturated-unsaturated flow in a rigid porous medium have been analysed above, showing the wide range of problems that can be considered. It also has been shown that the finite method (applied correctly) yields good results for the problems considered, both for results reported from other authors using finite element methods and from the writer using ADINAT. It is noted that the seepage face can cause errors and it is in this area that care needs to be exercised when using the finite element method.

6.12 Experiment verification using the finite element method.

6.12.1 Introduction.

In the previous chapter two experiments which had been performed by the writer were discussed. Various measurements were made while the experiments were in progress. A verification of the experiments is done by modelling the two problems, using the finite element program package which has been modified by the writer. The examples covered in section (6.11) show that the material models used in the program package do yield acceptable results.

6.12.2 Experiment No. 1: Unsteady flow through a rectangular dam.

Experiment number one, that was discussed in chapters 4 and 5 is analysed here by the finite element method. The problem consists of a rectangular earth dam, as shown in figure (6.19). The initial water level, at time t = 0, on both sides of the dam was 12,48 inches

(317 mm). The RHS water level was then lowered to the base (z=0) and this face was then regarded as a seepage outflow surface.

The functional relationship between ϕ, k_{rw} and c is given in Table (6.4), which was obtained from the experimental analysis in section (5.5.1). Figure (6.19) shows the observed positions of the phreatic surface obtained from the transducers in the experiment (See section 5.5) and those obtained numerically from ADINAT, using the finite

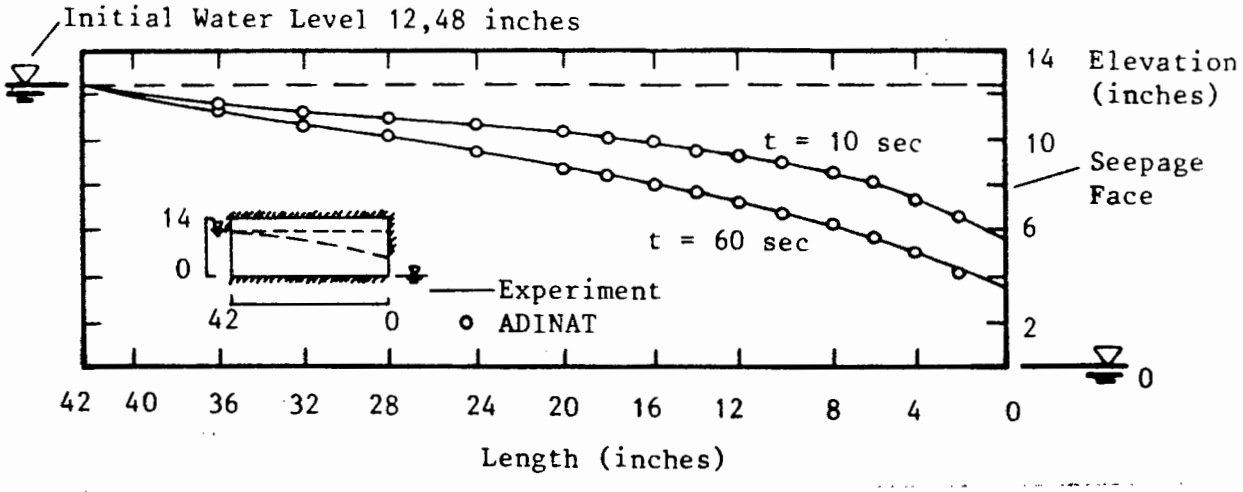

Fig 6.19: Decline of water table for the drainage experiment number one, of a saturated-unsaturated domain. Numerical results from ADINAT compared with calculated results from the experiment performed.

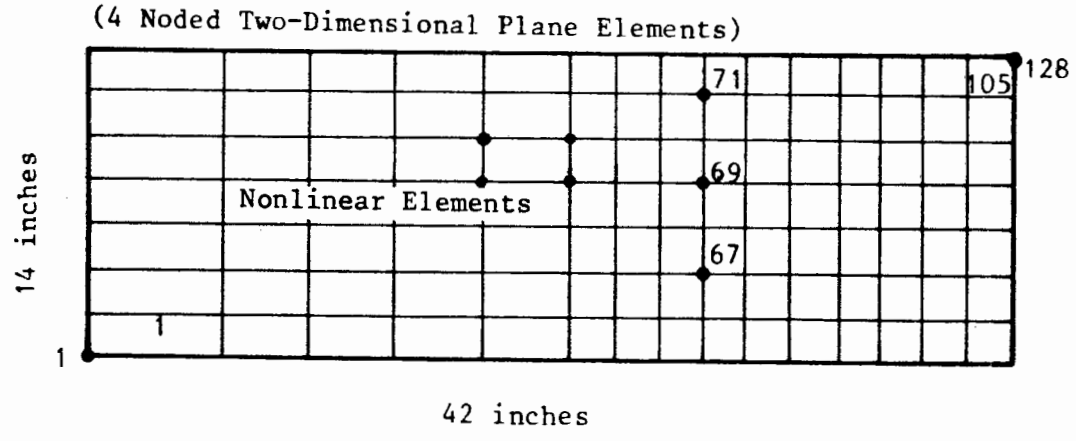

Fig 6.20: Finite element mesh used to model drainage experiment number one.

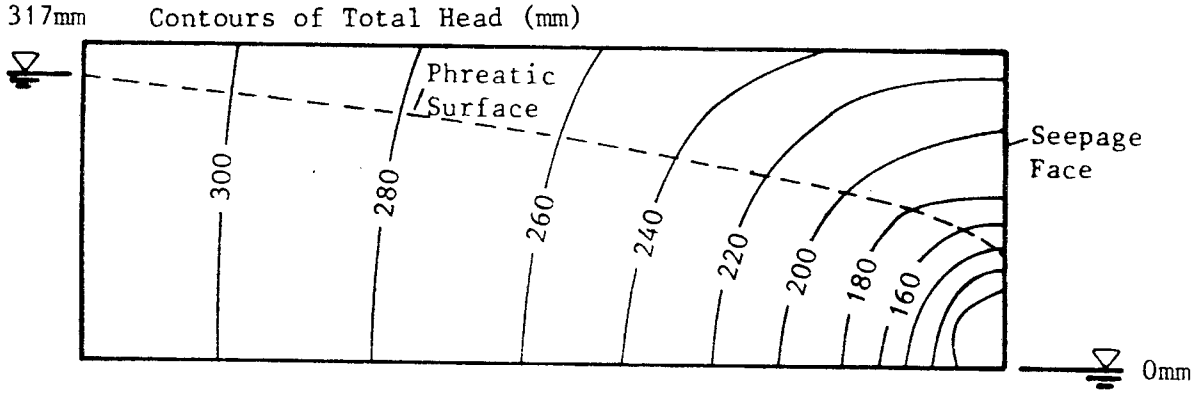

Fig 6.21: Contours of total head in the drainage experiment number one at time t = 15 sec. Obtained from the numerical analysis by ADINAT.

element mesh shown in figure (6.20). Figure (6.21) is a contour plot of the computed total heads at time t = 15 seconds. This can be compared with the observed values from figure (5.12), and it can be seen that the two are very similar. In figure (6.21) there is a problem, near the seepage face in that the contours are distorted. This is caused by the mesh size and the presence of the seepage face. Also shown, in figures (6.22), (6.23) and (6.24) are the results from pressure transducers, located at specific points in the domain, and the numerical results obtained by the finite element method ADINAT, for the nodes at the corresponding positions.

Table 6.4: Relationships between ϕ, k and c for drainage experiment number one.

ϕ (inches)	c (in^3/in)	k (in/s)
-50	0	$2,00 \times 10^{-4}$
-6	0	
-4,8		$2,00 \times 10^{-4}$
-4	$1,00 \times 10^{-1}$	$1,09 \times 10^{-2}$
-3	$1,00 \times 10^{-1}$	$6,33 \times 10^{-2}$
-2		$1,26 \times 10^{-1}$
-1	0	$1,555 \times 10^{-1}$
50	0	$1,555 \times 10^{-1}$

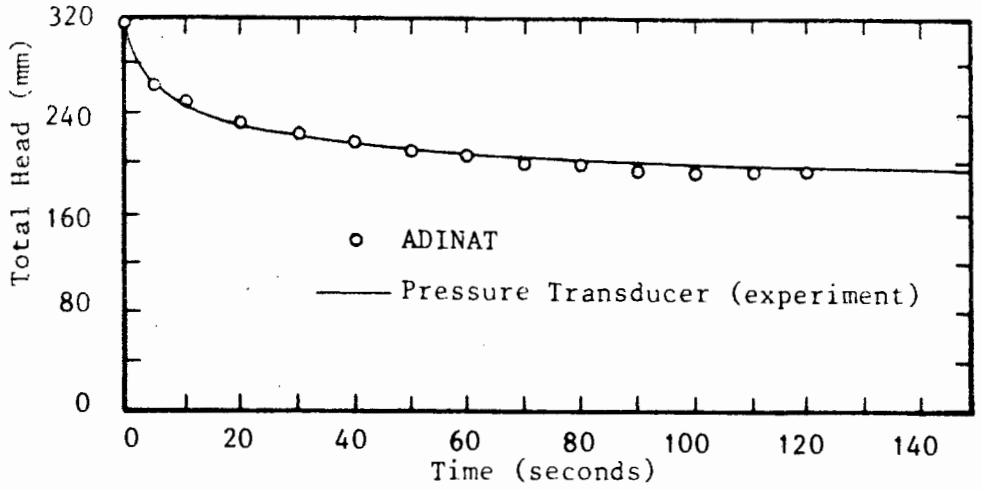

Fig 6.22: Comparison of the result for node 71 in the numerical analysis and the output for the pressure transducer, number "TB4", of experiment number one.

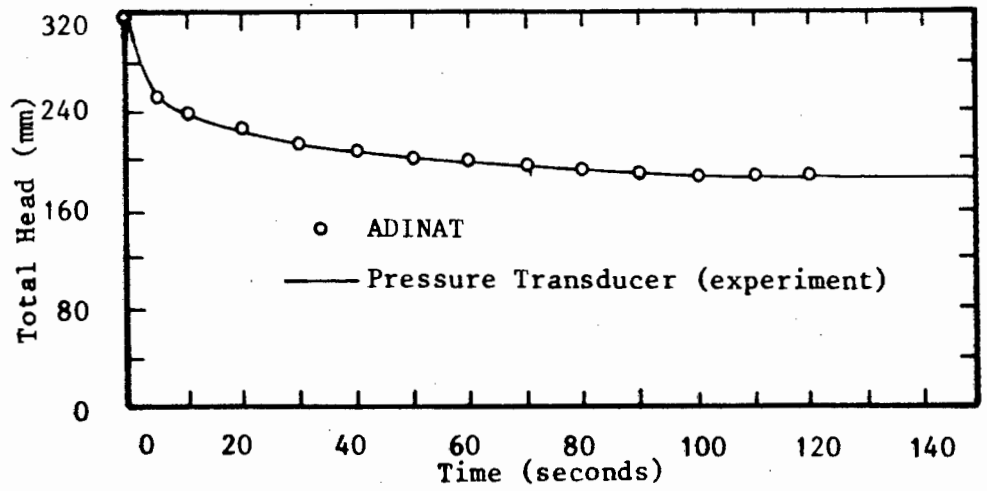

Fig 6.23: Comparison of the result for node 69 in the numerical analysis and the output for the pressure transducer, number "TB3", of experiment number one.

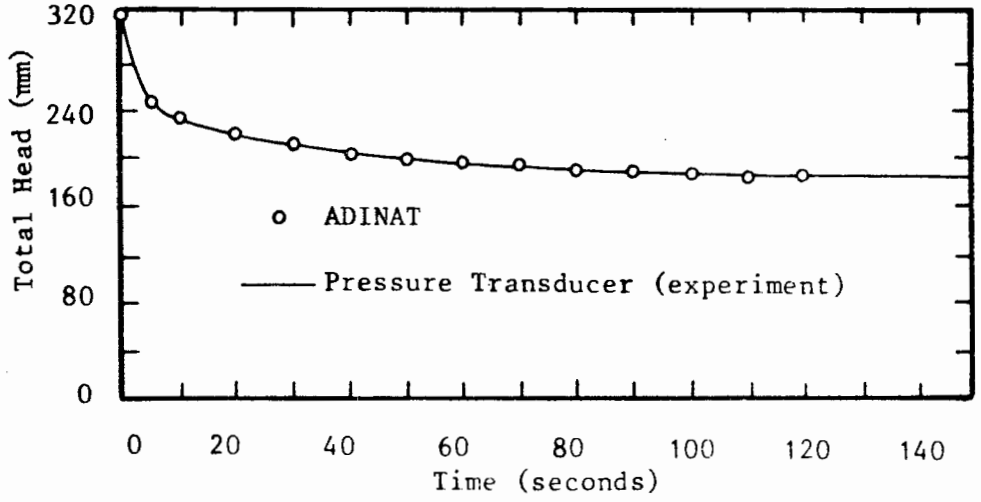

Fig 6.24: Comparison of the result for node 67 in the numerical analysis and the output for the pressure transducer, number "TB2", of experiment number one.

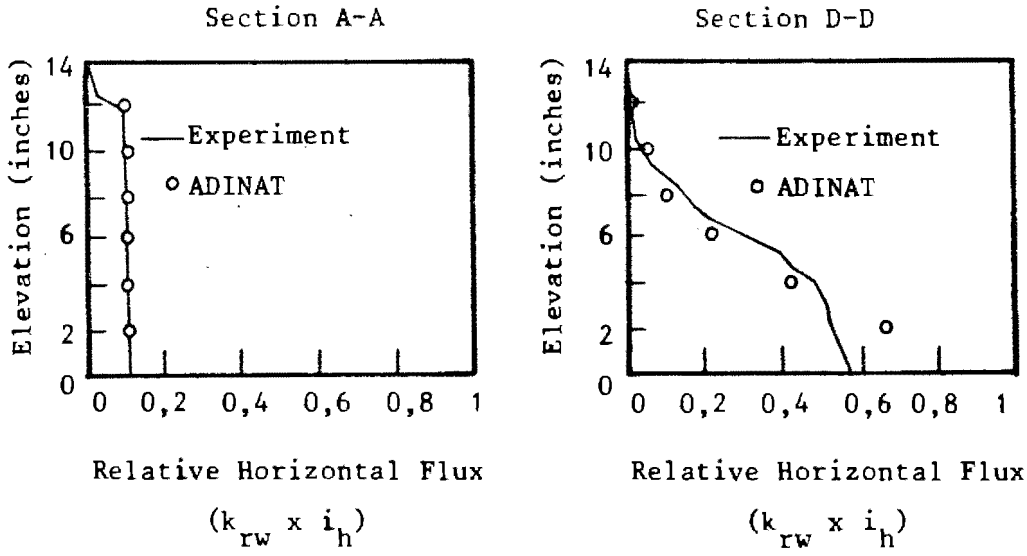

Fig 6.25: Comparison the horizontal components of the relative flux at section A-A and D-D, of the numerical analysis ADINAT and the calculated relative flux from the experimental results of experiment number one. (The actual superficial Darcian velocity is equal to the relative flux multiplied by k_{sat})

Figure (6.25) shows a comparison of the calculated relative flux (See section 5.5.5) at the sections A-A and D-D (See figure 5.12) with the results from the numerical analysis by ADINAT. As shown by the figures given above, the numerical results are in very good agreement with the results obtained from the experiment performed.

Based on the above, for experiment number one, it has been shown that the numerical analysis verifies the experimental results very accurately.

6.12.3 Experiment No. 2: Saturated-unsaturated flow in a slab of soil between drains after rapid drawdown.

Experiment number two, (discussed in chapters 4 and 5) is analysed here by the finite element method. The problem consists of a slab of soil with an impervious base and drained by a ditch with a zero water level, as shown in figure (6.26). The initial water level, at time t = 0, in the ditch was 15,0 inches (381 mm). The ditch water level was then lowered to the base (z=0) and the face treated as a seepage surface.

Table 6.5: Relationships between ϕ, k and c for drainage experiment number two.

ϕ (inches)	c (in^3/in)	k (in/s)
-50	0	$2,00 \times 10^{-4}$
-6	0	
-4,8		$3,00 \times 10^{-4}$
-4	$1,03 \times 10^{-1}$	$1,29 \times 10^{-2}$
-3	$1,03 \times 10^{-1}$	$7,53 \times 10^{-2}$
-2		$1,499 \times 10^{-1}$
-1	0	$1,85 \times 10^{-1}$
50	0	$1,85 \times 10^{-1}$

The functional relationship between ϕ, k_{rw} and c is given in Table (6.5), which was obtained from the experimental analysis in section (5.6.1). Figures (6.26a and b) show the comparisons of the phreatic surface determined from the experimental results, section (5.6) and the numerical results from ADINAT, at times t = 15 and 30 minutes respectively, after the start of experiment. Also shown are contour plots of the total heads, obtained from the numerical analysis, using the finite element mesh as shown in figure (6.29c). It is shown that the positions of the experimental phreatic surface do not aggree with the computed positions from the numerical analysis. As shown in figure (6.29c), the finite element mesh in the vertical direction is not very fine, especially near the seepage face. As shown earlier in section (6.11), the modelling of the outflow seepage face can affect the results. In this experiment number two, the shape of the drainage domain (ie. very long and horizontal) causes a horizontally inclined phreatic surface, even though drainage is occuring and the writer believes that the computer program ADINAT can provide incorrect results, especially if a coarse vertical spacing is used for the finite elements. The results of the numerical analysis have therefore been affected by the mesh size and seepage face. If a finer mesh had been used in the vertical direction the verification would have been better. Even with the present errors, the experiment is still modelled relatively accurately, in that the declining phreatic surface is about 16 % out at the worst place in relation to the overall vertical range of

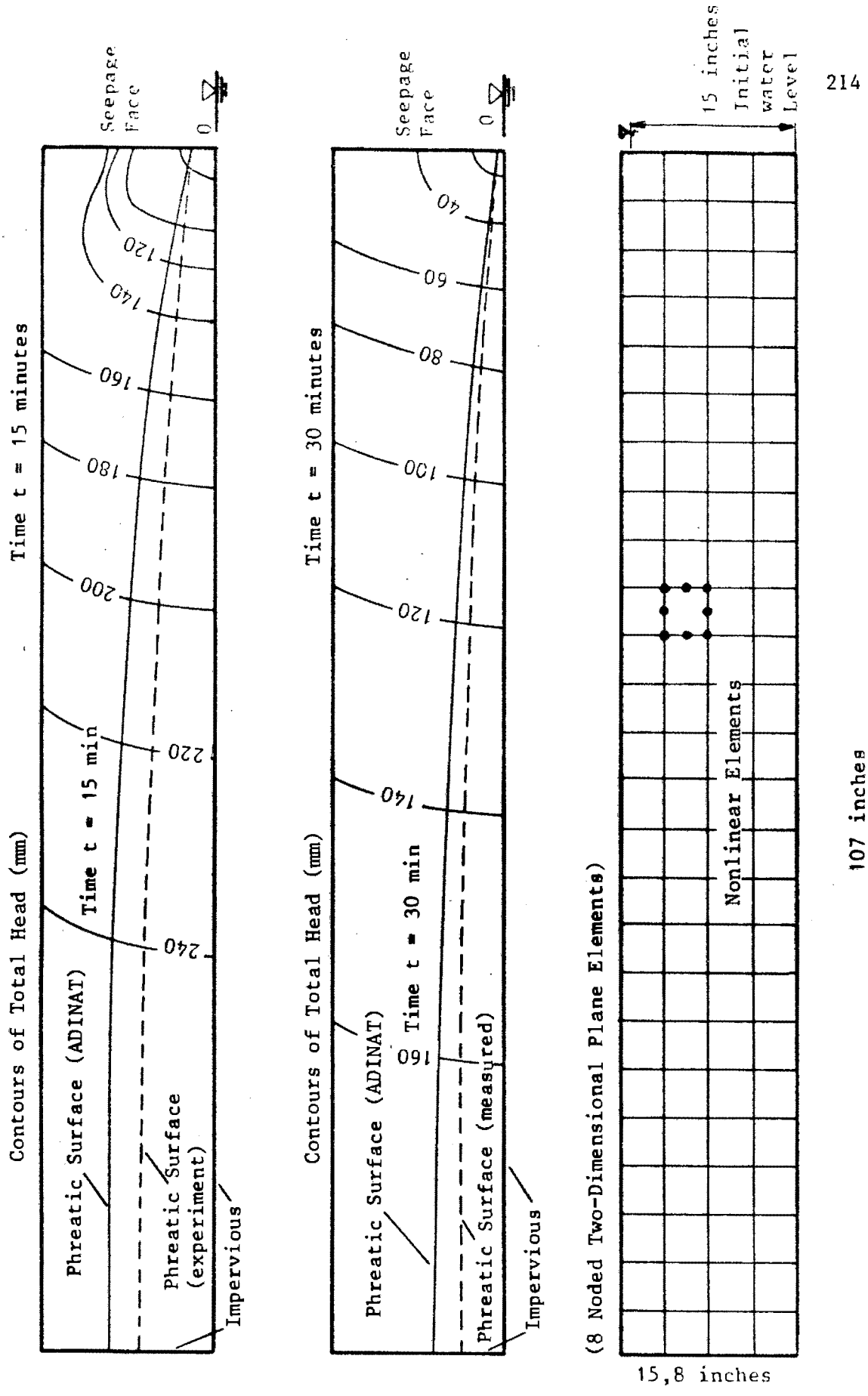

Fig 6.26: **Numerical results for experiment number two showing: Total head contours plot at (a) time t = 15 minutes; (b) time t = 30 minutes. (c) Finite element mesh used to model the drainage experiment number two.**

the drainage domain. The affect of the seepage face can be seen by the distorted contours in figure (6.26a). Near the drainage face the phreatic surface, calculated for the experiment and that predicted by the finite element method are about the same.

6.12.4 Conclusion.

For the results shown in figure (6.19) for experiment number one, the agreement between the numerical results and the experimental work is excellent. Based on these comparisons the writer feels that the experiment has been verified very accuratly by a numerical method. (ie. The finite element method.)

For the results shown in section (6.12.3) for experiment number two, the agreement between the numerical results and the experimental work is not as close as for experiment number one. Even with the slight error in the comparisons, which the writer feels with a finer mesh would be reduced, the results do show some form of similarity in the rate of decline of the phreatic surface. The difference in these results may be due to modelling errors.

In conclusion, the above shows that the experimental work can be verified by a numerical method and this can be done very accurately, as shown by the verification of experiment number one.

CHAPTER 7

SUMMARY AND CONCLUSIONS.

7.1 Comparison of experimental and numerical results.

The results in section (6.12), show good agreement between experimental and computed values.

For experiment number one, (Figure 6.19) the verification of the experimental work by the numerical method of finite elements is very accurate. For experiment number two (Figure 6.26) the numerical and experimental results show a lack of agreement, but the reason for this could be due to incorrect modelling of the problem by the finite element method, rather than inaccuracies in the experimental results.

Also contour plots of heads near drainage faces made from the ADINAT [2] finite element method results, show that errors exist near a drainage face. These errors result in the nodal values not reflecting a smooth contour plot of the total heads near the drainage face as would be expected or as was measured. A reason for this could be that the nodes on the drainage face are subject to errors in modelling boundary conditions. While the local pressure head at a node is zero, flux is allowed out of the drainage face. As soon as the local pressure head at the node turns negative, the node is considered part of the impermeable boundary. Therefore as time progresses, the phreatic surface at the drainage face above the tailwater drops in finite steps. Thus near the drainage face the results for the heads reflected could be slightly irregular and incorrect.

Overall, the finite element method is seen to be a very effective and accurate method for solving seepage problems. This is especially relevant in the case of transient problems of seepage in a saturated-unsaturated flow domain. The accuracy of the method has also been shown, both with numerous examples considered and with the experimental verification, to be reasonably good. The accuracy depends a lot on the user being able to model the problem correctly and

selecting the correct model for the material parameters. (eg. c, k as functions of ϕ).

7.2 Practical application.

The practical application of the work done in this thesis is mainly in the modifications of the finite element method as a numerical tool for the analysis of partly saturated drainage seepage problems. The experimental work was done to provide modelling experiments which could be used to check the finite element methods. The equipment designed for the experimental work can be used for future research or perhaps even in the practical use of monitoring of water pressures in the field. The writer feels that all the electrical noise observed with the data-acquisition equipment is not a serious problem in that the cause could be found with a small amount of investigation. (Personally, the writer thinks that the noise was caused by the transmission cables obtained with the transducers, in that the cables were short circuiting and causing a circular earth field. This assumption is based on the fact that 3 cables were found to be short circuiting initially, and that the noise only appeared when all the cables were used. This shortcircuiting occured in the plugs previously fitted by another student.)

The use of the finite element method is of great practical importance in that it allows transient flow problems with arbitrary shaped geometrical boundaries to be investigated. A problem is that a computer is required and if large transient problems are to be analysed, a computer with a large random access memory is needed. Also, to be able to model anything numerically the material parameters are needed. (ie. permeability and suction parameters).

7.3 Field and laboratory parameters required for the finite element method material model.

The required parameters vary depending on which material model in the finite element program package one intendeds to use. If a confined saturated seepage problem is to be analysed then the saturated hydraulic conductivity k_{sat} is required, and the specific moisture capacity is not required as the soil stays saturated. If a field problem needs to be analysed it is best to measure the saturated hydraulic conductivity in the field. Also, if only the saturated hydraulic conductivity is known, a steady-state unconfined problem with a free surface can be analysed. Once again the specific moisture capacity is not required as a steady-state analysis is made.

For a full investigation of the saturated-unsaturated flow domain, the number of parameters required is far greater than above. The saturated hydraulic conductivity k_{sat} needs to be known, as well as the relative hydraulic conductivity k_{rw} for the unsaturated zone, with respect to the local pressure head ϕ. The specific moisture capacity $c(\phi)$, with respect to the local pressure head ϕ, for the unsaturated zone is also required. (See figure 6.8) At present the hysteresis is not considered and therefore either the main drying or the wetting curve, or an average, is taken as the only relationship of the various parameters. If the material has an anisotropic hydraulic conductivity, the direction of the orthotropic principal axes and the ratio of the principal hydraulic conductivities is also required.

Once the required material parameters (from field measurement), and the boundary conditions that apply to the problem are known, a numerical analysis can be undertaken. As with any modelling the results must be checked, if possible by an alternative method, in order to ascertain that the problem has been analysed correctly.

7.4 Future possibilities.

Future possibilities in terms of the experimental drainage problems would be to first investigate better equipment with which to carry out the drainage experiments. With the experiments presented in this thesis, the degree of saturation within the experimental seepage domain was calculated from the suction pressures measured by the tensiometers and the use of the soil-moisture characteristic curve.

A more ideal system would be to continue to measure the suction pressure at various points within the soil, using the tensiometers, but also at the same time, to measure the degree of saturation near the respective positions of the tensiometers, using a neutron or gamma ray technique. This would then allow for both draining and wetting seepage problems to be investigated and the soil-moisture characteristic curve could be obtained. This would also mean that a separate soil-moisture characteristic curve test, as given in section (4.5), would not be necessary.

The modelling of the seepage face is a subject that could be further investigated. The method of modelling and the affect it has on the solution would need to be studied.

In terms of problems that need to be solved, future possibilities would include, investigating the toxic leaching into the soil from a waste dump and the problem of infiltration of water into the soil during ground water recharging due to flow in the unsaturated zone above the phreatic surface. Experimental work of this sort would be necessary to check the finite element material model under such conditions.

A future possibility with the finite element method would be to try and develop a material model which would only require the specific yield of the material rather than the specific moisture capacity. This would then allow for unconfined transient problems to be analysed with a free surface approach, rather than with the saturated-unsaturated seepage method. This type of approach would be much easier to apply to practical problems involving granular soil with a small capillary rise

or problems where the unsaturated seepage is not of importance.

7.5 Concluding remarks.

In order to achieve the principal aims of this thesis, as given in section (1.2), a number of secondary objectives were listed. These objectives have either been achieved or not achieved, as follows:

a) A literature survey on the soil-moisture relationships in connection with drainage has been covered in chapter 2.

b) A literature survey on the methods of obtaining the necessary parameters that are important in the drainage of soils has been covered in chapter 2.

c) The finite element method with application to solving seepage problems has been discussed in chapter 6.

d) An experimental program undertaken to investigate the flow of water in a saturated-unsaturated porous medium is covered in chapters 4 and 5.

e) Experimental equipment was needed and some of it was purchased while other parts were designed and built. Some of the equipment that was available required extensive modification to get it operational.

f) A data-acquisition unit was designed and built, using an A/D converter and an Apple IIe computer. The design and operation of the system is covered in chapter 3.

g) The finite element packages available at the University of Cape Town were investigated to find out if any could be used for the solving of saturated-unsaturated seepage problems. Of those available, namely: ADINAT [2]; NOSTUM [32]; PAFEC 75 [33]; ABAQUS [1], none could be used directly, in their present

version, at the time of investigation.

h) With the permission of Prof W S Doyle, the finite element package ADINAT [2] was altered to include a new material model so that the saturated-unsaturated seepage could be analysed.

i) The experimental results obtained were verified with the finite element method in section (6.12). A good comparison of the results was found where the modelling of the seepage domain was done correctly.

j) Suggestions for the use of the finite element method in a variety of seepage flow problems were made in section (6.11), where the method was actually used and the results are shown.

k) The seepage tank previously designed and constructed in the Soil Mechanics laboratory was large enough to provide meaningful results and sufficient delay in the experiments to allow the period of lowering the tailwater level to be neglected. The piezometer tubes in the walls of the tank showed a slow response time in the first experiment (Figure 6.19) and the electrical transducers provided excellent readings during this experiment which only lasted about 150 seconds. In the second experiment (Figure 6.26) the piezometer tubes in the walls provided good results. In this case the experiment lasted for about one hour.

In conclusion, the writer feels that the main aim of the thesis has been covered. The flow of water in a draining soil was investigated experimentally, and a numerical method was used for the verification of the results. The numerical method used, the finite element method, was shown to be a powerful method for the solving of seepage problems.

The problem with the finite element method, as with any numerical method, is that the necessary soil-moisture parameters are required for any material model of the method. The problem lies in trying to obtain these parameters. Field methods developed for determining the functional relationships between pressure head ϕ, relative

conductivity k_{rw} and moisture content θ under unsaturated conditions needs to be investigated in order to try and make them easier to use.

Finally, the reader is reminded of the fact that whichever method of analysis is applied the investigator should exercise careful judgement and not just blindly use the method nor the results.

REFERENCES

1. ABAQUS - User's Manual Version 4.5.151, HIBBITT, KARLSSON and SORENSON, Inc., Providence, Rhode Island, USA, 1984.

2. ADINAT - A Finite Element Program for Automatic Dynamic Incremental Nonlinear Analysis of Temperatures, Report AE 84-2, ADINA Engineering, December 1984.

3. H.G. Bass, Introduction to Engineering Measurement, McGraw-Hill, 1971

4. K.J. Bathe, Finite Element Procedures in Engineering Analysis, Prentice-Hall, 1982

5. K.J. Bathe, M.R. Khoshgoftaar, "Finite Element Free Surface Seepage Analysis without Mesh Iteration", Int. J. Numerical and Analytical methods in Geomechanics, 3, 13-22, 1979.

6. J. Bear, Hydraulics of Groundwater, McGraw-Hill, 1979.

7. H. Bouwer, Grounwater Hydrology, McGraw-Hill, 1978

8. J.E. Bowles, Engineering Properties of soils and their measurement, McGraw-Hill, 1970

9. G.M. Bragg, Principles of Experimentation and Measurement, Prentice-Hall, 1974

10. R.H. Brooks, A.T. Corey, "Properties of Porous Media affecting Fluid Flow", J. Irrig. Drain. Div., ASCE, 92, (IR2), 61-88, 1966

11. A.T. Corey, "Measurement of Water and Air Permeability in Unsaturated Soil", Soil Sci. Soc. Amer. Proc., 21, 7-10, 1957

12. C.S. Desai, "Finite Element Procedures for Seepage Analysis Using an Isoparametric Element", Proc., WES Symp. on Applications of the Finite Element Method in Geotechnical Engineering, Vicksburg, Miss., May 1972.

13. P.W. France, J.P. Chandrakant, J.C. Peters, C. Taylor, "Numerical Analysis of Free Surface Seepage Problems", J. Irrig. Drain. Div., ASCE, 97, (IR1), 165-179, 1971.

14. W.G. Gray, "Comparison of Finite Difference and Finite Element Methods", Proc. of the NATO Advanced Study Institute on Mechanics of Fluids in Porous Media, Newark, Delware, USA, July 18-27, 1982.

15. R.C. Hallgren, Interface Projects for the Apple II, Prentice-Hall, 1982

16. M.E. Harr, Groundwater and Seepage, McGraw-Hill, 1962.

17. Head, Manual of soil laboratory testing, Vol. 1: Soil classification and compaction testing, Pentech Press, 1980

18. D. Hillel, Fundamentals of Soil Physics, Academic Press, 1980.

19. D. Hillel, W.R. Gardner, "Measurement of unsaturated conductivity and diffusivity by infiltration through an impeding layer", Soil Sci., 109, 149-153, 1970

20. D Hillel, V.D. Krentos, Y. Stylianou, "Procedure and Test of an Internal Drainage Method for Measuring soil Hydraulics Characteristics in situ", Soil Sci., 114, 5, 395-400, 1972

21. R.D. Jackson, "On the Calculation of Hydraulic Conductivity", Soil Sci. Soc. Amer. Proc., 36, 380-383, 1972

22. D.J.P. Joubert, "Transducers for Soil Experiments and Windflow", B.Sc. Undergraduate Thesis No. 41, Dept. Civil Engineering, University of Cape Town, 1983

23. L.G. King, "Description of Soil Characteristics for Partially Saturated flow", Soil Sci. Soc. Amer. Proc., 29, 359-362, 1965

24. T.W. Lambe, Soil Testing for Engineers, Wiley, 1951

25. T.W. Lambe, R.V. Whitman, Soil Mechanics, Wiley, 1969

26. Y. Mualem, "A Conceptual Model of Hysteresis", Water Resour. Res., 10, (3), 514-520, 1974

27. Y. Mualem, "A New Model for Predicting the Hydraulic Conductivity of Unsaturated Porous Media", Water Resour. Res., 12, (3), 513-522, 1976

28. Y. Mualem, "Hydraulic Conductivity of Unsaturated Porous Media: Generalized Macroscopic Approach", Water Resour. Res., 14, (2), 325-334, 1978

29. Y. Mualem, E.E. Miller, "A Hysteresis Model based on an Explicit Domain-dependence function", Soil Sci. Soc. Amer. J., 43, 1067-1073, 1979

30. T.N. Narasimhan, S.P. Neuman, P.A. Witherspoon, "Finite Element Method for Subsurface Hydrology Using a Mixed Explicit-Implicit Scheme", Water Resour. Res., 14, (5), 863-877, 1978.

31 S.P. Neuman, "Saturated-unsaturated Seepage by Finite Elements", J. Hydraul. Div., ASCE, 99, (HY12), 2233-2250, 1973.

32. NOSTRUM - A Finite Element Program for Nonlinear Structural Mechanics, Technical Report No 18b, G.A. Duffett, T.B. Griffin, J.B. Martin, C.D. Mercer, B.D. Reddy, L. Resende, Applied Mechanics Research Unit, University of Cape Town, November, 1983

33. PAFEC LTD, PAFEC 75 User,s Manual level 4, Nottingham, U.K., 1982

34. J.Y. Parlange, "Capillary Hysteresis and Relationship Between Drying and Wetting Curves", Water Resour. Res., 12, (2), 224-228, 1976

35. K. Reichardt, P.L. Libardi, D.R. Nielsen, "Unsaturated Hydraulic Conductivity determination by a scaling Technique", Soil Sci., 120, 165-168, 1975

36. L.A. Richards, "Capillary Conduction of Liquids through Porous Media", Physics, 1, 318-333, 1931.

37. D.K. Todd, Ground water Hydrology, Wiley, 1959.

38. M. Vauclin, "Infiltration in unsaturated soils", Proc. of the NATO Advanced Study Institute on Mechanics of Fluids in Porous Media, Newark, Delware, USA, July 18-27, 1982.

39. G.T. Yeh, "On the Computation of Darcian Velocity and Mass Balance in the Finite Element Modeling of Groundwater Flow", Water Resour. Res., 17, (5), 1529-1534, 1981.

40. E.G. Youngs, "An Infiltration Method of Measuring the Hydraulic Conductivity of Unsaturated Porous Materials", Soil Sci., 97, 307-311, 1964

41. O.C. Zienkiewicz, The Finite Element Method, third edition, McGraw-Hill, 1977.

COURSES PASSED BY CANDIDATE

The following courses were completed in partial fulfilment of the requirements for the degree of Master of Science in Engineering at the University of Cape Town

Course		Date Credited	Credit Value
CE 5B7	Introduction to the Theory of Elasticity (Exam)	1984	2
CE 5B9	Introduction to the Finite Element Method (Exam)	1984	2
CE 5B10	Finite Element Analysis (Exam + Project)	1984	3
CE 5E4	Rock Mechanics (Exam)	1984	3
CE 5F1	Contracts and Contracts Administration (Exam)	1984	3
AM 344	Advanced Numerical Methods (Exam + Project)	1984	4
CE 5E6	Groundwater, Aquifer, Wells and Seepage (2 Projects)	1985	5
AM 363	Numerical Analysis (Exam + 2 Projects)	1985	3
		TOTAL	25

Course Credits : 25
Thesis Credits : 20
Total 45

Total credit requirements for the M.Sc. (Eng) Degree : 40 credits

TABLES OF THE SPECIFIC GRAVITY AND VISCOSITY CORRECTIONS FOR WATER WITH RESPECT TO TEMPERATURE.

Table. B-1: Specific Gravity of Water.* Lambe [24]

^0C	0	1	2	3	4	5	6	7	8	9
0	0,9999	0,9999	1,0000	1,0000	1,0000	1,0000	1,0000	0,9999	0,9999	0,9998
10	0,9997	0,9996	0,9995	0,9994	0,9993	0,9991	0,9990	0,9988	0,9986	0,9984
20	0,9982	0,9980	0,9978	0,9976	0,9973	0,9971	0,9968	0,9965	0,9963	0,9960
30	0,9957	0,9954	0,9951	0,9947	0,9944	0,9941	0,9937	0,9934	0,9930	0,9926
40	0,9922	0,9919	0,9915	0,9911	0,9907	0,9902	0,9898	0,9894	0,9890	0,9885
50	0,9881	0,9876	0,9872	0,9867	0,9862	0,9857	0,9852	0,9848	0,9842	0,9838
60	0,9832	0,9827	0,9822	0,9817	0,9811	0,9806	0,9800	0,9795	0,9789	0,9784
70	0,9778	0,9772	0,9767	0,9761	0,9755	0,9749	0,9743	0,9737	0,9731	0,9724
80	0,9718	0,9712	0,9706	0,9699	0,9693	0,9686	0,9680	0,9673	0,9667	0,9660
90	0,9653	0,9647	0,9640	0,9633	0,9626	0,9619	0,9612	0,9605	0,9598	0,9591

* Also the density or unit weight of water (g/cm^3)

Table. B-2: Viscosity corrections* η_T/η_{20} Bowles [8]

^oC	0	0,1	0,2	0,3	0,4	0,5	0,6	0,7	0,8	0,9
10	1,3012	1,2976	1,2940	1,2903	1,2867	1,2831	1,2795	1,2759	1,2722	1,2686
11	1,2650	1,2615	1,2580	1,2545	1,2510	1,2476	1,2441	1,2406	1,2371	1,2336
12	1,2301	1,2268	1,2234	1,2201	1,2168	1,2135	1,2101	1,2068	1,2035	1,2001
13	1,1968	1,1936	1,1905	1,1873	1,1841	1,1810	1,1777	1,1746	1,1714	1,1683
14	1,1651	1,1621	1,1590	1,1560	1,1529	1,1499	1,1469	1,1438	1,1408	1,1377
15	1,1347	1,1318	1,1289	1,1260	1,1231	1,1202	1,1172	1,1143	1,1114	1,1085
16	1,1056	1,1028	1,0999	1,0971	1,0943	1,0915	1,0887	1,0859	1,0803	1,0802
17	1,0774	1,0747	1,0720	1,0693	1,0667	1,0640	1,0613	1,0586	1,0560	1,0533
18	1,0507	1,0480	1,0454	1,0429	1,0403	1,0377	1,0351	1,0325	1,0300	1,0274
19	1,0248	1,0223	1,0198	1,0174	1,0149	1,0124	1,0099	1,0074	1,0050	1,0025
20	1,0000	0,9976	0,9952	0,9928	0,9904	0,9881	0,9857	0,9833	0,9809	0,9785
21	0,9351	0,9509	0,9487	0,9465	0,9443	0,9421	0,9399	0,9377	0,9355	0,9333
22	0,9531	0,9509	0,9487	0,9465	0,9443	0,9421	0,9399	0,9377	0,9355	0,9333
23	0,9311	0,9290	0,9268	0,9247	0,9225	0,9204	0,9183	0,9161	0,9140	0,9118
24	0,9097	0,9077	0,9056	0,9036	0,9015	0,8995	0,8975	0,8954	0,8934	0,8913
25	0,8893	0,8873	0,8853	0,8833	0,8813	0,8794	0,8774	0,8754	0,8734	0,8714

* Where the viscosity at 20^oC is: $\eta_{20} = 10,02 \times 10^{-3}$ g/cm sec

Fig C-1: **Pressure transducer and amplification circuit. Joubert [22]**

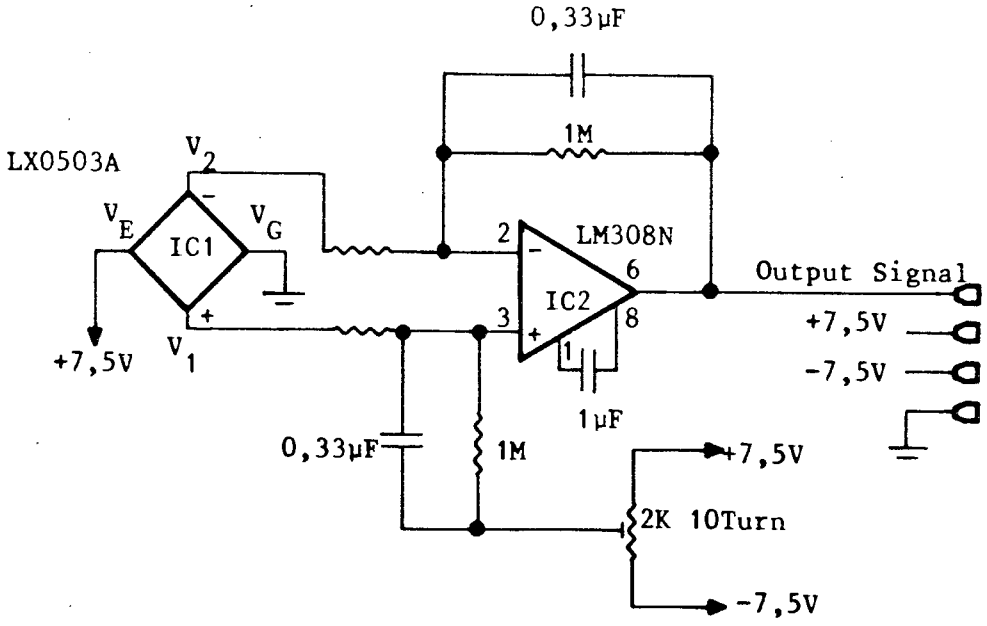

Number	Type	+7,5	-7,5	GND
IC1	LX0503A	3		8
IC2	LM308N	7	4	

C-2. Method of priming the transducer input interface with fluids.

To prime the input interfacing circuit, as shown in figure (3.12) with oil and de-aired water, the following procedure was adopted:

Firstly, only the interface block with the two vents C and E, the stop cock B and the connector F, were connected to the transducer via a heavy gauge nylon tube. The connection to the transducer was made with the connector G.

The nylon pipe that goes to the tensiometer point was then connected and the complete system pressure tested. This was done by using a mercury filled manometer, (See figure 3.18) and checking if there were any leaks. (ie. If there was a pressure loss with time.)

Stop cock B was then closed and vent E was opened. Through the open vent, oil was injected so that it travelled down the nylon tube to the transducer. When as much oil as could possibly be put into the pipe and the oil side of the interface block, under atmospheric conditions, vent E was closed. The stop cock was once again opened, but this time a changing pressure was applied to the system and the pipe GE was held vertical. Due to this changing pressure, (above and below atmospheric pressure) air bubbles flowed out of the transducer and up to the interface block. After no more air was seen to be left in the oil side of the system, except that trapped in the interface block, the stop cock B was closed. Vent C was now opened and oil injected into the interface block to replace the air in the oil side and fill the interconnecting tube D.

Once again a changing pressure was applied to the system until all the air was out of the oil side. At this stage the interconnecting pipe D was filled with oil and the nylon pipe to the transducer.

The nylon pipe to the tensiometer point was then disconnected

from the manometer and connected to the de-aired water supply line. Opening stop cock B and then vent C, the water side of the system was filled from the end A. Any air in this side was flushed out by allowing water to flow out of vent C.

On closing vent C the system was then in a primed condition, ready to be used.

Fig C-3: **Circuitry for high-speed A/D converter with a 32 channel multiplexer incorporated, for interfacing with the Apple IIe computer.**

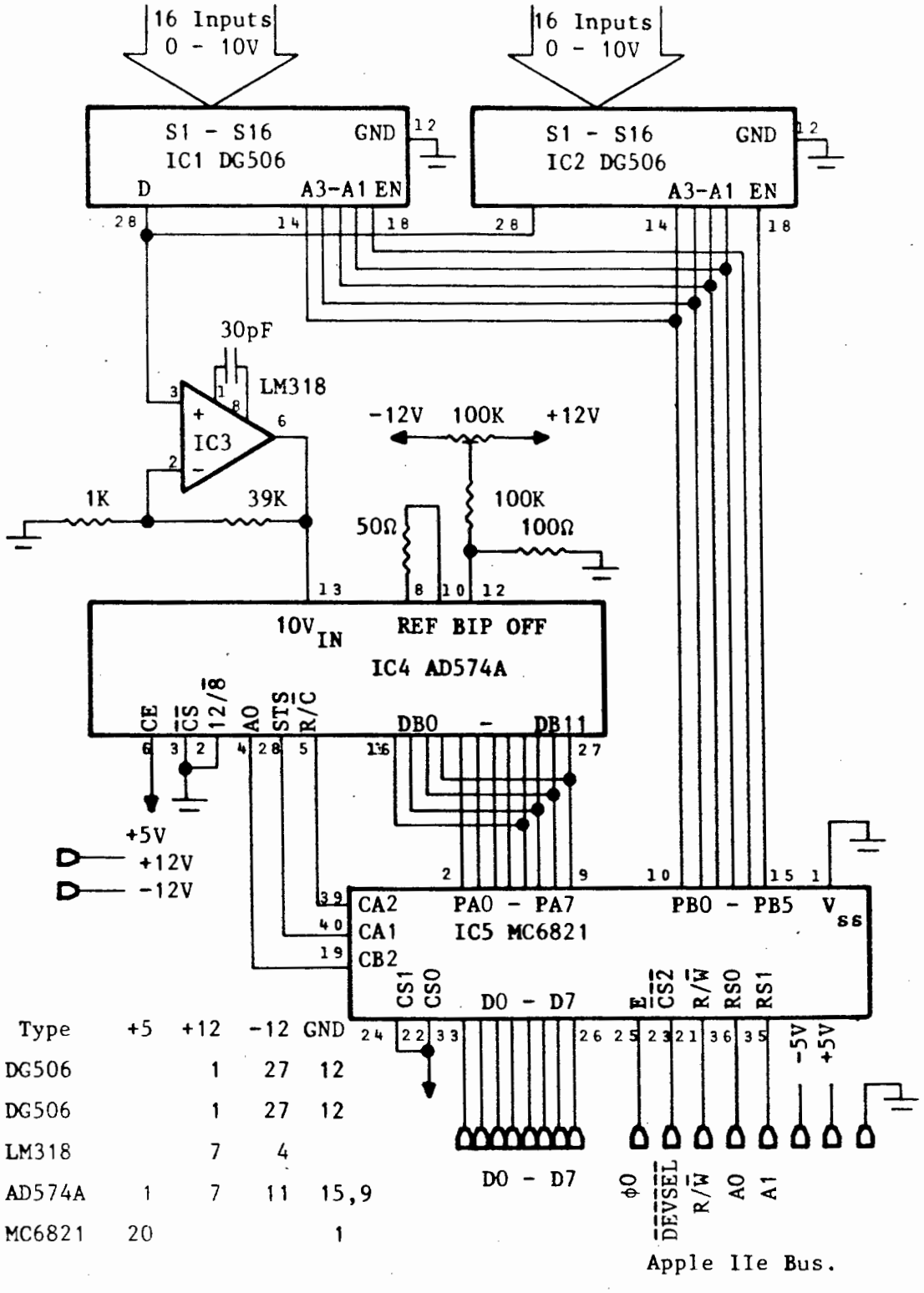

Number	Type	+5	+12	-12	GND
IC1	DG506		1	27	12
IC2	DG506		1	27	12
IC3	LM318		7	4	
IC4	AD574A	1	7	11	15,9
IC5	MC6821	20			1

Listing C-4: Machine language routines for the software control of the A/D converter and multiplexer.

Two Assembler language programs are used for the control of the A/D Converter system:

A/D_BINT
A/D_BOPT

A third assembler language program is listed for the control of the A/D Converter system for one conversion:

A/D_CON1

Program: A/D_BINT
Location $9010

This subroutine is called when the PIA interfacing the A/D Converter with the Apple IIe bus needs to be reset.

Program: A/D_BOPT
Location $9050

This subroutine is called to set the multiplexer switch to the correct channel, according to a look up table. (Starting at $8E00). Then to control the converter to do a set of conversions and to store the average of the results for each channel. (Starting at $6000). Each result uses up two addresses. If there are no more channels in the look up table, the program then gives a return back to the calling program.

Program: A/D_CON1
Location

This subroutine is called to set the multiplexer switch to channel number one. To do a single conversion and then to switch off the multiplexer.

Addresses used of the Apple IIe:

(Hexadecimal)

$05	Temporary data storage address pointer	
$06		
$07	Counter	(No. of Readings made for averaging)
$08	Counter	(Look up table counter)
$09	Counter	(No. of repeat cycles counter)

```
$0A          Data storage address Pointer
$0B

$0C          Look up Table Pointer
$0D

$0E          Counter check   (No. in look up table)
$0F          Counter check   (No. of read cycle repeats)
$10          Counter check   (No. of readings per channel to average)

$6000        Start of data storage area.

$8E00        Start of look up Table with Channel numbers

$8FA0        Start of Temporary storage area for averaging of results.

$9000        Temporary storage of Accumulator and X and Y Registers
$9001
$9002

$9010        Calling address of A/D_BINT

$9050        Calling address of A/D_BOPT


             PIA Registers. (Slot number 2)

$C0A0        Data Register A          DRA
$C0A1        Control Register A       CRA
$C0A2        Data Register B          DRB
$C0A3        Control Register B       CRB
```

Program: **A/D_BINT**

```
$A/D_BINT    STA   $9000      Save Accumulator
             STX   $9001      Save X Register
             STY   $9002      Save Y Register
             PHP              Save Processor Status
             LDA   #$00       Clear Accumulator
             NOP
             LDA   #$38
             STA   $C0A1      Access to Data Direction Reg. A of PIA
             LDA   #$30
             STA   $C0A3      Access to Data Direction Reg. B of PIA
             NOP
             LDA   #$00
             STA   $C0A0      Set Bus A as an input (A/D Converter)
             LDA   #$FF
             STA   $C0A2      Set Bus B as an output (Multiplexer)
             NOP
             LDA   #$3C
```

```
                STA     $C0A1       Close Access to DDR-A
                LDA     #$34
                STA     $C0A3       Close Access to DDR-B
                NOP
                LDA     #$00
                STA     $C0A2       Switch Off All Multiplexer channels
                NOP
                LDA     $9000       Restore Accumulator
                LDX     $9001       Restore X Register
                LDY     $9002       Restore Y Register
                PLP                 Restore Processor Status
                RTS                 Return to Calling Program
                BRK
```

Program: **A/D_BOPT**

```
$A/D_BOPT       STA     $9000       Save Accumulator
                STX     $9001       Save X Register
                STY     $9002       Save Y Register
                PHP                 Save Processor Status
                NOP
                LDA     #$00        Clear Accumulator
                LDX     #$00        Clear Registers
                LDY     #$00
                NOP
                LDA     #$00
                STA     $C0A2       Switch Off All Multiplexer channels
                STA     $0A         Start address of data storage
                LDA     #$60
                STA     $0B
                NOP
                LDA     #$00        Start address of look up Table
                STA     $0C         with channel no.
                LDA     #$8E
                STA     $0D
                NOP
                LDA     #$0B        No. of readings taken for averaging
                STA     $10
                LDA     $904F       No. of Channels in look up Table
                STA     $0E
                LDA     #$01        No. of times, read cycle is repeated
                STA     $0F
                NOP
                LDA     #$34        Set A/D so there is no conv.
                STA     $C0A3
                NOP
                LDA     #$01        No. of cycles counter.
                STA     $09
                LDA     #$00        Look up table counter.
                STA     $08
$START1         LDA     #$00        No. of readings for averaging, counter
                STA     $07
```

```
                NOP
                LDA     #$A2        Start address of averaging table
                STA     $05
                LDA     #$8F
                STA     $06
                NOP
                LDA     $08         Test if end of look up Table
                CMP     $0E
                BNE     $START3
                LDA     $09         Test if another cycle of reads
                CMP     $0F
                BNE     $START2
                NOP
                LDA     #$00        Clear Multiplexer
                STA     $C0A2
                NOP
                LDA     $9000       Restore Accumulator
                LDX     $9001       Restore X Register
                LDY     $9002       Restore Y Register
                PLP                 Restore Processor Status
                RTS                 Return to Calling Program
                BRK
                NOP
$START2         LDY     $09         Increment times counter
                INY
                STY     $09
                LDA     #$00        Restore look up table counter to zero
                STA     $08
                NOP
$START3         LDY     #$AF        Delay cycle
$LOOP1          DEY
                BNE     $LOOP1
                NOP
                LDY     $08         Set Multiplexer Channel from look up
                LDY     ($0C),Y     Table
                STA     $C0A2
                NOP
                LDY     #$AF        Delay cycle
$LOOP2          DEY
                BNE     $LOOP2
                NOP
                LDA     #$34        Start Conversion
                STA     $C0A1
                NOP
                LDA     #$3C
                STA     $C0A1
                NOP
$LOOP3          LDA     $C0A1       Check if conversion complete
                AND     #$80
                CMP     #$80
                BNE     $LOOP3
                NOP
                LDA     #$00        Switch off Multiplexer
                STA     $C0A2
                LDA     $C0A0       Take a dummy reading
                NOP
```

```
                LDY     #$4F            Delay cycle
$LOOP4          DEY
                BNE     $LOOP4
                NOP
                LDY     $08             Set Multiplexer Channel from look up
                LDY     ($0C),Y         Table
                STA     $C0A2
                INY                     Increment counter   (Look up table)
                STY     $08
                NOP
                LDY     #$64            Delay cycle
$LOOP5          DEY
                BNE     $LOOP5
                NOP
                LDA     #$34            Start Conversion
                STA     $C0A1
                NOP
                LDA     #$3C
                STA     $C0A1
                NOP
                LDA     #$3C            Set A/D for 4 LSB
                STA     $C0A3
                NOP
$LOOP6          LDA     $C0A1           Check if conversion complete
                AND     #$80
                CMP     #$80
                BNE     $LOOP6
                NOP
                LDA     $C0A0           Read 4 LSB from A/D
                AND     #$F0            Mask off 4 zero's
                STA     $8FA0           Store temporarily
                NOP
                LDA     #$34            Set A/D for 8 MSB
                STA     $C0A3
                NOP
                LDA     $C0A0           Read 8 MSB from A/D
                STA     $8FA1           Store temporarily
                NOP
                LDA     $8FA0           Roll 4 LSB to 4 LSB places
                LSR
                LSR
                LSR
                LSR
                STA     $8FA0
                NOP
                LDA     $8FA1           Roll 4 of 8 MSB to the MSB places
                AND     #$0F
                ASL
                ASL
                ASL
                ASL
                CLC
                ADC     $8FA0           Add up with previous 4 LSB to
                STA     ($05,X)         4 bits
                NOP
                INC     $05             Increment Temp. storage address
```

```
                BNE     $JMP1
                INC     $06
$JMP1           NOP
                LDA     $8FA1           Mask off 4 LSB of 8 MSB and roll to
                AND     #$F0            4 LSB
                LSR
                LSR
                LSR
                LSR
                STA     ($05,X)         Store 4 MSB
                INC     $05             Increment Temp. storage address
                BNE     $JMP2
                INC     $06
$JMP2           NOP
                LDY     #$01            Check if enough readings made
                INC     $07
                LDA     $07
                CMP     $10
                BNE     $LOOP5
                LDA     #$00            Switch off multiplexer
                STA     $C0A2
                NOP
                CLC                     Clear carry
                LDA     $10
                ADC     $10
                STA     $07
                LDA     #$00            Add up table of average readings
                TAY
                STA     $8FA0
                STA     $8FA1
$JMP3           CLC
                LDA     $8FA0
                ADC     $8FA2,Y
                STA     $8FA0
                INY
                LDA     $8FA1
                ADC     $8FA2,Y
                STA     $8FA1
                INY
                CPY     $07
                BNE     $JMP3
                NOP
                LDY     #$10            Divide the sum of the average values
                LDA     #$00
$JMP4           ASL     $8FA0
                ROL     $8FA1
                ROL
                CMP     $10
                BCC     $JMP5
                SBC     $10
                INC     $8FA0
$JMP5           DEY
                BNE     $JMP4
                NOP
                STA     $8FA2           Check remainder (< or > .5)
                SEC
```

```
                LDA     $10
                SBC     $8FA2
                CMP     $8FA2
                BCS     $JMP6
                INC     $8FA0
                BNE     $JMP6
                INC     $8FA1
$JMP6           LDA     $8FA0       Read and store 8 LSB
                STA     ($0A,X)
                INC     $0A         Increment storage address
                BNE     $JMP7
                INC     $0B
$JMP7           LDA     $8FA1       Read and store 4 LSB
                STA     ($0A,X)
                INC     $0A         Increment storage address
                BNE     $JMP8
                INC     $0B
$JMP8           JMP     $START1
```

Program: **A/D_CON1**

```
A/D_CON1        STA     $9000       Save Accumulator
                STX     $9001       Save X Register
                STY     $9002       Save Y Register
                PHP                 Save Processor Status
                JSR     $A/D_BINT   Initialize PIA.
                LDA     #$10
                STA     $C0A2       Switch Multiplexer to channel no. one.
                LDY     #$4F        Delay cycle
$LOOP1          DEY
                BNE     $LOOP1
                LDA     #$34        Start Conversion
                STA     $C0A1
                NOP
                LDA     #$3C
                STA     $C0A1
                LDA     #$3C        Set A/D for 4 LSB
                STA     $C0A3
$LOOP2          LDA     $C0A1       Check if conversion complete
                AND     #$80
                CMP     #$80
                BNE     $LOOP2
                LDA     $C0A0       Read 4 LSB from A/D
                STA     $ADDRESS1   Store 4 LSB
                LDA     #$34        Set A/D for 8 MSB
                STA     $C0A3
                LDA     $C0A0       Read 8 MSB from A/D
                STA     $ADDRESS2   Store 8 MSB
                LDA     #$00
                STA     $C0A2       Switch off multiplexer.
                RTS                 Return to calling program.
                BRK
```

Fig C-5: **A real-time-clock circuit relying on a crystal oscillator for its timebase. Provision is made for keeping the clock running when the computer is turned off.**

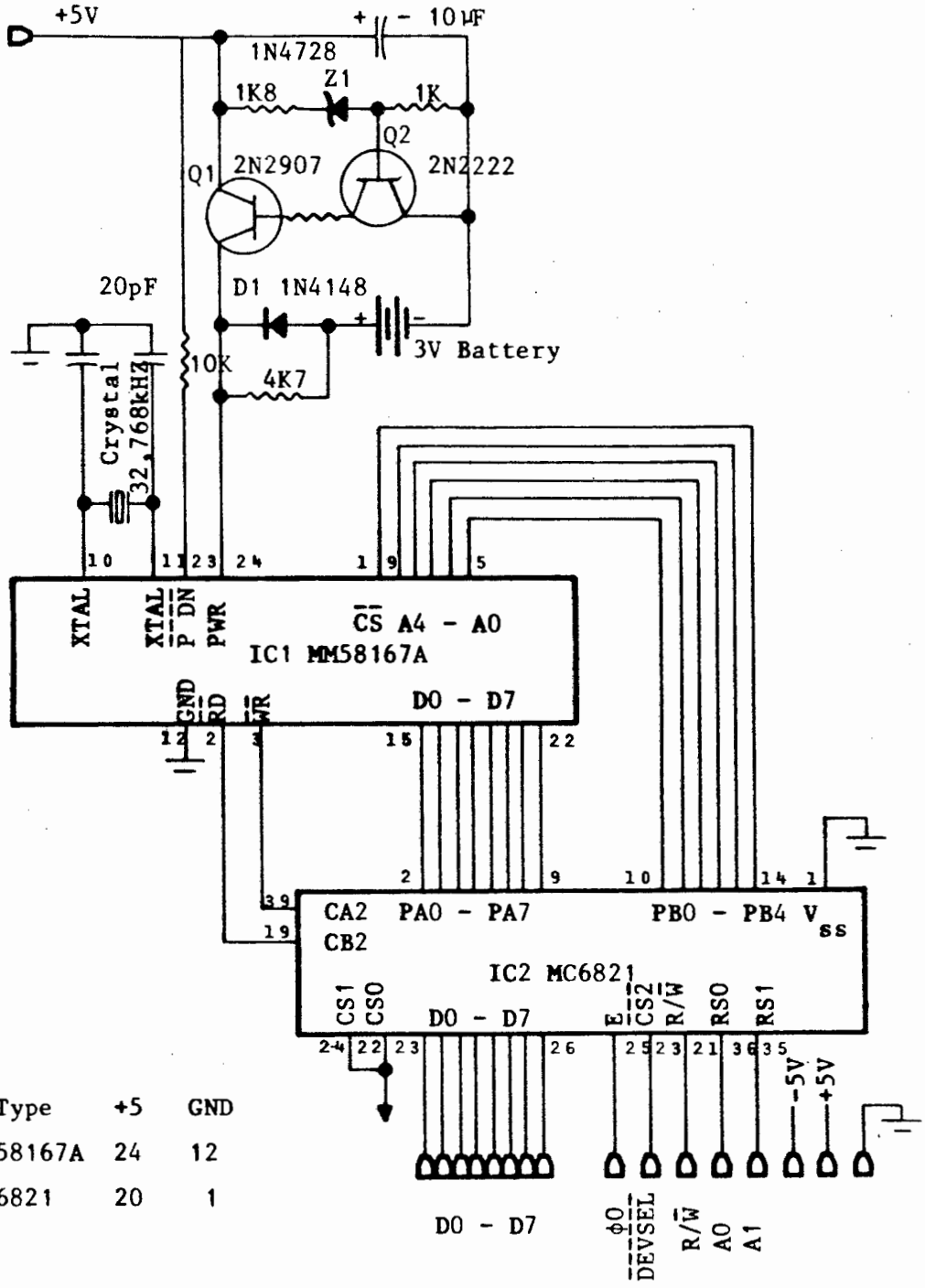

Apple IIe Bus.

Number	Type	+5	GND
IC1	MM58167A	24	12
IC2	MC6821	20	1

Listing C-6: Machine language routines for the reseting and reading of the real-time-clock register.

Four Assembler language programs are used for the control of the real-time-clock system:

C_BINT
C_READ
C_RESET
C_REG

Program: C_BINT
Location $0303

This subroutine is called when the PIA, interfacing the real-time-clock chip with the Apple IIe, bus needs to be reset.

Program: C_READ
Location $9380

This subroutine is called to read the real-time-clock registers. Either the second, minutes and hours (C_SEC) or the day-of-week, day-of-month and month (C_DAY) registers are read. The values of the registers read are stored in a table. (Starting at $6000).

Program: C_RESET
Location $9420

This subroutine is called to reset all the real-time-clock registers to there lowest value.

Program: C_REG
Location $9448

This subroutine is called to reset a selected register of the real-time-clock registers to a given value. The number of the register to be set is placed in address $05. The value to which it must be set is placed in address $06.

Addresses of the Apple IIe:

(Hexadecimal)

$04	Temporary data storage
$05	Temporary data storage address pointer
$06	Temporary data storage

```
$07          Counter  or data storage
$08          Counter  or data storage
$09          Counter  or data storage

$0A          Data storage address pointer
$0B

$0300        Temporary storage of Accumulator and X and Y Registers
$0301
$0302

$0303        Calling address of C_BINT

$6000        Start of data storage area.

$9380        Calling address of C_SEC
$9395        Calling address of C_DAY
$9420        Calling address of C_RESET
$9448        Calling address of C_REG


             PIA Registers. (Slot number 4)

$C0C0        Data Register A          DRA
$C0C1        Control Register A       CRA
$C0C2        Data Register B          DRB
$C0C3        Control Register B       CRB
```

Program: C_BINT

```
$C_BINT      STA   $0300      Save Accumulator
             PHP              Save Processor Status
             NOP
             LDA   #$3A
             STA   $C0C3      Access to Data Direction Reg. B of PIA
             LDA   #$FF
             STA   $C0C2      Set Bus B as an output.
             LDA   #$3E
             STA   $C0C3      Close Access to DDR-B
             NOP
             LDA   #$3A
             STA   $C0C1      Access to Data Direction Reg. A of PIA
             LDA   #$00
             STA   $C0C0      Set Bus A as an input.
             LDA   #$3E
             STA   $C0C1      Close Access to DDR-A
             NOP
             LDA   #$20
             STA   $C0C2      Disable real-time-clock chip.
             LDA   $0300      Restore Accumulator
             PLP              Restore Processor Status
             RTS              Return to Calling Program
```

Program: C_READ

```
$C_SEC      STA   $0300      Save Accumulator
            STX   $0301      Save X Register
            STY   $0302      Save Y Register
            PHP              Save Processor Status
            NOP
            LDA   #$02
            STA   $07        Register no. for seconds.
            LDA   #$03
            STA   $04        3 registers to be read.
            JMP   $START1
            NOP
$C_DAY      STA   $0300      Save Accumulator
            STX   $0301      Save X Register
            STY   $0302      Save Y Register
            PHP              Save Processor Status
            NOP
            LDA   #$05
            STA   $07        Register no. for day of week.
            LDA   #$03
            STA   $04        3 registers to be read.
            JMP   $START1
            NOP
$C_READ     STA   $0300      Save Accumulator
            STX   $0301      Save X Register
            STY   $0302      Save Y Register
            PHP              Save Processor Status
$START1     NOP
            LDA   #$00
            STA   $0A        Start address of data storage.
            LDA   #$60
            STA   $0B
            NOP
$LOOP2      LDX   $07        First clock register to be read
            LDY   #$00       Initialize Y register
$LOOP1      STX   $05
            NOP
            LDA   $05        Read clock register
            STA   $C0C2      No in address $05
            LDA   #$36
            STA   $C0C3
            NOP
            LDA   $C0C0
            STA   $06
            LDA   #$3E
            STA   $C0C3
            LDA   #$20
            STA   $C0C2
            NOP
            LDA   $06        Store result in data table
            STA   ($0A),Y
            INX              Increment storage and counters
```

```
                INY
                TYA
                CMP     $04             Chech if all clock registers have
                BNE     $LOOP1          been read.
                NOP
                LDA     #$14            Check if clock was not up-dated
                STA     $05             during read cycle.
                NOP
                LDA     $05             Read clock register
                STA     $C0C2           No in address $05
                LDA     #$36
                STA     $C0C3
                NOP
                LDA     $C0C0
                STA     $06
                LDA     #$3E
                STA     $C0C3
                LDA     #$20
                STA     $C0C2
                NOP
                LDA     $06             If clock was been up-dated. Then
                CMP     #$00            read time again.
                BNE     $LOOP2
                NOP
                LDY     #$00            Change output from Hex-decimal to
$LOOP3          LDA     ($0A),Y         decimal.
                AND     #$0F
                STA     $06
                LDA     ($0A),Y
                AND     #$F0
                LSR
                STA     $07
                LSR
                LSR
                CLC
                ADC     $07
                ADC     $06
                STA     ($0A),Y
                INY
                TYA
                CMP     $04
                BNE     $LOOP3
                NOP
                LDA     $0300           Restore Accumulator
                LDX     $0301           Restore X Register
                LDY     $0302           Restore Y Register
                PLP                     Restore Processor status
                RTS                     Return to Calling Program
                BRK
```

Program: C_RESET

```
STA   $0300      Save Accumulator
PHP              Save Processor status
NOP
LDA   #$3A
STA   $C0C1      Access to Data Direction Reg. A of PIA
LDA   #$FF
STA   $C0C0      Set Bus A as an output
LDA   #$3E
STA   $C0C1      Close Access to DDR-A
NOP
LDA   #$12
STA   $05
LDA   #$FF
STA   $06
NOP
LDA   $05        Write to clock register #$12
STA   $C0C2
LDA   $06        Value in address $06
STA   $C0C0
LDA   #$36
STA   $C0C1
LDA   #$3E
STA   $C0C1
LDA   #$20
STA   $C0C2
NOP
LDA   #$11
STA   $05
LDA   #$00
STA   $06
NOP
LDA   $05        Write to clock register #$11
STA   $C0C2
LDA   $06        Value in address $06
STA   $C0C0
LDA   #$36
STA   $C0C1
LDA   #$3E
STA   $C0C1
LDA   #$20
STA   $C0C2
NOP
LDA   #$3A
STA   $C0C1      Access to Data Direction Reg. A of PIA
LDA   #$00
STA   $C0C0      Set Bus A as an input
LDA   #$3E
STA   $C0C1      Close Access to DDR-A
LDA   $0300      Restore Accumulator
PLP              Restore Processor Status
RTS              Return to Calling Program
```

Program: C_REG

```
$C_REG      STA   $0300      Save Accumulator
            STX   $0301      Save X Register
            PHP              Save Processor Status
            NOP
            LDA   #$3A
            STA   $C0C1      Access to Data Direction Reg. A of PIA
            LDA   #$FF
            STA   $C0C0      Set Bus A as an output
            LDA   #$3E
            STA   $C0C1      Close Access to DDR-A
            NOP

            LDX   #$08
            LDA   #$0A
            STA   $08
            LDA   $06
            STA   $07
            LDA   #$00
$LOOP2      ASL   $07
            ROL
            CMP   $08
            BCC   $LOOP1
            SBC   $08
            INC   $07
$LOOP1      DEX
            BNE   $LOOP2
            STA   $06
            LDA   $07
            ASL
            ASL
            ASL
            ASL
            CLC
            ADC   $06
            STA   $06
            NOP
            LDA   $05        Write to a clock register
            STA   $C0C2      Register no in address $05
            LDA   $06        Value in address $06
            STA   $C0C0
            LDA   #$36
            STA   $C0C1
            LDA   #$3E
            STA   $C0C1
            LDA   #$20
            STA   $C0C2
            NOP
            LDA   #$3A
            STA   $C0C1      Access to Data Direction Reg. A of PIA
            LDA   #$00
            STA   $C0C0      Set Bus A as an input.
```

```
LDA     #$3E
STA     $C0C1           Close Access to DDR-A
NOP
LDA     $0300           Restore Accumulator
LDX     $0301           Restore X Register
PLP                     Restore Processor Status
RTS                     Return to Calling Program
BRK
```

Listing C-7: Program listing of the subroutine "TIME".

```
TIME        I = INT(I)
            IF  I > 0  AND  I < 4  THEN  GOTO  DIVIDE
            PRINT "ERROR.  Flag I not set for TIME call"
            END

DIVIDE      I = I + 1
            ON I GOTO  RESPIA , SEC , DAY , RESET , RESADD

RESPIA      CALL  C_BINT
            RETURN

SEC         CALL  C_SEC
            Sec = PEEK ($6002)
            Min = PEEK ($6001)
            Hr  = PEEK ($6000)
            RETURN

DAY         CALL  C_DAY
            Day_week = PEEK ($6002)
            Day_month = PEEK ($6001)
            Month = PEEK ($6000)
            RETURN

RESET       CALL  C_RESET
            RETURN

RESADD      POKE  ($05 , Set)
            POKE  ($06 , Value)
            CALL  C_REG
            RETURN

END
```

Listing C-8: Program listing of the subroutine "DATA".

```
DATA        I = INT(I)
            IF  I > 0  AND  I < 2  THEN  GOTO  DIVIDE
            PRINT "ERROR.  Flag I not set for DATA call"
            END

DIVIDE      I = I + 1
            ON I GOTO  RESET , TABLE , CONV

RESET       CALL  A/D_BINT
            RETURN

TABLE       FOR  I = 1 TO  (No. of Channels)
            POKE ($8DFF + I , $F + Channel No.(I))
            NEXT I
            POKE ($904F , No. of Channels)
            RETURN

CONV        CALL  A/D_BOPT
            FOR  I = 1 TO  (No. of Channels)
            L  =  2 * (I-1)
            L8B = PEEK ($6000 + L)
            M4B = PEEK ($6001 + L)
            Result (I) = M4B * 256 + L8B
            NEXT I
            RETURN

END
```

C-9. TRANSDUCER CALIBRATION.

A listing of the applied pressure head (mm of water head) versus the digital equivalent of the output from the transducers, (read by the computer during the calibration of the transducers) is given. Also the plot of the calibration curve for each transducer.

Data for the Calibration of 17 Pressure Transducers.

Pressure (mm) Water	Decimal Output from A/D Converter. Transducer No.																
	1	2	3	4	5	6	7	8	9	10	11	12	13	14	15	16	17
+5	1777	2009	1583	2282	1775	1857	2065	2007	1881	2081	2129	2103	1866	1920	1707	1843	1916
+5	1780	2010	1583	2279	1776	1857	2066	2008	1882	2083	2131	2105	1867	1921	1707	1845	1917
-105	2006	2143	1910	2454	1911	2026	2313	2219	2083	2248	2394	2368	2095	2082	2015	2159	2146
-105	2002	2141	1906	2451	1910	2024	2313	2217	2080	2247	2390	2366	2093	2080	2011	2156	2144
-200	2192	2257	2179	2592	2026	2165	2515	2399	2256	2386	2615	2589	2290	2219	2269	2426	2342
-200	2192	2258	2181	2591	2026	2166	2515	2400	2256	2387	2615	2590	2291	2220	2270	2427	2343
-300	2395	2379	2470	2760	2144	2319	2734	2591	2439	2533	2853	2830	2496	2364	2544	2708	2565
-300	2395	2379	2472	2755	2144	2320	2734	2591	2440	2533	2855	2831	2497	2364	2547	2709	2566
-243	2288	2315	2316	2657	2086	2243	2615	2489	2342	2463	2727	2697	2387	2285	2390	2558	2439
-243	2286	2317	2316	2666	2085	2242	2614	2488	2341	2462	2725	2696	2386	2284	2389	2548	2438
-150	2092	2206	2036	2530	1971	2097	2405	2302	2166	2325	2499	2472	2188	2155	2129	2281	2240
-150	2091	2205	2033	2524	1970	2095	2403	2301	2165	2324	2497	2471	2187	2153	2128	2280	2238
-50	1890	2080	1742	2370	1846	1945	2182	2111	1983	2172	2259	2234	1981	2008	1854	1999	2033
-50	1892	2082	1743	2370	1847	1946	2183	2112	1985	2173	2261	2235	1983	2010	1855	2000	2034
+40	1707	1974	1481	2239	1737	1813	1987	1942	1818	2036	2055	2024	1803	1878	1607	1744	1846
+40	1708	1974	1481	2240	1737	1813	1987	1942	1819	2036	2055	2024	1802	1878	1607	1744	1846
+150	1482	1837	1158	2065	1600	1641	1743	1729	1614	1880	1794	1762	1565	1715	1303	1431	1615
+150	1483	1837	1160	2064	1601	1641	1743	1729	1614	1880	1797	1763	1566	1714	1305	1432	1616
+250	1285	1710	867	1921	1476	1487	1520	1543	1428	1729	1550	1523	1357	1564	1033	1146	1405
+250	1282	1709	864	1924	1475	1485	1517	1545	1426	1727	1549	1521	1355	1562	1032	1141	1403
+350	1069	1584	572	1754	1351	1332	1299	1340	1240	1577	1305	1290	1145	1415	750	859	1194
+350	1069	1584	570	1753	1351	1330	1299	1338	1240	1577	1304	1290	1145	1415	748	858	1193
+300	1170	1646	716	1835	1412	1407	1406	1434	1332	1652	1421	1401	1249	1489	885	1000	1301
+300	1171	1646	716	1838	1413	1408	1406	1435	1333	1653	1423	1401	1249	1490	886	1000	1302
+200	1376	1770	1010	1978	1542	1561	1628	1629	1519	1806	1662	1640	1458	1637	1162	1292	1508
+200	1376	1770	1011	1978	1543	1560	1628	1628	1519	1807	1662	1639	1459	1637	1162	1292	1508
+110	1560	1882	1290	2122	1648	1699	1830	1808	1686	1935	1877	1855	1649	1771	1414	1549	1699
+110	1560	1881	1291	2125	1646	1696	1826	1805	1684	1932	1877	1851	1644	1768	1409	1550	1694
+5	1774	2014	1577	2282	1778	1860	2061	2004	1880	2089	2125	2097	1863	1925	1697	1834	1914
+5	1774	2014	1575	2279	1778	1859	2061	2005	1880	2088	2124	2097	1864	1925	1698	1835	1914

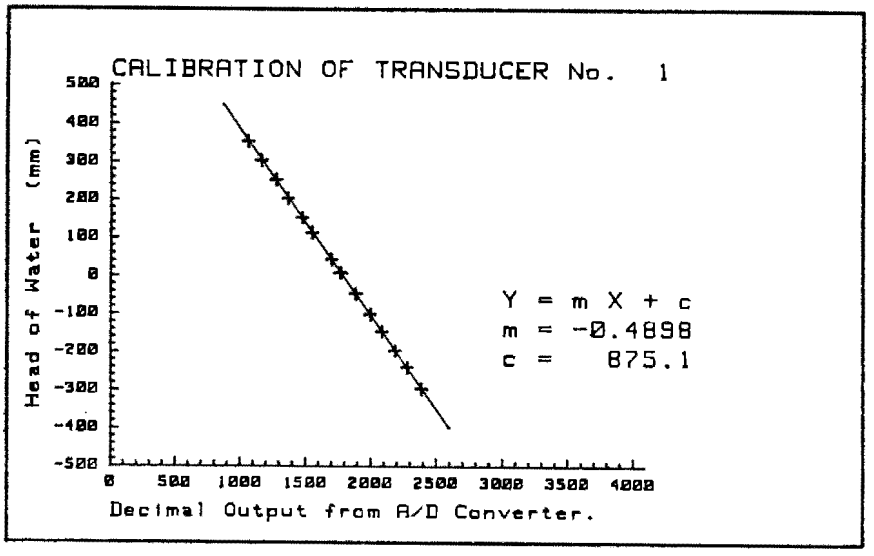

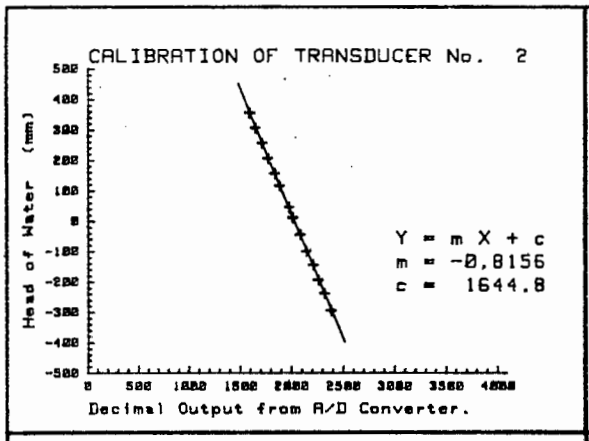
CALIBRATION OF TRANSDUCER No. 2
Head of Water (mm)
Decimal Output from A/D Converter.
Y = m X + c
m = -0.8156
c = 1644.8

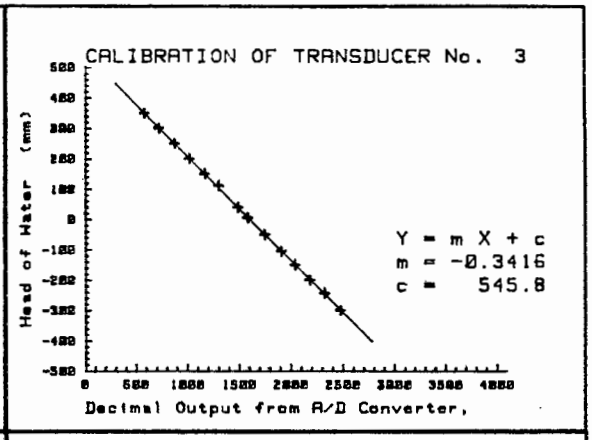
CALIBRATION OF TRANSDUCER No. 3
Head of Water (mm)
Decimal Output from A/D Converter.
Y = m X + c
m = -0.3416
c = 545.8

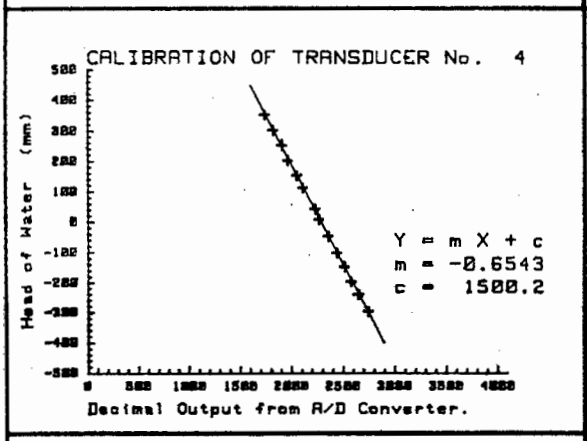
CALIBRATION OF TRANSDUCER No. 4
Head of Water (mm)
Decimal Output from A/D Converter.
Y = m X + c
m = -0.6543
c = 1500.2

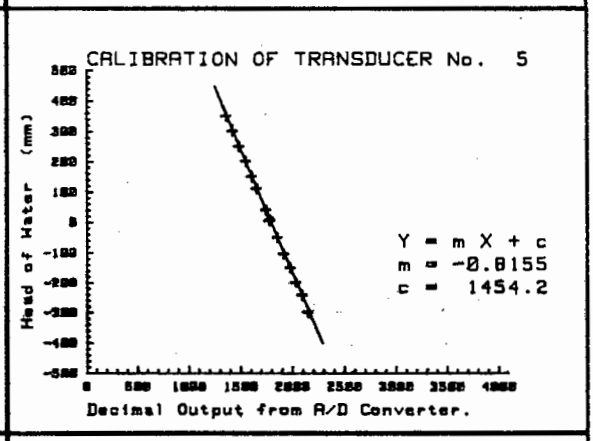
CALIBRATION OF TRANSDUCER No. 5
Head of Water (mm)
Decimal Output from A/D Converter.
Y = m X + c
m = -0.8155
c = 1454.2

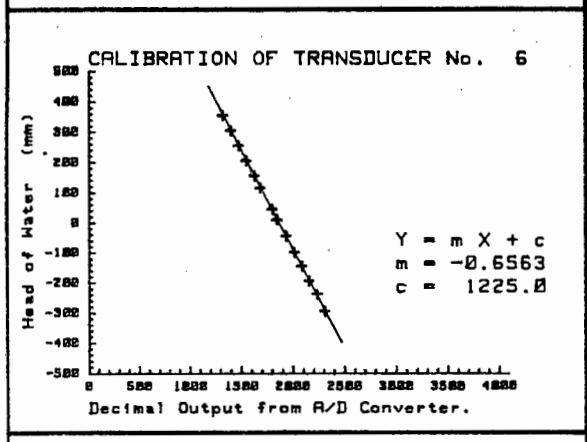
CALIBRATION OF TRANSDUCER No. 6
Head of Water (mm)
Decimal Output from A/D Converter.
Y = m X + c
m = -0.6563
c = 1225.0

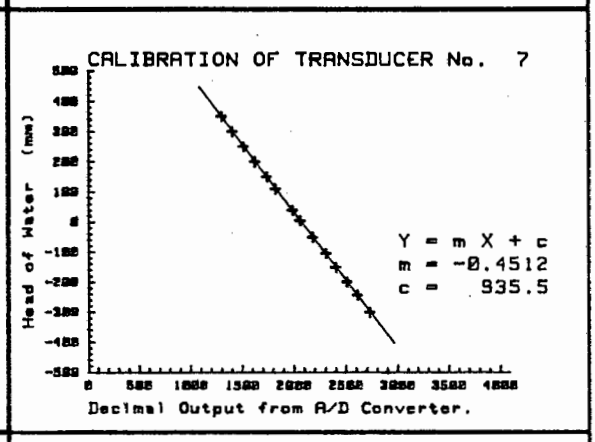
CALIBRATION OF TRANSDUCER No. 7
Head of Water (mm)
Decimal Output from A/D Converter.
Y = m X + c
m = -0.4512
c = 935.5

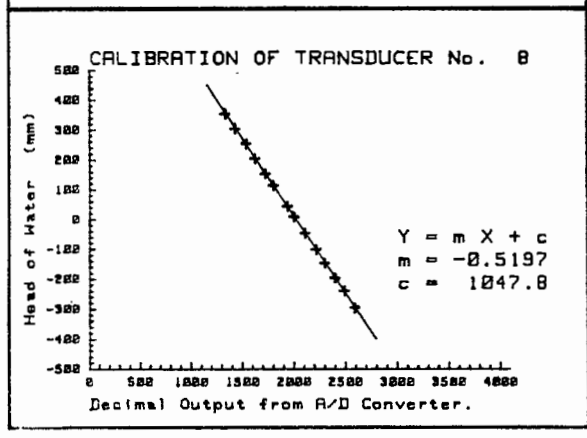
CALIBRATION OF TRANSDUCER No. 8
Head of Water (mm)
Decimal Output from A/D Converter.
Y = m X + c
m = -0.5197
c = 1047.8

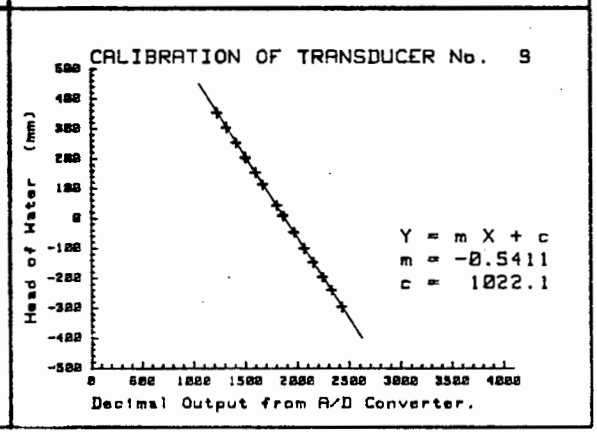
CALIBRATION OF TRANSDUCER No. 9
Head of Water (mm)
Decimal Output from A/D Converter.
Y = m X + c
m = -0.5411
c = 1022.1

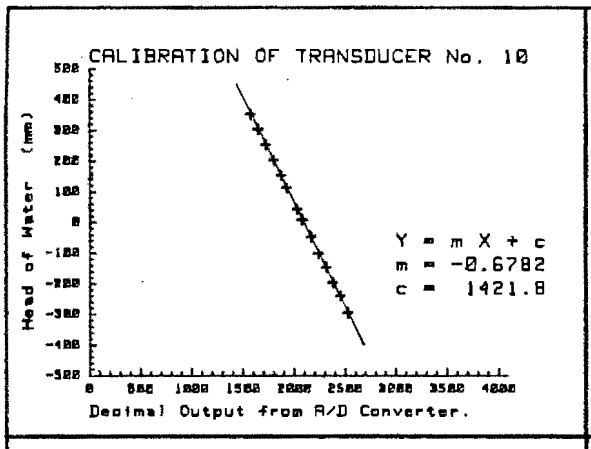
CALIBRATION OF TRANSDUCER No. 10
Head of Water (mm)
Decimal Output from A/D Converter.
Y = m X + c
m = -0.6782
c = 1421.8

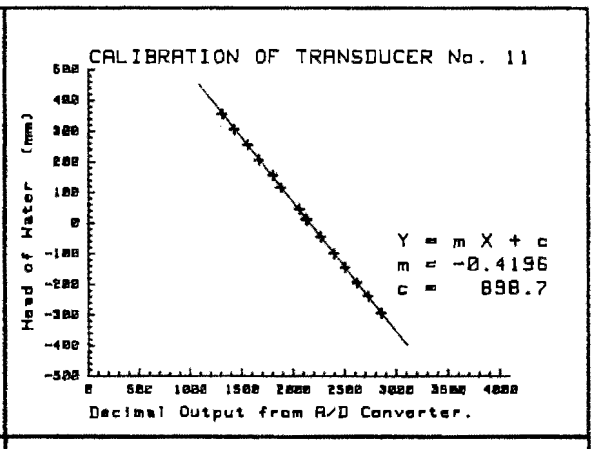
CALIBRATION OF TRANSDUCER No. 11
Head of Water (mm)
Decimal Output from A/D Converter.
Y = m X + c
m = -0.4196
c = 898.7

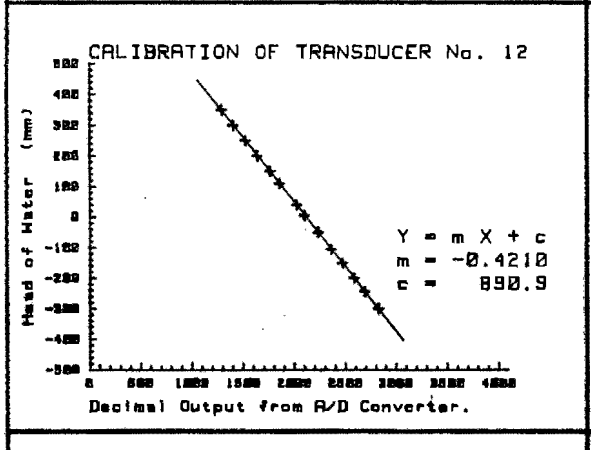
CALIBRATION OF TRANSDUCER No. 12
Head of Water (mm)
Decimal Output from A/D Converter.
Y = m X + c
m = -0.4210
c = 890.9

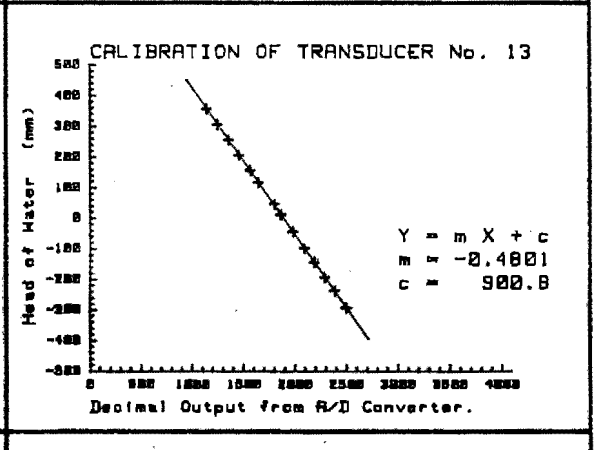
CALIBRATION OF TRANSDUCER No. 13
Head of Water (mm)
Decimal Output from A/D Converter.
Y = m X + c
m = -0.4801
c = 900.8

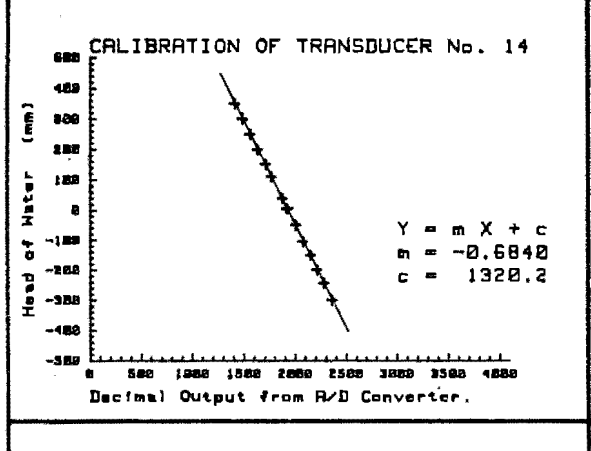
CALIBRATION OF TRANSDUCER No. 14
Head of Water (mm)
Decimal Output from A/D Converter.
Y = m X + c
m = -0.6840
c = 1320.2

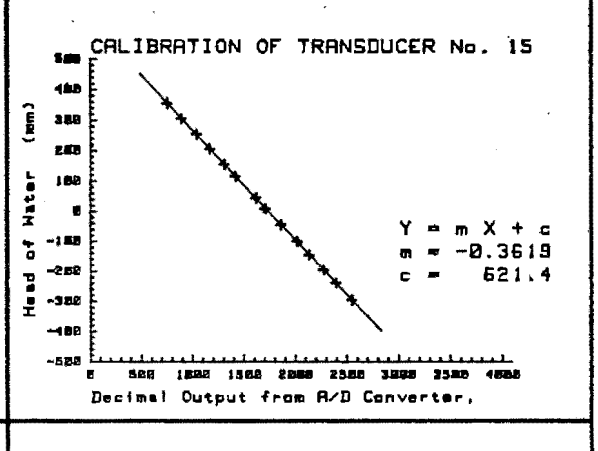
CALIBRATION OF TRANSDUCER No. 15
Head of Water (mm)
Decimal Output from A/D Converter.
Y = m X + c
m = -0.3619
c = 621.4

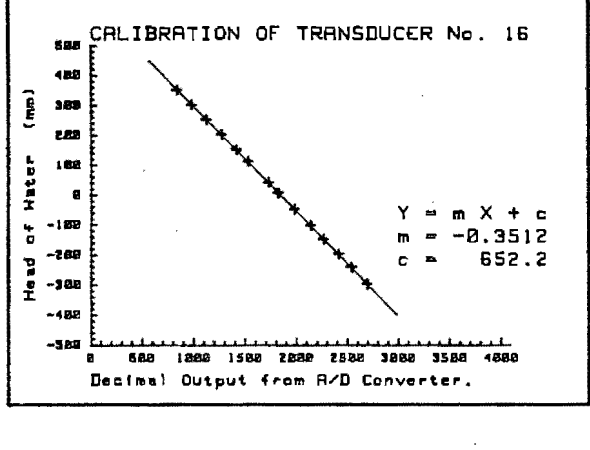
CALIBRATION OF TRANSDUCER No. 16
Head of Water (mm)
Decimal Output from A/D Converter.
Y = m X + c
m = -0.3512
c = 652.2

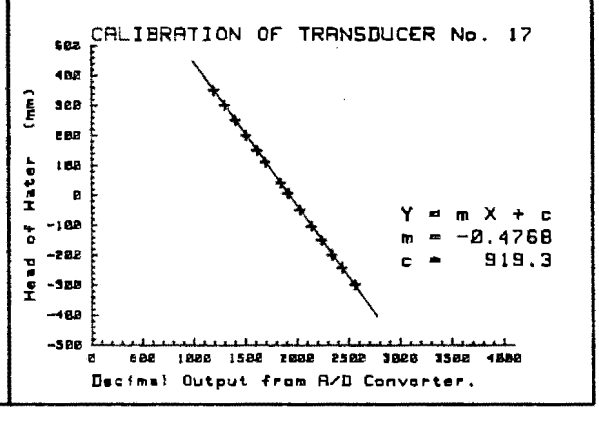
CALIBRATION OF TRANSDUCER No. 17
Head of Water (mm)
Decimal Output from A/D Converter.
Y = m X + c
m = -0.4768
c = 919.3

D-1. Specific Gravity. (ie. Relative Mass Density)

Introduction.

This test is done to determine the specific gravity (relative mass density) of the granular soil used for the experiments performed in this thesis. The method used is the same as that given in the 1975 British standard. (BS 1377:1975, Test 6(B)). Head [17]

Method.

The test was performed using a density bottle. This was washed, rinsed with acetone, dried with warm air and its mass found W_1. A random representative sample, of the original sample was obtained, by quartering down to about 50g. The soil was then oven dried at 105-110 ^{o}C and cooled in a desiccator. Using a funnel the soil was poured into the density bottle until about half-full. The mass of the density bottle with the sand was then found W_2. De-aired water was carefully added, so as not to trap air, to the bottle until the sand was covered. The bottle was then put inside a vacuum desiccator and a vacuum applied to remove any air trapped in the soil. After removal of all the air, the bottle was topped up to the full mark, and it was placed in a constant-temperature bath of temperature T. The bottle was left in the bath until it had attained the correct temperature. If the water level changed in the density bottle, this was corrected by adding de-aired water. The bottle was then removed, wiped dry and its mass found W_3. (ie. Bottle, soil and liquid).

The bottle was then cleaned out and completely filled with de-aired water and put back in the constant temperature bath as before. When the bottle had attained the correct temperature, it was removed, wiped dry and its mass found W_4. (ie. Bottle and liquid).

Calculation.

The specific gravity (ie. relative mass density) G_s of the soil was then calculated from the following equation.

$$G_s = \frac{G_T (W_2 - W_1)}{(W_4 - W_1) - (W_3 - W_2)}$$

where G_T is the specific gravity of the water at temperature T. (See Table. B-1) W_1 = mass of density bottle, W_2 = mass of bottle plus dry soil, W_3 = mass of bottle, soil plus water, W_4 = mass of bottle plus water only.

The average of the repeated test is reported as the specific gravity.

Results.

The specific gravity: G_s = 2,64 was obtained from the average of repeated tests. (See laboratory sheet following showing the specific gravity calculated for each test.)

SPECIFIC GRAVITY TEST

U.C.T. SOIL MECHANICS LABORATORY

SOIL SAMPLE. _____

TEST No. SGTA01

DATE. 8/85

TESTED By. G WARDLE

LOCATION. CAPE FLATS

BORING No. _____ SAMPLE DEPTH. _____

SAMPLE No. GW/MSC/01

SAMPLE No. & Ref.						
DETERMINATION No.			1	2	3	4
Pycnometer No.			GW1	GW2	GW3	GW4
Pycnometer mass	g	w_1	37,620	32,482	33,197	39,009
Pycnometer & soil.	g	w_2	78,600	70,267	78,543	86,661
Pycnometer, soil & water	g	w_3	112,952	105,865	111,301	118,539
Temperature	°C	T	23	23	23	23
Pycnometer & water	g	w_4	87,441	82,371	83,060	88,872
SPECIFIC GRAVITY OF WATER		G_t*	0,9976	0,9976	0,9976	0,9976
SPECIFIC GRAVITY OF SOIL		G_s	2,64	2,64	2,65	2,64

* From Table of Specific Gravity of water for temperature T.

REMARKS:

$$G_s = \frac{G_t.(w_2 - w_1)}{(w_4 - w_1)-(w_3 - w_2)}$$

G_s = 2,64

G.R.Wardle.
M.Sc. Thesis
U.C.T. 1984/85

D-2. Particle Size Analysis.

Introduction.

The object of a particle size analysis is to group the discrete particles of a soil into separate ranges of sizes and so as determine the relative proportions, by dry mass, of each size range.

A sieve analysis was performed to seperate the soil into different size ranges. The soil did not have many fine particles (< 0,2 mm) so a sedimentation procedure was not required. The method used is the same as that given in 1975 British Standard. (BS 1377: 1975, Test 7(B)) Head[17].

Method.

The test was performed using a simple dry sieving procedure. This was possible as the soil was a clean granular material. A random representative sample of the original sample was obtained, by quartering, to about > 100 g. (Based on BS 1377; 1975). This was oven dried at 105-110 ^{o}C, cooled in a desiccator and its mass found W_1. A set of sieves (manufactured to BS 410) was selected, with the size range from 2 mm down to 63 micron. After the set of sieves had been cleaned, each sieve's mass was found and then reassembled with the largest aperture sieve at the top.

The dried soil sample was placed in the topmost sieve (2 mm sieve size) and shaken long enough for all particles smaller than each aperture to pass through. A mechanical shaker was used to shake the set of sieves for a period of 15 minutes. (Greater then 10 minutes as specified by the Britsh Standard.)

After shaking, the set of sieves were carefully dismantled. The mass of the sieves, with retained soil, was found. The mass measured was recorded against the sieve aperture size. The mass of soil passing the

smallest sieve was also measured and recorded.

Calculations.

In order to draw a particle size distrbution curve and tabulate the data, it was necessary to calculate the cumulative percentage (by mass) of particles finer then each sieve aperture size. The cumulative mass passing each sieve was calculated first, from which the percentage passing was derived.

If the total initial mass is W_1. The mass retained in the first sieve W_{s1}. Then the mass passing the first sieve = $W_1 - W_{s1}$. The percentage passing the first sieve is given by:

$$P_1 = \frac{(W_1 - W_{s1})}{W_1} \quad 100$$

The mass passing the second sieve = $W_1 - W_{s1} - W_{s2}$. The percentage passing the second sieve is given by:

$$P_2 = \frac{W_1 - (W_{s1} + W_{s2})}{W_1} \quad 100$$

and so-on. The percentage passing any subsequent sieve can be written as:

$$P = \frac{W_1 - \Sigma W}{W_1} \quad 100$$

where ΣW denotes the sum of the masses retained on all the sieves down to and including the one in question. ($\Sigma W = W_{s1} + W_{s2} + \ldots$ etc). A check is that the mass passing the last sieve should, or very nearly equal, the mass collected in the pan at the bottom.

Results.

The results following are for the set of repeated sieve analysis tests performed. An average of the results is taken to give a grading curve as plotted.

The effective size (D_{10}), the largest size of the smallest 10 % is read off the graph as: 0,72

The uniformity coefficient (U), the ratio of the 60 % particle size (D_{60}) to the 10 % particle size (D_{10}) is: 1,3

SIEVE ANALYSIS

U.C.T. SOIL MECHANICS LABORATORY

SOIL SAMPLE. _____

TEST No. PSDA01

DATE. 1/8/85

TESTED By. G WARDLE

LOCATION. CAPE FLATS

BORING No. _____ SAMPLE DEPTH. _____

SAMPLE No. GW/MSC/01

SPECIFIC GRAVITY Gs. 2,64

SOIL SAMPLE WEIGHT

Container No. GW1

Dry soil & container. g 1721,4

Container. g 570,4

Dry soil. w1 g 1151,0

SIEVE No.	SIEVE OPENING (mm)	WT. SIEVE (g)	WT. SIEVE & SOIL (g)	SOIL RETAINED (g)	CUMULATIVE MASS PASSING	% PASSING
	2	472,5	473,3	0,8	1150,2	99,9
	1	436,5	645,1	208,6	941,6	81,8
	0,850	534,3	951,7	417,4	524,2	45,5
	0,710	434,0	903,4	469,4	54,8	4,8
	0,600	502,1	536,1	34,0	20,8	1,8
	0,425	385,5	402,4	16,9	3,9	0,3
	0,300	466,0	468,4	2,4	1,5	0,1
	0,125	340,1	341,2	1,1	0,4	0
	0,075	354,8	354,8	0,0	0,4	0
	PAN	335,6	335,6	0,0	0,4	0

REMARKS:

$$P\% = \frac{w1 - \sum w}{w1} \times 100$$

S.R. Wardle.
B.Sc. Thesis
U.C.T. 1984/88

SIEVE ANALYSIS

U.C.T. SOIL MECHANICS LABORATORY

SOIL SAMPLE. _____

TEST No. PSDA02

DATE. 1/8/85

TESTED By. G WARDLE

LOCATION. CAPE FLATS

BORING No. _____ SAMPLE DEPTH. _____

SAMPLE No. GW/MSC/01

SPECIFIC GRAVITY Gs. 2,64

SOIL SAMPLE WEIGHT

Container No. GW1

Dry soil & container. g 2023,9

Container. g 930,7

Dry soil. m_1 g 1093,2

SIEVE No.	SIEVE OPENING (mm)	WT. SIEVE (g)	WT. SIEVE & SOIL (g)	SOIL RETAINED (g)	CUMULATIVE MASS PASSING	% PASSING
	2	472,5	473,7	1,2	1092,0	99,9
	1	436,5	657,3	220,8	871,2	79,7
	0,850	534,7	911,0	376,3	494,9	45,3
	0,710	434,0	858,2	424,2	70,7	6,5
	0,600	501,9	546,4	44,5	26,2	2,4
	0,425	385,4	409,3	23,9	2,3	0,2
	0,300	465,9	467,8	1,9	0,4	0
	0,125	340,1	340,3	0,2	0,2	0
	0,075	354,8	354,8	0,0	0,2	0
	PAN	335,6	335,6	0,0	0,2	0

REMARKS:

$$P\% = \frac{m_1 - \sum m}{m_1} \times 100$$

G.R. Wardle.
B.Sc. Thesis
U.C.T. 1984/85

SIEVE ANALYSIS

U.C.T. SOIL MECHANICS LABORATORY

SOIL SAMPLE. _____

TEST No. PSDA03

DATE. 2/8/85

TESTED By. G WARDLE

LOCATION. CAPE FLATS

BORING No. _____ SAMPLE DEPTH. _____

SAMPLE No. GW/MSC/01

SPECIFIC GRAVITY Gs. 2,64

SOIL SAMPLE WEIGHT

Container No. GW1

Dry soil & container. g 1928,1

Container. g 820,3

Dry soil. w1 g 1107,8

SIEVE No.	SIEVE OPENING (mm)	WT. SIEVE (g)	WT. SIEVE & SOIL (g)	SOIL RETAINED (g)	CUMULATIVE MASS PASSING	% PASSING
	2	472,5	473,5	1,0	1106,8	99,9
	1	436,2	640,9	204,7	902,1	81,4
	0,850	534,6	922,1	387,5	514,6	46,5
	0,710	434,0	864,3	430,3	84,3	7,6
	0,600	502,0	549,1	47,1	37,2	3,4
	0,425	385,4	415,0	29,6	7,6	0,7
	0,300	465,9	469,2	3,3	4,3	0,4
	0,125	340,0	340,7	0,7	3,6	0,3
	0,075	354,8	354,8	0,0	3,6	0,3
	PAN	335,6	335,6	0,0	3,6	0,3

REMARKS:

$$Px = \frac{w1 - \sum w}{w1} \times 100$$

SIEVE ANALYSIS

U.C.T. SOIL MECHANICS LABORATORY

SOIL SAMPLE. _____

TEST No. PSDA04

DATE. 2/8/85

TESTED By. G WARDLE

LOCATION. CAPE FLATS

BORING No. _____ SAMPLE DEPTH. _____

SAMPLE No. GW/MSC/01

SPECIFIC GRAVITY Gs. 2,64

SOIL SAMPLE WEIGHT

Container No. GW1

Dry soil & container. g 1887,8

Container. g 717,6

Dry soil. wl g 1170,2

SIEVE No.	SIEVE OPENING (mm)	WT. SIEVE (g)	WT. SIEVE & SOIL (g)	SOIL RETAINED (g)	CUMULATIVE MASS PASSING	% PASSING
	2	472,5	473,9	1,4	1168,8	99,9
	1	436,3	670,0	233,7	935,1	79,9
	0,850	534,6	919,0	384,4	550,7	47,1
	0,710	433,9	884,6	450,7	100,0	8,5
	0,600	502,0	553,7	51,7	48,3	4,1
	0,425	385,4	420,0	34,6	13,7	1,2
	0,300	465,9	472,0	6,1	7,6	0,6
	0,125	340,0	346,9	6,9	0,7	0,1
	0,075	354,8	355,1	0,3	0,4	0
	PAN	335,6	335,8	0,2	0,2	0

REMARKS:

$$Px = \frac{wl - \sum w}{wl} \times 100$$

G.R. Wardle.
B.Sc. Thesis
U.C.T. 1984/85

PARTICLE SIZE DISTRIBUTION.

SUMMARY OF RESULTS.

U.C.T. SOIL MECHANICS LABORATORY

TEST No. PSD/A01/A02/A03/A04

DATE. 8/85

TESTED By. G WARDLE

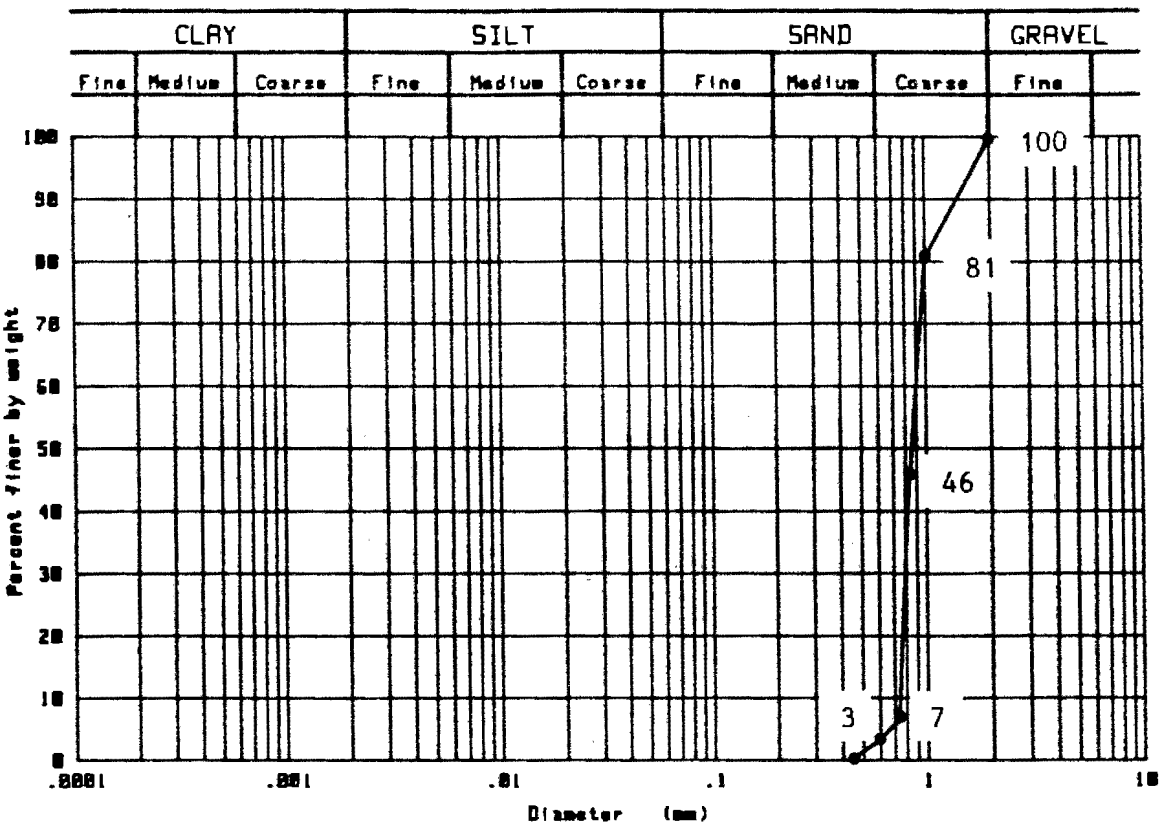

REMARKS: SUMMARY OF RESULTS FROM PARTICLE SIZE TESTS.

Sieve aperture size (mm)	Percent passing (By mass)
2	100
1	81
0,850	46
0,710	7
0,600	3
0,425	0,6
0,300	0,3

S.B.Wardle.
R.Sh. Thesis
U.C.T. 1985/88

E-1. Saturated hydraulic conductivity tests.

Listings of the results for the Constant-head tests performed are given in this appendix. The tests performed were:

CHPA01
CHPA02
CHPA03
CHPA04
CHPA05
CHPA06
CHPA07
CHPA08
CHPA09

Also given is the plot for each test of the hydraulic gradient versus the Darcian velocity, to determine the hydraulic conductivity for the test.

CONSTANT HEAD PERMEABILITY TEST

SOIL SAMPLE : COARSE SAND

TEST NO : CHPA01
DATE : 01/08/85
TESTED BY: G.Wardle

LOCATION : Cape Flats
SAMPLE NO : GW/MSC/01

SOIL SPEC.			PERMEAMETER.		
SPECIFIC GRAVITY:	2.64		DIAMETER :	7.37	cm
WT DRY SOIL :	2658.2	g	AREA =	42.61	sq cm
SAMPLE LENGTH :	34.3	cm	l1 :	12.75	cm
VOID RATIO e =	.452		l2 :	12.70	cm

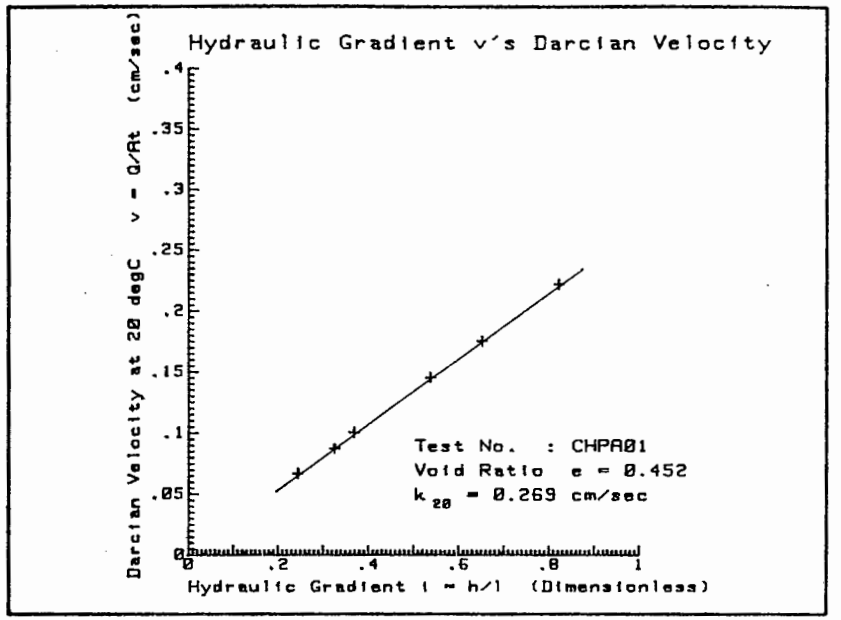

No.	Quantity Q cu cm	Time t sec	Temp.T deg C	Piezometers (cm) h1	h2	h3	Flow Rate Q/t cu cm/sec	Darcian Velocity Q/At at T	at 20 deg C	Hydraulic Gradient h/l i1	i2	i3	iaverage
1	880	270	15.5	46.6	42.5	38.3	3.26	.076	.086	.322	.331	.326	.326
2	720	290	15.5	43.2	40.3	37.0	2.48	.058	.065	.227	.260	.244	.244
3	925	246	15.5	48.5	43.9	39.1	3.76	.088	.099	.361	.378	.369	.369
4	825	151	15.5	56.0	49.4	42.3	5.46	.128	.144	.518	.559	.538	.538
5	913	138	15.5	61.5	53.6	44.9	6.62	.155	.174	.620	.685	.652	.652
6	965	115	15.5	69.9	59.8	49.0	8.39	.197	.221	.796	.850	.823	.823

CONSTANT HEAD PERMEABILITY TEST

SOIL SAMPLE : COARSE SAND

LOCATION : Cape Flats
SAMPLE NO : GW/MSC/01

TEST NO : CHPA02
DATE : 01/08/85
TESTED BY: G.Wardle

SOIL SPEC.

SPECIFIC GRAVITY: 2.64
WT DRY SOIL : 2658.2 g
SAMPLE LENGTH : 37.9 cm
VOID RATIO e = .604

PERMEAMETER.

DIAMETER : 7.37 cm
AREA = 42.61 sq cm
l1 : 12.75 cm
l2 : 12.70 cm

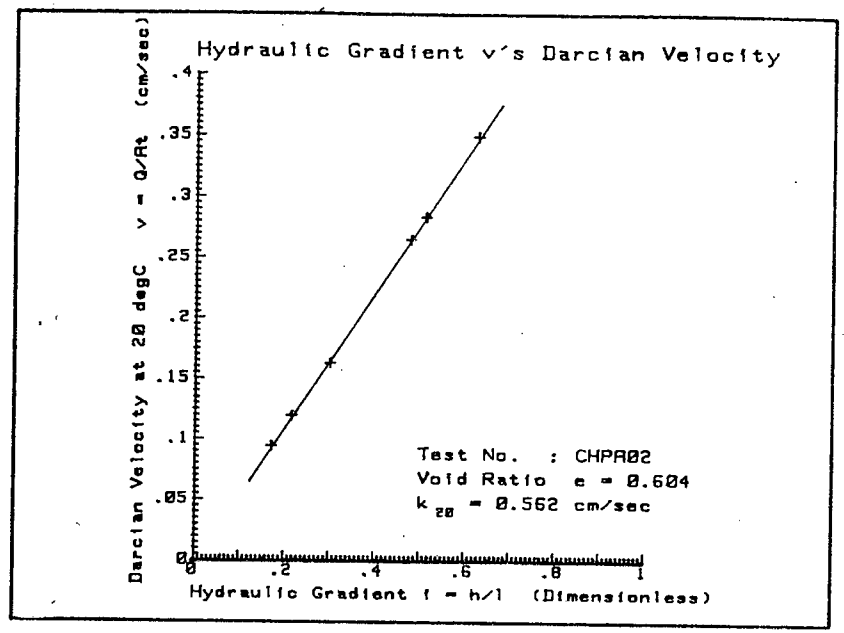

No.	Quantity Q cu cm	Time t sec	Temp T deg C	Piezometers (cm) h1	h2	h3	Flow Rate Q/t cu cm/sec	Darcian Velocity Q/At at T	at 20 deg C	Hydraulic Gradient h/l i1	i2	i3	iaverage
1	935	205	15.5	47.1	44.3	41.5	4.56	.107	.120	.220	.220	.220	.220
2	600	166	15.5	44.2	42.0	39.7	3.61	.085	.095	.173	.177	.175	.175
3	760	122	15.5	52.2	48.2	44.5	6.23	.146	.164	.310	.299	.305	.305
4	959	95	15.5	65.3	59.1	53.1	10.09	.237	.265	.490	.472	.481	.481
5	972	90	15.5	67.9	61.3	54.8	10.80	.253	.284	.518	.512	.515	.515
6	905	68	15.5	77.1	69.0	61.1	13.31	.312	.350	.635	.622	.629	.629

CONSTANT HEAD PERMEABILITY TEST

SOIL SAMPLE : COARSE SAND

TEST NO : CHPA03
DATE : 01/08/85
TESTED BY: G.Wardle

LOCATION : Cape Flats
SAMPLE NO : GW/MSC/01

SOIL SPEC.

SPECIFIC GRAVITY: 2.64
WT DRY SOIL : 2658.2 g
SAMPLE LENGTH : 36.6 cm
VOID RATIO e = .549

PERMEAMETER.

DIAMETER : 7.37 cm
AREA = 42.61 sq cm
l1 : 12.75 cm
l2 : 12.70 cm

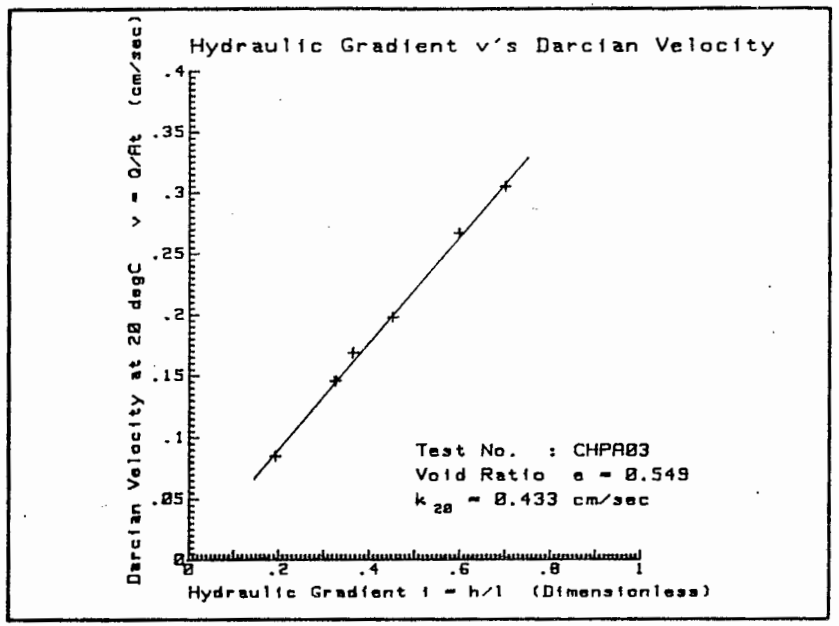

No.	Quantity Q cu cm	Time t sec	Temp T deg C	Piezometers (cm) h1	h2	h3	Flow Rate Q/t cu cm/sec	Darcian Velocity Q/At at T	at 20 deg C	Hydraulic Gradient h/l i1	i2	i3	iaverage
1	865	269	16.0	45.2	42.8	40.3	3.22	.075	.083	.188	.197	.193	.193
2	972	151	16.0	54.8	50.1	45.6	6.44	.151	.167	.373	.354	.363	.363
3	883	159	16.0	52.4	48.1	44.1	5.55	.130	.144	.337	.311	.324	.324
4	900	119	16.0	59.7	53.8	48.2	7.56	.177	.196	.463	.441	.452	.452
5	960	94	16.0	69.5	61.6	54.3	10.21	.240	.265	.620	.575	.597	.597
6	876	75	16.0	75.9	66.6	58.1	11.68	.274	.303	.729	.669	.699	.699

CONSTANT HEAD PERMEABILITY TEST

SOIL SAMPLE : COARSE SAND

TEST NO : CHPA04
DATE : 01/08/85
TESTED BY: G.Wardle

LOCATION : Cape Flats
SAMPLE NO : GW/MSC/01

SOIL SPEC.

SPECIFIC GRAVITY: 2.64
WT DRY SOIL : 2516.3 g
SAMPLE LENGTH : 33.4 cm
VOID RATIO e = .493

PERMEAMETER.

DIAMETER : 7.37 cm
AREA = 42.61 sq cm
l1 : 12.75 cm
l2 : 12.70 cm

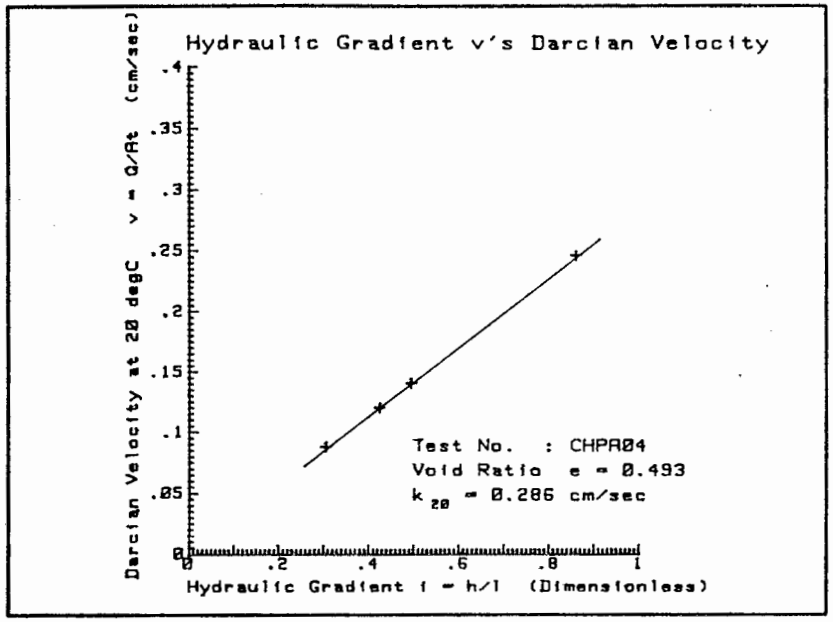

No.	Quantity Q cu cm	Time t sec	Temp T deg C	Piezometers (cm) h1	h2	h3	Flow Rate Q/t cu cm/sec	Darcian Velocity Q/At at T	at 20 deg C	Hydraulic Gradient h/l i1	i2	i3	iaverage
1	871	165	15.0	55.9	49.4	43.2	5.28	.124	.141	.510	.488	.499	.499
2	660	146	15.0	52.6	47.0	41.7	4.52	.106	.120	.439	.417	.428	.428
3	736	223	15.0	47.5	43.4	39.6	3.30	.077	.088	.318	.299	.308	.308
4	970	105	15.0	73.7	62.3	51.7	9.24	.217	.246	.898	.831	.864	.864

CONSTANT HEAD PERMEABILITY TEST

SOIL SAMPLE : COARSE SAND

LOCATION : Cape Flats
SAMPLE NO : GW/MSC/01

TEST NO : CHPA05
DATE : 01/08/85
TESTED BY: G.Wardle

SOIL SPEC.

SPECIFIC GRAVITY: 2.64
WT DRY SOIL : 2516.3 g
SAMPLE LENGTH : 35.4 cm
VOID RATIO e = .583

PERMEAMETER.

DIAMETER : 7.37 cm
AREA = 42.61 sq cm
l1 : 12.75 cm
l2 : 12.70 cm

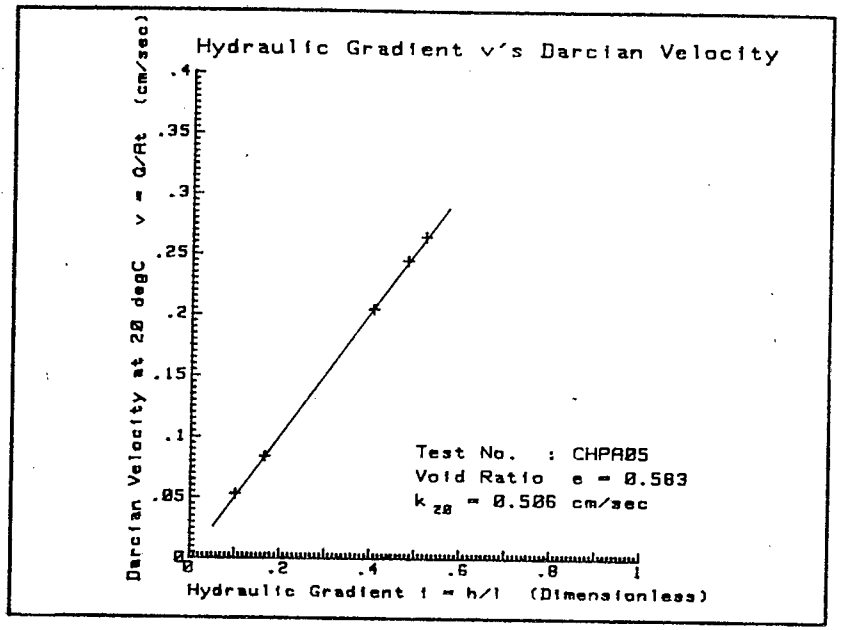

No.	Quantity Q cu cm	Time t sec	Temp T deg C	Piezometers (cm) h1	h2	h3	Flow Rate Q/t cu cm/sec	Darcian Velocity Q/At at T	at 20 deg C	Hydraulic Gradient h/l i1	i2	i3	iaverage
1	646	330	15.0	43.1	41.8	40.5	1.96	.046	.052	.098	.102	.100	.100
2	625	200	15.0	45.4	43.2	41.2	3.13	.073	.083	.169	.161	.165	.165
3	772	101	15.0	60.2	54.9	49.9	7.64	.179	.204	.416	.394	.405	.405
4	961	105	15.0	65.7	59.5	53.5	9.15	.215	.244	.486	.472	.479	.479
5	851	86	15.0	68.0	61.2	54.8	9.90	.232	.263	.533	.504	.519	.519

CONSTANT HEAD PERMEABILITY TEST

SOIL SAMPLE : COARSE SAND

LOCATION : Cape Flats
SAMPLE NO : GW/MSC/01

TEST NO : CHPA06
DATE : 01/08/85
TESTED BY: G.Wardle

SOIL SPEC.

SPECIFIC GRAVITY: 2.64
WT DRY SOIL : 2516.3 g
SAMPLE LENGTH : 37.2 cm
VOID RATIO e = .663

PERMEAMETER.

DIAMETER : 7.37 cm
AREA = 42.61 sq cm
l1 : 12.75 cm
l2 : 12.70 cm

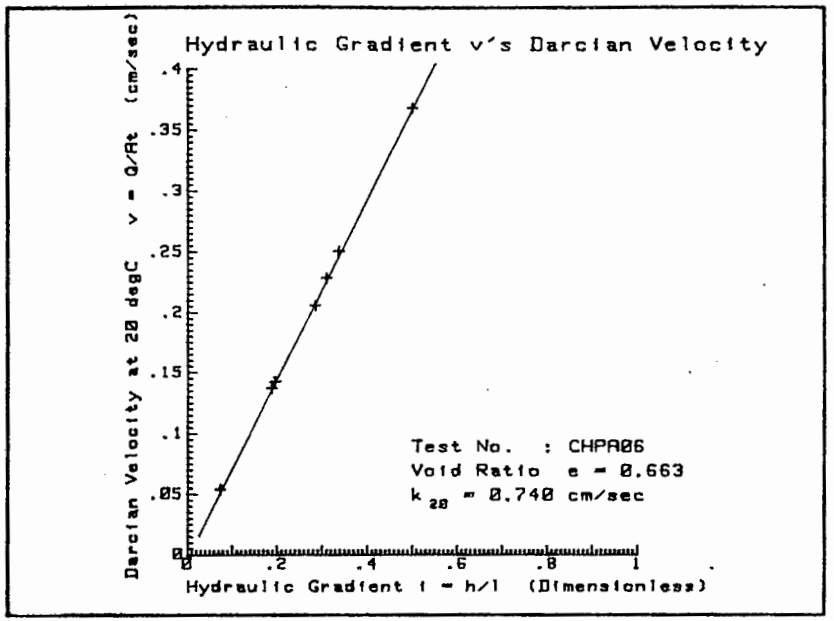

No.	Quantity Q cu cm	Time t sec	Temp T deg C	Piezometers (cm) h1	h2	h3	Flow Rate Q/t cu cm/sec	Darcian Velocity Q/At at T	at 20 deg C	Hydraulic Gradient h/l i1	i2	i3	iaverage
1	735	370	15.0	42.5	41.6	40.5	1.99	.047	.053	.067	.091	.079	.079
2	761	143	15.0	50.1	47.6	45.0	5.32	.125	.142	.200	.201	.200	.200
3	769	90	15.0	59.7	55.6	51.7	8.54	.201	.228	.322	.307	.314	.314
4	835	89	15.0	62.2	57.8	53.5	9.38	.220	.250	.349	.335	.342	.342
5	846	110	15.0	57.1	53.5	49.7	7.69	.180	.205	.282	.295	.289	.289
6	965	70	15.0	75.0	68.7	62.2	13.79	.324	.367	.498	.512	.505	.505
7	940	184	15.0	47.6	45.4	42.7	5.11	.120	.136	.176	.209	.193	.193

CONSTANT HEAD PERMEABILITY TEST

SOIL SAMPLE : COARSE SAND

TEST NO : CHPA07
DATE : 02/08/85
TESTED BY: G.Wardle

LOCATION : Cape Flats
SAMPLE NO : GW/MSC/01

SOIL SPEC.			PERMEAMETER.		
SPECIFIC GRAVITY:	2.64		DIAMETER :	7.37	cm
WT DRY SOIL :	2708.3	g	AREA =	42.61	sq cm
SAMPLE LENGTH :	36.5	cm	l1 :	12.75	cm
VOID RATIO e =	.516		l2 :	12.70	cm

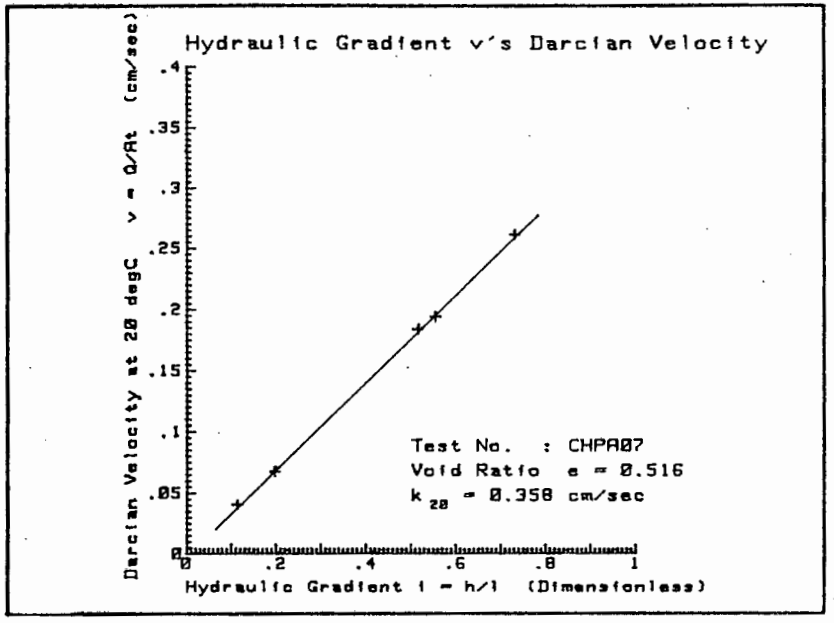

No.	Quantity Q cu cm	Time t sec	Temp T deg C	Piezometers (cm) h1	h2	h3	Flow Rate Q/t cu cm/sec	Darcian Velocity Q/At at T	at 20 deg C	Hydraulic Gradient h/l i1	i2	i3	iaverage
1	642	425	14.5	43.4	42.1	40.5	1.51	.035	.041	.106	.122	.114	.114
2	603	240	14.5	47.1	44.7	42.1	2.51	.059	.068	.192	.205	.198	.198
3	835	116	14.5	62.7	55.6	48.6	7.20	.169	.194	.561	.547	.554	.554
4	735	76	14.5	73.3	64.1	54.7	9.67	.227	.261	.722	.740	.731	.731
5	790	116	14.5	61.1	54.6	48.0	6.81	.160	.184	.510	.520	.515	.515

CONSTANT HEAD PERMEABILITY TEST

SOIL SAMPLE : COARSE SAND

TEST NO : CHPA08
DATE : 02/08/85
TESTED BY: G.Wardle

LOCATION : Cape Flats
SAMPLE NO : GW/MSC/01

SOIL SPEC.

SPECIFIC GRAVITY: 2.64
WT DRY SOIL : 2708.3 g
SAMPLE LENGTH : 38.4 cm
VOID RATIO e = .595

PERMEAMETER.

DIAMETER : 7.37 cm
AREA = 42.61 sq cm
l1 : 12.75 cm
l2 : 12.70 cm

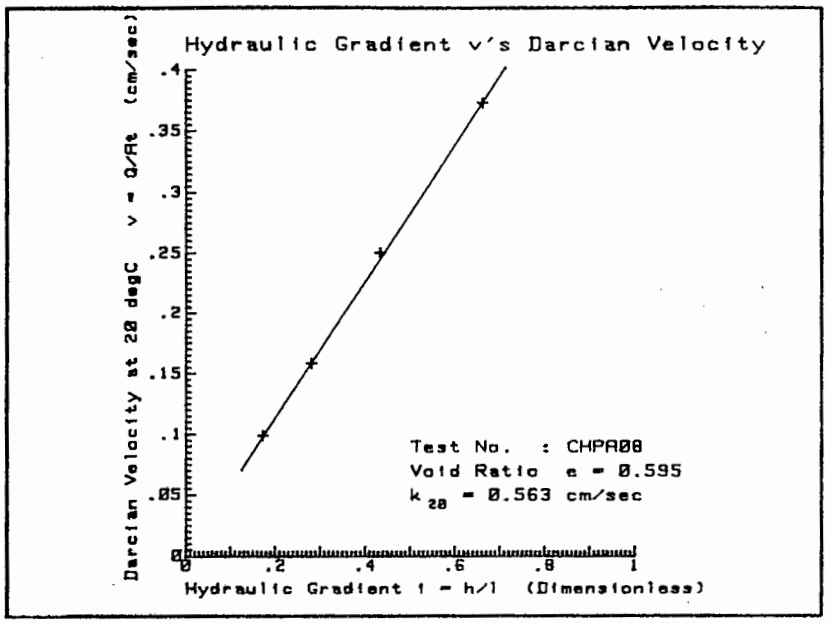

No.	Quantity Q cu cm	Time t sec	Temp T deg C	Piezometers (cm) h1	h2	h3	Flow Rate Q/t cu cm/sec	Darcian Velocity Q/At at T	at 20 deg C	Hydraulic Gradient h/l i1	i2	i3	iaverage
1	662	184	14.5	47.6	45.5	43.1	3.60	.084	.097	.161	.189	.175	.175
2	710	122	14.5	54.8	51.1	47.6	5.82	.137	.157	.290	.276	.283	.283
3	765	83	14.5	66.1	60.4	55.0	9.22	.216	.249	.447	.425	.436	.436
4	950	69	14.5	83.9	75.4	67.0	13.77	.323	.372	.667	.661	.664	.664

CONSTANT HEAD PERMEABILITY TEST

SOIL SAMPLE : COARSE SAND

TEST NO : CHPA09
DATE : 02/08/85
TESTED BY: G.Wardle

LOCATION : Cape Flats
SAMPLE NO : GW/MSC/01

SOIL SPEC.

SPECIFIC GRAVITY: 2.64
WT DRY SOIL : 2708.3 g
SAMPLE LENGTH : 37.8 cm
VOID RATIO e = .570

PERMEAMETER.

DIAMETER : 7.37 cm
AREA = 42.61 sq cm
l1 : 12.75 cm
l2 : 12.70 cm

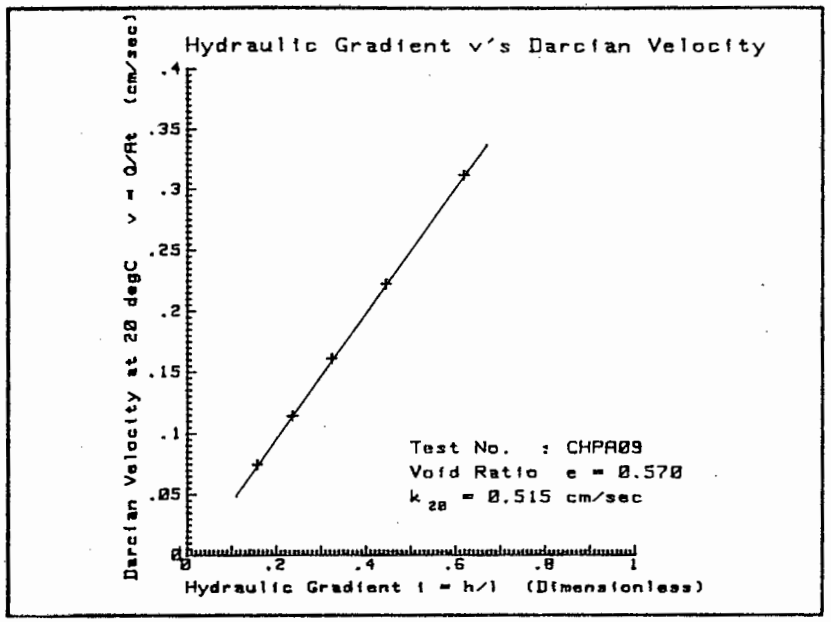

No.	Quantity Q cu cm	Time t sec	Temp T deg C	Piezometers (cm) h1	h2	h3	Flow Rate Q/t cu cm/sec	Darcian Velocity Q/At at T	at 20 deg C	Hydraulic Gradient h/l i1	i2	i3	iaverage
1	613	220	14.5	46.0	44.1	41.9	2.79	.065	.075	.149	.173	.161	.161
2	710	167	14.5	50.7	47.6	44.6	4.25	.100	.115	.243	.236	.240	.240
3	900	109	14.5	64.5	58.7	53.1	8.26	.194	.223	.455	.441	.448	.448
4	971	84	14.5	76.9	68.7	61.1	11.56	.271	.312	.643	.598	.621	.621
5	760	127	14.5	56.4	52.3	48.1	5.98	.140	.161	.322	.331	.326	.326

E-2. Unsaturated hydraulic conductivity tests.

Listings of the results for the tests performed to determine the unsaturated hydraulic conductivity, are given in this appendix. The tests performed were:

USPA01

USPA02

Also given is the plot of the results for each test, showing the relative permeability versus the degree of saturation.

UNSATURATED HYDRAULIC CONDUCTIVITY TEST.

SOIL SAMPLE : COARSE SAND

LOCATION : Cape Flats
SAMPLE No : GW/MSC/01

TEST NO : USPA01
DATE : 06/08/85
TESTED BY: G.Wardle

SOIL SPEC.

SPECIFIC GRAVITY: 2.64
WT DRY SOIL Ws : 2102.8 g
SAMPLE LENGTH : 83.7 cm
VOID RATIO e = .598
Sat. Perm. k(sat) .556 cm/sec
(From constant head test)

APPARATUS.

DIAMETER : 4.40 cm
AREA = 15.21 sq cm
WEIGHT Wa: 631.1 g
11 : 15.00 cm
12 : 15.05 cm
13 : 15.00 cm
14 : 15.00 cm

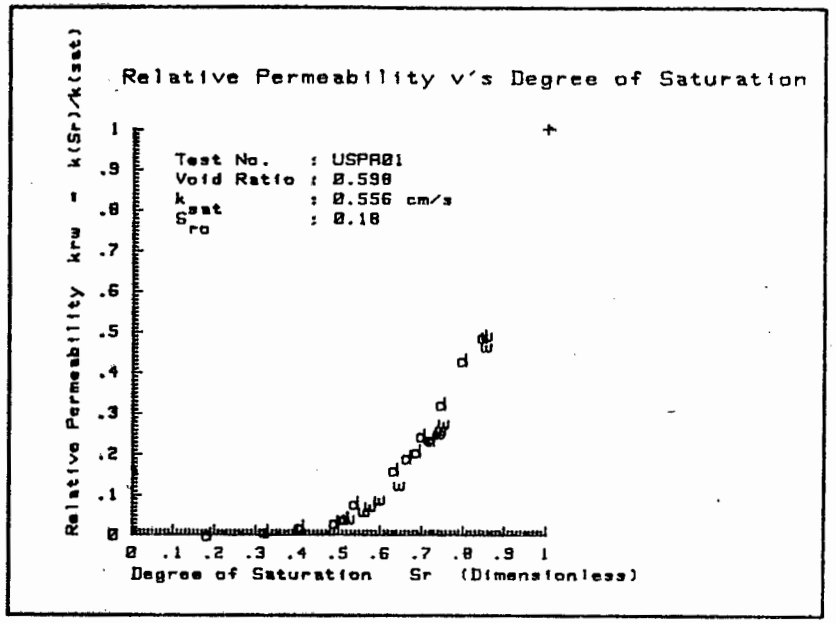

No.	Quantity Q cu cm	Time t sec	Temp T deg C	Weight Wt g	Tensiometers (cm) h1	h2	h3	h4	h5	Flow Rate Q/t cu cm/sec	Darcian Velocity Q/At at T	at 20 deg C	Hydraulic Gradient h/l i1	i2	i3	i4	iaverage	deg. Sat. Sr = Vw/Vv	krw Rel. Perm.
1w	318	957	15.5	2982.9	-9.6	-9.0	-9.7	-9.6	-10.9	.332	.022	.024	0.96	1.05	0.99	1.09	1.02	0.523	0.0431
2d	359	1132	15.5	2978.0	-8.9	-8.7	-10.0	-9.7	-9.2	.317	.021	.023	0.99	1.09	0.98	0.97	1.01	0.513	0.0418
3w	379	792	15.5	3000.0	-6.6	-7.2	-7.3	-8.0	-8.2	.479	.031	.035	1.04	1.01	1.04	1.02	1.03	0.559	0.0618
4d	158	646	15.5	2966.2	-8.8	-8.0	-10.3	-9.7	-10.2	.245	.016	.018	0.95	1.15	0.96	1.04	1.02	0.488	0.0316
5w	302	531	15.5	3007.0	-6.6	-5.8	-9.2	-6.9	-7.6	.569	.037	.042	0.95	1.23	0.85	1.04	1.02	0.574	0.0742
6w	400	587	15.5	3017.6	-5.8	-5.7	-8.2	-5.6	-5.5	.681	.045	.050	0.99	1.17	0.83	0.99	1.00	0.596	0.0907
7w	525	546	15.5	3040.2	-5.8	-5.6	-9.9	-6.2	-6.1	.962	.063	.071	0.99	1.29	0.75	1.00	1.01	0.643	0.1267
8w	491	318	15.5	3074.2	-7.9	+.2	-2.5	+0.0	+1.0	1.544	.102	.114	0.46	1.18	0.83	0.94	0.85	0.715	0.2402

No.	Quantity Q cu cm	Time t sec	Temp T deg C	Weight Wt g	Tensiometers (cm) h1	h2	h3	h4	h5	Flow Rate Q/t cu cm/sec	Darcian Velocity Q/At at T	at 20 deg C	Hydraulic Gradient h/l i1	i2	i3	i4	iaverage	deg. Sat. Sr = Vw/Vv	krw Rel. Perm.
9d	570	404	15.0	3060.0	-6.7	-6.0	-13.8	-5.8	-1.8	1.411	.093	.105	0.95	1.52	0.46	0.74	0.92	0.685	0.2062
10w	540	278	15.0	3086.0	+2.8	+4.6	-.7	+5.4	+1.1	1.942	.128	.145	0.88	1.35	0.59	1.29	1.03	0.739	0.2534
11w	420	203	15.0	3087.9	+5.0	+5.1	-2.4	+2.9	+1.2	2.069	.136	.154	0.99	1.50	0.64	1.12	1.06	0.743	0.2612
12w	415	197	15.0	3091.0	+1.6	+2.2	-3.7	+3.5	+.6	2.107	.139	.157	0.96	1.39	0.52	1.19	1.02	0.750	0.2780
13w	500	146	15.0	3139.6	-.8	+1.4	-4.8	+.3	-.1	3.425	.225	.256	0.86	1.41	0.66	1.03	0.99	0.852	0.4649
14d	355	199	15.0	3076.0	-6.7	-6.0	-13.0	-6.8	-8.0	1.784	.117	.133	0.95	1.46	0.59	1.08	1.02	0.718	0.2345
15w	475	129	15.0	3140.0	+10.5	+14.1	+11.1	+11.2	+10.2	3.682	.242	.275	0.76	1.19	1.00	1.06	1.00	0.853	0.4924
16d	414	132	15.0	3135.8	-.9	+4.1	+1.3	+6.9	+7.3	3.136	.206	.234	0.67	1.19	0.62	0.98	0.86	0.844	0.4873
17d	415	161	15.0	3112.5	-9.3	-7.5	-8.4	-1.0	+2.3	2.578	.170	.192	0.88	1.06	0.51	0.78	0.81	0.795	0.4285
18d	390	186	15.0	3088.2	-8.0	-6.9	-12.7	-5.7	-.4	2.097	.138	.156	0.93	1.39	0.53	0.65	0.87	0.744	0.3223
19d	375	227	15.0	3065.5	-8.0	-7.5	-12.9	-7.3	-2.4	1.652	.109	.123	0.97	1.36	0.63	0.67	0.91	0.696	0.2447
20d	375	279	15.0	3048.9	-9.6	-8.3	-14.0	-8.3	-6.3	1.344	.088	.100	0.91	1.38	0.62	0.87	0.94	0.662	0.1910
21d	365	314	15.0	3034.0	-9.3	-8.1	-12.0	-8.4	-7.4	1.162	.076	.087	0.92	1.26	0.76	0.93	0.97	0.630	0.1610
22d	329	572	15.0	2988.8	-11.0	-9.4	-15.3	-10.0	-10.3	.575	.038	.043	0.89	1.39	0.64	1.02	0.99	0.535	0.0781
23d	509	3359	15.0	2926.5	-11.0	-10.3	-16.8	-10.6	-11.1	.152	.010	.011	0.95	1.43	0.59	1.03	1.00	0.404	0.0203
24d	203	3642	15.0	2886.0	-11.7	-11.0	-16.1	-11.4	-10.0	.056	.004	.004	0.95	1.34	0.68	0.91	0.97	0.319	0.0077
25d	0	99999	15.0	2819.8	-15.5	-14.9	-20.6	-15.0	-13.8	0.000	0.000	0.000	0.96	1.38	0.62	0.92	0.97	0.180	0.0000

UNSATURATED HYDRAULIC CONDUCTIVITY TEST.

SOIL SAMPLE : COARSE SAND

LOCATION : Cape Flats
SAMPLE No : GW/MSC/01

TEST NO : USPA02
DATE : 09/08/85
TESTED BY: G.Wardle

SOIL SPEC.

SPECIFIC GRAVITY: 2.64
WT DRY SOIL Ws : 2102.8 g
SAMPLE LENGTH : 80.0 cm
VOID RATIO e = .527
Sat. Perm. k(sat) .388 cm/sec
(From constant head test)

APPARATUS.

DIAMETER : 4.40 cm
AREA = 15.21 sq cm
WEIGHT Wa: 631.1 g
11 : 15.00 cm
12 : 15.05 cm
13 : 15.00 cm
14 : 15.00 cm

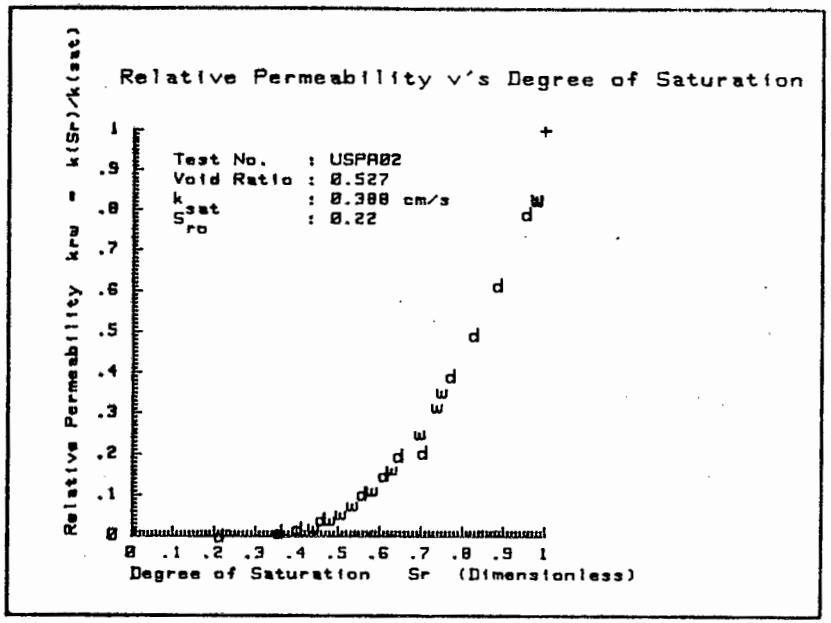

No.	Quantity Q cu cm	Time t sec	Temp T deg C	Weight Wt g	Tensiometers (cm) h1	h2	h3	h4	h5	Flow Rate Q/t cu cm/sec	Darcian Velocity Q/At at T	at 20 deg C	Hydraulic Gradient h/l i1	i2	i3	i4	iaverage	deg. Sat. Sr = Vw/Vv	krw Rel. Perm.
1w	578	125	15.5	3145.5	+.6	-1.1	-7.4	-2.7	-2.5	4.624	.304	.341	1.11	1.42	0.69	0.99	1.05	0.980	0.8342
2w	525	117	15.5	3146.0	-2.5	-2.5	-10.3	-4.5	-4.3	4.487	.295	.331	1.00	1.52	0.61	0.99	1.03	0.981	0.8276
3d	470	120	15.5	3136.0	-9.7	-9.1	-15.1	-7.7	-6.0	3.917	.258	.289	0.96	1.40	0.51	0.89	0.94	0.958	0.7920
4d	500	159	15.5	3107.0	-8.8	-8.7	-14.4	-10.3	-7.1	3.145	.207	.232	1.00	1.38	0.72	0.79	0.97	0.889	0.6136
5d	420	162	15.5	3082.5	-9.2	-8.8	-16.4	-9.8	-9.0	2.593	.171	.191	0.97	1.51	0.56	0.94	1.00	0.830	0.4941
6d	388	186	15.5	3059.5	-12.0	-11.5	-19.9	-11.9	-12.6	2.086	.137	.154	0.96	1.56	0.47	1.05	1.01	0.775	0.3919
7d	290	263	15.5	3031.1	-10.1	-9.6	-17.0	-10.4	-11.4	1.103	.073	.081	0.97	1.49	0.56	1.07	1.02	0.708	0.2047
8d	365	351	15.5	3006.5	-10.8	-9.9	-16.3	-10.1	-10.9	1.040	.068	.077	0.94	1.43	0.59	1.05	1.00	0.649	0.1969

No.	Quantity Q cu cm	Time t sec	Temp T deg C	Weight Wt g	Tensiometers (cm) h1	h2	h3	h4	h5	Flow Rate Q/t cu cm/sec	Darcian Velocity Q/At at T	at 20 deg C	Hydraulic Gradient h/l i1	i2	i3	i4	iaverage	deg. Sat. Sr = Vw/Vv	krw Rel. Perm.
9d	353	449	15.5	2991.7	-9.0	-9.3	-20.9	-10.5	-9.0	.786	.052	.058	1.02	1.77	0.31	0.90	1.00	0.614	0.1492
10d	316	590	15.5	2970.0	-10.4	-10.5	-22.2	-11.4	-9.2	.536	.035	.039	1.01	1.78	0.28	0.85	0.98	0.562	0.1037
11d	170	797	15.5	2928.3	-12.0	-11.0	-23.0	-11.6	-11.3	.213	.014	.016	0.94	1.80	0.24	0.98	0.99	0.463	0.0410
12d	174	1813	15.5	2904.8	-12.6	-11.3	-22.8	-12.1	-12.1	.096	.006	.007	0.92	1.76	0.29	1.00	0.99	0.407	0.0184
13d	104	2131	15.5	2885.3	-13.5	-12.2	-25.2	-13.6	-13.3	.049	.003	.004	0.91	1.87	0.23	0.98	1.00	0.361	0.0093
14d	0	99999	15.5	2825.5	-17.8	-16.8	-27.5	-16.2	-14.9	0.000	0.000	0.000	0.93	1.71	0.25	0.91	0.95	0.218	0.0000
15w	194	1459	15.5	2920.4	-7.9	-7.6	-20.2	-7.3	-9.9	.133	.009	.010	0.98	1.84	0.14	1.17	1.03	0.444	0.0244
16w	226	996	15.5	2937.0	-7.6	-7.4	-18.8	-7.9	-9.0	.227	.015	.017	0.99	1.76	0.28	1.07	1.02	0.484	0.0421
17w	416	1407	15.5	2948.0	-7.1	-7.0	-15.4	-6.8	-6.3	.296	.019	.022	0.99	1.56	0.43	0.96	0.99	0.510	0.0569
18w	612	1489	15.5	2959.8	-6.1	-6.5	-17.9	-7.1	-5.3	.411	.027	.030	1.03	1.75	0.28	0.88	0.99	0.538	0.0790
19w	649	1069	15.5	2979.4	-6.0	-6.7	-18.3	-7.2	-5.9	.607	.040	.045	1.05	1.77	0.26	0.91	1.00	0.585	0.1156
20w	588	679	15.5	2999.5	-6.7	-6.4	-15.1	-6.9	-6.1	.866	.057	.064	0.98	1.58	0.45	0.95	0.99	0.633	0.1660
21w	634	473	15.5	3027.5	-6.1	-6.0	-17.2	-6.0	-6.5	1.340	.088	.099	1.00	1.75	0.25	1.03	1.01	0.699	0.2527
22w	441	262	15.5	3045.0	-5.9	-5.9	-18.4	-7.4	-6.0	1.683	.111	.124	1.00	1.83	0.26	0.91	1.00	0.741	0.3190
23w	403	211	15.5	3049.7	-1.7	-1.8	-12.5	-2.7	-2.9	1.910	.126	.141	1.00	1.71	0.35	1.02	1.02	0.752	0.3555

E-3. Soil-moisture characteristic curve tests.

Listings of the results for the tests performed to determine the soil-moisture characteristic curve, (Suction head versus the degree of saturation) are given in this appendix. The tests performed were:

SMHA01

SMHA02

SMHA03

Also given is the plot for each test of the results showing the soil-moisture characteristic curve found.

SOIL - MOISTURE CHARACTERISTIC CURVE TEST.

SOIL SAMPLE : COARSE SAND

TEST NO : SMHA01
DATE : 22/10/85
TESTED BY: G.Wardle

LOCATION : Cape Flats
SAMPLE No : GW/MSC/01

SOIL SPEC.

SPECIFIC GRAVITY: 2.64
WT DRY SOIL Ws : 329.4 g
SAMPLE HEIGHT : 3.6 cm
VOID RATIO e = .593

APPARATUS.

DIAMETER : 8.35 cm
AREA = 54.76 sq cm
WEIGHT Wa: 239.3 g

No.	Temp T deg C	Weight Wt g	Tensiometer (cm)	deg. Sat. Sr = Vw/Vv
1d	19.5	643.4	+0	1.009
3d	20.0	642.5	-7	0.997
5d	20.0	642.5	-19	0.997
7d	20.0	641.7	-24	0.986
9d	20.5	641.1	-39	0.978
11d	20.5	639.6	-49	0.958
13d	20.5	638.5	-57	0.943
15d	20.5	637.4	-56	0.928
17d	21.0	626.9	-62	0.786
19d	20.0	602.9	-93	0.462
21d	20.0	600.9	-79	0.435
23d	20.0	595.7	-89	0.365
25d	20.0	589.3	-94	0.278
27d	20.0	582.7	-105	0.189
29d	20.0	579.2	-120	0.142
31d	20.0	577.7	-128	0.122
33d	20.0	577.7	-129	0.122
35d	20.0	577.0	-125	0.112
37d	20.0	578.5	-127	0.132
39d	19.0	576.6	-159	0.107
41w	19.0	577.2	-135	0.115
43w	19.0	578.3	-118	0.130
45w	19.5	579.6	-99	0.147
47w	19.5	580.3	-95	0.157
49w	19.5	581.8	-86	0.177
51w	19.5	584.0	-71	0.207
53w	19.5	588.5	-73	0.268
55w	19.0	584.5	-64	0.213
57w	19.0	587.0	-59	0.247
59w	20.0	602.5	-34	0.457
61w	19.0	608.3	-27	0.535
63w	19.0	614.3	-25	0.616
65w	19.0	619.5	-31	0.686
67w	19.0	625.1	-31	0.762
69w	19.0	630.5	-16	0.835
71w	18.0	635.0	-2	0.896
73w	18.0	639.4	+3	0.955

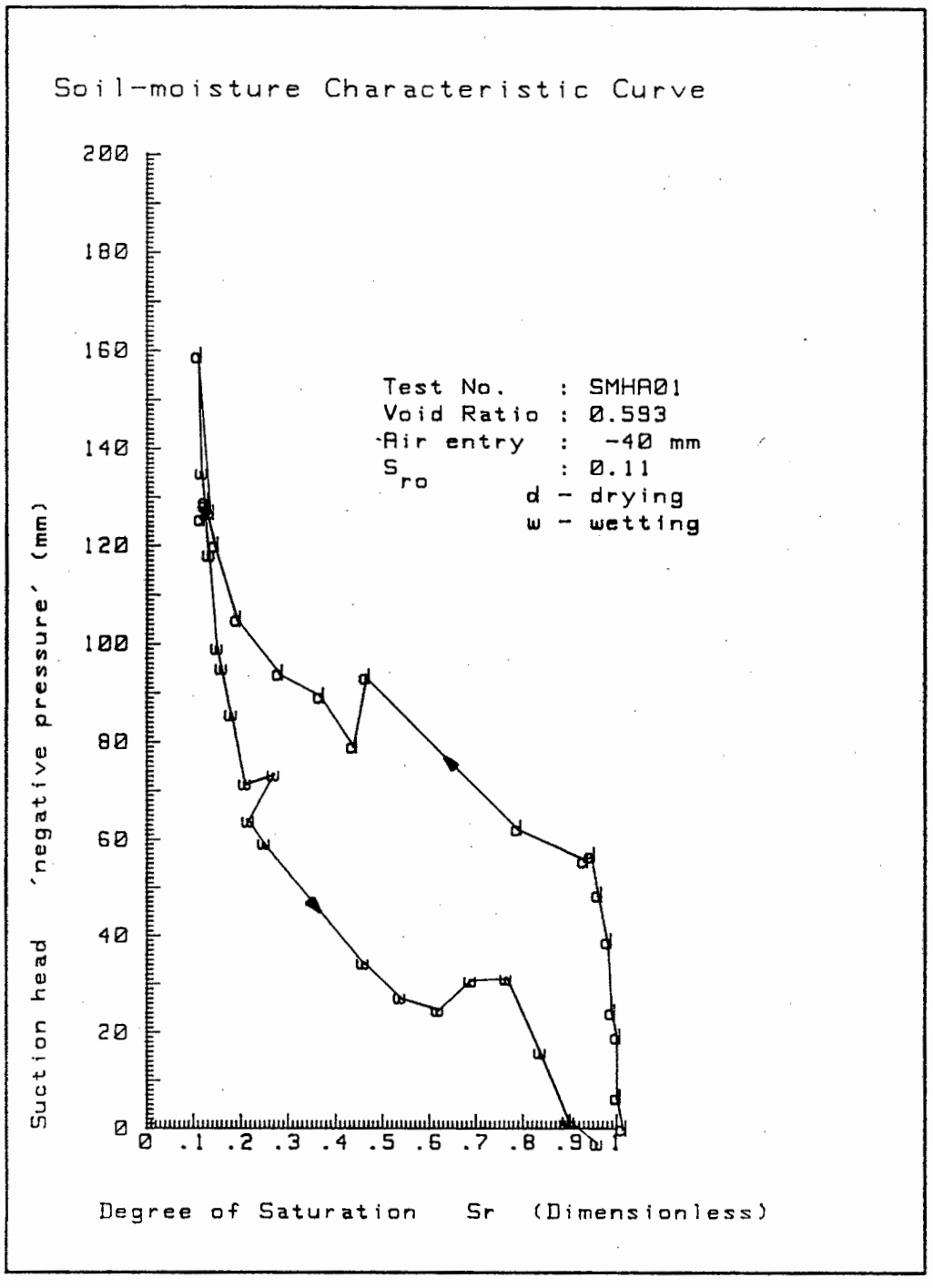
Soil-moisture Characteristic Curve
Test No. : SMHA01
Void Ratio : 0.593
Air entry : -40 mm
S ro : 0.11
d - drying
w - wetting
Suction head 'negative pressure' (mm)
200
180
160
140
120
100
80
60
40
20
0
0 .1 .2 .3 .4 .5 .6 .7 .8 .9 1
Degree of Saturation Sr (Dimensionless)

SOIL - MOISTURE CHARACTERISTIC CURVE TEST.

SOIL SAMPLE : COARSE SAND

TEST NO : SMWA02
DATE : 22/10/85
TESTED BY: G.Wardle

LOCATION : Cape Flats
SAMPLE No : GW/MSC/01

SOIL SPEC.

SPECIFIC GRAVITY: 2.64
WT DRY SOIL Ws : 304.6 g
SAMPLE HEIGHT : 3.3 cm
VOID RATIO e = .557

APPARATUS.

DIAMETER : 8.35 cm
AREA = 54.76 sq cm
WEIGHT Wa: 241.5 g

No.	Temp T deg C	Weight Wt g	Tensiometer (cm)	deg. Sat. Sr = Vw/Vv
1d	18.5	610.5	+0	1.003
3d	19.5	610.1	-1	0.997
5d	20.0	610.0	-0	0.995
7d	20.0	609.8	-18	0.992
9d	20.0	609.3	-21	0.984
11d	20.5	608.5	-37	0.972
13d	20.5	606.7	-49	0.944
15d	20.5	605.4	-56	0.924
17d	20.5	603.0	-60	0.886
19d	21.0	598.7	-70	0.819
21d	20.0	590.4	-100	0.690
23d	20.0	588.0	-88	0.653
25d	20.0	576.9	-101	0.480
27d	20.0	563.8	-111	0.276
29d	20.0	556.0	-128	0.155
31d	20.0	554.1	-136	0.125
33d	20.0	553.5	-143	0.116
35d	20.0	553.5	-146	0.116
37d	20.0	552.7	-149	0.103
39d	20.0	554.1	-143	0.125
41d	19.0	552.4	-190	0.099
43w	19.0	553.1	-183	0.110
45w	19.0	554.3	-159	0.128
47w	19.5	556.1	-113	0.156
49w	19.5	556.7	-109	0.166
51w	19.5	559.0	-99	0.202
53w	19.5	561.8	-85	0.245
55w	19.5	566.5	-86	0.318
57w	19.0	573.1	-74	0.421
59w	19.0	575.5	-77	0.458
61w	20.0	581.0	-51	0.544
63w	19.0	586.4	-40	0.628
65w	19.0	592.4	-34	0.721
67w	19.0	597.5	-31	0.801
69w	19.0	602.5	-15	0.879
71w	19.0	607.5	+4	0.956
73w	18.0	609.4	-8	0.986
75w	18.0	608.0	-14	0.964

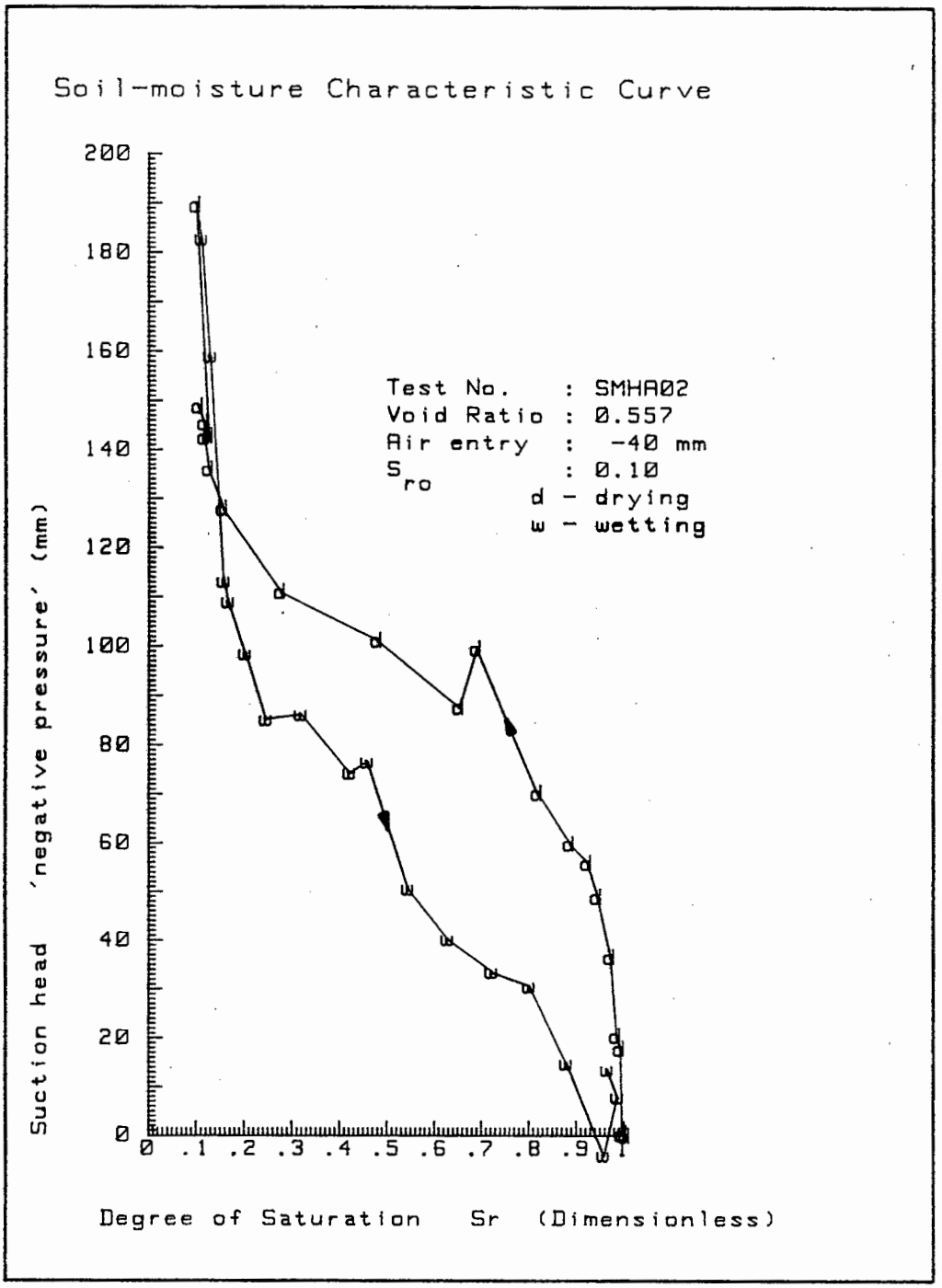
Soil-moisture Characteristic Curve
Test No. : SMHA02
Void Ratio : 0.557
Air entry : -40 mm
S ro : 0.10
d - drying
w - wetting
Suction head 'negative pressure' (mm)
200
180
160
140
120
100
80
60
40
20
0
0 .1 .2 .3 .4 .5 .6 .7 .8 .9 1
Degree of Saturation Sr (Dimensionless)

SOIL - MOISTURE CHARACTERISTIC CURVE TEST.

SOIL SAMPLE : COARSE SAND

TEST NO : SMKA03
DATE : 22/10/85
TESTED BY: G.Wardle

LOCATION : Cape Flats
SAMPLE No : GW/MSC/01

SOIL SPEC.

SPECIFIC GRAVITY: 2.64
WT DRY SOIL Ws : 315.2 g
SAMPLE HEIGHT : 3.4 cm
VOID RATIO e = .569

APPARATUS.

DIAMETER : 8.35 cm
AREA = 54.76 sq cm
WEIGHT Wa: 242.3 g

No.	Temp T deg C	Weight Wt g	Tensiometer (cm)	deg. Sat. Sr = Vw/Vv
1d	19.5	625.6	+0	1.003
3d	20.0	624.8	-4	0.991
5d	20.0	624.4	-19	0.985
7d	20.0	623.9	-24	0.978
9d	20.5	623.3	-38	0.969
11d	20.5	620.2	-50	0.924
13d	20.5	618.6	-54	0.900
15d	20.5	616.0	-60	0.862
17d	21.0	611.1	-68	0.790
19d	20.0	602.6	-96	0.664
21d	20.0	600.8	-90	0.638
23d	20.0	586.4	-105	0.426
25d	20.0	573.3	-118	0.233
27d	20.0	567.9	-131	0.153
29d	20.0	566.3	-139	0.130
31d	20.0	565.8	-145	0.122
33d	20.0	565.7	-148	0.121
35d	20.0	565.0	-147	0.110
37d	20.0	566.2	-139	0.128
39d	19.0	564.6	-177	0.105
41w	19.0	565.5	-149	0.118
43w	19.0	566.9	-129	0.138
45w	19.5	568.5	-110	0.162
47w	19.5	569.6	-105	0.178
49w	19.5	572.2	-94	0.217
51w	19.5	575.0	-85	0.258
53w	19.5	580.8	-84	0.343
55w	19.0	587.5	-77	0.442
57w	19.0	590.6	-79	0.488
59w	20.0	595.4	-52	0.558
61w	19.0	601.0	-43	0.641
63w	19.0	606.4	-34	0.720
65w	19.0	611.7	-30	0.798
67w	19.0	617.2	-19	0.879
69w	19.0	621.8	+4	0.947
71w	18.0	623.5	-6	0.972
73w	18.0	622.5	-15	0.958

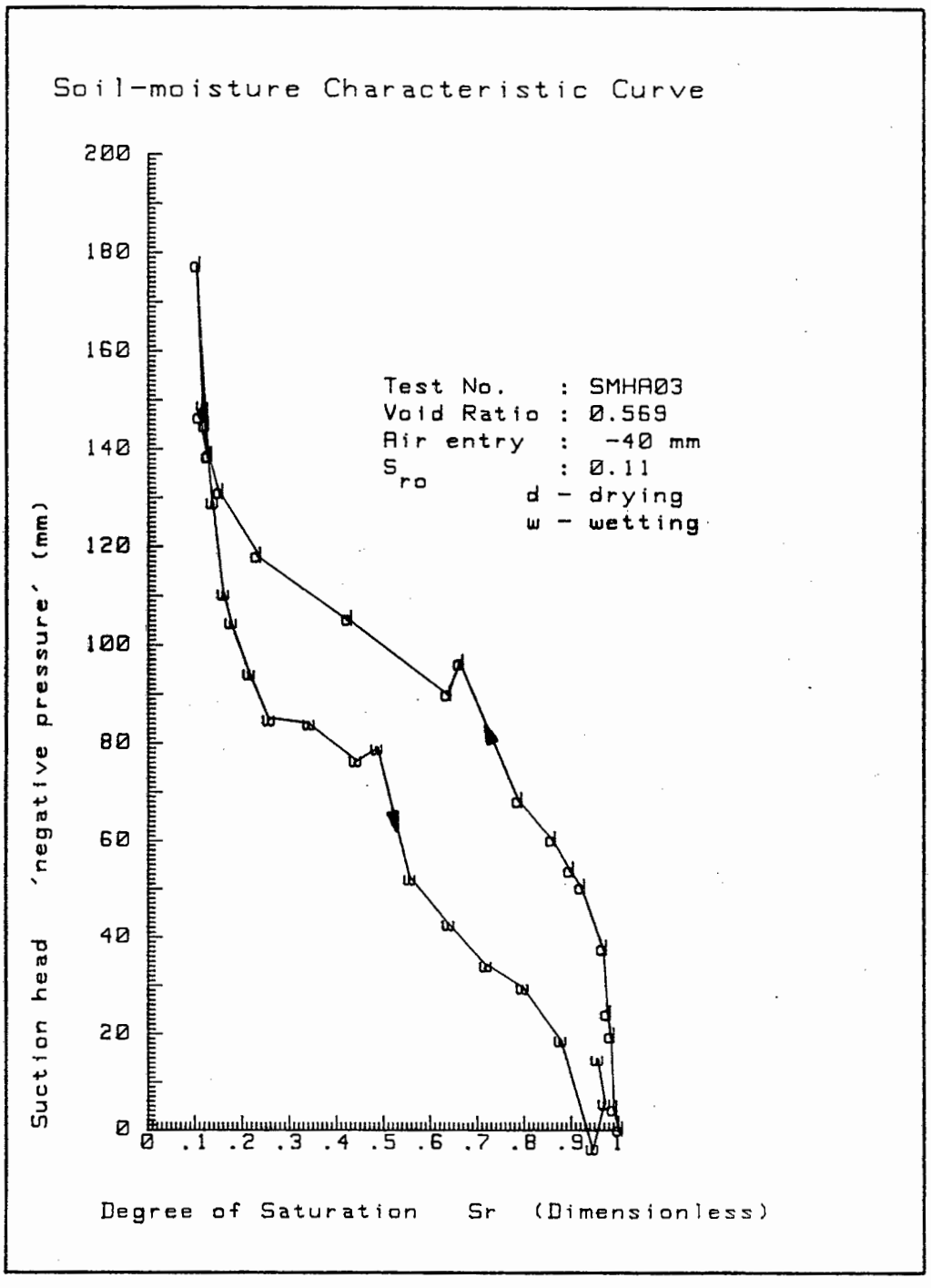
Soil-moisture Characteristic Curve
Test No. : SMHA03
Void Ratio : 0.569
Air entry : -40 mm
S ro : 0.11
d - drying
w - wetting
Suction head 'negative pressure' (mm)
200
180
160
140
120
100
80
60
40
20
0
0 .1 .2 .3 .4 .5 .6 .7 .8 .9 1
Degree of Saturation Sr (Dimensionless)

E-4. Measured Outflow from the drainage face. Experiment no. 1.

Listings of the results for the outflow measured from the drainage (Seepage) face for experiment no. 1 is given here. The outflow was measured for two runs of the experiment. The outflow is recorded as the quantity Q_t collected in time t draining from the experiment. Also listed is the reduction of the results showing the mid-interval flow rate calculated as Q_t/t and a plot of the results showing the calculated average mid-interval flow rate versus the mid-interval time from the start of the experiment.

Exp. #1. / Run # 1

Start (sec)	End (sec)	quantity Q (cu cm)	Time t (sec)	Time Step. (sec)	Flow Rate. (cu cm/sec)
10	15	600	5	12.5	120.0
15	20	470	5	17.5	94.0
20	25	500	5	22.5	100.0
25	30	550	5	27.5	110.0
30	35	450	5	32.5	90.0
35	40	400	5	37.5	80.0
40	45	520	5	42.5	104.0
45	50	340	5	47.5	68.0
50	55	360	5	52.5	72.0
55	60	360	5	57.5	72.0
70	75	360	5	72.5	72.0
75	80	360	5	77.5	72.0
80	85	360	5	82.5	72.0
85	90	350	5	87.5	70.0
90	95	340	5	92.5	68.0
95	100	330	5	97.5	66.0
100	105	320	5	102.5	64.0
105	110	320	5	107.5	64.0
110	115	320	5	112.5	64.0
115	120	320	5	117.5	64.0
120	125	320	5	122.5	64.0

Exp. #1. / Run # 2

Start (sec)	End (sec)	quantity Q (cu cm)	Time t (sec)	Time Step. (sec)	Flow Rate. (cu cm/sec)
10	15	580	5	12.5	116.0
15	20	580	5	17.5	116.0
20	25	540	5	22.5	108.0
25	30	460	5	27.5	92.0
30	35	470	5	32.5	94.0
35	40	420	5	37.5	84.0
40	45	410	5	42.5	82.0
45	50	440	5	47.5	88.0
50	55	410	5	52.5	82.0
55	60	400	5	57.5	80.0
60	65	370	5	62.5	74.0
65	70	370	5	67.5	74.0
70	75	360	5	72.5	72.0
75	80	360	5	77.5	72.0
80	85	310	5	82.5	62.0
85	90	350	5	87.5	70.0
90	95	360	5	92.5	72.0
95	100	320	5	97.5	64.0
105	110	350	5	107.5	70.0
110	115	350	5	112.5	70.0
115	120	300	5	117.5	60.0

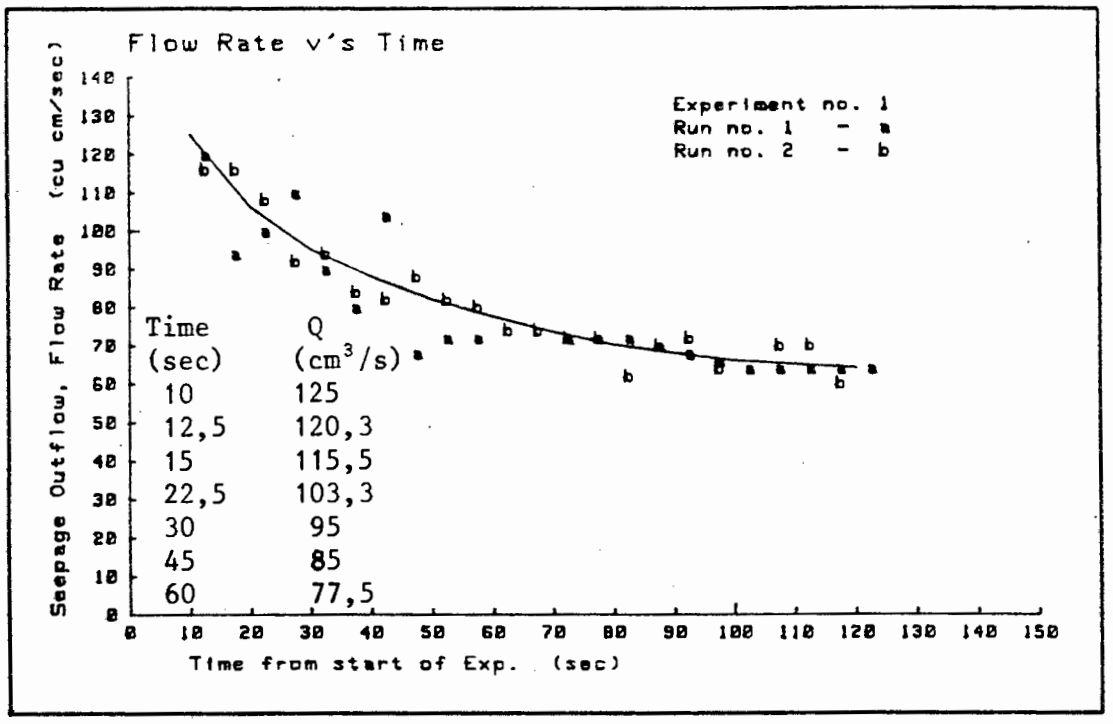
Flow Rate v's Time
Seepage Outflow, Flow Rate (cu cm/sec)
Experiment no. 1
Run no. 1 - a
Run no. 2 - b
Time (sec) Q (cm³/s)
10 125
12,5 120,3
15 115,5
22,5 103,3
30 95
45 85
60 77,5
Time from start of Exp. (sec)

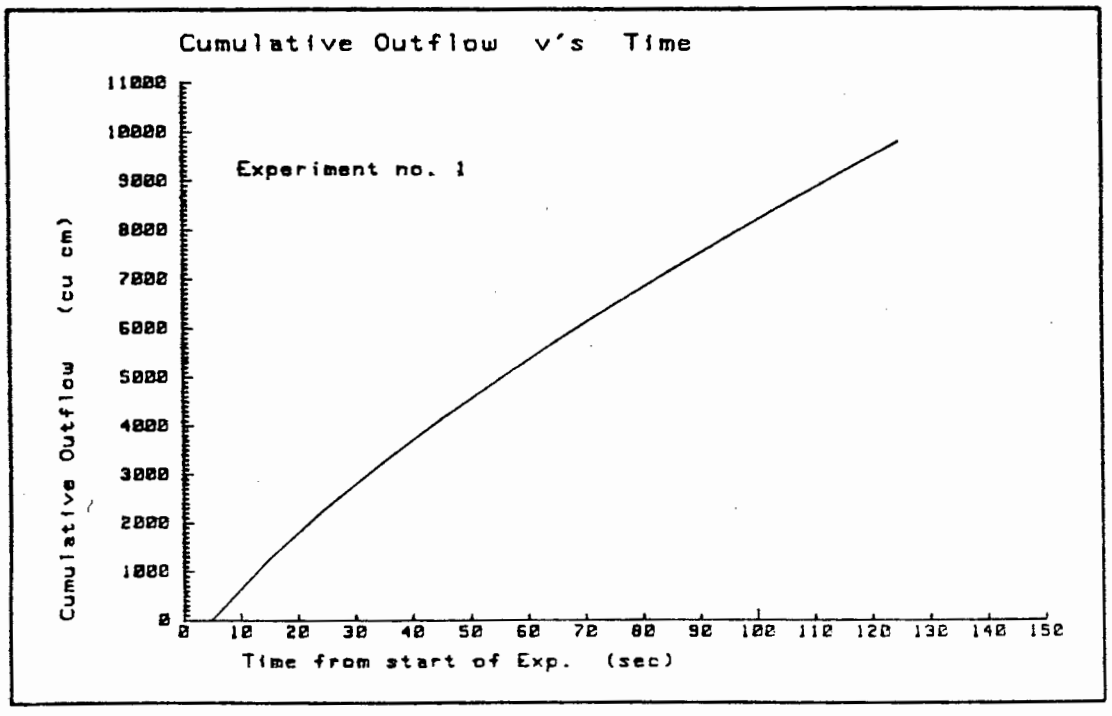
Cumulative Outflow v's Time
Cumulative Outflow (cu cm)
Experiment no. 1
Time from start of Exp. (sec)

E-5. Sidewall piezometer levels recorded. Experiment no. 1.

Listings of the results for the sidewall piezometer levels recorded for experiment no. 1, are given here. The readings are recorded with respect to time and the result given as the elevation (mm) above the base of the flume. The actual piezometer referenced is given by a reference number whose position is shown in figure (5.8)

Faulty piezometers are recorded as: Faulty (F)

Piezometer points falling above the phreatic surface are recorded as: AWT

Results that were not recorded, but can be interpolated are recorded as: I

Experiment no. 1 / Piezometer Results. / Time (sec) v's Total head (mm)

Time	Ref. no.							Time	Ref. no.						
	PA1	PA2	PA3	PA4	PA5	PA6	PA7		PB1	PB2	PB3	PB4	PB5	PB6	PB7
0	F	300	300	300	300	300	AWT	0	300	F	300	301	301	301	AWT
5	F	178	180	244	AWT	AWT	AWT	5	251	F	202	207	224	AWT	AWT
10	F	113	120	200	AWT	AWT	AWT	10	201	F	159	174	AWT	AWT	AWT
15	F	99	AWT	AWT	AWT	AWT	AWT	15	164	F	148	AWT	AWT	AWT	AWT
20	F	I	AWT	AWT	AWT	AWT	AWT	20	147	F	145	AWT	AWT	AWT	AWT
25	F	85	AWT	AWT	AWT	AWT	AWT	25	140	F	140	AWT	AWT	AWT	AWT
30	F	I	AWT	AWT	AWT	AWT	AWT	30	133	F	136	AWT	AWT	AWT	AWT
35	F	I	AWT	AWT	AWT	AWT	AWT	35	129	F	134	AWT	AWT	AWT	AWT
40	F	I	AWT	AWT	AWT	AWT	AWT	40	126	F	131	AWT	AWT	AWT	AWT
45	F	I	AWT	AWT	AWT	AWT	AWT	45	123	F	129	AWT	AWT	AWT	AWT
50	F	80	AWT	AWT	AWT	AWT	AWT	50	121	F	124	AWT	AWT	AWT	AWT
55	F	I	AWT	AWT	AWT	AWT	AWT	55	118	F	I	AWT	AWT	AWT	AWT
60	F	78	AWT	AWT	AWT	AWT	AWT	80	115	F	120	AWT	AWT	AWT	AWT
90	F	76	AWT	AWT	AWT	AWT	AWT	120	110	F	113	AWT	AWT	AWT	AWT
150	F	75	AWT	AWT	AWT	AWT	AWT	150	107	F	AWT	AWT	AWT	AWT	AWT

Experiment no. 1 / Piezometer Results. / Time (sec) v's Total head (mm)

Time	**Ref. no.**							**Time**	**Ref. no.**						
	PC1	PC2	PC3	PC4	PC5	PC6	PC7		PD1	PD2	PD3	PD4	PD5	PD6	PD7
0	F	304	305	F	305	305	AWT	0	F	305	F	306	F	306	AWT
5	F	222	218	F	265	AWT	AWT	5	F	287	F	267	F	262	AWT
10	F	192	190	F	230	AWT	AWT	10	F	272	F	243	F	AWT	AWT
15	F	178	180	F	AWT	AWT	AWT	15	F	259	F	225	F	AWT	AWT
20	F	175	178	F	AWT	AWT	AWT	20	F	243	F	212	F	AWT	AWT
25	F	168	173	F	AWT	AWT	AWT	25	F	231	F	205	F	AWT	AWT
30	F	164	166	F	AWT	AWT	AWT	30	F	221	F	198	F	AWT	AWT
35	F	160	163	F	AWT	AWT	AWT	35	F	213	F	195	F	AWT	AWT
40	F	155	158	F	AWT	AWT	AWT	40	F	205	F	192	F	AWT	AWT
45	F	152	155	F	AWT	AWT	AWT	45	F	200	F	189	F	AWT	AWT
60	F	149	153	F	AWT	AWT	AWT	50	F	194	F	185	F	AWT	AWT
80	F	145	145	F	AWT	AWT	AWT	60	F	189	F	177	F	AWT	AWT
90	F	141	142	F	AWT	AWT	AWT	70	F	183	F	177	F	AWT	AWT
120	F	138	139	F	AWT	AWT	AWT	80	F	179	F	173	F	AWT	AWT
150	F	136	137	F	AWT	AWT	AWT	120	F	170	F	168	F	AWT	AWT

Experiment no. 1 / Piezometer Results. / Time (sec) v's Total head (mm)

Time	Ref. no.							Time	Ref. no.						
	PE1	PE2	PE3	PE4	PE5	PE6	PE7		PF1	PF2	PF3	PF4	PF5	PF6	PF7
0	307	F	F	308	308	F	AWT	0	308	308	308	F	309	309	AWT
5	283	F	F	275	276	F	AWT	5	272	278	285	F	280	295	AWT
10	255	F	F	245	247	F	AWT	10	250	258	254	F	254	265	AWT
15	240	F	F	234	235	F	AWT	15	243	244	247	F	247	AWT	AWT
20	230	F	F	227	230	F	AWT	20	237	240	241	F	242	AWT	AWT
25	222	F	F	221	225	F	AWT	25	233	236	236	F	238	AWT	AWT
30	217	F	F	218	222	F	AWT	30	229	230	232	F	235	AWT	AWT
35	213	F	F	214	217	F	AWT	35	226	228	229	F	233	AWT	AWT
40	208	F	F	211	214	F	AWT	40	I	225	228	F	232	AWT	AWT
45	205	F	F	207	212	F	AWT	45	221	222	224	F	229	AWT	AWT
50	202	F	F	205	AWT	F	AWT	50	218	220	222	F	227	AWT	AWT
60	198	F	F	200	AWT	F	AWT	60	217	218	220	F	221	AWT	AWT
70	195	F	F	197	AWT	F	AWT	70	215	216	218	F	218	AWT	AWT
80	192	F	F	194	AWT	F	AWT	80	212	214	216	F	215	AWT	AWT
100	189	F	F	191	AWT	F	AWT	100	210	212	215	F	214	AWT	AWT
150	184	F	F	185	AWT	F	AWT	150	209	211	211	F	211	AWT	AWT

Experiment no. 1 / Piezometer Results. / Time (sec) v's Total head (mm)

Time	Ref. no.							Time	Ref. no.						
	PG1	PG2	PG3	PG4	PG5	PG6	PG7		PH1	PH2	PH3	PH4	PH5	PH6	PH7
0	310	F	310	310	311	311	311	0	312	F	313	313	314	F	315
5	280	F	270	276	285	300	AWT	5	294	F	297	290	288	F	AWT
10	258	F	260	267	275	282	AWT	10	280	F	286	274	274	F	AWT
15	253	F	255	260	267	270	AWT	15	273	F	276	266	271	F	AWT
20	249	F	252	255	259	261	AWT	20	268	F	270	265	267	F	AWT
25	246	F	249	252	255	AWT	AWT	25	266	F	268	264	265	F	AWT
30	243	F	247	250	252	AWT	AWT	30	264	F	265	262	262	F	AWT
35	238	F	244	247	250	AWT	AWT	35	260	F	262	260	260	F	AWT
50	I	F	I	244	245	AWT	AWT	50	257	F	259	258	257	F	AWT
60	234	F	241	240	241	AWT	AWT	60	255	F	257	256	255	F	AWT
70	I	F	239	I	I	AWT	AWT	70	252	F	253	253	252	F	AWT
90	233	F	236	236	237	AWT	AWT	90	247	F	251	250	250	F	AWT
100	231	F	233	234	234	AWT	AWT	100	246	F	250	249	248	F	AWT
120	228	F	232	233	232	AWT	AWT	120	244	F	248	247	247	F	AWT
150	227	F	230	231	231	AWT	AWT	150	244	F	247	245	245	F	AWT

Experiment no. 1 / Piezometer Results. / Time (sec) v's Total head (mm)

Time	Ref. no.							Time	Ref. no.						
	PI1	PI2	PI3	PI4	PI5	PI6	PI7		PJ1	PJ2	PJ3	PJ4	PJ5	PJ6	PJ7
0	315	F	316	316	316	F	317	0	318	318	318	319	319	319	320
5	307	F	305	305	308	F	312	10	301	301	301	303	305	308	312
10	300	F	295	295	297	F	AWT	15	296	297	298	299	301	302	AWT
15	293	F	285	290	294	F	AWT	25	293	294	295	297	298	299	AWT
25	286	F	282	285	287	F	AWT	40	289	290	292	294	296	295	AWT
30	281	F	279	281	283	F	AWT	60	285	286	290	292	294	294	AWT
40	278	F	277	278	281	F	AWT	100	284	285	287	289	291	292	AWT
50	275	F	273	275	279	F	AWT	150	284	284	285	286	288	290	AWT
60	271	F	271	273	277	F	AWT								
100	267	F	269	271	273	F	AWT								
150	264	F	266	269	271	F	AWT								

Experiment no. 1 / Piezometer Results. / Time (sec) v's Total head (mm)

Time	Ref. no.						
	PK1	PK2	PK3	PK4	PK5	PK6	PK7
0	F	320	321	321	321	322	322
10	F	315	315	316	316	315	314
15	F	310	313	313	315	315	I
25	F	308	312	312	313	313	I
30	F	300	311	311	I	I	I
40	F	303	309	310	312	312	I
60	F	303	308	309	311	311	I
100	F	302	306	308	310	310	I
150	F	301	305	307	309	309	310

E-6. Transducer monitored tensiometers. Experiment no. 1.

Listings of the results for the tensiometers, recorded for experiment no. 1, are given here. The recordings were made by the computer controlled data-acquisition unit. (See chapter 3) Five sets of readings are given for the five repeated experiment runs made. The readings are recorded with respect to time and the result given as the elevation (mm) above the base of the flume. The actual tensiometer referenced are given by a reference number whose position is shown in figure (5.8)

Also given are the plots, for each tensiometer recorded, showing the total pressure head versus time. The results for all five runs recorded by a tensiometer are show on a single plot.

Experiment no. 1 / Run no. 1

TIME	TA1	TA2	TA3	TA4	TB1	TB2	TB3	TB4	TC1	TC2	TC3	TC4
-60	300	300	300	300	307	307	307	307	317	317	317	317
-55	299	298	299	305	306	305	305	305	317	316	316	316
-51	300	299	300	300	306	306	305	306	317	317	317	317
-46	300	299	300	294	307	306	305	306	317	317	317	317
-42	300	300	300	296	307	306	305	306	317	317	317	317
-38	299	299	300	295	307	306	304	305	317	317	317	316
-32	269	268	269	263	276	276	273	275	285	334	286	285
-28	299	298	299	295	306	306	304	306	316	381	316	316
-23	300	298	300	297	307	306	306	306	316	310	317	316
-19	298	298	299	296	306	306	305	306	317	308	317	317
-14	296	295	296	296	304	303	304	304	315	394	316	316
-9	296	295	296	297	304	303	303	303	315	364	316	315
-5	296	295	296	297	304	304	304	303	316	317	316	315
0	295	294	295	299	303	303	303	303	314	316	316	315
5	159	163	206	286	240	255	268	270	304	317	304	304
9	79	124	189	272	220	228	241	254	298	308	298	298
14	80	121	181	328	217	220	228	245	297	392	297	297
19	141	118	174	247	214	218	226	241	296	392	296	296
24	77	114	165	247	208	212	220	234	294	388	294	294
28	46	82	129	207	175	178	186	200	262	271	262	262
32	76	111	155	237	203	206	215	228	292	386	292	292
38	44	77	158	212	169	172	182	190	261	267	261	261
42	75	106	142	242	197	201	255	286	292	297	291	291
48	74	104	139	244	195	197	262	217	290	296	291	290
52	73	102	136	240	193	195	260	217	290	297	289	289
56	74	103	133	244	193	195	261	217	291	296	290	290
62	73	100	130	241	190	192	200	214	290	384	289	289
67	42	68	97	207	157	160	167	181	258	267	258	258
72	72	97	125	242	185	188	198	210	288	297	288	287
76	71	97	124	234	184	187	196	209	287	296	287	287
81	71	96	123	238	184	186	195	210	288	297	288	288
86	70	94	121	236	184	185	194	209	287	384	287	287
91	40	63	90	207	153	153	163	177	257	266	256	256
97	70	93	119	240	182	183	193	207	288	299	287	287
101	69	93	118	245	179	182	190	206	286	296	286	286
105	70	93	118	240	181	182	190	206	287	298	286	287
111	70	92	117	237	179	181	188	205	287	297	286	286
116	39	61	86	205	149	149	157	174	256	267	254	255
121	69	91	116	233	178	180	188	204	287	298	285	286
125	68	90	116	236	177	178	188	203	286	299	285	285
129	69	90	116	240	178	178	187	203	286	299	285	285
134	68	89	115	241	177	177	186	201	285	298	284	285
138	68	90	115	237	178	177	187	201	286	298	285	285
143	68	89	115	243	177	177	186	201	286	385	285	285
147	68	88	113	237	176	176	185	200	286	299	284	285

Experiment no. 1 / Run no. 2

TIME	TA1	TA2	TA3	TA4	TB1	TB2	TB3	TB4	TC1	TC2	TC3	TC4
-60	300	300	300	300	307	307	307	307	317	317	317	317
-55	299	298	299	380	304	306	305	306	316	402	317	316
-51	300	299	299	385	306	306	305	306	316	317	316	317
-47	300	300	299	384	306	306	306	307	316	404	317	317
-42	299	299	299	299	304	305	305	305	316	315	316	316
-39	299	299	299	295	306	306	306	306	316	316	316	316
-33	298	298	298	380	304	305	305	306	316	402	317	317
-30	267	267	267	350	274	274	274	274	284	283	285	286
-26	297	297	297	295	304	304	304	305	314	399	315	316
-20	297	297	298	296	304	305	306	306	316	313	317	317
-17	298	298	298	294	305	306	306	306	316	316	317	317
-11	298	297	298	304	305	305	306	306	316	313	317	317
-7	298	297	298	298	306	306	306	306	316	313	317	317
-3	297	298	297	382	305	305	305	305	316	312	317	317
2	274	274	272	294	297	301	303	304	315	315	315	316
6	114	136	192	281	334	246	259	265	302	312	303	303
11	79	120	179	274	215	229	234	244	297	310	297	297
15	78	118	172	271	212	225	226	238	295	312	295	296
19	78	114	164	270	207	220	219	232	293	311	293	294
24	78	112	158	266	204	217	270	224	293	310	293	294
28	76	109	148	269	200	213	267	222	291	307	291	292
34	75	107	144	263	197	209	207	220	291	306	291	291
38	75	105	142	264	194	209	205	285	291	306	291	292
42	74	104	138	258	193	206	204	217	291	306	290	291
47	74	102	135	264	191	204	204	213	290	304	290	290
51	73	101	132	268	188	201	200	213	289	303	289	290
57	73	101	129	273	188	200	199	211	289	303	288	289
61	42	68	97	238	156	168	167	179	257	270	258	258
65	71	98	125	265	185	197	196	208	287	298	287	288
70	71	97	123	266	183	196	194	208	287	298	287	288
74	70	95	121	261	182	194	192	206	286	297	284	286
79	70	95	119	262	181	193	191	206	286	296	286	287
83	70	95	119	260	180	192	191	205	286	296	286	287
87	69	94	117	251	179	191	190	204	286	297	285	286
92	70	93	117	257	179	191	189	204	286	295	285	287
96	69	93	116	255	178	190	188	203	286	296	286	287
102	69	92	115	252	178	190	188	203	299	294	285	286
106	69	93	115	251	176	189	187	201	299	294	285	286
110	68	91	114	254	176	188	186	200	280	291	283	285
116	69	91	114	250	177	188	184	200	324	290	285	286
120	38	60	83	220	145	157	155	170	251	257	254	255
125	69	91	113	255	175	187	185	199	281	287	284	285
129	68	90	112	249	175	186	185	198	325	286	284	286
133	67	90	111	249	176	186	184	198	323	286	284	285
138	67	88	111	247	174	185	183	196	336	284	283	285
143	67	88	110	247	174	184	183	196	336	285	283	284
148	68	90	111	247	174	185	183	197	312	286	284	286

Experiment no. 1 / Run no. 3

TIME	TA1	TA2	TA3	TA4	TB1	TB2	TB3	TB4	TC1	TC2	TC3	TC4
-60	300	300	300	300	307	307	307	307	317	317	317	317
-56	299	299	299	296	306	306	304	306	316	316	318	316
-50	300	300	299	296	307	322	305	306	317	315	317	317
-46	300	299	299	302	306	306	303	306	317	312	317	317
-41	299	299	299	296	306	306	304	307	317	309	317	317
-36	299	299	299	298	305	306	305	306	316	311	317	317
-32	299	300	299	300	305	322	305	306	317	310	317	316
-27	299	298	299	301	306	305	305	306	317	311	317	316
-22	299	299	299	301	306	306	305	306	317	312	317	316
-17	300	299	299	300	306	322	306	306	317	314	318	316
-12	298	299	298	301	305	338	304	306	317	315	317	316
-8	298	297	298	300	305	322	305	306	317	315	318	317
-3	298	297	298	302	305	306	305	306	317	315	318	316
1	272	272	270	296	296	295	301	303	315	314	316	315
7	84	126	189	279	223	237	247	257	299	310	300	300
11	81	121	179	271	215	228	232	244	297	307	297	297
16	80	117	170	272	209	222	224	236	295	307	295	295
21	78	113	162	279	204	218	263	226	294	305	293	294
26	76	111	196	272	200	214	268	223	292	305	292	292
31	75	107	147	269	197	211	207	220	291	305	291	291
35	75	106	144	264	195	209	262	220	291	306	291	290
39	74	105	139	262	192	206	205	217	290	306	290	289
45	73	103	135	258	190	204	204	215	290	307	289	289
49	72	101	132	265	188	203	201	213	289	307	289	288
55	72	99	129	266	185	199	195	210	327	307	287	287
60	72	99	127	266	185	198	192	209	284	306	288	288
64	72	98	125	266	184	198	193	208	340	305	287	287
70	71	98	123	263	183	196	191	207	285	303	287	287
74	71	97	121	262	182	195	191	206	339	301	287	287
80	71	97	120	261	181	195	189	205	283	301	287	287
84	71	95	119	257	181	193	188	203	351	299	286	286
89	71	95	118	259	180	192	187	203	282	298	286	286
95	68	93	115	257	176	190	184	201	281	296	285	284
99	69	94	115	255	177	191	185	201	350	296	286	285
105	68	92	114	256	175	188	185	200	349	297	284	284
110	69	93	114	262	175	189	184	199	280	298	285	284
114	68	92	113	260	175	189	184	198	350	298	285	284
120	68	91	111	254	174	187	181	197	349	297	284	283
124	68	91	111	256	174	187	183	197	280	298	283	283
130	67	90	110	254	173	186	180	195	279	298	283	283
135	68	90	110	255	173	186	179	195	349	298	284	283
139	68	90	110	247	173	185	180	195	349	298	284	283
145	68	90	109	251	172	185	180	195	279	299	284	283
149	68	90	109	249	173	185	180	194	350	298	284	283

Experiment no. 1 / Run no. 4

TIME	TA1	TA2	TA3	TA4	TB1	TB2	TB3	TB4	TC1	TC2	TC3	TC4
-60	300	300	300	300	307	307	307	307	317	317	317	317
-54	300	300	299	256	306	391	307	306	318	316	317	316
-50	299	300	299	228	307	306	307	307	317	317	317	316
-46	300	300	299	217	305	391	307	306	318	316	317	316
-41	300	300	299	212	307	391	307	306	317	315	316	316
-38	300	300	300	218	307	392	309	307	317	317	317	317
-33	299	299	299	218	306	390	306	306	317	316	316	316
-29	299	300	299	299	307	307	306	306	318	316	317	317
-26	300	299	299	298	306	307	304	306	317	317	316	317
-21	299	299	299	258	306	307	306	306	318	316	317	317
-17	300	298	299	217	307	391	306	306	318	316	317	317
-12	299	298	299	299	307	306	305	306	318	316	317	317
-8	299	298	299	216	307	390	306	307	318	316	318	317
-5	299	298	299	228	306	307	306	306	318	316	318	317
1	292	291	291	220	303	389	306	305	317	316	317	316
4	140	147	200	187	240	258	272	274	304	309	306	307
10	81	122	182	170	218	229	295	312	297	301	297	297
14	80	118	216	167	213	223	231	240	297	298	296	295
17	79	115	166	168	208	217	226	235	294	297	294	293
22	77	112	159	174	203	213	220	229	293	296	291	292
26	77	110	154	172	201	209	217	226	293	295	291	291
31	76	107	148	171	197	206	211	223	292	293	290	290
35	75	105	143	169	193	202	208	219	290	292	289	289
39	75	103	139	171	192	200	205	216	290	291	288	288
44	74	102	135	178	189	196	201	214	289	290	287	287
48	73	100	132	182	187	194	199	212	288	290	286	286
53	73	98	128	178	185	192	196	209	287	289	285	285
56	72	97	127	176	182	191	194	208	287	289	285	285
60	71	97	125	174	181	189	193	207	287	289	285	285
65	71	95	122	179	180	187	190	206	286	288	284	284
69	70	95	121	177	178	186	189	205	285	288	283	284
74	70	93	119	174	178	184	188	204	286	288	283	283
78	70	93	117	177	176	183	186	202	285	287	282	282
82	70	91	117	172	175	182	185	201	284	286	283	282
87	69	91	115	169	175	181	184	200	284	285	282	281
91	68	90	115	173	174	180	183	199	284	285	282	281
96	68	89	113	173	172	180	181	198	283	285	281	281
100	68	89	113	170	173	178	182	198	283	284	281	281
104	68	88	113	171	172	179	182	197	284	285	283	281
110	68	87	111	181	172	177	179	196	283	284	281	280
114	68	88	111	179	171	177	179	195	283	285	280	280
119	68	87	111	175	170	177	180	195	283	284	281	280
123	68	87	110	171	170	177	179	194	283	284	281	280
127	67	86	110	169	169	177	178	194	283	284	280	280
132	67	86	109	171	169	175	177	193	283	284	281	280
136	67	85	108	170	168	174	176	192	282	284	280	279
141	67	85	108	179	168	175	176	192	283	284	280	280
146	66	85	107	172	168	174	176	191	282	284	280	279

Experiment no. 1 / Run no. 5

TIME	TA1	TA2	TA3	TA4	TB1	TB2	TB3	TB4	TC1	TC2	TC3	TC4
-60	300	300	300	300	307	307	307	307	317	317	317	317
-56	299	300	299	300	306	305	307	306	315	316	316	316
-51	299	298	299	301	306	305	306	306	315	316	316	316
-47	298	297	298	292	306	305	305	306	315	317	316	316
-44	298	298	299	295	307	305	303	306	316	316	316	316
-39	299	300	300	294	307	306	306	307	316	316	316	316
-36	299	299	299	295	307	306	306	307	317	316	317	316
-31	297	298	298	297	305	389	306	306	316	316	315	316
-27	298	297	299	293	307	305	306	306	316	317	317	316
-23	298	297	299	300	306	305	305	306	317	317	316	316
-19	298	297	298	296	305	304	307	306	315	316	315	316
-15	298	297	298	296	306	305	307	306	317	316	316	316
-10	298	297	298	301	306	305	307	306	317	317	317	316
-6	298	297	298	293	306	305	307	306	317	317	316	316
-2	297	296	298	298	306	304	306	305	316	315	315	315
3	250	249	250	276	285	292	298	296	377	313	311	312
6	167	127	188	234	227	235	254	257	298	302	298	299
12	76	115	219	224	217	221	236	246	295	298	295	296
15	75	111	170	220	213	217	232	309	296	298	293	294
19	74	109	164	218	210	214	229	238	294	297	292	293
24	73	106	156	214	204	209	222	234	294	330	291	291
28	72	104	151	213	202	205	219	231	293	362	291	291
33	71	100	144	211	198	201	214	226	291	292	289	290
37	69	98	139	215	195	198	210	223	290	375	288	289
40	69	96	136	205	193	195	206	221	290	374	287	288
46	68	94	130	209	190	191	203	218	290	287	287	288
50	68	93	128	213	187	189	199	216	289	373	286	287
55	67	91	125	211	185	187	197	214	288	286	285	286
59	67	90	122	201	183	184	195	213	287	286	284	285
63	66	90	120	209	181	183	193	212	288	372	284	285
68	66	87	118	201	180	180	190	210	286	371	283	284
71	65	86	116	205	178	179	189	209	286	284	282	283
77	64	85	114	203	176	177	187	208	285	283	282	283
81	64	85	113	204	175	176	186	207	285	372	282	282
85	64	84	112	202	174	175	185	206	284	283	281	282
90	63	82	110	200	173	174	183	205	284	370	281	281
94	63	82	110	193	173	174	182	205	284	284	280	281
100	62	81	108	205	171	171	180	204	283	283	280	280
103	62	82	108	201	171	171	181	203	283	370	279	280
107	63	81	108	192	171	171	180	202	284	283	280	281
112	63	80	107	274	169	169	178	202	283	283	279	280
116	62	80	107	201	170	170	178	202	283	283	280	280
121	61	78	105	271	169	168	178	201	282	283	279	280
124	61	79	105	193	169	168	177	200	283	284	278	280
128	62	79	105	188	168	168	176	200	284	283	278	279
133	62	78	105	188	169	168	176	200	283	284	279	280
137	62	78	104	189	167	167	175	200	283	283	279	280
141	62	77	103	187	166	168	175	199	283	283	279	279
145	62	77	104	186	167	167	175	199	283	284	280	280

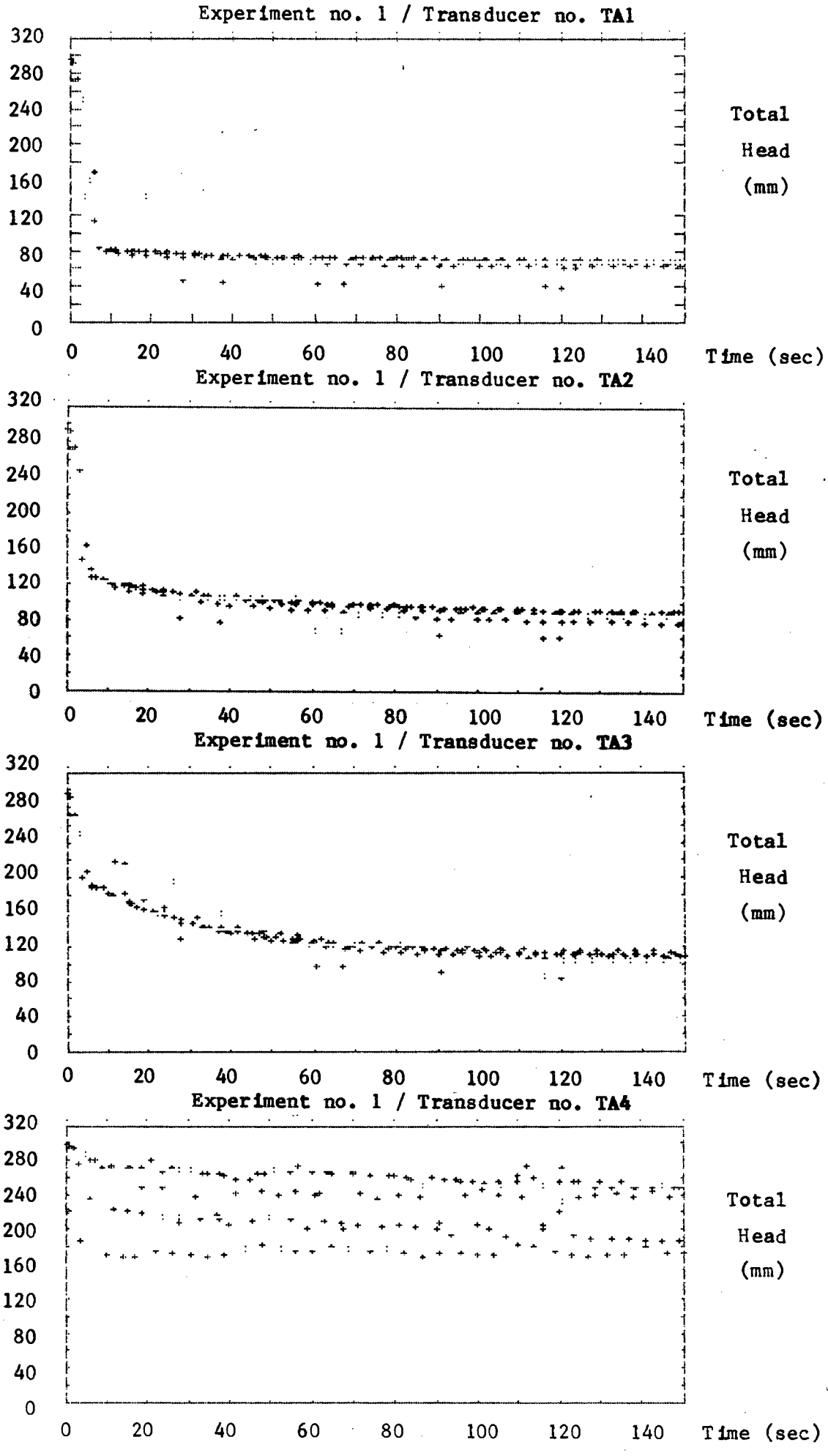
Experiment no. 1 / Transducer no. TA1
320
280
240
200
160
120
80
40
0
0
20
40
60
80
100
120
140
Time (sec)
Total
Head
(mm)
Experiment no. 1 / Transducer no. TA2
320
280
240
200
160
120
80
40
0
0
20
40
60
80
100
120
140
Time (sec)
Total
Head
(mm)
Experiment no. 1 / Transducer no. TA3
320
280
240
200
160
120
80
40
0
0
20
40
60
80
100
120
140
Time (sec)
Total
Head
(mm)
Experiment no. 1 / Transducer no. TA4
320
280
240
200
160
120
80
40
0
0
20
40
60
80
100
120
140
Time (sec)
Total
Head
(mm)

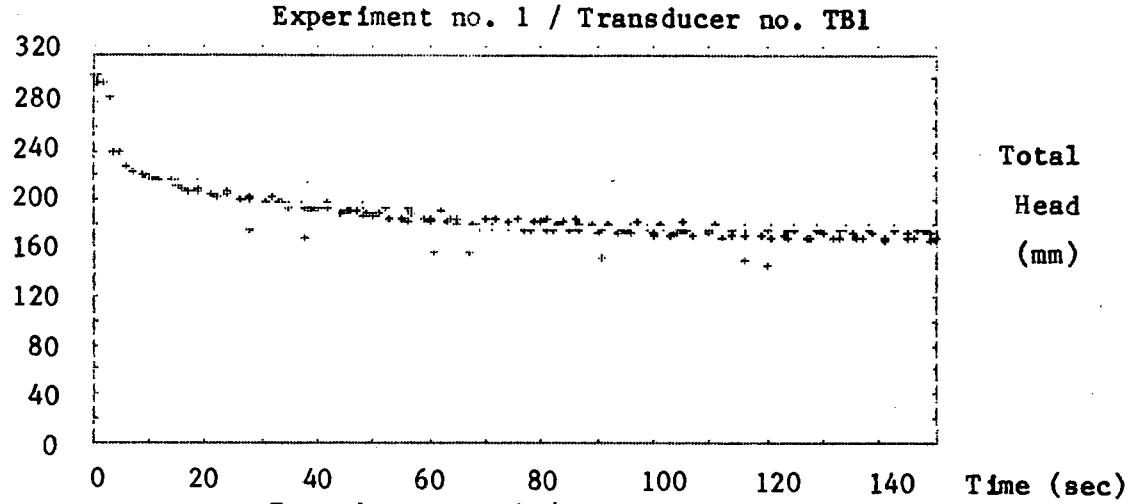
Experiment no. 1 / Transducer no. TB1
320
280
240
200
160
120
80
40
0
0
20
40
60
80
100
120
140
Time (sec)
Total
Head
(mm)

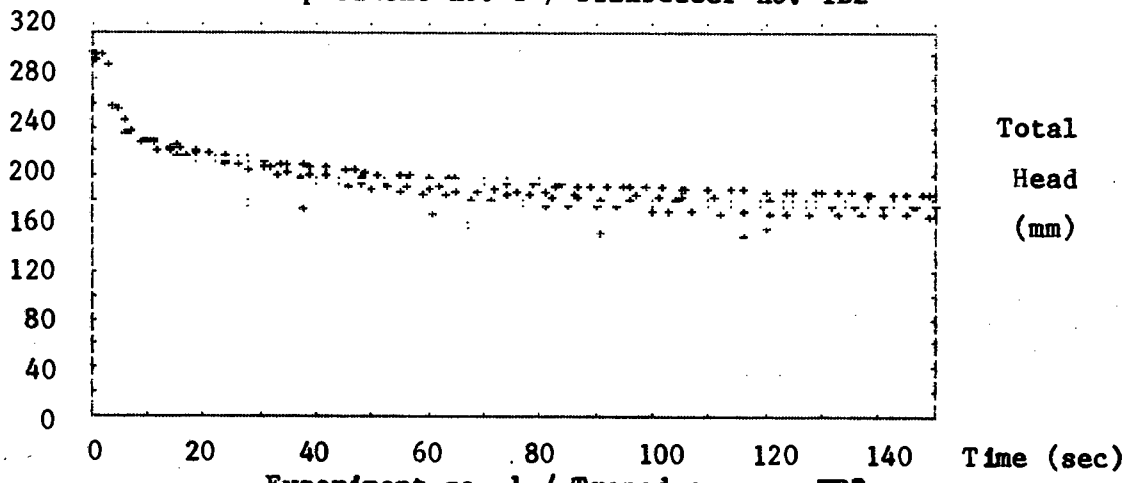
Experiment no. 1 / Transducer no. TB2
320
280
240
200
160
120
80
40
0
0
20
40
60
80
100
120
140
Time (sec)
Total
Head
(mm)

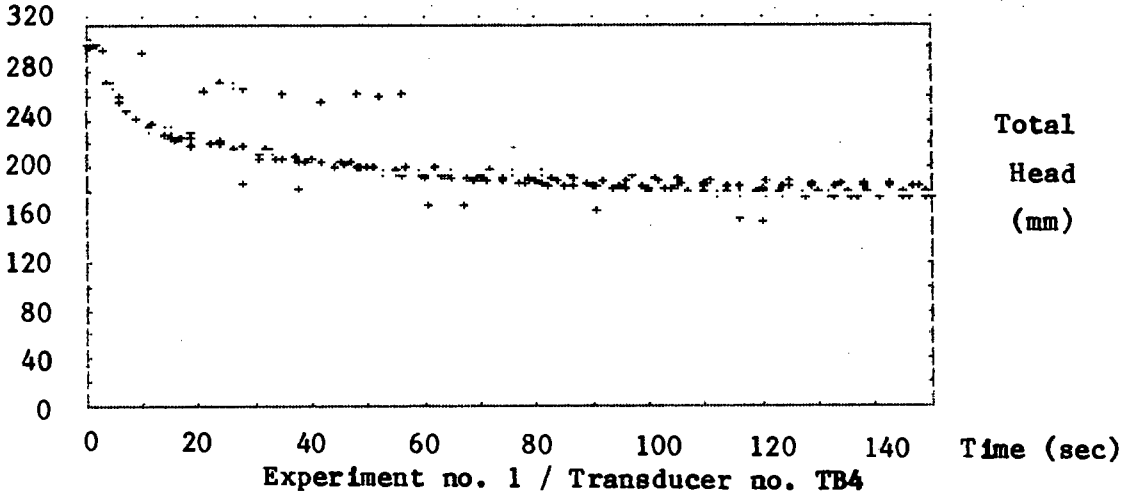
Experiment no. 1 / Transducer no. TB3
320
280
240
200
160
120
80
40
0
0
20
40
60
80
100
120
140
Time (sec)
Total
Head
(mm)

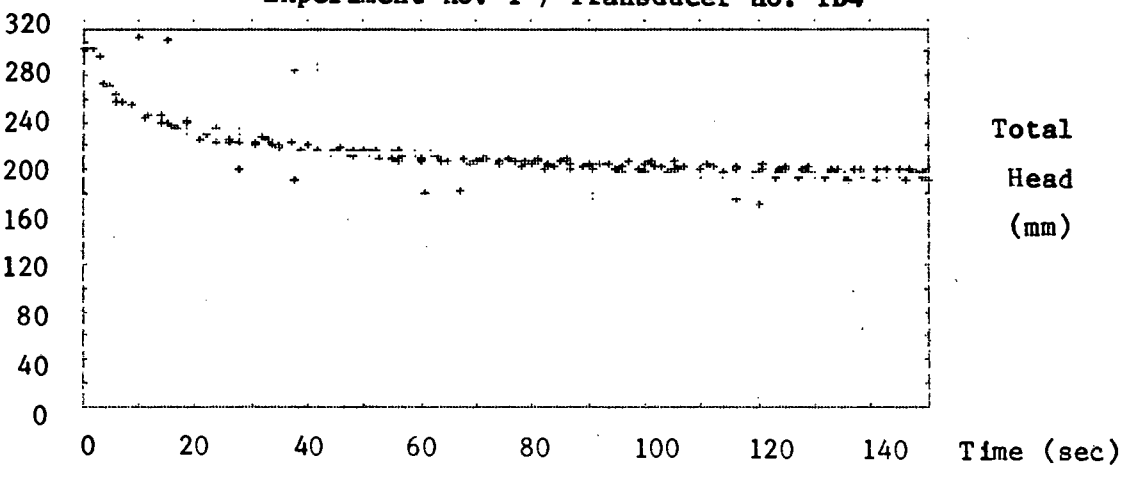
Experiment no. 1 / Transducer no. TB4
320
280
240
200
160
120
80
40
0
0
20
40
60
80
100
120
140
Time (sec)
Total
Head
(mm)

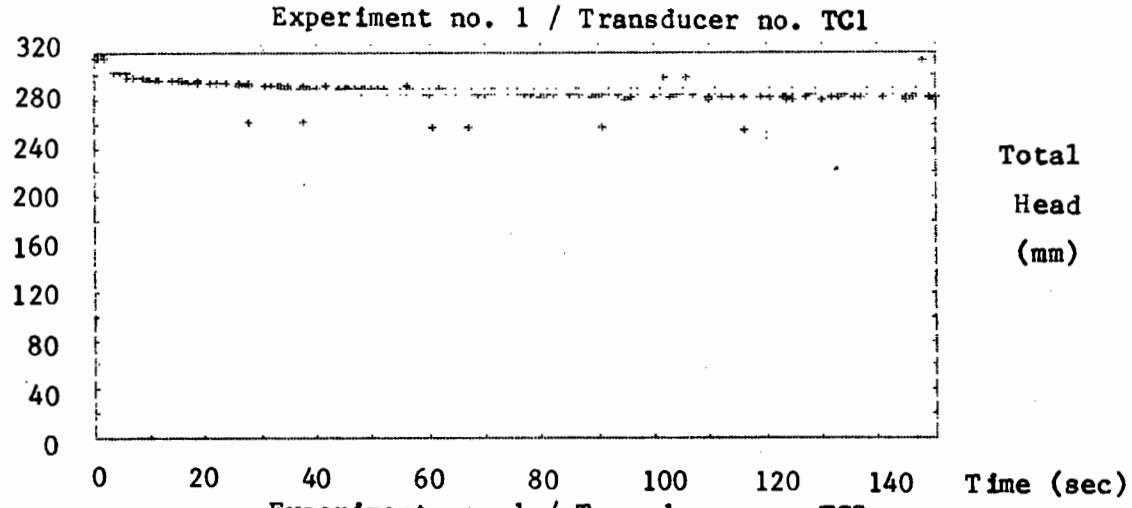
Experiment no. 1 / Transducer no. TC1
320
280
240
200
160
120
80
40
0
0
20
40
60
80
100
120
140
Time (sec)
Total
Head
(mm)

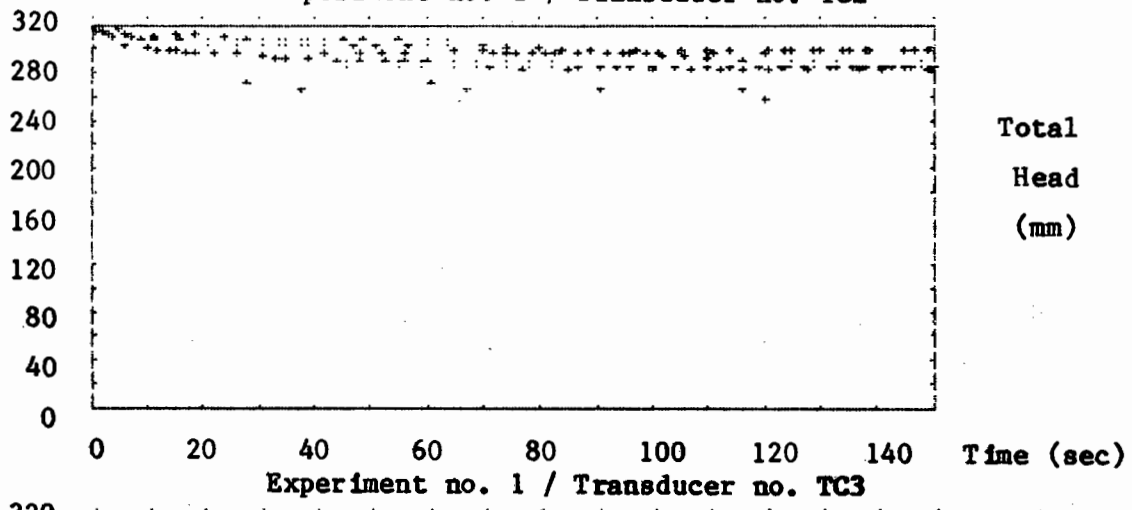
Experiment no. 1 / Transducer no. TC2
320
280
240
200
160
120
80
40
0
0
20
40
60
80
100
120
140
Time (sec)
Total
Head
(mm)

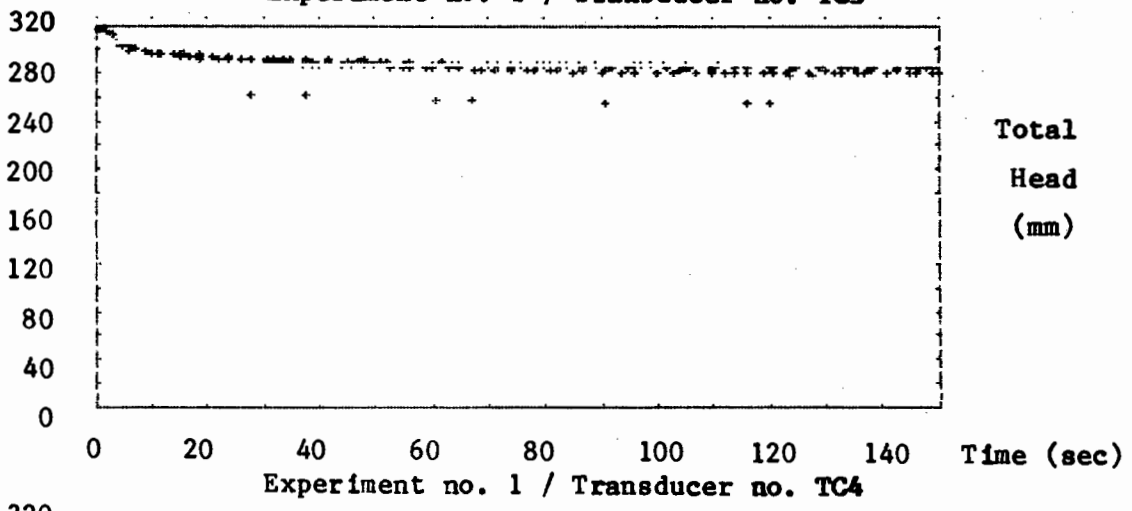
Experiment no. 1 / Transducer no. TC3
320
280
240
200
160
120
80
40
0
0
20
40
60
80
100
120
140
Time (sec)
Total
Head
(mm)

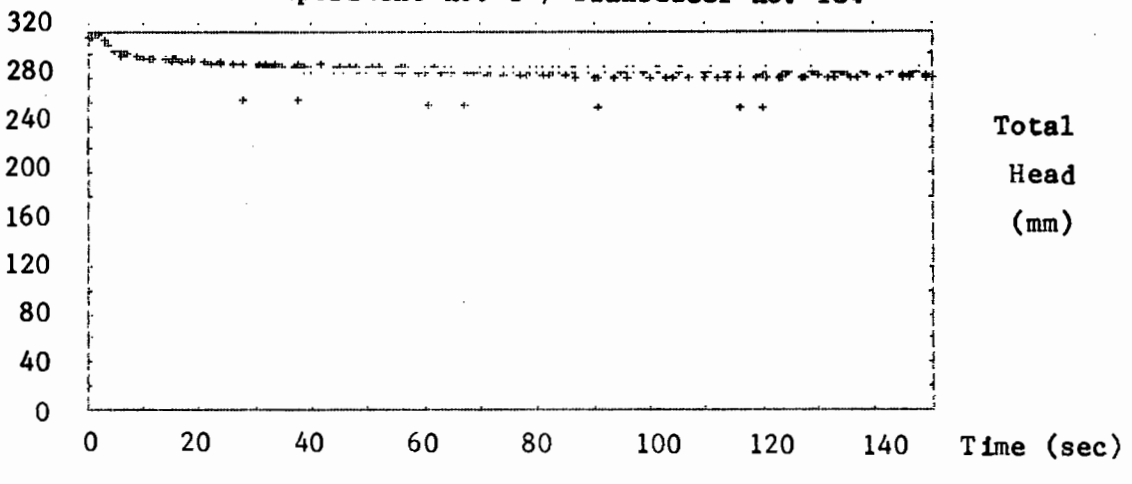
Experiment no. 1 / Transducer no. TC4
320
280
240
200
160
120
80
40
0
0
20
40
60
80
100
120
140
Time (sec)
Total
Head
(mm)

E-7. Approximate moisture transfer analysis. Experiment no. 1.

The results for the moisture mass transfer analysis of experiment no. 1, are given here. The times of: 10; 15; 30 and 60 seconds after the start of the experiment are considered. For each time considered the following results for the analysis is given:

A total head contour plot of the seepage domain.

A contour plot of the degree of saturation of the seepage domain.

Profile plots and their coordinates, for four vertical sections taken across the the seepage domain. The profile plots show the following with respect to elevation:

a) The pressure head;
b) Degree of saturation;
c) Relative hydraulic conductivity;
d) Horizontal hydraulic gradient; (Only sec. A & D)
e) Relative horizontal Darcian velocity. (Only sec. A & D)

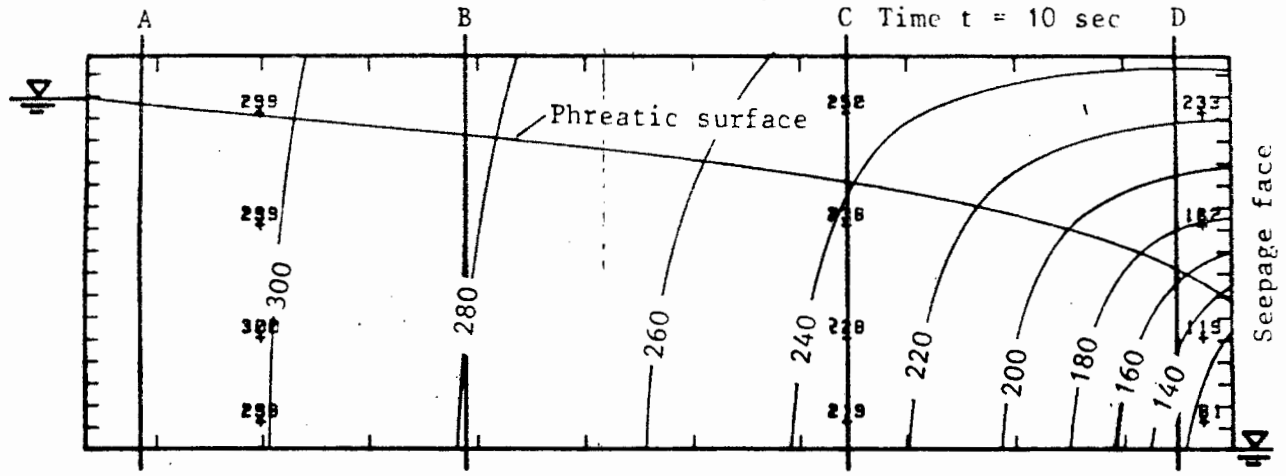
A
B
C Time t = 10 sec
D
Phreatic surface
Seepage face
300
280
260
240
220
200
180
160
140

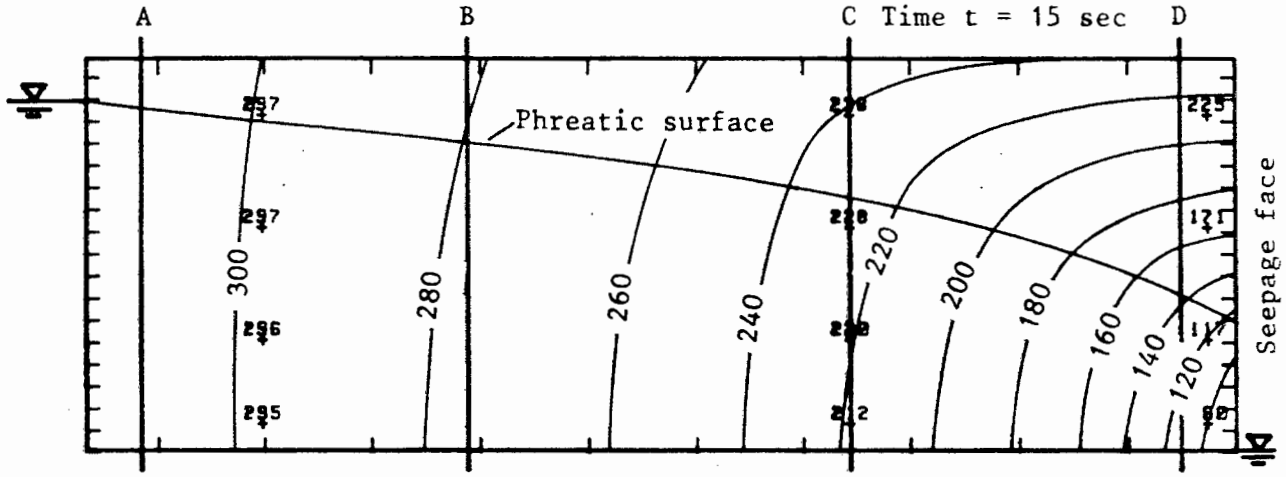
A
B
C Time t = 15 sec
D
Phreatic surface
Seepage face
300
280
260
240
220
200
180
160
140
120

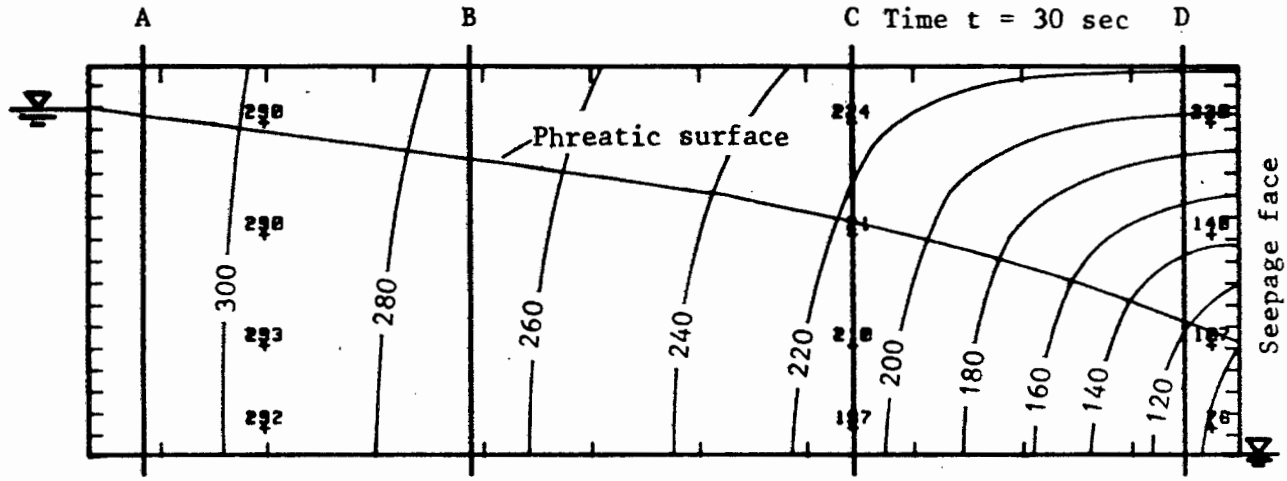
A
B
C Time t = 30 sec
D
Phreatic surface
Seepage face
300
280
260
240
220
200
180
160
140
120

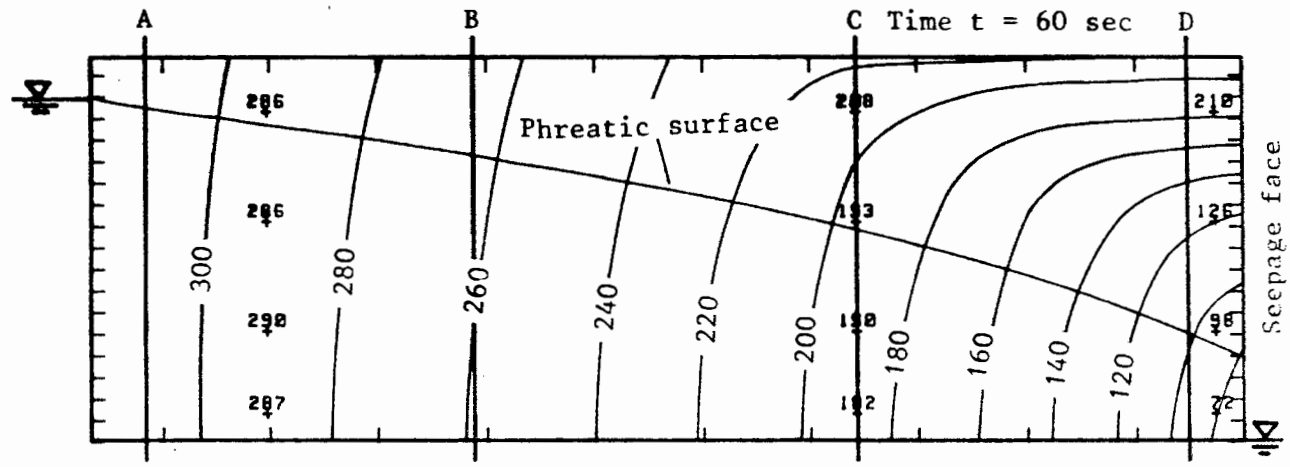
A
B
C Time t = 60 sec
D
Phreatic surface
Seepage face
300
280
260
240
220
200
180
160
140
120

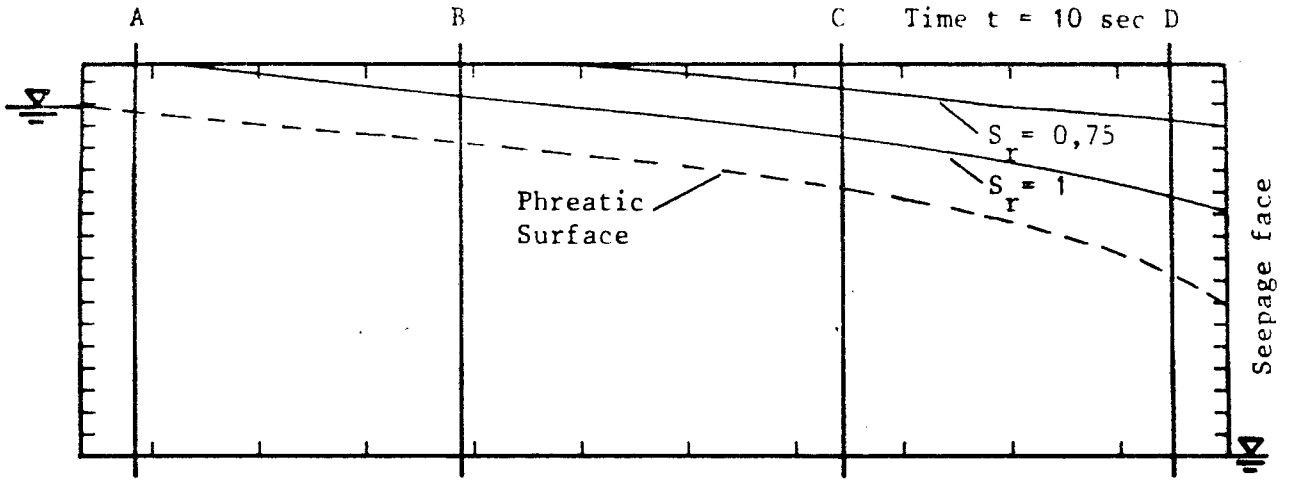
A
B
C
Time t = 10 sec
D
S_r = 0,75
S_r = 1
Phreatic Surface
Seepage face

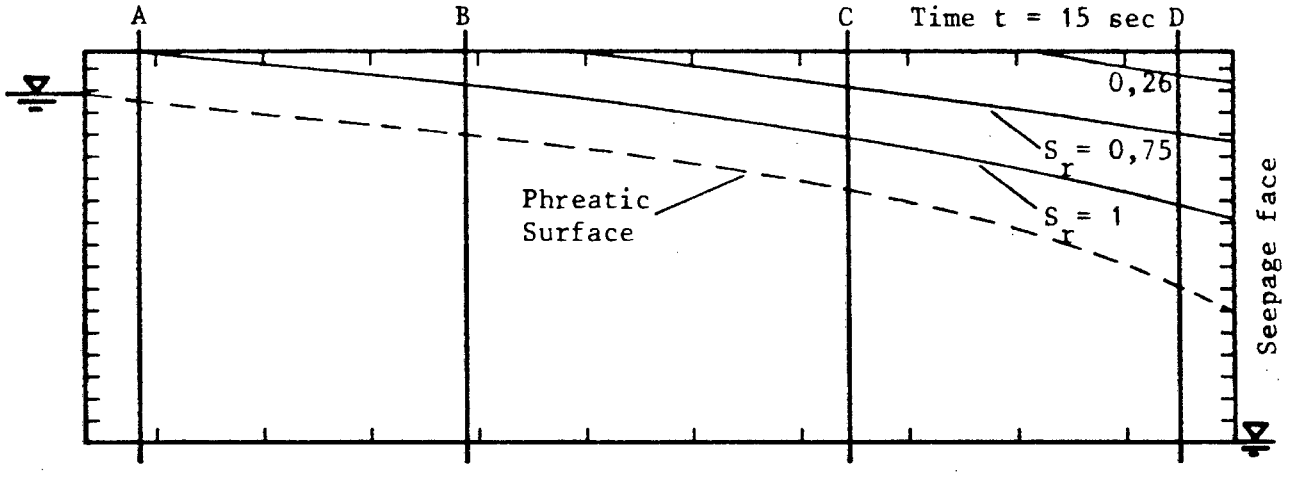
A
B
C
Time t = 15 sec
D
0,26
S_r = 0,75
S_r = 1
Phreatic Surface
Seepage face

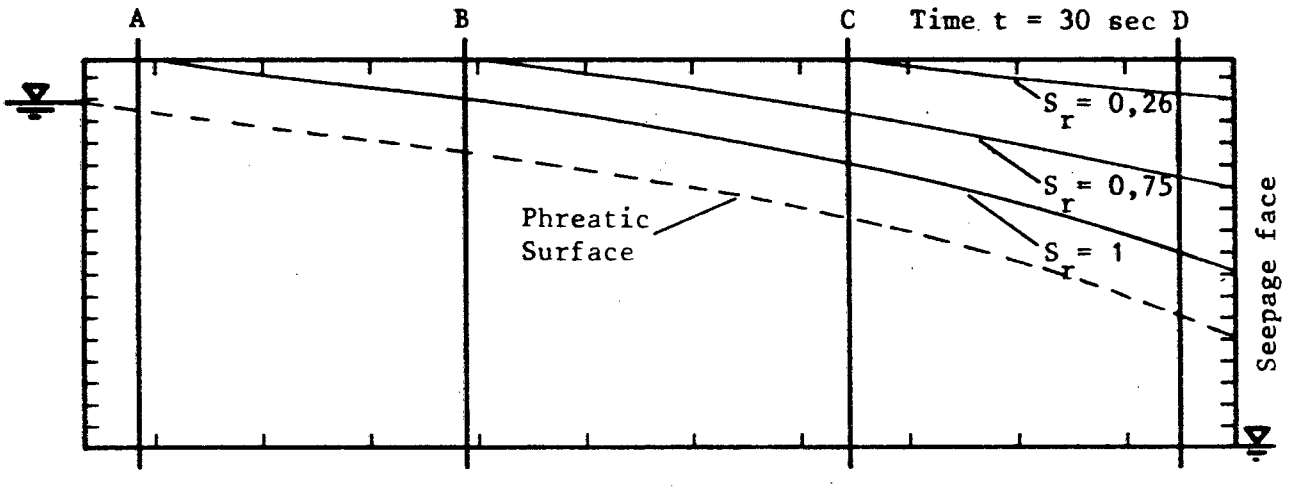
A
B
C
Time t = 30 sec
D
S_r = 0,26
S_r = 0,75
S_r = 1
Phreatic Surface
Seepage face

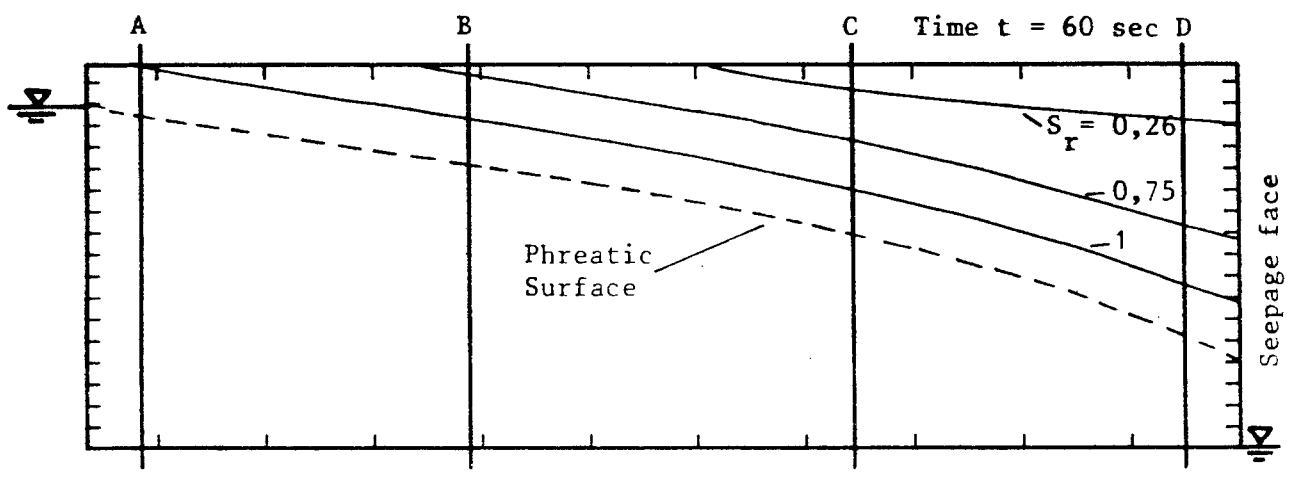
A
B
C
Time t = 60 sec
D
S_r = 0,26
0,75
1
Phreatic Surface
Seepage face

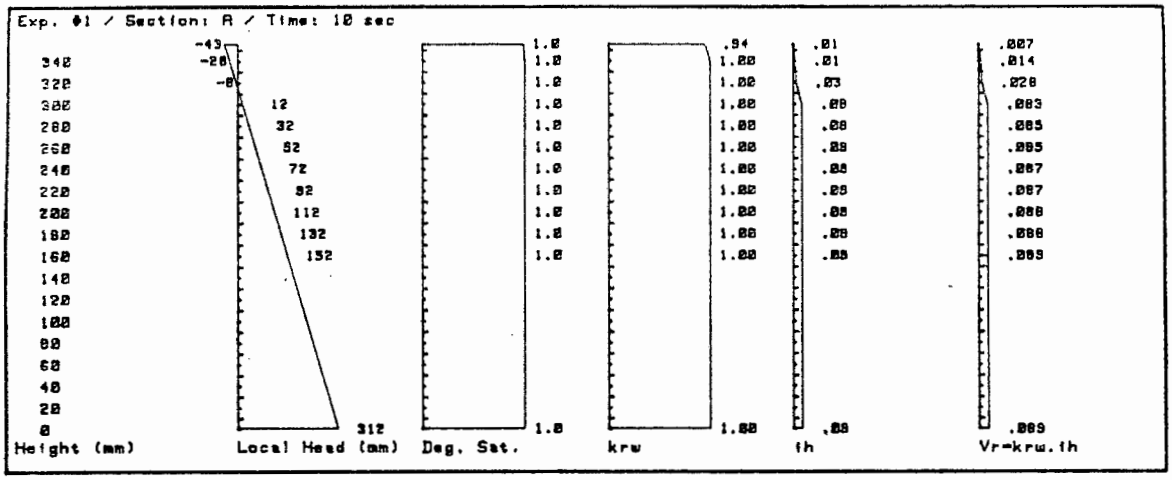
Exp. #1 / Section: A / Time: 10 sec
Height (mm)
Local Head (mm)
Deg. Sat.
krw
th
Vr=krw.th

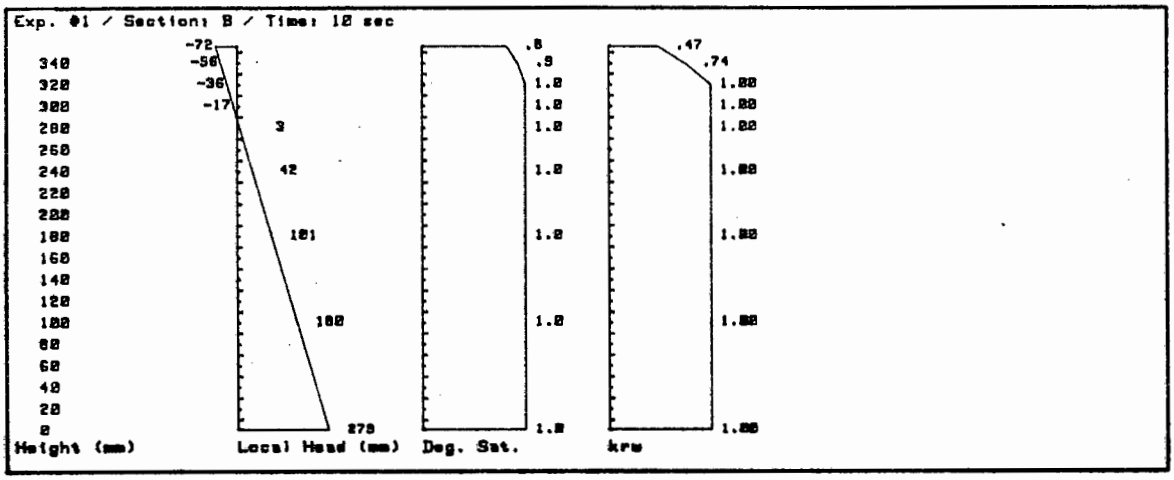
Exp. #1 / Section: B / Time: 10 sec
Height (mm)
Local Head (mm)
Deg. Sat.
krw

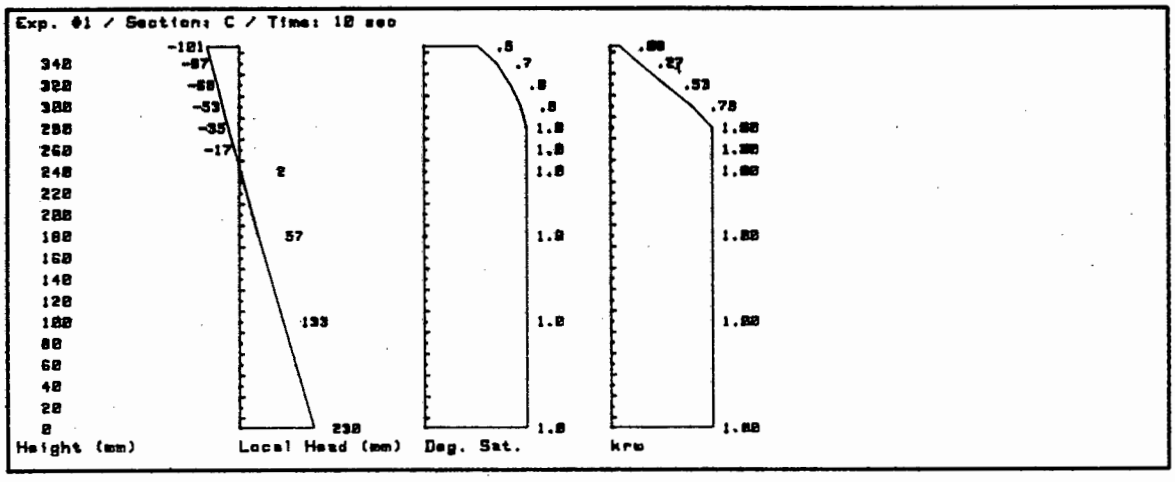
Exp. #1 / Section: C / Time: 10 sec
Height (mm)
Local Head (mm)
Deg. Sat.
krw

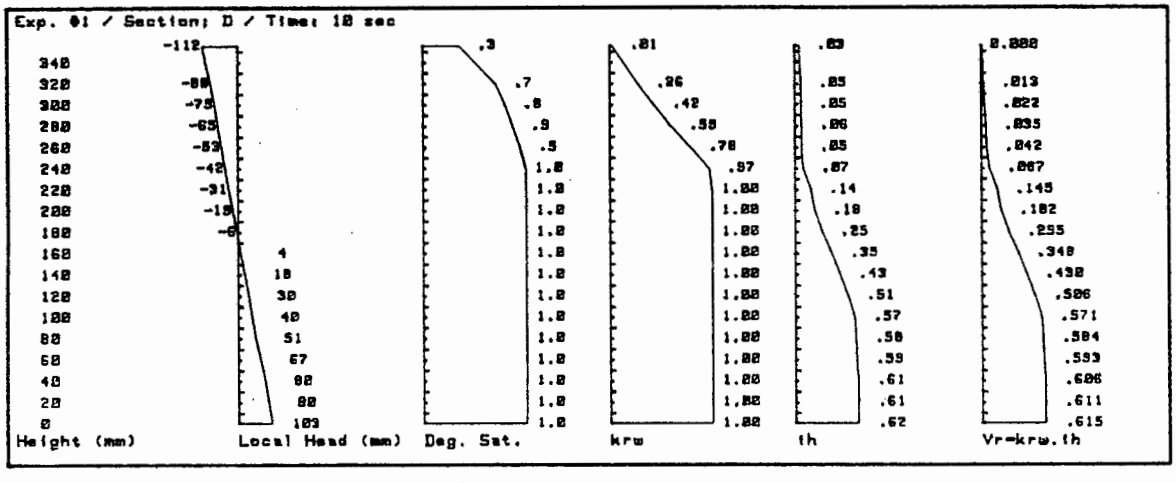
Exp. #1 / Section: D / Time: 10 sec
Height (mm)
Local Head (mm)
Deg. Sat.
krw
th
Vr=krw.th

Exp. #1 / Section: A / Time: 10 sec

Height (mm)	Local Head (mm)	Deg. Sat.	Rel. Perm.	Hydraulic Grad.	krw x ih
356	-43	0.98	0.943	0.01	0.007
340	-28	1.00	1.000	0.01	0.014
320	-8	1.00	1.000	0.03	0.028
300	12	1.00	1.000	0.08	0.083
280	32	1.00	1.000	0.09	0.085
260	52	1.00	1.000	0.09	0.085
240	72	1.00	1.000	0.09	0.087
220	92	1.00	1.000	0.09	0.087
200	112	1.00	1.000	0.09	0.088
180	132	1.00	1.000	0.09	0.088
160	152	1.00	1.000	0.09	0.089
0	312	1.00	1.000	0.09	0.089

Width : 312.4 mm
Void Ratio e : 0.547
Eff. Sat. Area : 125.7 mm
Temp T : 16.6 deg C
Sat. Perm. ks : 0.395 cm/sec
Rel. Flow Rate : 28.2 sq mm
Flow Rate : 34.8 cu cm/sec

Exp. #1 / Section: B / Time: 10 sec

Height (mm)	Local Head (mm)	Deg. Sat.	Rel. Perm.
356	-72	0.81	0.474
340	-56	0.92	0.736
320	-36	1.00	1.000
300	-17	1.00	1.000
280	3	1.00	1.000
240	42	1.00	1.000
180	101	1.00	1.000
100	180	1.00	1.000
0	279	1.00	1.000

Width : 312.4 mm
Void Ratio e : 0.547
Eff. Sat. Area : 124.7 mm

Exp. #1 / Section: C / Time: 10 sec

Height (mm)	Local Head (mm)	Deg. Sat.	Rel. Perm.
356	-101	0.52	0.081
340	-87	0.70	0.270
320	-68	0.84	0.526
300	-53	0.94	0.790
280	-35	1.00	1.000
260	-17	1.00	1.000
240	2	1.00	1.000
180	57	1.00	1.000
100	133	1.00	1.000
0	230	1.00	1.000

Width : 312.4 mm
Void Ratio e : 0.547
Eff. Sat. Area : 120.9 mm

Exp. #1 / Section: D / Time: 10 sec

Height (mm)	Local Head (mm)	Deg. Sat.	Rel. Perm.	Hydraulic Grad.	krw x ih
356	-112	0.34	0.012	0.03	0.000
320	-88	0.70	0.264	0.05	0.013
300	-75	0.79	0.422	0.05	0.022
280	-65	0.86	0.589	0.06	0.035
260	-53	0.93	0.784	0.05	0.042
240	-42	0.99	0.966	0.07	0.067
220	-31	1.00	1.000	0.14	0.145
200	-19	1.00	1.000	0.18	0.182
180	-6	1.00	1.000	0.25	0.255
160	4	1.00	1.000	0.35	0.348
140	18	1.00	1.000	0.43	0.430
120	30	1.00	1.000	0.51	0.506
100	40	1.00	1.000	0.57	0.571
80	51	1.00	1.000	0.58	0.584
60	67	1.00	1.000	0.59	0.593
40	80	1.00	1.000	0.61	0.606
20	90	1.00	1.000	0.61	0.611
0	103	1.00	1.000	0.62	0.615

Width : 312.4 mm
Void Ratio e : 0.547
Eff. Sat. Area : 115.6 mm
Temp T : 16.6 deg C
Sat. Perm. ks : 0.395 cm/sec
Rel. Flow Rate : 106.4 sq mm
Flow Rate : 131.4 cu cm/sec

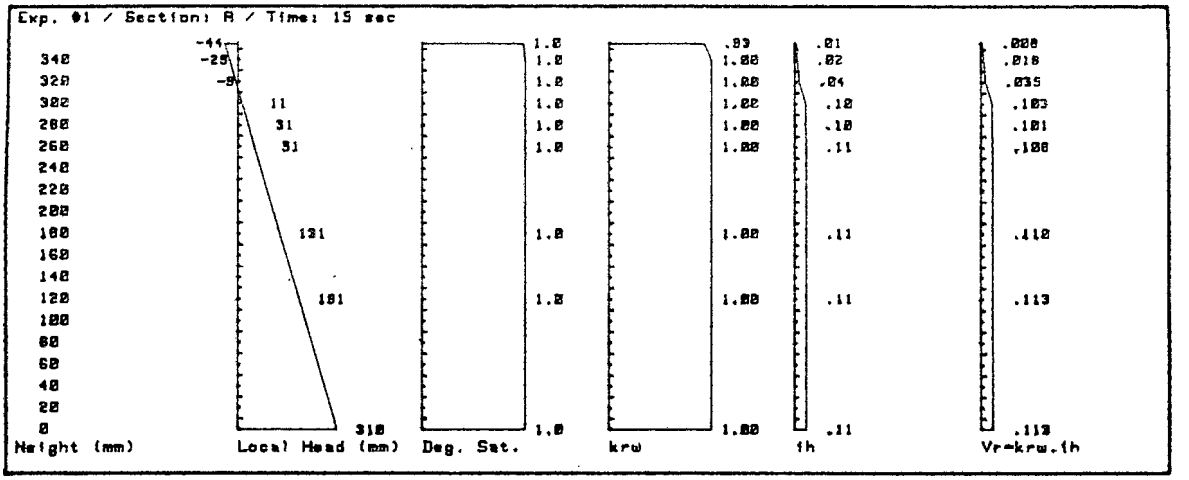
Exp. #1 / Section: A / Time: 15 sec
Height (mm)
Local Head (mm)
Deg. Sat.
krw
fh
Vr=krw.fh

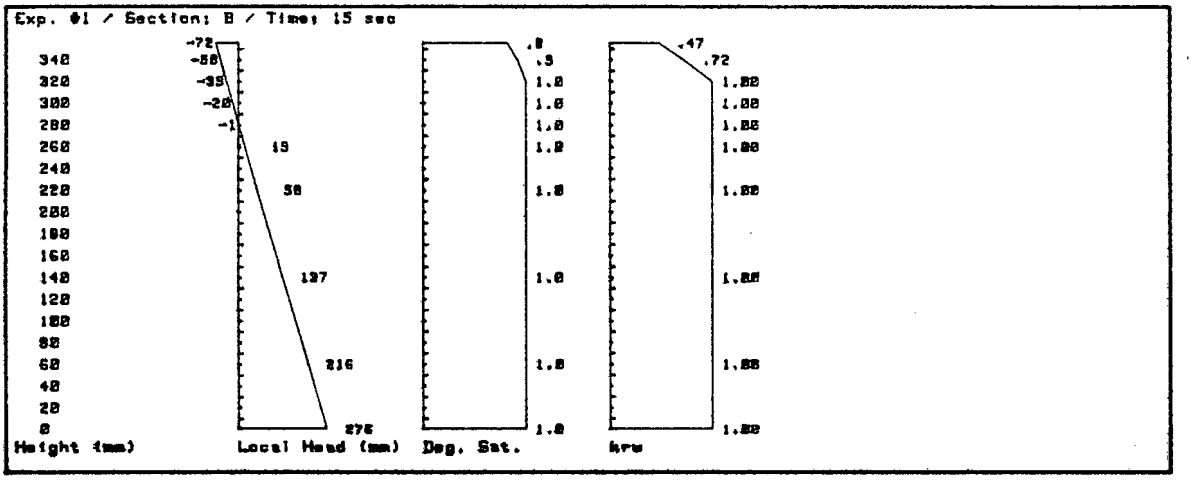
Exp. #1 / Section: B / Time: 15 sec
Height (mm)
Local Head (mm)
Deg. Sat.
krw

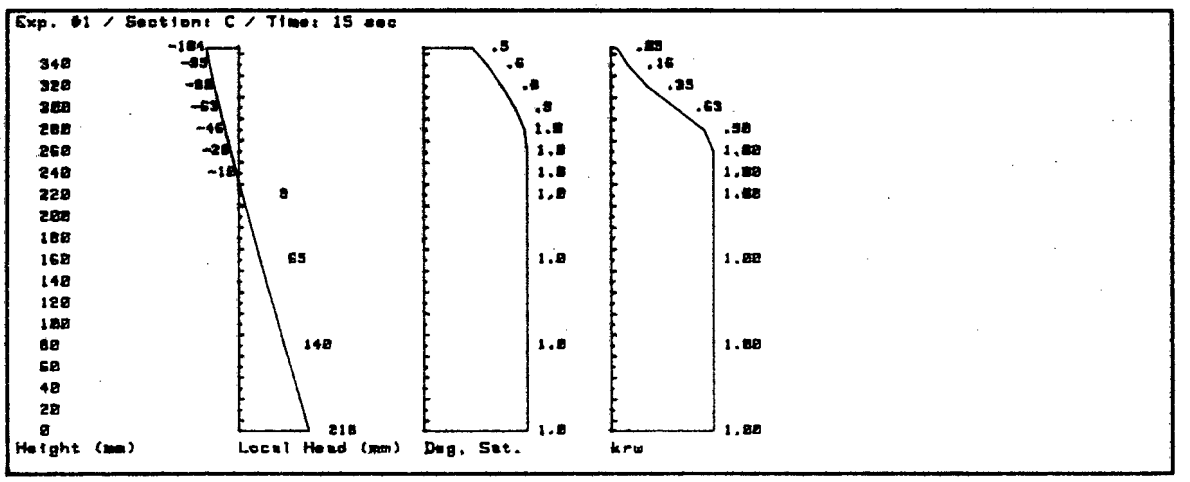
Exp. #1 / Section: C / Time: 15 sec
Height (mm)
Local Head (mm)
Deg. Sat.
krw

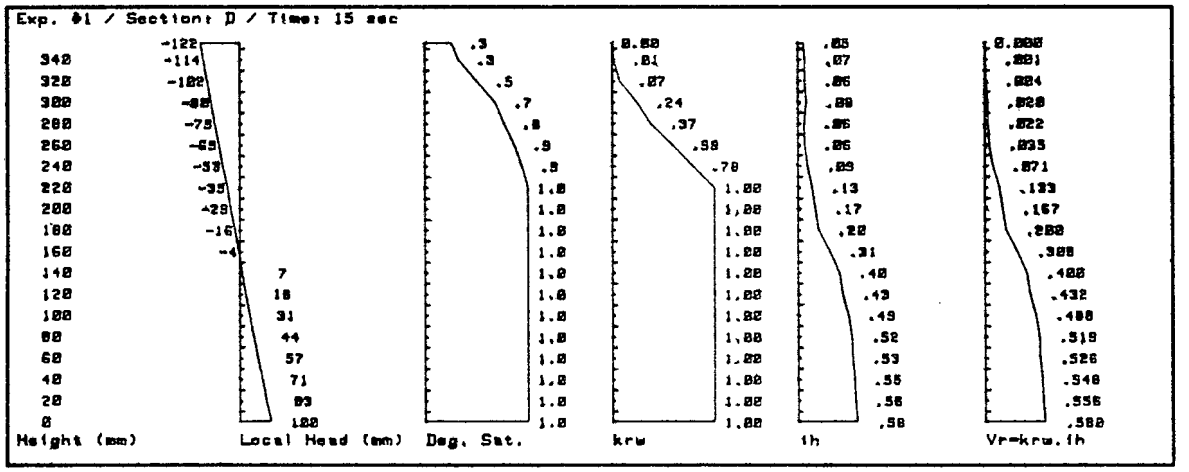
Exp. #1 / Section: D / Time: 15 sec
Height (mm)
Local Head (mm)
Deg. Sat.
krw
fh
Vr=krw.fh

Exp. #1 / Section: A / Time: 15 sec

Height (mm)	Local Head (mm)	Deg. Sat.	Rel. Perm.	Hydraulic Grad.	krw x ih
356	-44	0.98	0.926	0.01	0.008
340	-29	1.00	1.000	0.02	0.018
320	-9	1.00	1.000	0.04	0.035
300	11	1.00	1.000	0.10	0.103
280	31	1.00	1.000	0.10	0.101
260	51	1.00	1.000	0.11	0.106
180	131	1.00	1.000	0.11	0.110
120	191	1.00	1.000	0.11	0.113
0	310	1.00	1.000	0.11	0.113

Width : 312.4 mm
Void Ratio e : 0.547
Eff. Sat. Area : 125.7 mm
Temp T : 16.6 deg C
Sat. Perm. ks : 0.395 cm/sec
Rel. Flow Rate : 35.2 mm
Flow Rate : 43.4 cu cm/sec

Exp. #1 / Section: B / Time: 15 sec

Height (mm)	Local Head (mm)	Deg. Sat.	Rel. Perm.
356	-72	0.81	0.474
340	-58	0.91	0.717
320	-39	1.00	1.000
300	-20	1.00	1.000
280	-1	1.00	1.000
260	19	1.00	1.000
220	58	1.00	1.000
140	137	1.00	1.000
60	216	1.00	1.000
0	276	1.00	1.000

Width : 312.4 mm
Void Ratio e : 0.547
Eff. Sat. Area : 124.7 mm

Exp. #1 / Section: C / Time: 15 sec

Height (mm)	Local Head (mm)	Deg. Sat.	Rel. Perm.
356	-104	0.46	0.050
340	-95	0.61	0.158
320	-80	0.75	0.353
300	-63	0.88	0.627
280	-46	0.97	0.903
260	-28	1.00	1.000
240	-10	1.00	1.000
220	9	1.00	1.000
160	65	1.00	1.000
80	140	1.00	1.000
0	218	1.00	1.000

Width : 312.4 mm
Void Ratio e : 0.547
Eff. Sat. Area : 119.0 mm

Exp. #1 / Section: D / Time: 15 sec

Height (mm)	Local Head (mm)	Deg. Sat.	Rel. Perm.	Hydraulic Grad.	krw x ih
356	-122	0.25	0.002	0.05	0.000
340	-114	0.32	0.008	0.07	0.001
320	-102	0.50	0.069	0.06	0.004
300	-90	0.68	0.238	0.08	0.020
280	-79	0.76	0.373	0.06	0.022
260	-65	0.86	0.586	0.06	0.035
240	-53	0.93	0.784	0.09	0.071
220	-39	1.00	1.000	0.13	0.133
200	-29	1.00	1.000	0.17	0.167
180	-16	1.00	1.000	0.20	0.200
160	-4	1.00	1.000	0.31	0.308
140	7	1.00	1.000	0.40	0.400
120	18	1.00	1.000	0.43	0.432
100	31	1.00	1.000	0.49	0.488
80	44	1.00	1.000	0.52	0.519
60	57	1.00	1.000	0.53	0.526
40	71	1.00	1.000	0.55	0.548
20	83	1.00	1.000	0.56	0.556
0	100	1.00	1.000	0.58	0.580

Width : 312.4 mm
Void Ratio e : 0.547
Eff. Sat. Area : 110.4 mm
Temp T : 16.6 deg C
Sat. Perm. ks : 0.395 cm/sec
Rel. Flow Rate : 94.4 mm
Flow Rate : 116.5 cu cm/sec

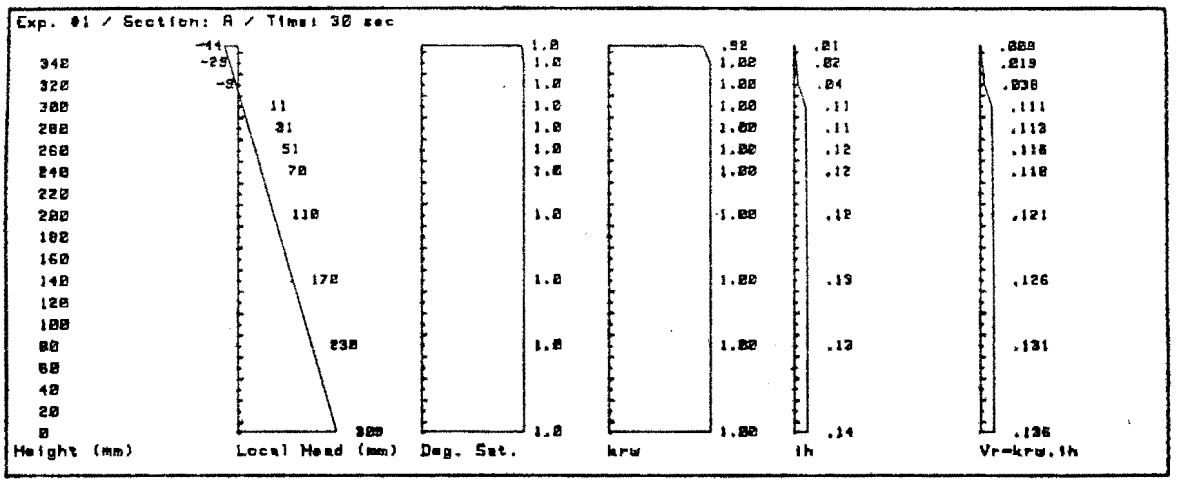
Exp. #1 / Section: A / Time: 30 sec
Height (mm)
Local Head (mm)
Deg. Sat.
krw
ih
Vr=krw.ih

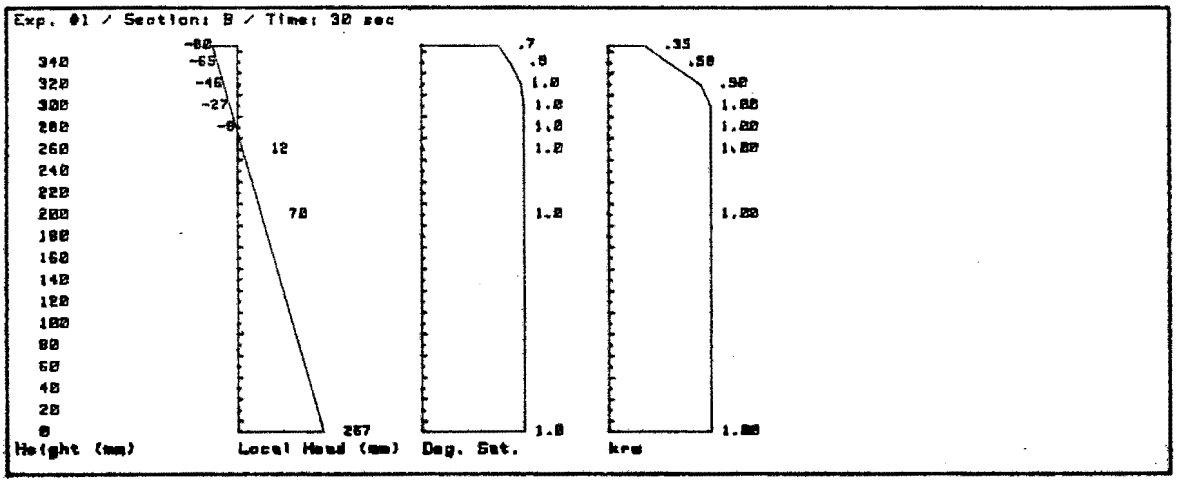
Exp. #1 / Section: B / Time: 30 sec
Height (mm)
Local Head (mm)
Deg. Sat.
krw

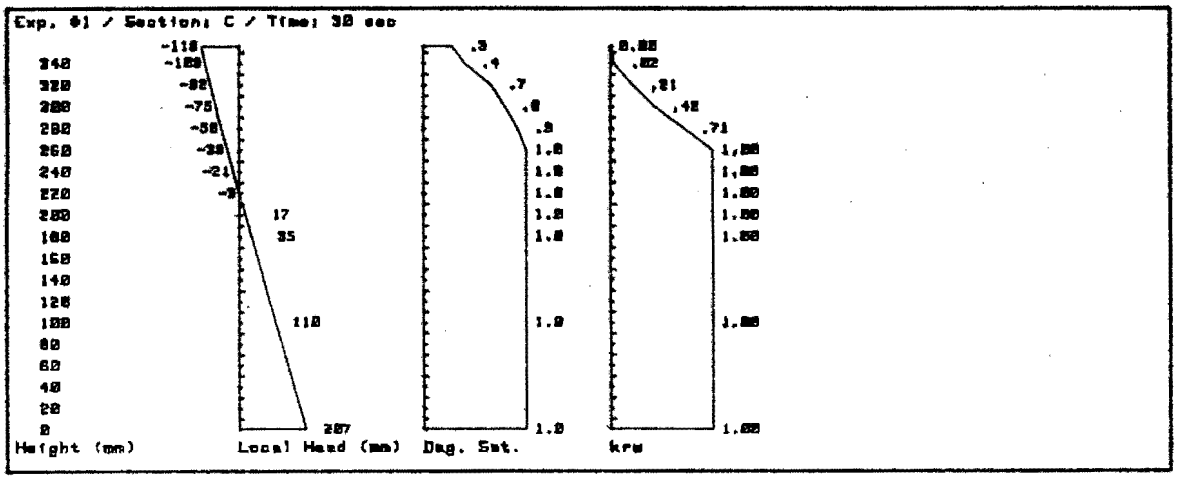
Exp. #1 / Section: C / Time: 30 sec
Height (mm)
Local Head (mm)
Deg. Sat.
krw

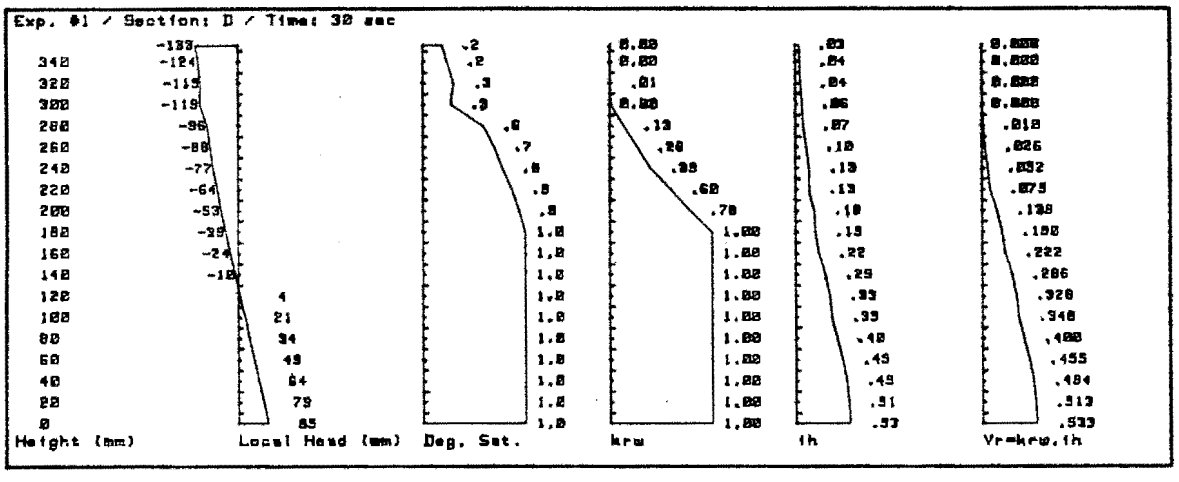
Exp. #1 / Section: D / Time: 30 sec
Height (mm)
Local Head (mm)
Deg. Sat.
krw
ih
Vr=krw.ih

Exp. #1 / Section: A / Time: 30 sec

Height (mm)	Local Head (mm)	Deg. Sat.	Rel. Perm.	Hydraulic Grad.	krw x ih
356	-44	0.98	0.925	0.01	0.009
340	-29	1.00	1.000	0.02	0.019
320	-9	1.00	1.000	0.04	0.038
300	11	1.00	1.000	0.11	0.111
280	31	1.00	1.000	0.11	0.113
260	51	1.00	1.000	0.12	0.116
240	70	1.00	1.000	0.12	0.118
200	110	1.00	1.000	0.12	0.121
140	170	1.00	1.000	0.13	0.126
80	230	1.00	1.000	0.13	0.131
0	309	1.00	1.000	0.14	0.136

Width : 312.4 mm
Void Ratio e : 0.547
Eff. Sat. Area : 125.7 mm
Temp T : 16.6 deg C
Sat. Perm. ks : 0.395 cm/sec
Rel. Flow Rate : 39.7 mm
Flow Rate : 49.0 cu cm/sec

Exp. #1 / Section: B / Time: 30 sec

Height (mm)	Local Head (mm)	Deg. Sat.	Rel. Perm.
356	-80	0.75	0.349
340	-65	0.86	0.580
320	-46	0.97	0.896
300	-27	1.00	1.000
280	-8	1.00	1.000
260	12	1.00	1.000
200	70	1.00	1.000
0	267	1.00	1.000

Width : 312.4 mm
Void Ratio e : 0.547
Eff. Sat. Area : 123.9 mm

Exp. #1 / Section: C / Time: 30 sec

Height (mm)	Local Head (mm)	Deg. Sat.	Rel. Perm.
356	-119	0.27	0.003
340	-109	0.39	0.023
320	-92	0.65	0.209
300	-75	0.79	0.422
280	-58	0.91	0.714
260	-39	1.00	1.000
240	-21	1.00	1.000
220	-3	1.00	1.000
200	17	1.00	1.000
180	35	1.00	1.000
100	110	1.00	1.000
0	207	1.00	1.000

Width : 312.4 mm
Void Ratio e : 0.547
Eff. Sat. Area : 115.3 mm

Exp. #1 / Section: D / Time: 30 sec

Height (mm)	Local Head (mm)	Deg. Sat.	Rel. Perm.	Hydraulic Grad.	krw x ih
356	-133	0.19	0.000	0.03	0.000
340	-124	0.23	0.001	0.04	0.000
320	-115	0.30	0.006	0.04	0.000
300	-119	0.27	0.003	0.06	0.000
280	-96	0.59	0.135	0.07	0.010
260	-88	0.70	0.264	0.10	0.026
240	-77	0.77	0.393	0.13	0.052
220	-64	0.87	0.597	0.13	0.075
200	-53	0.93	0.781	0.18	0.139
180	-39	1.00	1.000	0.19	0.190
160	-24	1.00	1.000	0.22	0.222
140	-10	1.00	1.000	0.29	0.286
120	4	1.00	1.000	0.33	0.328
100	21	1.00	1.000	0.35	0.348
80	34	1.00	1.000	0.40	0.400
60	49	1.00	1.000	0.45	0.455
40	64	1.00	1.000	0.49	0.494
20	79	1.00	1.000	0.51	0.513
0	95	1.00	1.000	0.53	0.533

Width : 312.4 mm
Void Ratio e : 0.547
Eff. Sat. Area : 100.5 mm
Temp T : 16.6 deg C
Sat. Perm. ks : 0.395 cm/sec
Rel. Flow Rate : 76.1 mm
Flow Rate : 93.9 cu cm/sec

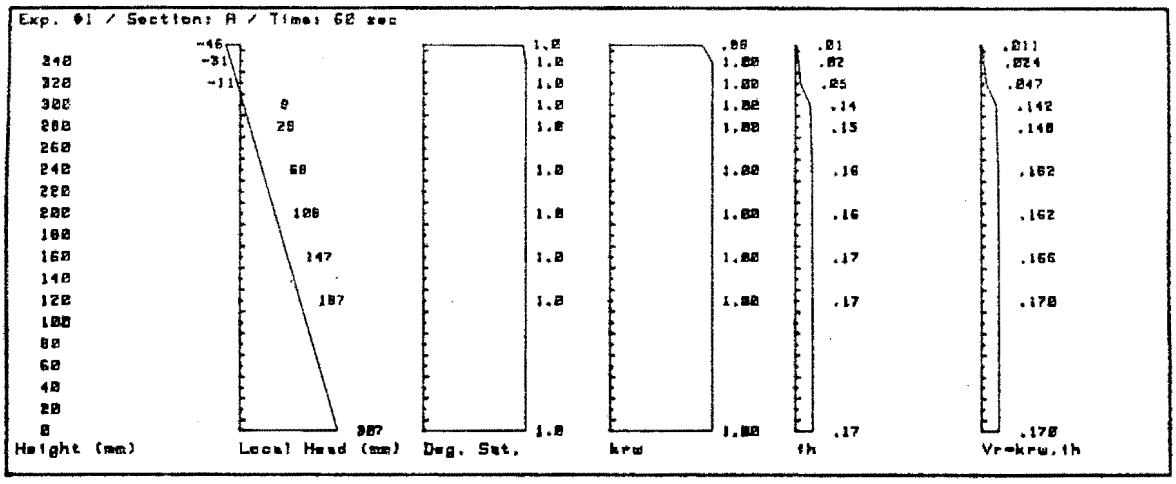
Exp. #1 / Section: A / Time: 60 sec
Height (mm)
Local Head (mm)
Deg. Sat.
krw
th
Vr=krw.th

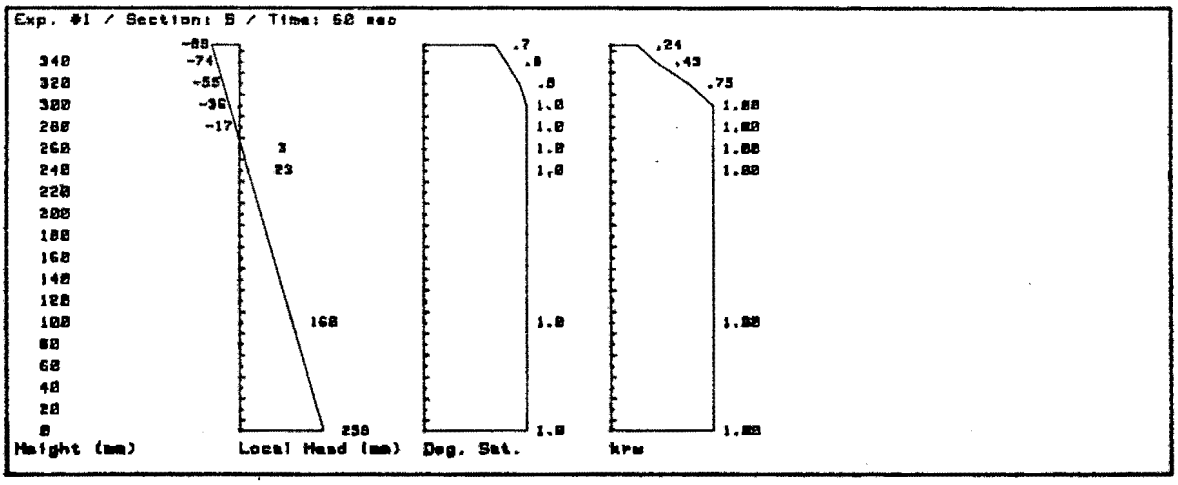
Exp. #1 / Section: B / Time: 60 sec
Height (mm)
Local Head (mm)
Deg. Sat.
krw

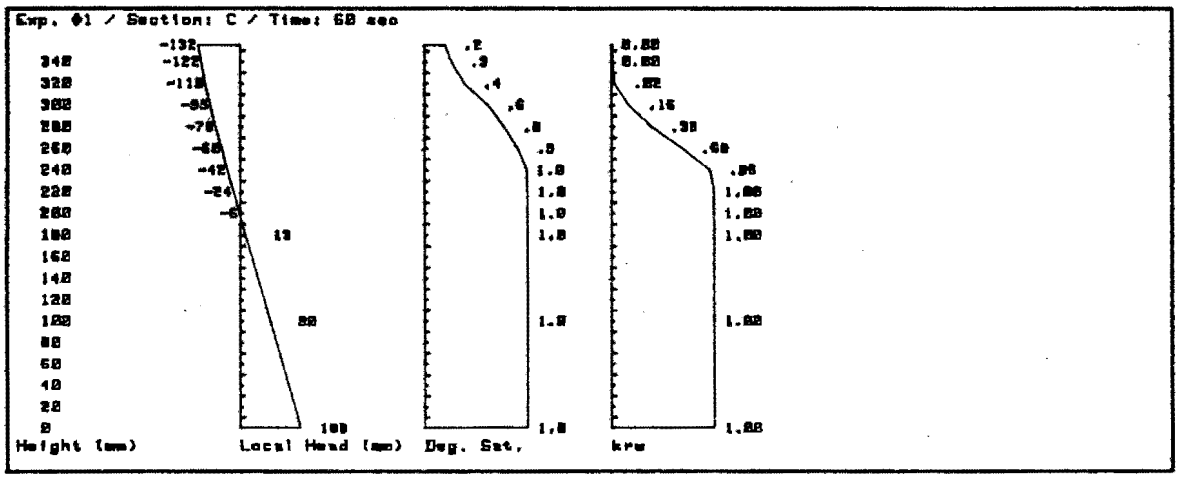
Exp. #1 / Section: C / Time: 60 sec
Height (mm)
Local Head (mm)
Deg. Sat.
krw

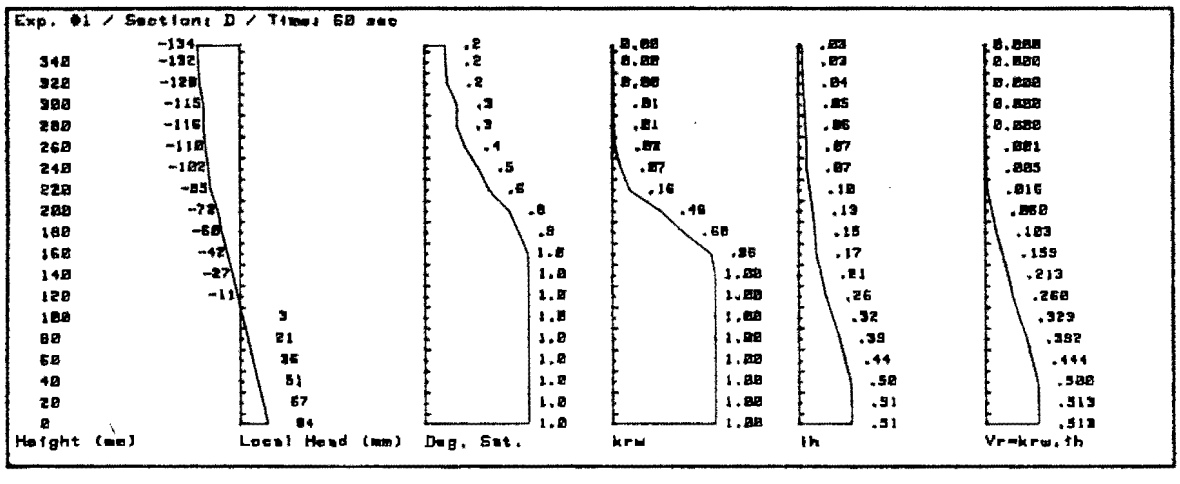
Exp. #1 / Section: D / Time: 60 sec
Height (mm)
Local Head (mm)
Deg. Sat.
krw
th
Vr=krw.th

Exp. #1 / Section: A / Time: 60 sec

Height (mm)	Local Head (mm)	Deg. Sat.	Rel. Perm.	Hydraulic Grad.	krw x ih
356	-46	0.97	0.893	0.01	0.011
340	-31	1.00	1.000	0.02	0.024
320	-11	1.00	1.000	0.05	0.047
300	9	1.00	1.000	0.14	0.142
280	29	1.00	1.000	0.15	0.148
240	68	1.00	1.000	0.16	0.162
200	108	1.00	1.000	0.16	0.162
160	147	1.00	1.000	0.17	0.166
120	187	1.00	1.000	0.17	0.170
0	307	1.00	1.000	0.17	0.170

Width : 312.4 mm
Void Ratio e : 0.547
Eff. Sat. Area : 125.6 mm
Temp T : 16.6 deg C
Sat. Perm. ks : 0.395 cm/sec
Rel. Flow Rate : 52.1 mm
Flow Rate : 64.3 cu cm/sec

Exp. #1 / Section: B / Time: 60 sec

Height (mm)	Local Head (mm)	Deg. Sat.	Rel. Perm.
356	-89	0.68	0.244
340	-74	0.79	0.429
320	-55	0.92	0.751
300	-36	1.00	1.000
280	-17	1.00	1.000
260	3	1.00	1.000
240	23	1.00	1.000
100	160	1.00	1.000
0	259	1.00	1.000

Width : 312.4 mm
Void Ratio e : 0.547
Eff. Sat. Area : 123.0 mm

Exp. #1 / Section: C / Time: 60 sec

Height (mm)	Local Head (mm)	Deg. Sat.	Rel. Perm.
356	-132	0.19	0.000
340	-122	0.25	0.002
320	-110	0.38	0.019
300	-95	0.61	0.158
280	-78	0.77	0.380
260	-60	0.90	0.681
240	-42	0.99	0.956
220	-24	1.00	1.000
200	-6	1.00	1.000
180	13	1.00	1.000
100	90	1.00	1.000
0	188	1.00	1.000

Width : 312.4 mm
Void Ratio e : 0.547
Eff. Sat. Area : 109.2 mm

Exp. #1 / Section: D / Time: 60 sec

Height (mm)	Local Head (mm)	Deg. Sat.	Rel. Perm.	Hydraulic Grad.	krw x ih
356	-134	0.19	0.000	0.03	0.000
340	-132	0.19	0.000	0.03	0.000
320	-128	0.21	0.000	0.04	0.000
300	-115	0.30	0.006	0.05	0.000
280	-116	0.30	0.005	0.06	0.000
260	-110	0.38	0.019	0.07	0.001
240	-102	0.50	0.073	0.07	0.005
220	-95	0.61	0.155	0.10	0.016
200	-72	0.81	0.461	0.13	0.060
180	-60	0.90	0.681	0.15	0.103
160	-42	0.99	0.956	0.17	0.159
140	-27	1.00	1.000	0.21	0.213
120	-11	1.00	1.000	0.26	0.260
100	3	1.00	1.000	0.32	0.323
80	21	1.00	1.000	0.39	0.392
60	36	1.00	1.000	0.44	0.444
40	51	1.00	1.000	0.50	0.500
20	67	1.00	1.000	0.51	0.513
0	84	1.00	1.000	0.51	0.513

Width : 312.4 mm
Void Ratio e : 0.547
Eff. Sat. Area : 90.0 mm
Temp T : 16.6 deg C
Sat. Perm. ks : 0.395 cm/sec
Rel. Flow Rate : 64.9 mm
Flow Rate : 80.1 cu cm/sec

E-8. Measured Outflow from the drainage face. Experiment no. 2.

Listings of the results for the outflow measured from the drainage (Seepage) face for experiment no. 2 is given here. The outflow was measured for four runs of the experiment. The outflow is recorded as the quantity Q_t collected in time t draining from the experiment. Also listed is the reduction of the results showing the mid-interval flow rate calculated as Q_t/t and a plot of the results showing the calculated average mid-interval flow rate versus the mid-interval time from the start of the experiment.

Exp. #2. / Run # 1

Start (sec)	End (sec)	quantity Q (cu cm)	Time t (sec)	Time Step. (sec)	Flow Rate. (cu cm/sec)
15	20	840	5	17.5	168.0
20	25	900	5	22.5	180.0
25	30	860	5	27.5	172.0
30	35	715	5	32.5	143.0
35	40	840	5	37.5	168.0
40	45	690	5	42.5	138.0
45	50	700	5	47.5	140.0
50	55	620	5	52.5	124.0
55	60	620	5	57.5	124.0
60	65	600	5	62.5	120.0
65	70	550	5	67.5	110.0
70	75	580	5	72.5	116.0
75	80	510	5	77.5	102.0
80	85	520	5	82.5	104.0
85	90	460	5	87.5	92.0
90	95	490	5	92.5	98.0
95	100	510	5	97.5	102.0
105	110	370	5	107.5	74.0
110	115	368	5	112.5	73.6

Exp. #2. / Run # 2

Start (sec)	End (sec)	quantity Q (cu cm)	Time t (sec)	Time Step. (sec)	Flow Rate. (cu cm/sec)
15	20	780	5	17.5	156.0
20	25	840	5	22.5	168.0
25	30	740	5	27.5	148.0
30	35	730	5	32.5	146.0
35	40	630	5	37.5	126.0
40	45	685	5	42.5	137.0
45	50	600	5	47.5	120.0
50	55	565	5	52.5	113.0
55	60	550	5	57.5	110.0
60	65	520	5	62.5	104.0
65	70	515	5	67.5	103.0
70	75	520	5	72.5	104.0
75	80	485	5	77.5	97.0
80	85	460	5	82.5	92.0
85	90	435	5	87.5	87.0
90	95	440	5	92.5	88.0
95	100	415	5	97.5	83.0
100	105	420	5	102.5	84.0
105	115	780	10	110.0	78.0
115	125	760	10	120.0	76.0
125	135	750	10	130.0	75.0
135	145	700	10	140.0	70.0
145	155	660	10	150.0	66.0
155	165	660	10	160.0	66.0
165	175	660	10	170.0	66.0
175	185	630	10	180.0	63.0
185	195	620	10	190.0	62.0
195	205	600	10	200.0	60.0
205	215	600	10	210.0	60.0
215	225	575	10	220.0	57.5
225	235	570	10	230.0	57.0
235	245	540	10	240.0	54.0
245	255	540	10	250.0	54.0
255	265	510	10	260.0	51.0
265	275	515	10	270.0	51.5
275	285	505	10	280.0	50.5
285	300	740	15	292.5	49.3
300	315	720	15	307.5	48.0
315	330	700	15	322.5	46.7
330	345	680	15	337.5	45.3
345	360	680	15	352.5	45.3
360	375	650	15	367.5	43.3
375	390	630	15	382.5	42.0
390	405	635	15	397.5	42.3
405	420	600	15	412.5	40.0
420	435	580	15	427.5	38.7
435	450	600	15	442.5	40.0
450	465	570	15	457.5	38.0
465	480	560	15	472.5	37.3
480	495	550	15	487.5	36.7
495	510	550	15	502.5	36.7
510	525	520	15	517.5	34.7
525	540	530	15	532.5	35.3
540	555	500	15	547.5	33.3
555	570	510	15	562.5	34.0
570	585	480	15	577.5	32.0
585	600	480	15	592.5	32.0
600	630	920	30	615.0	30.7
630	660	900	30	645.0	30.0

Exp. #2. / Run # 2

Start (sec)	End (sec)	quantity Q (cu cm)	Time t (sec)	Time Step. (sec)	Flow Rate. (cu cm/sec)
660	690	860	30	675.0	28.7
690	720	840	30	705.0	28.0
720	750	800	30	735.0	26.7
750	780	765	30	765.0	25.5
780	810	750	30	795.0	25.0
810	840	730	30	825.0	24.3
840	870	700	30	855.0	23.3
870	900	685	30	885.0	22.8
900	930	665	30	915.0	22.2
930	960	645	30	945.0	21.5
960	990	620	30	975.0	20.7
990	1020	610	30	1005.0	20.3
1020	1050	580	30	1035.0	19.3
1050	1080	570	30	1065.0	19.0
1080	1110	540	30	1095.0	18.0
1110	1140	550	30	1125.0	18.3
1140	1170	520	30	1155.0	17.3
1170	1200	510	30	1185.0	17.0
1200	1230	490	30	1215.0	16.3
1230	1260	475	30	1245.0	15.8
1260	1320	910	60	1290.0	15.2
1320	1380	870	60	1350.0	14.5
1380	1440	810	60	1410.0	13.5
1440	1500	775	60	1470.0	12.9
1500	1560	750	60	1530.0	12.5
1560	1620	700	60	1590.0	11.7
1620	1680	670	60	1650.0	11.2
1680	1740	645	60	1710.0	10.7
1740	1800	610	60	1770.0	10.2
1800	1860	580	60	1830.0	9.7
1860	1920	555	60	1890.0	9.3
1920	1980	535	60	1950.0	8.9
1980	2040	520	60	2010.0	8.7
2040	2100	480	60	2070.0	8.0
2100	2220	910	120	2160.0	7.6
2220	2340	835	120	2280.0	7.0
2340	2460	770	120	2400.0	6.4
2460	2580	705	120	2520.0	5.9
2580	2700	660	120	2640.0	5.5
2700	2820	605	120	2760.0	5.0
2820	2940	560	120	2880.0	4.7
2940	3060	525	120	3000.0	4.4
3060	3180	490	120	3120.0	4.1
3180	3300	455	120	3240.0	3.8
3300	3540	810	240	3420.0	3.4

Exp. #2. / Run # 3

Start (sec)	End (sec)	quantity Q (cu cm)	Time t (sec)	Time Step. (sec)	Flow Rate. (cu cm/sec)
15	20	810	5	17.5	162.0
20	25	880	5	22.5	176.0
25	30	745	5	27.5	149.0
30	35	740	5	32.5	148.0
35	40	640	5	37.5	128.0
40	45	650	5	42.5	130.0
45	50	590	5	47.5	118.0
50	55	550	5	52.5	110.0
55	60	540	5	57.5	108.0
60	65	515	5	62.5	103.0
65	70	495	5	67.5	99.0
70	75	495	5	72.5	99.0
75	80	470	5	77.5	94.0
80	85	445	5	82.5	89.0
85	90	420	5	87.5	84.0
90	95	440	5	92.5	88.0
95	100	435	5	97.5	87.0
100	110	805	10	105.0	80.5
110	120	775	10	115.0	77.5
120	130	730	10	125.0	73.0
130	140	720	10	135.0	72.0
140	150	705	10	145.0	70.5
150	160	650	10	155.0	65.0
160	170	640	10	165.0	64.0
170	180	620	10	175.0	62.0
180	190	620	10	185.0	62.0
190	200	590	10	195.0	59.0
200	210	560	10	205.0	56.0
210	220	570	10	215.0	57.0
220	230	560	10	225.0	56.0
230	240	540	10	235.0	54.0
240	250	540	10	245.0	54.0
250	260	490	10	255.0	49.0
260	270	530	10	265.0	53.0
270	280	510	10	275.0	51.0
280	290	470	10	285.0	47.0
290	300	500	10	295.0	50.0
300	315	700	15	307.5	46.7
315	330	660	15	322.5	44.0
330	345	685	15	337.5	45.7
345	360	640	15	352.5	42.7
360	380	830	20	370.0	41.5
380	400	840	20	390.0	42.0
400	420	780	20	410.0	39.0
420	440	775	20	430.0	38.8
440	460	760	20	450.0	38.0
460	480	720	20	470.0	36.0
480	500	700	20	490.0	35.0
500	520	695	20	510.0	34.8
520	540	685	20	530.0	34.3
540	560	645	20	550.0	32.3
560	580	635	20	570.0	31.8
580	600	615	20	590.0	30.7
600	630	910	30	615.0	30.3
630	660	860	30	645.0	28.7
660	690	825	30	675.0	27.5
690	720	810	30	705.0	27.0
720	750	800	30	735.0	26.7
750	780	750	30	765.0	25.0

Start (sec)	End (sec)	quantity Q (cu cm)	Time t (sec)	Time Step. (sec)	Flow Rate. (cu cm/sec)
780	810	730	30	795.0	24.3
810	840	715	30	825.0	23.8
840	870	680	30	855.0	22.7
870	900	665	30	885.0	22.2
900	930	630	30	915.0	21.0
930	960	625	30	945.0	20.8
960	990	595	30	975.0	19.8
990	1020	595	30	1005.0	19.8
1020	1050	565	30	1035.0	18.8
1050	1080	555	30	1065.0	18.5
1080	1110	540	30	1095.0	18.0
1110	1140	520	30	1125.0	17.3
1140	1170	510	30	1155.0	17.0
1170	1200	500	30	1185.0	16.7
1200	1260	945	60	1230.0	15.8
1260	1320	900	60	1290.0	15.0
1320	1380	845	60	1350.0	14.1
1380	1440	815	60	1410.0	13.6
1440	1500	780	60	1470.0	13.0
1500	1560	715	60	1530.0	11.9
1560	1620	700	60	1590.0	11.7
1620	1680	650	60	1650.0	10.8
1680	1740	640	60	1710.0	10.7
1740	1800	600	60	1770.0	10.0
1800	1860	570	60	1830.0	9.5
1860	1920	550	60	1890.0	9.2
1920	1980	520	60	1950.0	8.7
1980	2040	500	60	2010.0	8.3
2040	2100	480	60	2070.0	8.0
2100	2220	895	120	2160.0	7.5
2220	2340	820	120	2280.0	6.8
2340	2460	760	120	2400.0	6.3
2460	2580	690	120	2520.0	5.8
2580	2700	635	120	2640.0	5.3
2700	2820	590	120	2760.0	4.9
2820	2940	540	120	2880.0	4.5
2940	3060	500	120	3000.0	4.2
3060	3180	460	120	3120.0	3.8
3180	3300	430	120	3240.0	3.6
3300	3420	385	120	3360.0	3.2
3420	3540	370	120	3480.0	3.1
3540	3660	330	120	3600.0	2.8

Exp. #2. / Run # 4

Start (sec)	End (sec)	quantity Q (cu cm)	Time t (sec)	Time Step. (sec)	Flow Rate. (cu cm/sec)
15	20	850	5	17.5	170.0
20	25	780	5	22.5	156.0
25	30	780	5	27.5	156.0
30	35	690	5	32.5	138.0
35	40	650	5	37.5	130.0
40	45	650	5	42.5	130.0
45	50	560	5	47.5	112.0
50	55	570	5	52.5	114.0
55	60	540	5	57.5	108.0
60	65	510	5	62.5	102.0
65	70	530	5	67.5	106.0
70	75	460	5	72.5	92.0
75	80	460	5	77.5	92.0
80	85	480	5	82.5	96.0
85	90	445	5	87.5	89.0
90	95	440	5	92.5	88.0
95	100	420	5	97.5	84.0
100	110	830	10	105.0	83.0
110	120	760	10	115.0	76.0
120	130	800	10	125.0	80.0
130	140	700	10	135.0	70.0
140	150	670	10	145.0	67.0
150	160	670	10	155.0	67.0
160	170	640	10	165.0	64.0
170	180	640	10	175.0	64.0
180	195	880	15	187.5	58.7
195	210	880	15	202.5	58.7
210	225	845	15	217.5	56.3
225	240	830	15	232.5	55.3
240	255	790	15	247.5	52.7
255	270	750	15	262.5	50.0
270	285	740	15	277.5	49.3
285	300	750	15	292.5	50.0
300	320	935	20	310.0	46.8
320	340	890	20	330.0	44.5
340	360	885	20	350.0	44.3
360	380	840	20	370.0	42.0
380	400	835	20	390.0	41.7
400	420	800	20	410.0	40.0
420	440	785	20	430.0	39.3
440	460	760	20	450.0	38.0
460	480	770	20	470.0	38.5
480	500	700	20	490.0	35.0
500	518	590	18	509.0	32.8
518	540	770	22	529.0	35.0
540	560	650	20	550.0	32.5
560	580	650	20	570.0	32.5
580	600	620	20	590.0	31.0
600	630	920	30	615.0	30.7
840	870	720	30	855.0	24.0
870	900	695	30	885.0	23.2
900	930	675	30	915.0	22.5
1455	1500	605	45	1477.5	13.4
1500	1545	575	45	1522.5	12.8
1830	1860	300	30	1845.0	10.0
2280	2340	432	60	2310.0	7.2
2400	2460	420	60	2430.0	7.0

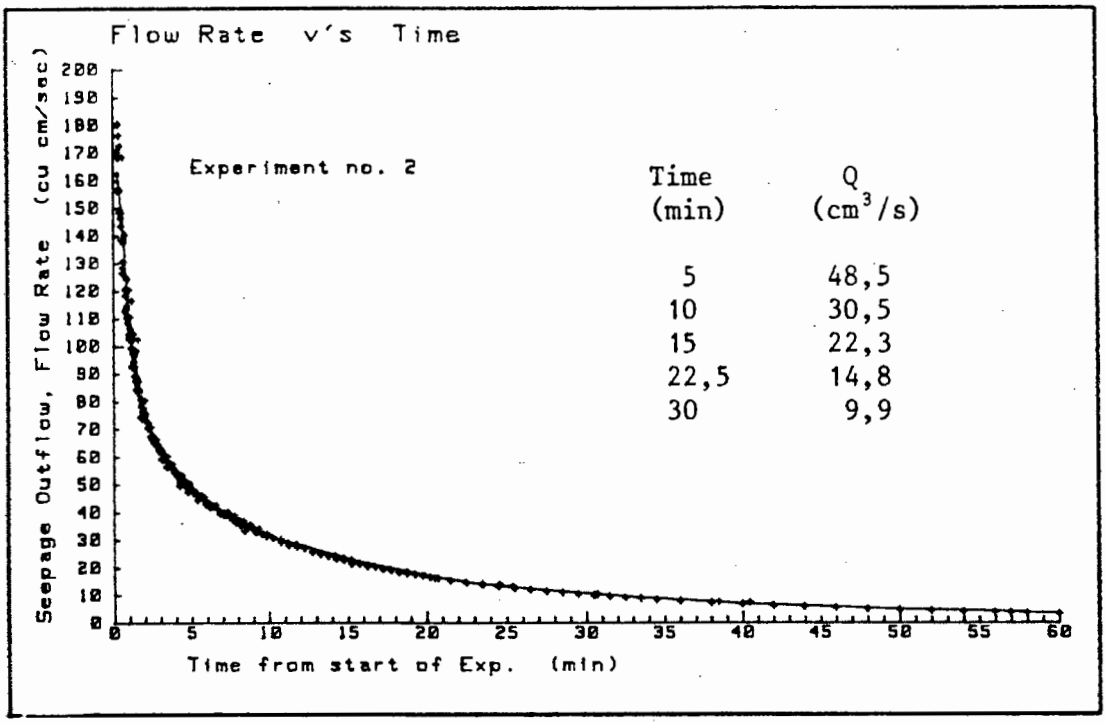

Time (min)	Q (cm^3/s)
5	48,5
10	30,5
15	22,3
22,5	14,8
30	9,9

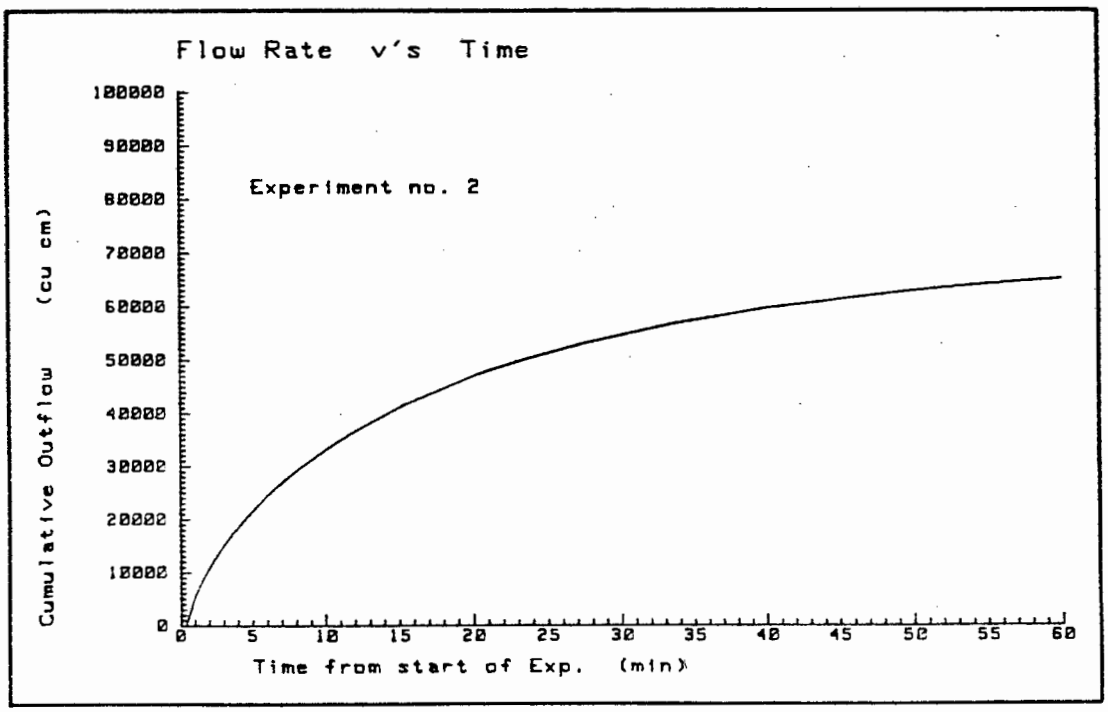

E-9. Sidewall piezometer levels recorded. Experiment no. 2.

Listings of the results for the sidewall piezometer levels recorded for experiment no. 2, are given here. The readings are recorded with respect to time and the result given as the elevation (mm) above the base of the flume. A single value for each vertical set of piezometers recorded, is given. The readings are referenced by a reference number as shown in figure (5.19)

Experiment no. 2 / Piezometer results. / Time (min) v's Total head (mm)

Piezometer Ref. no.	Time from start of experiment (min) 2	5	10	15	20	25	30
PA		80					
PB	140	105	82	69	60	55	51
PC	147	124	94	79	73	66	59
PD	173	138	110	85	78	71	65
PE	187	151	123	96	85	75	68
PF	206	168	134	108	93	81	72
PG	223	180	140	115	94	83	74
PH	234	187	147	120	97	84	76
PI	247	204	156	128	101	91	83
PJ	262	214	165	134	113	98	83
PK	270	222	171	139	118	100	84
PL	277	228	180	144	121	103	90
PM	284	235	184	149	124	107	95
PN	285	245	188	152	128	108	97
PO	292	250	194	156	130	112	100
PP	295	253	199	159	135	115	102
PQ	298	257	201	164	137	112	103
PR	302	264	209	168	140	118	103
PS	308	270	210	169	141	121	104
PT	308	275	212	171	143	123	109
PU	309	278	218	175	147	126	110
PV	309	280	218	177	149	126	111
PW	310	281	220	180	150	127	113
PX	310	284	223	182	152	129	113
PY	311	287	226	182	152	129	113
PZ	312	288	230	182	153	130	114

E-10. Transducer monitored tensiometers. Experiment no. 2.

Listings of the results for the tensiometers, recorded for experiment no. 2, are given here. The recordings were made by the computer controlled data-acquisition unit. (See chapter 3) Four sets of readings are given for the four repeated experiment runs made. The readings are recorded with respect to time and the result given as the elevation (mm) above the base of the flume. For each run a new set of tensiometers were monitored. The actual tensiometer monitored is referenced by a reference number whose position is shown in figure (5.8)

Also given are the plots, for each tensiometer recorded, showing the total head versus time.

EXPERIMENT NO. 2 / RUN NO. 1

TIME	TA0	TA4	TA8	TA12	TE0	TE4	TE8	TE12	TK0	TK4	TK8	TK12	TM4	TM12	T00	T08
-60	381	381	381	381	381	381	381	381	381	381	381	381	381	381	381	381
-55	380	381	380	384	380	381	381	381	380	381	380	381	381	381	380	381
-48	380	381	424	377	379	381	381	381	380	381	380	381	381	381	380	381
-43	380	380	380	379	380	381	381	380	379	380	380	381	380	381	380	381
-36	381	381	380	381	379	381	380	381	380	380	379	381	380	380	379	380
-31	380	380	424	381	379	381	380	380	380	380	380	381	380	380	380	380
-25	380	380	379	378	378	381	380	380	379	380	380	381	380	380	380	380
-20	380	379	379	377	379	380	380	381	379	380	379	380	380	380	379	380
-13	380	380	381	377	380	380	380	380	379	380	379	381	380	380	379	380
-8	380	380	424	382	381	380	380	381	380	380	379	381	380	380	379	380
-1	380	380	424	376	380	381	380	380	380	380	380	381	380	380	380	381
4	299	282	282	300	334	332	335	342	370	371	369	371	376	377	378	378
9	119	143	249	256	262	268	280	294	389	339	337	338	352	354	358	359
16	98	135	190	224	250	253	265	278	318	402	317	316	330	331	334	335
22	95	131	180	202	241	244	256	266	314	314	312	313	380	323	323	326
28	93	126	169	200	233	235	246	325	311	312	311	311	317	321	321	322
34	91	123	160	198	227	229	240	252	309	309	309	308	316	320	320	321
40	88	119	151	191	220	223	232	244	305	308	305	306	316	319	319	320
45	86	116	146	204	216	218	227	239	304	308	303	303	314	318	318	319
52	83	112	138	193	209	211	221	231	300	304	300	300	313	315	318	318
58	83	110	135	198	206	208	217	228	298	302	297	298	312	315	318	318
64	81	107	130	195	201	203	212	222	295	298	294	294	372	313	316	317
70	80	104	127	195	198	200	208	218	293	296	292	292	310	312	317	316
76	79	102	125	193	194	195	204	215	290	293	289	290	308	310	315	315
82	78	101	165	186	191	193	200	212	287	292	287	288	308	309	314	315
89	77	99	119	193	188	187	197	211	285	290	285	285	306	307	313	313
94	76	139	119	188	186	184	195	209	283	288	282	284	304	305	311	309
99	75	155	118	181	183	181	191	208	281	285	281	281	302	303	309	306
106	74	89	117	188	180	180	190	207	278	283	278	279	300	301	308	351
111	74	88	116	186	179	177	187	205	277	281	276	276	299	300	306	304
117	73	87	115	190	176	175	185	205	275	280	274	275	297	298	305	348
122	73	85	116	185	176	175	182	204	273	278	273	273	296	297	303	347
128	72	188	114	183	173	173	180	203	270	275	270	270	293	294	301	299
134	71	188	114	182	171	172	174	202	269	273	268	268	292	294	300	299
140	71	188	114	177	169	170	172	202	266	271	266	266	290	292	298	298
146	70	187	113	180	168	170	170	202	264	269	264	264	288	290	296	296
152	70	83	112	181	166	170	169	201	263	267	262	263	287	290	294	295
157	69	185	113	177	165	167	167	200	261	264	260	260	285	287	293	293
163	69	80	113	179	163	166	167	200	259	264	258	258	284	286	292	292
169	68	81	112	181	161	164	165	199	257	262	256	257	282	284	290	289
175	68	183	112	181	160	163	164	199	255	260	255	255	281	283	289	289
180	67	183	112	174	158	161	162	198	253	258	253	253	279	282	287	287
187	67	183	111	177	158	160	163	198	252	257	251	252	277	280	285	286
193	67	182	111	179	156	158	161	197	250	255	249	249	276	279	284	284
198	66	78	111	177	154	157	159	197	248	253	248	248	275	277	283	283
205	65	77	110	175	152	155	158	196	247	252	245	246	272	275	281	281
210	65	77	110	177	151	154	157	196	245	251	244	245	272	274	280	281
217	65	77	110	174	150	152	155	196	244	248	243	243	270	273	278	279
222	65	77	110	173	149	151	154	195	242	247	241	241	268	271	277	277
229	64	75	109	173	148	150	153	194	240	245	239	239	267	269	276	276
234	64	74	109	175	147	150	152	194	239	244	238	239	266	268	275	275
241	63	179	109	172	146	148	151	193	237	242	237	236	264	266	274	274
247	63	73	109	173	145	147	150	193	236	241	235	235	262	265	272	272
254	62	74	107	174	143	146	148	192	234	239	232	233	260	263	270	270
259	62	72	107	172	143	145	147	192	232	238	232	232	260	263	270	270
266	62	72	108	172	141	144	146	192	231	237	231	231	259	261	269	269
271	62	72	107	165	140	142	145	191	229	234	228	229	257	259	267	267
278	61	73	107	169	139	142	144	192	228	234	228	228	256	258	266	266
283	61	72	107	171	138	141	143	190	226	232	226	226	255	257	264	265

288	61	175	107	173	137	140	143	191	226	232	226	226	254	256	264	264
294	61	71	107	169	137	139	142	191	225	230	225	225	252	254	262	262
299	60	72	106	173	136	139	141	190	223	228	223	223	251	253	261	262
305	60	175	106	173	136	137	140	190	222	227	222	222	249	252	259	260
310	60	70	106	173	135	137	140	190	221	226	221	221	249	251	258	259
316	59	70	105	173	133	136	138	189	220	224	220	220	247	249	257	257
321	60	72	105	169	132	135	138	189	218	224	259	218	246	248	256	256
328	59	72	105	170	131	135	137	189	217	223	213	218	245	247	255	255
342	59	68	104	171	129	132	135	188	214	219	211	225	241	243	251	251
357	58	69	104	172	128	130	132	187	211	216	262	208	238	258	247	248
372	57	69	103	171	126	129	131	188	208	213	206	206	235	321	244	245
387	56	68	102	172	124	127	128	186	206	211	204	257	232	230	241	241
401	56	67	102	169	123	126	127	186	204	209	203	202	230	228	238	239
416	55	66	101	177	120	124	125	185	228	206	200	200	226	226	233	235
431	55	66	101	177	118	122	124	185	264	204	198	198	224	224	277	233
446	55	64	100	187	118	120	122	184	193	202	196	196	222	223	229	231
461	54	63	99	188	115	120	120	184	259	200	193	193	219	221	228	228
475	53	62	99	185	113	117	118	182	258	197	190	190	216	219	225	225
491	54	62	99	185	113	116	117	183	188	196	189	188	214	218	224	223
505	52	61	98	177	111	114	116	182	186	195	186	186	211	215	221	219
521	52	60	98	183	110	113	114	182	184	193	184	183	209	214	218	216
535	52	61	98	180	110	112	113	182	184	192	181	182	207	212	216	214
551	51	60	97	184	108	110	112	181	180	191	179	180	228	210	214	213
565	50	59	96	176	107	109	111	181	179	190	177	177	260	208	212	256
596	50	59	96	180	104	107	108	180	175	187	173	173	194	205	206	207
624	49	57	95	171	101	105	107	179	171	186	169	169	191	202	202	202
655	48	56	94	175	99	102	104	179	166	183	165	165	188	199	200	198
684	49	55	94	176	97	100	103	179	163	183	161	162	185	197	195	194
713	47	53	93	176	94	97	99	177	158	179	156	157	179	193	189	187
742	46	52	92	173	92	95	98	177	155	179	152	153	175	191	183	183
772	46	52	91	175	91	93	97	176	151	176	149	150	171	190	179	178
801	46	51	91	174	90	92	96	176	148	176	147	147	167	188	176	175
830	45	50	90	176	88	90	94	175	145	174	144	143	164	186	173	171
860	44	48	89	174	85	87	91	174	142	173	140	141	160	184	169	167
889	44	47	89	182	83	86	90	174	139	172	138	138	158	182	167	164
918	42	45	88	176	81	83	89	173	136	171	135	135	154	180	163	161
947	43	45	89	180	80	82	88	174	134	171	132	133	152	180	161	159
977	41	43	88	179	78	79	86	173	131	170	130	130	149	179	158	156
1005	41	44	88	181	78	79	85	173	129	170	127	128	146	177	154	153
1035	40	43	87	166	76	77	84	174	125	169	124	125	142	178	152	149
1064	40	43	87	162	74	76	83	172	124	169	123	123	140	178	148	147
1093	40	42	86	161	113	75	81	172	122	168	120	120	138	177	146	144
1122	39	41	86	162	152	74	81	172	118	168	117	117	135	175	141	141
1152	39	40	85	160	170	72	79	172	117	168	115	116	132	176	138	139
1181	38	39	85	174	168	72	78	172	114	167	113	113	130	175	136	136
1211	38	39	85	172	62	70	78	171	112	167	108	111	127	174	135	134
1240	37	38	84	171	62	68	77	171	110	167	105	109	125	174	134	173
1270	36	37	84	170	166	67	76	171	108	166	103	118	123	173	131	126
1298	37	37	84	164	164	66	75	171	107	166	156	146	120	172	129	124
1327	36	37	84	157	60	66	74	171	105	166	101	100	118	173	128	168
1357	35	35	83	153	162	64	73	171	104	166	100	152	116	172	123	120
1386	35	36	83	160	58	63	73	171	101	167	151	97	114	173	122	119
1416	47	34	82	162	56	61	71	170	100	165	96	97	111	172	122	116
1445	58	34	82	160	57	61	70	170	98	165	95	95	110	172	119	115
1475	69	33	82	149	57	59	71	170	98	165	95	93	108	171	117	113
1504	81	33	82	156	56	59	70	170	95	165	93	93	106	171	115	111
1564	29	32	82	153	54	58	68	170	93	165	90	90	103	171	111	107
1623	29	30	81	156	52	54	69	169	90	164	86	87	99	170	107	104
1683	28	29	81	177	52	53	67	169	88	163	84	85	96	169	105	100
1741	28	29	81	169	156	52	67	169	86	164	82	83	94	169	103	97
1802	27	27	80	182	50	50	67	168	83	163	79	80	91	169	100	94

1860	27	27	79	156	50	49	66	168	82	163	77	78	88	169	97	92
1920	53	51	105	195	74	73	89	194	105	188	101	102	111	194	122	115
1979	78	14	67	151	36	35	97	156	65	152	62	62	117	157	84	76
2038	27	24	79	157	46	45	108	168	76	162	71	72	139	167	95	86
2097	78	13	66	157	34	32	97	156	63	151	58	59	127	156	82	72
2155	27	25	78	166	45	43	62	168	74	163	68	69	74	168	92	81
2274	25	23	76	166	42	41	118	167	71	162	64	66	72	167	92	78
2391	24	22	76	165	40	40	59	167	69	162	61	63	69	167	91	74
2509	23	23	75	173	39	38	116	166	67	162	58	60	67	167	89	70
2626	23	20	75	168	38	36	59	166	65	162	56	57	64	166	89	67
2745	86	21	74	177	36	35	116	167	90	161	52	55	62	166	89	63
2862	23	19	75	176	34	32	58	167	127	160	50	53	58	163	89	61
2980	22	19	73	179	34	32	58	167	127	160	49	51	56	164	88	59
3098	11	8	62	167	21	20	45	155	116	148	35	37	42	152	78	45
3216	22	21	73	170	34	32	57	168	115	161	45	48	52	164	89	55
3333	11	8	62	162	21	20	44	156	47	149	33	35	39	153	77	41
3451	22	20	73	170	33	31	55	167	115	162	42	45	49	166	89	51
3568	20	22	71	171	32	31	54	166	63	162	39	42	46	166	86	47

EXPERIMENT NO. 2 / RUN NO. 2

TIME	TB0	TB4	TB8	TB12	TF0	TF4	TF8	TF12	TJ0	TJ4	TJ8	TJ12	TM0	TM8	TD0	TD8
-60	381	381	381	381	381	381	381	381	381	381	381	381	381	381	381	381
-53	380	381	380	379	381	380	381	381	381	380	381	380	380	380	380	380
-48	330	330	331	330	331	330	330	331	330	329	331	330	330	329	283	330
-42	319	318	320	324	320	319	319	319	319	319	320	320	319	406	273	319
-36	380	379	381	378	381	380	380	380	380	378	381	380	380	380	333	380
-30	381	380	381	381	382	380	381	381	381	379	381	381	380	380	379	380
-25	319	318	319	323	321	318	319	319	319	318	320	320	319	319	272	320
-19	380	379	380	376	381	379	381	381	380	379	381	380	380	466	333	381
-13	380	378	380	378	381	379	380	381	379	378	381	380	380	465	379	380
-6	319	317	320	323	319	318	319	319	319	317	319	319	319	406	273	319
-1	380	378	381	380	382	378	380	380	380	378	380	380	380	379	380	380
4	327	319	320	338	358	354	358	361	373	371	373	372	378	378	380	380
11	172	178	209	259	276	282	291	302	330	331	330	330	354	358	316	360
16	139	109	138	181	204	209	222	231	256	256	255	255	276	280	239	282
23	93	100	124	166	197	198	211	220	250	334	249	245	321	267	225	268
28	88	93	116	160	193	192	204	212	249	332	248	243	259	265	221	265
35	144	146	166	210	245	244	256	262	304	301	303	354	318	325	279	324
40	82	82	101	148	181	179	191	198	242	328	241	238	319	264	220	264
46	138	137	155	205	236	234	245	255	298	298	297	297	317	323	279	323
52	74	73	89	145	170	169	180	190	235	322	234	233	256	262	218	263
58	130	129	144	209	226	225	235	244	292	294	291	290	315	320	278	322
63	68	66	80	149	162	160	171	180	228	231	228	227	255	259	217	262
70	124	122	135	200	217	216	226	235	284	286	284	283	312	316	276	321
75	123	122	134	206	216	214	224	233	283	286	283	282	314	317	278	322
82	60	57	70	142	151	149	159	168	220	222	219	218	251	254	216	260
87	119	117	126	202	208	207	217	226	278	281	277	276	311	314	275	319
93	68	65	75	144	156	154	165	173	226	229	226	225	260	263	225	269
99	115	111	121	191	202	200	210	220	273	274	271	270	307	310	271	333
104	114	110	120	192	200	198	208	217	270	273	270	268	306	308	270	357
111	113	110	120	192	200	196	206	215	269	272	268	267	305	308	270	312
116	110	107	117	195	196	192	202	213	266	268	265	263	302	305	267	354
123	61	58	68	145	146	143	151	163	216	218	214	213	252	255	218	305
128	48	44	55	141	131	128	138	150	202	203	201	199	238	241	204	248
135	46	42	53	130	129	125	135	148	199	201	198	196	236	239	203	246
140	56	51	63	140	137	134	144	157	208	210	206	205	246	248	212	256
147	44	41	51	130	125	121	131	146	194	197	194	192	233	236	199	244
153	43	40	50	135	124	120	130	145	193	195	191	190	231	235	198	242
159	54	49	60	147	133	129	138	156	201	204	201	199	241	244	207	252
165	101	96	108	189	180	176	185	203	249	250	247	246	287	290	254	298
171	51	47	58	140	129	125	177	154	197	199	196	194	236	239	204	248
177	99	95	106	196	177	173	178	202	244	247	244	242	284	287	251	295
184	97	93	104	186	173	170	176	200	242	244	240	239	281	284	248	292
190	38	34	44	129	113	109	173	140	181	183	180	178	220	223	187	231
195	96	93	103	193	172	168	174	200	240	242	239	236	279	282	280	290
202	58	54	64	155	132	128	135	161	199	202	198	196	239	242	202	249
207	94	90	101	194	169	165	171	198	235	238	234	232	275	278	285	285
214	45	42	51	139	119	114	121	149	185	188	183	182	224	228	189	235
220	33	30	40	125	107	103	109	137	172	176	171	169	212	216	177	223
227	44	41	51	145	117	108	119	148	182	185	181	179	222	225	187	232
232	43	40	50	149	115	190	119	147	180	183	179	177	221	224	186	231
240	64	61	71	169	136	196	139	169	200	203	199	197	241	245	208	251
245	102	98	109	201	173	249	177	207	238	240	236	234	278	281	244	288
252	74	72	82	182	145	137	148	179	209	212	207	205	249	252	216	259
257	75	72	82	181	146	222	148	180	209	212	207	205	249	252	216	259
263	74	71	81	182	144	220	147	179	206	209	205	203	246	251	214	257
268	111	108	118	216	180	172	183	216	243	245	241	239	283	286	250	293
275	60	58	68	173	130	206	132	165	192	195	190	188	232	236	199	243
280	38	35	45	149	107	100	109	143	168	171	207	164	208	213	175	219
285	87	84	94	198	155	232	157	192	216	220	211	212	257	260	223	267

291	37	34	45	143	105	98	107	142	166	169	215	162	206	210	173	217
296	38	34	45	145	105	98	106	143	165	168	160	161	206	209	172	216
302	85	82	93	190	152	147	153	190	211	215	261	208	252	255	219	263
308	35	32	43	140	102	95	103	141	162	165	158	157	202	206	169	213
314	45	43	54	159	113	107	113	152	172	176	168	167	212	215	179	222
319	34	32	43	152	101	96	102	140	160	164	157	156	200	204	166	210
325	23	22	32	132	89	85	90	130	148	153	146	144	188	192	154	199
330	33	30	42	146	99	94	100	139	157	162	155	153	197	201	163	208
337	33	30	42	146	98	92	99	139	156	161	153	162	196	200	162	206
342	32	29	42	147	97	94	98	139	155	161	152	148	196	199	160	206
348	43	41	53	158	109	103	109	150	166	171	163	157	206	209	170	215
354	80	78	89	192	145	141	145	187	228	207	200	247	241	245	206	251
360	31	29	40	153	95	91	95	138	204	158	150	143	191	195	156	201
365	80	77	89	195	144	140	144	187	253	206	198	246	239	242	205	249
372	80	76	89	192	143	139	143	186	266	205	197	246	238	242	203	248
377	30	27	39	146	93	89	93	137	147	155	147	141	187	191	153	197
382	78	75	88	193	141	137	141	185	194	203	195	189	235	239	200	245
388	30	26	40	147	91	88	92	137	145	155	145	141	186	190	150	195
394	79	76	89	198	142	137	141	187	263	203	194	190	235	238	198	244
400	28	25	39	143	89	85	90	136	144	152	143	139	184	186	147	192
406	77	73	88	193	139	134	138	185	191	201	191	187	231	234	195	240
412	77	72	88	193	138	133	138	185	190	201	191	187	230	233	194	239
431	16	12	27	131	75	71	76	125	129	138	128	124	166	170	131	176
451	76	92	87	185	135	129	134	185	187	197	185	182	224	227	188	234
470	25	60	37	135	83	77	82	135	136	145	132	129	171	174	135	181
491	73	61	85	189	130	124	130	183	182	192	179	175	217	220	182	262
510	11	-2	24	120	67	61	66	121	119	129	115	111	154	151	117	206
530	70	162	84	178	125	119	126	182	176	188	173	169	211	208	175	220
549	9	-5	23	122	62	56	63	121	113	126	109	106	148	145	111	158
569	7	-6	22	128	60	54	61	120	110	125	107	102	202	142	108	155
588	68	159	82	185	118	113	120	181	169	184	165	161	200	203	167	213
607	66	55	82	180	117	110	118	180	166	183	163	158	198	199	164	210
627	66	157	81	181	115	109	117	180	163	182	160	156	196	197	161	207
646	5	-9	20	114	53	46	54	119	100	120	97	93	133	134	97	144
666	3	-10	19	120	50	44	52	118	97	119	94	90	132	130	93	140
685	64	51	80	178	110	103	112	179	156	179	153	149	189	188	197	199
706	2	-12	18	118	47	39	49	117	92	116	89	84	125	122	87	134
725	62	50	79	181	107	99	109	178	151	177	148	144	184	182	146	193
746	61	48	79	178	105	97	108	178	149	176	146	142	181	178	144	190
765	60	47	78	185	103	96	107	177	147	175	145	139	178	175	141	187
785	-1	-14	17	122	41	34	45	116	84	114	82	76	114	112	78	123
804	59	149	77	176	101	92	104	177	143	174	139	135	173	169	136	181
825	59	45	77	176	100	93	104	177	141	174	138	133	171	168	132	179
844	-4	-15	15	120	36	28	41	115	77	113	75	69	106	103	69	114
865	-4	-16	15	117	35	28	40	115	76	113	73	68	104	101	67	112
884	-4	-17	15	121	34	26	39	114	75	112	71	66	102	99	64	110
905	56	42	75	171	94	85	99	175	133	172	130	125	161	156	123	169
924	55	43	75	171	93	85	98	176	132	173	129	124	159	156	121	167
943	55	42	74	174	93	84	97	175	130	173	127	122	157	154	119	165
964	55	42	75	176	92	83	96	175	129	173	126	121	156	152	117	164
983	-8	-19	14	118	30	21	34	114	66	111	63	58	93	89	53	101
1004	-8	-21	13	125	29	19	34	113	65	111	61	56	91	86	52	98
1023	-7	-22	13	122	28	18	33	113	64	111	60	55	89	85	49	97
1044	52	38	72	181	87	77	92	174	123	171	119	113	148	143	108	155
1063	51	37	72	187	86	77	91	174	121	172	118	112	146	141	106	154
1084	-11	-24	11	112	24	14	30	112	58	110	55	49	84	78	43	90
1103	50	36	72	164	84	75	91	174	119	172	115	109	143	138	103	150
1124	-11	-26	10	110	21	11	28	112	55	110	92	46	80	74	39	87
1143	50	34	71	168	82	72	88	174	115	171	162	106	139	133	98	147
1163	49	34	70	127	121	71	88	173	113	170	107	104	137	131	96	145
1182	48	34	70	167	81	70	87	173	113	171	106	103	136	130	95	143

1202	-13	-28	9	106	97	8	25	112	51	110	98	41	74	67	34	89
1221	47	32	69	174	157	67	85	172	110	170	103	100	132	126	91	181
1240	47	32	70	178	72	67	86	172	109	170	104	109	131	124	92	180
1260	-14	-29	8	115	11	5	24	111	46	109	42	33	69	62	29	74
1279	46	30	69	173	175	65	84	172	106	169	101	137	127	121	87	132
1299	45	28	68	175	174	63	83	172	105	168	101	91	126	118	86	131
1317	44	28	67	172	172	61	82	171	103	168	99	144	124	117	84	130
1337	44	27	67	171	68	60	82	172	103	168	98	90	123	115	83	130
1356	56	27	67	175	170	60	81	172	102	168	97	143	121	114	81	128
1386	78	26	66	171	66	59	79	171	99	168	95	87	118	111	78	125
1415	40	26	67	165	171	58	80	172	99	168	94	86	117	110	78	124
1444	40	27	68	177	65	58	80	173	99	169	93	86	116	108	77	123
1473	38	25	67	172	65	56	79	172	97	168	92	85	114	106	73	121
1503	37	24	66	169	64	54	78	172	95	167	90	83	112	103	71	118
1531	38	-38	4	115	2	-8	16	110	33	106	27	20	49	40	8	55
1561	36	23	65	177	63	53	76	171	92	167	86	79	107	99	76	113
1590	36	21	65	175	63	51	76	171	91	167	84	78	106	98	109	112
1620	35	21	65	174	165	51	76	171	91	167	84	77	104	96	108	111
1649	35	21	64	173	62	49	87	171	89	167	82	75	103	94	58	109
1678	35	21	64	176	59	49	109	172	88	168	81	74	102	93	58	108
1708	35	-41	3	112	-1	-13	57	110	26	106	18	12	38	30	-4	44
1736	35	21	65	177	60	48	118	171	87	168	79	72	100	90	104	105
1766	33	19	64	180	58	46	71	170	86	167	77	70	97	88	55	102
1795	34	18	64	178	58	45	70	171	85	166	77	70	96	87	56	101
1825	33	17	62	173	56	43	69	169	82	165	74	67	93	84	56	98
1854	35	-43	2	113	-5	-17	9	109	22	105	13	6	31	23	-6	37
1884	96	17	62	225	55	42	127	170	81	167	73	65	91	83	52	96
1913	32	16	63	148	54	43	70	170	81	166	72	64	90	82	51	95
1943	31	15	62	165	56	40	69	169	79	165	70	62	122	79	49	93
1972	31	14	61	151	54	39	68	168	78	164	69	61	82	77	48	91
2002	32	13	62	166	53	38	68	168	77	165	68	60	80	76	47	90
2030	-30	-49	-1	106	-9	-24	64	106	15	103	5	-2	18	13	-16	27
2060	32	13	61	174	53	37	69	168	77	165	65	58	78	74	45	88
2089	93	12	60	167	50	36	126	167	76	163	64	57	78	73	44	87
2118	30	12	61	167	51	35	69	168	76	164	63	56	78	71	48	85
2147	28	11	59	180	50	33	125	167	74	163	61	54	138	70	47	83
2176	91	10	59	167	48	33	124	166	72	162	60	53	74	68	45	81
2206	29	11	60	164	49	34	68	167	74	163	61	53	74	70	45	81
2235	-33	-50	-2	104	-13	-27	65	106	12	102	-1	-9	13	8	-17	19
2265	29	9	58	210	48	32	125	167	43	162	58	50	133	67	42	78
2294	28	10	59	151	47	32	126	167	111	163	57	50	73	66	41	77
2324	-32	-54	-4	169	-14	-31	64	105	5	101	-5	-13	9	4	-21	14
2353	29	9	58	238	47	31	125	166	66	162	55	48	70	65	39	75
2383	28	9	58	236	46	31	125	166	68	163	54	47	70	65	39	74
2412	28	8	57	238	44	30	67	166	135	162	54	46	69	64	38	72
2471	28	9	57	148	45	30	125	166	65	162	53	45	66	63	36	71
2530	28	8	57	152	44	28	67	166	133	163	51	44	65	62	36	69
2590	-34	-53	-4	92	-17	-34	6	105	3	102	-11	-19	2	-1	-26	6
2649	27	8	57	165	44	27	67	166	132	163	48	41	62	61	35	65
2709	-35	-55	-5	105	-19	-36	64	105	1	101	-14	-22	-1	-2	-27	2
2768	-35	-55	-5	108	-21	-37	6	105	1	100	-15	-23	-2	-2	-28	1
2826	-34	-56	-4	151	-20	-38	64	105	1	99	-16	-24	-3	-3	-28	0
2887	25	5	56	168	40	23	125	165	61	161	44	37	56	59	32	59
2945	25	5	56	165	39	22	67	165	131	160	42	35	54	58	32	57
3006	25	4	56	160	38	21	68	165	61	160	42	34	53	57	34	57
3064	24	3	55	181	37	19	68	165	60	159	40	32	51	56	31	64
3124	24	1	56	155	36	18	125	165	62	159	40	31	50	57	33	96
3183	23	1	54	153	35	17	67	164	130	157	38	30	48	56	31	86
3243	-37	-59	-6	114	-26	-44	7	104	1	97	-24	-32	-13	-4	-29	33
3302	-37	-59	-6	108	-25	-44	64	105	0	99	-24	-32	-14	-3	-27	-13
3363	23	2	55	169	35	17	125	165	61	160	36	28	46	58	33	47

EXPERIMENT NO. 2 / RUN NO. 3

TIME	TC12	TC8	TC4	TC0	TG12	TG8	TG4	TG0	TL12	TL8	TL4	TL0	TN12	TN4	TD8	TD0
-60	381	381	381	381	381	381	381	381	381	381	381	381	381	381	381	381
-54	381	381	381	393	381	381	381	381	381	381	381	381	441	380	381	381
-49	381	381	381	387	381	380	380	380	379	380	381	381	381	380	381	381
-44	380	379	380	389	380	379	380	380	379	379	380	380	440	379	380	380
-39	380	379	380	377	379	379	379	380	379	380	379	380	380	379	380	380
-34	379	379	380	374	379	379	379	380	378	379	380	380	441	379	380	380
-29	380	379	380	380	381	379	380	379	379	379	381	380	380	380	381	380
-23	380	380	381	376	381	380	380	381	379	379	380	380	380	380	381	381
-18	380	379	380	378	380	379	380	379	379	379	380	380	441	379	380	380
-13	379	379	379	374	380	379	379	379	378	378	380	379	379	379	379	379
-8	379	378	379	373	379	378	379	379	378	378	379	379	379	378	379	379
-2	379	378	379	374	379	379	379	378	378	378	379	379	441	378	380	379
3	368	364	364	360	374	373	373	371	377	377	379	379	379	379	380	380
10	277	250	268	214	305	302	298	295	347	347	348	346	362	357	358	360
15	261	234	212	204	293	288	285	282	331	331	333	332	345	340	344	343
20	250	225	206	192	289	283	279	276	322	321	323	323	335	329	333	375
26	235	214	197	186	280	276	271	268	313	314	316	315	326	320	324	324
32	229	206	191	226	275	270	265	263	309	310	312	311	321	309	319	319
38	223	192	184	253	268	263	259	256	306	306	308	307	318	306	315	315
44	221	290	178	164	263	252	255	251	304	304	307	306	315	390	312	312
50	231	181	172	161	256	330	249	245	302	302	305	303	313	302	310	310
56	214	176	169	162	253	244	245	242	301	301	305	303	312	302	309	309
63	265	173	164	156	247	241	241	238	301	300	305	303	311	302	309	309
68	212	172	160	153	243	321	237	234	299	298	303	302	310	300	308	308
75	212	167	157	148	239	235	234	230	298	297	302	300	309	299	307	306
80	210	163	154	156	235	232	228	227	296	295	301	298	309	298	306	306
87	210	160	151	151	232	229	224	224	296	295	300	298	309	298	306	306
92	209	158	149	149	228	226	224	221	295	293	299	297	308	299	305	305
99	210	155	146	142	224	222	220	218	293	292	297	295	307	296	304	304
104	209	152	177	133	222	220	219	215	291	290	296	293	307	296	303	303
109	271	150	140	134	221	218	216	213	290	288	294	292	306	296	303	303
115	208	147	182	129	217	214	215	211	288	286	292	290	305	295	302	303
120	269	146	137	127	215	212	213	208	287	285	292	289	305	295	302	302
127	208	144	180	110	233	210	211	207	286	285	291	288	305	295	303	302
132	208	142	135	113	205	209	209	204	284	283	289	286	303	296	302	301
139	207	140	177	108	202	205	206	202	282	281	287	284	303	295	301	301
144	268	139	133	105	200	204	205	200	280	279	285	283	302	294	301	300
150	206	137	132	104	197	202	203	248	279	278	284	281	301	293	301	300
156	205	135	130	108	196	200	201	193	278	276	282	279	300	292	300	299
162	205	133	129	106	196	198	199	191	276	274	280	278	300	291	299	298
167	205	132	128	111	196	196	198	191	275	274	279	277	299	290	299	298
174	204	131	126	92	192	194	196	189	273	272	277	275	297	290	297	297
180	204	129	125	92	296	193	194	188	272	270	276	273	297	289	296	296
186	205	129	124	87	190	191	192	253	297	268	274	272	296	288	295	295
192	202	126	123	95	189	189	191	186	332	267	272	270	295	286	294	293
198	202	125	122	93	188	188	189	184	331	266	271	268	294	285	293	292
203	204	124	120	91	186	186	187	183	261	264	269	267	292	283	291	291
209	201	123	119	90	186	184	186	181	328	263	268	265	290	282	290	290
215	203	123	119	89	186	182	185	182	258	262	267	265	290	281	290	289
221	202	121	118	84	184	181	183	180	326	260	265	263	289	280	289	288
228	202	120	116	88	184	180	182	179	257	258	264	261	288	279	287	286
233	201	120	116	87	183	178	181	177	256	257	263	260	286	278	286	286
240	201	120	115	84	184	177	179	176	325	256	261	259	285	277	285	284
245	201	118	114	86	184	176	178	175	253	255	260	257	284	276	284	283
252	201	118	114	89	183	175	177	174	253	254	279	256	284	274	283	282
262	201	117	112	82	183	174	175	173	320	251	254	254	282	274	281	281
273	200	115	111	87	180	172	173	170	249	249	252	251	279	270	297	278
283	200	115	111	94	181	171	172	169	248	247	251	261	278	269	321	277
294	200	115	110	83	181	169	171	168	247	246	304	290	276	267	273	275

303	199	113	108	79	179	167	168	166	244	239	301	243	273	264	270	272
314	198	112	106	78	178	165	166	163	241	236	245	240	270	261	268	269
322	198	110	105	77	177	163	165	162	239	235	245	239	268	260	266	267
333	197	111	104	80	176	162	163	160	237	320	242	237	265	257	264	264
343	197	109	103	69	176	160	161	159	235	231	239	236	286	254	262	261
353	196	108	102	71	176	158	160	157	233	229	237	233	256	252	259	259
363	196	109	101	72	175	158	158	157	231	229	235	234	254	250	257	257
373	196	108	101	71	175	157	158	155	229	228	234	231	314	248	255	254
388	195	107	99	70	174	153	154	152	225	224	230	228	249	244	250	249
402	196	108	99	72	174	153	154	152	224	225	229	227	248	242	248	247
418	196	108	98	76	174	152	153	150	222	225	227	224	248	240	245	261
432	193	105	95	64	172	148	149	147	218	220	223	220	242	235	240	237
448	193	104	93	78	172	146	147	144	215	217	220	217	239	232	237	234
462	193	104	92	72	171	144	145	143	213	215	218	215	237	230	235	233
477	192	102	92	68	172	143	144	142	211	213	217	213	235	228	233	232
491	192	101	91	79	170	141	142	139	208	210	214	211	233	225	231	231
507	193	101	91	74	171	140	142	139	207	208	213	209	232	223	229	229
521	191	100	89	66	168	136	139	136	204	204	210	206	229	219	226	226
537	190	99	88	60	167	135	137	134	201	202	208	203	226	217	224	223
551	190	97	87	56	167	133	135	133	198	199	207	201	224	214	222	221
565	190	97	87	59	167	132	135	132	197	199	207	199	223	213	221	220
581	190	98	86	55	168	131	133	132	196	197	206	198	222	212	218	219
596	190	96	85	66	167	129	132	129	194	194	204	195	220	209	217	216
611	189	97	85	65	167	128	131	128	192	192	203	194	217	207	214	214
626	188	95	83	62	165	126	128	126	188	189	201	191	215	204	212	211
641	189	94	82	63	164	125	127	125	187	187	200	189	214	202	210	209
655	189	95	81	57	164	123	126	123	185	185	199	186	212	199	207	207
676	189	95	81	60	165	123	125	123	183	185	199	185	211	199	206	206
705	188	94	80	56	165	120	122	120	179	180	197	181	208	194	202	201
735	187	92	77	51	163	116	118	116	173	175	193	176	204	188	195	196
764	188	93	77	51	165	116	118	115	172	173	193	173	204	186	193	193
794	186	91	74	57	163	112	168	111	167	168	190	169	201	180	187	187
823	186	90	73	45	161	110	107	109	163	164	189	165	199	176	180	183
853	186	91	72	38	163	109	106	108	160	161	188	162	198	173	223	179
882	185	88	70	41	161	105	163	105	156	157	186	158	195	168	173	175
911	185	89	69	42	161	104	103	103	153	154	186	155	194	165	171	171
941	185	89	68	42	161	103	103	101	151	152	185	152	193	162	169	169
969	186	89	67	37	162	102	101	100	149	150	185	151	193	161	167	167
1029	185	87	65	21	160	98	98	96	144	144	184	145	190	154	160	161
1087	184	86	63	21	160	95	94	92	138	139	181	190	188	148	155	155
1147	184	84	61	18	159	125	92	89	133	134	182	133	187	143	150	148
1205	185	84	61	17	160	87	90	87	183	130	182	131	187	135	146	146
1265	184	83	67	25	158	168	86	84	191	125	180	126	186	130	140	142
1324	184	83	90	21	158	82	84	81	119	121	179	122	185	127	135	137
1383	185	84	54	12	158	80	81	80	115	116	179	118	184	124	131	133
1442	183	82	51	17	157	78	78	75	113	113	179	113	183	122	125	128
1502	186	83	52	22	159	80	77	75	112	111	178	112	184	120	123	126
1560	185	82	51	41	158	80	75	73	109	108	178	109	183	117	119	122
1620	183	78	49	36	156	74	70	68	103	101	175	103	180	108	113	116
1679	183	78	48	36	156	74	69	80	101	99	175	101	180	106	111	113
1738	182	78	47	26	155	73	67	114	97	95	174	98	179	103	108	109
1797	183	80	47	16	156	74	66	126	95	94	174	96	180	101	106	107
1856	182	78	46	33	155	73	64	124	92	91	173	93	179	97	103	104
1916	181	76	44	35	156	72	61	121	88	87	173	90	177	94	99	100
2033	184	79	45	26	157	75	62	56	86	84	174	89	180	90	98	97
2152	181	75	41	26	154	154	56	51	80	77	171	84	176	82	127	90
2270	181	74	39	20	154	71	53	49	76	73	171	81	176	78	86	85
2389	181	74	37	-4	154	70	50	48	71	150	170	78	176	73	85	80
2506	181	73	36	18	154	69	48	46	67	59	171	77	176	70	83	77
2625	180	72	34	6	153	67	46	43	64	58	170	75	174	64	82	73
2897	178	71	30	73	153	67	40	38	56	138	167	72	173	57	77	106

EXPERIMENT NO. 2 / RUN NO. 4

TIME	TD12	TD8	TD4	TD0	TH12	TH8	TH4	TH0	TI12	TI8	TI4	TI0	TN8	TN0	TO8	TO0
-60	381	381	381	381	381	381	381	381	381	381	381	381	381	381	381	381
-55	380	381	381	390	380	380	323	446	382	382	382	381	381	381	418	381
-49	444	382	381	385	380	381	324	447	382	381	382	392	382	382	420	382
-44	445	382	383	386	381	382	382	448	382	382	437	393	383	382	383	383
-37	382	382	381	390	381	381	325	382	381	382	382	412	382	382	428	382
-32	443	381	381	389	380	380	324	446	380	381	382	381	381	381	419	381
-25	381	381	382	379	381	380	323	434	380	381	383	391	381	381	419	381
-20	379	380	379	378	377	378	380	378	379	380	380	390	380	379	379	380
-14	379	379	379	382	379	379	322	445	379	380	382	400	381	380	418	380
-8	442	379	380	383	379	379	380	444	378	379	381	380	381	379	418	380
-2	380	378	380	379	379	379	321	444	379	379	381	389	380	379	426	380
3	343	330	324	393	358	356	300	357	361	360	366	363	378	378	378	378
10	289	261	249	249	312	307	251	307	315	315	326	321	356	356	361	358
15	277	250	237	236	302	296	240	295	306	305	314	308	341	339	346	340
21	266	239	229	222	296	289	231	287	298	297	307	301	330	327	334	331
28	254	231	222	222	291	284	226	281	293	293	304	297	323	321	328	324
33	248	223	216	210	287	280	222	278	291	291	303	295	320	319	325	321
40	239	215	209	206	281	274	229	272	287	287	299	291	317	315	321	318
45	234	209	204	201	277	270	267	268	283	284	295	287	315	314	319	316
51	229	202	199	197	272	265	206	263	279	279	292	283	314	312	318	315
57	225	199	194	188	267	261	203	259	276	276	285	280	313	310	316	313
64	223	193	189	188	263	256	199	255	272	272	334	275	311	309	315	312
69	222	189	185	184	260	253	196	313	269	269	279	293	311	308	314	311
76	219	184	182	184	255	249	192	243	266	265	276	265	310	308	314	311
81	219	181	179	177	252	246	189	241	263	263	274	264	310	308	313	310
88	219	179	177	173	249	243	187	241	261	261	273	317	310	307	314	311
93	217	176	174	179	245	241	184	237	258	258	269	260	309	306	313	310
100	215	171	170	173	241	236	179	233	253	254	265	257	307	305	311	308
106	215	169	168	180	239	233	177	232	252	252	263	255	308	305	311	308
111	216	167	167	179	237	231	176	231	251	249	261	253	307	304	311	308
117	215	164	165	174	233	229	173	229	247	247	258	250	306	303	310	307
122	214	162	163	173	232	227	171	226	246	245	256	248	306	302	309	307
129	213	159	169	167	228	224	168	223	243	241	254	245	304	301	308	305
134	213	159	157	153	226	222	166	222	241	240	251	243	304	300	308	305
140	212	155	154	148	224	219	163	219	238	237	249	241	348	299	308	304
145	212	154	154	235	222	218	162	217	236	236	248	239	359	298	308	304
161	211	150	194	147	216	212	157	212	231	231	242	234	357	295	306	303
175	210	144	148	140	212	207	152	207	226	226	237	229	355	292	303	299
191	210	141	146	139	209	203	150	204	223	223	234	225	293	290	302	297
205	208	137	143	139	206	198	146	201	219	218	229	221	290	285	298	294
220	208	133	140	133	203	194	141	196	215	213	225	217	287	281	295	291
235	207	130	138	137	202	191	138	193	212	210	222	214	285	278	289	288
250	205	127	135	138	197	187	135	190	208	205	218	210	281	274	285	284
264	205	126	133	131	197	185	132	187	205	203	216	207	278	271	283	282
280	202	121	130	123	194	180	128	183	200	198	213	203	272	265	280	276
295	204	121	130	123	194	179	127	182	199	197	213	201	271	263	278	274
309	204	118	128	123	193	239	125	179	196	193	212	198	267	258	274	270
325	202	116	125	123	190	250	121	176	192	190	209	195	263	254	270	265
339	202	110	124	123	190	250	120	175	190	187	208	193	261	251	267	264
355	201	107	122	114	189	163	117	171	182	185	206	190	257	247	263	259
370	202	109	122	120	189	162	116	170	182	184	207	189	255	246	262	255
385	197	206	117	113	185	158	110	164	245	177	202	183	249	239	256	249
400	199	206	117	107	186	159	110	164	176	177	202	182	248	238	254	249
430	198	205	114	110	183	155	105	160	173	171	199	176	241	225	247	244
459	198	100	112	114	184	153	103	157	172	168	199	173	236	223	243	240
490	197	97	110	110	183	149	143	153	168	164	198	169	232	218	238	235
518	195	200	106	115	181	144	92	149	163	160	196	195	225	213	232	229
548	195	95	105	103	182	142	91	146	160	153	194	213	222	213	228	225
577	194	197	102	111	180	139	88	142	156	150	193	156	217	207	223	220

607	192	92	99	109	179	135	85	138	152	231	192	152	212	202	217	214
636	192	90	96	97	178	131	82	135	148	143	190	149	207	197	213	210
665	192	89	96	98	178	129	80	133	146	141	191	147	204	194	209	207
724	193	89	93	98	179	124	76	128	140	138	188	142	195	186	201	199
782	192	86	89	92	178	118	71	123	135	133	188	136	187	176	237	190
842	190	83	85	90	177	113	65	169	128	128	187	130	173	168	184	181
900	188	80	82	90	175	107	60	109	122	121	183	124	167	160	175	173
959	189	79	80	101	175	105	57	175	119	117	186	120	166	154	171	168
1018	187	75	76	92	174	99	52	105	113	111	183	115	158	147	164	160
1077	188	74	109	81	173	97	49	103	111	107	184	113	154	142	161	159
1136	187	73	114	79	174	95	46	99	107	103	204	109	150	137	155	154
1196	186	72	80	83	171	91	43	96	103	100	223	106	144	132	150	148
1254	186	72	79	78	173	91	40	95	100	98	233	104	140	129	145	144
1313	184	70	74	75	172	88	37	90	96	94	232	100	135	123	140	139
1372	181	66	69	65	169	84	32	86	92	88	176	95	127	117	133	132
1432	182	66	68	70	168	82	30	83	89	85	230	93	124	113	129	128
1490	182	65	69	75	170	82	28	82	87	84	177	93	121	110	127	125
1550	181	63	68	73	168	80	25	79	84	81	176	90	116	105	122	120
1609	180	63	66	62	167	78	23	77	81	78	231	89	114	102	119	117
1667	179	61	64	59	168	75	20	73	78	74	229	86	109	97	115	113
1727	179	60	63	64	168	75	18	72	76	72	175	85	106	95	112	110
1786	179	58	61	58	166	73	16	70	73	69	175	83	103	90	152	107
1846	178	57	59	68	166	71	13	67	70	67	174	81	99	86	103	103
1963	179	59	58	58	168	71	12	65	68	65	176	81	96	85	100	99
2081	176	57	54	46	165	68	6	60	63	59	173	76	90	77	96	91
2199	176	59	53	39	167	69	4	58	61	58	173	75	89	74	94	88
2318	175	59	52	42	166	68	1	54	58	54	173	73	84	67	90	82
2435	176	60	51	33	167	66	-1	53	55	52	174	72	81	64	88	76
2554	175	60	49	36	167	66	-4	50	53	49	172	71	79	144	86	73
2672	174	62	47	41	167	65	-7	47	90	47	172	70	77	53	83	69
2790	175	66	47	53	169	67	-7	47	46	47	172	70	77	140	84	68
2908	175	65	46	43	171	66	-9	45	44	46	227	70	77	138	83	66
3027	177	65	46	34	170	65	-10	44	43	43	176	70	78	49	84	64
3144	176	63	45	30	169	63	-25	41	110	40	174	69	76	46	83	61
3417	177	65	43	36	170	63	-19	39	39	37	229	68	75	40	82	55

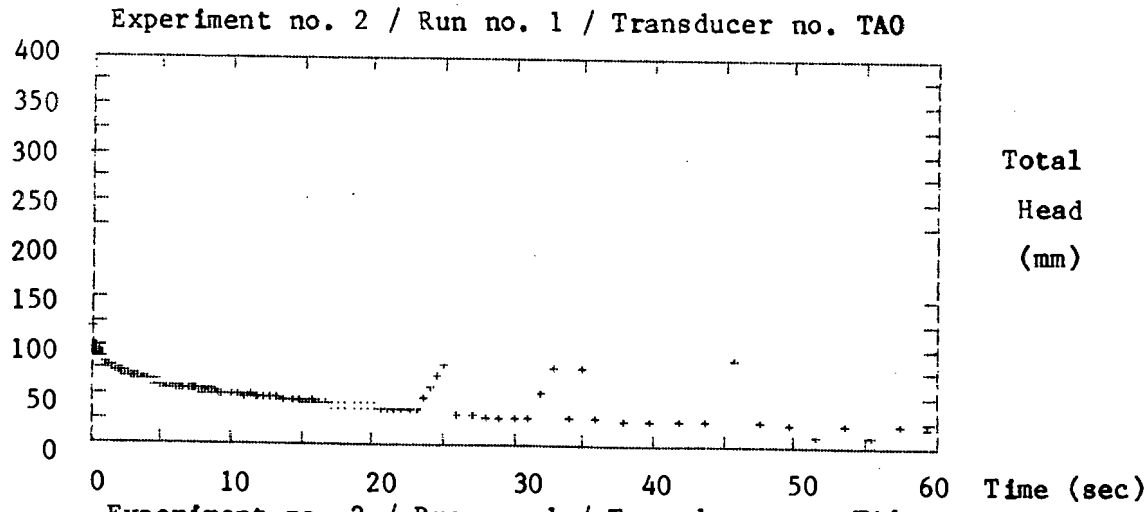
Experiment no. 2 / Run no. 1 / Transducer no. TA0
400
350
300
250
200
150
100
50
0
0
10
20
30
40
50
60
Time (sec)
Total
Head
(mm)

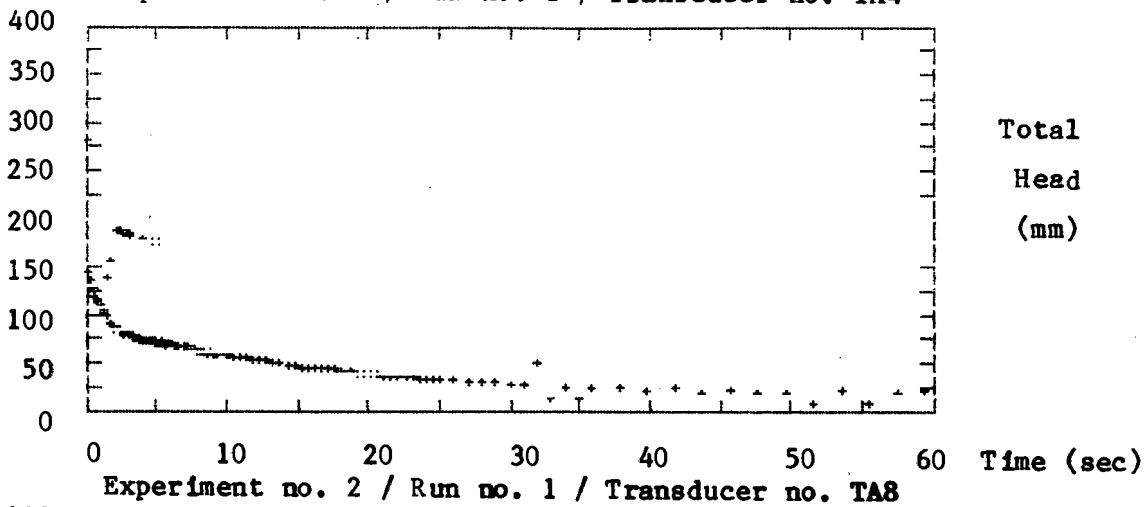
Experiment no. 2 / Run no. 1 / Transducer no. TA4
400
350
300
250
200
150
100
50
0
0
10
20
30
40
50
60
Time (sec)
Total
Head
(mm)

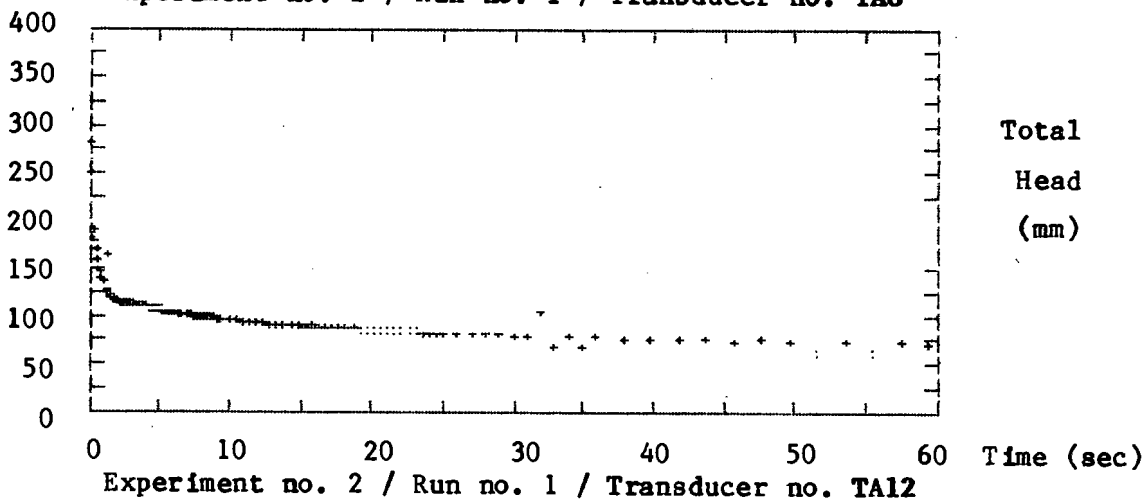
Experiment no. 2 / Run no. 1 / Transducer no. TA8
400
350
300
250
200
150
100
50
0
0
10
20
30
40
50
60
Time (sec)
Total
Head
(mm)

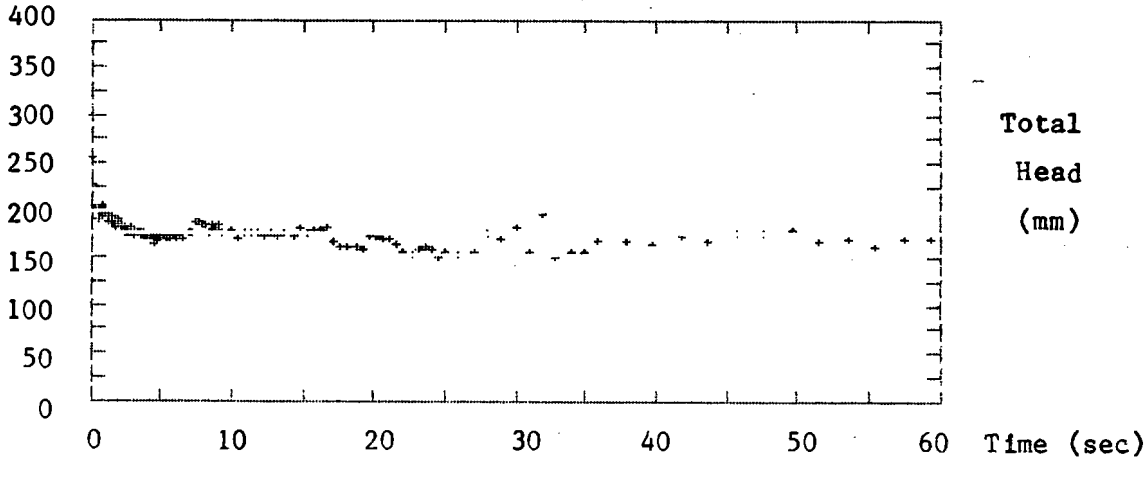
Experiment no. 2 / Run no. 1 / Transducer no. TA12
400
350
300
250
200
150
100
50
0
0
10
20
30
40
50
60
Time (sec)
Total
Head
(mm)

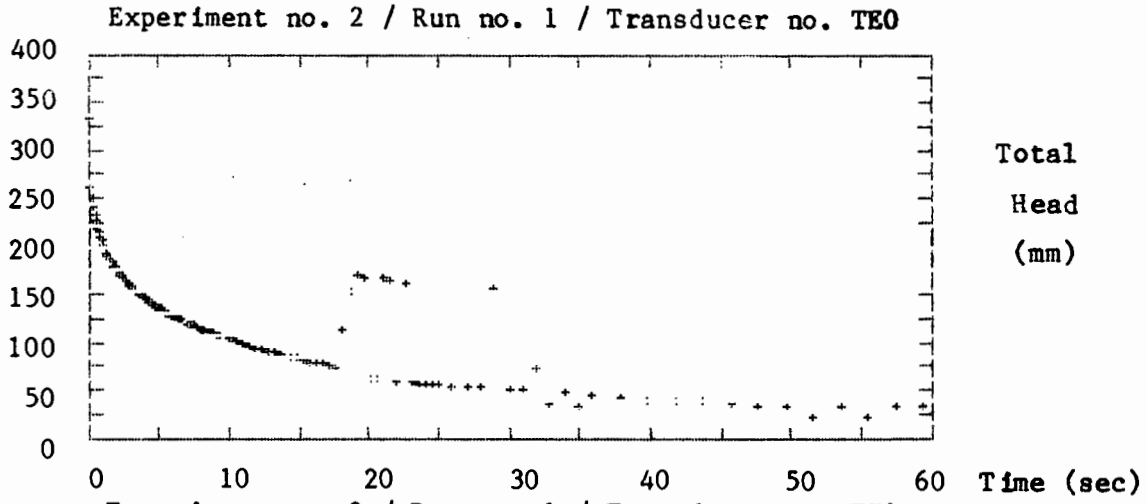
Experiment no. 2 / Run no. 1 / Transducer no. TE0
400
350
300
250
200
150
100
50
0
Total
Head
(mm)
0
10
20
30
40
50
60
Time (sec)

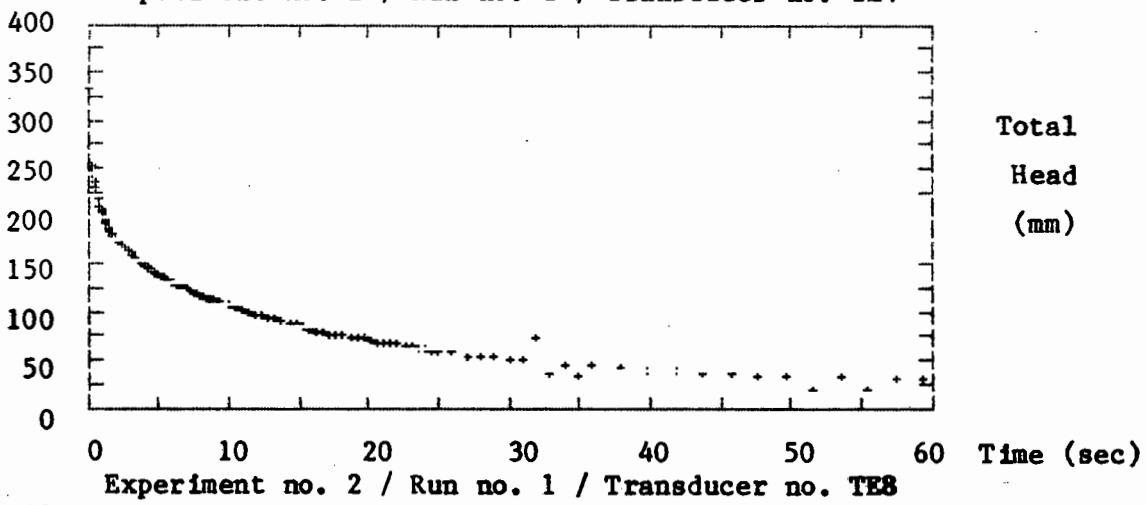
Experiment no. 2 / Run no. 1 / Transducer no. TE4
400
350
300
250
200
150
100
50
0
Total
Head
(mm)
0
10
20
30
40
50
60
Time (sec)

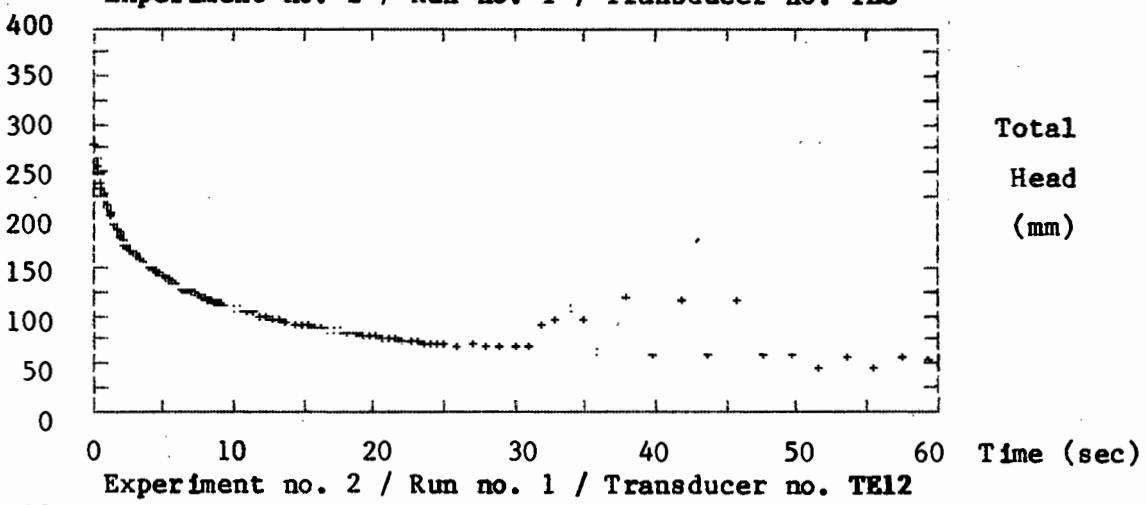
Experiment no. 2 / Run no. 1 / Transducer no. TE8
400
350
300
250
200
150
100
50
0
Total
Head
(mm)
0
10
20
30
40
50
60
Time (sec)

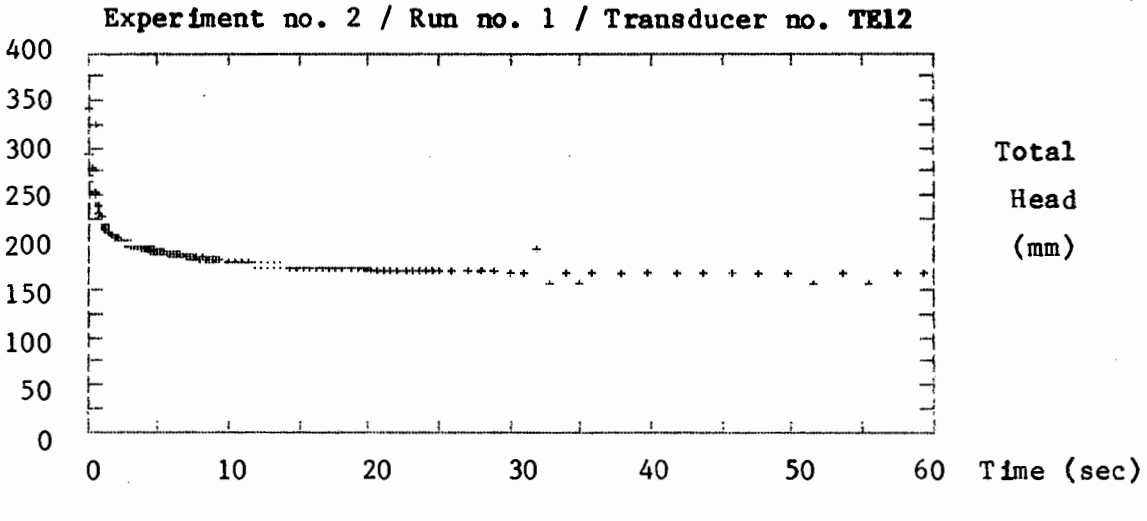
Experiment no. 2 / Run no. 1 / Transducer no. TE12
400
350
300
250
200
150
100
50
0
Total
Head
(mm)
0
10
20
30
40
50
60
Time (sec)

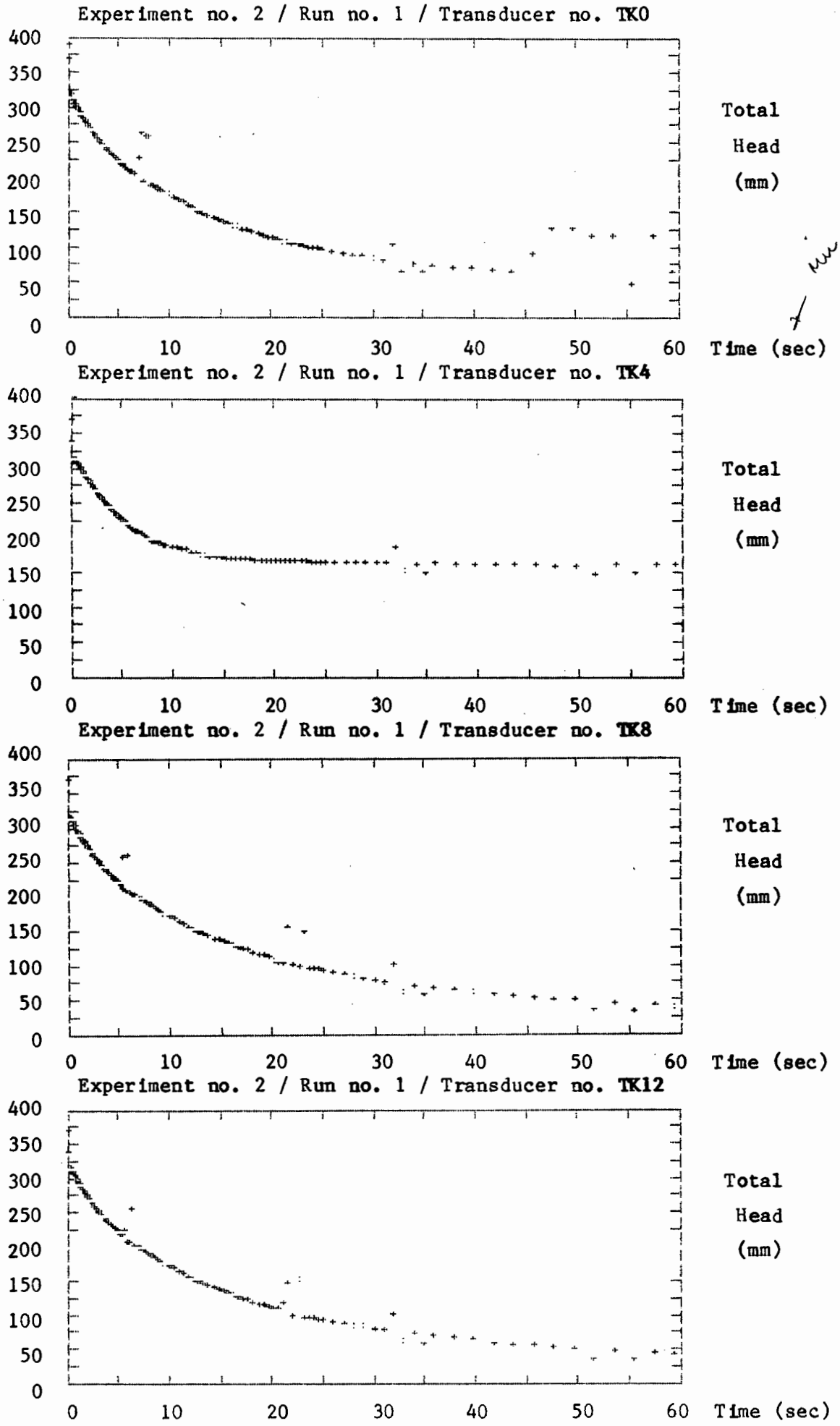
Experiment no. 2 / Run no. 1 / Transducer no. TK0
Total Head (mm)
Time (sec)
Experiment no. 2 / Run no. 1 / Transducer no. TK4
Total Head (mm)
Time (sec)
Experiment no. 2 / Run no. 1 / Transducer no. TK8
Total Head (mm)
Time (sec)
Experiment no. 2 / Run no. 1 / Transducer no. TK12
Total Head (mm)
Time (sec)

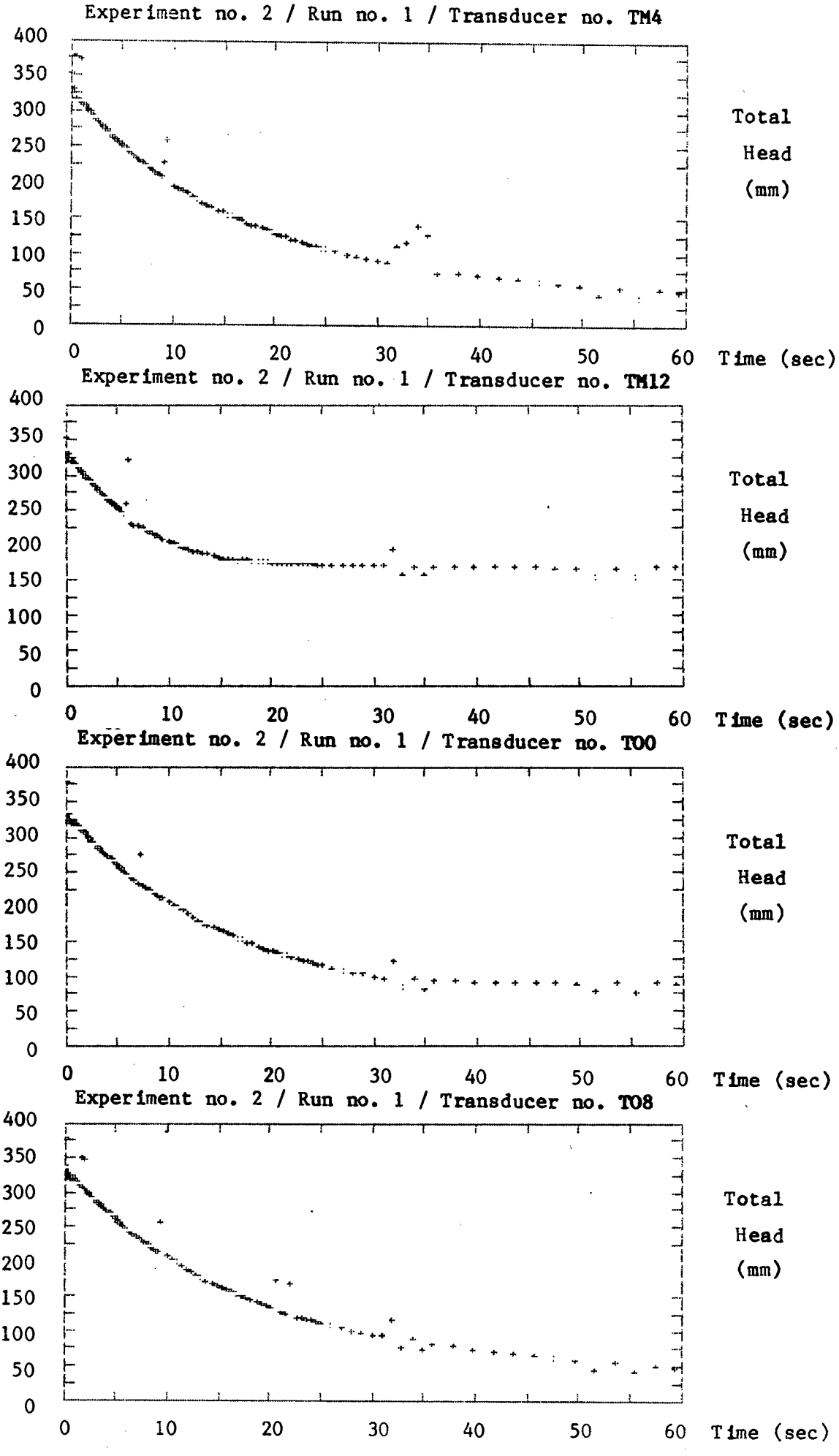
Experiment no. 2 / Run no. 1 / Transducer no. TM4
Total Head (mm)
Time (sec)
Experiment no. 2 / Run no. 1 / Transducer no. TM12
Total Head (mm)
Time (sec)
Experiment no. 2 / Run no. 1 / Transducer no. T00
Total Head (mm)
Time (sec)
Experiment no. 2 / Run no. 1 / Transducer no. T08
Total Head (mm)
Time (sec)

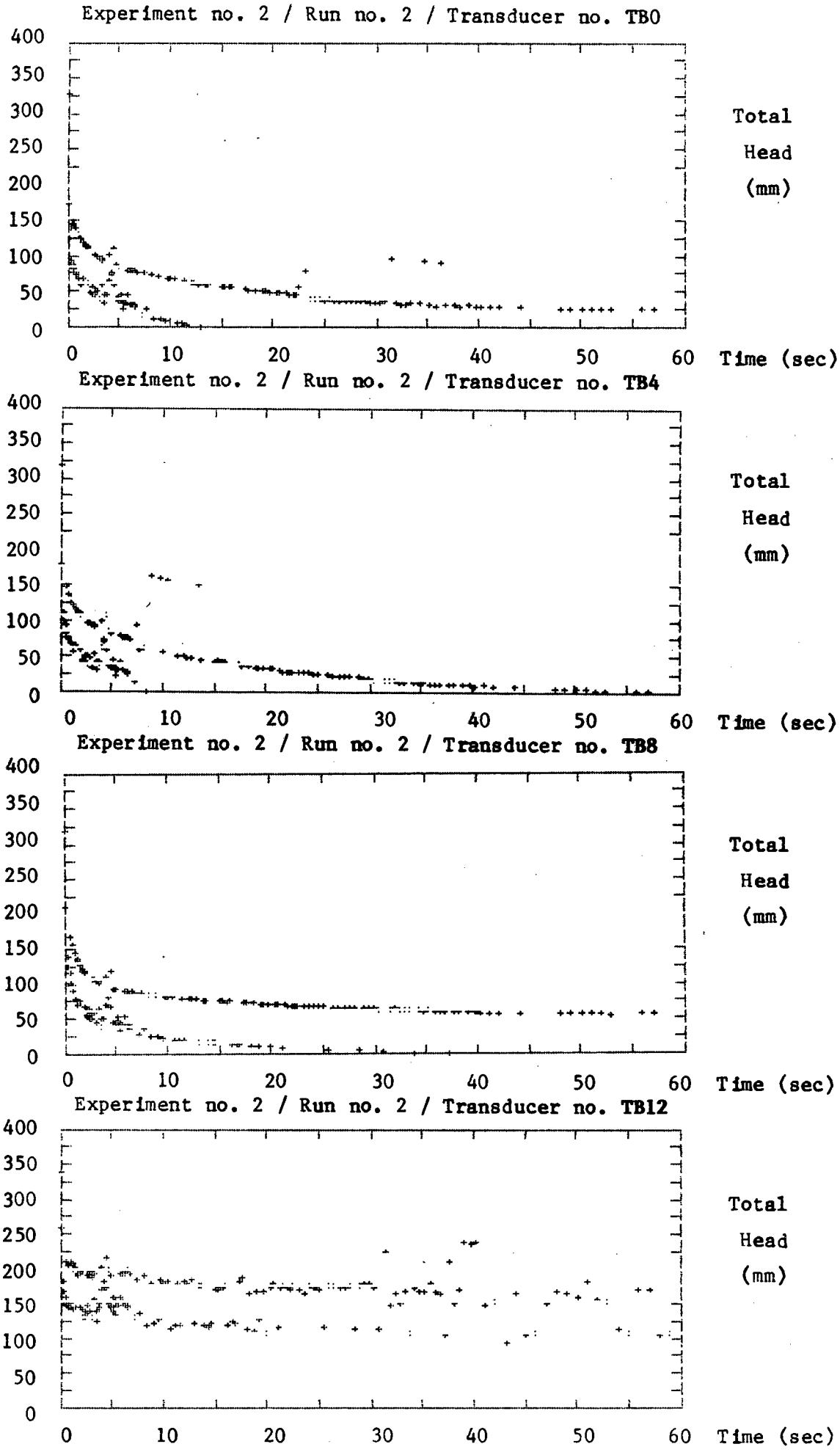
Experiment no. 2 / Run no. 2 / Transducer no. TB0
Total Head (mm)
Time (sec)
Experiment no. 2 / Run no. 2 / Transducer no. TB4
Total Head (mm)
Time (sec)
Experiment no. 2 / Run no. 2 / Transducer no. TB8
Total Head (mm)
Time (sec)
Experiment no. 2 / Run no. 2 / Transducer no. TB12
Total Head (mm)
Time (sec)

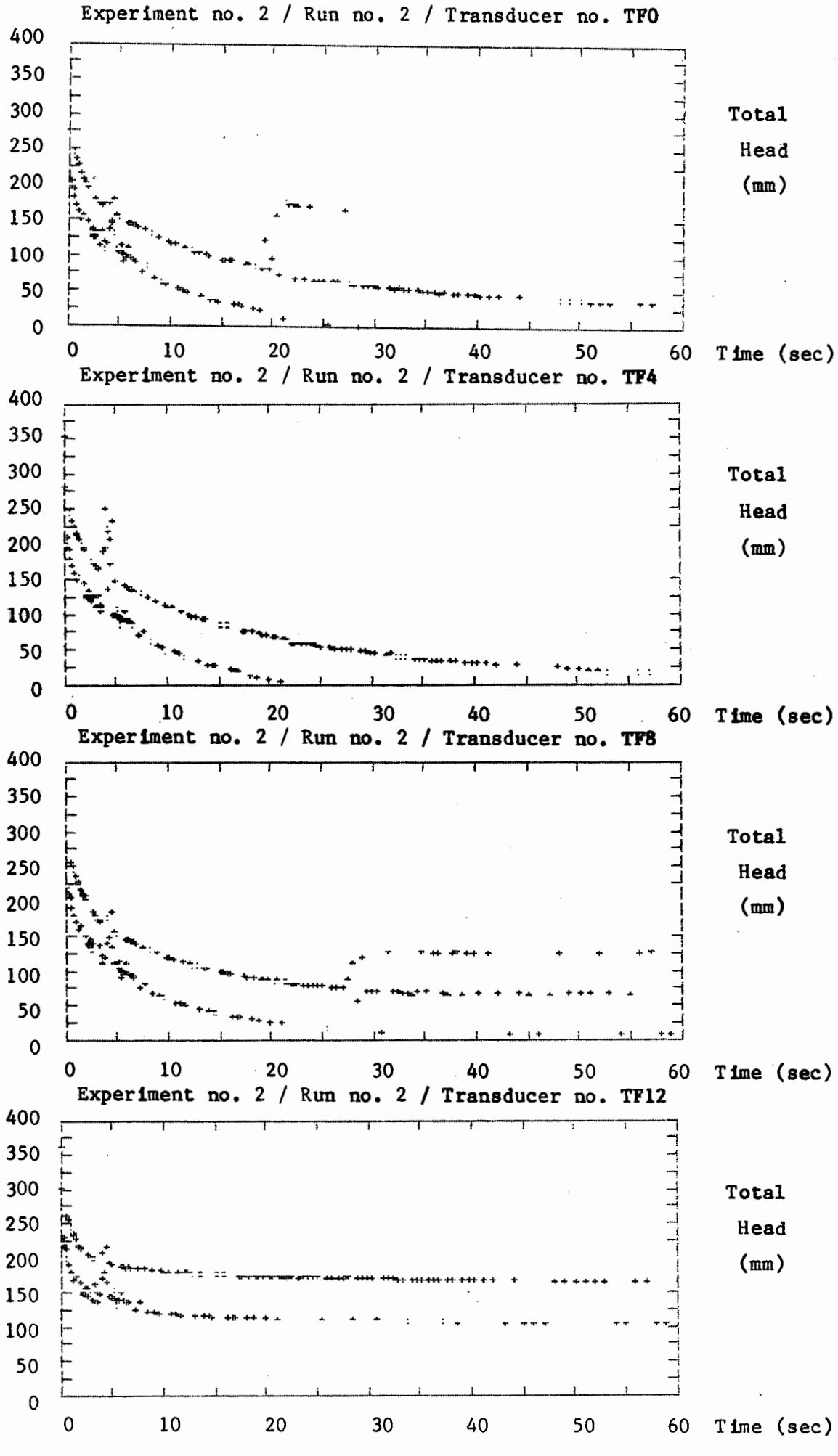
Experiment no. 2 / Run no. 2 / Transducer no. TF0
Total Head (mm)
Time (sec)
Experiment no. 2 / Run no. 2 / Transducer no. TF4
Total Head (mm)
Time (sec)
Experiment no. 2 / Run no. 2 / Transducer no. TF8
Total Head (mm)
Time (sec)
Experiment no. 2 / Run no. 2 / Transducer no. TF12
Total Head (mm)
Time (sec)

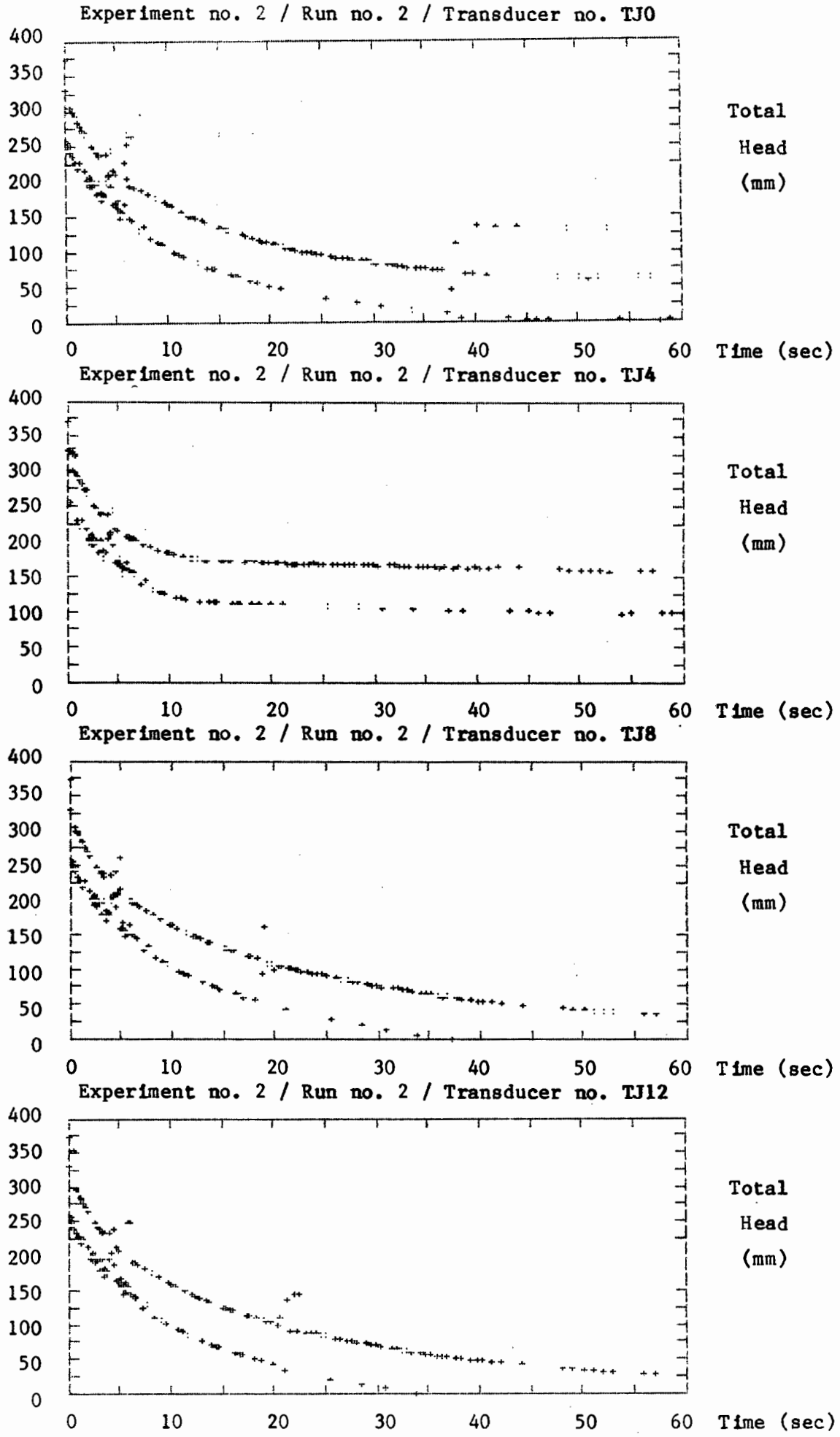
Experiment no. 2 / Run no. 2 / Transducer no. TJ0
Total Head (mm)
Time (sec)
Experiment no. 2 / Run no. 2 / Transducer no. TJ4
Total Head (mm)
Time (sec)
Experiment no. 2 / Run no. 2 / Transducer no. TJ8
Total Head (mm)
Time (sec)
Experiment no. 2 / Run no. 2 / Transducer no. TJ12
Total Head (mm)
Time (sec)

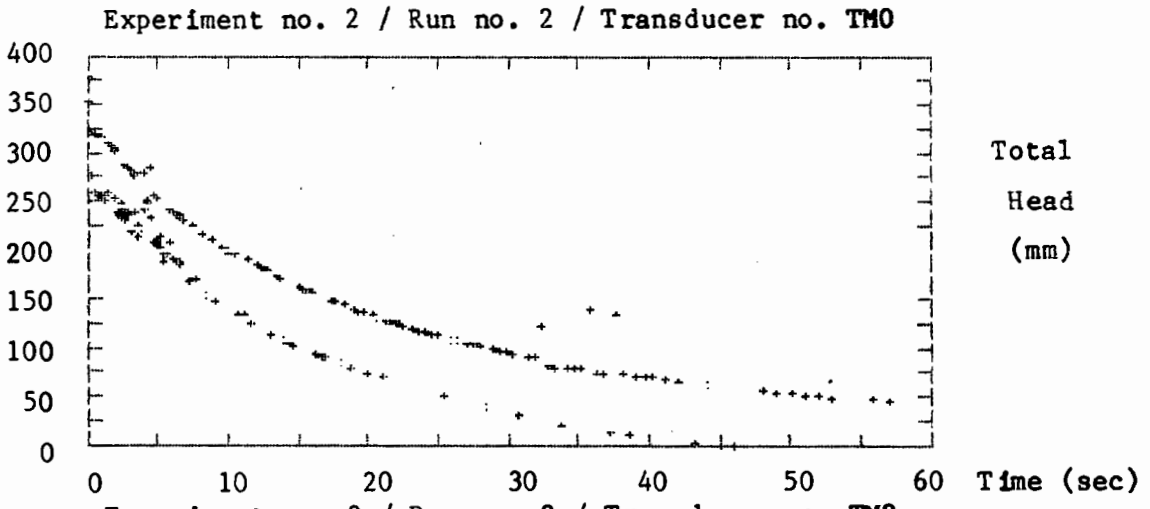
Experiment no. 2 / Run no. 2 / Transducer no. TM0
400
350
300
250
200
150
100
50
0
0
10
20
30
40
50
60
Time (sec)
Total
Head
(mm)

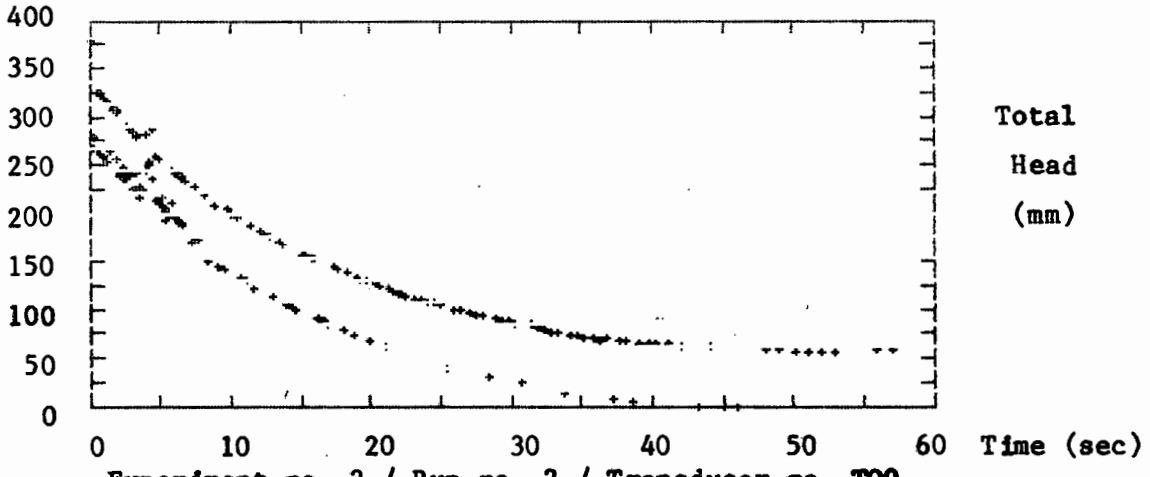
Experiment no. 2 / Run no. 2 / Transducer no. TM8
400
350
300
250
200
150
100
50
0
0
10
20
30
40
50
60
Time (sec)
Total
Head
(mm)

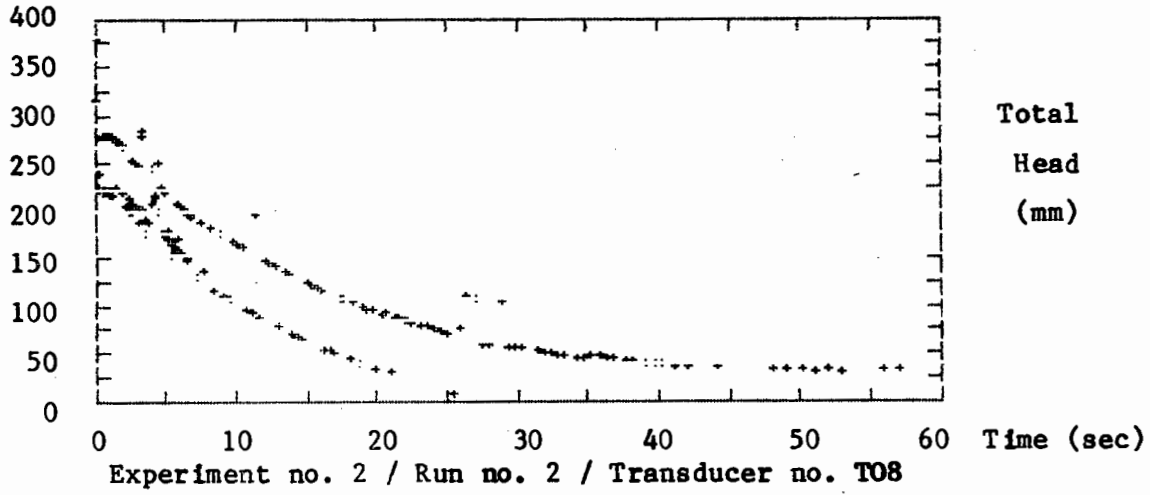
Experiment no. 2 / Run no. 2 / Transducer no. TO0
400
350
300
250
200
150
100
50
0
0
10
20
30
40
50
60
Time (sec)
Total
Head
(mm)

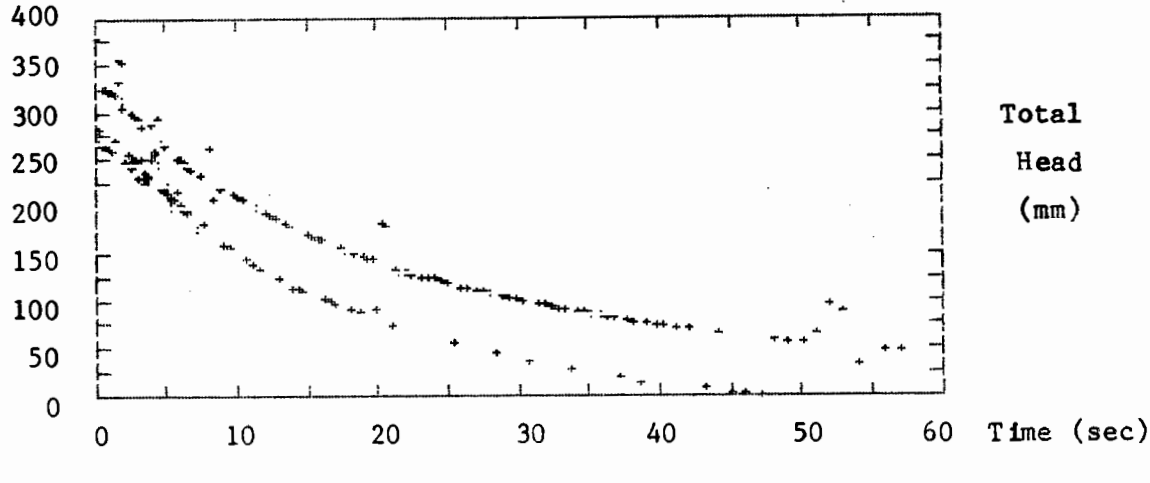
Experiment no. 2 / Run no. 2 / Transducer no. TO8
400
350
300
250
200
150
100
50
0
0
10
20
30
40
50
60
Time (sec)
Total
Head
(mm)

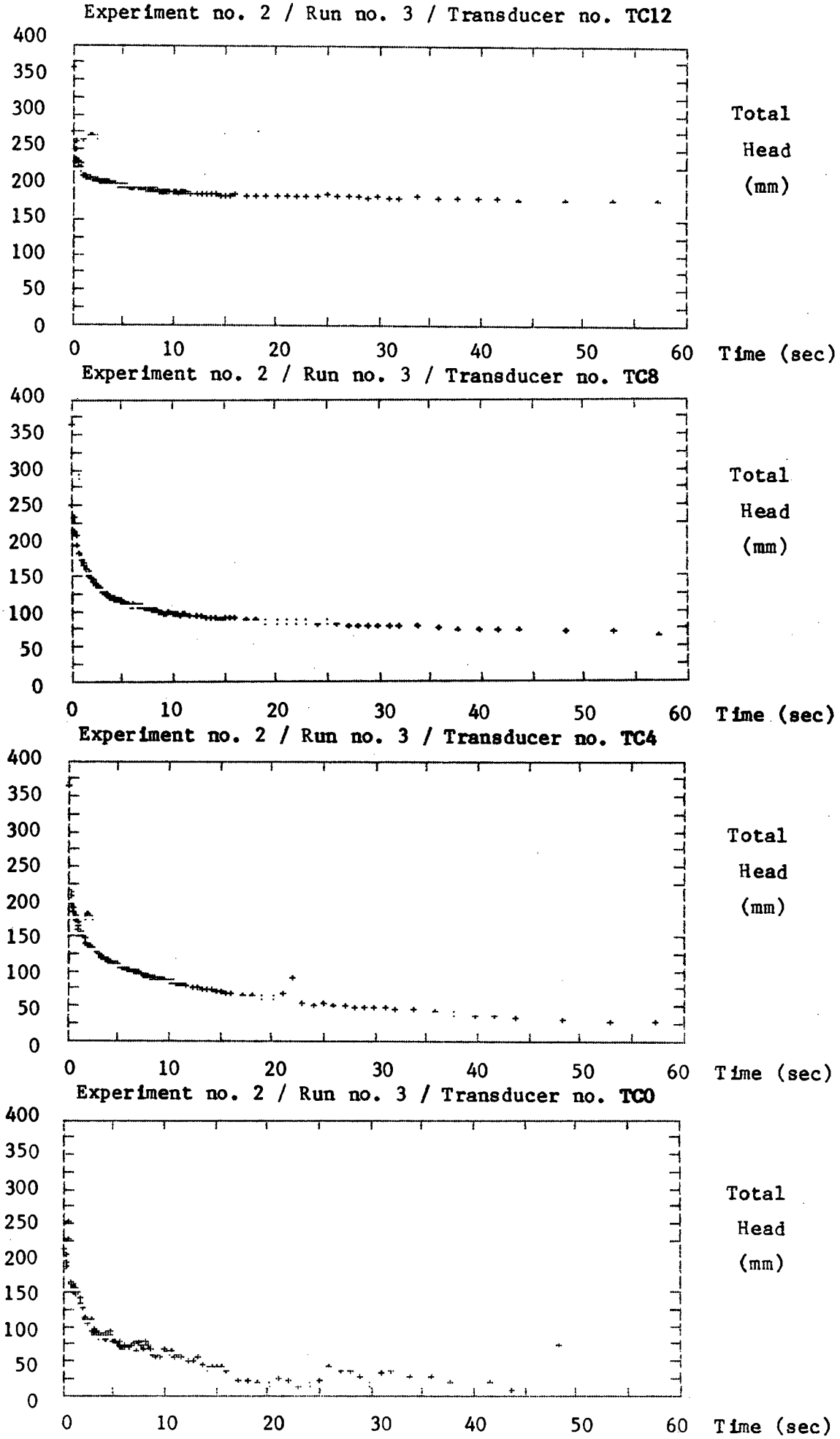
Experiment no. 2 / Run no. 3 / Transducer no. TC12
Total Head (mm)
Time (sec)
Experiment no. 2 / Run no. 3 / Transducer no. TC8
Total Head (mm)
Time (sec)
Experiment no. 2 / Run no. 3 / Transducer no. TC4
Total Head (mm)
Time (sec)
Experiment no. 2 / Run no. 3 / Transducer no. TC0
Total Head (mm)
Time (sec)

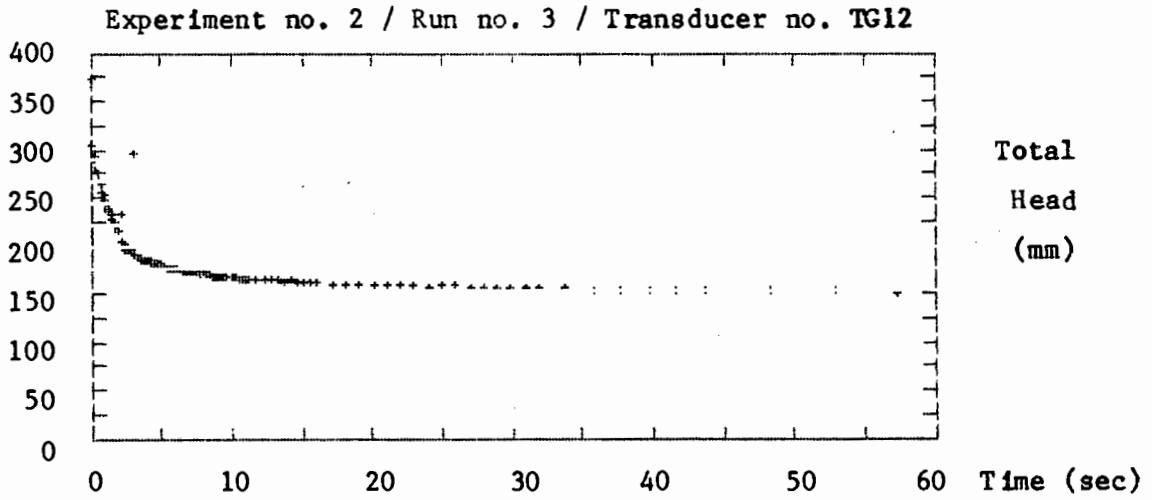
Experiment no. 2 / Run no. 3 / Transducer no. TG12
400
350
300
250
200
150
100
50
0
Total
Head
(mm)
0
10
20
30
40
50
60
Time (sec)

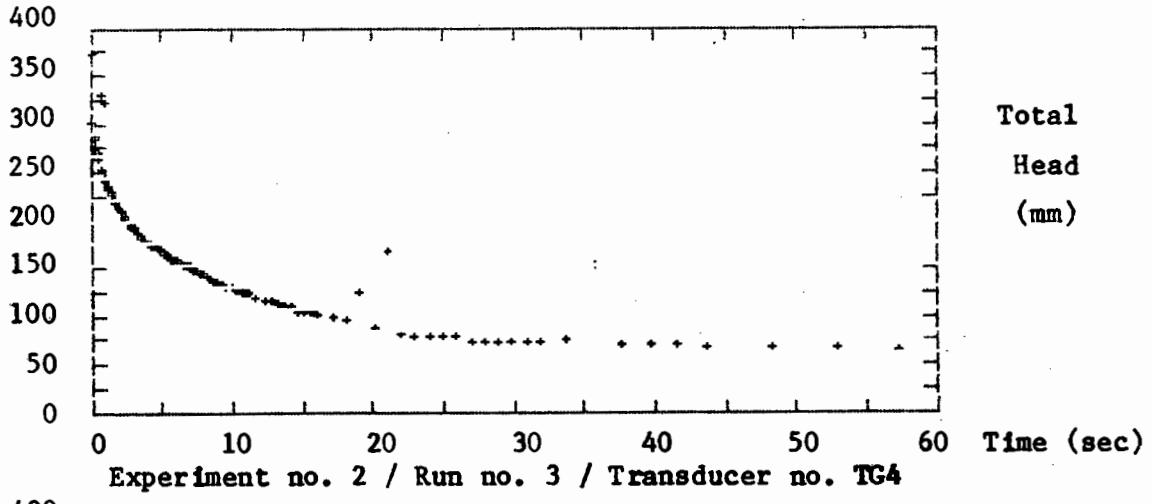
Experiment no. 2 / Run no. 3 / Transducer no. TG8
400
350
300
250
200
150
100
50
0
Total
Head
(mm)
0
10
20
30
40
50
60
Time (sec)

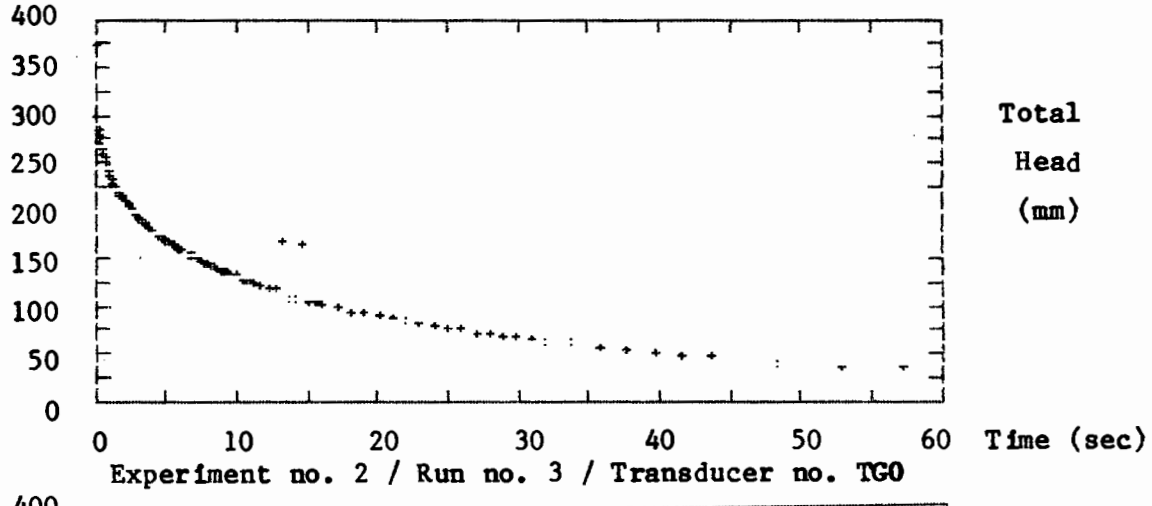
Experiment no. 2 / Run no. 3 / Transducer no. TG4
400
350
300
250
200
150
100
50
0
Total
Head
(mm)
0
10
20
30
40
50
60
Time (sec)

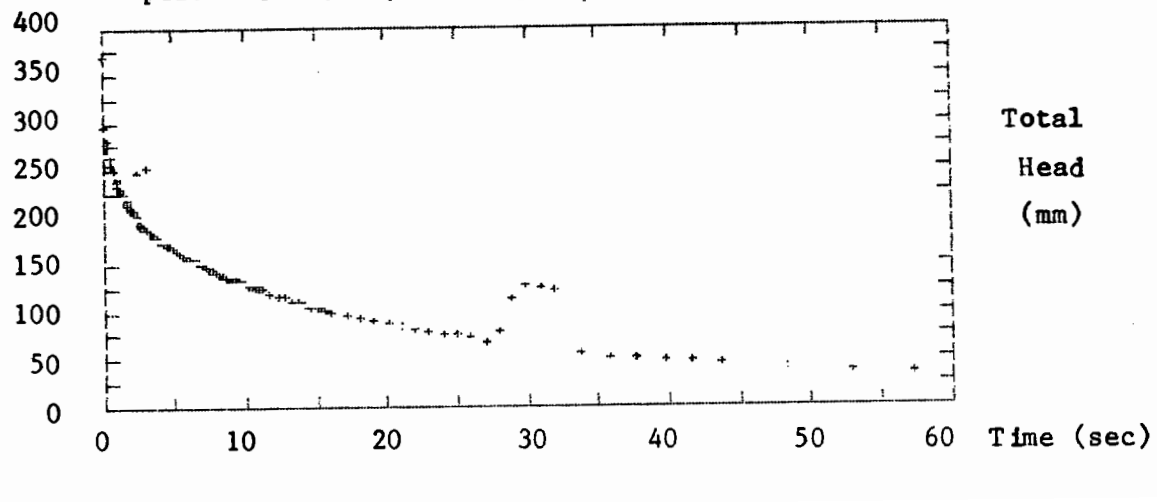
Experiment no. 2 / Run no. 3 / Transducer no. TG0
400
350
300
250
200
150
100
50
0
Total
Head
(mm)
0
10
20
30
40
50
60
Time (sec)

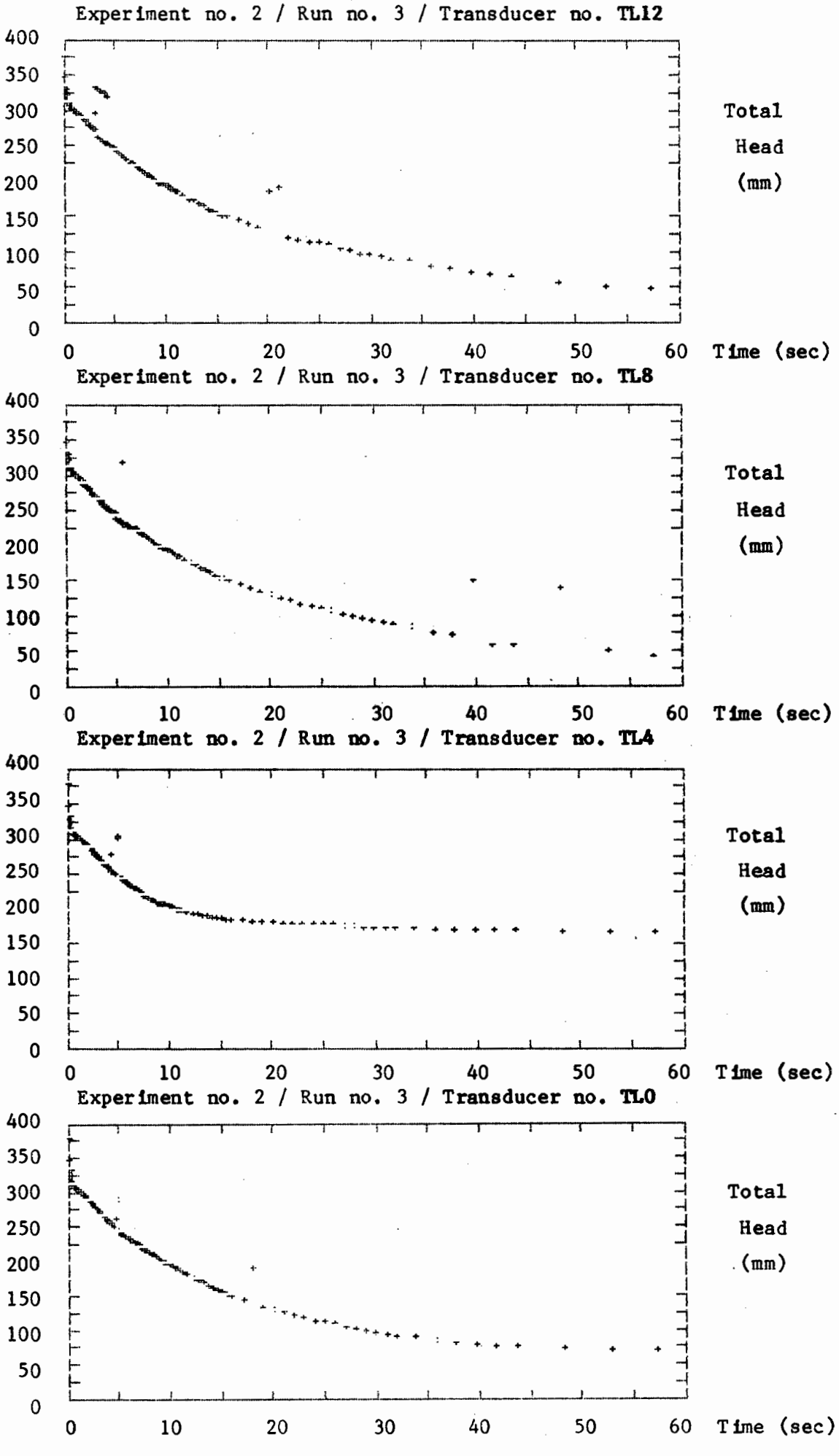
Experiment no. 2 / Run no. 3 / Transducer no. TL12
Total Head (mm)
Time (sec)
Experiment no. 2 / Run no. 3 / Transducer no. TL8
Total Head (mm)
Time (sec)
Experiment no. 2 / Run no. 3 / Transducer no. TL4
Total Head (mm)
Time (sec)
Experiment no. 2 / Run no. 3 / Transducer no. TL0
Total Head (mm)
Time (sec)
0
50
100
150
200
250
300
350
400
0
10
20
30
40
50
60

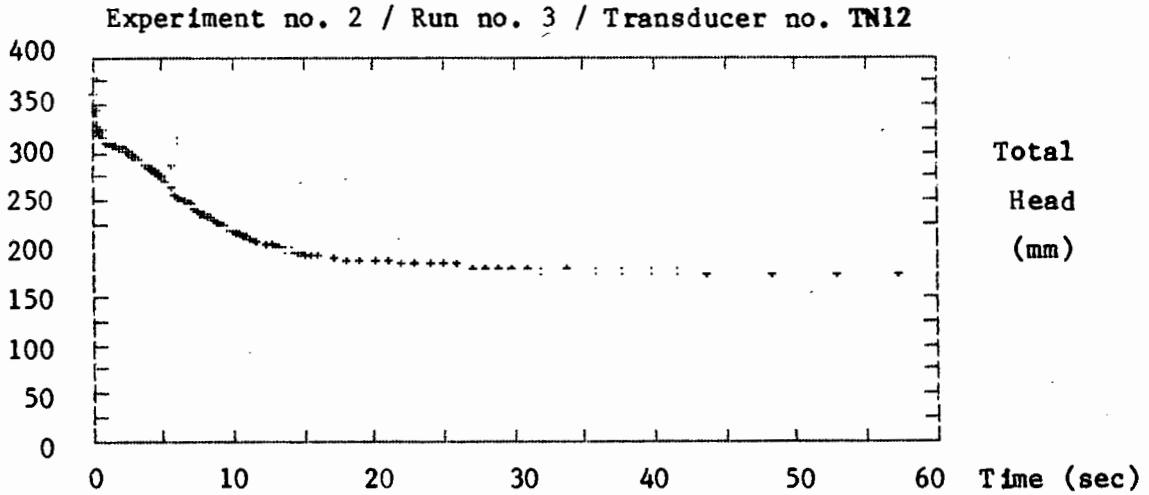
Experiment no. 2 / Run no. 3 / Transducer no. TN12
400
350
300
250
200
150
100
50
0
0
10
20
30
40
50
60
Time (sec)
Total
Head
(mm)

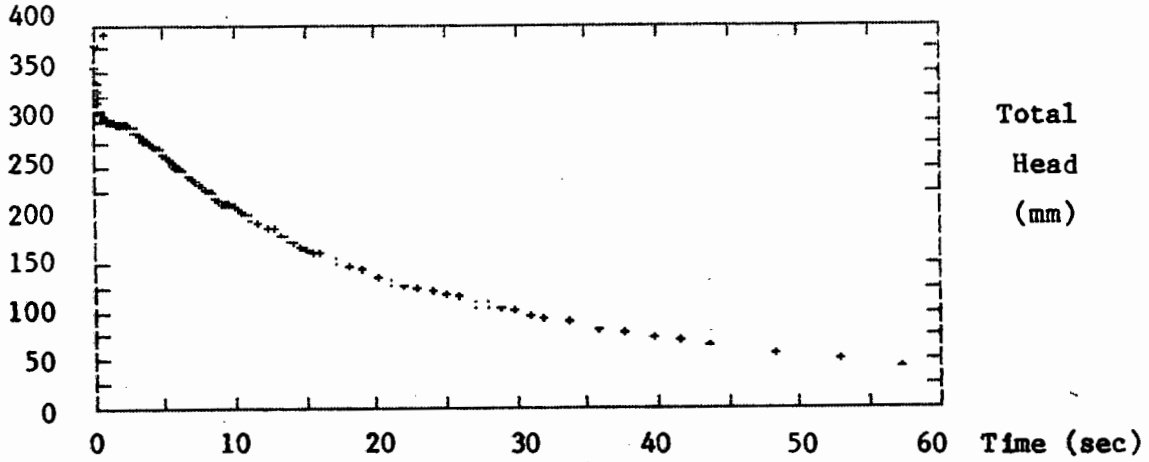
Experiment no. 2 / Run no. 3 / Transducer no. TN4
400
350
300
250
200
150
100
50
0
0
10
20
30
40
50
60
Time (sec)
Total
Head
(mm)

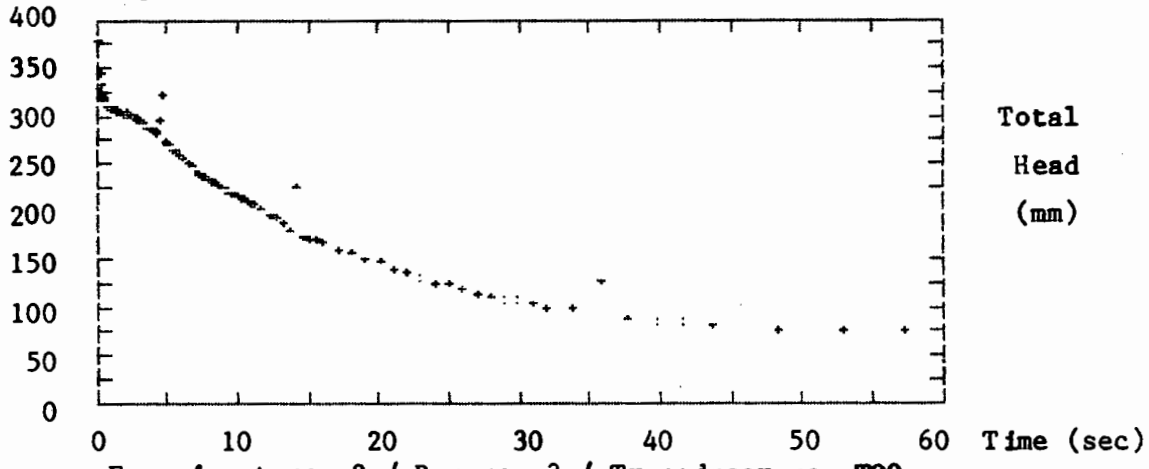
Experiment no. 2 / Run no. 3 / Transducer no. TO8
400
350
300
250
200
150
100
50
0
0
10
20
30
40
50
60
Time (sec)
Total
Head
(mm)

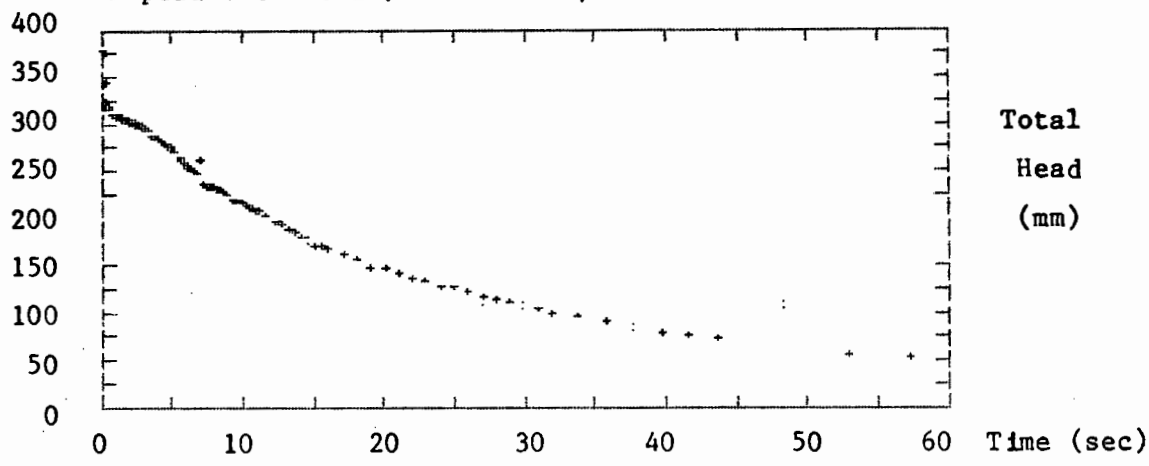
Experiment no. 2 / Run no. 3 / Transducer no. TO0
400
350
300
250
200
150
100
50
0
0
10
20
30
40
50
60
Time (sec)
Total
Head
(mm)

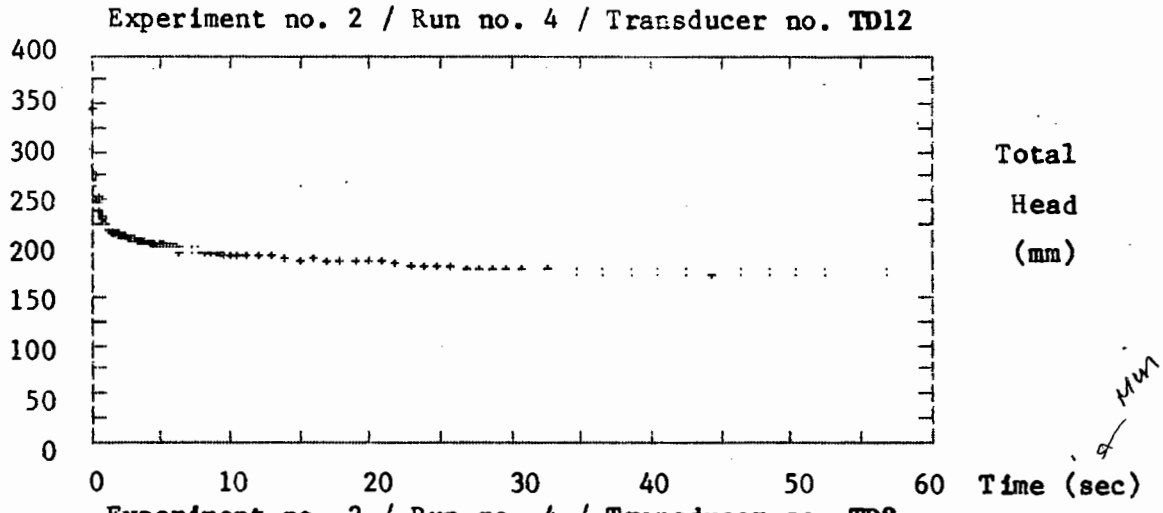
Experiment no. 2 / Run no. 4 / Transducer no. TD12
400
350
300
250
200
150
100
50
0
0
10
20
30
40
50
60
Time (sec)
Total
Head
(mm)

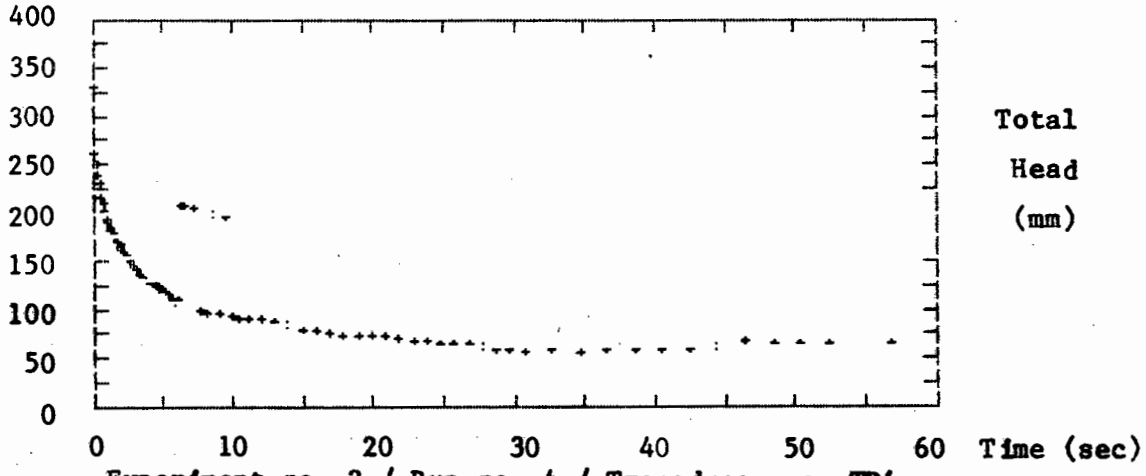
Experiment no. 2 / Run no. 4 / Transducer no. TD8
400
350
300
250
200
150
100
50
0
0
10
20
30
40
50
60
Time (sec)
Total
Head
(mm)

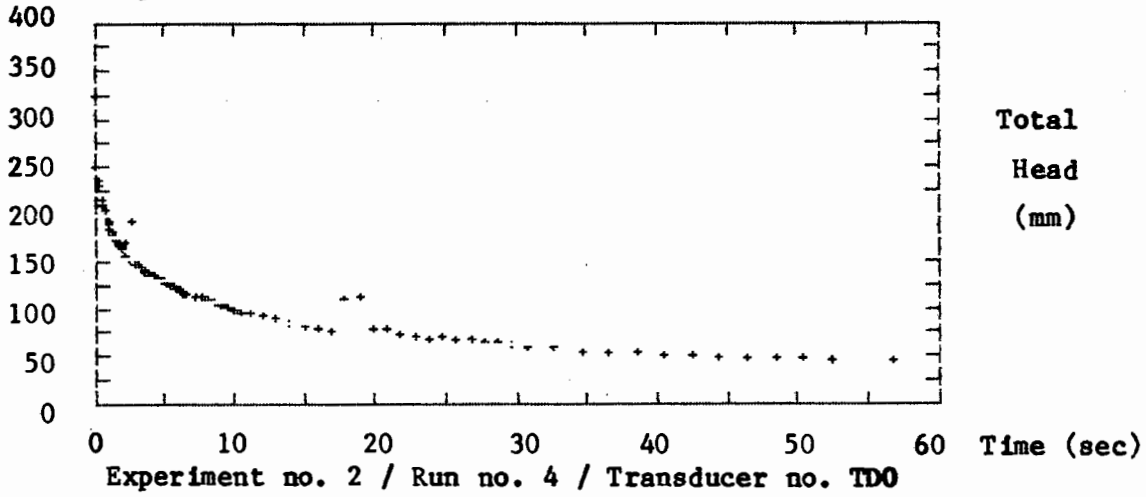
Experiment no. 2 / Run no. 4 / Transducer no. TD4
400
350
300
250
200
150
100
50
0
0
10
20
30
40
50
60
Time (sec)
Total
Head
(mm)

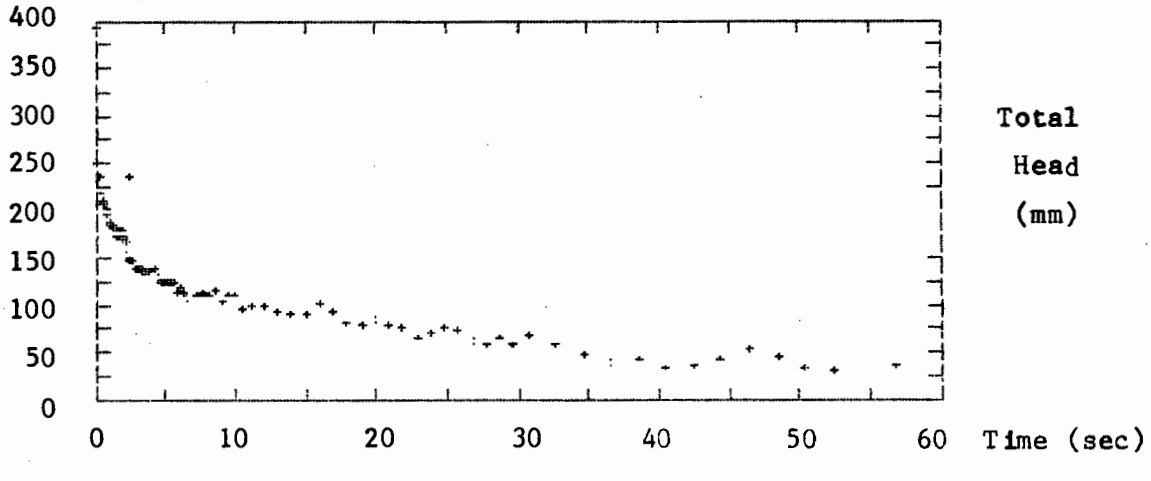
Experiment no. 2 / Run no. 4 / Transducer no. TD0
400
350
300
250
200
150
100
50
0
0
10
20
30
40
50
60
Time (sec)
Total
Head
(mm)

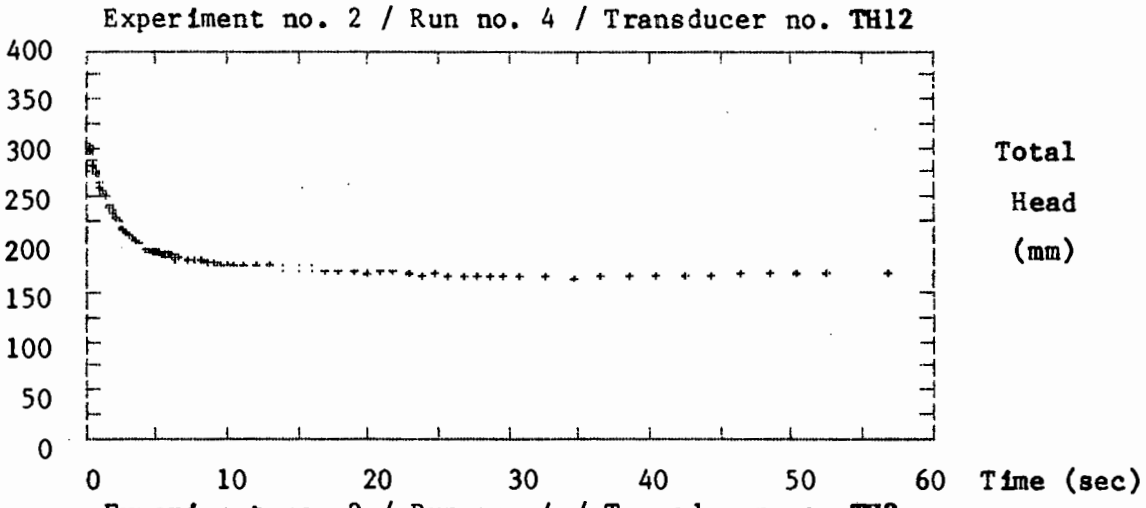
Experiment no. 2 / Run no. 4 / Transducer no. TH12
400
350
300
250
200
150
100
50
0
0
10
20
30
40
50
60
Time (sec)
Total
Head
(mm)

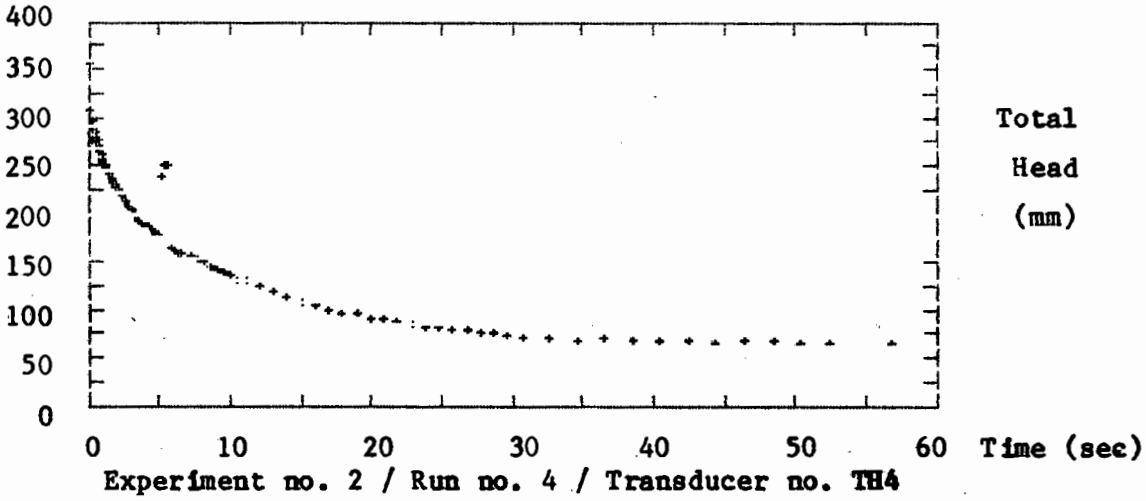
Experiment no. 2 / Run no. 4 / Transducer no. TH8
400
350
300
250
200
150
100
50
0
0
10
20
30
40
50
60
Time (sec)
Total
Head
(mm)

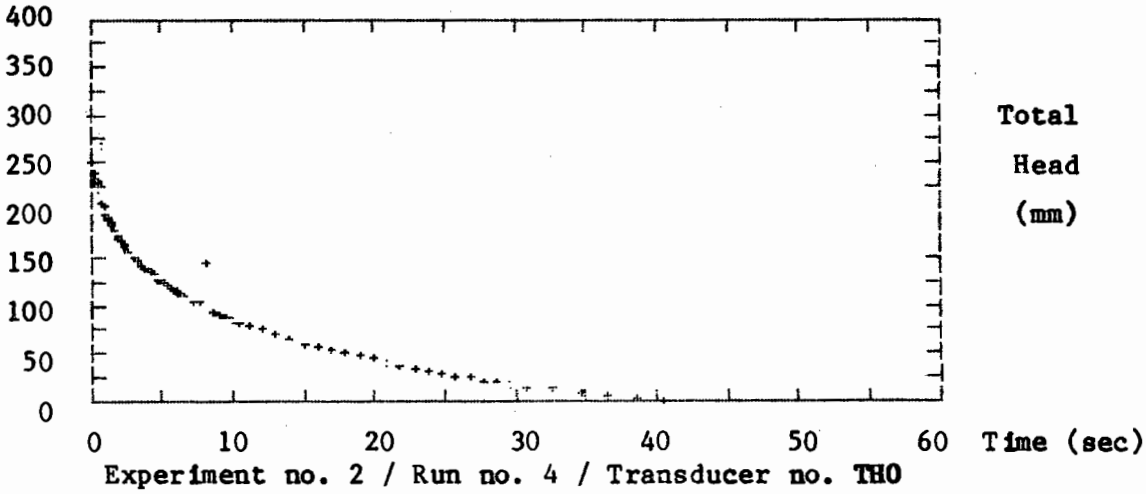
Experiment no. 2 / Run no. 4 / Transducer no. TH4
400
350
300
250
200
150
100
50
0
0
10
20
30
40
50
60
Time (sec)
Total
Head
(mm)

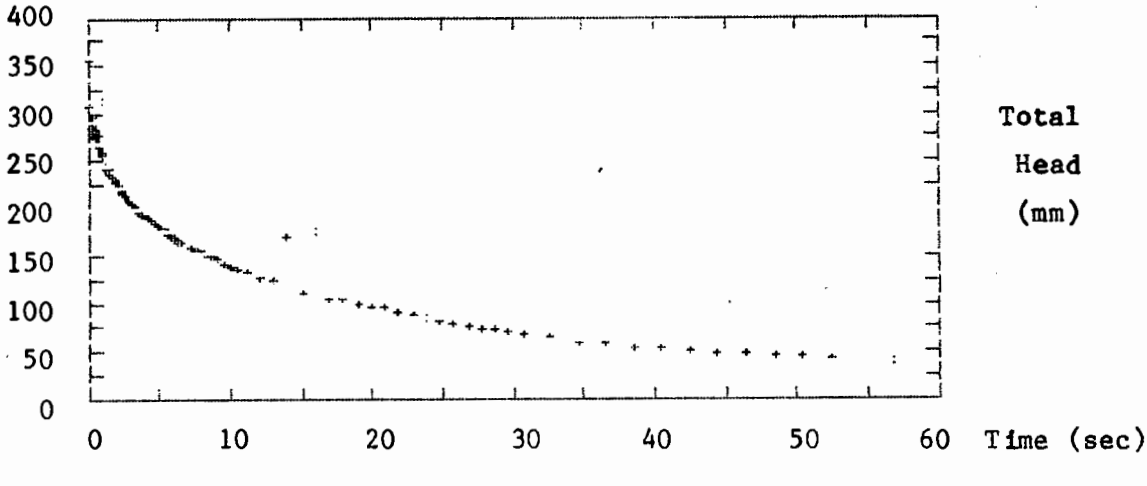
Experiment no. 2 / Run no. 4 / Transducer no. TH0
400
350
300
250
200
150
100
50
0
0
10
20
30
40
50
60
Time (sec)
Total
Head
(mm)

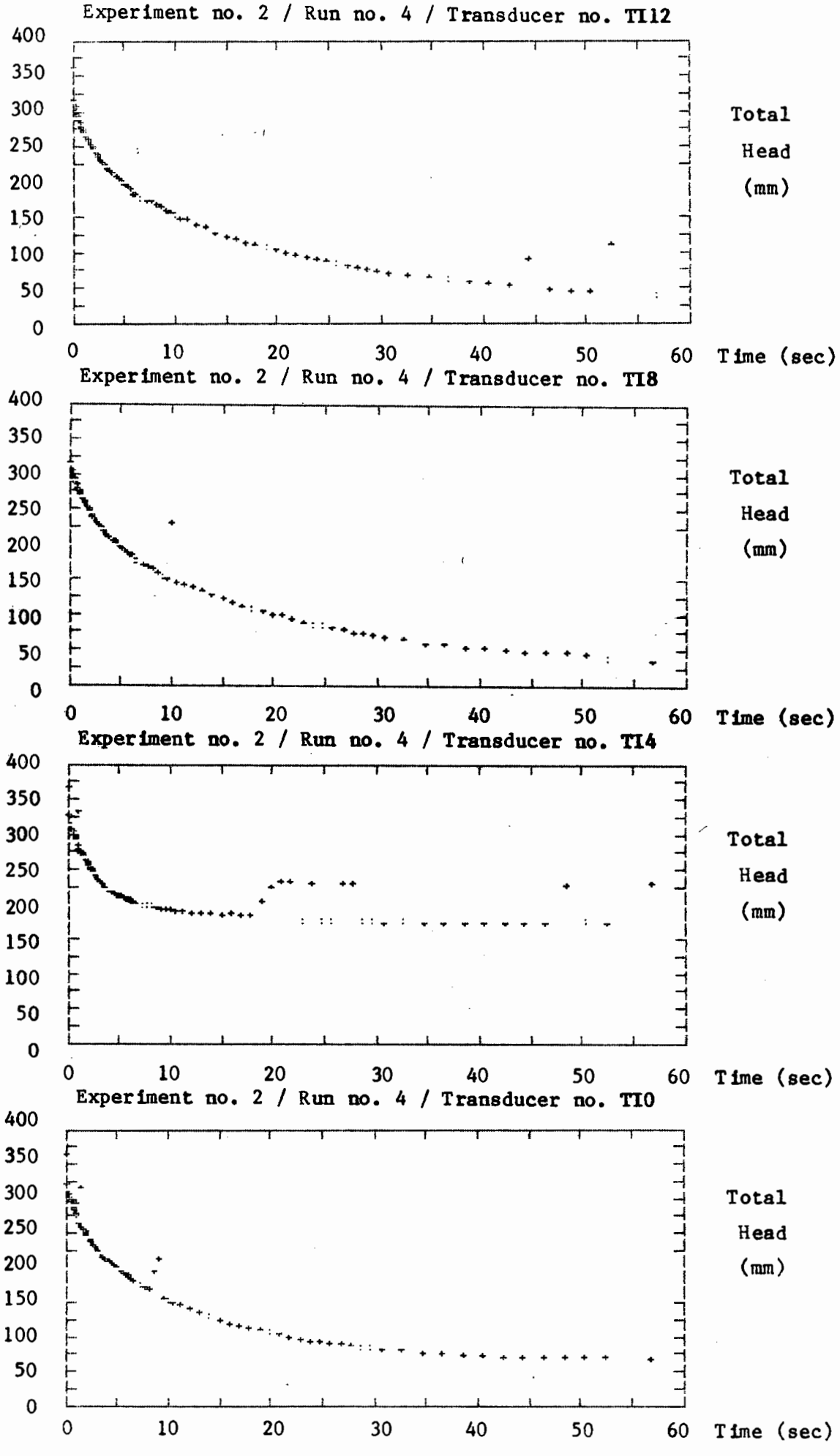
Experiment no. 2 / Run no. 4 / Transducer no. TI12
Total Head (mm)
Time (sec)
Experiment no. 2 / Run no. 4 / Transducer no. TI8
Total Head (mm)
Time (sec)
Experiment no. 2 / Run no. 4 / Transducer no. TI4
Total Head (mm)
Time (sec)
Experiment no. 2 / Run no. 4 / Transducer no. TI0
Total Head (mm)
Time (sec)
0
50
100
150
200
250
300
350
400
0
10
20
30
40
50
60

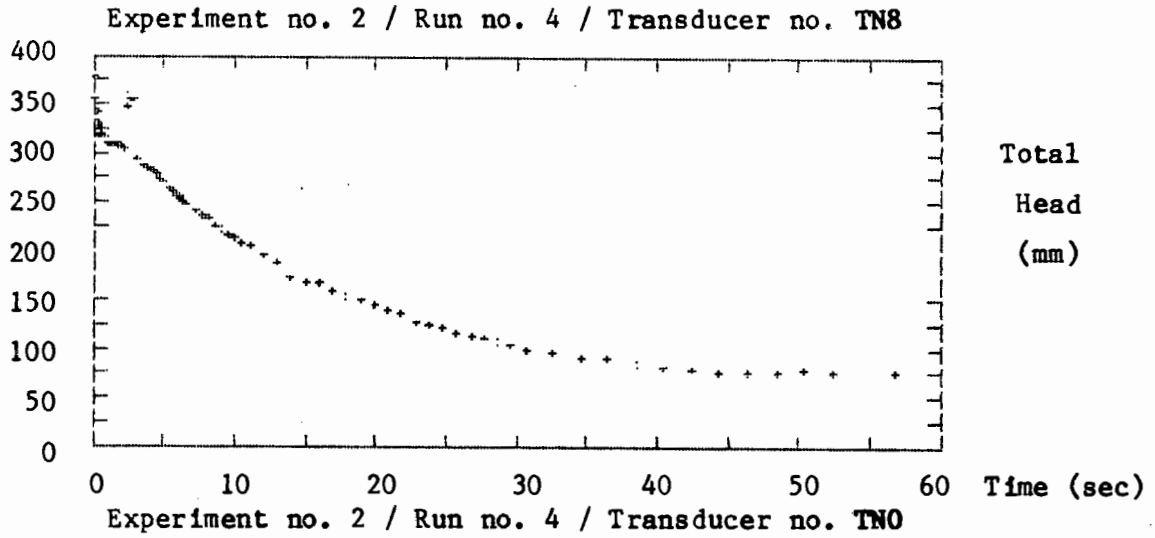
Experiment no. 2 / Run no. 4 / Transducer no. TN8
400
350
300
250
200
150
100
50
0
0
10
20
30
40
50
60
Time (sec)
Total
Head
(mm)

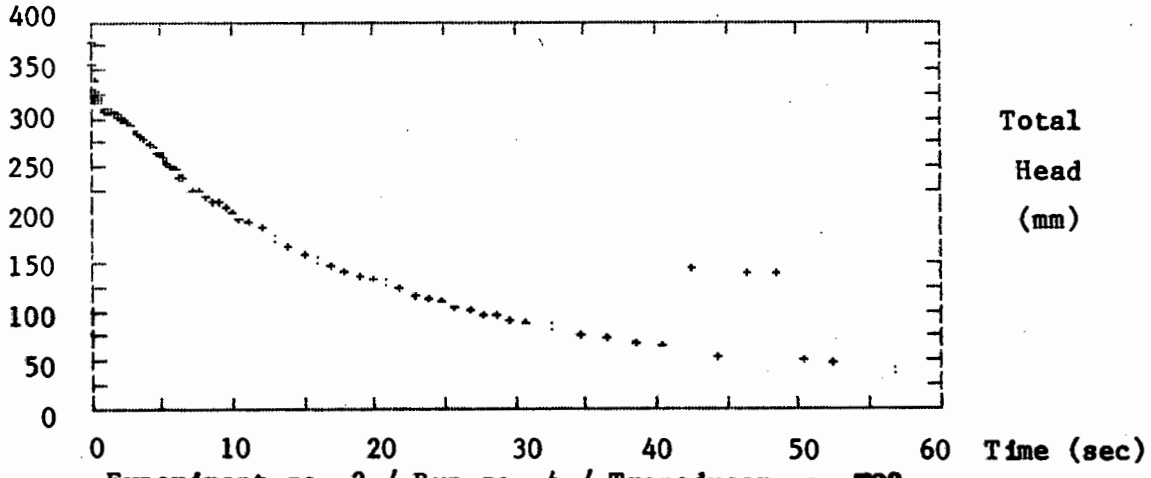
Experiment no. 2 / Run no. 4 / Transducer no. TN0
400
350
300
250
200
150
100
50
0
0
10
20
30
40
50
60
Time (sec)
Total
Head
(mm)

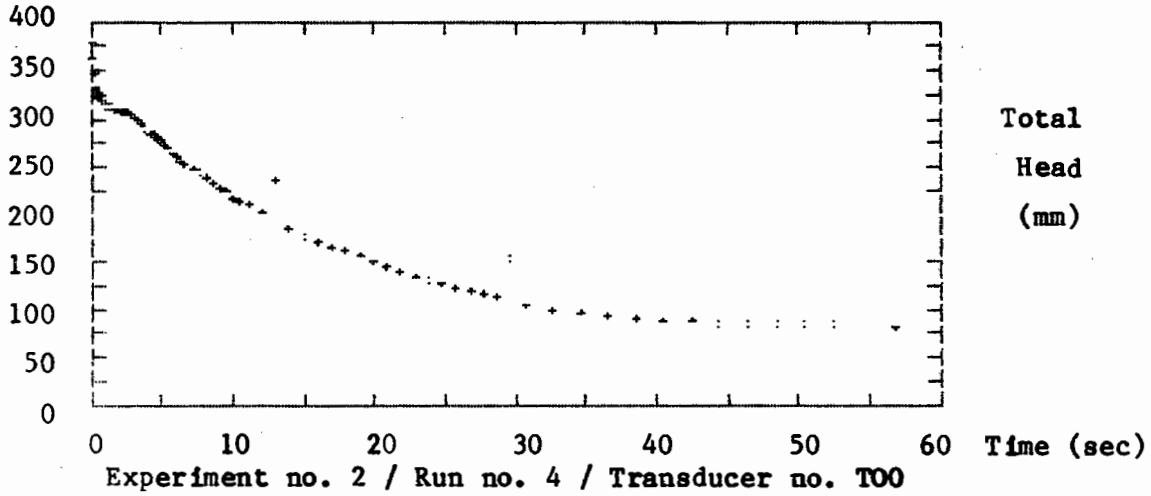
Experiment no. 2 / Run no. 4 / Transducer no. T08
400
350
300
250
200
150
100
50
0
0
10
20
30
40
50
60
Time (sec)
Total
Head
(mm)

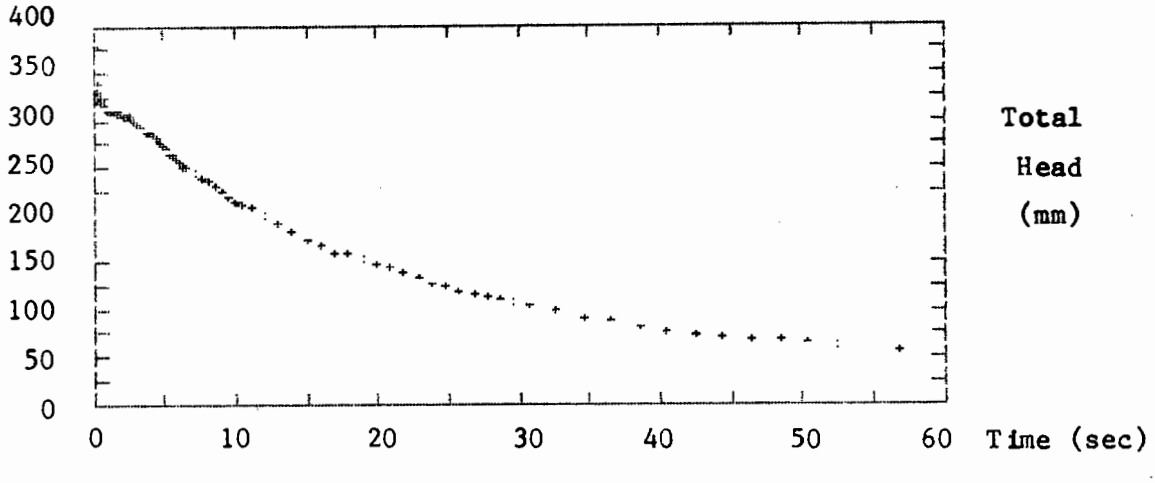
Experiment no. 2 / Run no. 4 / Transducer no. T00
400
350
300
250
200
150
100
50
0
0
10
20
30
40
50
60
Time (sec)
Total
Head
(mm)

E-11. Approximate moisture transfer analysis. Experiment no. 2.

The results for the moisture mass transfer analysis of experiment no. 2, are given here. The times of: 5; 15 and 30 minutes after the start of the experiment are considered. For each time considered the following results for the analysis is given:

A total head contour plot of the seepage domain.

A contour plot of the degree of saturation of the seepage domain.

Profile plots and their coordinates, for four vertical sections taken across the the seepage domain. The profile plots show the following with respect to elevation:

a) The pressure head;
b) Degree of saturation;
c) Relative hydraulic conductivity;
d) Horizontal hydraulic gradient; (Only sec. A & D)
e) Relative horizontal Darcian velocity. (Only sec. A & D)

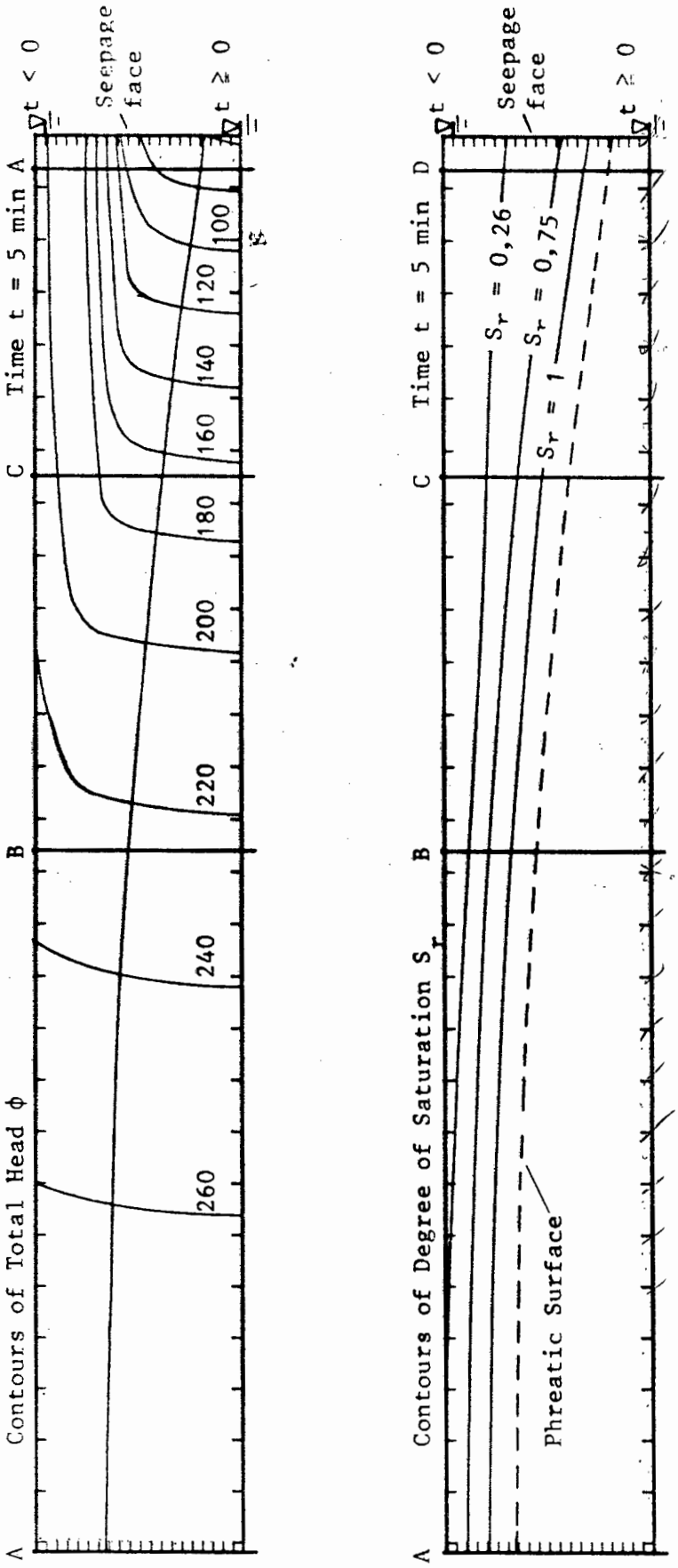
Contours of Total Head ϕ
Time t = 5 min
t < 0
t ≥ 0
Seepage face
A
B
C
D
100
120
140
160
180
200
220
240
260

Contours of Degree of Saturation S_r
Time t = 5 min
t < 0
t ≥ 0
Seepage face
S_r = 0,26
S_r = 0,75
S_r = 1
Phreatic Surface
A
B
C
D

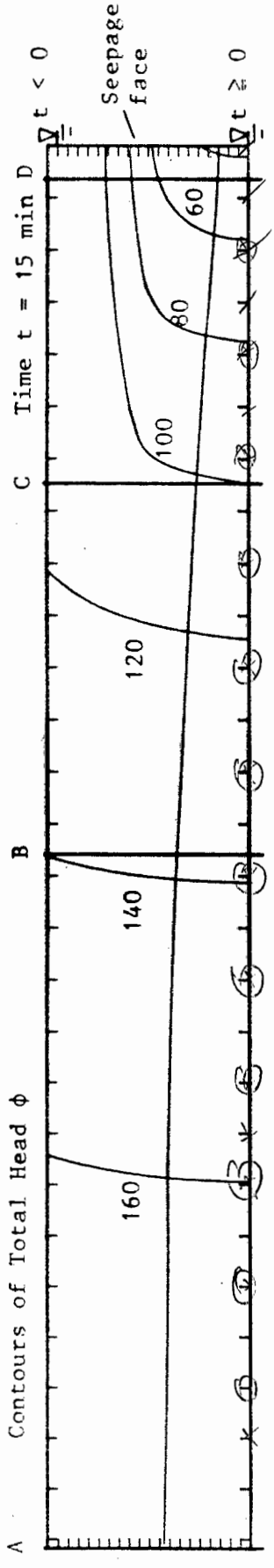
Contours of Total Head ϕ
A
B
C
D
Time t = 15 min
Seepage face
t < 0
t ≥ 0
60
80
100
120
140
160

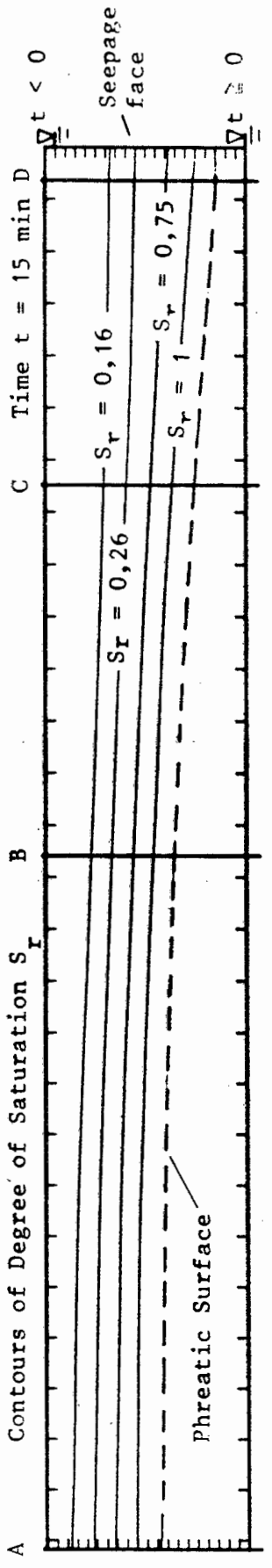
Contours of Degree of Saturation S_r
A
B
C
D
Time t = 15 min
Seepage face
t < 0
t ≥ 0
S_r = 0,16
S_r = 0,26
S_r = 0,75
S_r = 1
Phreatic Surface

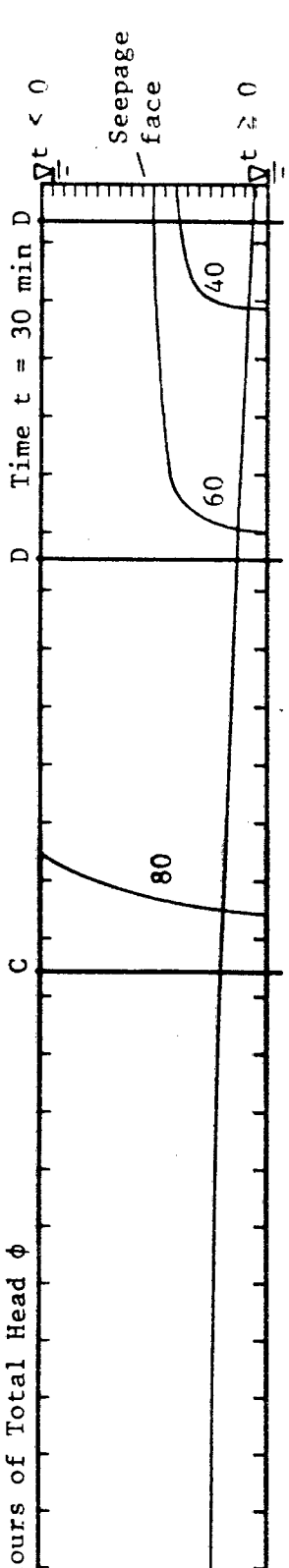
Contours of Total Head ϕ
Time t = 30 min
Seepage face
t < 0
t ≥ 0
A
C
D
100
80
60
40

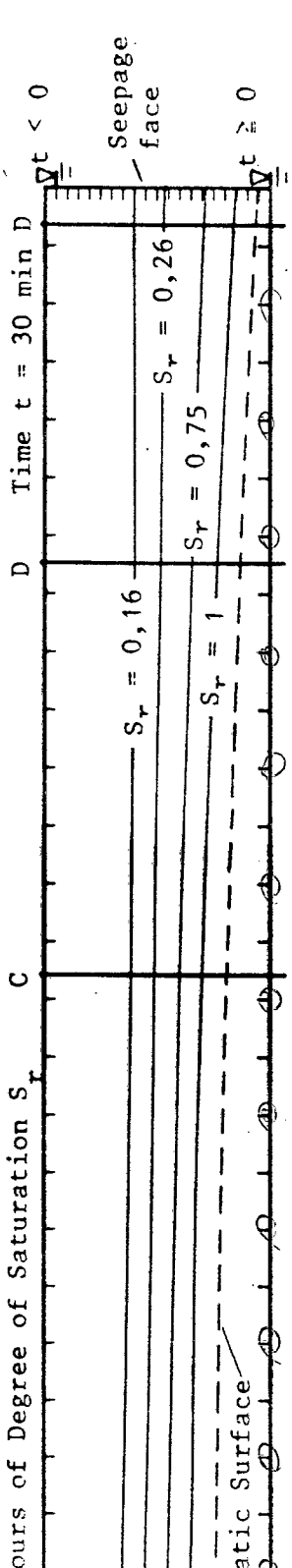
Contours of Degree of Saturation S_r
Time t = 30 min
Seepage face
t < 0
t ≥ 0
A
C
D
S_r = 0,16
S_r = 0,26
S_r = 0,75
S_r = 1
Phreatic Surface

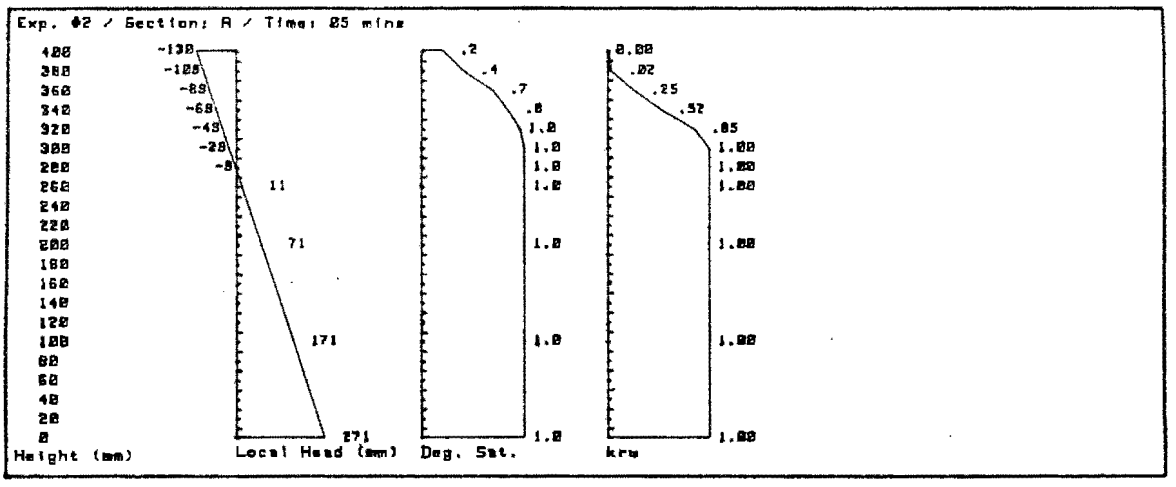
Exp. #2 / Section: A / Time: 05 mins
Height (mm)
Local Head (mm)
Deg. Sat.
krw

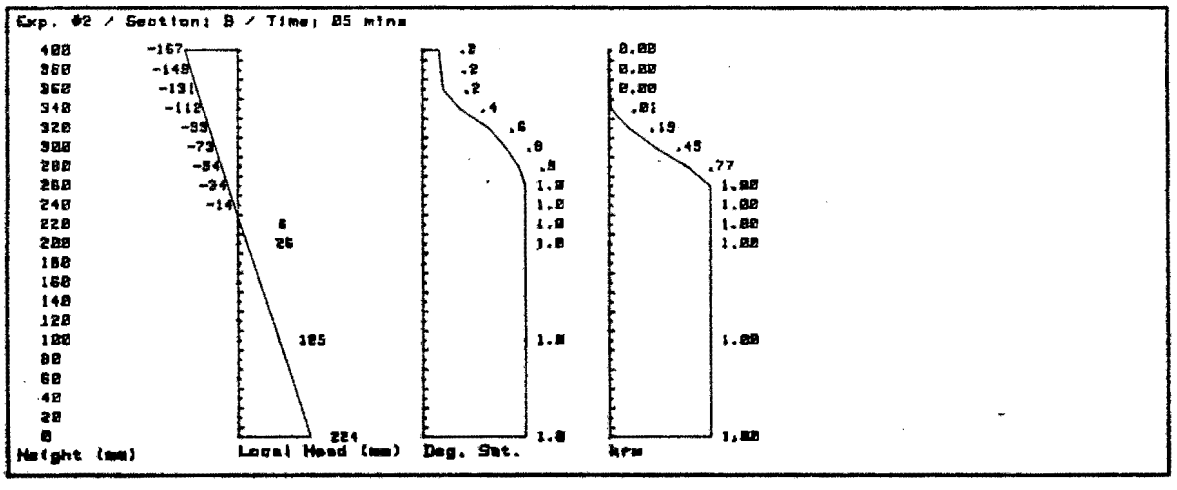
Exp. #2 / Section: B / Time: 05 mins
Height (mm)
Local Head (mm)
Deg. Sat.
krw

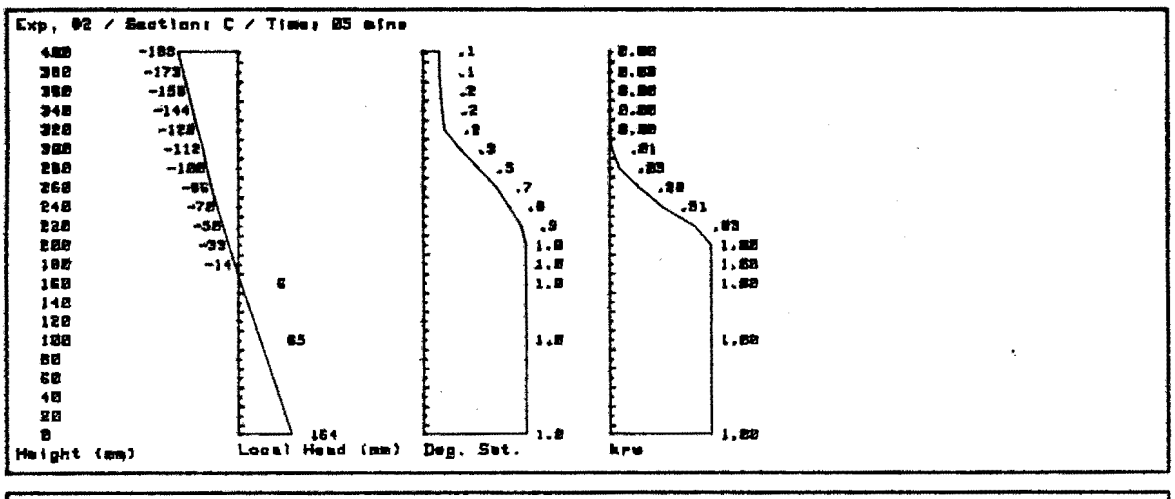
Exp. #2 / Section: C / Time: 05 mins
Height (mm)
Local Head (mm)
Deg. Sat.
krw

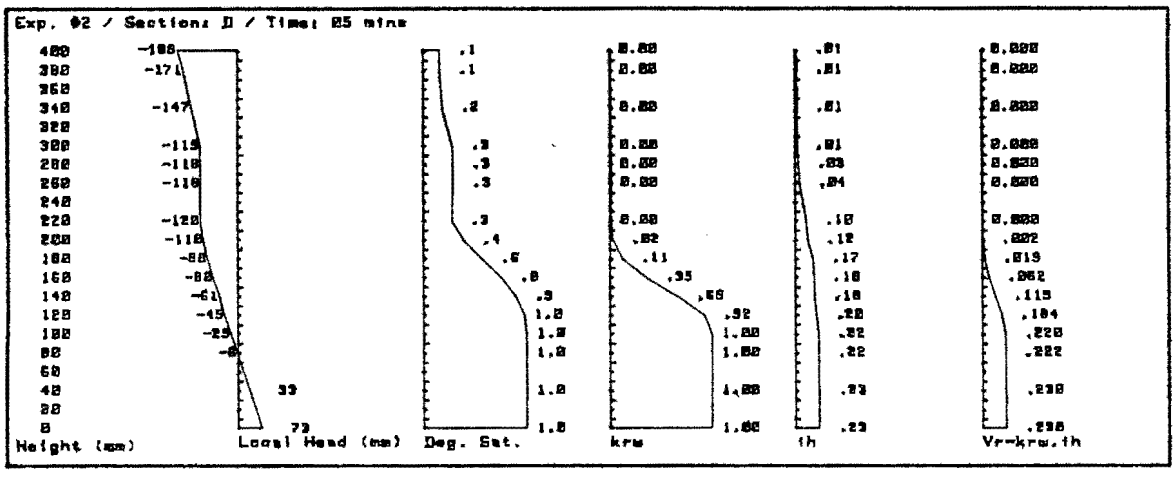
Exp. #2 / Section: D / Time: 05 mins
Height (mm)
Local Head (mm)
Deg. Sat.
krw
th
Vr=krw.th

Exp. #2 / Section: A / Time: 05 mins

Height (mm)	Local Head (mm)	Deg. Sat.	Rel. Perm.
401	-130	0.19	0.000
380	-109	0.39	0.023
360	-89	0.68	0.248
340	-69	0.83	0.516
320	-49	0.95	0.847
300	-29	1.00	1.000
280	-9	1.00	1.000
260	11	1.00	1.000
200	71	1.00	1.000
100	171	1.00	1.000
0	271	1.00	1.000

Width : 312.4 mm
Void Ratio e : 0.574
Eff. Sat. Area : 134.8 mm

Exp. #2 / Section: B / Time: 05 mins

Height (mm)	Local Head (mm)	Deg. Sat.	Rel. Perm.
401	-167	0.15	0.000
380	-149	0.17	0.000
360	-131	0.19	0.000
340	-112	0.36	0.014
320	-93	0.64	0.191
300	-73	0.80	0.452
280	-54	0.93	0.770
260	-34	1.00	1.000
240	-14	1.00	1.000
220	6	1.00	1.000
200	26	1.00	1.000
100	125	1.00	1.000
0	224	1.00	1.000

Width : 312.4 mm
Void Ratio e : 0.574
Eff. Sat. Area : 121.6 mm

Exp. #2 / Section: C / Time: 05 mins

Height (mm)	Local Head (mm)	Deg. Sat.	Rel. Perm.
401	-189	0.15	0.000
380	-173	0.15	0.000
360	-158	0.16	0.000
340	-144	0.18	0.000
320	-129	0.20	0.000
300	-112	0.35	0.013
280	-100	0.53	0.088
260	-86	0.71	0.281
240	-70	0.83	0.508
220	-50	0.95	0.827
200	-33	1.00	1.000
180	-14	1.00	1.000
160	6	1.00	1.000
100	65	1.00	1.000
0	164	1.00	1.000

Width : 312.4 mm
Void Ratio e : 0.574
Eff. Sat. Area : 106.7 mm

Exp. #2 / Section: D / Time: 05 mins

Height (mm)	Local Head (mm)	Deg. Sat.	Rel. Perm.	Hydraulic Grad.	krw x ih
401	-189	0.15	0.000	0.01	0.000
380	-171	0.15	0.000	0.01	0.000
340	-147	0.17	0.000	0.01	0.000
300	-119	0.27	0.003	0.01	0.000
280	-118	0.28	0.003	0.03	0.000
260	-118	0.28	0.004	0.04	0.000
220	-120	0.27	0.003	0.10	0.000
200	-110	0.38	0.019	0.12	0.002
180	-98	0.56	0.112	0.17	0.019
160	-80	0.75	0.353	0.18	0.062
140	-61	0.89	0.660	0.18	0.119
120	-45	0.98	0.921	0.20	0.184
100	-25	1.00	1.000	0.22	0.220
80	-6	1.00	1.000	0.22	0.222
40	33	1.00	1.000	0.23	0.230
0	73	1.00	1.000	0.23	0.230

Width : 312.4 mm
Void Ratio e : 0.574
Eff. Sat. Area : 81.9 mm

Temp T : 18.0 deg C
Sat. Perm. ks : 0.470 cm/sec
Rel. Flow Rate : 32.6 mm
Flow Rate : 47.9 cu cm/sec

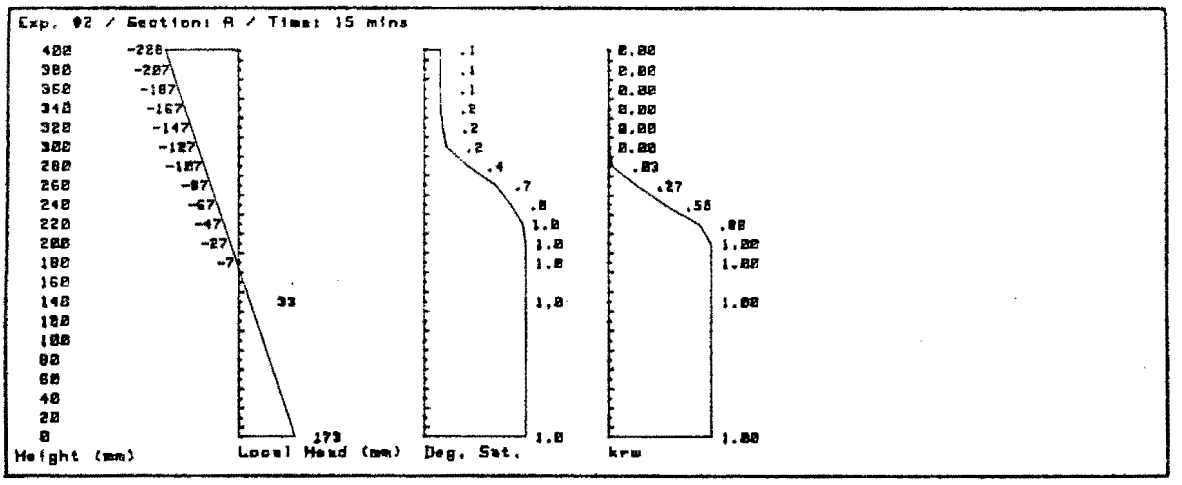
Exp. 02 / Section: A / Time: 15 mins
Height (mm)
Local Head (mm)
Deg. Sat.
krw

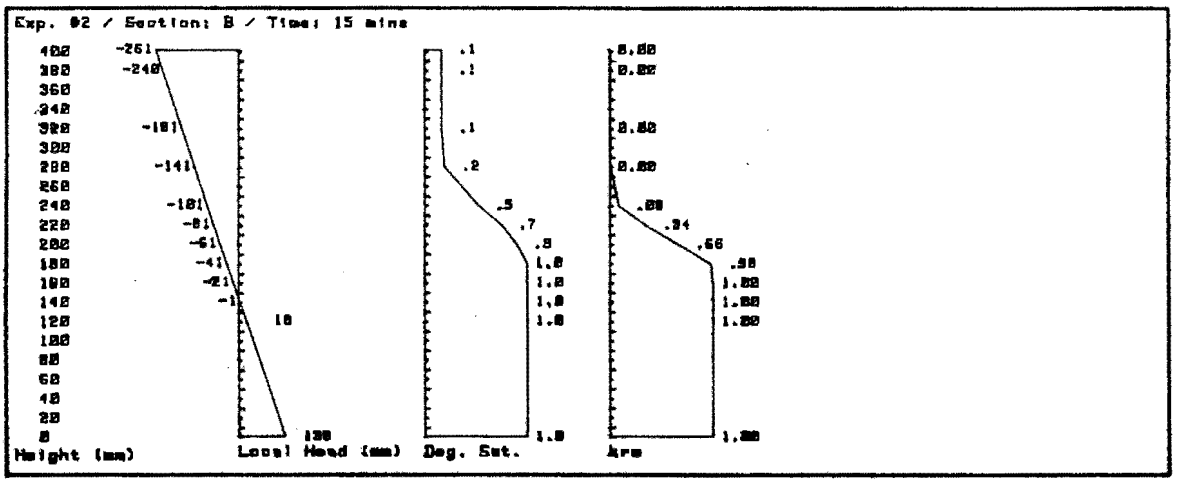
Exp. 02 / Section: B / Time: 15 mins
Height (mm)
Local Head (mm)
Deg. Sat.
krw

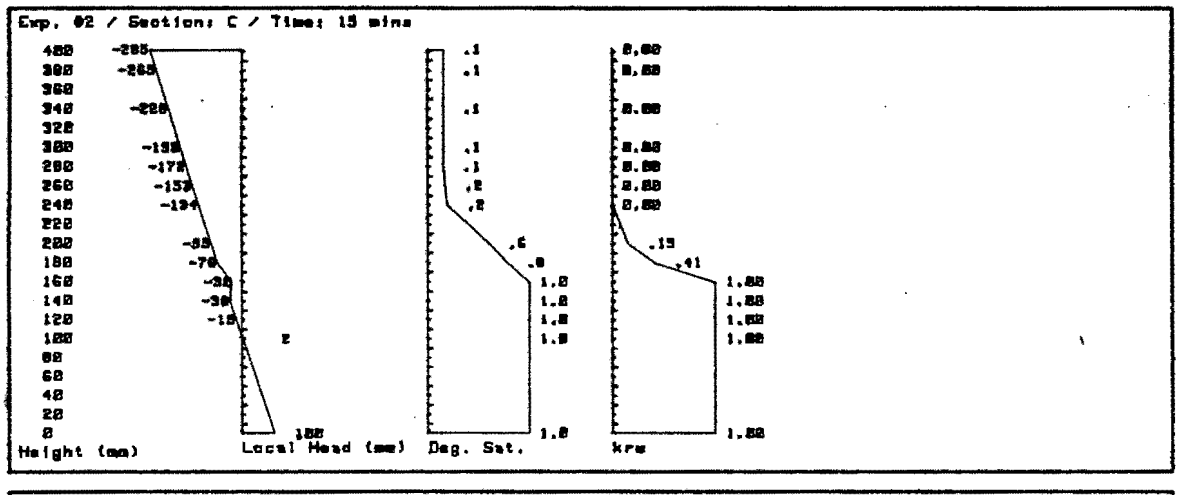
Exp. 02 / Section: C / Time: 15 mins
Height (mm)
Local Head (mm)
Deg. Sat.
krw

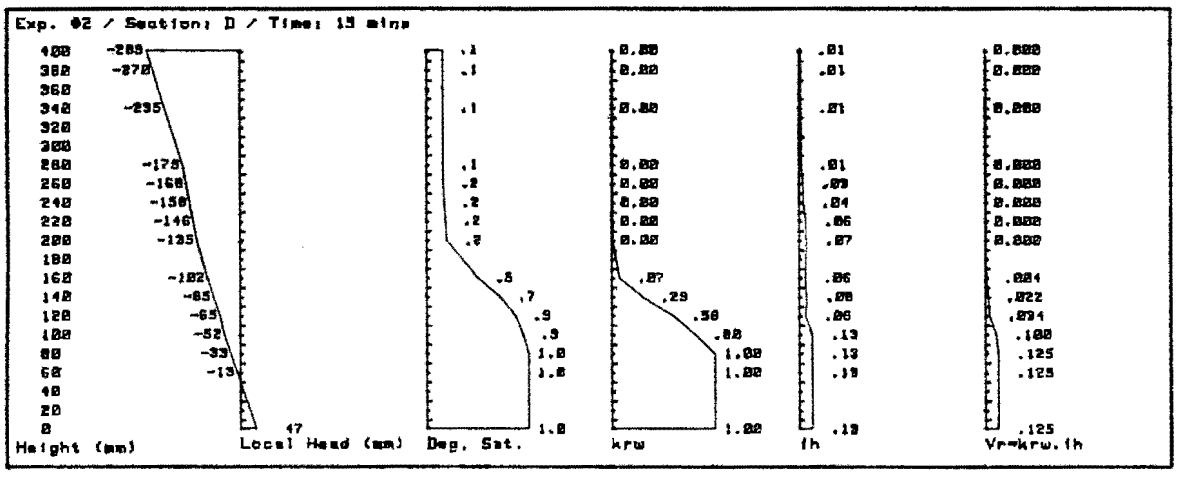
Exp. 02 / Section: D / Time: 15 mins
Height (mm)
Local Head (mm)
Deg. Sat.
krw
th
Vr=krw.th

Exp #2 / Section: A / Time: 15 mins

Height (mm)	Local Head (mm)	Deg. Sat.	Rel. Perm.
401	-228	0.15	0.000
380	-207	0.15	0.000
360	-187	0.15	0.000
340	-167	0.15	0.000
320	-147	0.17	0.000
300	-127	0.21	0.000
280	-107	0.42	0.033
260	-87	0.70	0.270
240	-67	0.85	0.550
220	-47	0.96	0.879
200	-27	1.00	1.000
180	-7	1.00	1.000
140	33	1.00	1.000
0	173	1.00	1.000

Width : 312.4 mm
Void Ratio e : 0.574
Eff. Sat. Area : 104.7 mm

Exp. #2 / Section: B / Time: 15 mins

Height (mm)	Local Head (mm)	Deg. Sat.	Rel. Perm.
401	-261	0.15	0.000
380	-240	0.15	0.000
320	-181	0.15	0.000
280	-141	0.18	0.000
240	-101	0.51	0.078
220	-81	0.74	0.339
200	-61	0.89	0.660
180	-41	0.99	0.979
160	-21	1.00	1.000
140	-1	1.00	1.000
120	18	1.00	1.000
0	138	1.00	1.000

Width : 312.4 mm
Void Ratio e : 0.574
Eff. Sat. Area : 94.9 mm

Exp. #2 / Section: C / Time: 15 mins

Height (mm)	Local Head (mm)	Deg. Sat.	Rel. Perm.
401	-285	0.15	0.000
380	-265	0.15	0.000
340	-228	0.15	0.000
300	-190	0.15	0.000
280	-172	0.15	0.000
260	-153	0.17	0.000
240	-134	0.19	0.000
200	-95	0.60	0.148
180	-76	0.78	0.406
160	-30	1.00	1.000
140	-38	1.00	1.000
120	-19	1.00	1.000
100	2	1.00	1.000
0	100	1.00	1.000

Width : 312.4 mm
Void Ratio e : 0.574
Eff. Sat. Area : 84.7 mm

Exp. #2 / Section: D / Time: 15 mins

Height (mm)	Local Head (mm)	Deg. Sat.	Rel. Perm.	Hydraulic Grad.	krw x ih
401	-289	0.15	0.000	0.01	0.000
380	-270	0.15	0.000	0.01	0.000
340	-235	0.15	0.000	0.01	0.000
280	-179	0.15	0.000	0.01	0.000
260	-168	0.15	0.000	0.03	0.000
240	-158	0.16	0.000	0.04	0.000
220	-146	0.18	0.000	0.06	0.000
200	-135	0.19	0.000	0.07	0.000
160	-102	0.49	0.067	0.06	0.004
140	-85	0.71	0.292	0.08	0.022
120	-65	0.86	0.593	0.06	0.034
100	-52	0.94	0.804	0.13	0.100
80	-33	1.00	1.000	0.13	0.125
60	-13	1.00	1.000	0.13	0.125
0	47	1.00	1.000	0.13	0.125

Width : 312.4 mm
Void Ratio e : 0.574
Eff. Sat. Area : 69.4 mm

Temp T : 18.0 deg C
Sat. Perm. ks : 0.470 cm/sec
Rel. Flow Rate : 14.5 mm
Flow Rate : 21.3 cu cm/sec

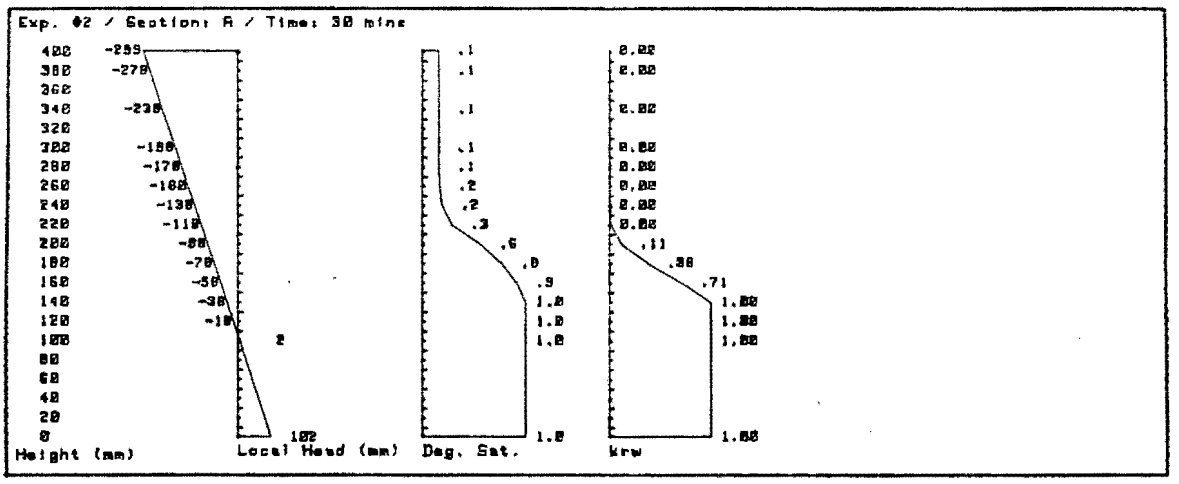
Exp. #2 / Section: A / Time: 30 mins
Height (mm)
Local Head (mm)
Deg. Sat.
krw

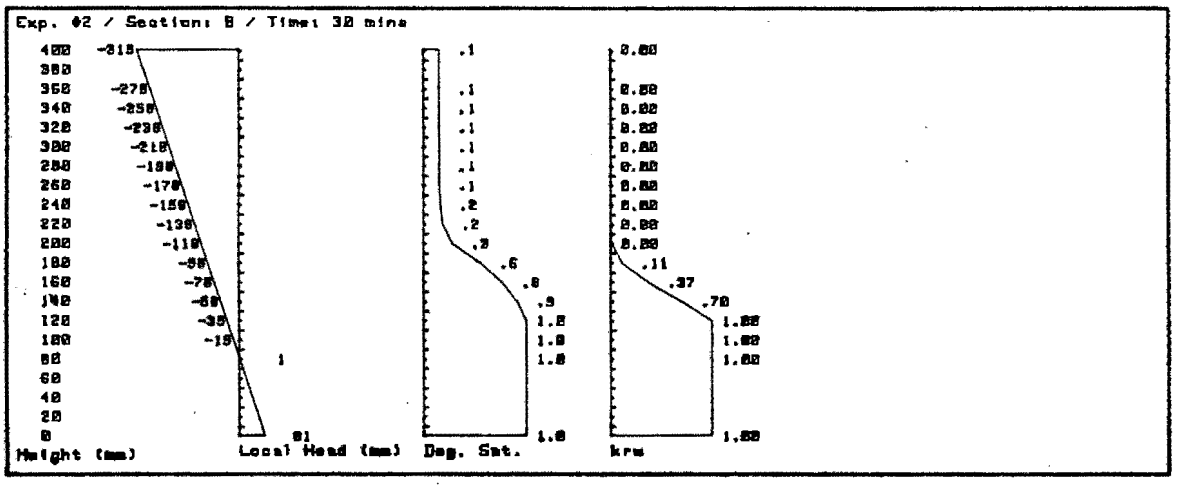
Exp. #2 / Section: B / Time: 30 mins
Height (mm)
Local Head (mm)
Deg. Sat.
krw

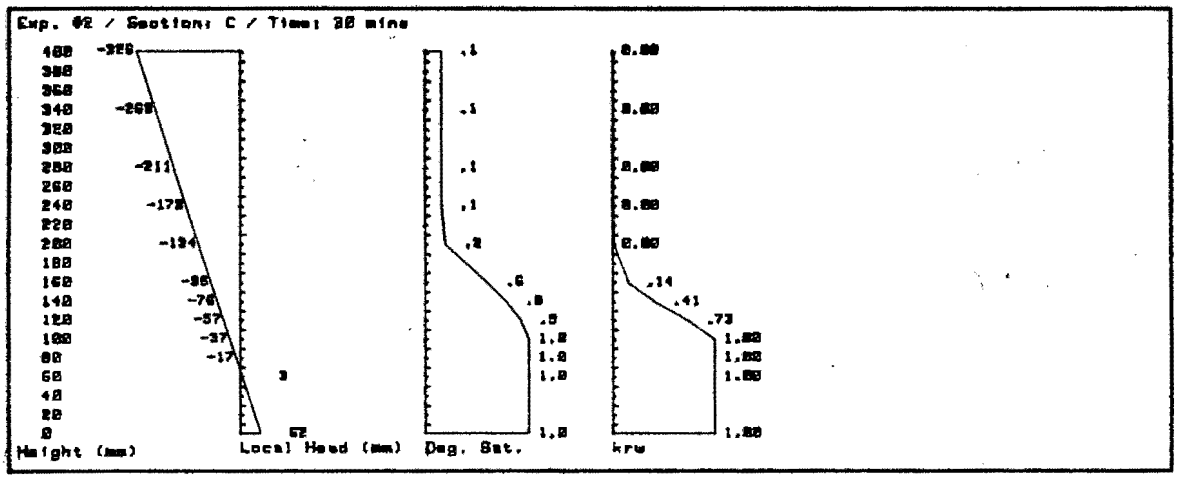
Exp. #2 / Section: C / Time: 30 mins
Height (mm)
Local Head (mm)
Deg. Sat.
krw

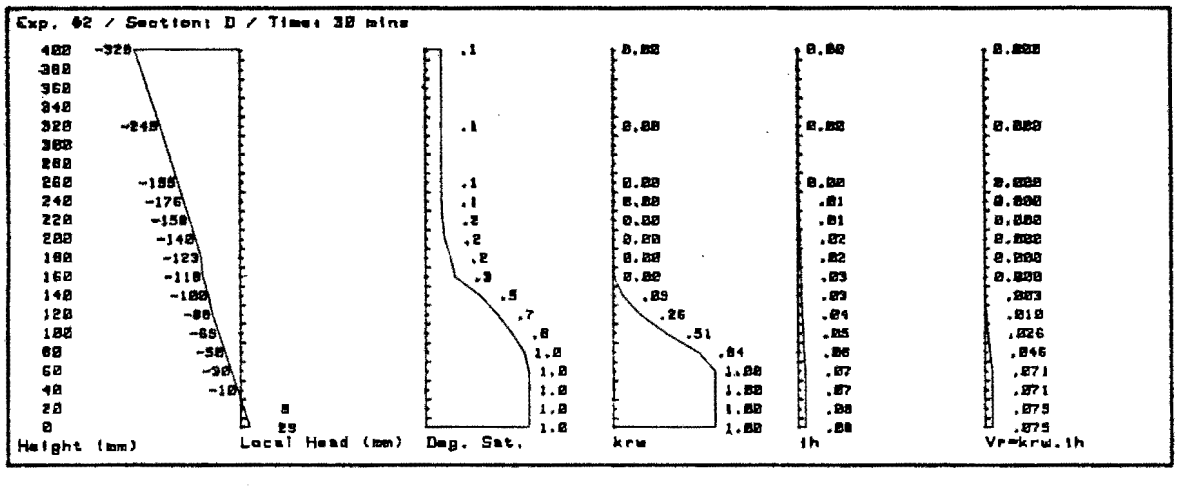
Exp. #2 / Section: D / Time: 30 mins
Height (mm)
Local Head (mm)
Deg. Sat.
krw
ih
Vr*krw.ih

Exp. #2 / Section: A / Time: 30 mins

Height (mm)	Local Head (mm)	Deg. Sat.	Rel. Perm.
401	-299	0.15	0.000
380	-278	0.15	0.000
340	-238	0.15	0.000
300	-198	0.15	0.000
280	-178	0.15	0.000
260	-160	0.16	0.000
240	-138	0.18	0.000
220	-118	0.28	0.004
200	-98	0.56	0.110
180	-78	0.77	0.380
160	-58	0.91	0.710
140	-38	1.00	1.000
120	-18	1.00	1.000
100	2	1.00	1.000
0	102	1.00	1.000

Width : 312.4 mm
Void Ratio e : 0.574
Eff. Sat. Area : 82.7 mm

Exp. #2 / Section: B / Time: 30 mins

Height (mm)	Local Head (mm)	Deg. Sat.	Rel. Perm.
401	-319	0.15	0.000
360	-278	0.15	0.000
340	-258	0.15	0.000
320	-238	0.15	0.000
300	-218	0.15	0.000
280	-198	0.15	0.000
260	-178	0.15	0.000
240	-158	0.16	0.000
220	-138	0.18	0.000
200	-118	0.28	0.003
180	-98	0.55	0.105
160	-78	0.76	0.374
140	-58	0.91	0.703
120	-39	1.00	1.000
100	-19	1.00	1.000
80	1	1.00	1.000
0	81	1.00	1.000

Width : 312.4 mm
Void Ratio e : 0.574
Eff. Sat. Area : 76.4 mm

Exp. #2 / Section: C / Time: 30 mins

Height (mm)	Local Head (mm)	Deg. Sat.	Rel. Perm.
401	-326	0.15	0.000
340	-268	0.15	0.000
280	-211	0.15	0.000
240	-173	0.15	0.000
200	-134	0.19	0.000
160	-96	0.59	0.143
140	-76	0.78	0.407
120	-57	0.92	0.731
100	-37	1.00	1.000
80	-17	1.00	1.000
60	3	1.00	1.000
0	62	1.00	1.000

Width : 312.4 mm
Void Ratio e : 0.574
Eff. Sat. Area : 71.7 mm

Exp. #2 / Section: D / Time: 30 mins

Height (mm)	Local Head (mm)	Deg. Sat.	Rel. Perm.	Hydraulic Grad.	krw x ih
401	-328	0.15	0.000	0.00	0.000
320	-249	0.15	0.000	0.00	0.000
260	-195	0.15	0.000	0.00	0.000
240	-176	0.15	0.000	0.01	0.000
220	-158	0.16	0.000	0.01	0.000
200	-140	0.18	0.000	0.02	0.000
180	-123	0.24	0.001	0.02	0.000
160	-118	0.28	0.004	0.03	0.000
140	-100	0.53	0.088	0.03	0.003
120	-88	0.69	0.257	0.04	0.010
100	-69	0.83	0.514	0.05	0.026
80	-50	0.95	0.835	0.06	0.046
60	-30	1.00	1.000	0.07	0.071
40	-10	1.00	1.000	0.07	0.071
20	9	1.00	1.000	0.08	0.075
0	29	1.00	1.000	0.08	0.075

Width : 312.4 mm
Void Ratio e : 0.574
Eff. Sat. Area : 63.1 mm

Temp T : 18.0 deg C
Sat. Perm. ks : 0.470 cm/sec
Rel. Flow Rate : 6.8 mm
Flow Rate : 10.0 cu cm/sec

Listing F-1: Example of typical input and output of an ADINAT analysis.
(Steady-state anaylsis of simple 3 element problem.)

```
**********************************************************************************************
**********************************************************************************************
**                                                                                          **
**                                                                                          **
**                                  A FINITE ELEMENT PROGRAM FOR                            **
**                  AUTOMATIC DYNAMIC INCREMENTAL NONLINEAR ANALYSIS OF TEMPERATURES        **
**                                                                                          **
**                                                                                          **
**      AAAAAAAAAA    DDDDDDDDD      IIIIIIIIIII  NN       NN   AAAAAAAAAA   TTTTTTTTTTT  **
**     AAAAAAAAAAAA   DDDDDDDDDD     IIIIIIIIIII  NNN      NN  AAAAAAAAAAAA  TTTTTTTTTTT  **
**     AA      AA     DD      DD        II        NNNN     NN  AA      AA        TT       **
**     AA      AA     DD       DD       II        NN NN    NN  AA      AA        TT       **
**     AA      AA     DD       DD       II        NN  NN   NN  AA      AA        TT       **
**     AAAAAAAAAAAA   DD       DD       II        NN   NN  NN  AAAAAAAAAAAA    TT       **
**     AAAAAAAAAAAA   DD       DD       II        NN    NN NN  AAAAAAAAAAAA    TT       **
**     AA      AA     DD       DD       II        NN     NNNN  AA      AA        TT       **
**     AA      AA     DD       DD       II        NN      NNN  AA      AA        TT       **
**     AA      AA     DD      DD        II        NN       NN  AA      AA        TT       **
**     AA      AA     DDDDDDDDD      IIIIIIIIIII  NN        N  AA      AA        TT  & S  **
**                                                                                          **
**                                                                                          **
**                                      VERSION - 84.00                                     **
**                              REFERENCE- ADINA ENGINEERING REPORT AE 84-2                  **
**                                                                                          **
**                                                                                          **
**********************************************************************************************
**********************************************************************************************
```

THIS PROGRAM IS IN ITS ENTIRETY PROPRIETARY TO AND IS SUPPORTED AND MAINTAINED BY

ADINA ENGINEERING AB
MUNKGATAN 20D
S-722 12 VASTERAS SWEDEN
TEL 021-14 40 50
TELEX 40630 ADINA S

ADINA ENGINEERING INC
71 ELTON AVENUE
WATERTOWN MA USA
TEL (617) 926-5199
TELEX 951-772 ADINA US WTWN

FOLLOWING IS A CARD IMAGE LISTING OF THE INPUT DATA

```
                                        COLUMN NUMBER
CARD          1       2       3       4       5       6       7       8
NUMBER 12345678901234567890123456789012345678901234567890123456789012345678901234567890
------ --------------------------------------------------------------------------------
  1    LIST
  2     THREE LAYER SOIL FLOW PROBLEM.          G.WARDLE.
  3       4   1   0   1.1       0.  1   0   0   0   0   0   0
  4       0
  5       0
  6       0   0   0       0
  7           0
  8       0   0
  9
 10       0   0   0
 11       1
 12           1
 13       1   0       0       0       0   1
 14       4   0       0       0      12   0
 15       0   0      20
 16       1   2       2
 17       1   2
 18           0       1       1       1
 19       1   1       8       0
 20       4   1      20       0
 21      1  3  0  0                                           1  3  0  0
 22       1       1
 23           .5
 24
 25       2       1
 26           1.
 27
 28       3       1
 29           2.
 30
 31       1   1   1   2   1   0       0   0
 32       2   1   2   3   2   0       0   0
 33       3   1   3   4   3   0       0   0
 34    STOP
------ --------------------------------------------------------------------------------
CARD          1       2       3       4       5       6       7       8
NUMBER 12345678901234567890123456789012345678901234567890123456789012345678901234567890
                                        COLUMN NUMBER
```

********** END OF INPUT LISTING **********

Appendix F.4

MASTER CONTROL CARDS

CARD NUMBER 1

NUMBER OF NODAL POINTS . . . . . (NUMNP) = 4

NUMBER OF LINEAR ELEMENT GROUPS . . . . . (NEGL) = 1

NUMBER OF NONLINEAR ELEMENT GROUPS . . . . (NEGNL) = 0

SOLUTION MODE . . . . . (MODEX) = 1
EQ.0, DATA CHECK
EQ.1, EXECUTION
EQ.2, RESTART

NUMBER OF SOLUTION PERIODS . . . . . (NPER) = 1

TIME AT SOLUTION START . . . . . (TSTART) = .0000

PRINTING INTERVAL . . . . . (IPRI) = 1

TEMPERATURE TAPE INDICATOR . . . . . (ITP56) = 0

INDICATOR FOR WRITING INPUT DATA IN
GENERATED FORM . . . . . (IPDATA) = 0
EQ.0, DETAILED PRINTING OF ALL GENERATED
INPUT DATA
EQ.1, SAME AS EQ.0 EXCEPT NO PRINTING OF
EQUATION NUMBERS (ID ARRAY)
EQ.2, SAME AS EQ.0 EXCEPT NO PRINTING OF
GENERATED NODAL POINT DATA
EQ.3, COMBINATION OF EQ.1 AND EQ.2
GT.3, NO PRINTING OF GENERATED INPUT DATA

BLANK COMMON STORAGE REQUEST . . . . . (MTOTK) = 20

INDICATOR FOR THE PREPROCESSOR ADINA-IN . . (IADIN) = 0
EQ.0, ADINA-IN NOT USED
EQ.1, INPUT DATA GENERATED USING ADINA-IN

DIRECT ACCESS FILES RECORD LENGTH IN WORDS (LREC) = 3000

INDICATOR FOR PRINTING STORAGE INFORMATION (ICORE) = 0
EQ.0, NO PRINTING
EQ.1, PRINT STORAGE INFORMATION

CARD NUMBER 2

HEAT CAPACITY MATRIX CODE . . . . . .(IHEAT) = 0
EQ.0, NO HEAT CAPACITY EFFECTS
EQ.1, LUMPED HEAT CAPACITY
EQ.2, CONSISTENT HEAT CAPACITY

NUMBER OF CONCENTRATED NODAL HEAT CAPACITIES (IHEATN) = 0

NUMBER OF PHASE INTERFACES. . . . . .(NLATHT) = 0

CARD NUMBER 3

FREQUENCIES SOLUTION CODE . . . . . (IE 5) = 0
EQ.0, NO FREQUENCIES SOLUTION
EQ.1, FREQUENCIES AND MODE SHAPES
ARE DETERMINED

CARD NUMBER 4

NUMBER OF TIME STEPS BETWEEN REFORMING
EFFECTIVE CONDUCTIVITY MATRIX . . . . . (ISREF) = 2
(NOT APPLICABLE FOR LINEAR ANALYSIS)

NUMBER OF TIME STEPS BETWEEN
EQUILIBRIUM ITERATIONS . . . . . (IEQUIT) = 2
(NOT APPLICABLE FOR LINEAR ANALYSIS)

MAXIMUM NUMBER OF EQUILIBRIUM
ITERATIONS PERMITTED . . . . . (ITEMAX) = 15

CONVERGENCE TOLERANCE . . . . . (RTOL) = .1000-002

CARD NUMBER 5

TIME INTEGRATION CODE . . . . . (IOPE) = 1
EQ.1, EULER BACKWARD METHOD
EQ.2, EULER FORWARD METHOD
EQ.3, TRAPEZOIDAL RULE
EQ.4, ALPHA, FAMILY METHOD

TIME INTEGRATION FACTOR . . . . . (ALPHA) = .1000+001

CARD NUMBER 6

NUMBER OF BLOCKS OF NODAL PRINTOUT . . . . (NPB) = 1

LATENT HEAT PRINT FLAG . . . . . (ILHFLG) = 0

CARD NUMBER 7

PRINT-OUT BLOCK 1

FIRST NODE OF THIS BLOCK . . . . . (IPNODE(1,1) = 1

LAST NODE OF THIS BLOCK . . . . . (IPNODE(2,1) = 4

CARD NUMBER 8

PORTHOLE PARAMETER . . . . . (JNPORT) = 0
EQ.0, PORTHOLE NOT WRITTEN
EQ.1, PORTHOLE WRITTEN

NODAL RESULTS INTERVAL SAVING ON PORTHOLE . (IPRNOD) = 1

ELEMENT RESULTS INTERVAL SAVING ON PORTHOLE (IPRELM) = 1

A N A L Y S I S T Y P E (ESTABLISHED USING .HEAT,.RES,.NON)

TIME DEPENDENCY CODE . . . . . (ISTAT) = 0
EQ.0, STEADY STATE ANALYSIS
EQ.1, TRANSIENT ANALYSIS

NONLINEARITY CODE . . . . . (KLIN) = 0
EQ.0, LINEAR ANALYSIS
EQ.1, NONLINEAR ANALYSIS

T I M E S T E P D A T A

NUMBER OF STEPS	TIME STEP INCREMENT
1	.1000+001

N O D A L P O I N T D A T A

INPUT DATA AT NODES

NODE N	TEMPERATURE CONDITION CODE - ID(N)	NODAL POINT COORDINATES X	Y	Z	MESH GENERATING CODE KN
1	0	.00000	.00000	.00000	1
4	0	.00000	.00000	12.00000	0

GENERATED NODAL DATA

NODE N	TEMPERATURE CONDITION CODE - ID(N)	NODAL POINT COORDINATES X	Y	Z
1	0	.00000	.00000	.00000
2	0	.00000	.00000	4.00000
3	0	.00000	.00000	8.00000
4	0	.00000	.00000	12.00000

EQUATION NUMBERS

N	EQ. NUMBER	N	EQ. NUMBER	N	EQ. NUMBER	N	EQ. NUMBER
1	1						
2	2						
3	3						
4	4						

I N I T I A L C O N D I T I O N S

INITIAL CONDITIONS CODE (ICON) = 0
EQ.0, REFERENCE TEMPERATURE TREF
EQ.1, DEVIATIONS FROM REFERENCE TEMPERATURE TREF ARE READ (BUT RESTART OVER-RIDES ICON)

INITIAL CONDITIONS PRINT-OUT CODE (IPRIC) = 0
EQ.0,DO NOT PRINT
EQ.1, PRINT

REFERENCE TEMPERATURE (TREF) = .2000000+032

EXTERNAL HEAT FLOW INPUT CONTROL DATA

NUMBER OF TIME FUNCTION CURVES . . . . . (NTTF) = 1

MAXIMUM NUMBER OF POINTS IN TIME FUNCTION CURVES (NPTM) = 2

LINEAR CONVECTION CODE . . . . . (ILCOV) = 0
EQ.0, NO LINEAR CONVECTION BOUNDARY CONDITIONS
EQ.1, LINEAR CONVECTION BOUNDARY CONDITIONS

NUMBER OF SPECIFIED NODAL POINT TEMPERATURE . . . (NTEMP) = 2

NUMBER OF BOUNDARY CONVECTION NODES . . . . . (NBCV) = 0

NUMBER OF BOUNDARY RADIATION NODES . . . . . (NBRA) = 0

NUMBER OF CONCENTRATED HEAT FLOW INPUTS . . . . . (NLOAD) = 0

NUMBER OF 2/D HEAT FLUX INPUTS . . . . . (NLOAD2) = 0

NUMBER OF 3/D HEAT FLUX INPUTS . . . . . (NLOAD3) = 0

NUMBER OF INTERNAL HEAT GENERATION DATA SETS . . . (NIHT) = 0

TOTAL NUMBER OF ELEMENTS WITH INTERNAL
HEAT GENERATION . . . . . (NTOT) = 0

HEAT FLOW INPUT

TIME FUNCTION CURVE NUMBER = 1

NUMBER OF TIME POINTS = 2

TIME VALUE	FUNCTION
.00000	.1000+001
1.00000	.1000+001

SPECIFIED NODAL POINT TEMPERATURES

NODE	TIME FUNCTION CURVE NO.	FUNCTION MULTIPLIER	STARTING TIME	KN
1	1	.8000+001	.0000	0
4	1	.2000+002	.0000	0

E L E M E N T G R O U P D A T A

C O N D U C T I O N E L E M E N T G R O U P ..... = 1 (LINEAR CONDUCTION)

E L E M E N T D E F I N I T I O N

ELEMENT TYPE . . . . . .(NPAR(1)). . = 1
   EQ.1, 1-DIM CONDUCTION ELEMENTS
   EQ.2, 2-DIM CONDUCTION ELEMENTS
   EQ.3, 3-DIM CONDUCTION ELEMENTS
   EQ.4, BOUNDARY CONVECTION ELEMENTS
   EQ.5, BOUNDARY RADIATION ELEMENTS

NUMBER OF ELEMENTS. . . . . .(NPAR(2)). . = 3

TYPE OF NONLINEAR ANALYSIS. . . . . .(NPAR(3)). . = 0
   EQ.0, LINEAR
   EQ.1, MATERIALLY NONLINEAR ONLY

ELEMENT BIRTH AND DEATH OPTIONS . . . .(NPAR(4)). . = 0
   EQ.0, OPTION NOT ACTIVE
   EQ.1, BIRTH OPTION ACTIVE
   EQ.2, DEATH OPTION ACTIVE

M A T E R I A L D E F I N I T I O N

MATERIAL MODEL. . . . . .(NPAR(15)). . = 1
   EQ.1, CONSTANT CONDUCTIVITY AND CONSTANT
          SPECIFIC HEAT
   EQ.2, TEMPERATURE-DEPENDENT CONDUCTIVITY AND
          CONSTANT SPECIFIC HEAT
   EQ.3, CONSTANT CONDUCTIVITY AND TEMPERATURE-
          DEPENDENT SPECIFIC HEAT
   EQ.4, TEMPERATURE-DEPENDENT CONDUCTIVITY AND
          TEMPERATURE-DEPENDENT SPECIFIC HEAT
   EQ.5, TIME-DEPENDENT CONDUCTIVITY AND
          CONSTANT SPECIFIC HEAT

NUMBER OF DIFFERENT SETS OF MATERIAL
   CONSTANTS . . . . . .(NPAR(16)). . = 3

NUMBER OF MATERIAL CONSTANTS PER SET. .(NPAR(17)). . = 1
(CONDUCTIVITY)

NUMBER OF MATERIAL CONSTANTS PER SET. .(NPAR(18)). . = 1
(SPECIFIC HEAT)

```
SET NO.  ..... =       1
AREA     ..... =  .100000+001

CONDUCTIVITY  ..... =  .500000+000

SPECIFIC HEAT  ..... =  .000000

SET NO.  ..... =       2
AREA     ..... =  .100000+001

CONDUCTIVITY  ..... =  .100000+001

SPECIFIC HEAT  ..... =  .000000

SET NO.  ..... =       3
AREA     ..... =  .100000+001

CONDUCTIVITY  ..... =  .200000+001

SPECIFIC HEAT  ..... =  .000000
```

E L E M E N T I N F O R M A T I O N

N	IPS	II	JJ	MAT. SET	KG	ETIME	ISVPH
1	1	1	2	1	1	.0000	0
2	1	2	3	2	1	.0000	0
3	1	3	4	3	1	.0000	0

TOTAL SYSTEM DATA

```
NUMBER OF EQUATIONS . . . . . .(NEQ) =     4

NUMBER OF MATRIX ELEMENTS . . . . . .(NWK) =     7

MAXIMUM HALF BANDWIDTH . . . . . .(MA ) =     2

MEAN HALF BANDWIDTH . . . . . .(MAM) =     2

MAXIMUM BLOCK LENGTH . . . . . .(ISTOH) =     7

NUMBER OF BLOCKS . . . . . .(NBLOCK) =     1

MAXIMUM TOTAL STORAGE AVAILABLE . . . . . .(MTOT) =  52648


NUMBER OF COLUMNS PER BLOCK AND 1ST COUPLING BLOCK
  NUMBER OF BLOCK              1
  NUMBER OF COLUMNS PER BLOCK  4
  FIRST COUPLING BLOCK         1
```

F-2. Using ADINAT [2] with modifications.

The finite element program ADINAT [2] including the modifications made by the writer of this thesis, is available at the University of Cape Town. With the permission of Prof. W S Doyle, (Dept. of Civil Engineering.) the program may be used. Information on how to use the program, and the input required, is given by the user manual [2]. In conjunction with the user manual [2], the following three pages are used. They give the layout of the input required for the use of "MODEL 9". "MODEL 9" is the nonlinear saturated-unsaturated seepage material model that has been included by the writer, (See section 6.9.3) in ADINAT [2].

XI. TWO-D CONDUCTION ELEMENTS (continued)

For MODEL "9" (NPAR(15).eq.9)

Skip this set of cards if NPAR(15).NE.9, otherwise, input NPAR(16) sets of cards.

conductivity card(s) (8F10.0)

note	columns	variable	entry
(1)	1 - 10	PROP(1,N)	Local Pressure Head at pt. 1, ϕ_1
	11 - 20	PROP(2,N)	Local Pressure Head at pt. 2, ϕ_2
	.	.	.
	.	.	.
		PROP(NCON/2,N)	Local Pressure Head at pt. NCON/2
		PROP(NCON/2+1,N)	Conductivity at pt. 1, k_{a1}
		PROP(NCON/2+2,N)	Conductivity at pt. 2, k_{a2}
		.	
		.	
		PROP(NCON,N)	Conductivity at pt. NCON/2
		PROP(NCON+1,N)	RATIO OF k_a/k_b EQ.0; default set to "1"

specific moisture card(s) (8F10.0)

note	columns	variable	entry
(1)	1 - 10	PROPS(1,N)	Local Pressure Head at pt. 1, ϕ_1
	11 - 20	PROPS(2,N)	Local Pressure Head at pt. 2, ϕ_2
	.	.	.
	.	.	.
		PROPS(NCONS/2,N)	Local Pressure Head at pt NCONS/2
		PROPS(NCONS/2+1,N)	Specific moisture per unit volume at pt. 1, c_1
		PROPS(NCONS/2+2,N)	Specific moisture per unit volume at pt. 2, c_2
		.	
		.	
		PROPS(NCONS,N)	Specific moisture per unit volume at pt. NCONS/2

NOTES/

(1) MODEL 9 is a nonlinear material model, in which the conductivity and the specific moisture are local pressure head dependent. Linear interpolation is used to obtain the conductivity and specific moisture of the material at points between the points input on the above cards. (See figure XI.2-4). The constants (k_a, k_b) are defined in a material coordinate system (a, b). (See figure XI.2-5). The axes a, b, are principal material axes, and β is read individually for each element in section XI.4 of the user manual [2]. The ratio k_a/k_b is entered in as the variable PROP (NCON+1,N).

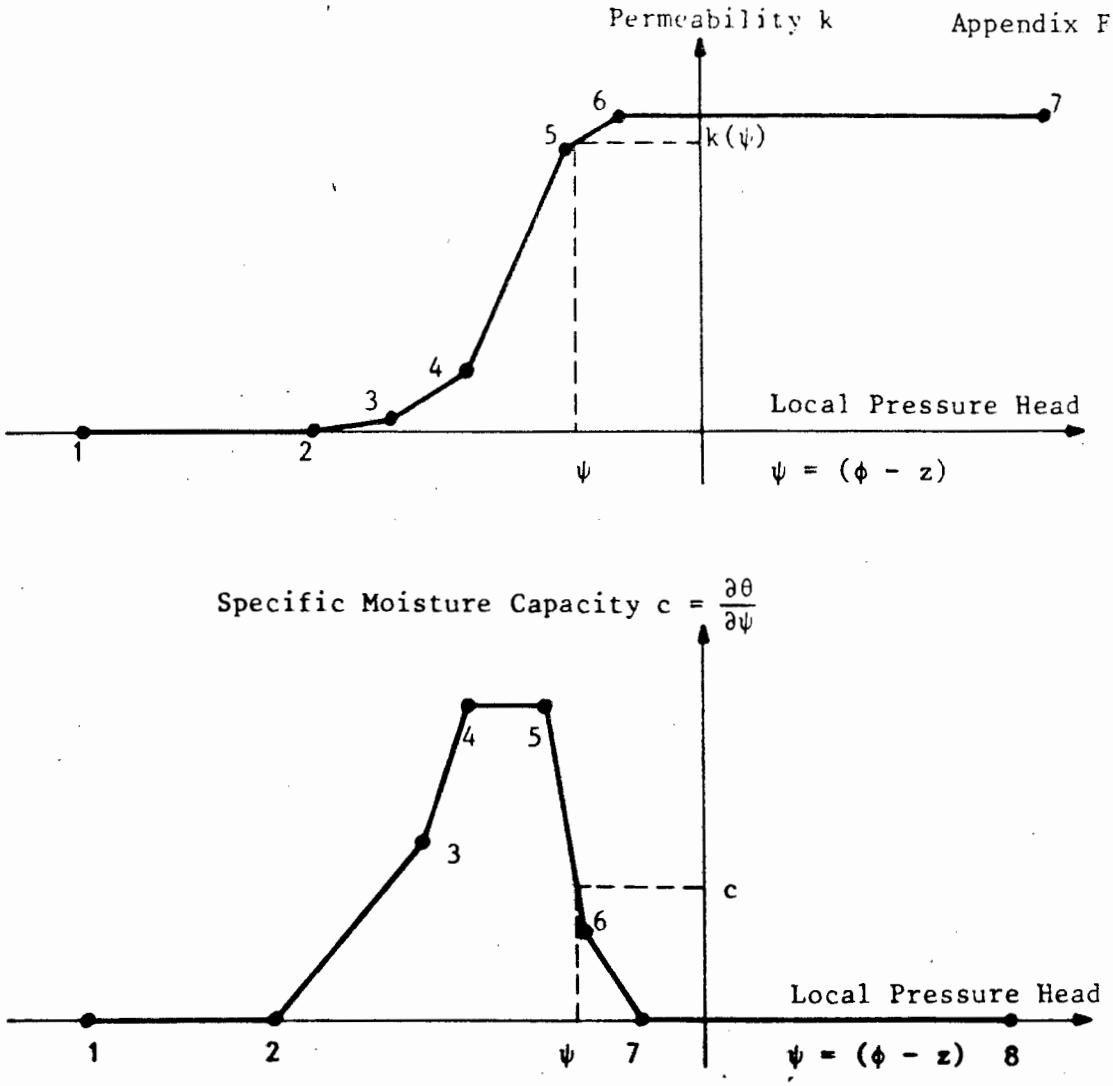

Fig XI.2-4: Material behaviour for two-dimensional saturated-unsaturated seepage model. Interpolation shown as a function of pressure head for: (a) The current conductivity; (b) The specific moisture capacity.

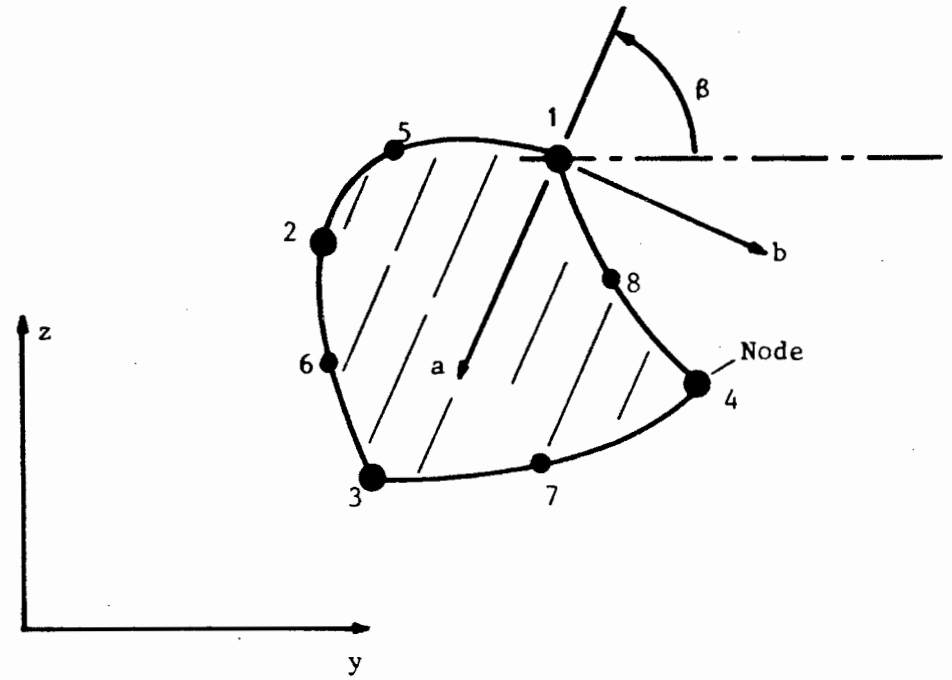

Fig XI.2-5: Principal in-plane material axes orientation for the saturated-unsaturated orthotropic seepage material model.

Modifications made to ADINAT [2].

Modifications made to the program ADINAT [2], to incorporate the nonlinear saturated-unsaturated seepage material model are as follows:

Subroutines ELCAL, TODMFE, TDFE and MATRT2 were altered so that the data for the non-linear material models could be entered with the input data. A new material model (No. 9) was chosen and this allows the hydraulic conductivity to be entered in a tabular form, as a nonlinear function, with respect to the pressure head. The specific moisture capacity is also entered in a tabular form, as a nonlinear function, also with respect to the pressure head.

Subroutines TDFE, QUADS and STSTL were altered so that the non-linear hydraulic conductivity was taken as a function of the pressure head in the formulation of the stiffness matrix.

Subroutines NLSP2H, QUADM and TDFE were altered so that the non-linear specific moisture capacity was taken as a function of the pressure head in the formulation of the mass matrix.

Subroutines MATRT2 and TDFE were also altered so that results were printed with the headings relating to pressure and not temperature.

The modifications made to the program where checked by comparing the results from the program with those given in papers. (See 6.11)

PRINT-OUT FOR TIME STEP 1 (AT TIME .100+000)

NO EQUILIBRIUM ITERATION IN THIS TIME STEP
CONDUCTIVITY REFORMED FOR THIS TIME STEP

NODAL POINT TEMPERATURES

NODE	TEMPERATURE	NODE	TEMPERATURE	NODE	TEMPERATURE	NODE	TEMPERATURE
1	.800000+001						
2	.148571+002						
3	.182857+002						
4	.200000+002						

HEAT FLUX CALCULATIONS FOR ELEMENT GROUP 1 (ONE-D CONDUCTION)

ELEMENT	HEAT FLUX
1	-.857143+000
2	-.857143+000
3	-.857143+000

SOLUTION TIME LOG (IN SEC)

FOR PROG

THREE LAYER SOIL FLOW PROBLEM. G.WARDLE.

INPUT PHASE	18.42
ASSEMBLAGE OF LINEAR CONDUCTIVITY , HEAT CAPACITY MATRICES	1.22
ASSEMBLAGE OF HEAT FLOW VECTORS	1.22
FREQUENCY ANALYSIS	.00
TRIANGULARIZATION OF LINEAR (EFFECTIVE) CONDUCTIVITY MATRIX	.01
STEP-BY-STEP SOLUTION (1 TIME STEPS)	
CALCULATION OF EFFECTIVE HEAT FLOW VECTORS	.00
UPDATING EFFECTIVE CONDUCTIVITY MATRICES AND HEAT FLOW VECTORS FOR NONLINEARITIES . .	.00
SOLUTION OF EQUATIONS	.00
EQUILIBRIUM ITERATIONS	.00
CALCULATION AND PRINTING OF TEMPERATURES .	.03
STEP-BY-STEP TOTAL .	.04
TOTAL SOLUTION TIME (SEC)	27.91

SUBROUTINE ELCAL

```
C.....................................................................
C.                                                                    .
C.   P R O G R A M                                                    .
C.      . TO CALL THE APPROPRIATE ELEMENT ROUTINES FOR READING,       .
C.        GENERATING AND STORING THE ELEMENT DATA                     .
C.                                                                    .
C.....................................................................


C     2/D CONDUCTION MATERIAL MODELS
*1    2 IF (MODEL.LT.1 .OR. MODEL.GT.9) GO TO 820
      IF (MODEL.GT.2) GO TO 230
C
      IF (INDNL.EQ.0) GO TO 20
      IF (IDEATH.GT.0) GO TO 20
      GO TO 810
C
```

SUBROUTINE TODMFE

```
C.....................................................................
C.                                                                    .
C.   M O D E L S                                                      .
C.                                                                    .
C.   MODEL = 1   LINEAR HOMOGENEOUS                                   .
C.           2   LINEAR ORTHOTROPIC                                   .
C.           3-6 CURVE DESCRIPTION MODEL                              .
C.           7   TIME-DEPENDENT CONDUCTIVITY MODEL                    .
*1           8   SEEPAGE MODEL                                        .
C.           9   SATURATED - UNSATURATED SEEPAGE MODEL                .
C.                                                                    .
C.   S T O R A G E                                                    .
C.                                                                    .
C.         N110   YZ ARRAY (ELEMENT COORDINATES)                      .
C.         N120   BETA                                               .
C.         N130   THICK                                              .
C.         N140   RLH                                                .
C.         N150   PROPS                                              .
C.         N160   PROP                                               .
C.         N170   ETIMV                                              .
C.         N180   LM ARRAY (ELEMENT CONNECTIVITY)                    .
C.         N190   IELT                                               .
C.         N200   IPS                                                .
C.         N210   MATP                                               .
C.         N220   NOD5                                               .
C.         N230   ITABLE                                            .
C.         N240   ISVPH                                             .
C.         N250   ISO                                                .
C.                                                                    .
C.....................................................................


      COMMON A(1)
      REAL A
*1    DIMENSION NMCON(9)
C     ------ ---- -
C
C
*1    DATA NMCON /1,2,0,1,2,0,0,1,0/
C
C
```

```
      SUBROUTINE TDFF (D,Y,Z,PMT,YZ,BETA,THICK,RLH,PROPS,PROP,FTREV,
     1                 LM,IELT,IPST,MATP,NODS,ITAPE,ISUPH,ISO,
     2                 NTABLE,NCON,NCONS,NOM,ND5DIM,NCOR,NDOF,NLTNHT)
C
C
C
C     R E A D   A N D   G E N E R A T E   E L E M E N T
C     I N F O R M A T I O N
C
C
      IF (IDATWR.NE.0) GO TO 5
      WRITE (NFLIST,2050) NPAR1,NUME,INDNL
      WRITE (NFLIST,2051) IDEATH,ITYP2D
      WRITE (NFLIST,2015) MXNODS,ISPISO,NINT,NTABLE
    5 CONTINUE
C
      NCONT = NCON
      IF (MODEL.EQ.9) NCONT = NCONT - 1
      DO 10 I=1,NUMMAT
      IF (MODEL.EQ.9) READ (NFREAD,1005) N,PROP(NCON,N)
      IF (PROP(NCON,N).EQ.0.D0) PROP(NCON,N) = 1.D0
      IF (MODEL.NE.9) READ (NFREAD,1000) N
      IF(NLATHT.GT.0)READ (NFREAD,1001)(RLH(J,N),J=1,NLATHT)
      READ (NFREAD,1001) (PROP(J,N), J=1,NCONT)
      READ (NFREAD,1001) (PROPS(J,N),J=1,NCONS)
      CALL MATRT2 (N,PROP(1,N),PROPS(1,N),RLH(1,N),NLATHT)
   10 CONTINUE
C
C
C     A S S E M B L E   L I N E A R   C O N D U C T I V I T Y
C     M A T R I X
C
C
  440 IF (IDEATH.GT.0 .OR. (MODEL.EQ.3.OR.MODEL.EQ.6) ) RETURN
      IF (IDEATH.GT.0 .OR. (MODEL.EQ.7 .OR. MODEL.EQ.8)) RETURN
      IF (IDEATH.GT.0 .OR. MODEL.EQ.9) RETURN
C
C     A S S E M B L E   S P E C I F I C   H E A T   M A T R I C E S
C
C
  560 CONTINUE
      IF(LHASMB.EQ.1)GO TO 901
      IF(LHSHAS.EQ.1)GO TO 950
      IF (IDEATH.GT.0 .OR. (MODEL.GT.3 .AND. MODEL.LT.7)) RETURN
      IF (IDEATH.GT.0 .OR. MODEL.EQ.9) RETURN
C
C     TWO D SPECIFIC HEAT VECTOR FOR LATENT HEAT ANALYSIS
C
  950 INDP=IND
      IND=4
      DO 960 I=1,NLATHT
      DO 962 J=1,9
  962 EDIS(J)=THF(I)+DTHF(I)*.5D0
      DO 952 N=1,NUME
      IF (MODEL.EQ.9) GO TO 970
      IF (MODEL.LE.3 .OR. MODEL.GE.7) GO TO 952
  970 CONTINUE
```

```
C
C     A S S E M B L E   N O N L I N E A R   F I N A L   S Y S T E M
C     C O N D U C T I V I T Y   A N D   E F F E C T I V E   H E A T
C     F L O W S
C
C
      CALL QUADS (N,ND,B,S,YZ(1,N),PROP(1,MTYPE),RE,EDIS,H,P,NOD5(1,N))
C
   15 IF (ISTAT.EQ.0) GO TO 30
      IF (IDEATH.EQ.0 .AND. MODEL.EQ.9) GO TO 980
      IF (IDEATH.EQ.0 .AND. MODEL.LE.3) GO TO 20
      IF (IDEATH.EQ.0 .AND. MODEL.GE.7) GO TO 20
  980 CONTINUE
C
C
C     H E A T   F L O W   C A L C U L A T I O N S
C
      IF (IPRNT.NE.1) GO TO 802
      IF (MODEL.NE.8 .AND. MODEL.NE.9) WRITE (NFLIST,2020) NG
      IF (MODEL.EQ.8 .OR. MODEL.EQ.9) WRITE (NFLIST,2021) NG
      IF (ITYP2D.EQ.0) WRITE (NFLIST,2022)
      IF (ITYP2D.EQ.1) WRITE (NFLIST,2024)
      IF (MODEL.NE.8 .AND. MODEL.NE.9) WRITE (NFLIST,2030)
      IF (MODEL.EQ.8 .OR. MODEL.EQ.9) WRITE (NFLIST,2031)
  802 MTYPE=MATP(N)
C
C     CALCULATE HEAT FLOWS IN Y AND Z DIRECTION
C
      ZELEV=0.D0
      TEMP=TIME
      IF (MODEL.EQ.7) GO TO 850
C
C     MODEL=7 IS A TIME-DEPENDENT CONDUCTIVITY MODEL
C     MODEL=8 IS A SEEPAGE MODEL
C
      TEMP=0.D0
      DO 834 I=1,ND
  834 TEMP=TEMP + H(I)*EDIS(I)
C
      IF (MODEL.LT.8.OR.MODEL.GT.9) GO TO 850
C
C     CALCULATE THE ELEVATION FOR SEEPAGE MODEL
C
  851 ZELEV=ZELEV + H(NDPT)*XX(IX)
      HTFLX1=-(C(1,1)*DISD1 + C(1,2)*DISD2)
      HTFLX2=-(C(2,1)*DISD1 + C(2,2)*DISD2)
      PRESS = (TEMP - ZELEV)
      IF (IPS.NE.0 .AND. KPRI.EQ.0 .AND. MODEL.EQ.9) WRITE
     1   (NFLIST,2041) IPT,HTFLX1,HTFLX2,PRESS
      PRESS = PRESS * PROPS(1,MTYPE)
      IF (PRESS .LE. 0.D0) PRESS = 0.D0
      IF (IPS.NE.0 .AND. KPRI.EQ.0 .AND. MODEL.NE.8.AND.
     1   MODEL.NE.9) WRITE (NFLIST,2040) IPT,HTFLX1,HTFLX2
      IF (IPS.NE.0 .AND. KPRI.EQ.0 .AND. MODEL.EQ.8) WRITE
     1   (NFLIST,2041) IPT,HTFLX1,HTFLX2,PRESS
      XYZINT(1,IPT)=HTFLX1
      XYZINT(2,IPT)=HTFLX2
```

```
      SUBROUTINE MATRT2 (N,PROP,PROPS,RLH,NLATHT)
C
C
C     SUBROUTINE TO PRINT OUT MATERIAL PROPERTIES
C     FOR TWO-DIMENSIONAL ELEMENTS
C
C
C
      IF (MODEL.EQ.9) ISEEP=2
      IF (MODEL.EQ.8) ISEEP=1
      NCONT = NCON
      IF (MODEL.EQ.9) NCONT = NCONT - 1
      IF (N.EQ.1 .AND. IDATWR.EQ.0) WRITE (NFLIST,2000) MODEL
      IF (N.EQ.1 .AND. IDATWR.EQ.0 .AND. MODEL.NE.9)
     1    WRITE (NFLIST,2050) NUMMAT,NCON,NCONS
      IF (N.EQ.1 .AND. IDATWR.EQ.0 .AND. MODEL.EQ.9)
     1    WRITE (NFLIST,2060) NUMMAT,NCONT,NCONS
      IF (IDATWR.EQ.0) WRITE (NFLIST,2100) N
      IF(NLATHT.LE.0)GO TO 30
      IF (IDATWR.EQ.0) WRITE (NFLIST,2309)
      IF (IDATWR.EQ.0) WRITE (NFLIST,2310)(I,RLH(I),I=1,NLATHT)
   30 CONTINUE
C
      GO TO (1,2,3,3,8,3) , MODEL1
C
C
C.... MODEL = 3   C U R V E   D E S C R I P T I O N   M O D E L
C
    3 IP=NCONT/2
      IF (IDATWR.EQ.0 .AND. MODEL1.NE.4 .AND. MODEL1.NE.6)
     1    WRITE (NFLIST,2200)
      IF (IDATWR.EQ.0 .AND. MODEL1.EQ.6) WRITE (NFLIST,2070) PROP(NCON)
      IF (IDATWR.EQ.0 .AND. MODEL1.EQ.4) WRITE (NFLIST,2320)
      DO 45 I=1,IP
   45 IF (IDATWR.EQ.0) WRITE (NFLIST,2210) I,PROP(I),PROP(IP+I)
C
   10 IF (MODEL.GT.3 .AND. MODEL.LT.7) GO TO 5
      IF (MODEL.EQ.9) GO TO 5
C
      IF (IDATWR.EQ.0) WRITE (NFLIST,2010) PROPS(1)
      ILSH=1
      GO TO 999
C
    5 IP=NCONS/2
      IF (IDATWR.EQ.0 .AND. MODEL1.NE.6) WRITE (NFLIST,2220)
      IF (IDATWR.EQ.0 .AND. MODEL1.EQ.6) WRITE (NFLIST,2080)
      DO 50 I=1,IP
   50 IF (IDATWR.EQ.0) WRITE (NFLIST,2210) I,PROPS(I),PROPS(IP+I)
      GO TO 999
C
 2000 FORMAT (38H M A T E R I A L   D E F I N I T I O N///,
     F        52H    EQ.7,   TIME-DEPENDENT ISOTROPIC                  /,
     G        52H            CONDUCTIVITY AND CONSTANT SPECIFIC HEAT   /,
     I        52H    EQ.8,   SEEPAGE MODEL .                           //,
     9        52H    EQ.9,   SATURATED-UNSATURATED SEEPAGE.            //)
```

```
 2060 FORMAT (40H NUMBER OF DIFFERENT SETS OF MATERIAL                 /,
     1        14H     CONSTANTS,13(2H ,),16H( NPAR(16)). . =,I5       //,
     2        40H NUMBER OF MATERIAL CONSTANTS PER SET. .              ,
     3        16H( NPAR(17)). . =,I5                                  / ,
     4        20H ( PERMEABILITY )                                    //,
     5        40H NUMBER OF MATERIAL CONSTANTS PER SET. .              ,
     6             16H( NPAR(18)). . =                          ,I5/
     7        32H ( SPECIFIC MOISTURE CAPACITY )              //)
 2200 FORMAT (//5X,5HPOINT,6X,11HTEMPERATURE,8X,12HCONDUCTIVITY /)
 2070 FORMAT (//5X,16HRATIO :  KA/KB =,E14.6,
     1        //5X,5HPOINT,5X,13HPRESSURE HEAD,7X,12HPERMEABILITY /)
 2220 FORMAT (//5X,5HPOINT,6X,11HTEMPERATURE,8X,13HSPECIFIC HEAT /)
 2080 FORMAT (//5X,5HPOINT,5X,13HPRESSURE HEAD,7X,15HSPECIFIC WEIGHT /)
 2210 FORMAT (I9,4X,E14.6,6X,E14.6)
 2309 FORMAT(///,10X,12HLATENT HEATS,///,10X,15HPHASE INTERFACE,4X,
     1       21HLATENT HEAT/UNIT VOL. /)
 2310 FORMAT(1H ,10X,I5,13X,E14.6)
 2320 FORMAT (//5X,5HPOINT,13X,4HTIME,8X,12HCONDUCTIVITY/)
 2330 FORMAT (/10X,23HPERMEABILITY  ..... =,E14.6//,
     1         10X,23HSPECIFIC WEIGHT  .... =,E14.6)
C
      END
```

```
      SUBROUTINE QUADS (NEL,ND,B,S,YZ,PROP,RE,EDIS,H,P,NOD5)
C
C
C . . . . . . . . . . . . . . . . . . . . . . . . . . . . . . . . . . .
C
C     ISOPARAMETRIC FORMULATION OF QUADRILATERAL ELEMENT CONDUCTIVITY
C     FOR AXISYMMETRIC GEOMETRY
C
C . . . . . . . . . . . . . . . . . . . . . . . . . . . . . . . . . . .
C
C
C     MODEL=7 IS A TIME-DEPENDENT CONDUCTIVITY MODEL
C     MODEL=8 IS A SEEPAGE MODEL
C     MODEL=9 IS A SATURATED-UNSATURATED SEEPAGE MODEL.
C
      TEMP=0.D0
      DO 120 I=1,ND
  120 TEMP=TEMP + H(I)*EDIS(I)
C
      IF (MODEL.LT.8.OR.MODEL.GT.9) GO TO 125
C
C     CALCULATE THE ELEVATION FOR SEEPAGE MODEL
C
      CALL FUNCT2 (E1,E2,H,P,NOD5,XJ,DET,YZ,NEL,1)
      KK=0
      DO 121 K=1,IEL
      KK=KK + 2
  121 ZELEV=ZELEV + H(K)*YZ(KK)
C
  125 CONTINUE
C
```

```
      SUBROUTINE STSTL (NEL,XX,PROP,C,TEMP,ZELEV)
C
C
C     TO GENERATE THE GLOBAL CONDUCTIVITY TENSOR FOR
C .      ISOTROPIC AND ORTHOTROPIC MATERIALS
C
C
C
      GO TO (1,2,3,1,2,3,3,8,9) , MODEL
C
 C
C .... MODEL = 9  SATURATED - UNSATURATED   S E E P A G E.
C
    9 PSI = TEMP - ZELEV
      IP = (NCON - 1)/2
      DO 900 I = 2,IP
      L = I
      IF (PSI.LE.PROP(I)) GO TO 910
  900 CONTINUE
      WRITE (NFLIST,2020) NEL
      STOP
  910 DC = PROP(IP+L) - PROP(IP+L-1)
      DT = PROP(L) - PROP(L-1)
      COND = PROP(IP+L-1) + DC*(PSI-PROP(L-1))/DT
C
      IF (PROP(NCON).NE.1.D0.AND.PROP(NCON).NE.0.D0) GO TO 90
C
      C(1,1) = COND
      C(2,2) = COND
      C(1,2) = 0.D0
      C(2,1) = 0.D0
      GO TO 100
C
C
   90 PI = 4.D0*ATAN(1.D0)
      BETR=BET*PI/1.8D2
C
C     COMPUTE THE ANGLE BETWEEN THE MATERIAL A-AXIS AND GLOBAL X-AXIS
C
      GAM= BETR
      PI2=2.D0*PI
C***DEL:MASSCOMP***
      IF (ABS(GAM).GE.PI2) GAM=AMOD(GAM,PI2)
C***END:MASSCOMP***
C
C     TRANSFORM MATERIAL PROPERTIES TO OBTAIN GLOBAL CONDUCTIVITY MATRIX
C
      COND1 = COND / PROP(NCON)
C
      SG = SIN(GAM)
      CG = COS(GAM)
      C(1,1)=COND*CG*CG + COND1*SG*SG
      C(2,2)=COND*SG*SG + COND1*CG*CG
      C(1,2)=(COND - COND1)*SG*CG
      C(2,1)=C(1,2)
C
C
  100 RETURN
C
```

```
      SUBROUTINE QUADM (NEL,ND,XM,CM,XX,PROPS,RE,EDIS,
     1                  EDIST,H,P,NODS)
C
C
C     SUBROUTINE TO CALCULATE THE HEAT CAPACITY MATRIX OF
C           A QUADRILATERAL ELEMENT.
C
C
C
      TEMP=0.D0
      ZELEV=0.D0
      DO 265 I=1,ND
  265 TEMP=TEMP + H(I)*EDIS(I)
C
      IF (MODEL.NE.9) GO TO 269
C
C .... CALCULATE THE ELEVATION FOR SAT. UNSATURATED MODEL
C
      DO 267 K = 1,IEL
  267 ZELEV = ZELEV + H(K) * XX(2,K)
C
```

```
      SUBROUTINE NLSP2H (NEL,PROPS,SH,TEMP,ZELEV)
C
C
C     TO CALCULATE SPECIFIC HEAT  ( SH )
C
C
C
      IF (MODEL.EQ.9) GO TO 10
      IF (MODEL.GT.3) GO TO 4
C
C
C .... MODEL = 9   ( PSI.  DEPENDENT SPECIFIC HEAT )
C
   10 PSI = TEMP - ZELEV
      IP = NCONS/2
      DO 900 I = 2,IP
      L = I
      IF (PSI.LE.PROPS(I)) GO TO 910
  900 CONTINUE
      WRITE (NFLIST,2000) NEL
      STOP
  910 DS = PROPS(IP+L) - PROPS(IP+L-1)
      DT = PROPS(L) - PROPS(L-1)
      SH = PROPS(IP+L-1) + DS*(PSI - PROPS(L-1))/DT
C
```